OCS Study BOEM 2012-012

Chukchi Sea Offshore Monitoring in Drilling Area (COMIDA): Chemical and Benthos (CAB)
Final Report

Prepared By:
Kenneth H. Dunton, Co-Principal Investigator
University of Texas Marine Science Institute
750 Channel View Drive, Port Aransas, TX 78373
(email of corresponding author: ken.dunton@mail.utexas.edu)

Prepared For:
Bureau of Ocean Energy Management
Department of the Interior
3801 Centerpoint Drive, Suite 500
Anchorage, AK 99503

Contract Number M08PC20056

Lead Project Scientists:
Lee W. Cooper
Kenneth H. Dunton
Jacqueline M. Grebmeier
H. Rodger Harvey
Brenda Konar
David Maidment
Susan V. Schonberg
John Trefry

March 2012

OCS Study BOEM 2012-012

Chukchi Sea Offshore Monitoring in Drilling Area (COMIDA): Chemical and Benthos (CAB)
Final Report

Prepared By:
Kenneth H. Dunton, Co-Principal Investigator
University of Texas Marine Science Institute
750 Channel View Drive, Port Aransas, TX 78373
(email of corresponding author: ken.dunton@mail.utexas.edu)

Prepared For:
Bureau of Ocean Energy Management
Department of the Interior
3801 Centerpoint Drive, Suite 500
Anchorage, AK 99503

Contract Number M08PC20056

March 2012

Study, design, oversight, and funding were provided by the U.S. Department of the Interior, Bureau of Ocean Energy Management, Alaska Outer Continental Shelf Region, Anchorage, Alaska, as part of the BOEM Environmental Studies Program, under Contract Number M08PC20056.

Chukchi Sea Offshore Monitoring in Drilling Area (COMIDA): Chemical and Benthos (CAB)
Final Report

Lead Project Scientists:

Lee Cooper
University of Maryland
Center for Environmental Science
P.O. Box 38
Solomons, MD 20688
cooper@umces.edu

Kenneth H. Dunton
University of Texas
Marine Science Institute
750 Channel View Drive
Port Aransas, TX 78373
ken.dunton@mail.utexas.edu

Jacqueline Grebmeier
University of Maryland
Center for Environmental Science
PO Box 38
Solomons, MD 20688
jgrebmei@umces.edu

H. Rodger Harvey
Old Dominion University
Ocean, Earth, and Atmospheric Sciences
4600 Elkhorn Ave
Norfolk, VA 23529
rharvey@odu.edu

Brenda Konar
University of Alaska Fairbanks
Global Undersea Research Unit
217 O'Neill P.O. Box 757220
Fairbanks, AK 99775-7220
bkonar@guru.uaf.edu

David Maidment
University of Texas at Austin
Center for Research in Water Resources
1 University Station C1786
Austin, TX 78712-0273
maidment@mail.utexas.edu

Susan V. Schonberg
University of Texas
Marine Science Institute
750 Channel View Drive
Port Aransas, TX 78373
susan.schonberg@mail.utexas.edu

John Trefry
Florida Institute of Technology
Department of Marine and Environmental Systems
College of Engineering
Edwin A Link, 101
jtrefry@fit.edu

COMIDA Principal Investigators and Science Tasks

Lee Cooper
Sediment Chlorophyll
Water Column Chlorophyll
Sediment Tracers
Associated Students and Staff:
- Marisa Guarinello
- Reagan Simpson

Kenneth H. Dunton
Food Web Structure
Infaunal Species Diversity and Abundance
Nutrient Fluxes
Associated Students and Staff:
- Nathan McTigue
- Afonso C. Souza
- Susan V. Schonberg
- K. Dana Sjostrom

Jacqueline Grebmeier
Infaunal Biodiversity
Infaunal Respiration
Sediment Grain Size
Associated Students and Staff:
- Linton Beaven
- Christian Johnson
- Stephanie Soquez
- Lisa Wilt

H. Rodger Harvey
Hydrocarbon Extraction
Sediment Screening
Associated Students and Staff:
- Karen Taylor
- Hanna Fink

Brenda Konar
Epifaunal Composition and Abundance
Associated Students:
- Alexandra Ravelo

David Maidment
GIS and Data Management
Associated Students:
- Eric Hersh
- Harish Sangireddy

John Trefry
Trace Metal Analyses in Sediments and Water Column
Trace Metal Analyses in Biota
Associated Students and Staff:
- Austin Fox
- Emily Hughes
- Robert Trocine

Table of Contents

The COMIDA-CAB Project: An Overview of the Biological and Chemical Characteristics of the Northern Chukchi Sea Benthos

Dunton, K.H., J.M. Grebmeier, J.H. Trefry, and L.W. Cooper

Kenneth H. Dunton
Marine Science Institute
The University of Texas at Austin, Port Aransas, Texas 78373

Jacqueline M. Grebmeier and Lee W. Cooper
Chesapeake Biological Laboratory,
University of Maryland, Solomons, MD 20688

John H. Trefry
Department of Marine and Environmental Systems
Florida Institute of Technology, Melbourne, Florida 32901

Introduction

The interest in Lease Sale Area 193 in the northeastern Chukchi Sea by the oil and gas industry resulted in a significant effort by the Bureau of Ocean Energy and Management (BOEM) to explore and characterize the chemical and biological environment of the seabed prior to any construction activities. It was also important to document the character of the seabed prior to any significant loss of seasonal ice that is expected to occur as a consequence of climate change and a warming Arctic Ocean. This report summarizes the results of a two-year field effort by a team of scientists from The University of Texas at Austin (main campus and Marine Science Institute), Florida Institute of Technology (FIT), Chesapeake Biological Laboratory (CBL) at the University of Maryland Center for Environment Science (UMCES), Old Dominion University, and the University of Alaska Fairbanks under a BOEM solicitation entitled, "Chukchi Sea Offshore Monitoring in Drilling Area (COMIDA): Chemical and Benthos (CAB)." Our sampling plan was designed as a robust, comprehensive effort to characterize the lease area (#193) benthic biota and chemistry in the Chukchi Sea, which would generate data that is comparable to current and past sampling efforts within the area. The oil industry concurrently collected data through monitoring programs required for Federal exploration permits. Both Shell Oil and Conoco-Phillips began conducting pre-drilling baseline benthic environmental studies in summer 2008. These private data collections will serve as a significant complement to the datasets collected under this BOEM-funded project.

Objectives

This collaborative research effort aimed to provide baseline information on the biological, physical and chemical characteristics of the Chukchi Sea lease area #193. Biological surveys documented the abundance and spatial distributions of benthic infauna and epifauna. Sediments within the COMIDA study area were examined for grain size, organic carbon, radioisotopes for

down core dating, trace metals and concentrations of straight chain and polycyclic aromatic hydrocarbons. Lastly, this research related organic carbon dynamics to the sources, cycles and fates of selected trace metals within the coastal Chukchi Sea.

Station Selection and Location

In 2009, station locations were determined using 1) a general randomized tessellation stratified design (GRTS) in the core COMIDA area (30 stations), and 2) a spatially-oriented, nearshore-to-offshore, south to north grid overlaying the GRTS design (20 stations). This arrangement resulted in the placement of 30 GRTS core stations in a spatial grid. Of the 30 GRTS stations, 10 were chosen as overlap stations to cross-calibrate and provide QA/QC between the UTMSI and CBL benthic laboratories. In 2010, the project added sites in the upstream Bering Strait/SE Chukchi region and to the core grid. The science team also reoccupied a subset of the 2009 stations (Figure 1) and expanded scientific sampling to enable a systems approach for understanding of the Chukchi Sea ecosystem.

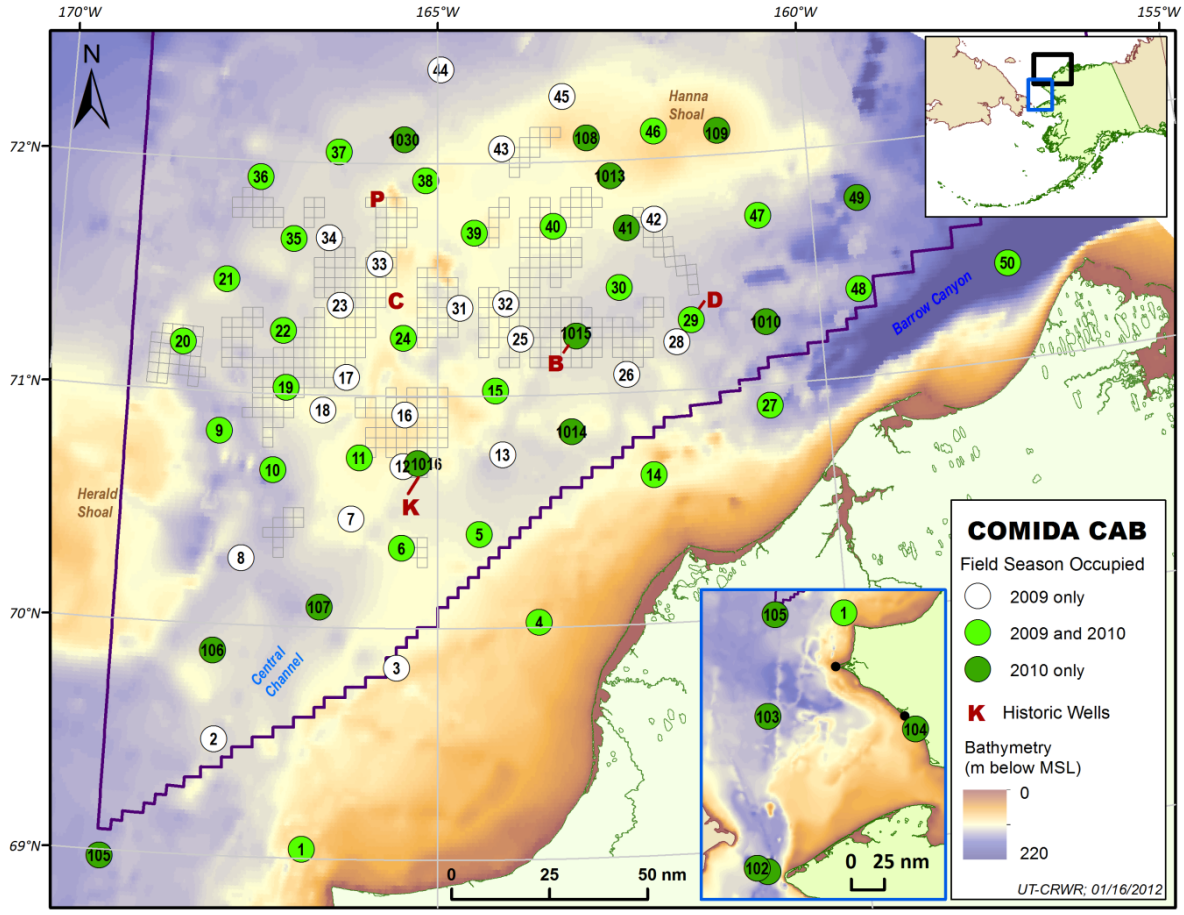

Figure 1. Station locations occupied during the COMIDA CAB program in the Chukchi Sea, Alaska, superimposed on tracts in Lease Area 193. A total of 61 stations were sampled over two field seasons, between 24 July and 12 August in 2009 and 2010. Old drill sites or prospects are denoted in red. Overall, ice conditions were more variable in 2009, with large ice fields common in the northern part of the study area. In 2010, the area was predominantly ice-free.

Data Management

In support of the extensive data sets generated by the COMIDA CAB scientists, this project included a significant data management component that is outlined in the final chapter (Hersh et al). Data management was accomplished using an Observations Data Model (ODM) relational database that incorporated a significant ArcGIS component. The graphical displays produced from this effort are illustrated throughout this report. In addition, field products, reports, data, and shapefiles are available on the COMIDA CAB website maintained at The University of Texas at Austin (http://www.comidacab.org).

Organic Contaminants, Trace Metals and Sedimentary Organic Processes

Three major water masses transit through the Chukchi Shelf and transport enormous volumes of water, nutrients, and particulate material. A significant fraction of the particulate matter is deposited in the sediments, which reflects a mixture of both natural and anthropogenic sources of hydrocarbons and trace metals. Harvey et al. determined concentrations of organic contaminants (aliphatic hydrocarbon and polycyclic aromatic hydrocarbons, PAHs) in surface sediments throughout the study area. In general, with one exception, PAH concentrations in surface sediments on the Chukchi shelf measured at background levels (< 1500 ng/g).

Harvey also measured the concentration of aliphatic n-alkanes in surface sediments. The Arctic Ocean receives significant inputs of terrigenous material from rivers and coastal erosion, and the n-alkane distribution seen in Chukchi shelf surface sediments represents a mixture of terrestrial and petroleum hydrocarbon sources (Figure 2). Unlike PAHs, which decreased in larger organisms per unit weight, aliphatic n-alkanes in *Neptunea* gastropod muscle increased in larger organisms. Consequently, *Neptunea* represents an ideal indicator species for which to monitor changes in the loadings of organic contaminants to the system. In addition, it appears that these animals are omnivorous, and rely on multiple food sources, despite their common description as "benthic predators" (Figure 3).

Similarly, Trefry et al. examined the concentrations of trace metals across the study area from 207 sediment samples. The values of all 17 trace metals were essentially at natural, background levels. Trefry et al. used the ratios of metals/Al as a model for determining background metal concentrations and identifying anthropogenic inputs. Anomalies were linked to old drill sites in the Chukchi Sea (Figure 1) and the Red Dog mine (near station 104). Trefry's work concerning trace metal concentrations in the biota also revealed that mercury is a reliable indicator of trophic level, as reported by Fox et al. (Figure 4). The data presented by Fox et al. confirms the trophic position of several key fauna reported by McTigue et al. using stable isotopes of carbon and nitrogen.

Cooper and Grebmeier used gamma spectroscopy in sediment cores collected throughout the COMIDA continental shelf study area to characterize sedimentation rates and patterns. Their work implied an averaged sedimentation rate of ~0.25 cm $year^{-1}$ without accounting for the impacts of bioturbation. Souza and Dunton explored nutrient and gas fluxes at the sediment-water interface. Their preliminary work (Table 1) showed large oxygen fluxes into the sediments

and a significant flux of both phosphate and nitrate into the water column at two of their four stations. The efflux of NO_3^- from the sediments is concomitant with an efflux of N_2 at stations 9 and 103, which suggests that benthic NO_3^- production exceeds its consumption by denitrification. It is therefore possible to infer that benthic nitrification compensates for N removal and maintains a supply of NO_3^- to benthic primary producers from the oxidation of porewater ammonium. In contrast, fluxes of nitrogen decreased significantly at station 1015 (0.4 μmoles N m^{-2} h^{-1}) and reversed direction into the sediment at station 48 (-0.8 μmoles N m^{-2} h^{-1}). Future research should investigate the relationship between sedimentation rates and benthic nutrient fluxes.

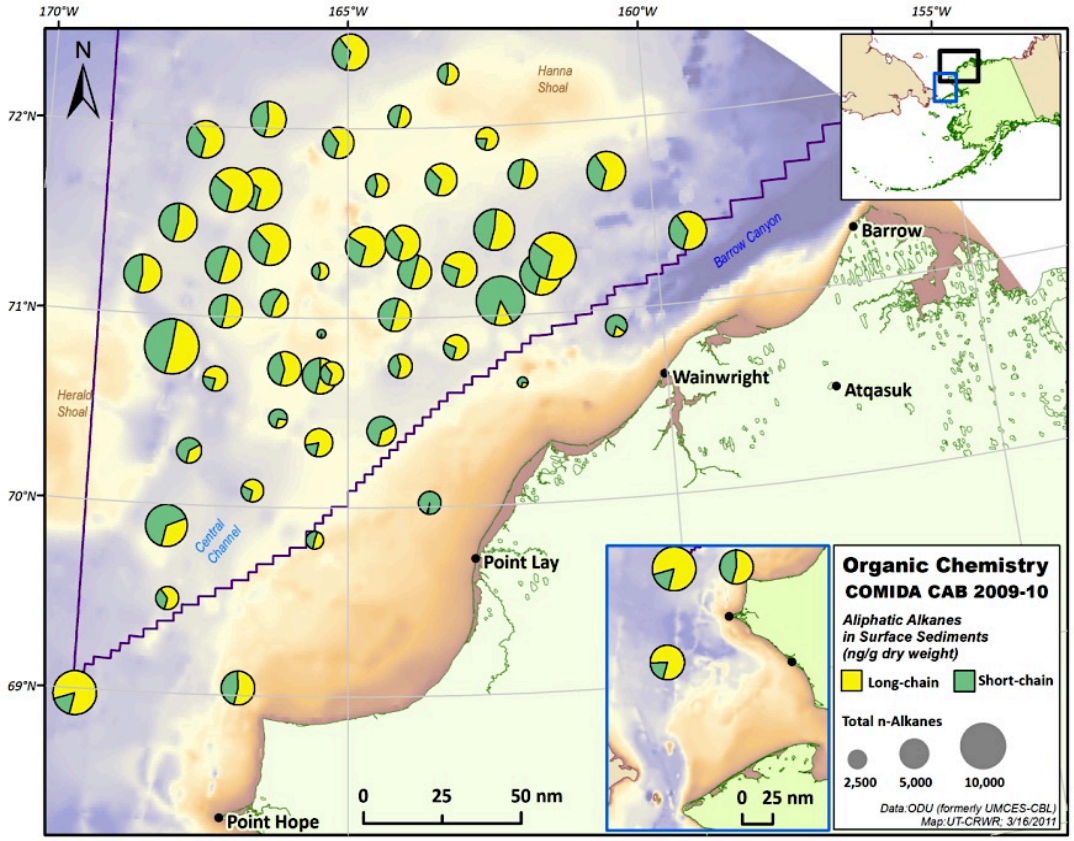

Figure 2. The concentration of aliphatic n-alkanes in surface sediments of the Chukchi Sea. Circles illustrate the total concentration and relative contribution of long and short-chain hydrocarbons across the study region. From Harvey et al.

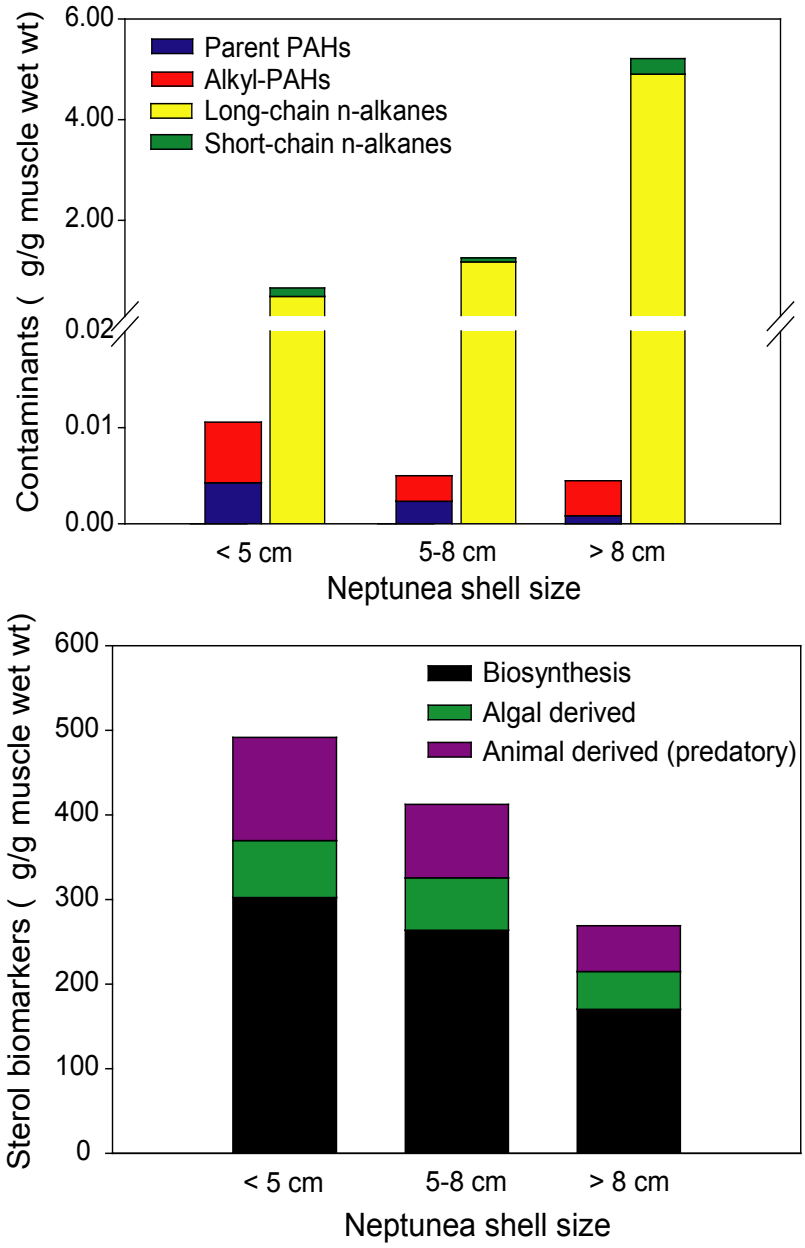

Figure 3. Trophic transfer of organic contaminants is selective in the whelk, as accumulation was only observed for some compound classes. The distribution of sterols shows that whelks rely on multiple food sources over the life of the animal. From Harvey et al.

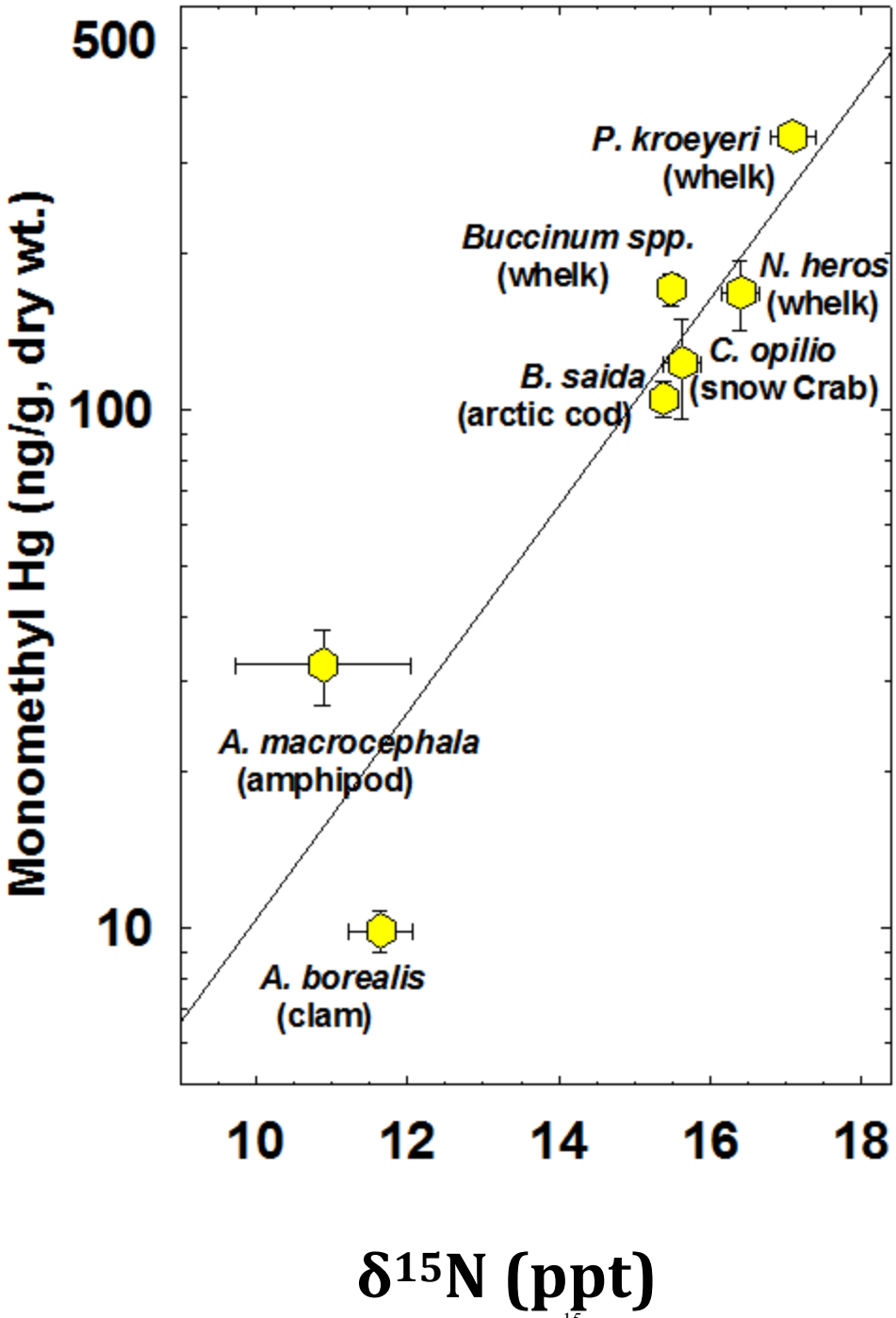

Figure 4. Mercury concentrations as a function of $\delta^{15}N$ in the muscle tissue of benthic invertebrates and the arctic cod. The increase in mercury concentrations is highly correlated with biomagnification of $\delta^{15}N$ with trophic level. From Fox et al.

Table 1: Gas and nutrient fluxes at the sediment-water interface over the Chukchi Sea shelf. Negative values reflect fluxes into the sediment (water → sediment). From Souza and Dunton.

Stations	*Depth*	*Net* N_2	O_2	NO_3^-	PO_4^{-3}
	(m)	(μmoles m^{-2} h^{-1})			
48	46	24.2 (9.9)	-268.7 (55.2)	-0.8 (0.2)	1.1 (0.1)
1015	46	8.2 (6.5)	-209.5 (42.4)	0.4 (0.9)	-0.9 (0.3)
9	45	260.1 (25.0)	-131.3 (18.6)	1.7 (0.1)	1.0 (0.2)
103	43	73.2 (2.3)	-601.9 (33.1)	6.1 (2.2)	3.6 (0.5)

Benthic and Epibenthic Community Structure

The northern Chukchi Sea is universally recognized as a region with an abundant and diverse benthic fauna that exhibits high spatial and temporal variability in carbon production. Grebmeier and Cooper found appreciable benthic chlorophyll concentrations reflective of export production from phytoplankton to the underlying sediments (Figure 5). Chl *a* values in surface sediments of the northern offshore Chukchi Sea waters were generally higher than in nearshore coastal areas influenced by Alaska Coastal water. The availability of fresh, ungrazed chlorophyll undoubtably contributes to the low C:N ratios of surface sediments observed in the northern regions of the study area (Figure 6). The low C:N ratios in this area, particularly in the vicinity of Hanna Shoal and Barrow Canyon, are correlated with high abundances of infaunal and epifaunal invertebrate grazers collected in grab samples (Figure 7, 8) by Schonberg and Dunton. Similarly, Grebmeier and Cooper also noted high biomass of these faunal groups in the northern Chukchi Sea.

a.

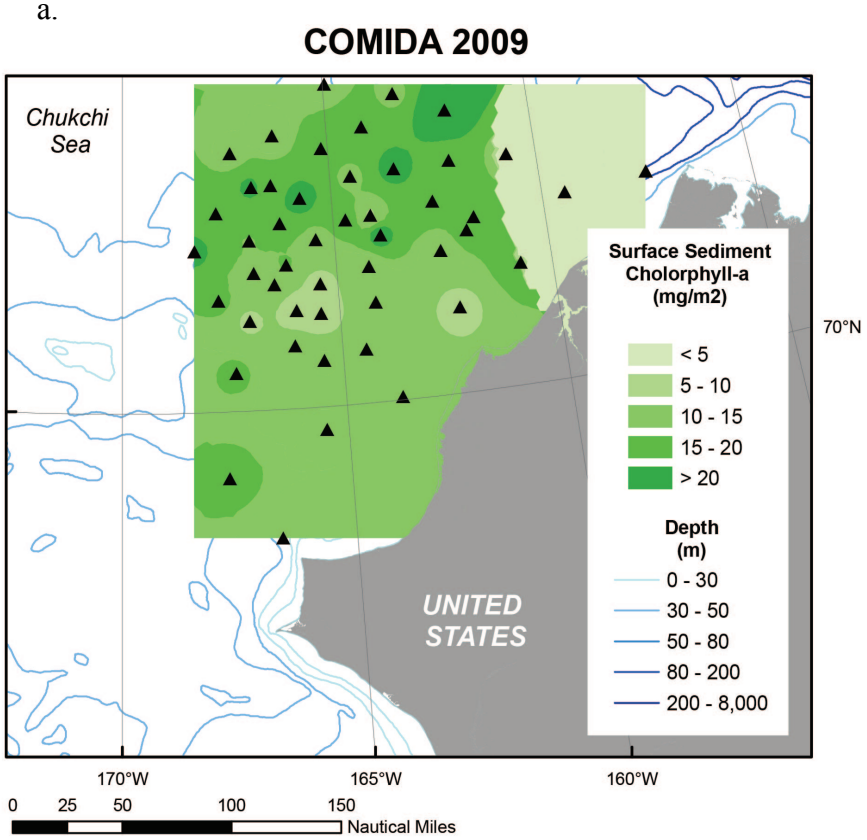

b.

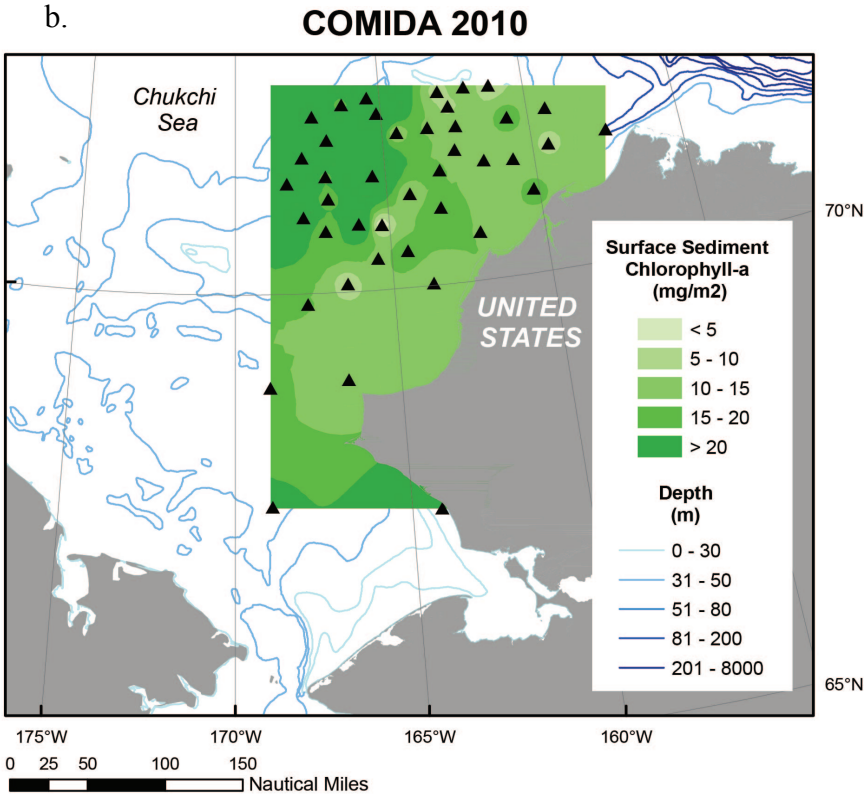

Figure 5. Spatial distribution of a.) surface sediment chlorophyll *a* (chl *a*) during COMIDA2009 and b.) surface sediment chl *a* during COMIDA2010.

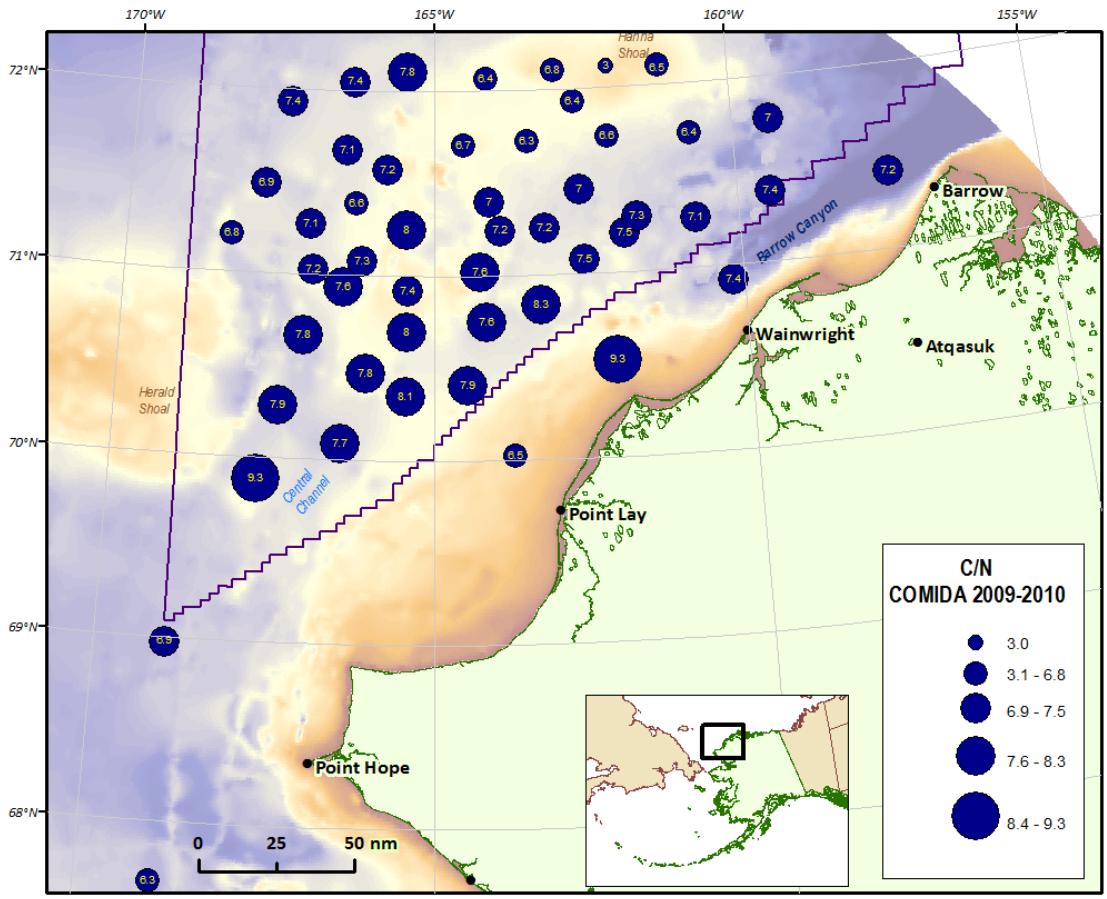

Figure 6. Surface sediment C:N ratios recorded in 2009 and 2010. These ratios provide an indication of the lability of organic matter on the seabed, with lower values reflective of higher N-content, and thus, nutritional value to primary benthic and epibenthic consumers.

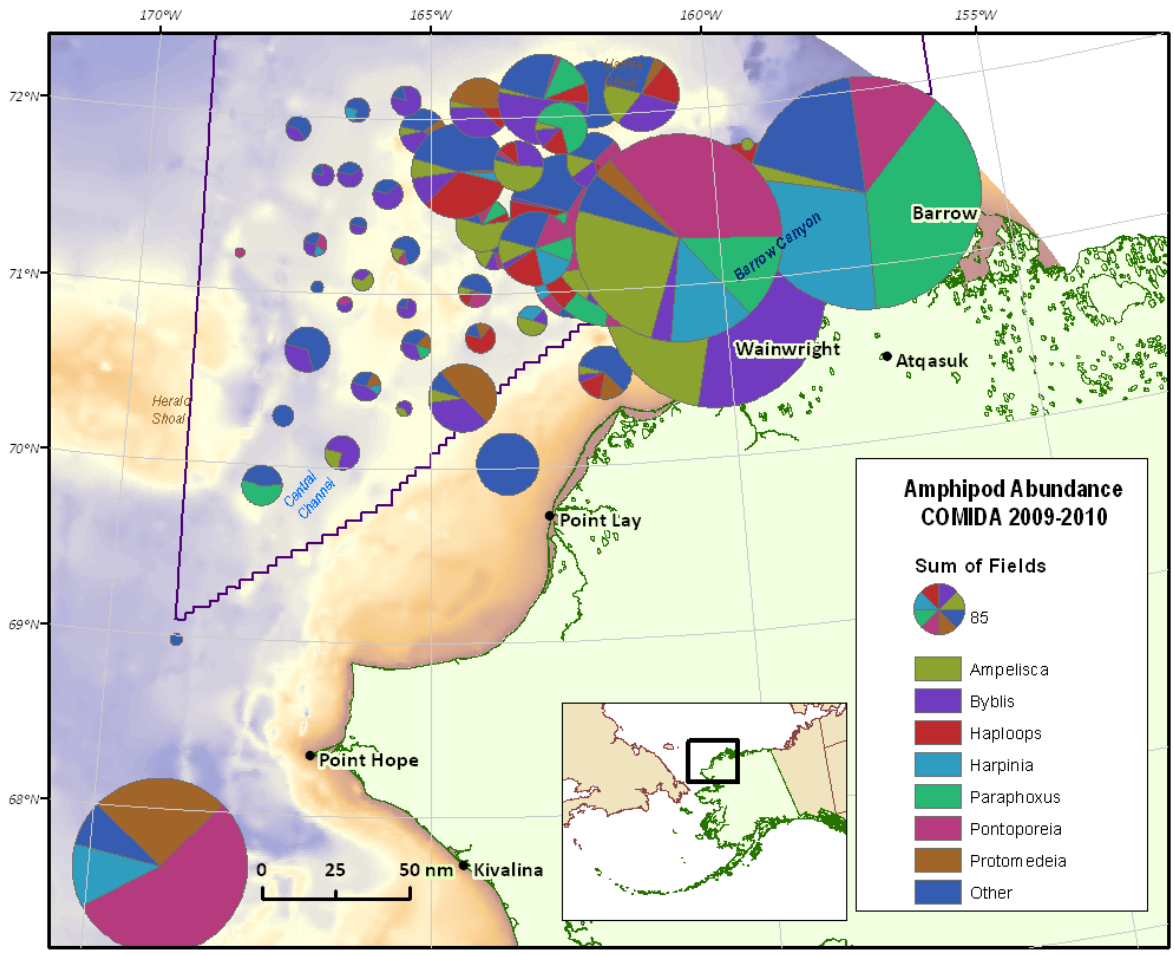

Figure 7. The spatial distribution in dominant amphipod species abundance. Highest concentrations were found in the northern area of the Chukchi Sea. A total of 64 amphipod species were identified from the study area.

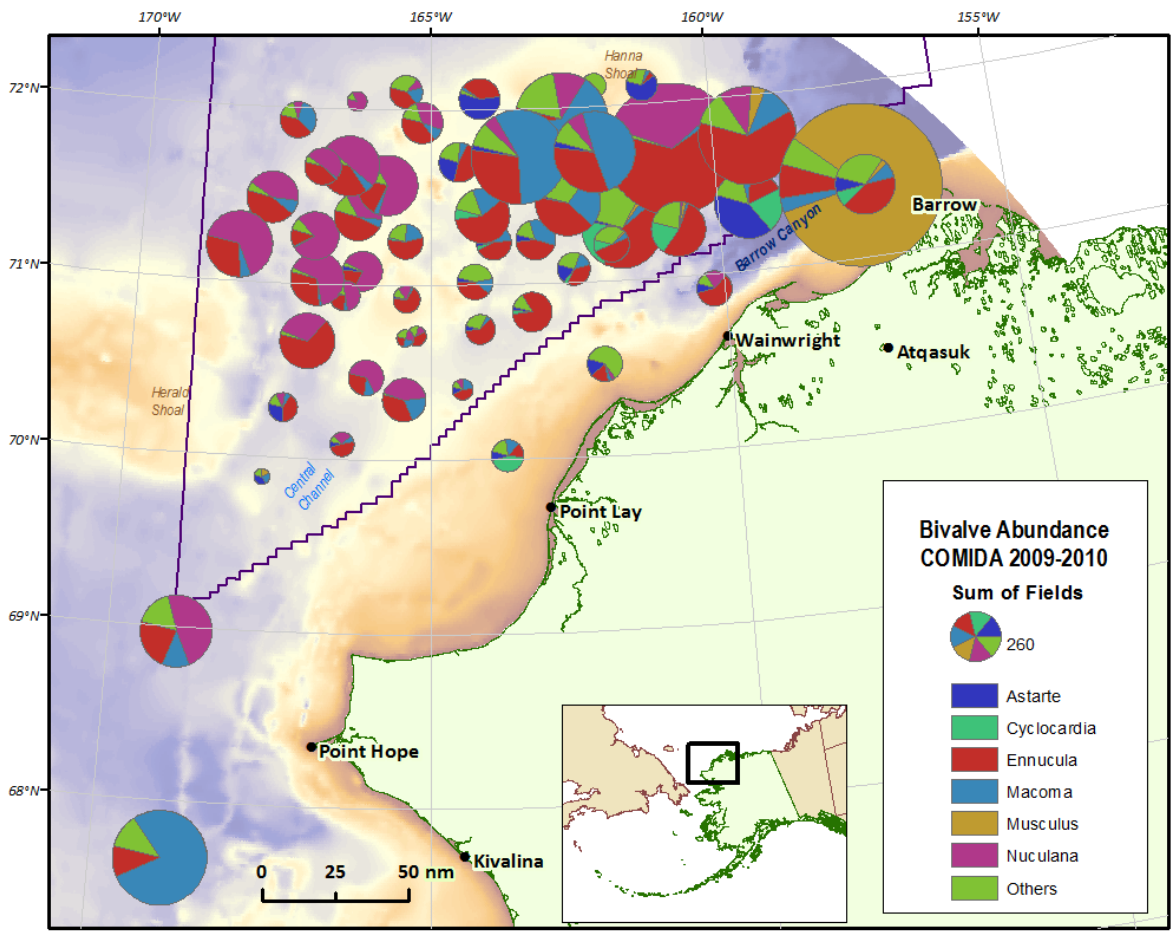

Figure 8. The spatial distribution in dominant bivalve abundance. Densities were generally highest in Barrow Canyon and in the vicinity of Hanna Shoal. A total of 39 bivalve species were identified from the study area.

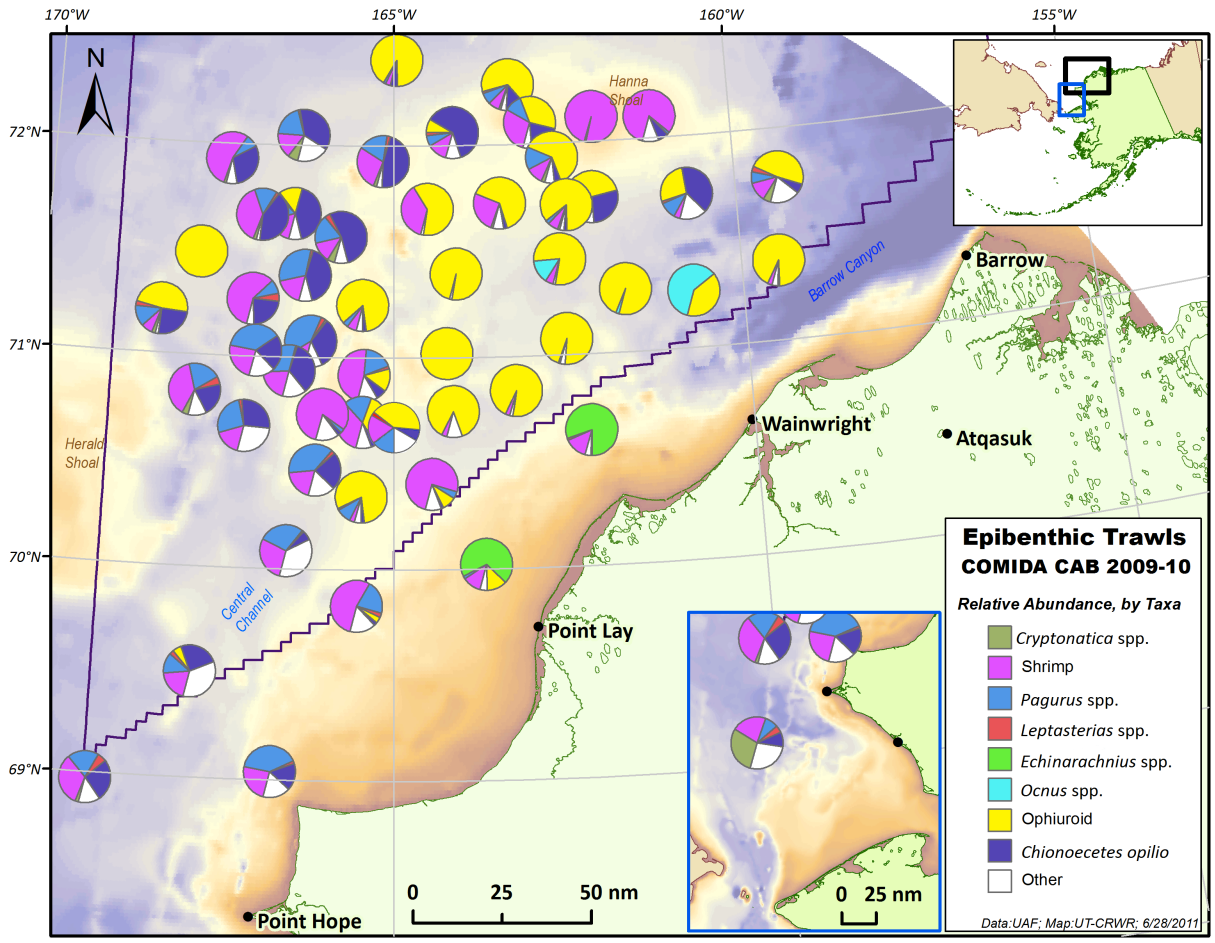

Figure 9. Relative abundance of taxa selected by the BEST analysis, including taxa of high abundance or biomass that were not selected as important in the community composition (e.g. *Ocnus* spp. and *Leptasterias* spp.). From Ravelo et al.

Konar et al. collected valuable baseline data on size frequency distributions for a number trophically important epibenthic species including *Chionoecetes* and *Hyas* crabs, the gastropods *Plicifusus, Colus*, *Cryptonatica*, and *Neptunea*, and the echinoderms *Gorgonocephalus, Leptasterias,* and *Echinarachnius*. Although no major changes in community composition were observed from data spanning the last 20 years, the information contained here provides an invaluable reference for assessing future change. Konar's group (Ravelo et al.) noted that the epibenthic communities of the northeastern Chukchi Sea were dominated by either crustaceans or echinoderms (Figure 9). Communities dominated by crustaceans exhibited higher diversity and evenness index values compared to communities dominated by echinoderms. As noted by Grebmeier and Cooper for the infauna, assemblages dominated by different taxa followed a distinct distributional pattern that matched the path of distinct water masses within the region.

Sources and Fates of Organic Carbon: Food Web Implications

A team led by Dunton investigated the trophic structure of the northeastern Chukchi Sea from stable carbon and nitrogen isotopic measurements. Isotopic analyses included an enormous number of specimens collected from the seabed and water column. Based on these measurements, McTigue et al. developed a food web model including two distinct carbon source end-members preferred by benthic consumers (Figure 10). Energy moves from pelagic carbon, one of the two end-members, to zooplankton, amphipods, holothurians, Echinarachniidae (sand dollars), isopods, and forams. These groups rely little on benthic microalgal carbon, and therefore, assimilate almost exclusively pelagic carbon. Pisces ascertains most of its carbon from these groups, although some carbon is also obtained from other groups that rely on benthic microalgae carbon (or ice algal carbon deposited to the benthos earlier in the season). Bivalves, bryozoans, hydrozoans, Porifera (sponges), and ascidians appear to derive a major portion of their carbon from benthic microalgae (or ice algae). Carbon from these organisms is transferred to benthic predators, including gastropods, cephalopoda, priapulids, decapods, and polychaetes. Third trophic level omnivores, including sipunculids, ophiuroids, and polychaetes obtain carbon from both primary producers and primary consumers. As indiscriminant feeders, they assimilate both benthic microalgae and pelagic carbon. Both pelagic carbon and benthic algal carbon seem to play an important role in the benthic food web of the Chukchi Sea. These data provide an invaluable opportunity to assess the potential exposure effects and uptake of anthropogenic contaminants to key prey species in Chukchi Sea food webs (Figure 11).

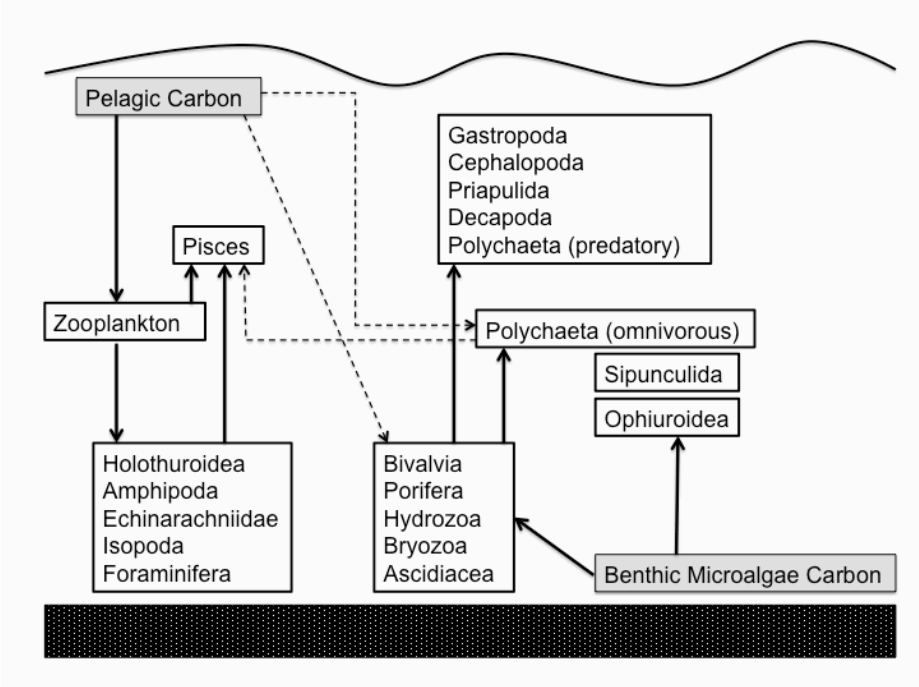

Figure 10. A conceptual food web that incorporates benthic taxa from the Chukchi Sea. Solid arrows represent pathways of energy flow from ultimate carbon sources (grey boxes). Dashed arrows represent weaker connections of energy flow.

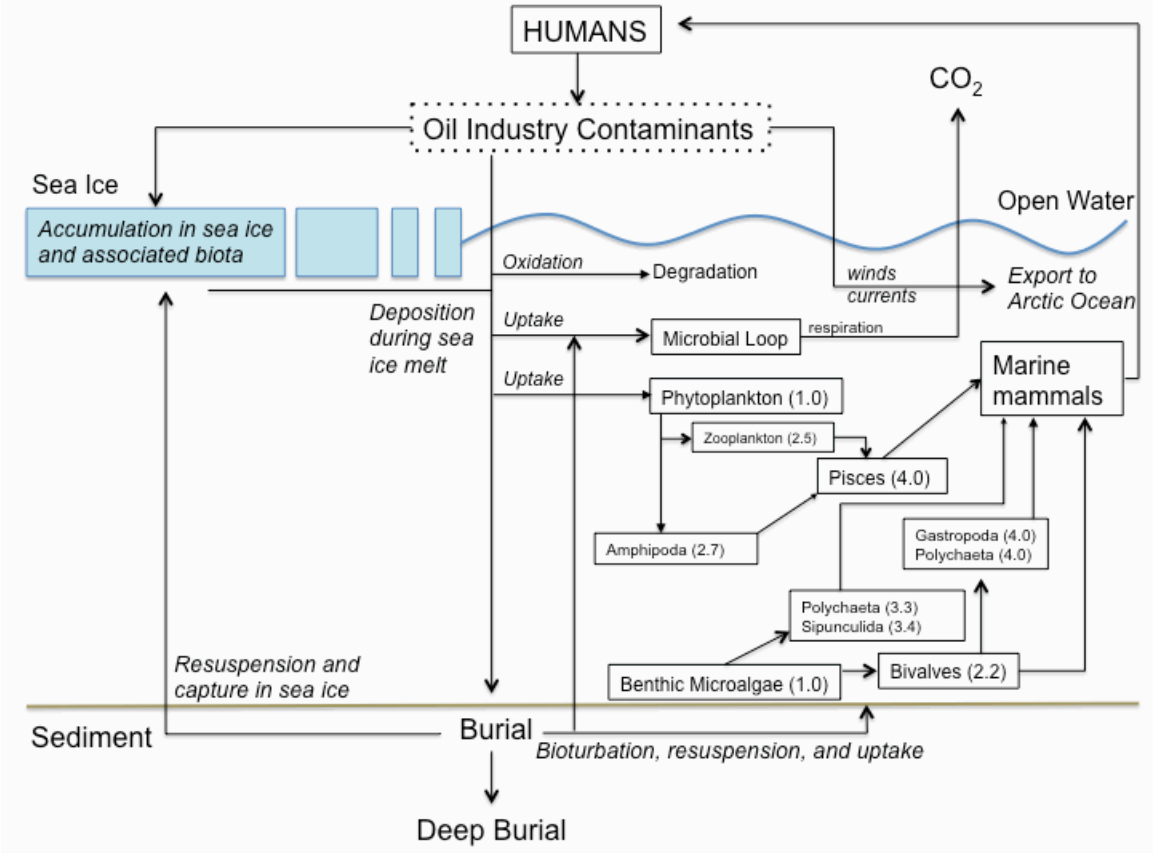

Figure 11. Simplified schematic of potential pathways for an anthropogenic contaminant exposed to the Chukchi Sea ecosystem. Average trophic level contained in parentheses after each taxonomic group name.

Acknowledgements

We thank the Bureau of Ocean Energy and Management (BOEM), U.S. Department of Interior, for funding and providing us with the opportunity to work collaboratively on this project for over three years. We are especially appreciative to Dr. Dick Prentki of BOEM for his participation on the research cruises, unqualified support of our research, and active role in project planning throughout the COMIDA project period. His enthusiasm for our science stimulated great work and dedication to the project by us all. We salute Captain John Seville and crews of both *R/V Alpha Helix* and *R/V Moana Wave* for their dedication and work to make collection of our diverse datasets possible. We are extremely grateful to Jackie Grebmeier who provided leadership, humor, and vision as Chief Scientist on both cruises. She will continually be awarded a supply of dark chocolate in appreciation of her efforts. Finally, as COMIDA CAB science team lead, KHD would like to express his sincere thanks to the COMIDA CAB PIs, their students and associates for their teamwork and friendship that resulted in commendable science over the past three years.

Distribution and Provenance of Trace Metals in Recent Sediments of the Northeastern Chukchi Sea

Trefry, J.H., R.P. Trocine, and L.W. Cooper

John H. Trefry and Robert P. Trocine
Department of Marine and Environmental Systems
Florida Institute of Technology, Melbourne, Florida 32901

Lee W. Cooper
Chesapeake Biological Laboratory,
University of Maryland, Solomons, MD 20688

Abstract

Concentrations of 17 trace metals (Ag, As, Ba, Be, Cd, Cr, Cu, Hg, Mn, Ni, Pb, Sb, Se, Sn, Tl, V and Zn) in 207 bottom sediment samples from the eastern Chukchi Sea were essentially all at natural, background values. Ratios of metals/Al were used as a model for determining background metal concentrations and identifying anthropogenic inputs. Minor exceptions were observed in 29 of 3105 data points; some natural diagenetic enrichment of As and Mn also was observed. Fifteen of the 29 anomalies were for concentrations of Ba at an old drill site in the Klondike lease area where the highest Ba value was 1,290 μg/g; this value was ~700 μg/g higher than average background and is equivalent to ~0.3% of the drilling mud additive barite. Another 3 anomalies, 1 each for Hg, Ni and Pb were found at the Klondike site; the anomalous Hg value was 0.090 μg/g, relative to background values of 0.034 μg/g, and the Hg was most likely present in a sulfide mineral that was part of the oil formation cuttings. Drilling mud, as identified by elevated Ba concentrations in the sediments, was not an identifiable source of Hg in the COMIDA study area. Included in the other anomalies were higher values for Zn, Cu and Pb at one station where a natural metal sulfide was most likely present and two values for both Ni and Cr that were elevated at the port for the Red Dog mine that extracts Zn and Pb; no anomalies for Zn or Pb were found at the site. All concentrations of the potentially toxic metals Ag, Cd, Hg, Pb and Zn were below all sediment quality criteria. The highest Ba concentrations were ~50 times lower than a tested value that showed no impact. The sediments of the eastern Chukchi Sea are presently free of metal contamination with the likely exception of small areas around old drill sites. Provenance of sediment metals was evaluated using Fe/Al and Cr/Al ratios; most ratios from the COMIDA area were within 20% of values obtained for the Yukon River and Norton Sound. Such agreement is consistent with previous studies that showed the importance of the Yukon River as a source of sediment and metals to the Chukchi Sea. Sediments from two nearshore stations and 11 stations in the northern portion of the study area had Fe/Al and Cr/Al ratios that support additional sources of sediments including coastal erosion and transport from the west.

Introduction

The broad shelf of the Chukchi Sea is presently at a crossroad with respect to sea-ice retreat, northward migration of species, coastal erosion and offshore energy development. These ongoing events follow a long geological history of extensive sea level changes that have greatly influenced both the sedimentary environment and human activity in the Chukchi Sea (Hopkins, 1967). Six major sea level regressions exposed the seabed in the Chukchi Sea during the Pleistocene and Holocene epochs with the most recent exposure occurring just 13,000 to 17,000 years BP (Creager and McManus, 1965). Even with such a dynamic history, only 2 to 10 m of sediment were deposited throughout most of the Chukchi Sea during the past 1.8 million years (Pleistocene and Holocene, (Grantz et al., 1982). Thicker deposits of 12 to >30 m have been noted in the North Chukchi basin, offshore from Wainwright and at a few other locations (Phillips, 1984). Present-day events are likely to have a significant impact on the Chukchi Sea, one that is just beginning to be recorded in the sediments.

Silt and clay comprise <10 to >90% of the surface sediments on the Chukchi shelf; the provenance of these sediments is considered to be the Yukon and other rivers, with transport from the Bering Sea to the Chukchi Sea by the Alaska Coastal Current (McManus et al., 1969). Ortiz et al. (2009) show that the dominant clay mineral in the COMIDA area is illite as part of the Arctic illite band. On Herald and Hanna Shoal, sand and gravel sediments are reported to have formed by winnowing of the fine fraction by currents following resuspension by ice gouging of the seafloor (Tomil and Grantz, 1976).

Sediments in the Chukchi Sea support a vibrant benthic habitat and provide a record of both sediment sources from continental weathering and anthropogenic inputs of various contaminants. With a specific focus on the COMIDA study area in the eastern Chukchi Sea, the objectives of this report are as follows: (1) identify the geographical distribution of trace metals in surface and subsurface sediments, (2) determine background concentrations of trace metals in sediments and identify any anthropogenic inputs of metals to the sediments, (3) assess the ecological implications of any anthropogenic metals, and (4) determine the provenance of metals in area sediments by specifically identifying the likely importance of the Yukon River as a key sediment source to the eastern Chukchi Sea.

Methods

Study Area

The COMIDA study area is located in the northeastern Chukchi Sea (Figure 1). Exploratory drilling for oil was carried out at 5 locations between 1989 and 1992. The sediments are silty sand and mud with <10% silt plus clay in nearshore areas and >90% silt plus clay in offshore areas (Naidu et al., 1997). These sediments support an infaunal assemblage characterized by polychaete worms, small mollusks and crustaceans (Feder et al., 1994b). Biota from higher trophic levels include arctic cod, walrus, seals, polar bears, sea birds and migrating bowhead whales.

Sample Collection

Sampling for this study took place during July and August 2009 and 2010 using the vessels *R/V Alpha Helix* and *R/V Moana Wave*, respectively. Sample stations were selected using a probability-based grid for each section of the study area and randomly choosing locations within each grid cell. Sampling was conducted at 49 stations in 2009 and 44 stations in 2010 (Figure 1).

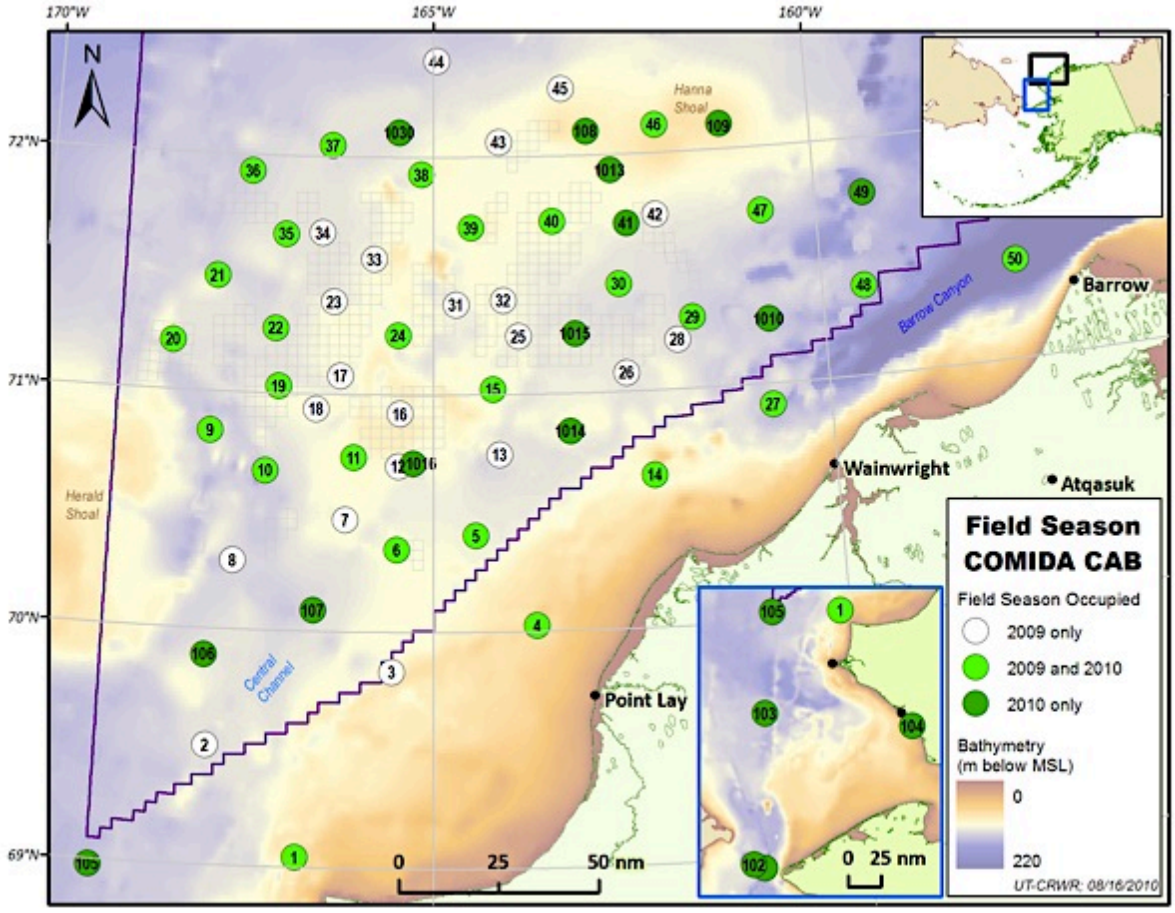

Figure 1. Maps showing sampling stations for 2009 and 2010 field surveys for the COMIDA Project. Lower inset map shows stations to the south of those shown on the larger map and upper inset map shows location of study area off the northwest coast of Alaska.

Sediments were collected using a pre-cleaned, double van Veen grab that obtained two side-by-side samples, each with a surface area of 0.1 m^2 and a depth of ~15 cm. Samples (top 1 cm and subsurface layers) were carefully collected from one of the two grabs and placed in separate containers for analysis of metals, organic C and grain size. The companion grab was used for sampling benthic biota. A HAPS corer (Kanneworff and Nicolaisen, 1973) with a 30-cm acrylic liner was deployed at numerous sites and a Benthos gravity core with a 1-m long barrel, 7.5-cm diameter plastic liner, and no core catcher, was deployed into stiff sediments at several sites.

Core samples were split into 1- to 2-cm thick layers aboard ship under clean conditions. All sediments samples, except those for grain size analysis, were frozen shipboard.

Laboratory Methods

Sediment samples for metal analysis were homogenized and a wet portion was set aside for Hg analysis. The remaining sample was freeze-dried to provide percent water content and dry sediment for acid digestion. A separate, wet sediment sample from each location was set aside for grain size analysis.

Sediment digestion for Hg was carried out using high-purity HNO_3 and H_2SO_4. Concentrations of the remaining metals were determined using dry sediment that was totally dissolved by high-purity HF, HNO_3 and $HClO_4$. The sediment digestions included the Certified Reference Material MESS-3 (National Research Council of Canada) and the Standard Reference Material (SRM) #2709 from the National Institute of Standards and Technology.

Analysis of the sediment solutions was carried out using established laboratory methods (Trefry et al, 2003) with the following instruments: (1) a Perkin-Elmer Model 4000 atomic absorption spectrometer for Al, Cr, Cu, Fe, Mn, V and Zn, (2) a Varian Model 820-MS inductively coupled plasma mass spectrometer for Ag, As, Ba, Be, Cd, Ni, Pb, Se, Sn and Tl and (3) a Laboratory Data Control cold vapor atomic absorption spectrometer for Hg. All values for reference materials were within the 95% confidence intervals for certified values. Analytical precision ranged from 1% (Al, Cu, Fe, and Pb) to 4% (Hg). Method detection limits were 25 (Cu) to >5,000 (Ba, Pb) times lower than the lowest value obtained for field samples.

Sediment TOC concentrations were determined by treating freeze-dried sediment with 10% phosphoric acid to remove inorganic carbon, followed by high-temperature combustion and infra-red CO_2 quantification. Grain size analyses of surface sediment samples were carried out using the classic method of Folk (1974) that includes a combination of wet sieving and pipette techniques.

Results and Discussion

Metal Distributions in Sediments

Concentrations of Ag, Al, As, Ba, Be, Cd, Cr, Cu, Fe, Hg, Mn, Ni, Pb, Sb, Se, Sn, Tl, V and Zn were determined for surface sediments (0-1 cm) collected from the COMIDA study area during 2009 (n = 49) and 2010 (n 40); 25 of the sites were sampled during both years (See Figure 1). Metal data also were obtained for sediment cores collected during 2009 (5 cores, 77 samples) and 2010 (4 cores, 41 samples).

Large ranges in values for each metal were found throughout the study area with maximum/minimum concentrations that varied from ~2 (Ag and Ba) to 18 (Hg, Table 1). Average metal concentrations for surface sediments collected in 2009 were within 20% of values found for sediments collected in 2010 due to repeat sampling of more than half the sites (Table 1). Concentrations of Al, Ba and other metals obtained for samples collected during 2009 corresponded well with values obtained for the same sites in 2010 (Figure 2). Thus, we have combined the two data sets to obtain an overall perspective on the distribution of sediment metals.

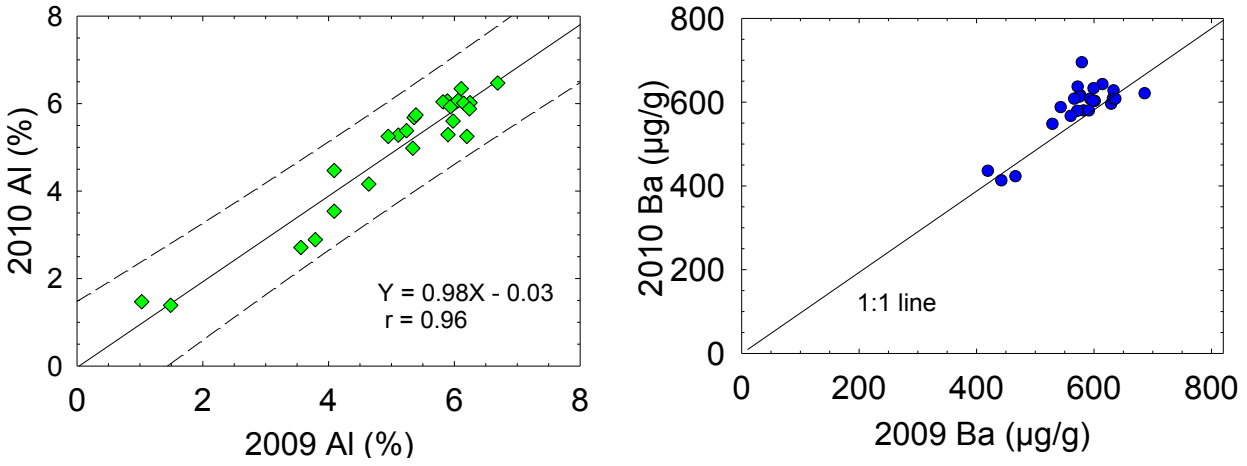

Figure 2. Concentrations of (a) Al and (b) Ba for surface sediments collected at the same locations during 2009 and 2010. Solid line and equation on (a) are from a linear regression calculation, dashed lines show 99% prediction interval and *r* is the correlation coefficient. Solid line on (b) shows 1:1 correspondence for 2009 and 2010 Ba values.

The overall variations and patchwork distribution of metal concentrations are shown using Al as an example (Figure 3). The lowest Al and metal values were found closer to shore in sand and gravel and the highest concentrations were found offshore in silt- and clay-rich sediments. Data from the present study agree very well with and complement previous results for Al, Fe, Mn, Cu, Cr, V, Ni and Zn by Naidu et al. (1997, Table 1). Metal concentrations were directly correlated with sediment grain size (Figure 4). Concentrations of Al and other trace metals generally correlate well with concentrations of silt + clay because concentrations of both Al and most metals are very low in coarse-grained quartz sand or carbonate shell material and much higher in fine-grained aluminosilicates (Figure 4). Aluminum is rarely introduced by anthropogenic activities and is present at percent levels in most sediment relative to part per million (ppm or µg/g) levels for trace metals. Thus, for this study, concentrations of trace metals were normalized to Al (i.e., use of metal/Al ratios) as a proxy for the metal controlling variables of grain size, organic carbon content and mineralogy.

Table 1. Summary data for metals in surface sediments of the COMIDA study area, eastern Chukchi Sea.

Samples		Ag (µg/g)	Al (%)	As (µg/g)	Ba (µg/g)	Be (µg/g)	Cd (µg/g)	Cr (µg/g)	Cu (µg/g)	Fe (%)	Hg (µg/g)
2009	Mean	0.11	5.12	14	609	1.2	0.16	73	14	2.93	0.029
(n = 49)	± SD	± 0.01	± 1.24	± 5	± 78	± 0.3	± 0.06	± 22	± 5	± 0.99	± 0.014
2010	Mean	0.13	5.01	15	577	1.2	0.17	72	14	2.93	0.034
(n = 40)	± SD	± 0.02	± 1.46	± 7	± 57	± 0.2	± 0.04	± 17	± 4	± 0.77	± 0.011
All	Mean	0.12	5.07	14.6	591	1.2	0.17	72	14	2.93	0.032
(n = 89)	± SD	± 0.02	± 1.34	± 6.0	± 57	± 0.3	± 0.05	± 19	± 4	± 0.87	± 0.013
	Max.	0.17	7.80	43.6	823	2.05	0.38	104	28.6	4.70	0.090
	Min.	0.07	1.03	4.1	412	0.35	0.04	9.7	2.7	0.38	0.005
	Max/Min	2.4	7.6	10.6	2.0	5.9	9.5	10.7	10.6	12.4	18.0
Naidu et	Mean	-	4.7	-	-	-	-	86	17	3.0	-
al. (1997)	± SD		1.9					26	6	1.3	

		Mn (µg/g)	Ni (µg/g)	Pb (µg/g)	Sb (µg/g)	Se (µg/g)	Sn (µg/g)	Tl (µg/g)	V (µg/g)	Zn (µg/g)	Silt + Clay (%)
2009	Mean	374	26	11	0.62	0.78	1.4	0.43	108	74	64
(n = 49)	± SD	± 100	± 6	± 2	± 0.11	± 0.17	± 0.4	± 0.06	± 29	± 19	± 29
2010	Mean	334	24	12	0.62	0.69	1.3	0.40	99	69	66
(n = 40)	± SD	± 117	± 8	± 3	± 0.14	± 0.19	± 0.4	± 0.08	± 32	± 24	± 25
All	Mean	356	25	11	0.62	0.74	1.4	0.41	104	72	65
(n = 89)	± SD	± 109	± 7	± 2	± 0.12	± 0.19	± 0.4	± 0.07	± 31	± 22	± 27
	Max.	646	41.6	21.5	1.06	1.03	2.4	0.66	164	108	98
	Min.	41	2.9	5.4	0.28	0.19	0.2	0.22	16	8	5
	Max/Min	15.8	14.3	4.0	3.8	5.4	12.0	3.0	10.2	13.5	19.5
Naidu et	Mean	252	22	-	-	-	-	-	88	61	
al. (1997)	± SD	97	7						33	22	

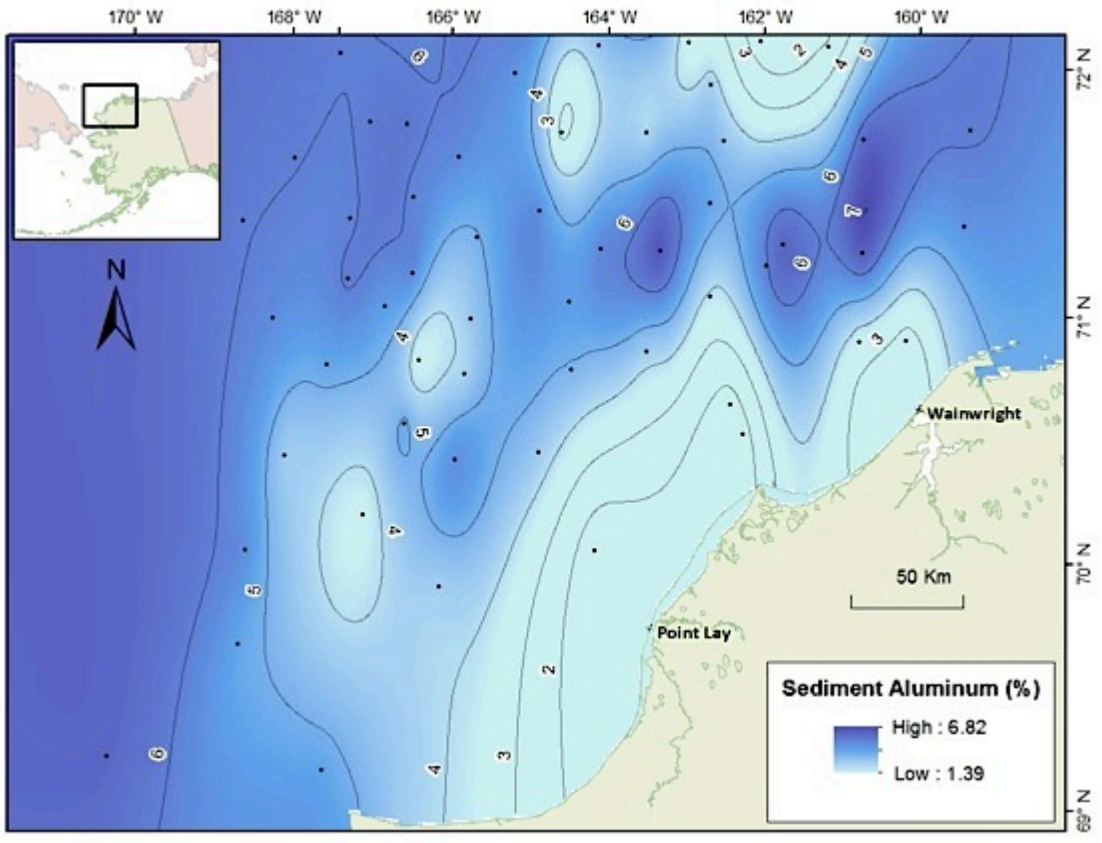

Figure 3. Contour map for concentrations of aluminum in surface sediments.

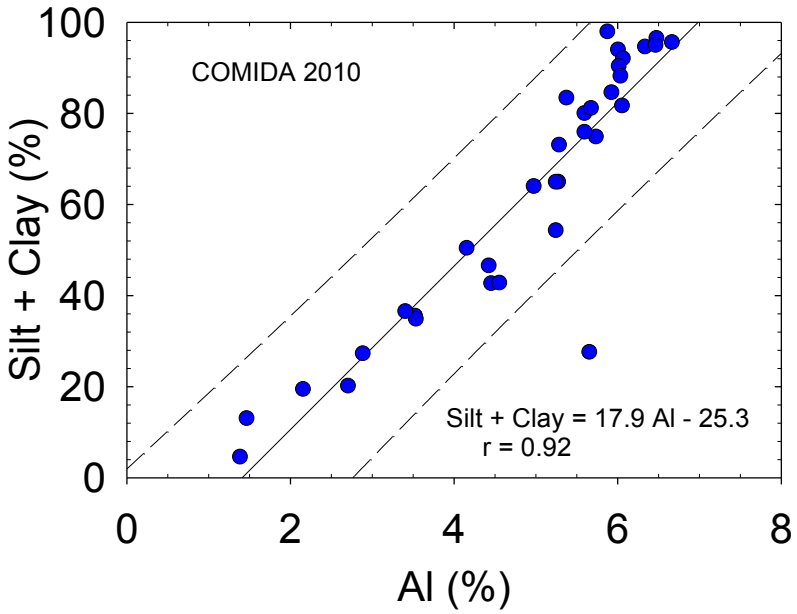

Figure 4. Concentrations of Al versus silt + clay for data from 2010.

In the ideal case, a strong linear correlation is observed between concentrations of a trace metal and Al. Significant, positive deviations from this linear trend, as explained in more detail below, can be used to identify metal contamination. Plots of trace metal concentrations versus Al or Fe have been used in various forms for many years to help determine background concentrations of metals in a given depositional basin as well as to identify sediment metal contamination (e.g., (e.g., Bruland et al., 1974; Schropp et al., 1990; Trefry et al., 1985; Trefry and Presley, 1976)

Graphs for V, Se, Sb and Sn versus Al show that all 207 data points for each metal plotted within the 99% prediction intervals established using the combined 2009 and 2010 data for surface sediments and sediment cores (Figure 5). Thus, even though individual metal concentrations were quite variable from site to site, differences in absolute concentrations can be explained by variations in grain size, TOC and/or mineralogy when normalized to Al. Once again, concentrations of V and other metals follow Al in that higher values are found in aluminosilicate clays and lower values are found in quartz and carbonate sands. Thus, the plots and linear regression equations shown in Figure 5 describe the natural trend (i.e., V/Al ratio) for metals in the northeastern Chukchi Sea.

For Ag, Hg, Cd, Cr, Be, Zn, Cu, Pb and Ni, one to three data points plotted at >10% above the upper prediction interval (Figures 5-7). By definition ~2 data points would plot outside a 99% prediction interval for 207 data points. The small number of anomalous data points suggests that the COMIDA study area is essentially uncontaminated with respect to any of these metals. For these 9 metals, 13 of 1,863 data points (0.75% of the data points) were anomalous. Three of the data points were from a sediment core at site 1015 near the Burger drill site (1 each for Zn, Cu and Pb); these anomalies are believed to be due to the presence of a trace amount of a natural sulfide mineral as described in more detail below. Two data points each for Cr and Ni were from sediments collected at station 104 near the offshore loading zone for ships carrying ore away from the port serving the Red Dog Mine, a Zn-Pb mine. No anomalies for Zn or Pb were found at this site. One unexplained anomaly was found for Ag (station 109), Hg (station 13), Cd (station 103) and Be (station 40). Some scatter was observed in the Tl data and no prediction interval was used at this time (Figure 7b).

Barium has been used historically as a sensitive indicator for the presence of petroleum drilling mud in sediment because barite ($BaSO_4$) is such a common and distinctive additive (e.g., Chow et al., 1978; Trefry et al., 2003). The graph for Ba versus Al for the COMIDA data (Figure 7c) shows 15 samples with elevated Ba values, all from a core collected at station 1016 near an old drill site in the Klondike lease area. Barium anomalies were previously reported for stations in both the Klondike and Burger areas (Neff et al., 2010) with Ba concentrations as high as 2,420 µg/g. One elevated value each for Ni and Pb also was found at station 1016, possibly due to drilling mud or cuttings.

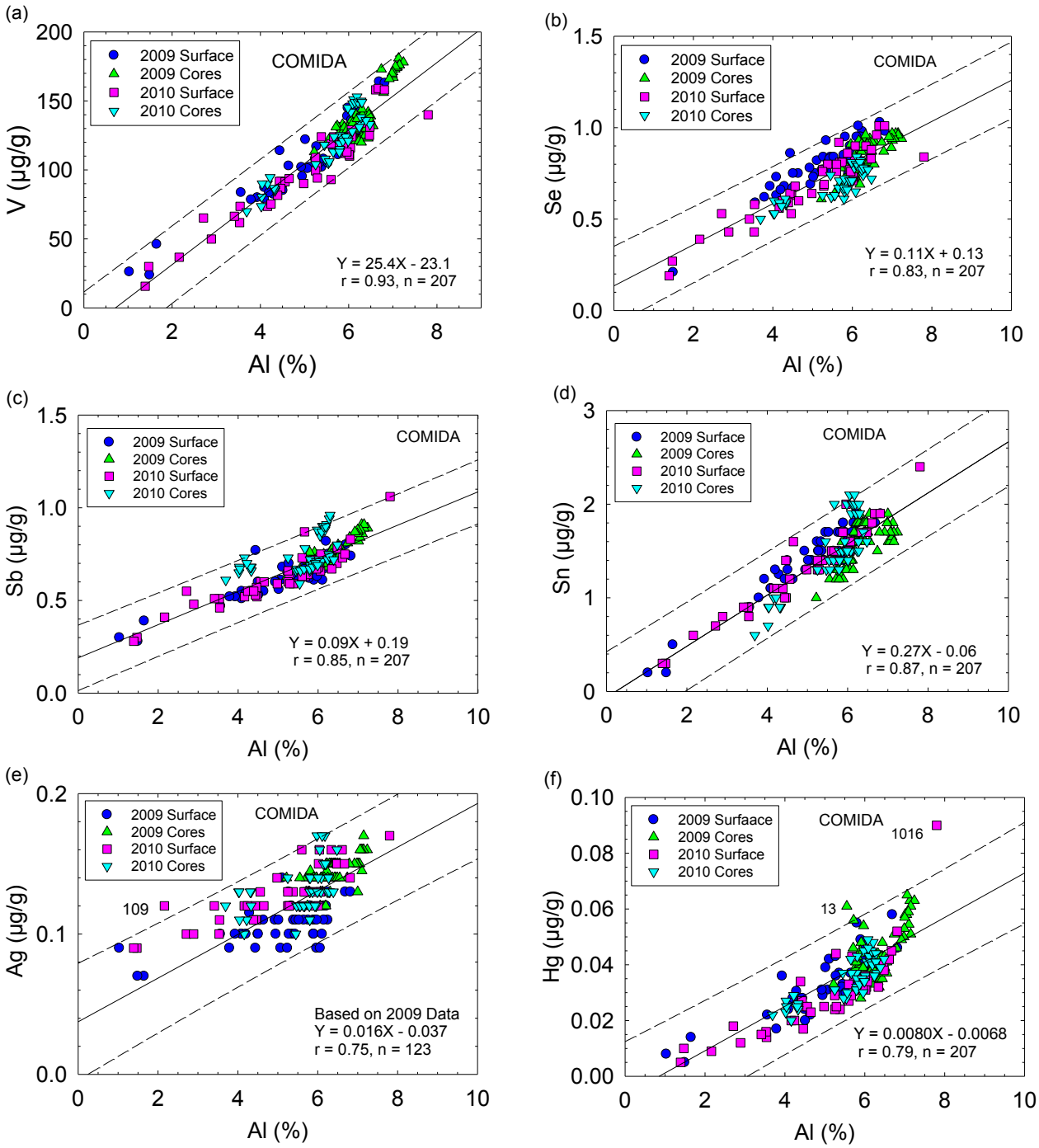

Figure 5. Concentrations of Al versus (a) V, (b) Se, (c) Sb, (d) Sn, (e) Ag and (f) Hg for surface sediments and sediment cores collected during 2009 and 2010. Equations and solid lines are from linear regression calculations, dashed lines show 99% prediction intervals, r is the correlation coefficient and n is the number of samples for the linear regression.

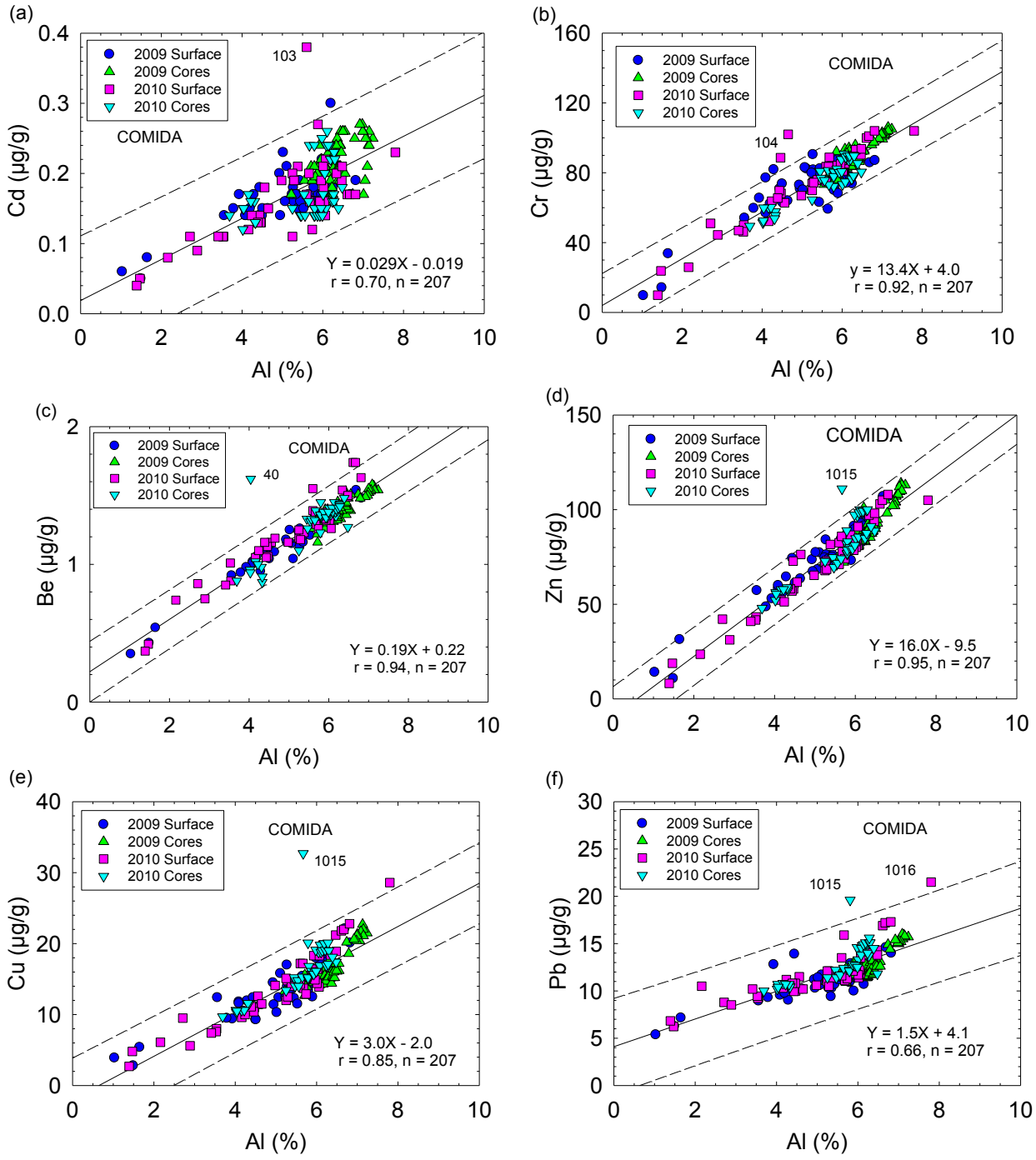

Figure 6. Concentrations of Al versus (a) Cd, (b) Cr, (c) Be, (d) Zn, (e) Cu and (f) Pb for surface sediments and sediment cores collected during 2009 and 2010. Equations and solid lines are from linear regression calculations, dashed lines show 99% prediction intervals, *r* is the correlation coefficient and *n* is the number of samples for the linear regression.

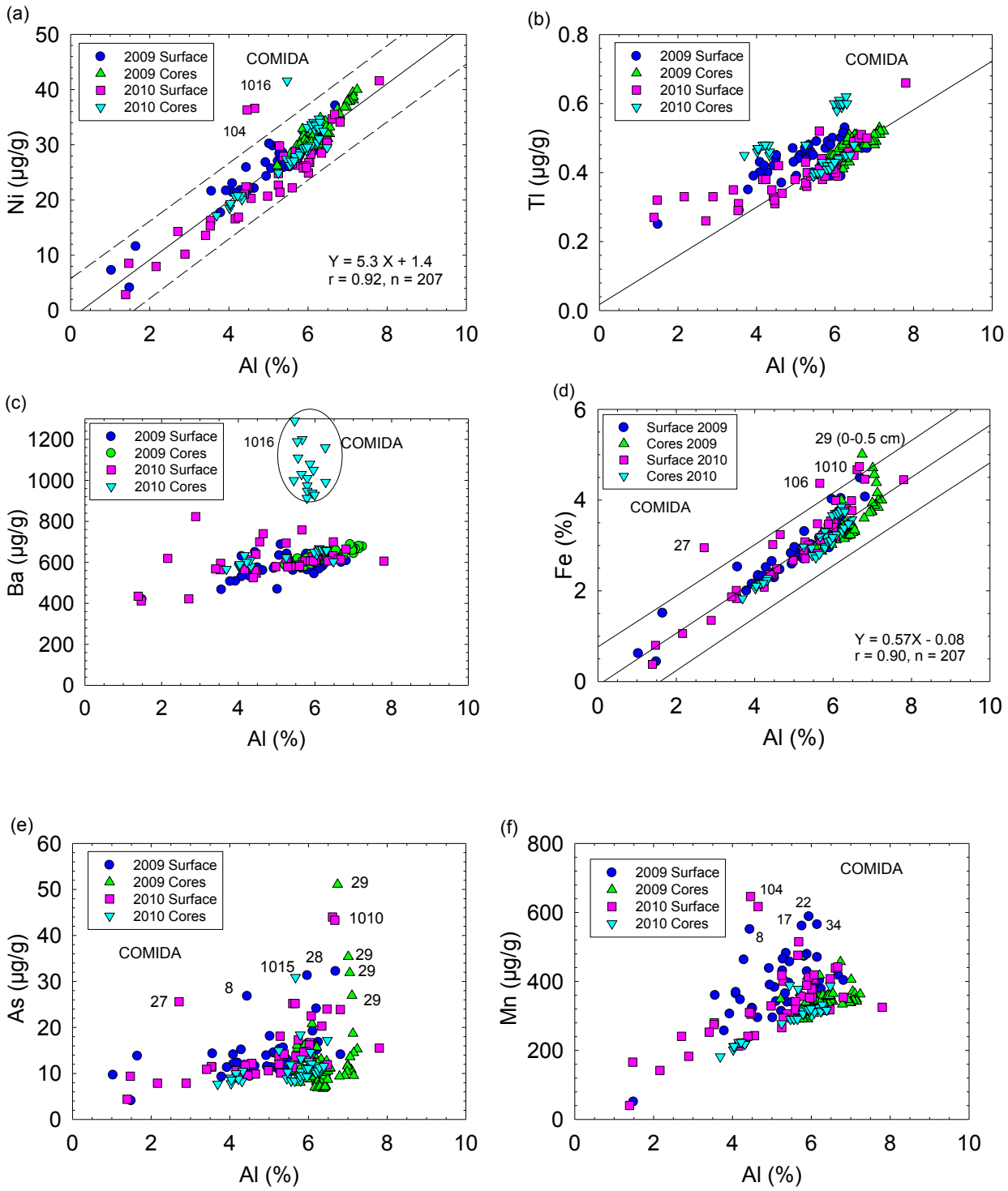

Figure 7. Concentrations of Al versus (a) Ni, (b) Tl, (c) Ba, (d) Fe, (e) As and (f) Mn for surface sediments and sediment cores collected during 2009 and 2010. Equations and solid lines are from linear regression calculations, dashed lines show 99% prediction intervals, *r* is the correlation coefficient and *n* is the number of samples for the linear regression.

Concentrations of Fe, relative to Al, were elevated in surface sediments at stations 27, 106, 1010 and 29 (Figure 7d), three of the same stations where As concentrations plotted above the upper prediction interval (Figure 7e). Observed enrichment of Fe, As and Mn (Figure 7) is most likely related to either early chemical diagenesis in the sediments or scavenging by fine-grained iron oxides. These possibilities will be discussed in more detail below when vertical profiles for metals in sediment cores are introduced.

Vertical profiles for metals were obtained for nine cores (stations 6, 13, 20, 29, 37, 40, 49, 1015 and 1016). Profiles for station 29 show that metal concentrations and metal/Al ratios were relatively uniform for Ba, Pb, Hg, Se, V and Zn (shown in Figure 8) as well as for Ag, Be, Cd, Cr, Cu, Ni, Sb, Sn and Tl. Surface enrichment of Fe, As and Mn (Figure 8) are related to early chemical diagenesis and will be discussed below.

Detailed vertical profiles for Pb in all 9 cores show the straight-line trends for 7 of the 9 locations (Figure 9). The Pb profile for station 40 showed a 30% decrease in the Pb/Al ratio between 3 cm and the top of the core. This decrease occurred along with a 60% decrease in Al concentrations as a thin layer of clay-rich sediments covered more silty-sand from 3 cm to the base of the short core. Sometimes such sharp shifts in sediment texture and mineralogy lead to shifts in metal/Al ratios. In addition to Pb, similar trends of decreased metal/Al ratios in the top layer of sediment from the core at station 40 were observed for Ba, Sb and Tl. In the core from station 1015, a peak in values for Pb and the Pb/Al ratio was observed at 2-3 cm (Figure 9). Concentrations of As, Cd, Cu, Sn and Zn also were elevated in the 2-3 cm layer of the core from station 1015 (Figure 10). These metals are commonly found to occur together in sulfide minerals (Bendel et al., 1993; Halbach et al., 1998) and the source of these anomalies is believed to be a trace amount of a naturally occurring sulfide mineral in the sediment column.

Sediment profiles for Hg/Al show relatively straight lines in most cases (Figure 11) with an average Hg/Al ratio of 6.0 ± 1.3 for all COMIDA sediments. The two highest Hg/Al ratios in the sediment cores are for the top 0.5 cm at station 6 (Hg/Al = 9.8) and in the 0.5-1 cm layer at station 13 (Hg/Al = 11.0). These small anomalies may represent recent anthropogenic inputs; however, no data or information is available to support an anthropogenic source for Hg at the two locations.

The most variable profiles were observed for As. For example, the concentration of As in the top 0.5 cm of sediment at station 29 was 50 µg/g relative to an overall average of 15 µg/g for As in the eastern Chukchi Sea (Figure 12). These As enrichments are most likely due to natural diagenetic remobilization of As under reducing conditions that leads to dissolution of As in subsurface sediments and coprecipitation and enrichment of upwardly diffusing, dissolved As with Fe oxides in oxidizing surface sediments (Farmer and Lovell, 1986). Such behavior for As was recently reported by Neff et al. (2010) for the eastern Chukchi Sea. The As/Al ratio in surface sediments can provide a simple indication of areas with oxic sediments that overlie mildly reducing sediments. Such behavior is suggested for stations 8, 27, 28, 29, 48, 50 and 1010. Each of the sites with a higher As/Al ratio in the surface layer contained relatively high values for TOC in the study area (>1%), and these sites were generally closer to shore where sedimentation rates may be higher.

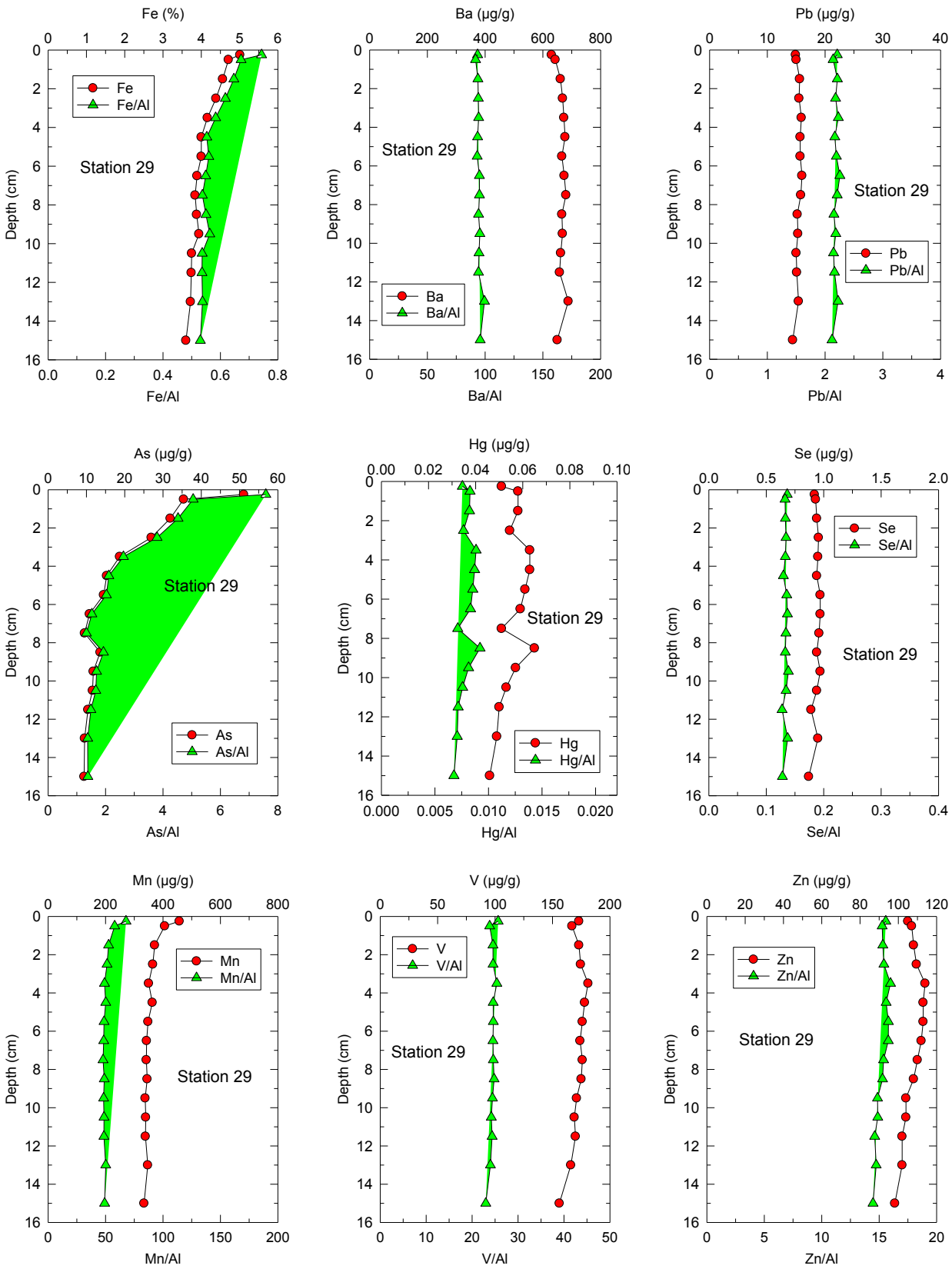

Figure 8. Vertical profiles for metals and metal/Al ratios for sediment core from stations 29.

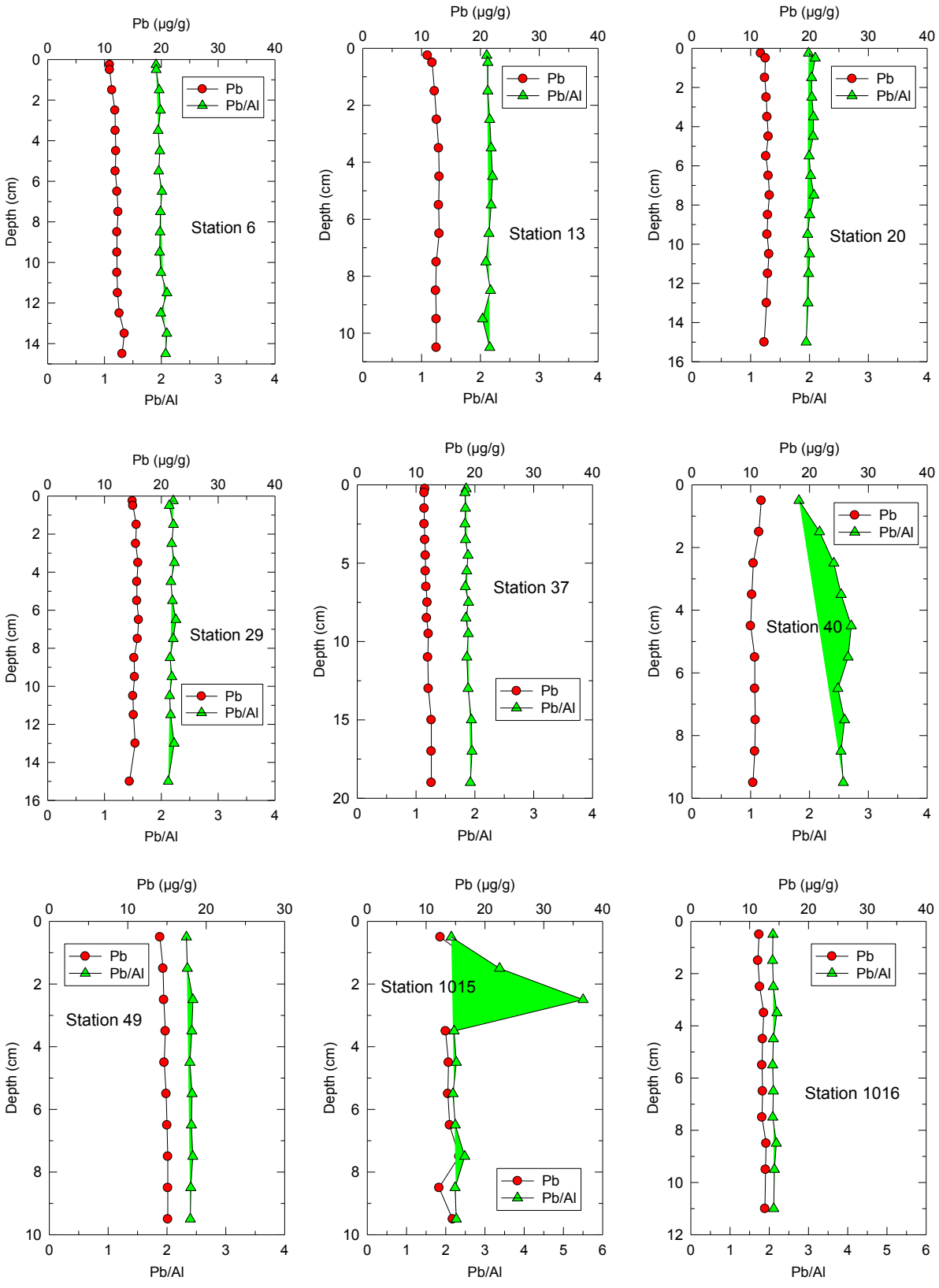

Figure 9. Vertical profiles for Pb and Pb/Al ratios for all sediment cores from COMIDA study.

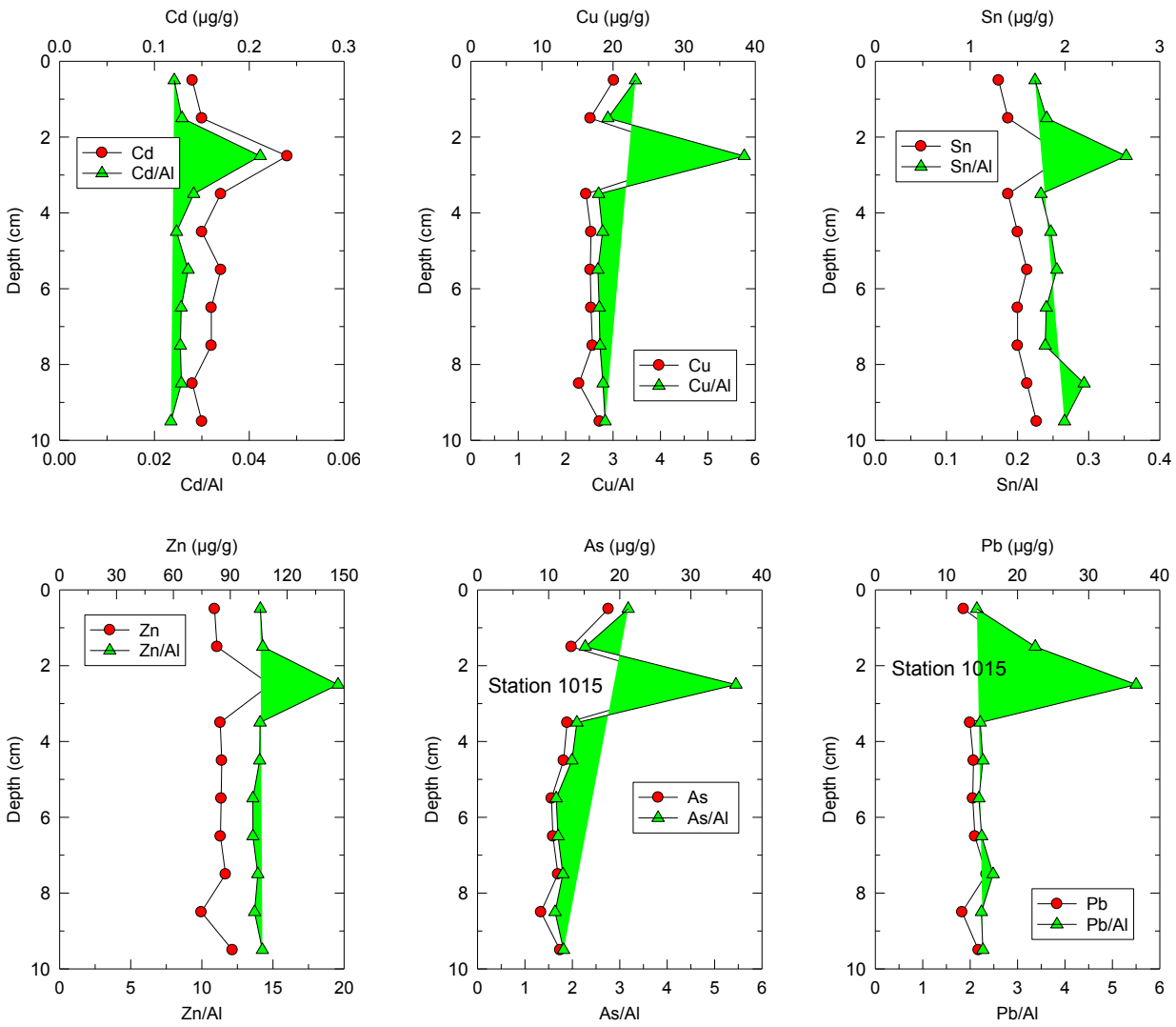

Figure 10. Vertical profiles for metals and metal/Al ratios for metals with enrichment in the 2-3 cm layer from the core collected at station 1015.

Enrichment of sediment Mn concentrations also was observed at several locations (stations 8, 17, 22, 29, 34 and 104; Figures 7e and 8). Diagenetic impacts on Mn distribution in sediments are well studied and can lead to a variety of perturbations in concentrations of Mn (Gobeil et al., 1997; Trefry and Presley, 1982). In the top 1 cm of the core from station 29 (Figure 8), the Mn/Al ratio is ~40% higher than found in deeper layers of the core. One possible explanation for this observation is similar to that described above for As whereby Mn undergoes reductive dissolution at depth with diffusion of dissolved Mn^{2+} upward in the sediment column where it can precipitate as an oxide phase or pass into the overlying water column (Gobeil et al., 1997; Trefry and Presley, 1982).

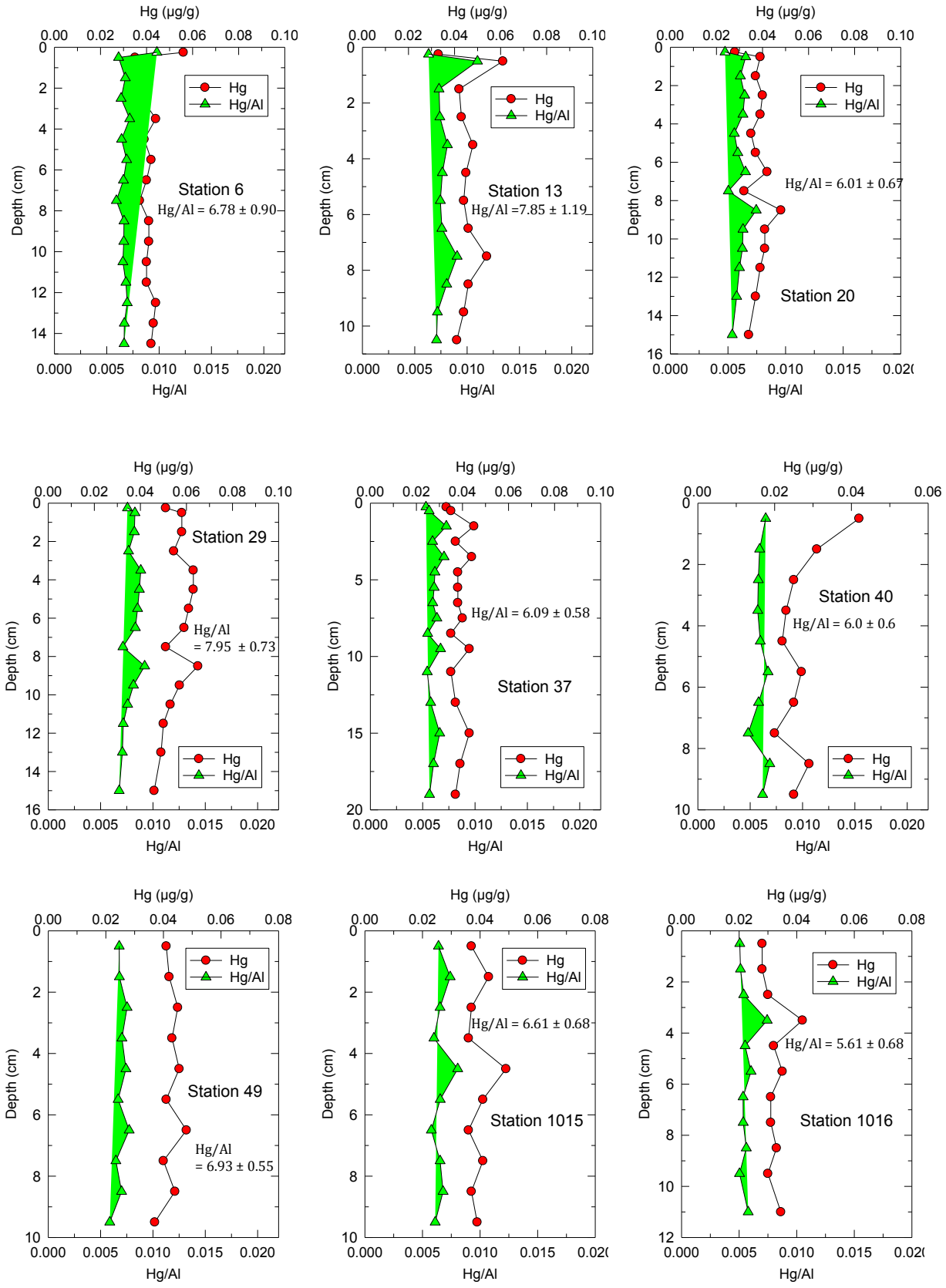

Figure 11. Vertical profiles for Hg and Hg/Al ratios for all sediment cores from COMIDA study.

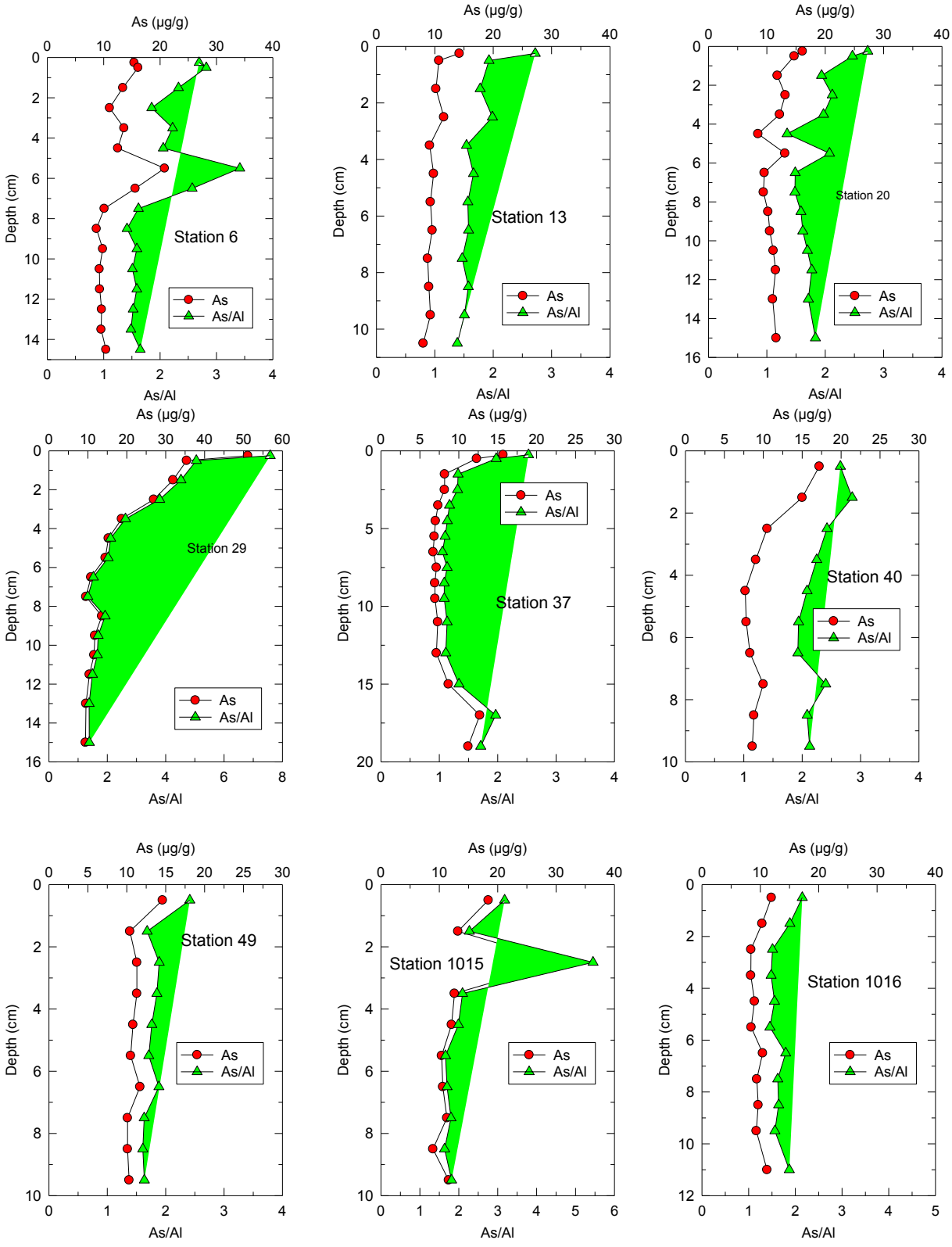

Figure 12. Vertical profiles for As and As/Al ratios for all sediment cores from COMIDA study.

Ecological Implications of Trace Metal Data

When data points plot above the upper prediction interval on a metal versus Al graph, a common question that follows is "Do those concentrations produce adverse biological effects?" Various investigators have developed sediment quality guidelines to help assess possible adverse biological effects from sediment contaminants (e.g., Field et al., 1999; Long et al., 1995; MacDonald et al., 1996). The guidelines introduced by Long et al. (1995) use an Effects Range Low (ERL) and Effects Range Median (ERM) that are based on field, laboratory, and modeling studies conducted in North America that coupled concentrations of contaminants in sediment with adverse biological effects. The ERL and ERM are defined as the 10^{th} and 50^{th} percentile, respectively, from an ordered list of concentrations of substances in sediments that are linked to a biological effect.

Several authors have noted that sediment quality guidelines should be used cautiously with an appropriate understanding of their limitations. For example, Field et al. (2002) noted that the ERL is not a concentration threshold for a chemical in sediment, above which toxicity is possible and below which toxicity is impossible. Instead, according to O'Connor (2004), the ERL is a concentration "at the low end of a continuum roughly relating bulk chemistry with toxicity." O'Connor (2004) also stated that concentrations of more than one chemical that are above the ERL do not increase the probability of toxicity. The utility of the sediment quality criteria is to call attention to a specific site where additional study, such as determining benthic biomass and community structure, may be warranted. The application of ERLs and ERMs to the sediment data from the eastern Chukchi Sea are presented here with these caveats.

Five metals (Ag, Cd, Hg, Pb and Zn) of the 17 trace metals investigated during this study have been assigned realistic values for the ERL and ERM by Long et al. (1995). These guidelines are continually evolving as demonstrated by the extensive efforts of Field et al. (2002; 1999) to validate values for Hg, Pb and Zn. Some difficulties still exist with ERL values for As, Cr and Cu as discussed below.

All concentrations of Ag, Cd, Hg, Pb and Zn were below both the ERM and ERL (Table 2). As mentioned above, there are difficulties with values for the ERL for Cr, Cu and Ni (Long et al., 1995) because the ERL concentrations are lower than concentrations in typical continental crust (Wedepohl, 1995). The published ERL values for Cr, Cu and Ni are 81, 34 and 21 µg/g (Long et al., 1995). These values are close to or less than values for average marine sediment or average continental crust. For example, average concentrations of Cr, Cu and Ni in continental crust are 126, 25 and 56 µg/g (Wedepohl, 1995). Background Cr, Cu and Ni values for sediments in the Chukchi Sea are 72, 14 and 25 µg/g (Table 1). The choice of ERL values for Cr and Cu were most likely taken from a database compiled by Long et al. (1995) that used metal concentrations from an acid leach of the sediment rather than a total digestion. For example, only a minor fraction (<25%) of the total Cr is removed by a strong acid leach (Sinex et al., 1980; Trefry and Presley, 1976). Thus, a leachable Cr value equal to the ERL level of 81 µg/g is more likely comparable with a total Cr level of >300 µg/g, a value considerably higher than Cr values for continental crust or any samples from this study. O'Connor (2004) noted that the original ERL for Cu was 70 µg/g in (Long and Morgan, 1990). Clearly, the ERL values for Cr and Cu need to be revised

Table 2. Summary of maximum metal values from this study with number of values that exceed the upper prediction interval (PI) on metal versus Al plot, the Effects Range Low (ERL) and Effects Range Median (ERM).

Metal	Max this study (µg/g)	# Values >10% above upper PI (station ID)	ERL (µg/g)[a]	# Values >ERL	ERM (µg/g)[a]	# Values >ERM
V	164	0	NA	-	NA	-
Se	1.0	0	NA	-	NA	-
Sb	1.1	0	NA	-	NA	-
Sn	2.4	0	NA	-	NA	-
Ag	0.17	1 (109)	1.0	0	3.7	0
Hg	0.090	2 (13, 1016)	0.150	0	0.710	0
Cd	0.38	1 (103)	1.2	0	9.6	0
Cr	104	2 (104)	-	-	370	0
Zn	108	1 (1015)	150	0	410	-
Cu	29	1 (1015)	34	0	270	0
Pb	22	2 (1015, 1016)	46.7	0	218	0
Be	2.0	1 (40)	NA	-	NA	-
Ni	42	3 (104, 1016)	-	-	-	-
Ba	823	15 (1016)	NA	-	NA	-

[a]Long et al. (1995).

in future iterations of the sediment quality criteria. Similarly, the ERL for As of 8.2 µg/g is close to the value of 7.7 µg/g for average marine sediments (Salomons and Förstner, 1984) and much lower than the background, natural value of 15 µg/g for the eastern Chukchi Sea.

No sediment quality criteria are available for Ba. Toxicity studies using barite are limited; however, Starczak et al. (1992) found no significant differences in the growth rates for the polychaete *Mediomastus ambiseta* between natural sediments and sediments containing 10% barite (Ba ~50,000 µg/g). All sediment samples from this study contained <0.1% Ba (<1,000 µg/g) or 50 times less Ba than in the experiment that showed no impacts.

Provenance of Chukchi Sediments and Associated Metals

The Yukon River and other much smaller rivers have been considered to be important sources for sediments found in the Chukchi Sea (McManus et al., 1969). In a study of trace metals in suspended sediments from the Yukon River estuary, adjacent Norton Sound and the northeastern shelf of the Bering Sea, Feely et al. (1981) used various metal/Al ratios to define the particles derived from the Yukon River. Ratios for Fe/Al and Cr/Al are used here to compare suspended sediment from the Yukon River with bottom sediments from the Chukchi Sea (Table 3). The Fe/Al and Cr/Al ratios for most sediments from the COMIDA area were within 20% of values obtained for the Yukon River and Norton Sound (Table 3). Such agreement is certainly consistent with a Yukon River source.

Table 3. Ratios of Fe and Cr to Al for suspended sediments from the Yukon River and Norton Sound (from Feely et al. 1981) along with ratios for stations from the COMIDA study area.

Location	Fe/Al
Yukon River estuary[a]	0.66
Central Norton Sound[a]	0.66
W. Norton Sound/Bering Sea[a]	0.66
Most COMIDA stations (n = 57)	0.57 ± 0.05
COMIDA stations 14, 27	0.92, 1.09
COMIDA stations 39, 46, 109, 1013	0.47, 0.28, 0.49, 0.49
Location	Cr/Al (x 10^{-4})
Yukon River estuary[a]	13.4
Central Norton Sound[a]	15.7
W. Norton Sound/Bering Sea[a]	15.9
Yukon and Norton (Mean ± SD)[a]	15.0 ± 1.4
Most COMIDA stations (n = 45)	14.5 ± 0.9
COMIDA stations 2, 3, 14, 27, 104	17.2, 19.1, 20.4, 18.8, 20.4,
COMIDA stations 25, 31, 32, 38, 40, 44, 46, 47, 109	12.1, 10.5, 11.8, 11.6, 12.5, 12.8, 9.5, 12.1, 12.0

[a]Feely et al. (1981)

Results for several COMIDA stations were more than 25% above or below the values found for source particles from the Yukon River estuary. For example, results for nearshore COMIDA stations 14 and 27 showed that both ratios were 25 to 65% greater than found for the Yukon River and Norton Sound (Table 3). These nearshore sediments certainly contain some fraction of sediment from coastal erosion (Figure 13). Ratios of Fe/Al and/or Cr/Al were more than 20% lower than found for the Yukon River estuary for 11 COMIDA stations (Table 3). These stations cluster around Hanna Shoal and the northern portion of the study area where other sources of sediment certainly may contribute to the sediments (Figure 13). This brief consideration of the

provenance of sediments and sediment metals is certainly consistent with many previous studies citing the importance of the Yukon River as a source of sediments to the Chukchi Sea. Development of an algorithm to define the fraction of Chukchi Sea sediments that might be derived from Yukon River sediments may be possible with more sediment data and use of more than two metal/Al ratios.

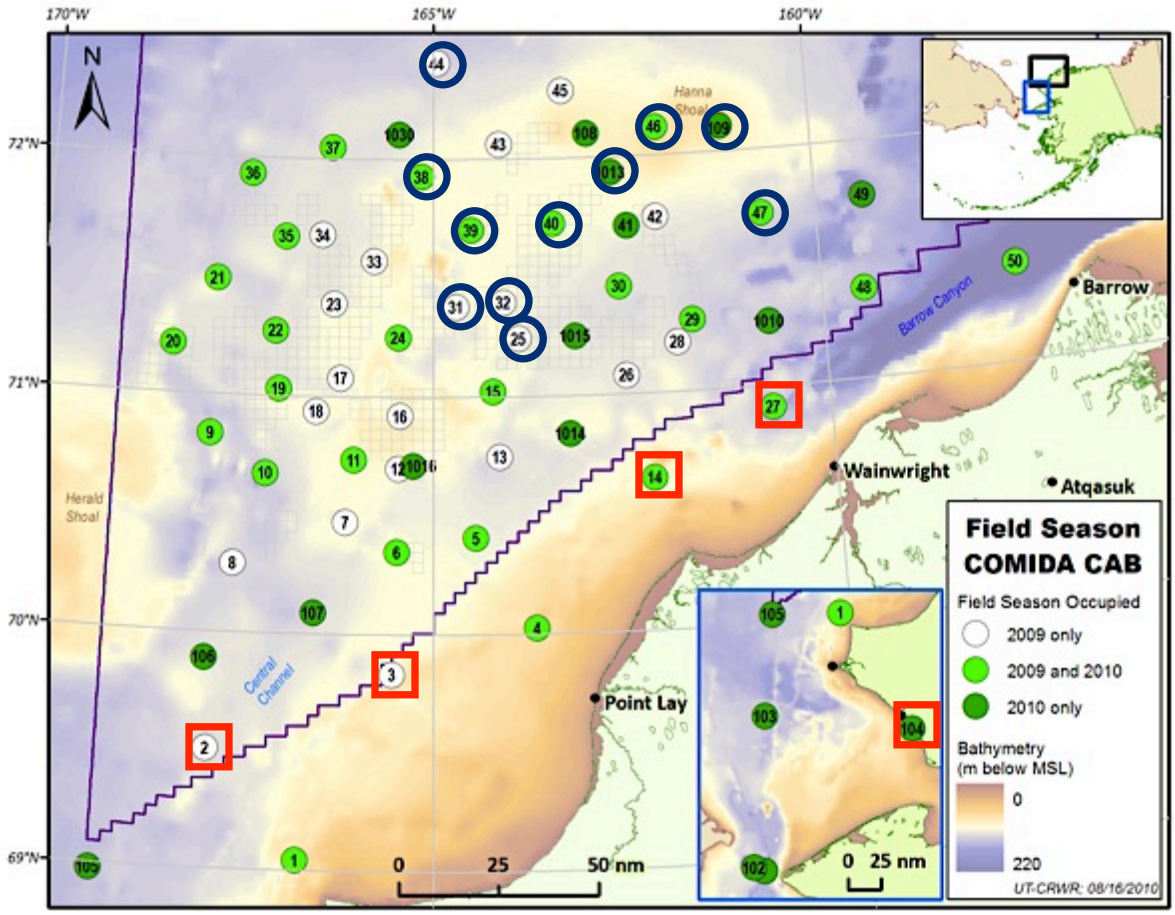

Figure 13. Maps showing 2009 and 2010 stations for the COMIDA Project. Red squares identify stations where bottom sediments have distinctly higher Fe/Al and/or Cr/Al ratio than suspended sediments from the Yukon River estuary. Blue circles identify stations where bottom sediments have distinctly lower Fe/Al and/or Cr/Al ratios than suspended sediments from the Yukon River estuary. The remaining stations have Fe/Al and Cr/Al ratios that are consistent with a Yukon River source.

Summary and Conclusions

Concentrations of 17 trace metals (Ag, As, Ba, Be, Cd, Cr, Cu, Hg, Mn, Ni, Pb, Sb, Se, Sn, Tl, V and Zn) in 207 bottom sediment samples from the eastern Chukchi Sea were essentially all at natural, background values. Ratios of metals/Al were used as a model for determining background metal concentrations and identifying anthropogenic inputs. Minor exceptions were

observed in 29 of 3105 data points; some natural diagenetic enrichment of As and Mn also was observed. No Zn or Pb anomalies were found in sediments from the offshore loading area for the Red Dog Mine, a Zn-Pb mine; and, the higher Cr and Ni values found for sediments in the loading zone were not observed in the primary COMIDA CAB study area. Fifteen of the 28 anomalies were for concentrations of Ba at an old drill site in the Klondike lease area; another 3 anomalies, 1 each for Hg, Ni and Pb, were found at the Klondike site. The highest Ba concentration in the sediment core from the Klondike site (station 1016) was 1290 μg/g, only ~700 μg/g higher than the average background value of ~600 μg/g. Concentrations of Ba in sediments with abundant drilling mud have been reported to have Ba concentrations as high as 200,000 μg/g (Trefry et al., 2007); thus, the excess Ba found to date is relatively small. The anomalous Hg value mentioned above was 0.090 μg/g (relative to background values of 0.034 μg/g) and was not found to be an impurity in barite, but was most likely present in a sulfide mineral that may have been part of the oil formation cuttings.

The other anomalous values included higher values for Zn, Cu and Pb at one station where a natural metal sulfide was most likely present. Two values for both Ni and Cr were elevated at the port for the Red Dog mine that extracts Zn and Pb; no anomalies for Zn or Pb were found at the site. Four other single and unexplained values (one each for Ag, Hg, Cd and Be) also were observed.

All concentrations of Ag, Cd, Hg, Pb and Zn were below all the sediment quality criteria. The highest Ba concentrations were 50 times lower than a tested value that showed no impact. The sediments of the eastern Chukchi Sea are presently free of metal contamination with the likely exception of small areas around old drill sites.

Provenance of sediment metals was evaluated using Fe/Al and Cr/Al ratios; most ratios from the COMIDA area were within 20% of values obtained for the Yukon River and Norton Sound. Such agreement is consistent previous studies that showed the importance of the Yukon River as a source of sediment and metals to the Chukchi Sea. Sediments from two nearshore stations and 11 stations in the northern portion of the study area had Fe/Al and Cr/Al ratios that suggest additional sources of sediments including coastal erosion or transport from the west.

Acknowledgments

We thank the Bureau of Ocean Energy Management (BOEM), U.S. Department of Interior for funding to support this study. We especially thank Dick Prentki of BOEM for his participation in the cruises, his active role in project planning and in scientific discussions as well as his continued support and enthusiasm for the COMIDA Project. We thank Ken Dunton for his leadership as Chief Scientist for the COMIDA Project and Jackie Grebmeier for her leadership as Chief Scientist on the two COMIDA cruises. We greatly appreciate the hard work and "can do" attitude of Captain John Seville and his crews on the *R/V Alpha Helix* and *R/V Moana Wave*. We thank Eric Hersh and Harish Sangireddy for support at sea and after with cruise operations and data cataloging. We thoroughly enjoyed our sea voyages with all the COMIDA scientists and thank them for such a strong sense of camaraderie. We thank Austin Fox, Emily Hughes and Cory Hodes of Florida Institute of Technology for help at sea, in the laboratory and in data processing and graphing.

Organic Contaminants in Chukchi Sea Sediments and Biota and Toxicological Assessment in the Arctic cod, *Boreogadus saida*

Harvey, H.R., K.A. Taylor, H.V. Fink, and C.L. Mitchelmore

H. Rodger Harvey and Karen A. Taylor
Department of Ocean, Earth, and Atmospheric Sciences
Old Dominion University, Norfolk, VA 23529

Hannah V. Fink and Carys L. Mitchelmore
Chesapeake Biological Laboratory
University of Maryland Center for Environmental Science
Solomons, MD 20688

Abstract

As part of the Chukchi Sea Offshore Drilling Area (COMIDA) project, we determined concentrations of organic contaminants (aliphatic hydrocarbon and polycyclic aromatic hydrocarbons, PAHs) in surface sediments (0-1 cm) from 52 sites in the Chukchi Sea. Up to 31 total PAHs, including parent and alkyl-homologues, were detected with total concentrations ranging over 20-fold in surface sediments from 149 ng g^{-1} at station 16 to 2956 ng g^{-1} at station 26 (Figure 2). Alkyl PAHs are dominant among all stations and contribute 54-93% of the total. PAH concentrations in surface sediments at 51 of 52 sites on the Chukchi shelf measured at background levels (< 1600 ng g^{-1}). The exception was station 26, where total PAHs (2956 ng g^{-1}) are 2 to 20-times greater than at other baseline sites. At three sites concentrations of total PAHs and aliphatic hydrocarbons were determined at multiple depths from collected cores. A general decrease in total PAHs is seen downcore with alkyl-substituted PAHs ranging from 50-81% of the total among all sediment depths analyzed. In biota, foot muscle of the Northern whelks, *Neptunea heros,* contained total concentrations of PAHs from 4.5 to 10.7 ng g^{-1} wet tissue wt. which decreased in larger organisms. In contrast, aliphatic n-alkanes in *Neptunea* muscle ranged from C_{19}-C_{33} and increased in larger organisms from 0.66 to 5.2 μg g^{-1} wet tissue. Muscle tissues were dominated by long-chain (C_{23}-C_{33}) n-alkanes that contribute 73-94% of the total among all size classes. Assays of exposure response were conducted on the common Arctic cod, *Boreogadus saida*. Levels of gene expression and enzymatic activity of cytochrome P4501A1 (CYP1A1/EROD), glutathione-*S*-transferase (GST), and Cu/Zn superoxide dismutase (SOD) were measured in liver tissue and correlation analyses between gene expression and enzyme activity were conducted. DNA damage in liver was measured using the Comet assay. Arctic cod exhibited liver EROD activity from 1.17-24.24 pmol min^{-1} mg^{-1} protein, cytosolic GST activity from 85.61-717.38 nmol min^{-1} mg^{-1} protein, and cytosolic SOD activity from 1.34-24.65 U min^{-1} mg^{-1} protein. The CYP1A1, GST, and SOD enzyme levels are comparable to baseline levels reported in previous field studies and other polar fish. Although some significant differences were seen between specific stations in the Arctic cod examined, there were no overall differences between stations in liver *cyp1a1* and *gst* gene expressions, EROD enzyme activity, and DNA

damage. No significant correlations between gene expression and enzyme activity were observed for the three biomarkers examined.

Introduction

The Chukchi Sea may be one of the last non-exploited areas in North America with potential as a significant source of oil and natural gas. Located between northern Alaska and the Siberian coast, the Chukchi Sea is part of the largest continental shelf in the world and its northern location puts it at the crossroads of recent observed changes in global climate. Recent decadal scale observations of warming temperatures makes it highly susceptible to the effects of sea-ice retreat, ecosystem shifts and offshore energy development (Grebmeier et al., 2010). The Chukchi Sea is estimated to contain 15 billion barrels of oil recoverable by conventional methods (MMS, 2006), and interest in exploring this area has increased dramatically over the past decade. In 2008, the Chukchi Sea Lease sale 193 leased 487 block areas of the Chukchi Sea primarily to Shell and Conoco-Phillips for rights to future oil and natural gas extraction (BOEMRE, 2011).

Aliphatic n-alkane and polycyclic aromatic hydrocarbons (PAHs) were targeted for this study. Their ability to trace specific sources of anthropogenic contamination (i.e. fossil fuel combustion) and natural inputs (i.e. oil seeps, terrestrial debris) is important due to increased interest in recoverable oil reserves on the Chukchi shelf and the possibility of hydrocarbon contamination as a result of petroleum exploration. Hydrocarbon biomarkers found in the Arctic represent a mixture of natural background and petroleum hydrocarbon sources with concentrations of aliphatic n-alkanes significantly greater than those of PAHs. Major contributors to the elevated n-alkane signal (C_{27} and C_{29}) in Arctic Ocean sediments derive from persistent inputs of terrigenous material from rivers and coastal erosion (Belicka and Harvey, 2009; Belicka et al., 2002; Yamamoto et al., 2008; Yunker et al., 2005).

Although PAHs represent only a small (0.2-7%) fraction of the total composition of crude oil, their aromatic structures represent one of the major contributors to its toxicity (Neff, 2002b; NRC, 2003). As one of the most abundant and widely distributed circumpolar Arctic fish species (Gillespie et al., 1997), the Arctic cod, *Boreogadus saida* is an important component of the marine food web within the Chukchi Sea (Craig et al., 1982; Welch et al., 1991). Arctic cod is considered a key species in the transformation of energy from lower to higher trophic levels as they feed on zooplankton, copepods, amphipods, and other fish, while being the major prey source of many seabirds (fulmars, kittiwakes, murres, and guillemots) and marine mammals including ringed and harp seals, narwhals, and belugas (Bradstreet and Cross, 1982; Bradstreet et al., 1986). Given its abundance, economic and ecological importance, the Arctic cod was targeted for evaluation of baseline health status of a native organism.

In vertebrate organisms like fish, the most commonly used biomarker for studying exposure to petroleum PAHs in marine vertebrate organisms is hepatic cytochrome p4501A1 (CYP1A). CYP1A is a phase I metabolism enzyme involved in the biotransformation and excretion of xenobiotic (and endogenous) compounds as well as oxidative stress (van der Oost et al., 2003; Whyte et al., 2000). In *B. saida,* the ethoxyresorufin *O*-deethylase (EROD) enzyme activity assay (a measurement of CYP1A activity) has been shown to exhibit a time and dose-dependent

induction from exposure to dispersed and the water-soluble fraction of North Sea crude oil (Jonsson et al., 2010; Nahrgang et al., 2010b). In some species (often invertebrates) metabolism of PAHs by CYP1A and CYP1A-like enzymes can also lead to oxidative stress by the activation of PAHs (Livingstone, 2003). However, cells contain multiple antioxidant enzymes that can neutralize these ROSs and prevent oxidative stress such as superoxide dismutase (SOD), which catalyzes the dismutation of superoxide anion radicals into hydrogen peroxide and oxygen. SOD gene expression and enzyme activity have been examined for use as biomarkers for pollution monitoring in *B. saida* and other marine fish (Benedetti et al., 2007; Livingstone et al., 1992; Nahrgang et al., 2009; Nahrgang et al., 2010b; Olsvik et al., 2009). If these antioxidant systems are overwhelmed, the oxidative stress caused by ROSs can lead to DNA damage, particularly single-strand DNA breaks. Exposure to PAHs and other pollutants have been shown to result in DNA strand breaks in both the liver and blood cells of *B. saida* and other marine fish (Curtis et al., 2011; Hartl et al., 2007; Mitchelmore and Chipman, 1998a, b; Nacci et al., 1996; Nahrgang et al., 2010b).

This component of the overall COMIDA-CAB study was to document organic contaminant levels in sediments as seen as PAH and aliphatic hydrocarbons, establish concentrations in a common invertebrate (e.g. *Neptunea heros*) and determine if environmental concentrations had resulted in observable responses by the native fish *B. saida.*

Methods

Sample Collection

Sediments

Sampling in the Chukchi Sea was accomplished aboard the *R/V Alpha Helix* during July 27-August 11, 2009 by scientists H. Rodger Harvey and Karen Taylor from Old Dominion University. In 2010, sampling was accomplished aboard the *R/V Moana Wave* during July 25-August 11, 2010 by the same scientists listed above plus Hannah Fink from UMD. Collections included a suite of sediments, particles and associated biota. Surface sediment (0-1 cm) samples in 2009 were collected using a Van-Veen grab, while a double Van-Veen sampler was used in 2010 (Figure 1). The grab samplers were protected from stack smoke, grease drips from winches and wire, and other potential airborne contamination during sampling. Subsurface sediment samples were collected at selected sites during 2009 from undisturbed cores using a HAPS or Pouliot 0.06 m^2 box corer. Only the HAPS corer was used in 2010. On shipboard all cores were sectioned into 1 cm intervals in the upper 10 cm of sediment, and 2 cm intervals below for chemical analysis. During the collection and handling of sediment samples, extreme care was taken to avoid contact with potential hydrocarbon sources. Contamination blanks for deck and laboratory processing of all samples are described in the QA/QC section. Only clean glassware and other materials of high purity that may come in contact with the samples were used. All sediments for PAH and hydrocarbon analysis were stored in pre-cleaned plastic I-Chem jars with Teflon-lined screw cap lids and immediately frozen.

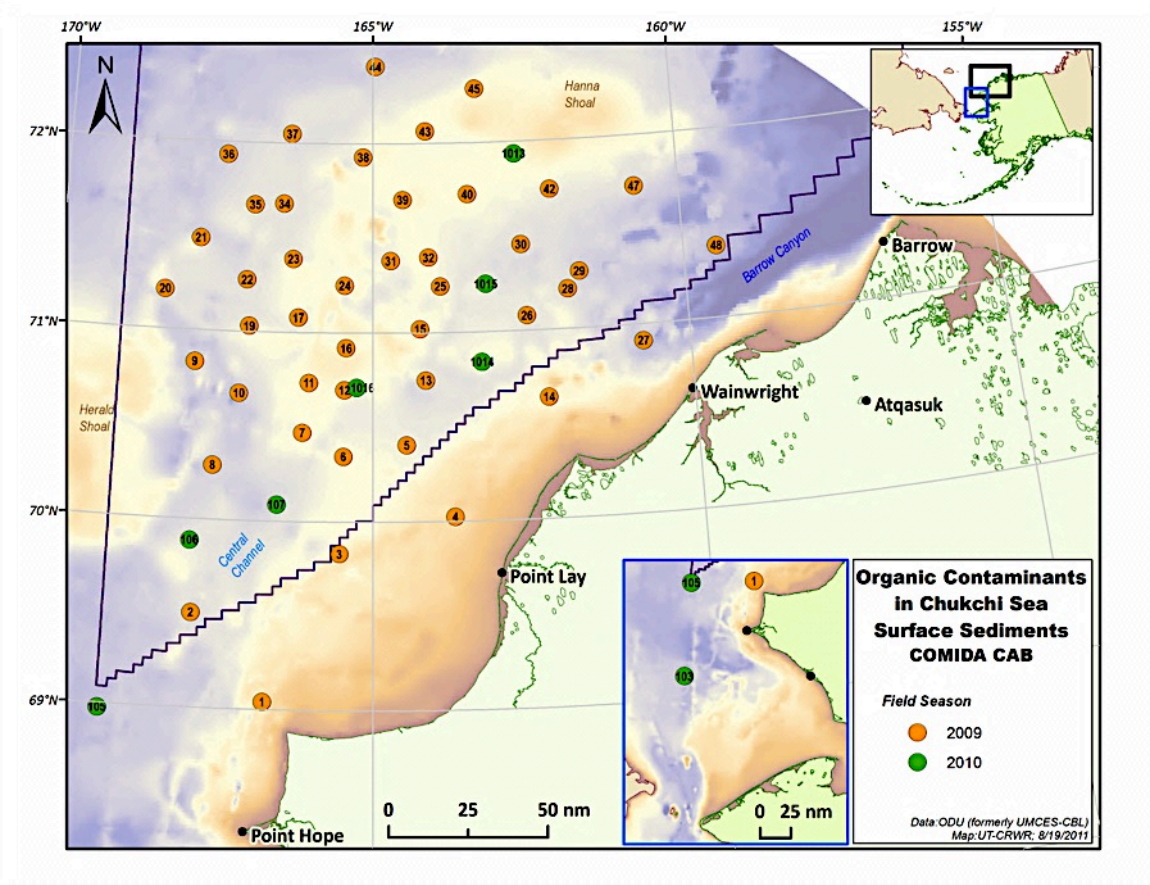

Figure1. Map of stations sampled during COMIDA09 and COMIDA10 for organic contaminants. Detailed information on individual stations is provided in appendices.

Invertebrates

Northern Neptune whelks (*Neptunea heros*) were sampled using an epibenthic otter trawl from selected stations. Trawls were approximately 10 min in duration and catches were immediately sorted. *Neptunea* shells were measured and organisms pooled by size (< 5, 5-8, and >8 cm). Sterile tools were used for the dissection and removal of foot muscles on the ship, which were stored in pre-combusted foil and immediately frozen.

Fish

Arctic cod (72-140 mm) were collected by LGL fisheries scientists by benthic trawling using demersal fishing nets in 2010. We refer to this species of Gadidae as Arctic cod and not polar cod, as Arctic cod is the name recognized by the American Fisheries Society (Robins et al., 1980). Locations, dates, water quality and depth are given in Table 1 below for the depth trawled at each station.

Table 1. Sampling location for Arctic Cod collected in the Chukchi Sea. Ancillary water quality parameters at trawl depth were measured with an YSI Sonde attached to the trawl frame. For illustration of station locations see Figure 1.

Station Code	Sampling Date	Location		Water Temperature (°C)	pH	DO (mg/L)	Salinity (ppt)	Trawling Depth (m)
		Latitude	Longitude					
6	7/30/10	70°20.400'	-165°22.900'	-0.26	7.80	11.13	33.13	47
10	7/31/10	70°41.670'	-167°07.000'	-0.31	7.78	11.57	32.53	40
22-24	8/10/10	71°16.289'	-166°02.553'	-0.78	7.74	11.82	32.27	43
30	8/5/10	71°27.780'	-162°37.150'	-1.69	7.34	10.10	32.91	50
47-49	8/4/10	71°44.750'	-160°01.300'	-1.66	7.32	9.44	33.19	43
103	7/26/10	67°40.223'	-168°57.467'	3.1	7.73	10.06	32.80	51

Upon collection, fish from trawls were transferred to aerated buckets of seawater (4-5°C) and examined for any gross physical abnormalities (e.g. lesions and tumors). Fish in good condition were sacrificed and total body length was measured (Table 2 below). The livers were dissected immediately on ice and a subsample of fresh liver tissue was directly used for the COMET assay, while the rest was flash frozen and stored in liquid N_2 to be processed at the shore based laboratory

Table 2. Sampling descriptions of sample size, total body length and range of Arctic cod, *B. saida*, used for analyses. Length represents mean ± SE.

Station Code	N	Length (mm)	Length Range (mm)
103	4	103±2.16	100-105
6	3	112±4.58	108-117
10	5	89.8±13.1	78-111
22-24	4	86.25±7.54	79-95
47-49	5	119±23.56	80-140
30	3	94±27.62	72-125

Laboratory analysis of hydrocarbons in COMIDA sediments and *Neptunea* foot muscle

Extraction of hydrocarbons

Surface sediments (0-1 cm) from 52 sites, including 3 sediment cores from station 37, 40 and 1016, and foot muscle from *Neptunea* were analyzed for both aromatic and aliphatic hydrocarbons. Each sediment sample was lyophilized to a fine powder and thoroughly homogenized prior to chemical analysis. *Neptunea* muscle was cut into smaller pieces and extracted wet. About 6 g of lyophilized sediment or 13 g of muscle tissue were transferred to

Green Chem glass vessels with Teflon screw-cap lids. Six perdeuterated PAHs (Acenaphthene-d_{10}, Phenanthrene-d_{10}, Benz(a)anthracene-d_{12}, Benzo(a)pyrene-d_{12} and Benzo(g,h,i)perylene-d_{12}, and n-Octadecane-d_{38}) were added prior to extraction and served as internal standards for calculation of recoveries and hydrocarbon concentrations (refinement of EPA Method 8270). Sediments and muscle tissues were extracted with hexane: acetone (1:1, 35ml) at 80^{o}C for 30 min and stirred on high using a MARS microwave assisted extraction system (CEM Corp., Matthews, NC) operating at 800-1200 W depending on the number of samples (refinement of EPA Method 3546). After extraction, vessels were allowed to cool to room temperature before being opened. The supernatant was first filtered through pre-cleaned and combusted glass wool and then combined with 2-4 ml hexane: acetone (1:1) rinses of the extraction vessel containing the sample. Sediment and muscle tissue extracts were concentrated to 3 ml using rotary evaporation and then split for the analysis of PAHs and aliphatic hydrocarbons.

Labware used in the extraction process was washed in Alconox, soaked in RBS-35 detergent, and then 15% HCl each for 24 hr and then rinsed three times with RO or UV Nanopure water after each washing step. Glassware was dried and then combusted at 450^{o}C for 4 hr to remove any possibility of remaining organics. Labware was pre-rinsed with solvent three times before sample addition. A procedural blank was prepared with each round of samples extracted.

Gas Chromatography-Mass Spectrometry analysis of PAHs

PAHs were analyzed by capillary gas chromatography (GC) with an Agilent 6890 system coupled to an Agilent 5973 Network Mass Selective Detector (MS) operated in electron ionization mode. The GC-MS system was equipped with a J&W Scientific DB-5MS fused silica column (30 m, 0.25 mm id, 0.25 film thickness) and operated in selected ion monitoring (SIM) mode. Samples were injected in splitless mode at an initial oven temperature of 50^{o}C and an injector temperature of 250^{o}C with helium as the carrier gas. The oven temperature was ramped at 15^{o}C/min to 120^{o}C and then 3.5^{o}C/min to 300^{o}C before holding at 300^{o}C for 10 min. The base peak area response of selected ions was adjusted relative to that of the appropriate perdeuterated-PAH internal standard, which is based on the number of carbons (refinement of EPA Method 8270D). Target PAHs and those detected in COMIDA09 and COMDA10 samples, including method detection limits, are listed in Table 3.

Table 3.Target polycyclic aromatic hydrocarbons (PAHs) measured in COMIDA samples, including number of rings and method detection limit values (MDL). (*) denotes PAHs that have been detected in COMIDA09/10 sediments.

PAH Targets	# of rings	MDL (ng/g dry wt.)	PAH targets (continued)	# of rings	MDL (ng/g dry wt.)
Naphthalene*	2	1.12	Fluoranthene*	4	0.22
2-Methylnapthalene*	2	0.57	Pyrene*	4	0.20
1-Methylnapthalene*	2	0.28	Benzo(a)fluorene	4	0.03
Biphenyl*	2	0.18	Retene*	4	0.15
2,7-Dimethylnapthalene*	2	0.07	Benzo(b)fluorine*	4	0.02
1,3-Dimethylnapthalene*	2	0.08	Cyclopenta(c,d)pyrene	4	0.02
1,6-Dimethylnapthalene*	2	0.09	Benz(a)anthracene*	4	0.03
1,4-Dimethylnapthalene*	2	0.04	Chrysene+Triphenylene	4	0.03
1,5-Dimethylnapthalene*	2	0.03	Napthacene*	4	0.08
Acenapthylene	2	0.02	4-Methylchrysene*	4	0.02
1,2-Dimethylnapthalene	2	0.02	Benzo(b)fluoranthene	4	0.04
1,8-Dimethylnapthalene	2	0.39	Benzo(k)fluoranthene	4	0.02
Acenapthene	2	0.11	Dimethylbenz(a)anthracene	4	0.03
2,3,5-Trimethylnapthalene*	2	0.03	Benzo(e)pyrene	5	0.04
Fluorene	2	0.11	Benzo(a)pyrene*	5	0.08
1-Methylfluorene*	2	0.05	Perylene*	5	0.06
Dibenzothiophene*	3	0.04	3-Methylchloanthrene	5	0.08
Phenanthrene*	3	0.62	Indeno(1,2,3-c,d)pyrene	5	0.01
Anthracene	3	0.03	Dibenz(a,h+ac)anthracene	5	0.02
2-Methyldibenzothiophene*	3	0.09	Benzo(g,h,i)perylene*	6	0.02
4-Methyldibenzothiophene*	3	0.04	Anthanthrene	6	0.01
2-Methylphenanthrene*	3	0.15	Corenene	7	0.00
2-Methylanthracene*	3	0.03			
4,5-Methylenephenanthrene	3	0.04	Internal standards:		
1-Methylanthracene*	3	0.04	Acenaphthene-d_{10}	3	
1-Methylphenanthrene*	3	0.13	Phenanthrene-d_{10}	3	
9-Methylanthracene	3	0.03	Benz(a)anthracene-d_{12}	4	
3,6-dimethylphenanthrene*	3	0.10	Benzo(a)pyrene-d_{12}	5	
9,10-Dimethylanthracene*	3	0.16	Benzo(g,h,i)perylene-d_{12}	6	

Purification and GC/GC-MS analysis of aliphatic hydrocarbons

Due to the complex matrix and organic matter content of sediments and muscle tissue, it was necessary to further purify extracts through hydrolysis and fractionation by normal phase-high performance liquid chromatography (HPLC). In brief, a fraction of each sediment extract was subjected to alkaline hydrolysis with a solution of 0.5 N KOH in methanol. The resulting neutral fractions were concentrated to 250 μl and separated with an Agilent HPLC system equipped with

a Luna silica analytical column (5 μm; 250 mm x 4.6 mm id) and guard column cartridge of similar material (Phenomenex Torrance, CA). Separation of fractions was achieved at ambient temperature with an injection volume of 50 μl and flow rate of 0.5 ml min^{-1} with the following solvent gradient (modified slightly from Tolosa and de Mora, 2004): 100% A (0-10 min); 80% A and 20% B (at 15 min); 100% B (at 20 min) and then isocratic hold to 30 min, followed by 50% B and 50% C (at 35 min) and then isocratic hold to 60 min (where A = hexane, B = methylene chloride and C = MeOH; all HPLC grade). Once fractions were collected, the flow rate was increased to 1 ml $min^{-1}$and the column re-equilibrated before the start of the next run with 100% B (to 65 min); 100% A (to 70 min) and then isocratic hold to 80 min. The elution of n-alkanes occurs in the first fraction (0-10 min). Once collected, solvent was concentrated to 80 μl with a stream of N_2 gas before GC and GC-MS analysis.

Aliphatic n-alkanes were quantified by capillary GC using Agilent 6890N Network GC System and flame ionization detection (FID) with hydrogen as the carrier gas. The base peak area response of n-alkanes was adjusted relative to that of the perdeuterated internal standard (n-Octadecane-d_{38}). Identification of n-alkanes was carried out by GC-MS operated in full scan mode. The column and temperature programs are similar to that described above. Target n-alkanes including those detected in COMIDA09 and COMIDA10 samples are shown in Table 4.

Table 4. Target n-alkanes measured in COMIDA samples, including method detection limit values (MDL). (*) denotes n-alkanes detected in COMIDA 09/10 sediments samples.

n-Alkane Targets	n-Alkane Targets (continued)
n-C_{10}	n-C_{27}*
n-C_{11}	n-C_{28}*
n-C_{12}	n-C_{29}*
n-C_{13}	n-C_{30}*
n-C_{14}	n-C_{31}*
n-C_{15}*	n-C_{32}*
n-C_{16}*	n-C_{33}*
n-C_{17}*	n-C_{34}
n-C_{18}*	n-C_{35}
n-C_{19}*	n-C_{36}
n-C_{20}*	n-C_{37}
n-C_{21}*	n-C_{38}
n-C_{22}*	n-C_{39}
n-C_{23}*	n-C_{40}
n-C_{24}*	Internal
n-C_{25}*	Standard:
n-C_{26}*	n-C_{18}-d_{38}

Quality Assurance and Quality Control

A quality assurance (QA) plan that includes quality control (QC) procedures and analyses were applied during the COMIDA-CAB program. Important QC components of this plan included analytical balance calibration, instrument tuning and calibration (MARS, GC-MS), standard recoveries, procedural and field blank analysis, and duplicate sample analysis. The MARS solvent sensor was calibrated with acetone vapors prior to each round of sample extractions. Calibration and tuning of the mass spectrometer was carried out after each set of 10 samples using perfluorotributylamine (PFTBA) as the calibrant to automatically adjust the MS parameters to meet the predefined criteria for operation in EI mode. Internal standard recoveries of perdeuterated PAH (83-102%) and n-alkane (9%) standard reference compounds were determined based on measurements obtained both before and after microwave assisted extraction and processing (MARS system). Detailed information for all samples is provided in Appendix 5. For each round of 12 samples, one procedural blank was prepared to monitor potential contamination resulting from glassware, solvents, and processing procedures. These blanks were processed along with field samples and followed the same handling and analytical scheme. Procedural blanks accounted for $\leq$ 16% and $\leq$ 0.15% of the PAH and n-alkane concentrations observed in samples, respectively. Refer to Appendix 6 for detailed information.

Field blanks collected during COMIDA cruises were processed in parallel to field samples and followed the same handling and analytical scheme. Field blanks, including ship laboratory air and DI water blanks were obtained on glass-fiber filters at the start and end of each cruise. Target hydrocarbon concentrations detected in field blanks were subtracted from those in field samples and accounted for $\leq$7% and $\leq$0.14% of the total PAH and n-alkane concentrations observed in samples, respectively. Refer to Appendix 6 for detailed information. Duplicate sample analysis was prepared for 17% of the total samples and provided a measure of processing and analytical precision.

Laboratory analysis of contaminant exposure and response in Arctic cod

Enzyme activity level measures

Liver samples were homogenized on ice in a potassium-phosphate buffer (100mM) pH 7.4 containing 150mM KCl, 1 mM EDTA, and 1mM dithiothretiol. Homogenates were centrifuged (10,000 x g, 4°C) for 30 min and the S9 fraction, supernatant, was collected. The S9 fraction was then centrifuged (100,000g, 4°C) for 60 min to collect the supernatant cytosolic fraction, which was stored in liquid N_2 for the GST and SOD assays. The resulting pellet was resuspened in homogenization buffer and centrifuged (100,000 x g, 4°C) for 45 min. The subsequent supernatant was discarded and the microsomal pellet was resuspended in homogenization buffer containing 20% glycerol. The microsomal fraction was stored in liquid N_2 for the EROD assay. Total protein concentrations in microsomal and cytosolic fractions were determined colometrically in a 96-well quartz microplate using the Pierce BCA Protein Assay kit with bovine serum albumin (BSA) as the standard reference (0-2,000µg/mL), following manufacturer's microplate procedures.

Hepatic microsome ethoxyresorufin *O*-deethylase (EROD) activity was determined spectrofluorometrically using a modified method (Eggens and Galgani, 1992; Nahrgang et al., 2010a; Nahrgang et al., 2009; Nahrgang et al., 2010b). The reaction mixture contained 10 or 30 µL microsomal fraction, 190 µL 7-ethoxyresorufin deethylase (2.5 µM), and 10 µL NADPH (100 µM; Applichem St. Louis, MO) in potassium-phosphate buffer (100 mM) pH 7.0 for 250 µL total. The production of resorufin was measured in triplicate in a 96-well quartz plate over 10 min (23°C) with a SpectraMax Gemini (Molecular Devices) Fluorometer at 530/590 nm, excitation/emission, respectively. Enzyme activities were quantified using a resorufin standard curve (0-2.5 µM) and then normalized against total protein contents in microsome samples to be expressed as pmol min^{-1} mg^{-1} microsomal protein. Detection limit of resorufin was determined to be 0.5 nM.

Glutathione *S*-transferase (GST) activity was determined spectrophotometrically following a modified method from Nahrgang et al. (2010a; 2009; 2010b). The reaction mixture contained 10 or 20 µL cytosolic fraction (depending on protein concentration), 10 µL reduced glutathione (GSH 1mM, Agros Organics New Jersey), and 5 µL 1-chloro,2,4-dinitrobenzene (CDNB, 1mM, Agros Organics New Jersey) as the substrate in potassium-phosphate buffer (100 mM) pH 7.0 for 200 µL total. The production of conjugated glutathione formed by the reaction of GSH with CDNB was measured in triplicate using a 96-well quartz plate for 3 min (25°C) with a Spectramax Plus 384 Microplate Reader (Molecular Devices) at 340nm (ϵ=9.6 mM^{-1} cm^{-1}).

Superoxide dismutase (SOD) activity was determined spectrophotometrically by measuring the degree of inhibition of the reduction of cytochrome c generated by the xanthine oxidase/ hypoxanthine reaction (McCord and Fridovich, 1969). The reaction mixture contained 10 µL hypoxanthine (50 µM), 10 µL cytochrome c (10 µM), 10 µL sample (or dilution), 210 µL phosphate buffer (50 mM) pH 7.8, and 10 µL xanthine oxidase (XOD, 1.8m U/mL) in a 96-well quartz microplate. Samples were diluted as necessary to keep the percent inhibition within the linear phase (30%-60%) of the reaction. The reduction of cytochrome c was followed on a Spectramax Plus 384 Microplate Reader (Molecular Devices) at 550nm over 5 min at 25°C. A standard curve was determined with commercial SOD from bovine erythrocytes at 0.5-25 U/mL (0.02-1.0 U in assay). SOD activity was calculated from the linear regression of the standard curve by substituting the linearized rate for each sample as described in Cayman Chemical Company's Superoxide Dismutase Assay Kit (http://www.caymanchem.com/pdfs/706002.pdf). The amount of SOD required to cause 50% inhibition of cytochrome c is equal to 1 unit of SOD activity (McCord and Fridovich, 1969). Results are expressed as units of SOD per milligram protein.

DNA damage analyses

The alkaline single cell gel electrophoresis (COMET) assay was conducted following a modified method described by Mitchelmore et al. (1998a, b). Briefly, microscope slides were coated with 1% normal melting point agarose (NMPA) in phosphate buffered saline (PBS) and allowed to dry (~24h) at 37°C in the dark. During dissection, a small section of fresh liver tissue was removed and minced in 300µL Hank's Balanced Salt Solution-Hepes buffer pH 7.6 (HBSS-Hepes, 4°C). From this cell suspension, 10µL were added to 100µL of 0.6% low melting point agarose (LMPA, 37°C) in HBSS-Hepes pH 7.6 and layered over the NMPA layer. Coverslips

were place onto and agarose allowed to polymerize for 5 min on a metal tray over ice. A final layer of 100 µL of 0.6% LMPA in HBSS-Hepes pH 7.6 was added. Following solidification, the coverslips were removed and slides placed into cold (4°C) lysing solution (10% DMSO, 1% Triton X-100, 2.5M NaCl, 100 mM EDTA, 10 mM Tris Base, 1% sodium sarconsinate; pH 10) for at least 1 h at 4°C in the dark.

Slides were rinsed with distilled water, placed on a horizontal gel electrophoresis tray, and covered with cold (4°C) electrophoresis buffer (0.20M NaOH, 1mM EDTA; pH>12) for 10 min to allow DNA to unwind. Electrophoresis was conducted at 25V, 300mA for 10 min. Slides were removed and placed in cold (4°C) neutralization solution (0.4M Tris, pH 7.5) for 5 min and repeated three times. Slides were then drained and placed in 100% ethanol (4°C) for 5 min, allowed to dry in a dark container overnight, and then placed in a desiccated slide box until processing.

For analyses, slides were reconstituted with 2 µM/mL ethidium bromide diluted with HBSS-Hepes and examined using a epifluorescent microscope (Olympus BX50) with a green filter at 40x magnification (Q Imaging Retiga 1300 camera). The Komet 5.5 Software's (Kinetic Imaging, Liverpool, UK) image analysis package was used to score the cells. From each duplicate slide, 50 non-overlapping cells were randomly selected for quantification. Results are expressed as means ± standard error of the means in terms of percentage DNA in tail, tail length and tail olive moment.

Statistical analyses

Statistical analyses for enzyme assays were performed using SAS (9.2) and R (2.12.2). Normality and homogeneity of variances of all biomarkers were examined first with the Shapiro-Wilk and Fligner-Killeen tests, respectively. When these requirements were met, a one-way ANOVA and Tukey-Kramer multiple comparison of means test were used to determine significant differences between means of biomarker results in Arctic cod from the six stations. When normality was not met, the non-parametric Wilcoxon rank-sum test was used to compare means of the biomarkers between stations. Correlations between gene expression and enzyme activity were examined using the non-parametric Spearman's rank correlation coefficient. The significance level chosen for all analyses was α=0.05.

Results

Concentrations and Distribution of PAHs in sediments

Surface sediment (0-1 cm) concentrations and distributions were determined for organic contaminants at 52 sites spanning the study area. Up to 31 total PAHs, including parent and alkyl-homologues were detected. Total concentrations ranged over 20-fold in surface sediments from 149 ng g^{-1} sed wt at station 16 to 2956 ng g^{-1} sed wet at station 26 (Figure 2). At all stations alkyl PAHs were dominant and contributed 54-93% of the total PAHs seen (Figure 2). See Appendix 1 for concentration information of individual PAHs which are based on weight.

Organic carbon concentrations of sediments (%TOC) are available in the Trefry et al. chapter for all surface sediments should alternative descriptions be of interest.

In addition to surface sediments, hydrocarbons were determined in three subsurface sediment cores at stations 37 (to 20 cm), 40 (to 10 cm), and 1016/K3 (to 12 cm). Concentrations of total PAHs vary with depth of sediment at station 37 and range from 130-975 ng g^{-1} (Figure 4). A general decrease in total PAHs is seen downcore at stations 40 and 1016/K3 with concentrations ranging from 101-2776 ng g^{-1} and 244-1310 ng g^{-1}, respectively (Figure 4). Alkyl-substituted PAHs ranged from 50-81% of the total among all cores with contributions varying with depth. Refer to Appendix 3 for detailed concentration information.

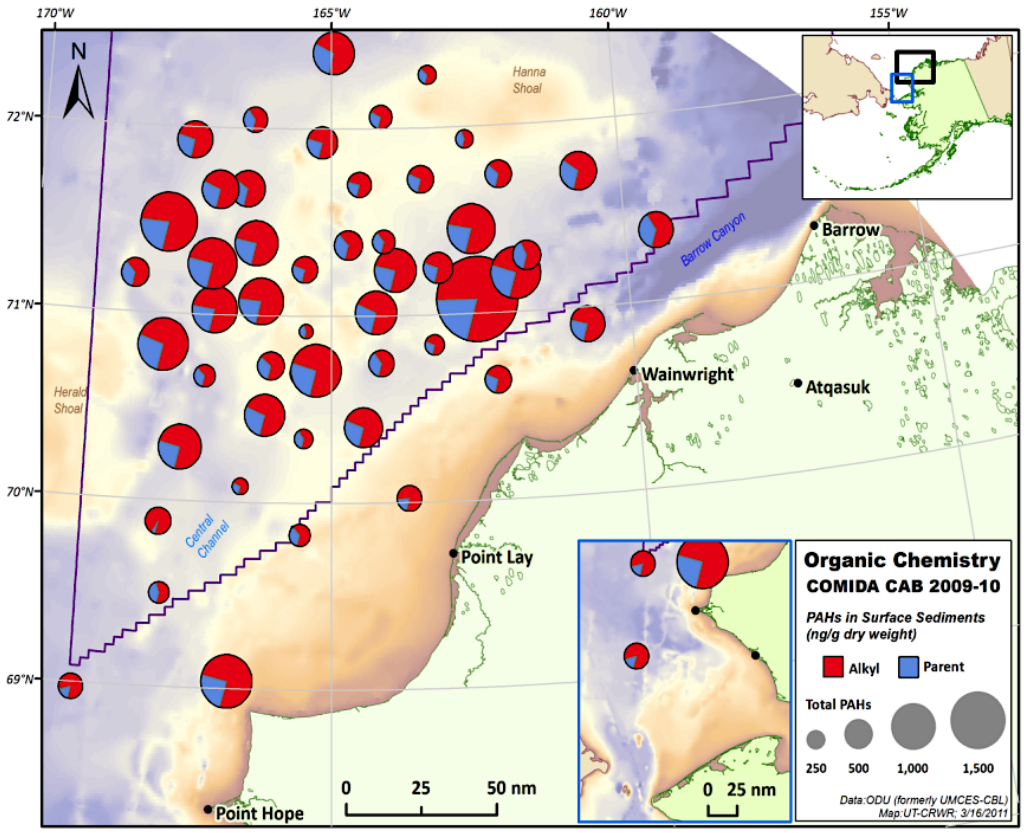

Figure 2. The concentration and distribution of PAHs in surface sediments as the sum and relative contribution of the parent and alkyl-substituted compounds.

Aliphatic n-alkanes in COMIDA sediments

Aliphatic normal-alkanes with 15 to 33 carbons (C_{15} to C_{33}) were detected in surface sediments with concentrations ranging from 1.8 μg g^{-1} at Station 14 to 17 μg g^{-1} at Station 9 (Figure 3). The distribution of short (C_{15}-C_{22}) versus long-chain (C_{23}-C_{33}) n-alkanes varied in surface sediments with significantly higher concentrations of shorter n-alkanes observed at station 26 (10.3 μg g^{-1})

than other stations (Figure 3). See Appendix 2 for concentration information of individual n-alkanes.

Concentrations of total n-alkanes vary with depth of sediment at stations 37 and 1016/K3 and range from 7.2-23 μg g^{-1} and 3.1-5.5 μg g^{-1}, respectively (Figure 4). A general decrease in total n-alkanes is seen downcore at station 40 with concentrations ranging from 1.8-10.5 μg g^{-1} (Figure 4). Long-chain n-alkanes contribute 58-91% of the total among all sediment cores, and distributions of long versus short-chain n-alkanes vary with depth. Appendix 3 contains concentration information for all individual structures observed.

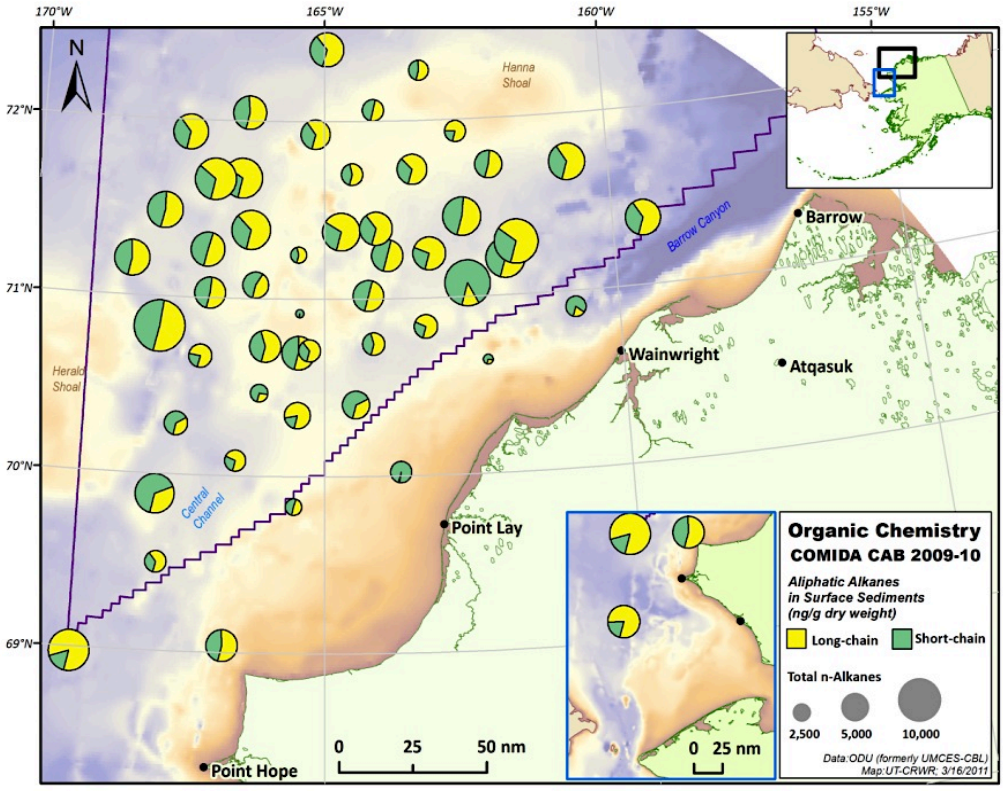

Figure 3. The concentration of aliphatic n-alkanes in surface sediments of the Chukchi Sea. Circles illustrate the total concentration and relative contribution of long and short-chain hydrocarbons across the study region.

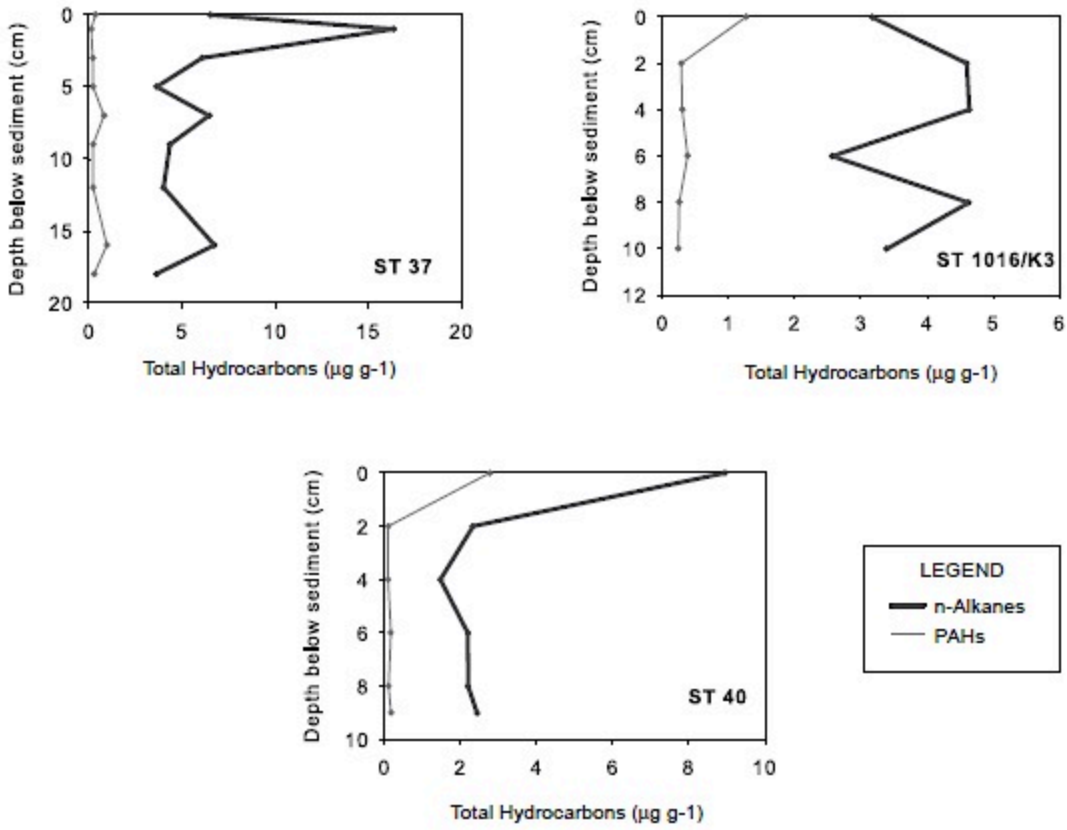

Figure 4. The vertical profiles of total PAH (grey lines) and n-alkane hydrocarbons (black lines) with depth in the three sediment cores examined from the Chukchi Sea.

Alkane and PAH hydrocarbons in *Neptunea heros*

Foot muscle from 35 *Nepuntea* were collected at station 7 and pooled by shell size (< 5, 5-8, > 8 cm) for the investigation of organic contaminants. A diversity of PAHs were found in muscle tissues with alkyl-substituted compounds dominating over parent species and contributing 54-81% of the total among all size classes (Figure 5). Total concentrations of PAHs decrease in larger organisms and range from 0.005 µg g^{-1} wet tissue wt. Aliphatic n-alkanes in *Neptunea* muscle from C_{19}-C_{33} show the opposite trend with concentrations increasing in larger organisms from 0.66-5.2 µg g^{-1} (Figure 5). Muscle tissues are dominated by long-chain (C_{23}-C_{33}) n-alkanes that contribute 73-94% of the total among all size classes. See Appendix 4 for detailed concentration information.

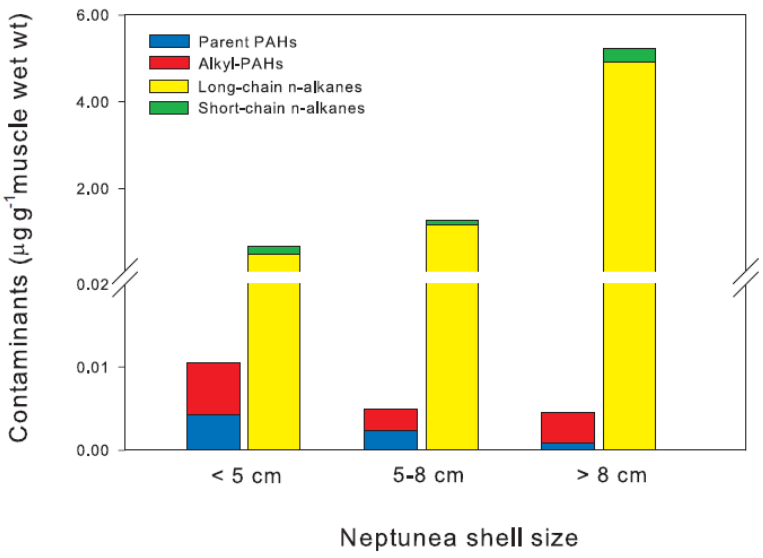

Figure 5. The concentrations of alkane and PAH hydrocarbons in *Neptunea* foot muscle shown as the sum of parent and alkyl-substituted PAHs and the sum of long and short-chain n-alkanes.

Enzymatic activity in Arctic cod

Detectible EROD activities ranged from 1.17-24.24 pmol min^{-1} mg^{-1}protein (Figure 6). Three individuals from stations 10 and 30 had EROD activities below the detection limit of the assay and were therefore not included in the final analyses. The mean liver EROD activity in Arctic cod from station 47/49 were significantly higher than the liver EROD activity of fish from station 103 (p-value<0.05). There were no other significant differences in liver EROD activity of Arctic cod between stations.

Overall, cytosolic GST activity showed a high individual variability between and within the six stations. GST activities ranged from 85.61-717.38 nmol min^{-1} mg^{-1} protein with a median of 228.6 nmol min^{-1} mg^{-1} protein (Figure 7). There were no significant differences in GST activity levels in the liver tissue of Arctic cod between the six stations.

The SOD activities in Arctic cod ranged from 1.34-24.65 U mg^{-1} protein (Figure 8). Liver SOD activity levels of Arctic cod from station 6 were significantly higher than fish from station 10 (p value<0.05). However, there were no other significant differences in SOD activity of Arctic cod between stations.

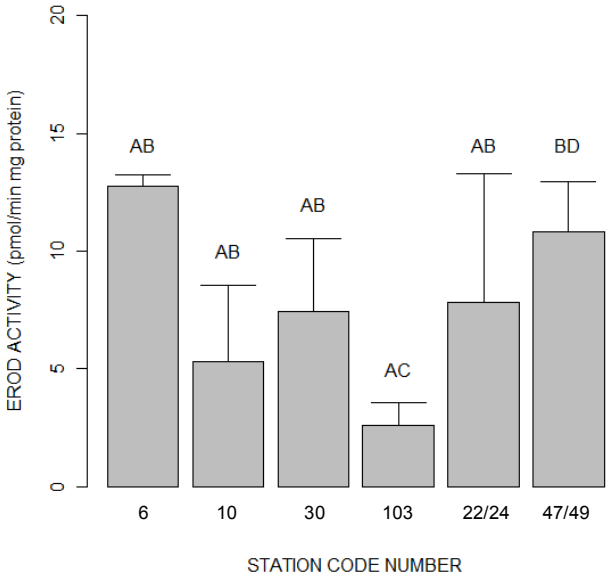

Figure 6. Ethoxyresorufin *O*-deethylase (EROD) activity in livers of Arctic cod, *B. saida*, from the Chukchi Sea from July-August 2010. Values represent means ± SE (n=2-5). Different letters signify significant differences in means (p value <0.05).

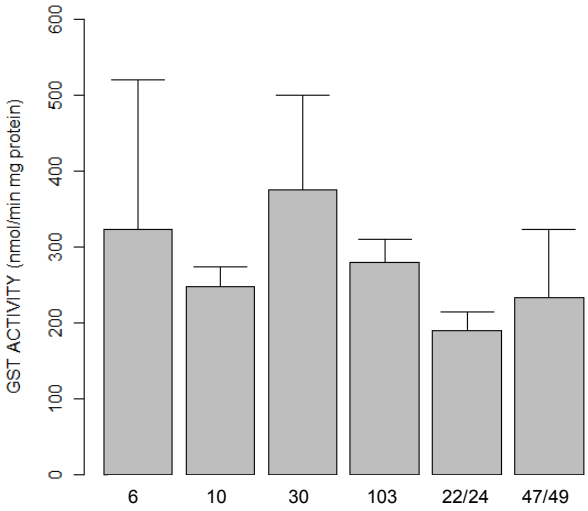

Figure 7. Glutathione *S*-transferase (GST) activity in livers of Arctic cod, *Boreogadus saida*, caught in the Chukchi Sea from July-August 2010. Values represent means ± SE (n=3-5).

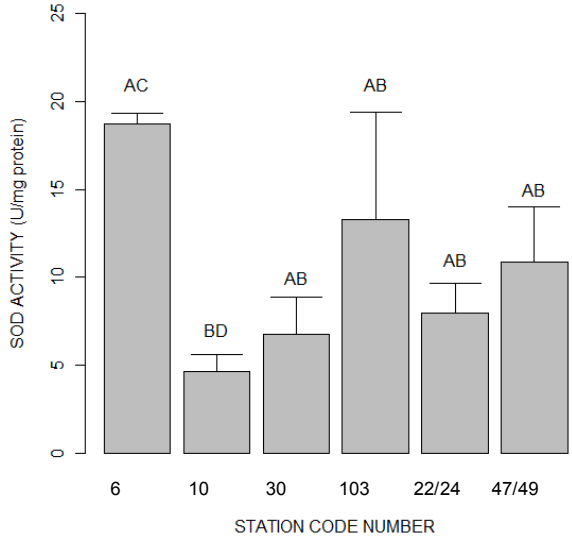

Figure 8. Superoxide dismutase (SOD) activity (U mg^{-1} protein) in livers of Arctic cod, *Boreogadus saida*, caught in the Chukchi Sea from July-August 2010. Values represent means ± SE. Different letters signify significant differences in means (p value <0.05).

Gene expression in Arctic cod

RT-PCR was able to detect all three target genes (*cyp1a1, sod,* gst) and normalization gene (β-*act)*. The relative gene expression was highest for superoxide dismutase, *sod*, which had the lowest ΔCT values of target genes examined (Table 5). Arctic cod from station 103 had significantly higher relative gene expression for superoxide dismutase, *sod,* than Arctic cod from both stations 10 and 47/49 (p-values < 0.05). There were no other significant differences in relative gene expressions of Arctic cod between stations for the three target genes. There was a significant negative correlation between relative gene expression (ΔCT) of *sod* and SOD activity levels in Arctic cod from stations examined (p value < 0.05). However, there was no significant correlation between gene expression and enzymatic activity for either cytochrome p450 1a1 or glutathione *S*-transferase.

Table 5. Relative gene expression of Arctic cod liver *cyp1a1, gst,* and *sod* normalized β-*act*. Values represented as means ± SE. Different letters designate significant differences in relative gene expression (p-value < 0.05).

	Relative Gene Expression Ratio of Target Gene/β-actin		
Station Code	*cyp1a1*	*gst*	*sod*
6	6.05±0.69	4.66±0.59	2.69±0.36 a, b
10	5.52±0.60	3.85±0.51	3.44±0.31 a, c
30	5.13±0.69	3.51±0.59	2.72±0.36 a, b
103	5.90±0.60	4.34±0.51	2.73±0.31 b, d
22/24	6.21±0.60	4.48±0.51	3.49±0.31 a, b
47/49	5.46±0.60	4.09±0.51	3.46±0.31 a, c

DNA damage in Arctic cod liver cells

The DNA damage in liver cells was found to be minimal with very low levels of DNA single strand breaks. For the six stations, average percent tail DNA in *Boreogadus saida* ranged from 2.86-3.96% with the highest individual cod having only 6.95% tail DNA. The tail length and olive moment were also very low for all stations (Table 6). There were no significant differences in percent tail DNA, tail length, or olive moment between the stations.

Table 6. Results of Comet assay to measure DNA damage in Arctic cod, *Boreogadus saida*. Values represented as means ± SE.

Station Code	Percent Tail DNA	Tail Length	Olive Tail Moment
6	2.86±0.87	2.39 ± 0.82	0.12 ± 0.047
10	3.96±0.68	4.10 ± 0.64	0.20 ± 0.037
22/24	3.68±0.76	3.92 ± 0.71	0.16 ± 0.041
30	3.35±0.87	3.62 ± 0.82	0.14 ± 0.047
47/49	3.01±0.76	2.54 ± 0.71	0.13 ± 0.041
103	3.00±0.76	2.19 ± 0.71	0.11 ± 0.041

Discussion

PAHs in Surface Sediments

Surface and subsurface sediments collected from the Chukchi shelf during the COMIDA 2009 and 2010 field seasons establish a baseline data set to identify future impacts from oil and gas exploration in this region. PAH concentrations in surface sediments (0-1cm) spanning the study area were spatially variable and ranged from 149-2956 ng g^{-1} (Figure 2; see Appendix 1 for detailed concentration information). The mean ± SD concentrations observed here (683 ± 483 ng g^{-1}) are considered at background levels and comparable to total PAH values of 500 ng g^{-1} (Yunker et al., 2011) and 614 ± 611 ng g^{-1} (Naidu et al., 2001) reported in other Arctic sediments. Our results were low, however, relative to total PAH measurements in Camden Bay (961 ± 334 ng/g; Brown et al., 2010), Elson Lagoon (1299 ± 1698 ng/g; Naidu et al., 2003) and Canadian Beaufort shelf sediments (1900 ± 470 ng/g; Yunker et al., 1993).

The PAH concentrations in Chukchi shelf surface sediments comprised both parent and alkyl-substituted PAHs, which represent a mixture of pyrogenic, petrogenic and biogenic sources that are typical of this region. Alkyl-PAHs account for a large fraction of the total (54-93%) and are dominated by methyl-naphthalenes, phenanthrenes and anthracenes, which are likely derived from petroleum inputs throughout the study area. This dominance of alkyl-PAHs appears widespread and has also been also reported in sediments from the Chukchi (Yunker et al., 2011) and Beaufort Sea (Yunker et al., 1993; Yunker et al., 1996) shelves. While it is possible that these petrogenic markers originate in oil from seeps on the Chukchi shelf (Gautier et al., 2009), organic-rich peat, shales and bitumens that cover Alaska's North Slope tundra also provide likely sources and stable matrices for the transport of alkyl-PAHs over long distances via turbidity currents or ice rafting of sediments (Jones and Yu, 2010; Mull, 1995). Similarly, the Mackenzie River is credited with supplying the Beaufort Sea with elevated concentrations of alkyl-PAHs through the delivery of eroded bitumens from within the watershed to the Canadian shelf (Yunker et al., 1993; Yunker et al., 1996).

Additional sources of parent PAHs to the Arctic region include sea-ice (Kawamura et al., 1994; Masclet and Hoyau, 1994) and snow (Welch et al., 1991), which arrive in the Arctic through long-range atmospheric transport of emissions from fossil fuel and biomass burning in temperate

regions and sequestered (Becker et al., 2006; Patton et al., 1991). This is corroborated by the significant amount of pyrogenic PAHs detected in airborne particles from Alert, a long-term air monitoring site on Northern Ellesmere Island, Canada (Becker et al., 2006; Halsall et al., 1997; Patton et al., 1991). While parent PAHs (excluding perylene) in Chukchi shelf surface sediments contribute a mean of 29 ± 6% to the total PAH signal, several studies (Yunker et al., 2002; Yunker and MacDonald, 1995) suggest that atmospheric transport of PAHs have a minor influence on sedimentary PAH distributions in the Arctic Ocean due to their volatility and substantial losses from the particulate phase during snow/ice-melt and passage through the water column. This leaves the resulting sediment composition with a much lower proportion of pyrogenic PAHs than the original combustion sources.

Among the suite of PAHs measured in Chukchi shelf surface sediments, perylene is one of the most abundant structures (47 ± 30 ng g^{-1}) observed. This compound is found naturally in many sedimentary environments and generally thought to originate from organic matter diagenesis (Meyers and Ishiwatari, 1993). Values observed in Chukchi sediments for this biogenic PAH is comparable to the estimate of 60 ng g^{-1} reported by Yunker et al. (2011) in a surface sediment from the same region. Overall, however, total PAH concentrations in surface sediments at 51 of 52 sites on the Chukchi shelf are present at levels considered to be background values for pristine areas (< 1600 ng g^{-1}). The exception is station 26, where total PAHs (2956 ng g^{-1}) are 2 to 20-times greater than at other sites (see Figure 2). This increased value is the result of elevated amounts of alkyl-PAHs, mainly phenanthrenes and naphthalenes. While further study is required, these elevated levels may be derived result from petroleum seeps or may have been impacted by Burger, a former drill site approximately 30 km distant. Alternatively, this station might represent a localized high depositional region for sediment transport from the Alaskan coast.

Compared to overall PAH values, alkane hydrocarbons in surface sediments (0-1cm) spanning the study area varied spatially and showed higher concentrations (1.8 and 17 μg g^{-1}). Average total n-alkane concentrations (7.4 ± 3.2 μg g^{-1}) were comparable to that reported in surface sediments from the Beaufort Sea inner shelf (7.2 ± 5.1μg/g; Naidu et al., 2001), but lower relative to Mackenzie shelf sediments (9.8 ± 1.7 μg/g; Yunker and MacDonald, 1995), which are much closer to direct inputs of terrigenous organic matter. Among subsets of the alkanes, the mean value for the long-chain $C_{23\text{-}33n}$-alkanes (4.8 ± 2.1 μg g^{-1}) was very similar to that measured by Yunker et al. (2011) for select sites on the Chukchi shelf (4.8 μg g^{-1}).

Aliphatic n-alkanes in surface sediments

Though concentrations varied spatially, surface sediments throughout the study area showed the greatest average abundance of C_{27}, C_{29} and C_{31} n-alkanes (0.94, 0.75, 0.85 μg g^{-1}, respectively) and reflected a distinct odd-over-even carbon predominance of higher molecular weight compounds. Higher molecular weight n-alkanes have also been documented in the Beaufort Sea nearshore sediments with a dominance of C_{27} or C_{29} and a well-defined odd-over-even predominance (Wainwright and Humphrey, 1984; Yunker et al., 1993); an indication of terrestrial source material (Bianchi et al., 1989; Kalkreuth et al., 1998; Tuo et al., 2003). The

carbon preference index (CPI), a common indicator of odd-carbon predominance of higher molecular weight n-alkanes, supports the input of terrigenous carbon sources in Chukchi shelf surface sediments. The CPI for Chukchi surface sediments was calculated for the range C_{23}-C_{33} using the following formula from Vonk et al. (2008):

$$CPI = 1/2(\Sigma(X_i + X_{i+2} + \ldots + X_n)/ \Sigma(X_{i-1} + X_{i+1} + \ldots + X_{n-1})) + 1/2(\Sigma(X_i + X_{i+2} + \ldots + X_n) / \Sigma(X_{i+1} + X_{i+3} + \ldots + X_{n+1}))$$

where X is the n-alkane concentration for carbon numbers ranging from *i* to *n*. CPI values for surface sediments from 49 of 52 sites were >2 and indicate inputs from vascular plant sources. Stations 4, 9 and 11 were the exceptions with a CPI values ranging from 0.3 to1.2.

A number of studies (e.g. Belicka et al., 2002; Belicka et al., 2004; Boucsein and Stein, 2000; Goñi et al., 2000; Schubert and Calvert, 2001; Stein et al., 1994; Taylor and Harvey, 2011) have used various suites of organic carbon signatures (i.e. long-chain n-alkanes, fatty acids and alcohols, triterpenoids) to quantify the input and movement of terrestrial carbon to the western Arctic. The Arctic Ocean receives significant inputs of terrigenous material from rivers and coastal erosion and the n-alkane distribution seen in Chukchi shelf surface sediments represent a mixture of terrestrial and petroleum hydrocarbons sources (Figure 3). The sources for such alkanes include major inputs eastward of our study area in the Beaufort Sea where annual sediment loads from the Mackenzie River alone have been estimated at 127 Mt (Macdonald et al., 1998). These inputs are supplemented with terrestrial contributions by rapid erosion (0.5 to 6 m yr^{-1}) of the peat-enriched Alaskan coastline (Are et al., 2008; Macdonald et al., 1998; Solomon, 2005). Sea-ice transport provides one mechanism to link plant alkanes seen in sediments with their terrestrial origin. Sediment resuspension and coastal erosion near the Alaskan shoreline allow sea-ice to entrain significant quantities of terrigenous material during freezing (Eicken et al., 2005). This material is subsequently redistributed to the Chukchi Sea upon thawing, with predicted trajectories of sea-ice movement showing a westward direction (Eicken et al., 2005).

The Yukon River serves as another potential source of terrigenous organic matter and n-alkanes to the Chukchi shelf. The Yukon River discharges annual sediment loads of approximately 60 Mt into Bering Sea (Brabets et al., 2000), which become entrained in the northward flowing Alaskan Coastal Current (Guay and Falkner, 1997). Naidu et al. (1982) traced the movement and subsequent deposition of clay minerals originating from the Yukon River northward through Bering Strait and into the Chukchi Sea, supporting another potential mechanism of the delivery of terrestrial organic carbon to Chukchi shelf sediments.

The distribution of lower molecular weight n-alkanes (C_{15-22}) seen in Chukchi shelf surface sediments likely represent a mixture of both algae/bacteria and petroleum sources (Figure 3). Contributions of C_{17} and C_{19} n-alkanes suggest algal and photosynthetic bacterial activity (Cranwell et al., 1987; Giger et al., 1980; Wakeham, 1990; Xiao et al., 2008), while inputs of even carbon short-chain n-alkanes (C_{16-22}) are indicative of petroleum sources (Boehm et al., 1990; Boehm et al., 1987; Brown et al., 2004; Steinhauer and Boehm, 1992). Similar to PAH distributions, n-alkanes in Chukchi shelf sediments are detected at background levels and represent a combination of natural background biogenic and petrogenic hydrocarbons.

Hydrocarbon concentrations in sediment cores

Total PAH concentrations measured with depth in sediment cores taken from stations 40 and 1016 on the Chukchi shelf decrease downcore and are accompanied by a decrease in the relative proportion of alkyl to parent PAHs (Figure 4; refer to Appendix 3 for detailed concentration information). This trend differs compared to other measurements of PAHs in core sediments taken from the Chukchi shelf, but is consistent with PAH profiles in Arctic basin cores (Yunker et al., 2011). Surface sediments reveal 20 and 4-times higher concentrations of total PAHs (station 40 and 1016, respectively) relative to deeper sediments, which are fairly uniform at depth.

Similarly, n-alkanes from station 40 are nearly 4-times greater in surface versus subsurface sediments; however the relative abundance of perylene increases from 2% at the surface to an average of 29% with depth (Figure 4). While perylene is often found to increase downcore as diagenetic processes primarily occur in deeper, suboxic and anoxic layers (Wakeham and Farrington, 1980), this change between surface and deeper sediment layers is likely the result of mixing due to the abundant benthic communities that inhabit the Chukchi shelf (Grebmeier et al., 1989b; Grebmeier et al., 1988).

In contrast, the sediment core from station 37 reveals a very different PAH profile. PAH abundance peaks at 7 cm and 16 cm (816 ng g^{-1} and 975 ng g^{-1}, respectively) relative to all other core depths, which average 234 $\pm$69 ng g^{-1} (Figure 4). Similarly, an increase in the relative proportion of alkyl-substituted PAHs is observed at 7 cm and 16 cm and represents 75% of the total compared to other sediment depths (57 ± 4%). Perylene contributions also differ at 7 cm and 16 cm with reduced contributions (7% of all PAHs) compared to the remaining core sediments (24 ± 4%). It seems evident that the hydrocarbon signal preserved in deeper Arctic sediments from station 37 reveals changes in the source, transport and deposition of organic matter during two different time periods in geologic history.

Vertical profiles of alkanes exhibit no systematic trends in concentration with core depth at stations 37 and 1016 on the Chukchi shelf with the exception of predominance in odd-carbon higher molecular weight n-alkanes indicative of terrestrial source material (Figure 4). Alkane concentrations peak just below the surface interface (at 1cm) at station 37, which could be the result of organic matter mixing and consolidation by benthic and epibenthic organisms. The core taken from station 1016 is located approximately 40 m from the former drill site, Klondike; and exhibited average values of hydrocarbon concentrations (Figure 4).

Hydrocarbons in *Neptunea heros* foot muscle

Hydrocarbons are often bioaccumulated by benthic invertebrates through desorption from sediments and ingestion of food items. A relationship is often observed between hydrocarbons in benthic marine invertebrates and the sediment in which they reside. In the Chukchi Sea, *Neptunea* of increasing size show a greater relative abundance of alkyl-substituted PAHs in muscle tissues (54-81% of the total), however, all organisms contain substantially lower total PAH concentrations (4.5-11 ng g^{-1} wet wt) than their corresponding surfaces sediment (893 ng

g^{-1}). Total PAH concentrations decrease with animal size and suggest that whelks are able to actively depurate organic contaminants (Figure 5). A similar trend was seen for one clam (*Astarte*) and one worm sample collected at Klondike, a historic drill site on the Chukchi shelf, where tissue samples contained only 5% and 10%, respectively, of the total PAH concentrations seen the surface sediment (Neff et al., 2010). This is further corroborated by low PAH concentrations obtained for polychaete worms in the more contaminated, offshore sediments of Prince William Sound, Alaska that contain PAHs from natural oil seeps, oil from the *Exxon Valdez* oil spill and pyrogenic sources (Neff et al., 2003). PAHs in invertebrate tissues can be attributed to the variety of sources contributing to the background hydrocarbon concentrations in sediments (i.e. coastal erosion, terrestrial plant material, natural hydrocarbon seeps) and their long-range transport and deposition to the Chukchi Sea shelf.

In contrast to PAHs, n-alkanes in *Neptunea* muscle showed a different pattern with higher concentrations and a shift in distribution from short to long-chain n-alkanes relative to surface sediment at station 7 (Figure 5). While long-chain (C_{23}-C_{33}) n-alkanes accounted for 52% of the total in surface sediment, contributions of 73%, 93% and 94% were measured in < 5 cm, 5-8 cm and > 8 cm *Neptunea*, respectively. These data suggest that northern Neptune whelks are selectively depurating lower molecular weight n-alkanes, resulting in elevated concentrations of high molecular weight fractions. Similar observations for other marine invertebrates are common, including early reports by Oudot and Fusey (1981). In this work, the sponges (*Halichondria panacea, Grantia compresa*), anemone (*Actinia equine*), mollusk (*Patella vulgata*) and echinoderm (*Leptosynapta galliennei*) collected from the offshore waters of Brittany, France following the Amoco Cadiz oil spill were all found to remove petrogenic n-alkanes from their tissues after non-selective feeding on petroleum-contaminated sediments (Oudot et al., 1981). Depuration of invertebrates is believed to include a major passive excretion of petroleum residuals and a minor active metabolism of lower molecular weight hydrocarbons (Malins, 1977). Our results suggest that northern Neptune whelks from the Chukchi Sea appear to have the ability to remove petrogenic materials from their muscle tissues at the levels experienced in the Chukchi Sea.

Enzyme activity and DNA damage in Arctic cod

In addition to hydrocarbon burdens of invertebrates, an important goal was to characterize the baseline levels of various petroleum PAH biomarkers in Arctic cod, *Boreogadus saida*. While other studies have examined biomarkers for oil exposure in *B. saida* from the western Arctic (George et al., 1995; Jonsson et al., 2010; Nahrgang et al., 2010a; Nahrgang et al., 2009; Nahrgang et al., 2010b), to our knowledge there had been no analysis conducted on Arctic cod or any other species within the Chukchi Sea. Our measurements of EROD activity levels (1.17-24.24 pmol min^{-1} mg^{-1}protein) in wild *B. saida* were comparable to those reported in *B. saida* from the eastern Arctic at Kongsfjorden, Svalbard (3-33 pmol min^{-1} mg^{-1} protein (avg. 11.9±6.7 pmol min-1 mg-1 protein; Nahrgang et al., 2010a). In addition, the GST activities measured in this study (85.61-717.38 nmol min^{-1} mg^{-1} protein with a median of 228.6 nmol min^{-1} mg^{-1} protein) were similar to previously observed levels in wild caught *B. saida*, from Kongsfjorden, Svalbard that averaged 139 ± 13 nmole min^{-1} mg^{-1} protein (Nahrgang et al., 2010a). The SOD activity levels measured here (1.34-24.65 U mg^{-1} protein) are within the other baseline levels

measured in red-blooded polar fish (0.69-22.17 U mg^{-1} protein; Cassini et al., 1993; Speers-Roesch and Ballantyne, 2005).
Baseline EROD and GST activity levels from wild Arctic cod examined in this study appear very low and indeed are below or comparable to laboratory control studies exposing *B. saida* to benzo(*a*)pyrene, water soluble fraction of crude oil, and dispersed crude oil (George et al., 1995; Jonsson et al., 2010; Nahrgang et al., 2009; Nahrgang et al., 2010b). These studies showed that exposed *B. saida* had significantly higher EROD activities (and GST activities for Nahrgang et al. (2010b) than control fish. Nahrgang et al. (2010b) demonstrated a dose-dependent induction of both EROD and GST activity in *B. saida* exposed to water soluble fraction of crude oil (>25 pmol min^{-1} mg $protein^{-1}$, >700 nmol min^{-1} mg $protein^{-1}$ respectively). Jonsson et al. (2010) observed *B. saida* exposed to a nominal exposure concentration of 1 ppm dispersed crude oil with hepatic microsomal EROD activities ranging from 9.5 - 80.7 pmol min^{-1} mg^{-1} protein. Additionally, Nahrgang et al. (2010b) observed a delay in EROD and GST activity levels returning to baseline following depuration, which indicates that impacts of oil exposure may be observed weeks after an isolated incident. The clear induction of EROD (and to a lesser extent GST) activities in *B. saida* with exposure to both the water soluble fraction and dispersed crude oil makes these markers good tools for monitoring impacts of oil on Arctic cod.

While other studies have examined relative gene expression for cytochrome p4501a1, glutathione *S*-transferase, and Cu/Zn superoxide dismutase in *B. saida* and other cod species (Nahrgang et al., 2009; Nahrgang et al., 2010b; Olsvik et al., 2009), their results could not be directly comparable to this study as they converted ΔCT to either relative gene expression by a standard dilution curve (*geNorm* software) or mean fold change in mRNA expression with a reference site using the $2^{-\Delta\Delta CT}$ method. However, Nahrgang et al. (2010b) suggests that that *cyp1a1* is a promising marker with *gst* as a suitable complement for examining exposure to water soluble fractions of crude oil.

The DNA damage observed in Arctic cod hepatic cells was very low, with all station averages <5% tail DNA. While DNA damage in Arctic cod hepatic cells has not been reported before, the levels observed in this study are comparable to or below the levels found in various cell types isolated from laboratory control fish. For example, in *B. saida* blood cells exhibited levels >9% tail DNA (Nahrgang et al., 2010b) and brown trout (*Salmo trutta*) hepatic cells averaged 3.7-5.0% tail DNA (Mitchelmore and Chipman, 1998a, b). These experiments also showed that the DNA damage assay was responsive to oil or components contained within oil mixtures. Additionally, a dose-dependent increase in hepatic DNA damage has been observed in demersal fish exposed to PAH contaminated sediment (French et al., 1996; Roy et al., 2003). Given the low baseline levels of hepatic DNA damage observed in Arctic cod from the Chukchi and evidence for responses in hepatic and blood cells to PAH exposure, DNA strand breaks should be a useful biomarker to monitor for future impacts of oil drilling. These low baseline biomarker levels observed in Arctic cod correspond to the low levels of PAHs and heavy metals measured within the region of the Chukchi Sea surveyed. For all stations where fish were collected, the levels of heavy metals (Ag, Be, Cd, Cr, Ni, Sb, Zn, Hg, Cu, and Pb) were all at a background level (see Trefry report). For example, Zn levels ranged from 67-87 µg g dry $weight^{-1}$ and Cd levels from 48-76 µg g dry $weight^{-1}$ for stations where trawling occurred. Heavy metal levels observed during the 2009 and 2010 COMIDA cruise were comparable to those measured in the northeastern Chukchi by Naidu et al. (1997) and significantly below threshold levels suggested

to have potential adverse biological effects (Long et al., 1995). Overall, the low levels of PAH, heavy metals, and biological markers within the Chukchi Sea indicate that this ecosystem is still relatively pristine.

When using biomarkers for monitoring the impacts of oil drilling, it is important to be aware of potential confounding factors that can limit the effectiveness and accuracy of the assessment including the reproductive status, sex, age/size, food availability, and origin/mobility of the organisms (Martinez-Gomez et al., 2010; Thain et al., 2008). Reproductive status can greatly influence various biological responses, particularly EROD activity levels, within organisms. EROD activity has been shown to decrease with increasing steroid hormone levels during sexual maturation in fish (Arukwe and Goksoyr, 1997; Stegeman and Hahn, 1994), which is hypothesized to be an adaptive response necessary for active reproductive processes (Arukwe et al., 2008). Therefore, suggested sampling time should occur outside of spawning periods to limit the effects on the responses (Martinez-Gomez et al., 2010; Thain et al., 2008). The influence of reproductive status should be limited for this study as the survey was conducted outside of spawning periods of Arctic cod, which occur between late November and early February (Craig et al., 1982).

While the effects of seasonal reproductive status on biomarker levels were limited, other factors such as size, age, and sex of the Arctic cod could be potential confounding factors in the biomarker results for this study. Differences in biomarker responses can be up to orders of magnitude different between males and females depending on the life stage and reproductive status of the fish (Hop et al., 1995; Stegeman et al., 1982; Thain et al., 2008). For this study, the sex of the Arctic cod was not identified. Therefore, significant differences in biomarker levels potentially attributable to sex cannot be determined, which could be important given the range in size and age of fish from this survey. The total body length of Arctic cod collected (72 mm-140 mm) indicates that the fish were between ages 1 and 3, as compared to previous otolith/body length measurements in Arctic cod of the Chukchi and Beaufort Seas (Barber et al., 1997; Craig et al., 1982). Most male Arctic cod mature at age 2-3 and females at age 3 (Craig et al., 1982). Therefore, this study could be including biomarker results of mature cod with those of juveniles, which could explain some variation in biomarker levels between individuals and stations. Splitting up the data into size classes would have been a possible way to account for this. However, the sample size collected was not large enough to allow this. Therefore, size, age, and sex of the Arctic cod could be potential confounding factors in the biomarker results for this study, and these factors should be addressed in any future studies by identifying sex in individual fish as well as collecting a larger sample size to allow for separation (if needed) of size/age and sex in statistical analysis of biomarkers.

A confounding factor and potential limitation to this study is the movement or migration of the species being examined. Biological effects examined in species that are known to be highly migratory might not be indicative of exposure in areas collected. Even though Arctic cod are the most abundant fish species within the Chukchi Sea, baseline levels examined in this study might not fully reflect the environmental conditions at stations where fish were caught. As the Chukchi Sea is generally covered with ice from November through July (Aagaard, 1984), it is hypothesized that Arctic cod move southward to the northern Bering Sea every fall with the advancing ice edge and back northward into Arctic waters every spring and summer with the

receding ice edge (Lowry and Frost, 1981). However, this migration pattern has never been demonstrated. *B. saida* have been shown to undertake long distance spawning migrations within the Arctic Ocean (Ponomarenko, 1968). The potentially high mobility of Arctic cod could result in misinterpretation of biomarker levels if the organisms were exposed to contaminants during migration.

Overall, this study represents a crucial examination of spatial explicit concentrations of hydrocarbons across the Chukchi shelf and the response of various petroleum PAH markers to native fish. The low levels seen across the stations surveyed indicate that this ecosystem is relatively pristine and uncontaminated. The use of both an array of biomarkers (including genes, enzymes, and DNA damage) in this study as well as chemical analysis of sediment will be helpful for continued environmental monitoring of the Chukchi Sea.

Summary

Chukchi shelf surface sediments contain both parent and alkyl-substituted PAHs that represent a mixture of pyrogenic, petrogenic and biogenic sources at low concentrations. Multiple transport paths are likely responsible for the distribution and concentrations observed.

Aliphatic n-alkane concentrations in Chukchi shelf surface sediments are significantly greater than PAHs and represent a mixture of natural background and petroleum hydrocarbon sources with significant inputs of vascular plant debris from the Alaskan shoreline.

Vertical profiles of PAH and n-alkane concentrations in sediment cores suggest intense mixing by benthic organisms with some indication of diagenetic activity as well as changes in organic matter inputs during geologic history.

The resident northern Neptune whelks (*Neptunea heros*), appears to actively depurate petrogenic materials taken-up during feeding on sediments.

In Arctic cod, *B. saida*, multiple measures of enzymatic activity (CYP1A1, GST, and SOD) were comparable to baseline levels reported in previous field studies. Although some significant differences were seen between specific stations in the Arctic cod examined, there were no overall differences between stations in liver *cyp1a1* and *gst* gene expressions, EROD enzyme activity, and DNA damage with all showing low levels of oxidative stress.

Regulation of Zinc and Biomagnification of Mercury in Biota of the Northeastern Chukchi Sea

Fox, A.L, E.A. Hughes, R.P. Trocine, J.H. Trefry, N.D. McTigue, B.K. Lasorsa, and B. Konar

Austin L. Fox, Emily A. Hughes, Robert P. Trocine and John H. Trefry
Department of Marine and Environmental Systems
Florida Institute of Technology, Melbourne, Florida 32901

Nathan D. McTigue
Marine Science Institute
The University of Texas at Austin, Port Aransas, Texas 78373

Brenda K. Lasorsa
Battelle Marine Science Laboratory
Sequim, Washington 98382

Brenda Konar
School of Fisheries and Ocean Sciences
University of Alaska Fairbanks, Fairbanks, Alaska 99775

Abstract

Mercury contamination in the atmosphere, snow and marine mammals of the Arctic has been a long-term environmental concern and the focus of many investigations. Much less is known about the distribution of Hg in seawater, sediments and organisms from lower trophic levels. Mercury values were obtained during the COMIDA Project for eight different species of organisms (the isopod *Synidotea bicuspida,* amphipod *Ampelisca macrocephala,* clam *Astarte borealis,* whelk *Buccinum sp.,* whelk *Neptunea heros,* crab *Chionoecetes opilio, Arctic cod Boreogadus saida,* whelk *Plicifusus kroeyeri)* from the northeastern Chukchi Sea. Concentrations of total Hg (THg) and monomethyl Hg (MMHg) vary greatly within and among species. The lowest values for THg (30 ng/g dry weight) and % MMHg (32%) were in *A. borealis*; the highest average values for THg (336 ng/g dry weight) and % MMHg (>95%) were in *P. kroeyeri*. Variations in Hg concentrations among and within species followed a complex pattern that could be partly explained by concentrations of sediment Hg and total organic carbon, latitude, bottom water temperature and diet. Zinc, a well regulated metal in marine biota, was used as a reference metal because concentrations varied by <10% within each species over the entire study area. For example, average Zn concentrations of 73 ± 1 μg/g dry weight and 114 ± 2 μg/g dry weight were found for *N. heros* and *C. opilio*, respectively. The main source of Zn was believed to be diet, including ingestion of suspended sediments. Concentrations of both THg and MMHg increased with trophic level as determined using data for $\delta^{15}N$. Mercury was shown to biomagnify following the relationship $\log_{10}[THg] = 0.17(\delta^{15}N) - 0.43$ ($r^2 = 0.83$). Unlike Hg, no biomagnification of Zn was observed.

Introduction

The Chukchi Sea, located between northern Alaska and the Siberian coast, is part of the largest continental shelf in the world. This entire region is currently at a crossroads with respect to global climate change and warming arctic temperatures. As a result, the Chukchi Sea is highly susceptible to the effects of sea-ice retreat, northward migration of species, coastal erosion and offshore energy development (Grebmeier et al., 2010).

Mercury is a persistent, toxic heavy metal that is introduced to the Arctic mainly through atmospheric deposition (Ariya et al., 2004). The Arctic can be affected by long range atmospheric transport of Hg from anthropogenic sources such as coal burning in Asia (Jaeger et al., 2009; Pacyna, 2005). Transport of anthropogenic Hg to the Arctic perpetuates concerns about observed biomagnification of Hg in marine mammals.

The more toxic monomethyl mercury (MMHg) is produced from inorganic Hg in sediments by bacteria (Oremland et al., 1991) and then bioaccumulated by biota through their diet. In the Arctic, MMHg biomagnifies from lower trophic level organisms such as plankton, bivalves and crabs to high trophic level organisms such as sea birds, marine mammals and humans (Jaeger et al., 2009). For example, polar bears from Canada had a maximum total Hg (THg) concentration in hair of 23,900 ng/g (Cardona-Marek et al., 2009) relative to 20 ng/g for plankton (Neff et al., 2010).

Mercury concentrations can be variable within species due to environmental parameters such as total organic carbon (TOC) and Hg in sediments (Chen et al., 2009; Hammerschmidt et al., 2004). Conditions where organic carbon is present at 1 to 5% and temperatures are >2^{o}C favor methylation of Hg (Knoblauch and Jorgensen, 1999; Mason and Lawrence, 1999). In contrast with Hg, some metals, such as Zn, are accumulated and regulated by biota because they are essential elements (Neff, 2002a). Regulated metals are not greatly affected by water or sediment concentrations and are more dependent on accumulation from food sources (Willis and Sunda, 1984; Young, 1977).

In this report, we contrast the distribution and behavior of Zn with Hg in biota from the northeastern Chukchi Sea with the following objectives: (1) establish a baseline for concentrations of Zn, THg and MMHg in biota, (2) determine possible sources of these trace metals to the biota, and (3) determine the extent that regulation and/or biomagnification of these metals occur in Chukchi Sea biota.

Methods

Study Area

The COMIDA study area is located in the northeastern Chukchi Sea (Figure 1). This region contains numerous leased blocks where future offshore oil development may occur. Concentrations of THg and MMHg in biota, sediments and water were determined to help

establish baseline values and to aid in assessing any future natural or anthropogenic inputs that could alter body burdens of Hg in biota from this environment. Our study focuses on selected benthic organisms; however, this ecosystem supports a much broader array of organisms including seabirds, polar bears, walrus, seals and bowhead whales. Potential sources of Hg to the Chukchi Sea include: atmospheric transport (Fitzgerald et al., 1998), river runoff (Leitch et al., 2007), inputs from local on-shore mines, introduction of Hg from the Pacific Ocean via the Bering Sea, as well as very localized occurrences of Hg from ancient formation cuttings discharged during exploratory drilling (Neff et al., 2010). Sources of Zn to the Chukchi Sea include inputs from the Bering Sea, river runoff and possibly dust from ores at offshore loading zones (Station 104 in Figure 1).

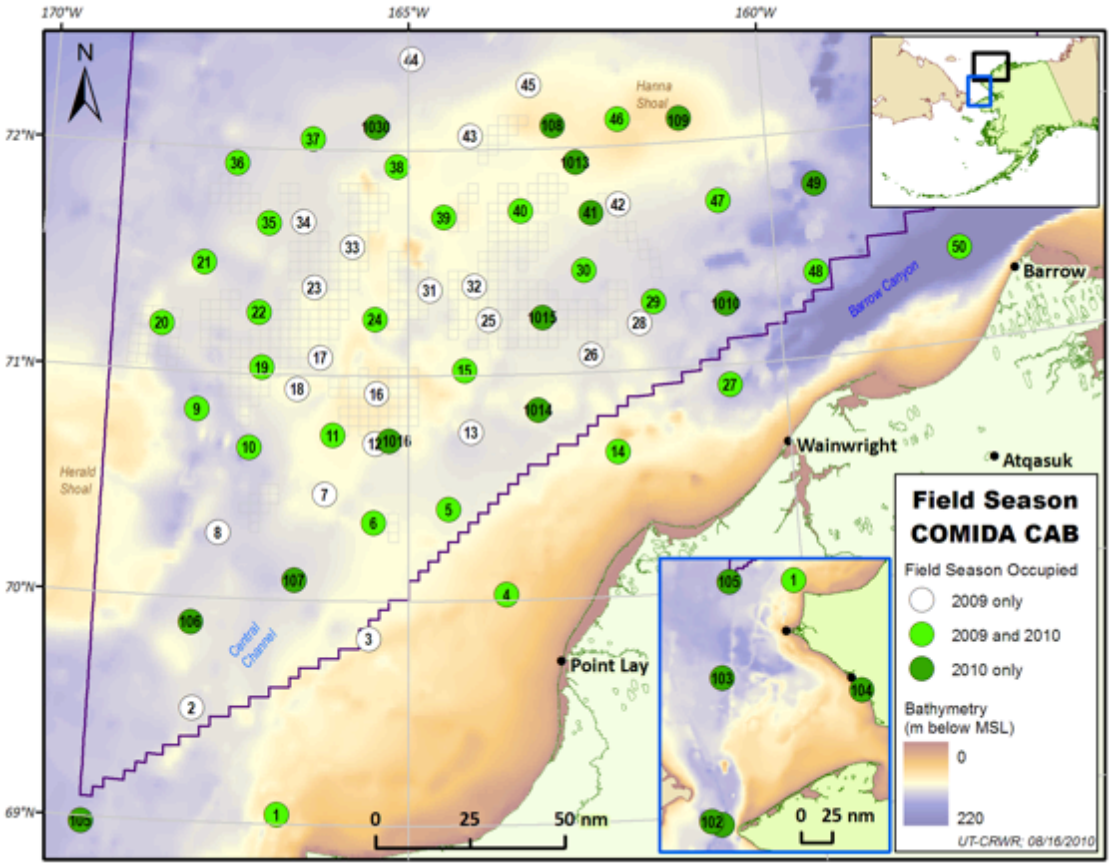

Figure 1. Map showing sample stations for 2009 and 2010 field surveys for the COMIDA Project. Lower inset map shows stations to the south of those shown on the larger map and upper inset map shows location of study area off the northwest coast of Alaska.

Sample Collection

Sampling took place during July and August of 2009 and 2010 using the research vessels *R/V Alpha Helix* and *R/V Moana Wave*, respectively. Sample stations were selected using a probability based grid for each section of the study area and randomly choosing locations within each grid cell. Sampling was conducted at 49 stations in 2009 and 44 stations in 2010 (Figure 1).

Biota were collected using an epibenthic trawl with a 3-m diameter beam trawl, 7-mm mesh and a 4-mm mesh cod end. An area of ~260 m^2 was sampled by trawling for 2 to 5 minutes along the bottom while the vessel moved at 1 to 1.5 knots. A 3-m pipe, positioned forward of the net, held the mouth of the net open for a swath of 2.3 m and vertical opening of 1.2 m. Eight different species were collected for metal analysis (Table 1). Organisms from each trawl were sorted, counted and measured to the nearest mm. Gastropods were de-shelled and the foot muscle dissected for analysis, fish were filleted for muscle tissue, crabs were dissected for their leg muscle tissue, bivalves were removed from their shells to obtain soft tissue and amphipods and isopods were analyzed whole. All samples were dissected using stainless steel blades, washed with deionized water and kept frozen until analysis.

Table 1. Taxonomic and common names for biota collected at specified stations (see map in Figure 1) from the northeastern Chukchi Sea plus abbreviations (Code).

Taxonomic Name	**Common Name**	**Code**	**Stations**
Synidotea bicuspida	Isopod	IS	47, 49, BF3A*, BF3B*, BF4*
Ampelisca macrocephala	Amphipod	AM	46, 108, 1010
Astarte borealis	Astarte (clam)	AS	15, 41, 47, 49, 103, HR6
Buccinum sp.	Buccinum (whelk)	BC	11, 19, 22, 105, 1016
Neptunea heros	Hero (whelk)	NP	1, 5, 9, 11, 15, 19, 20, 40, 41, 49, 105, 107, 108, 1016
Chionoecetes opilio	Snow crab	SC	10, 11, 19, 21, 22, 35, 38, 40, 48, 49, 108, 1016
Boreogadus saida	Arctic cod	AC	4, 9, 22, 24, 38, 40, 41, 47, 49, 103, 109, 1013
Plicifusus kroeyeri	Plicifusus (whelk)	PL	9, 47, 49, 107

* Samples from adjacent Beaufort Sea.

Sediments were collected using a pre-cleaned, double van Veen grab that obtained two side-by-side samples, each with a surface area of 0.1 m^2 and a depth of ~15 cm. Samples (top 1 cm and subsurface layers) were carefully collected from one of the two grabs and placed in separate containers for metals, organic carbon and grain size. The companion grab was used for sampling benthic biota. A HAPS corer (Kanneworff and Nicolaisen, 1973) with a 30-cm acrylic liner was deployed at numerous sites and a Benthos gravity core with a 1-m long barrel, 7.5-cm diameter plastic liner, and no core catcher, was deployed into stiff sediments at several sites. Core samples were split into 1- to 2-cm thick layers aboard ship under clean conditions. All sediments samples, except those for grain size analysis, were frozen shipboard.

Water column samples were collected at 12 stations in 2009 and 16 stations in 2010 using a peristaltic pump with acid washed tubing attached to a Teflon weight and equipped with a HOBO pressure and temperature sensor. Samples were collected in 5-L, acid-washed, low density polyethylene bottles after the first 15 L of water were discarded.

Laboratory Methods

Tissue samples were homogenized, completely digested in Fisher Trace Metal Grade HNO_3 and H_2O_2 and analyzed for Zn and Fe using a Perkin-Elmer Model 4000 atomic absorption spectrometer and for THg using a Laboratory Data Control cold vapor atomic absorption spectrometer according to established laboratory methods (Trefry et al., 2003). Standard reference material (SRM) #1566b (oyster tissue) from the National Institute of Standards and Technology (NIST) was processed with each batch of samples; all values were within the 95% confidence intervals for the certified values (Table 2). Analytical precision was better than 6% for all analytes. Method detection limits (MDL) were as follows: Fe (2.5 μg/g), THg (1.0 ng/g) and Zn (0.4 μg/g). All metal concentrations in tissue samples were reported on a dry weight basis.

Monomethyl mercury in biota was isolated by acid bromide/methylene chloride extraction and the aqueous phase was analyzed by ethylation, isothermal GC separation, and cold vapor atomic fluorescence spectrometry (CVAFS) detection following methods from Bloom and Crecelius (1983) and Bloom (1989). Analytic precision averaged 6% and the MDL was 2 ng/g. Concentrations of inorganic mercury were calculated by subtracting MMHg from THg.

Table 2. Results for analysis of Zn, THg and Fe (Mean ± SE) in SRM 1566b (Oyster Tissue) and MMHg in SRM DORM-2 (Dogfish Muscle). *n* represents the number of standards analyzed.

Element	***N***	**Certified Value**	**This Study**
Zn	13	1424 ± 46 μg/g	1430 ± 18 μg/g
THg	17	37 ± 1.3 ng/g	36.3 ± 3.2 ng/g
Fe	13	205.8 ± 6.8 μg/g	206.0 ± 1.1 μg/g
MMHg	5	0.355 ± 0.056 μg/g	0.326 ± 0.012 μg/g

Sediment samples for metal analysis were homogenized and a wet portion was set aside for THg analysis. The remaining sample was freeze-dried to provide percent water content and dry sediment for acid digestion. A separate, wet sediment sample from each location was set aside for grain size analysis. Sediment samples for metal analysis, except THg, were homogenized, completely digested in Fisher Trace Metal Grade HF, HNO_3 and $HClO_4$ and analyzed for Zn and Fe using a Perkin-Elmer Model 4000 atomic absorption spectrometer according to established laboratory methods (Trefry et al., 2003). The SRM #2709 from the NIST was processed with each batch of samples; all values were within the 95% confidence intervals for certified values. Analytical precision was as follows: 1% for Fe and 2% for Zn.

Sediment digestion for THg was carried out using high-purity HNO_3 and H_2SO_4. The sediment Certified Reference Material (CRM) MESS-3 from the National Research Council of Canada (NRC) was digested and analyzed with each group of sediment samples. All values were within the 95% confidence interval for the CRM, precision was 4% and the MDL was 1 ng/g.

Sediment TOC concentrations were determined by treating freeze-dried sediment with 10% phosphoric acid to remove inorganic carbon, followed by high-temperature combustion and infra-red CO_2 quantification. Grain size analyses of surface sediment samples were carried out using the classic method by Folk (1974) that includes a combination of wet sieving and pipette techniques.

Zinc concentrations in seawater were determined on extracts obtained using a reductive precipitation procedure by Nakashima et al. (1988). In this procedure, ultra-high purity Pd, Fe and $NaBH_4$ were used to precipitate metals that were then collected by filtration and redissolved in ultra-high purity HNO_3 and HCl. This procedure was carried out using 400-mL portions of seawater and a seawater CRM (CASS-3 issued by the NRC) with final extract volumes of ~4mL (by weighing and determining density), resulting in a ~100-fold increase in concentrations of the seawater metals prior to analysis. The extracts were transferred to acid-washed 7.5-mL LDPE bottles, sealed, labeled and then stored in a plastic bag until analysis by inductively coupled plasma mass spectrometry.

Total dissolved Hg concentrations in seawater were determined by treating water samples in the field with bromine monochloride solution (Szakacs et al., 1980) to oxidize organic ligands and preserve the samples until analysis. Total dissolved Hg concentrations were determined by CVAFS using a Brooks-Rand Model III Mercury System following preconcentration by gold amalgamation. Concentrations of dissolved MMHg followed extraction and then the method described for the biota.

Stable Isotope Analysis

Samples for stable isotope analysis were treated with acid, rinsed with distilled water to remove carbonates and then dried at 60°C. All samples were analyzed for $\delta^{15}N$ using a Finnegan MAT Delta Plus mass spectrometer. Results are expressed in standard δ notation relative to atmospheric nitrogen. Precision was ± 0.2‰.

Results and Discussion

Values for Zn, Fe, THg, MMHg and $\delta^{15}N$ were determined for the eight species of organisms collected from the COMIDA study area in 2010 (Table 3). The main focus of this report is on THg and MMHg in biota because of a keen interest and concern for Hg contamination in the Arctic (Ariya et al., 2004; Campbell et al., 2005). Results for Zn are included here to demonstrate the distribution of a metal that is essential for life and well regulated by marine biota. Iron concentrations are used to help assess possible inclusion of sediment associated Zn and Hg in biota samples. Data for Zn and Hg in water and sediments are introduced and discussed as needed to help explain distribution patterns for Zn and Hg in biota.

Table 3. Mean (±SE), *n*, range and median values for Zn, Fe, THg, MMHg, inorganic Hg, water content, $\delta^{15}N$ and trophic level in biota collected in the northeastern Chukchi Sea during 2010.

Organism	Zn (µg/g d.w.)	*N*	Range	Median	Fe (µg/g d.w.)	*n*	Range	Median
IS	88 ± 9	5	57-107	94	5420 ± 708	5	3210-7,190	5,810
AM	207 ± 31	6	132-285	206	346 ± 102	6	130-772	291
AS	93 ± 9	6	76-124	83	1460 ± 336	6	651-2,720	1,150
BC	70 ± 1	6	67-75	69	65 ± 12	5	44-111	55
NP	73 ± 1	33	65-92	72	102 ± 6	34	33-198	98
SC	114 ± 2	25	107-138	114	36 ± 5	25	12-96	31
AC	63 ± 4	12	48-94	60	6.0 ± 0.4	12	4-8	6
PL	67 ± 2	4	64-73	65	62 ± 4	3	53-67	65

Organism	THg (ng/g d.w.)	*N*	Range	Median	MMHg (ng/g d.w.)	*n*	Range	Median
IS	37 ± 8	6	10-61	38	30.0 ± 5.1	5	12.3-40.6	32.4
AM	32 ± 7	4	14-50	33	32.0 ± 5.4	4	19.5-43.8	32.7
AS	32 ± 2	7	25-42	33	9.9 ± 0.9	6	7.6-13.3	9.7
BC	249 ± 60	8	50-532	197	171 ± 12	2	159-183	171
NP	189 ± 25	36	30-677	155	172 ± 26	19	25.0-525	143
SC	134 ± 11	25	46-288	123	105 ± 8.5	25	34.0-197	101
AC	130 ± 24	14	12-276	137	122 ± 27	11	22.0-228	146
PL	336 ± 166	3	69-641	298	641	1		

Organism	Inorganic Hg (ng/g d.w.)	*N*	Range	Median	Water Content (%)	*n*	Range	Median
IS	5.3 ± 2.5	2	2.8-7.7	5.3	73.3 ± 0.3	3	72.8-73.6	73.6
AM	12 ± 3	4	4.2-17	13	76.1 ± 0.7	6	73.2-77.6	76.5
AS	22 ± 3	5	15-33	21	80.5 ± 0.6	6	78.0-82.6	80.5
BC	26 ± 11	2	15-36	26	77.4 ± 0.4	9	76.3-78.8	77.1
NP	11 ± 5	19	0-47	14	76.5 ± 0.3	45	71.1-81.8	76.3
SC	30 ± 4	25	4.4-91	23	87.3 ± 0.3	25	84.6-89.6	87.2
AC	16 ± 5	11	0-48	7.1	85.0 ± 0.5	12	83.5-87.7	84.3
PL	-	-	-	-	78.0 ± 0.7	4	76.3-79.4	78.1

Organism	$\delta^{15}N$ (‰)	*n*	Range	Median	Trophic Level*
IS	11.3 ± 0.3	3	10.7-11.8	11.4	3.3
AM	11.7 ± 1.2	3	10.4-14.0	10.7	3.4
AS	12.1 ± 0.4	5	11.3-13.3	11.4	3.5
BC	14.3 ± 0.2	2	14.2-14.5	14.3	4.2
NP	15.0 ± 0.3	4	14.5-15.7	15.0	4.4
SC	15.0 ± 0.2	8	14.4-15.8	15.0	4.4
AC	15.9 ± 0.3	2	15.7-16.2	15.9	4.6
PL	17.4 ± 0.3	4	16.8-18.1	17.4	5.1

*Trophic Level = 2 + [(δ^{15}Nconsumer-δ^{15}Nbase)/Δ δ^{15}N] (modified after (Lavoie et al., 2010).

Zinc

Average Zn concentrations in biota ranged from 50 to 114 µg/g, excluding the amphipod *A. macrocephala* with an average Zn value of 207 µg/g (Table 3, Figure 1). Concentrations of Zn within each of the eight species analyzed were uniform throughout the study area (Figure 2). Relative standard errors [RSE = (Standard Error / Mean) x 100] for Zn in each organism had an overall average of 6% and ranged from 1.3% in *N. heros* to 15% in *A. macrocephala*.

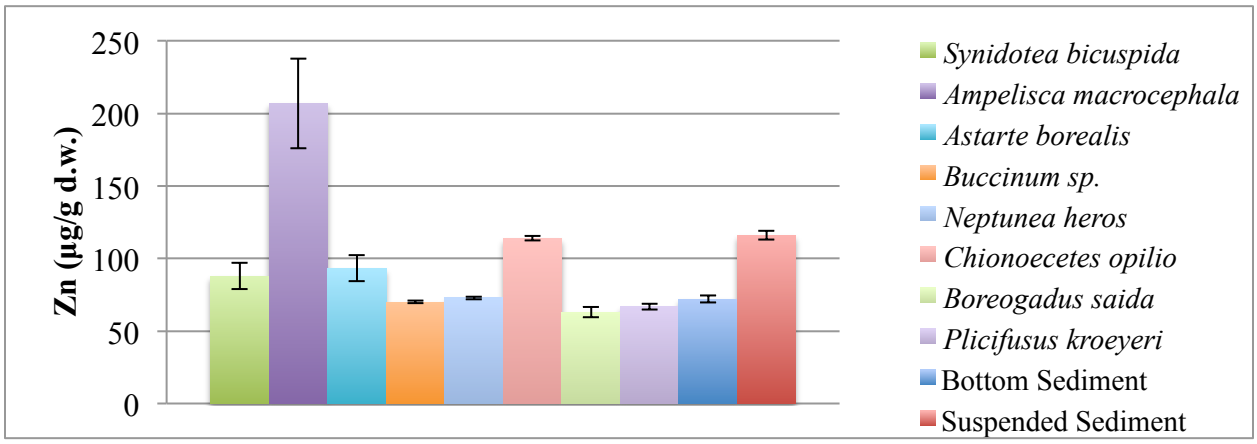

Figure 2. Concentrations of Zn (mean ± SE in µg/g) in biota, bottom sediment and suspended sediment collected in 2010 from the northeastern Chukchi Sea.

Zinc concentrations in *Neptunea heros*, *Chionoecetes opilio*, and *Boreogadus saida*, the three most sampled organisms (Table 1), were uniform throughout the northeastern Chukchi Sea with RSE values equal to 1.3, 1.5 and 5.8%, respectively. For example, average Zn concentrations for *N. heros* from the northeast stations (40, 41, 49, 108, all north of 71.5°N) and southwest stations (1, 105, 107, all south of 70.1°N) were 71 ± 1 µg/g and 72 ± 2 µg/g, respectively (Figure 3). Likewise, Zn concentrations for *C. opilio* from the northeast stations (38, 40, 48, 49, 108) and central stations (10, 11, 19, 1016) were 115 ± 3 µg/g and 121 ± 3 µg/g, respectively (Figure 3), despite differences in bottom water temperature, sediment TOC and grain size. Such uniform Zn values are commonly observed in marine biota because Zn is used as a micronutrient and as a cofactor in nearly 300 enzymes; this requirement leads to strong regulation of Zn within organisms (Neff, 2002a).

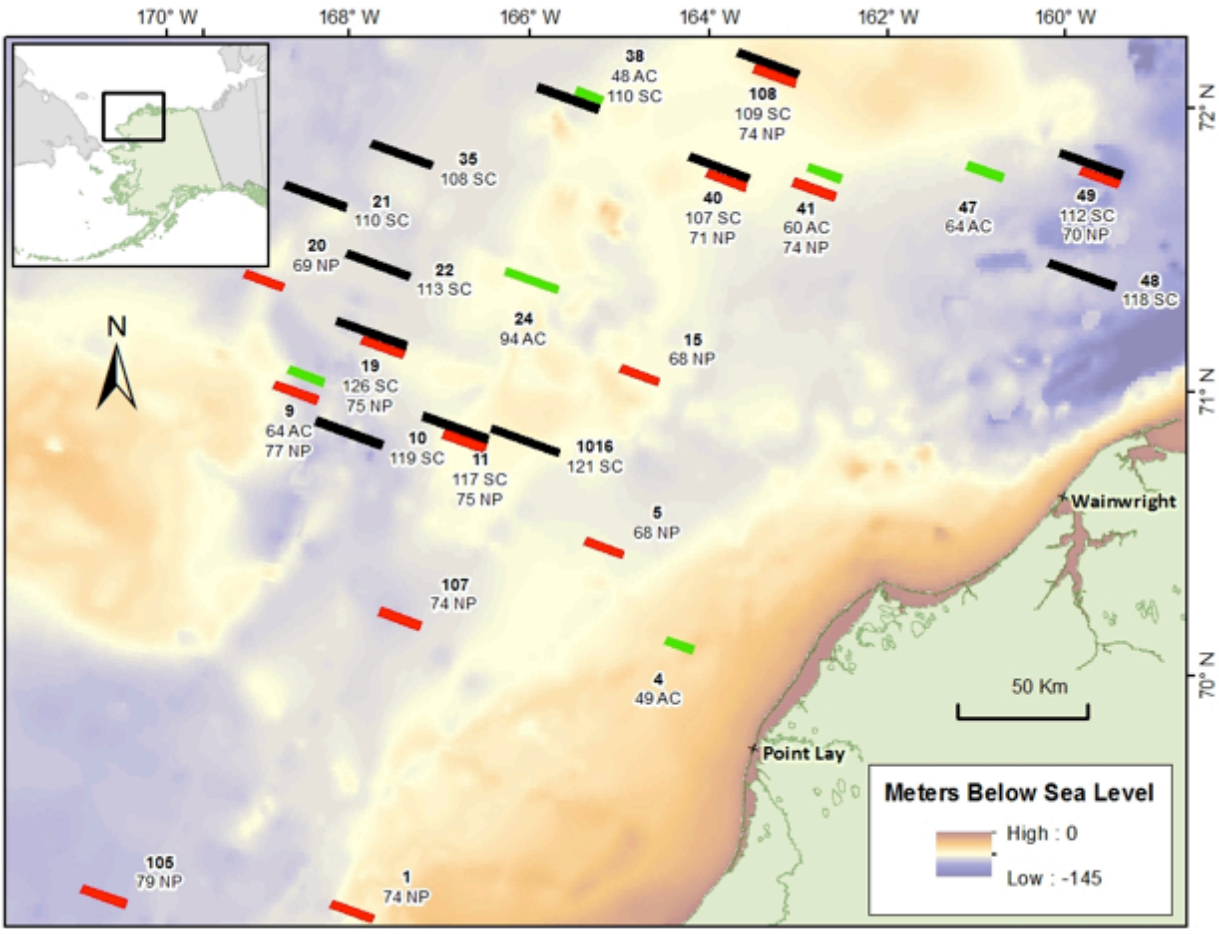

Figure 3. Mean Zn concentrations (µg/g) in *Neptunea heros* (NP, red bars), *Chionocetes opilio* (SC, black bars) and *Boreogadus saida* (AC, green bars) at stations where these biota were collected.

White and Rainbow (1982) showed that marine invertebrates exposed to a range of dissolved Zn concentrations were still able to regulate the metal in tissues at seawater Zn concentrations of up to 100 µg/L. Chan (1988) found that with increasing concentrations of dissolved Zn in water, concentrations of Zn in tissues of the green mussel *P. viridis* remained constant around 100 µg/g when exposed to dissolved Zn concentrations from 178 to 362 µg/L over 7 days.

Data were obtained for Zn in water, suspended particles and sediments (Table 4). Despite similarities in Zn values between tissue and sediments, Zn values in tissues did not seem to be directly related to the presence of residual sediment in the biota sample. Concentrations of Zn and Fe in bottom sediment from the Chukchi Sea averaged 72 µg/g and 30,000 µg/g, respectively. When sediment is present in a biota sample, concentrations of Fe can be greatly elevated. In some sediment-dwelling organisms, such as isopods (*S. bicuspida*), concentrations of other metals also can be enhanced by the presence of sediment. Tissue samples from this study contained Fe at concentrations that ranged from 3.8 µg/g (*B. saida*) to 7,190 µg/g (*S. bicuspida*) (Table 3). However, for 5 of the 8 species analyzed, Fe concentrations were less than

~100 µg/g (Table 3 and Figure 4) and most likely this Fe was in tissues and not associated with sediment that was included in the organism, as discussed below.

Table 4. Mean ± SE for concentrations of Zn in bottom water, suspended sediments, bottom sediments and all biota collected from the northeastern Chukchi Sea.

	Units	*n*	Zn	Range	Median
Bottom Water	µg/L	14	0.46 ± 0.05	0.16-0.84	0.37
Suspended Sediment	µg/g	88	116 ± 28	18-320	131
Bottom Sediment	µg/g	89	72 ± 22	8-108	76
Biota	µg/g	97	93 ±4	48-285	76

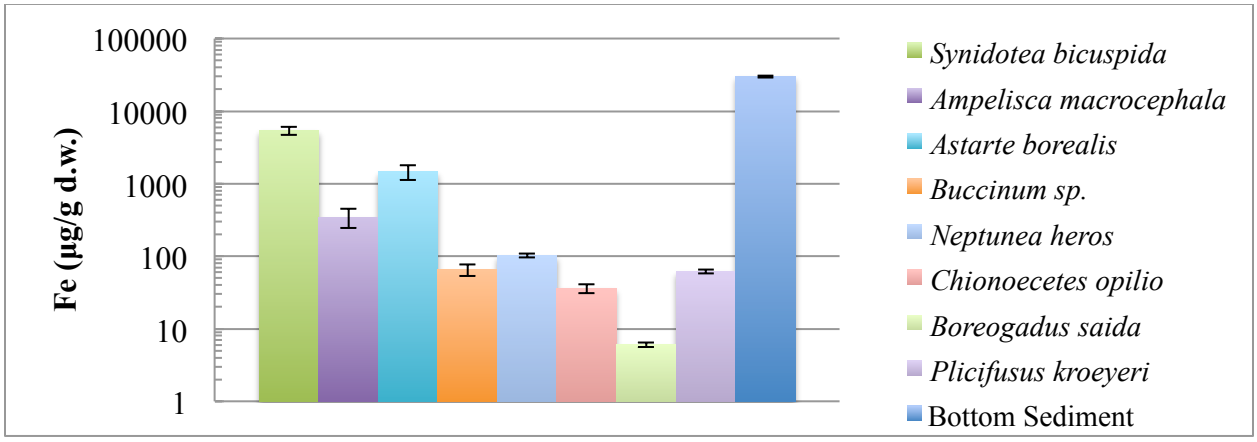

Figure 4. Concentrations of Fe (mean ± SE in µg/g) in biota and bottom sediment collected in 2010 from the northeastern Chukchi Sea.

The amount of Zn in a biota sample that may be due to sediment present in the sample can be calculated using Fe concentrations in the sediment and biota. For example, if we assume that essentially all of the Fe at 7,190 µg/g in a *S. bicuspida* sample (the most extreme case) was from sediment, then the corresponding amount of Zn associated with that sediment would be 17 µg/g [(7,190/30,000) x 79 µg/g] or 24% of the measured total Zn value of 79 µg/g for *S. bicuspida*. A more typical Fe concentration in biota samples from this study was ~70 µg/g; if that Fe were completely associated with sediment, an unlikely assumption, then the corresponding amount of sediment-associated Zn would be 0.17 µg/g, relative to the total tissue Zn concentrations of 48 to 285 µg/g. Overall, an average of < 2% of the Zn content of all samples of *A. macrocephala*, *Buccinum sp.*, *N. heros*, *C. opilio*, *B. saida*, and *P. kroeyeri* can be linked with the presence of sediment in the tissue sample. For *A. borealis* and *S. bicuspida,* maxima of 9 and 24% and averages of 5 and 17%, respectively, of the total Zn may be associated with sediment inclusion in the sample.

Concentrations of metals in biota are often compared with values for water and sediment by calculating enrichment factors (EF in Eq. 1 and 2) to evaluate the potential or likelihood for metal accumulation from environmental sources or to assess the possibility that enhanced metal concentrations may be due to sediment metal contamination. As previously mentioned, dissolved Zn concentrations averaged 0.46 ± 0.05 μg/L in bottom water over the entire study area. Therefore, Zn in *C. opilio* and *N. heros* was enriched relative to the bottom water by factors of 36,000 and 40,000, respectively. Enrichment factors of this magnitude suggest that water is not likely a direct source for Zn in these organisms because such a high degree of bioaccumulation from water has not been observed. For example, Milner (1982) reported that <10% of the total Zn in the marine fish *Pleuronectes platessa* was accumulated from the water column. Wang and Ke (2002) concluded that <10% of intake of Zn in gastropods was directly from the water and that the main source of Zn was food.

$$\mathrm{EF}_{\mathrm{H_2O}} = \frac{\text{μg metal/g biota wet weight}}{\text{μg metal/g water}} \quad (1)$$

$$\mathrm{EF}_{\mathrm{SED}} = \frac{\text{μg metal/g biota dry weight}}{\text{μg metal/g sediment}} \quad (2)$$

Enrichment factors for Zn in *C. opilio* and *N. heros,* relative to surface sediments, were 1.6 ± 0.1 and 1.2 ± 0.1, respectively. Previous investigators have used sediment EFs to show that sediments may be a source of Zn to biota (Thomann et al., 1995; Trefry et al., 1996). Although concentrations of Zn in the surface sediments showed a large variation across the COMIDA study area (8 to 108 μg/g), a weak relationship between concentrations of Zn in sediments and biota was found ($r^2 < 0.27$). Furthermore, all of the sediment Zn in the Chukchi Sea was at natural levels with no anthropogenic inputs.

Previous investigators have shown that the dominant source of Zn to biota is food. The bioaccumulation efficiency of Zn to marine organisms from food depends on the quantity and quality of the food. Organisms that have a diet consisting of plankton and algae do not bioaccumulate Zn as efficiently as organisms that prey on those with higher trophic levels, as described below (Neff, 2002a). Average Zn concentrations in plankton from the Chukchi Sea were reported to be ~20 μg/g (Neff et al., 2010). Willis and Sunda (1984), using ^{65}Zn in a laboratory setting, showed that up to 82% of accumulated Zn in marine fishes was directly from their diet. A study on dogwhelk using ^{65}Zn-labeled seawater and prey demonstrated that the main source of Zn to the tissues was from diet rather than from dissolved Zn (Young, 1977). Another study using the crab *Pugetta producta* showed that more than 65% of the Zn accumulated directly from macroalgal food (Boothe and Knauer, 1972).

Detrital feeders in the northeastern Chukchi Sea also have access to Zn through abundant amounts of suspended matter (detritus) in the bottom water that averaged ~2 mg/L. Suspended particles contained an average of 8% organic carbon and were >8 times richer in organic carbon than the surface sediments. These particles also were richer in Zn (by 60%) than surface sediments (Table 4). A large fraction of the metal enrichment in the suspended particles was

associated with the organic matter and would be more easily bioaccumulated than metals in bottom sediments.

Mercury

Introduction

Concentrations of THg and MMHg in organisms from the northeastern Chukchi Sea varied greatly among species and location. Total Hg concentrations in biota, ranged from 10 to 677 ng/g. Concentrations of Hg in each of the eight species were highly variable throughout the study area (Figure 5 and Table 3). The RSE for THg averaged 21% and ranged from 8% in *A. borealis* to 49% in *P. kroeyeri* (Table 3).

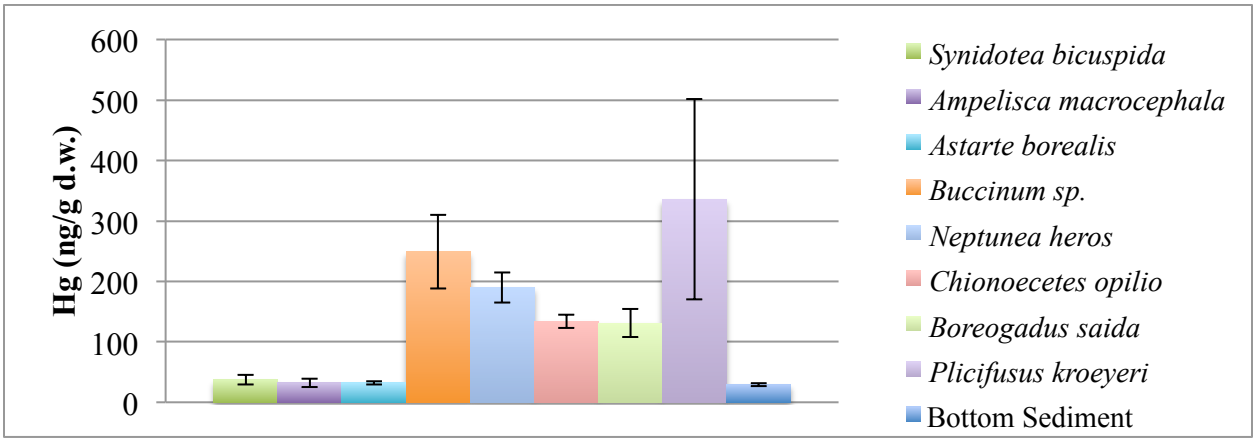

Figure 5. Concentrations of THg (mean ± SE in ng/g) in biota and sediment collected in 2010 from the northeastern Chukchi Sea.

As previously mentioned, observed variations of Hg concentrations in biota, may be partly explained using data for sediment Hg and TOC, temperature, latitude and food sources. Latitude is listed as a possible variable because atmospheric deposition of Hg has been reported to decrease by 3 fold from latitudes south of 69°N to ~80°N (Outridge et al., 2008). The distribution of these potentially important variables is discussed briefly before more detailed assessment of trends in Hg values for biota.

Dissolved Hg

Concentrations of total dissolved Hg (THg_d), determined for 51 samples from 13 stations in the COMIDA study area, showed a pattern that seems to be partly linked to primary productivity, and thus, may be a factor in explaining trends in the biota Hg data. Values for THg_d averaged 0.53 ± 0.29 ng/L (2.6 ± 1.4 pM) and ranged from 0.16 to 1.40 ng/L (0.8 to 7.0 pM). No other THg_d data for the Chukchi Sea have been identified to date; however, Outridge et al. (2008) used an average value of 0.15 ng/L with a range of 0.11 to 0.38 ng/L for the Bering Strait, based on results from Laurier et al. (2004). Our concentrations for the northeastern Chukchi Sea are

consistent with results from other studies that range from 0.2 to 1.0 ng/L (1 to 5 pM) in the open ocean and 0.2 to 2.0 ng/L (1 to 10 pM) in coastal seawater (Fitzgerald et al., 2007).

Vertical profiles for THg_d from the COMIDA study showed three different types of trends. At stations 20 (Figure 6a), 49, and 103, maximum values were found at the surface; these concentrations decreased across the pycnocline and were more uniform in bottom water. In contrast, at stations 10 (Figure 6b), 14 and 37, the lowest THg_d was at the surface, with an increase below the pycnocline, to a maximum concentration in the near bottom water. A third trend was identified at stations 107 (Figure 6c), and 46 where a mid-depth maximum was observed, between the pycnocline and the chlorophyll *a* maximum, as discussed below.

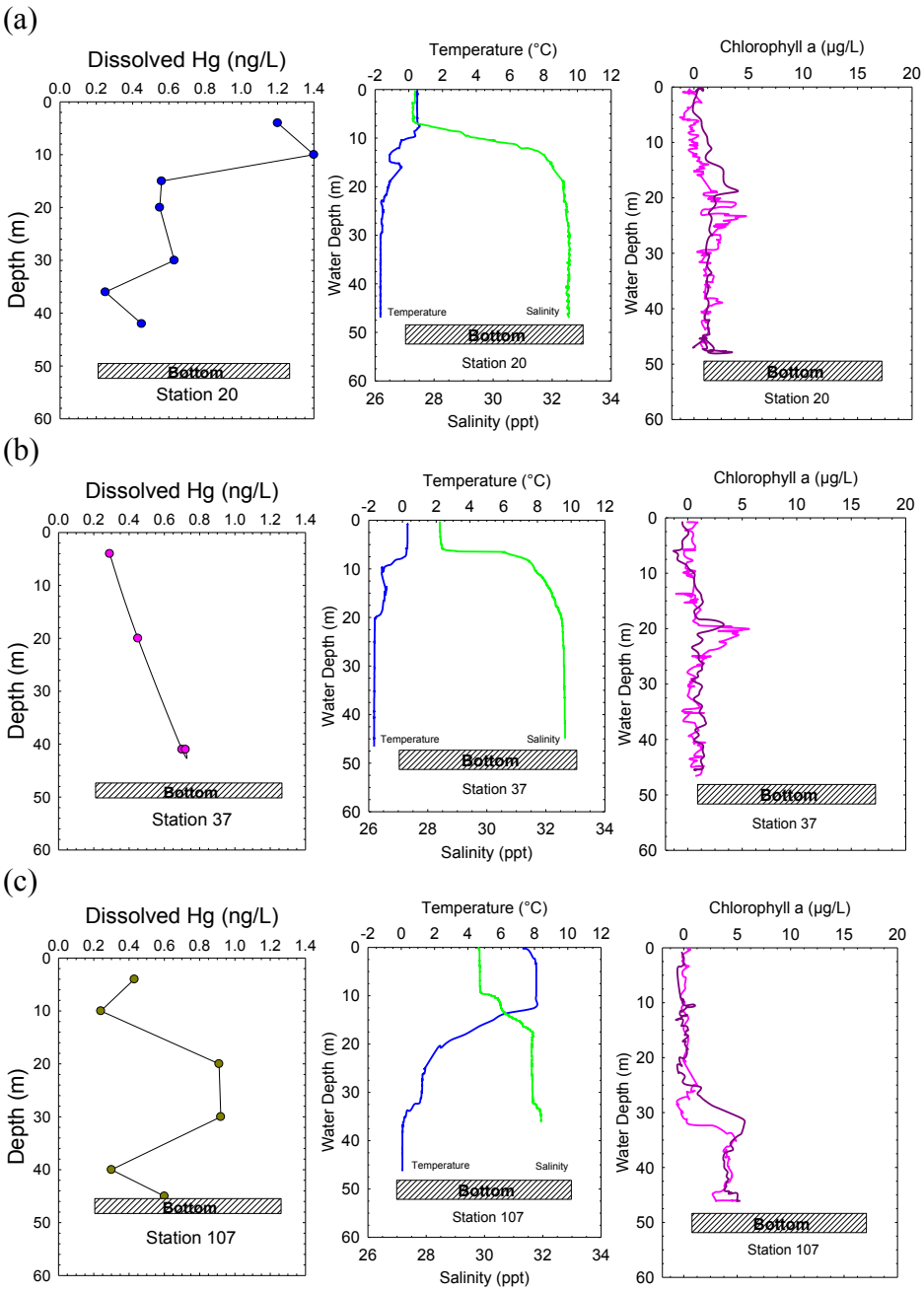

Figure 6. Vertical profiles for total dissolved Hg, salinity, temperature and chlorophyll *a* for COMIDA 2010 (a) station 20, (b) station 37 and (c) station 107.

Distribution patterns for THg_d in the water column are often influenced by biological and photochemical reactions (Fitzgerald et al., 2007). Increases in algal biomass during a bloom can be accompanied by simultaneous depletions of Hg and some other metals from the dissolved phase (Luengen and Flegal, 2009).

The diverse trends observed for vertical profiles of Hg in the Chukchi Sea, may be related to primary productivity in the water column. For example, Luengen and Flegal (2009) reported that

an algal bloom significantly depleted dissolved MMHg concentrations in San Francisco Bay, followed by a significant increase in dissolved MMHg as the bloom decayed. In our study, when concentrations of THg_d were >0.8 ng/L (>4 pM, Figure 7), values for chlorophyll *a* were low (<1.5 µg/g). In contrast, at lower concentrations of THg_d (<0.5 ng/L, <2.5 pM), higher values of chlorophyll *a* (>1.5 µg/g) were found in some samples, most likely due to the uptake of Hg by primary producers (Figure 7). However, at stations where bloom conditions were not occurring, as determined by low concentrations of chlorophyll *a*, low values of THg_d were sometimes observed. We believe this to be the result of post bloom conditions when concentrations of both dissolved Hg and chlorophyll *a* were depleted. Finally, no high THg_d concentrations >0.8 ng/L (>4 pM) were observed during conditions of high chlorophyll *a* (>1.5 µg/g). This final observation is most likely due to depletion of THg_d during bloom conditions. This generally indirect relationship between THg_d and chlorophyll *a* is a dynamic process that removes Hg from the water column; however, the stages of chlorophyll *a* production, removal of dissolved Hg, and breakdown of chlorophyll *a* are not clearly distinguishable without continuous, long-term measurements.

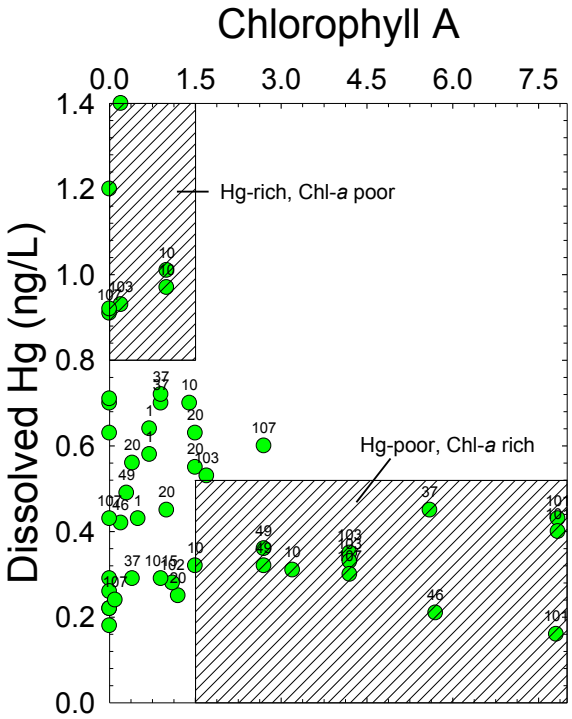

Figure 7. Chlorophyll *a* versus THg_d from fourteen stations sampled in the COMIDA 2010 study area. Shaded boxes identify water samples with Hg-rich and chlorophyll *a*-poor conditions and Hg-poor and chlorophyll *a*-rich conditions. Numbers identify sample stations.

Superimposed on the relationship between chlorophyll *a* and dissolved Hg was a geographic distribution pattern. The lowest concentrations of THg_d were found in the Bering Strait with an average for stations 101 and 102 of 0.30 ng/L (1.5 pM). In contrast, the highest concentrations of THg_d (0.64 ± 0.33 ng/L) were at stations 107, 10 and 20 in the western portion of the study area.

The lowest concentrations north of the Bering Strait (0.37 ± 0.17 ng/L) were at stations 46, 49 and 1015 in the north.

Mercury in Sediment

As previously mentioned, Hg concentrations were determined for surface sediments (0 to 1 cm) in the COMIDA study area during 2009 (n = 49) and 2010 (n = 40); 25 of the sites were sampled during both years (see Figure 1). Mercury data also were obtained for sediment cores collected during 2009 (5 cores, 77 samples) and 2010 (4 cores, 41 samples).

Sediment mercury concentrations in the study area ranged from 5 to 90 ng/g. The lowest mercury values were found in coarse-grained sediments and the highest concentrations were found offshore in silt- and clay-rich sediments. Mercury and other trace metals generally correlated well with grain size and thus were very low in Hg-poor, coarse-grained quartz sand or carbonate shell material and much higher in Hg-rich, fine-grained aluminosilicates.

Concentrations of Hg were normalized to Al (i.e., use of Hg/Al ratios) as a proxy for the Hg controlling variables of grain size, organic carbon content and mineralogy. Aluminum is rarely introduced by anthropogenic activities and is present at percent levels in most sediment relative to part per billion (ng/g) levels for Hg. In the ideal case, a strong linear correlation is observed between concentrations of Hg and Al. Significant, positive deviations from this linear trend, can be used to identify metal contamination (Figure 8). Surface sediment at station 1016 contained Hg at a concentration that was above background based upon the Hg/Al graph (Figure 8). Station 1016 was located in the Klondike lease area near an exploratory drill site that was occupied during 1989. Mercury is an impurity of variable concentrations in barite ($BaSO_4$) that is used as a weighting agent in drilling mud. Barite was identified as an important source of Hg in sediment containing drilling mud in the Gulf of Mexico (Trefry et al., 2007). Sediment from station 1016 with an elevated Hg value contained Ba at a background value of 606 µg/g, far below values in excess of 100,000 µg/g found in the Gulf of Mexico. Therefore, the Hg anomaly is most likely due to the presence of a metal sulfide present in the formation cuttings. Slightly enhanced Hg concentrations also were found at station 13 that is located ~15 km east of station 1016 (Figure 8) where the Ba concentration was 570 µg/g. No evidence was found that drilling mud and cuttings were a significant source of Hg in the COMIDA CAB area.

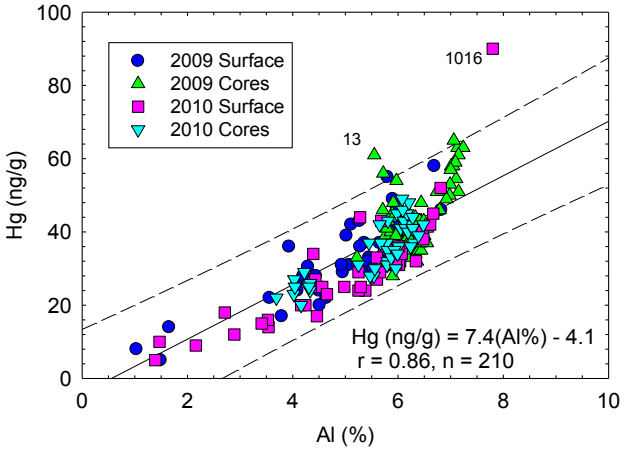

Figure 8. Mercury versus sediment aluminum from surface sediments and cores from 2009 and 2010. Solid line and equation are from a linear regression calculation, dashed lines show 99% prediction interval, *r* is the correlation coefficient and *n* is the number of samples.

Sediment profiles for Hg/Al show relatively uniform distribution with an average Hg/Al ratio of 6.0 ± 1.3 ng/% for all COMIDA sediments. The two highest Hg/Al ratios in the sediment cores are for the top 0.5 cm at station 6 (Hg/Al = 9.8) and in the 0.5 to 1 cm layer at station 13 (Hg/Al = 11.0) (Figure 9). These anomalies may represent recent anthropogenic inputs.

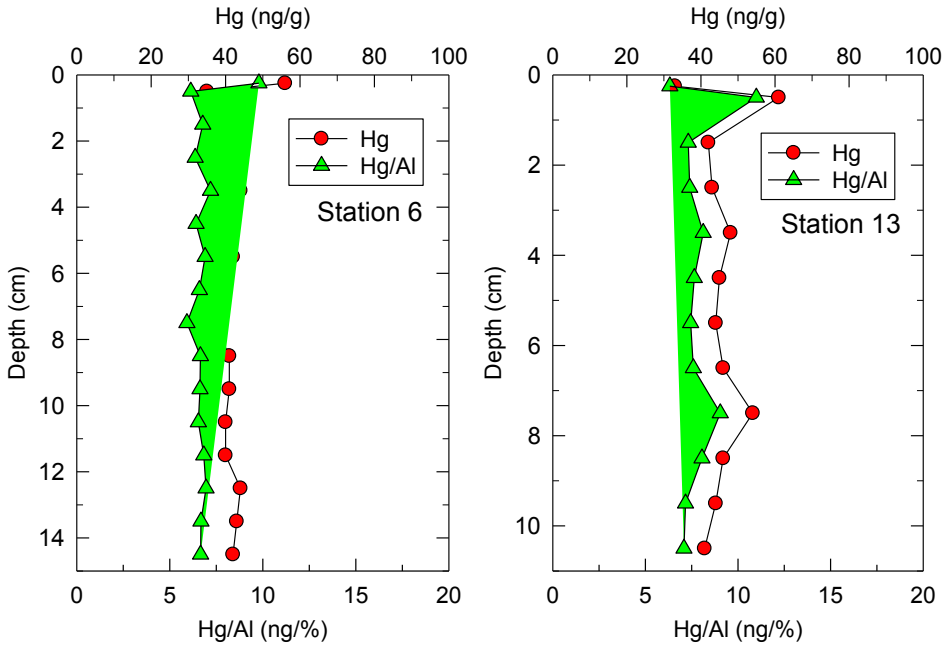

Figure 9. Sediment cores from stations 6 and 13. Hg concentrations in ng/g (red circles), Hg/Al ratio (green triangles).

A large range in concentrations of sediment TOC was found throughout the study area with TOC values that ranged from 0.03% to 1.79%. The lowest TOC was in coarse grained sediment at station 46 and the highest concentrations were found offshore at station 50 in silt and clay rich sediments.

Metals have a high affinity for organic carbon. This high affinity can limit bioavailability due to Hg retention by TOC (Chen et al., 2009). Furthermore, as the TOC content of sediments increases, production of H_2S increases and precipitation of HgS inhibits methylation of Hg. Previous investigations have shown that sulfide inhibition of Hg methylation occurs as TOC values approach 3% (Trefry et al., 2007). Chukchi Sea sediments were low in TOC with an average of less than 1%. These measurements are consistent with those reported in the Chukchi Sea by Feder et al. (1994). In sediments with low TOC, a more likely occurrence is a decline in methylation rates as a result of limited organic material available to methylating bacteria (Mason and Lawrence, 1999).

Temperature also is important in regulating the rate of Hg methylation and the bioavailability of sediment Hg to biota. Bacteria from arctic sediments have been shown to live at -1.8°C, the freezing point of seawater; however, the greatest rates of methylation and sulfate reduction occurred at higher temperatures between 2 and 9°C in the Arctic. Within the range of temperatures measured in the Chukchi Sea, sulfate reduction rates were shown to increase exponentially with temperature (Knoblauch and Jorgensen, 1999). Temperatures in bottom water of the study area ranged from 7.4°C (station 104) to -1.7°C (station 36). Bottom water temperatures were highest in the southernmost stations, located within the Bering Strait and the southern Chukchi Sea. In contrast the lowest temperatures were north of 71.5^{o}N, underlying Chukchi Winter Water.

The distribution of benthic organisms within the study area is believed to be regulated by several environmental parameters, including depth, sediment grain size, TOC, TON, and temperature. Not all organisms shared the same distribution patterns; for example, some organisms such as snow crabs and shrimp were relatively uniform throughout the study area. In contrast, organisms such as sand dollars and brittle stars were found in some regions but not others. The variability in organism distribution was believed to influence predator-prey interactions and may have resulted in dietary shifts between regions. Such shifts impact food web structure and are believed to be important in regulating organism THg and MMHg concentrations.

Hg in Isopods (Synidotea bicuspida), Amphipods (Ampelisca macrocephala) and Clams (Astarte borealis)

Concentrations of THg in *S. bicuspida*, *A. macrocephala*, and *A. borealis* ranged from 10 to 61 ng/g (Table 3). The grand average THg concentration for all three organisms was relatively uniform at 33 ± 4 ng/g. In contrast with values for THg, average concentrations of MMHg in *S. bicuspida* and *A. macrocephala* (31 ± 5 ng/g) were 3 times greater than found for *A. borealis* (10 ± 1 ng/g; Table 3). Thus, *A. borealis* contained only 32% MMHg (as a percent of THg) relative to 73% MMHg in *S. bicuspida* and *A. macrocephala*. Mason and Lawrence (1999) also found

that concentrations of MMHg were much higher in isopods (48 ± 15 ng/g) from Baltimore Harbor than in clams (4 ± 3 ng/g).

Concentrations of THg in *S. bicuspida*, *A. macrocephala*, and *A. borealis*, were similar to those for sediments, and thus, the EF values for these organisms were 0.87 ± 0.15, 1.8 ± 1.1 and 1.2 ± 0.17, respectively. These low EF values may be observed because, these organisms are deposit and filter feeders at the sediment-water interface. By feeding at the sediment-water interface, Mason and Lawrence (1999) suggest that these organisms may provide a reasonable estimate of the bioavailability of Hg in sediment to other biota.

Using the same type of calculation as demonstrated above for Zn, the amount of Hg that may have been introduced by any trace amounts of sediment incorporated into the biota sample was calculated. Like Zn, an average of < 2% of the Hg content of *A. macrocephala*, *Buccinum sp.*, *N. heros*, *C. opilio*, *B. saida*, and *P. kroeyeri* could be linked with the presence of sediment in the tissue samples. In the extreme case of 7,190 ng/g Fe in *S. Bicuspida*, assuming that all Fe in the sample was the result of sediment, then 24% of the THg in the sample was due to trace amount of sediment. (Fe at 7,190 µg/g; [(7,190/30,000) x 10ng/g = 2.4 ng/g = 24%]) For *A. borealis* and *S. bicuspida* maxima of 9 and 24% and averages of 4 and 17%, respectively, of the total Hg may be associated with sediment inclusion in the sample. Thus, the relationship between sediment Hg and organism Hg is the result of the bioaccumulation and incorporation into tissues of available Hg and MMHg from the sediments and food sources, not by inclusion of sediments in biota samples.

The concentrations of Hg and TOC in sediments have been reported to strongly influence Hg availability to biota (Muhaya et al., 1997). In order to bioaccumulate, Hg must first be methylated (Jaeger et al., 2009); this process is mediated by several environmental factors. Bacterial activity is reduced at low TOC values and at low temperature (Kostka et al., 1999; Mason and Lawrence, 1999; Knoblauch and Jorgensen, 1999). As a result, in sediments with limited TOC or low temperature, the rate of Hg methylation may be low. Low methylation rates in the sediments can lead to low MMHg concentrations in resident biota. The amount of MMHg in sediments has been shown to increase with increasing TOC up to values of 2 to 3% (Trefry et al., 2007). Production of H_2S at TOC values >2 to 5% inhibit MMHg formation (Mason and Lawrence, 1999; Trefry et al., 2007). Sediment in the COMIDA study averaged less than 1% TOC with a maximum of 1.79% at station 50. Under conditions observed in the Chukchi Sea, H_2S production was unlikely. Methylation in this study was not limited by high TOC and accompanying metal-sulfide precipitation; instead, methylation was more likely limited by the low organic carbon content of the sediment. Organisms living in sediments with low TOC (<0.75%), were generally lower in THg and MMHg concentrations than organisms in sediments with high TOC (>1% for this study).

Hg in Snow Crab (Chionoecetes opilio)

Concentrations of Hg in *C. opilio* ranged from 46 to 228 ng/g with an average of 134 ± 11 ng/g. Specimens of *C. opilio* were separated into two size classes: 3-6 cm and 6-8 cm. At stations where both size classes were sampled, the THg concentrations in the larger *C. opilio* size class

(6-8 cm) were typically higher than for the smaller size class (3-6 cm). For example, at station 22, the average THg concentration for the larger *C. opilio* size class was 176 ng/g relative to the lower 125 ng/g for the smaller *C. opilio* size class. This size-Hg trend was generally observed throughout the COMIDA study area and the grand average THg concentration of 157±26 for *C. opilio* 6-8cm was higher than that of the grand average THg concentration, 125 ± 6 ng/g for *C. opilio* 3-6cm. To account for the effects of size on concentrations of THg and MMHg in *C. opilio*, only the most abundant size class (3-6 cm) was used to assess geographic variations in Hg concentrations. Samples from the 3-6 cm size class were available at all 12 stations where *C. opilio* were sampled.

The lowest concentrations of Hg in the 3-6 cm size class of *C. opilio*, 95 ± 15 ng/g, were found in the northern area underlying Chukchi Winter Water. In contrast, the highest Hg concentrations in the 3-6 cm size class of 172 ± 20 ng/g were found in the southern area underlying Alaskan Coastal Water, with intermediate values (119 ± 17 ng/g) to the west, underlying Bering Sea Water. To help explain this general geographic distribution, the bioavailability of sediment Hg was considered. The lowest concentration of THg in *C. opilio* was at station 49 in the northeast portion of the study area. At this station, the bottom water temperature (-1.63˚C) was believed to limit the rate of Hg methylation by bacteria in the sediments. In contrast, the highest concentration of THg in *C. opilio* was found for station 19 where the bottom water temperature of 0.26˚C was believed to be more favorable for bacterial methylation.

Hg in gastropods (Buccinum sp., Neptunea heros, Plicifusus kroeyeri)

Gastropods in this study had the highest and most variable Hg concentrations of the organisms analyzed. Of the three species, *Neptunea heros* was most abundant and had the most variable Hg concentrations. *N. heros* specimens were separated into six, 2-cm size classes that ranged from 2-14 cm; the most abundant size class was 4-6 cm. At stations where three or more size classes were collected, the THg concentrations were plotted versus size (e.g., Figure 10). Size correlated well with THg concentrations ($r^2 = 0.58$) for *N. heros* at individual stations. To account for the effects of size on THg and MMHg concentrations in *N. heros*, only the most abundant size class (4 to 6 cm) was used to assess geographic variations in Hg concentrations. Samples from the 4-6 cm size class were available at 12 of 14 stations where *N. heros* were sampled.

The highest concentration of THg for *N. heros* in the 4-6 cm size class was 401 ng/g at station 105. At this station, the sediment Hg and TOC concentrations were 38 ng/g and 1.38%, respectively. The bottom water temperature at this station was 2.3°C. These conditions were likely more favorable for Hg methylation and probably contributed to the high MMHg concentrations observed in *N. heros* from station 105. In contrast, the lowest THg concentrations for *N. heros* in the 4-6 cm size class were at stations 40 (76 ng/g THg) and 108 (68 ng/g THg); both sites are located north of 71.5˚N. Concentrations of sediment Hg, TOC, as well as bottom water temperatures, at stations 40 and 108 were below average. At station 108, sediment THg was 15 ng/g, TOC was 0.41% and bottom water temperature was -1.6°C. Values for THg, TOC and temperature were similar at station 40. Low values for THg, TOC, and temperature at stations 40 and 108 were not conducive to Hg methylation and may help explain the low THg and MMHg values.

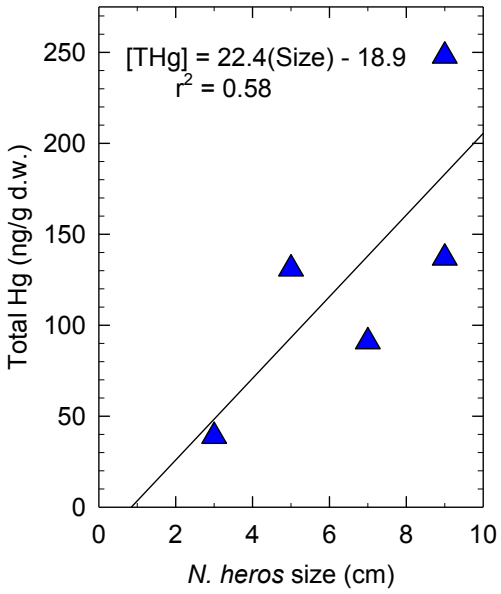

Figure 10. Concentrations of THg (ng/g) in *N. heros* versus size in cm based, 2-cm size intervals.

Hg in Arctic Cod (Boreogadus saida).

Concentrations of THg in *B. saida* ranged from 12 to 276 ng/g. The average concentration of THg of *B. saida* in this study, 130 ± 24 ng/g, was between values of 190 ± 30 and 85 ± 5 ng/g reported in past studies (Atwell et al., 1998; Stern and Macdonald, 2005). In this study, *B. saida* also were separated into different size classes; there were 5, 2-cm size classes ranging from 6 to 18 cm in length. There were no stations where more than 2 size classes of *B. saida* were sampled; therefore no size-THg relationship could be reliably determined.

The variability in THg concentrations for *B. saida* in this study was best related to sediment THg concentrations ($r^2 = 0.47$). Concentrations of MMHg ranged from 22 to 228 ng/g with an average of 122 ± 27.4. The percent MMHg averaged 91 ± 2%, consistent with Bloom (1992) who reported that the %MMHg in *B. saida* was >90%.

Biomagnification

The trophic levels of the eight species analyzed in this study were determined using average $\delta^{15}N$ concentrations. Values for $\delta^{15}N$ in biota from this study ranged from 10.7 in *A. macrocephala* to 17.4 in *P. kroeyeri*. Trophic level values in Table 3 were calculated for organisms based on $\delta^{15}N$ values using equation 3 from Lavoie et al., (2010). Fractionation for $\delta^{15}N$ is 3.4‰ per trophic level based on results from Hobson and Welch, (1992). Distinct trophic levels are not commonly observed in marine benthic communities due to omnivorous species interactions (Hobson and

Welch, 1992; Atwell et al., 1998). Instead, in marine benthic systems, small changes in $\delta^{15}N$ are often observed.

$$TL_{consumer} = 2 + [(\delta^{15}N_{consumer} - \delta^{15}N_{base})/\Delta\ \delta^{15}N] \quad (3)$$

The lowest trophic level calculated for the organisms in this study was 3.3 for *S. bicuspida* and the highest trophic level was 5.1 for *P. kroeyeri*. *Echinarachnius parma,* a sand dollar with a $\delta^{15}N$ value of 6.9, was used as the base of the food web and set as trophic level 2. Fractionation of $\delta^{15}N$ between a known trophic step was calculated using POM/phytoplankton with a fractionation of 3.4‰.

Trace metals, with the notable exception of Hg, generally do not biomagnify (Neff 2001; Campbell et al., 2005). In this study, using average Zn concentrations and $\delta^{15}N$ values from the organisms sampled, no biomagnification of Zn was observed in the Chukchi Sea ($r^2 = 0.01$).

Concentrations of THg in organisms correlated positively with $\delta^{15}N$ showing Hg biomagnification ($r^2 = 0.83$, Figure 11). A biomagnification power of 0.17 was determined for Hg from the slope of the linear regression between Log_{10}[THg] versus $\delta^{15}N$ (Figure 11). Atwell et al. (1998) reported a biomagnification power of 0.2 for benthic organisms in Lancaster Sound; Lavoie et al. (2010) reported a biomagnification power of 0.17 from the Gulf of St. Lawrence.

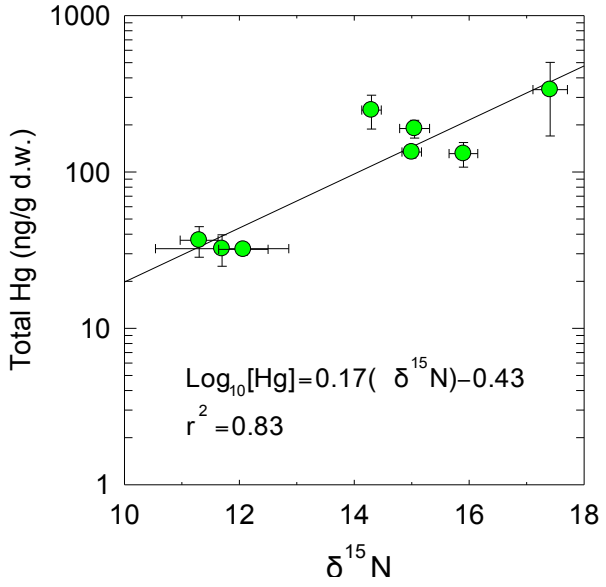

Figure 11. Mean (±SE) THg concentrations (ng/g) versus $\delta^{15}N$.

A higher biomagnification power of 0.23 was determined for MMHg relative to THg (Figure 12). Lavoie et al. (2010) also observed a biomagnification power of 0.23 for MMHg. The inorganic component of the THg was relatively uniform for each species (Table 3) and did not show any biomagnification. The difference in the slopes between THg versus $\delta^{15}N$ (0.17) and

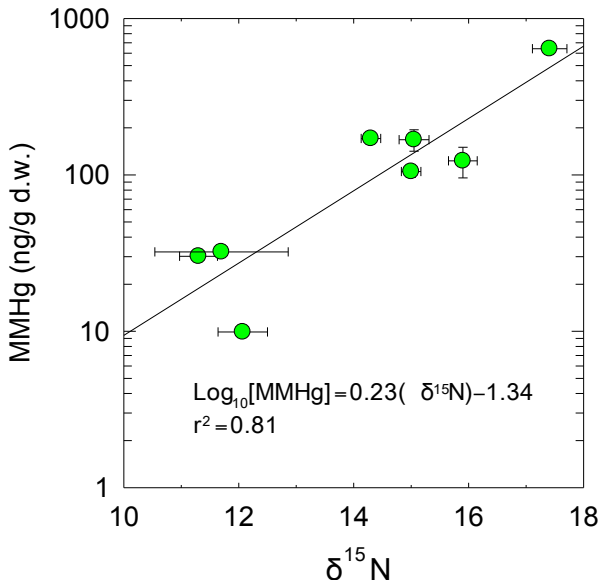

Figure 12. Mean (±SE) MMHg concentrations (ng/g) versus $\delta^{15}N$.

MMHg versus $\delta^{15}N$ (0.23) are due to the inorganic form of Hg included in THg that does not biomagnify. The highest percent inorganic Hg (68%) was found for *A. borealis* compared to the lowest percent inorganic Hg (7%) was found for *N. heros*.

The %MMHg was uniform for each species over a wide range of THg concentrations. For example, a > 20 fold range in THg concentrations were found for a *N. heros*; however, the %MMHg was 93 ± 3%. Similarly, *C. opilio* THg concentrations ranged from 46 to 288 ng/g whereas the %MMHg was 78 ± 2%. The strong correlations between THg and MMHg in *N. heros* and *C. opilio* were $r^2 = 0.97$ and $r^2 = 0.92$, respectively (Figure 13).

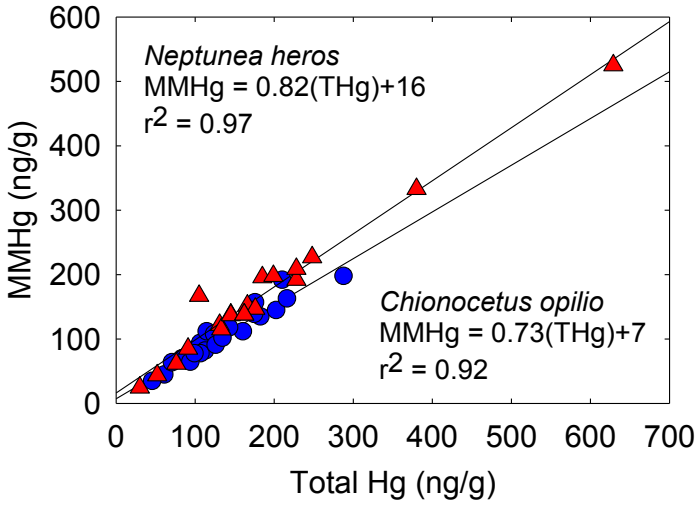

Figure 13. Concentrations of MMHg versus THg in *N. heros* (red triangles) and *C. opilio* (blue circles) from the COMIDA study area.

Summary and Conclusions

Mercury values were obtained during the COMIDA Project for eight different species of organisms (*Synidotea bicuspida, Ampelisca macrocephala, Astarte borealis, Buccinum sp., Neptunea heros, Chionoecetes opilio, Boreogadus saida, Plicifusus kroeyeri)* from the northeastern Chukchi Sea. Concentrations of total Hg and MMHg varied greatly within and among species. The lowest values for THg (30 ng/g) and % MMHg (32%) were in *A. borealis* and the highest average values for THg (336 ng/g) and % MMHg (>95%) were in *P. kroeyeri*. Variations in Hg concentrations among and within species followed a complex pattern that could be partly explained by concentrations of sediment Hg and total organic carbon, latitude, bottom water temperature and diet. Concentrations of both THg and MMHg increased with trophic level as determined using data for $\delta^{15}N$. Mercury was shown to biomagnify following the relationship log THg = $0.17(\delta^{15}N) - 0.43$ ($r^2 = 0.83$). Values for %MMHg were uniform (81 ± 2%) among species despite the large range in Hg concentrations.

Acknowledgements

We thank the Bureau of Ocean Energy Management (BOEM), U.S. Department of Interior for funding to support this study. We especially thank Dick Prentki of BOEM for his interest and support in studies of metals in biota. We thank Ken Dunton and Jackie Grebmeier for serving as Chief Scientists and for helping to create a strong collegial environment at sea. We are grateful for the hard work of Captain John Seville and his crews on the *R/V Alpha Helix* and *R/V Moana Wave*. We thoroughly enjoyed our sea voyages with all the COMIDA scientists and thank them for all of their hard work and dedication to the COMIDA CAB project. We thank Cory Hodes of Florida Institute of Technology for help in data processing and graphing.

Sedimentation Rate Analyses

Cooper, L.W. and J.M. Grebmeier

Lee W. Cooper and Jacqueline M. Grebmeier
Chesapeake Biological Laboratory,
University of Maryland, Solomons, MD 20688

Abstract

Short (~20 cm) sediment cores were collected throughout the COMIDA continental shelf study area, particularly during the 2009 field effort. Gamma spectroscopy of ten cores was completed, with the goal of characterizing sedimentation rates and patterns. All cores collected show significant bioturbation by organisms, but some sedimentation patterns are preserved in many cores. For example, a bomb fallout radionuclide that adheres to clay particles, ^{137}Cs, is found throughout the sediments declining to levels at or near detection limits (~0.1 mBq cm^{-2}) at 20 cm depth. Relatively low activities are typically found in surface sediments, increasing to maxima of 2 mBq cm^{-2} that are observed at approximately 8-10 or 10-12 cm depth. The preservation in many cores of muted activity maxima suggest that while bioturbation is a dominant process in turning over the sediments, some sedimentation patterns are preserved. Given the 45 years between the time of the bomb fallout peak deposition of ^{137}Cs (~1963-64) and the collection of cores in 2009, preservation of peak activities from 1963-4 at 10-12 cm implies an averaged sedimentation rate of ~0.25 cm year $^{-1}$ without accounting for the impacts of bioturbation. As of this date, two cores with strong declines in ^{137}Cs with depth have also been evaluated for sedimentation using the ^{210}Pb method. Excess (above background) ^{210}Pb activities derived from atmospheric deposition were estimated and declines in excess ^{210}Pb were plotted against depth. The slope of the decline on a logarithmic scale was divided by the appropriate activity decay coefficient for ^{210}Pb to produce a sedimentation rate that is independent of the ^{137}Cs sedimentation estimate. Both of these cores, which were collected on the outer continental shelf boundary of the study area showed lower sedimentation rates using the ^{210}Pb methodology, 0.14 cm year^{-1} and 0.02 cm year $^{-1}$.

Introduction

Sedimentation rate determinations have value for characterizing the cycling of anthropogenic as well as natural materials within marine sediments. Because of high biological activity and related bioturbation in many Chukchi shelf sediments (Grebmeier et al., 2006b), this study of sedimentation rates was initiated with the understanding that precise sedimentation determinations might not be possible. Nevertheless, understanding the ultimate impacts of industrial development activities in the Chukchi Sea is of critical interest, and a predictive capability to understand the ultimate fate of materials added to the sediments is linked intrinsically to an understanding of sedimentation rates and bioturbation patterns.

Methods

Study Area

Sampling for sedimentation rate determinations was undertaken in the COMIDA study area in the northeastern Chukchi Sea, primarily in 2009. Given the time consuming nature of the gamma spectroscopy counting procedures, we were able to collect more than enough sediment cores in 2009, so 2010 sediment collections focused on other components of the project.

Sample Collection

Sampling for sedimentation rates took place primarily during July and August 2009 using the vessel *R/V Alpha Helix*. Sample stations were selected using a probability-based grid for each section of the study area and randomly choosing locations within each grid cell, as described elsewhere in this report.

Sediment cores were collected using a 133 cm^2 HAPS corer (Kanneworff and Nicolaisen, 1973) with a 30-cm polycarbonate liner. Core samples were sectioned in 1-cm increments to 4-cm depth, and then every 2-cm thereafter to the bottom of the core. Sediments were canned in 90 cm^3 aluminum cans shipboard and returned to the laboratory frozen.

Laboratory Methods

The canned sediments were directly assayed by gamma spectroscopy. Our gamma spectroscopy system is a Canberra GR4020/S reverse 109 electrode closed-end coaxial detector, and we used methods described by Cooper et al. (2005). Briefly, ^{137}Cs and ^{210}Pb inventories were calculated as the sum of total activity detected in each sediment interval taken from an individual core, taking into account the area of the core (133 cm^2), as well as volume of sediment in each core interval that was counted (90 cm^3). Every sample was individually counted for 160,000 to 200,000 seconds to lower counting errors. A certified mixed standard was counted for 10 minutes between each sample assay to assure data integrity and to confirm that the instrument performance met manufacturer's specifications, specifically the peak width for ^{60}Co at 1332 KeV. Background counts were also undertaken in the empty low-background shield and subtracted from each sample; we used the self-absorption corrections of Cutshall et al. (1983) to determine ^{210}Pb activities by assaying samples with a ^{210}Pb source compared to an empty can and the same source. ^{137}Cs activities are presented as an inventory of the radionuclide cm^{-2} and ^{210}Pb activities (in mBq g^{-1}) are derived from dry weights determined after counting. Errors shown are one sigma.

Results and Discussion

^{137}Cs Results

Ten cores were counted for ^{137}Cs (Figure 1). In part because the study was conducted almost exclusively over the continental shelf, all ten cores that have been assayed to date show significant bioturbation by organisms, while general sedimentation patterns are nevertheless preserved in many cases. For example, on most of the cores, ^{137}Cs activities show mid-depth peaks, with low activities in surface sediments, which is consistent with nil deposition of ^{137}Cs in recent decades. Low activities are also found at the base of the deeper cores, with activities declining to levels at or near detection limits (~0.1 mBq cm^{-2}) at 20 cm depth. Maximum activities of 2 mBq cm^{-2} are typically observed at approximately 8-10 or 10-12 cm depth. The preservation in many cores of muted activity maxima suggest that while bioturbation is a dominant process in turning over the sediments, some sedimentation patterns are preserved. Given the 45 years between the time of the bomb fallout peak deposition of ^{137}Cs (~1963-64) and the collection of cores in 2009, preservation of peak activities from 1963-4 at 10-12 cm implies an averaged sedimentation rate of ~0.25 cm year^{-1} without accounting for the impacts of bioturbation. By comparison, Pirtle-Levy et al. (2009), who also sampled on the Chukchi shelf and slope in generally deeper waters (126 to 2227m) found similar mid-depth ^{137}Cs peaks in sediment cores, which were observed in sediment core increments ranging from 4-6 cm to 10-12 cm. In many cases, these mid-depth maxima were more focused than we observed in the COMIDA study area, presumably due to lower degrees of sediment bioturbation at deeper water depths. In one particularly focused core collected at 526 m, Pirtle-Levy et al. (2009) estimated sedimentation rates of approximately 0.06 cm per year. Nevertheless it is somewhat surprising that in the COMIDA study area, on the shallow continental shelf, that general sedimentation patterns are, in part, preserved. In typical sediment cores from the Bering Sea and the southern Chukchi Sea, by comparison, bioturbation is great enough that almost no structure is preserved for fallout ^{137}Cs (Cooper et al., 1998; Cooper et al., 1995).

^{210}Pb Results

Analysis of two of the cores assayed for ^{137}Cs has also been completed for ^{210}Pb, which provides an independent indication of sedimentation, based upon the decline in excess (atmospherically-derived) ^{210}Pb in sediment cores (Figure 2). The two cores chosen, UTX21-20, and CBL15-47, showed declines in ^{137}Cs to near detection limits at the base of each core, indicating that they might also preserve the independent sedimentation record for ^{210}Pb. Our analysis of excess ^{210}Pb sedimentation entailed determination of the background (non-atmospherically derived) ^{210}Pb activities, which we estimated by using the mean activities determined in several of the deepest core increments for each core. For core UTX21-20 we estimated a background activity of 67.80 mBq g^{-1} dry weight (average of 3 measurements) and for core CBL 15-47, we estimated a background activity of 44.05 mBq g^{-1} dry weight (average of two measurements). These background activities are consistent with the previous work of Pirtle-Levy et al. (2009) who estimated a background activity of 41.4 mBq g^{-1} dry weight for the core they analyzed from the outer Chukchi shelf, but higher than estimates of 20.6 mBq g^{-1} observed by Baskaran and Naidu (1995) northwest of Hanna Shoal. We subtracted our calculated background activities from the measured ^{210}Pb activities in each of the two cores and plotted the decline in excess ^{210}Pb over

depth after excluding surface increments that varied little in excess ^{210}Pb due to bioturbation. Consequently, the plotted core increments for UTX21-20 are from 6-14 cm and for CBL15-47 are from 8 to 18 cm (Figure 2). The slope of the decline on a logarithmic scale was divided by the appropriate activity decay coefficient for ^{210}Pb to produce sedimentation rate estimates of 0.02 cm year^{-1} and 0.14 cm year^{-1} for cores UTX21-20 and CBL15-47, respectively. These estimates differ from those suggested by ^{137}Cs deposition, but as noted previously, significant bioturbation in these shallow continental shelf sediments will make definitive sedimentation rate estimates with small errors challenging.

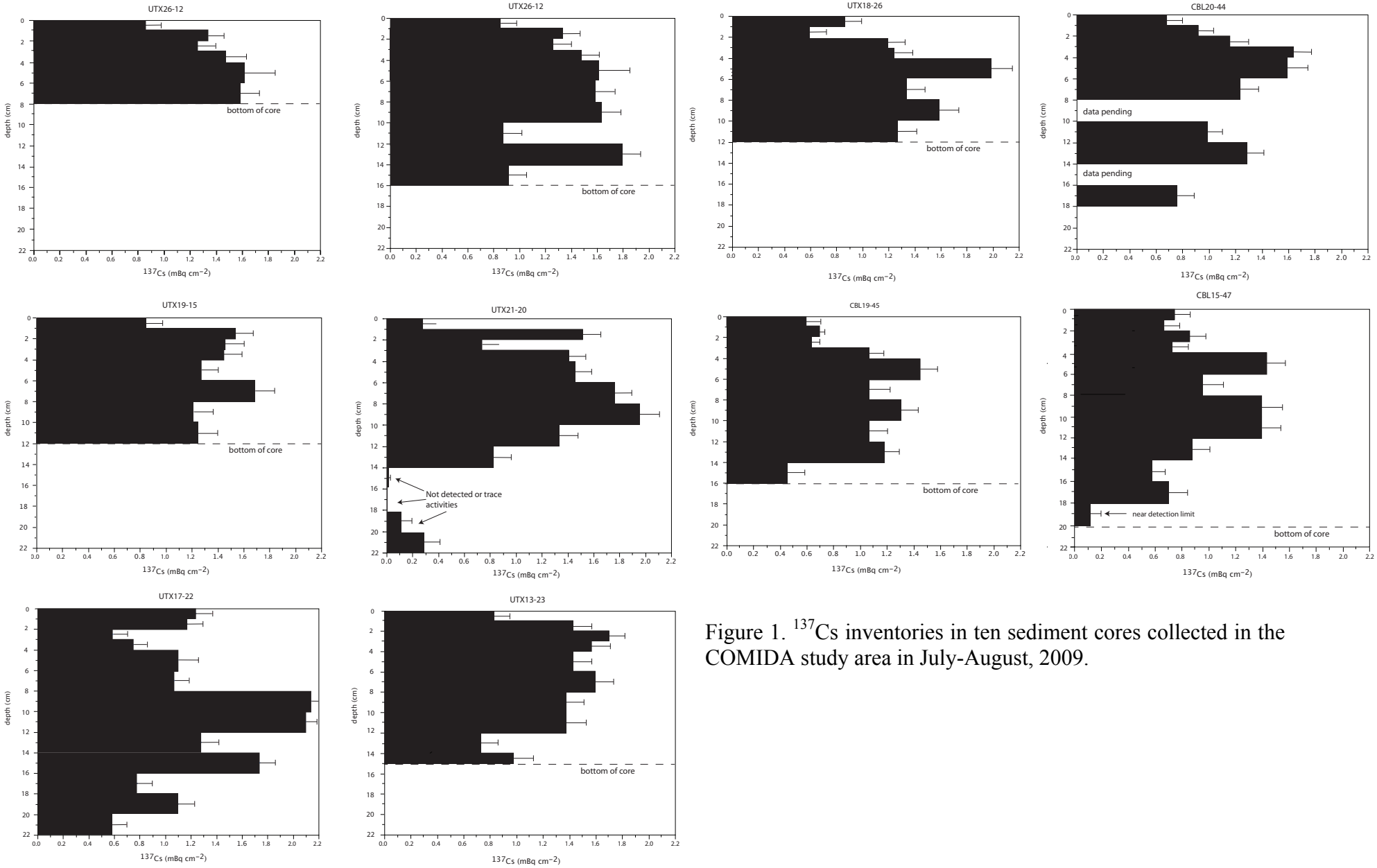

Figure 1. ^{137}Cs inventories in ten sediment cores collected in the COMIDA study area in July-August, 2009.

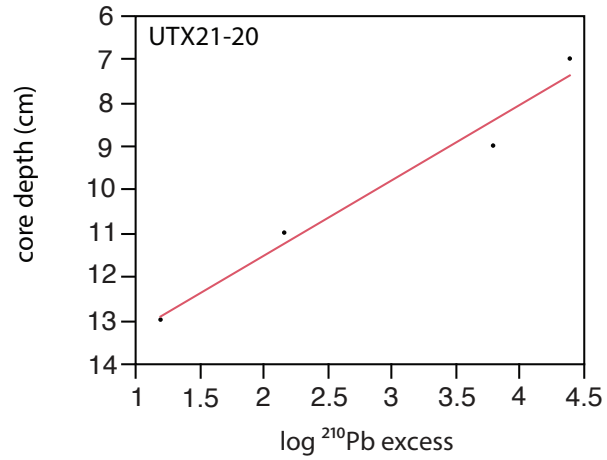

log ^{210}Pb=-0.56* mid-depth of core increment (cm) + 8.49 r^2 = 0.97

decay coefficient for ^{210}Pb (-0.01352 year^{-1}) divided by slope implies a sedimentation rate of 0.02 cm year^{-1}

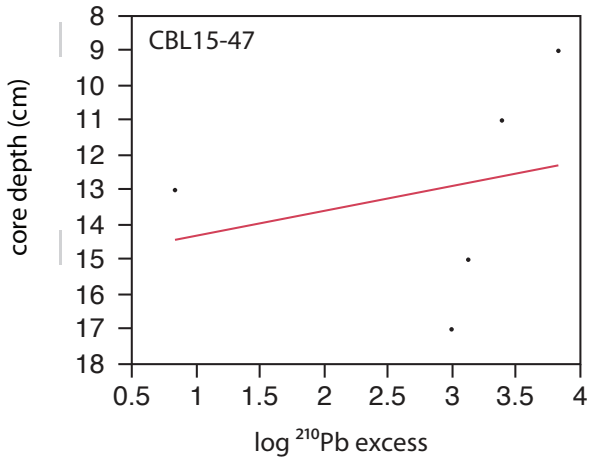

log ^{210}Pb= -0.096 * mid-depth of core increment (cm) + 4.09 r^2 = 0.47

decay coefficient for ^{210}Pb (-0.01352 year^{-1}) divided by slope implies a sedimentation rate of 0.14 cm year^{-1}

Figure 2. Declining excess ^{210}Pb activities with depth in two COMIDA cores.

Implications for industrial activities in the COMIDA study area

These studies show that bioturbation is a significant factor in re-distribution of materials within the top 20 cm of the sediments over decadal time periods. Anthropogenic materials introduced during industrial activities associated with oil and gas extraction will be cycled within the sediments by resident benthic fauna for periods of decades or more. Averaged sedimentation rate estimates are not as reliable as on the outer continental shelf, but can be estimated here unlike

many more biologically productive portions of the northern Bering and southern Chukchi Seas. These averaged sedimentation rates range from 0.02 to 0.25 cm $year^{-1}$, reasonably in agreement with rates estimated from the outer Chukchi continental shelf (0.06 to 0.075 cm $year^{-1}$) that were observed in other studies (Pirtle-Levy et al. 2009) (Pirtle-Levy et al., 2009).

Acknowledgments

We thank the Bureau of Ocean Energy Management (BOEM), U.S. Department of Interior for funding and the participants of the COMIDA cruises for facilitating the collection of these samples. Thanks are also extended to Captain John Seville and his crew on the *R/V Alpha Helix* and *R/V Moana Wave* for providing the vessel platform, navigational expertise and shipboard skills to collect the samples. Dr. Dan Marsh of Oak Ridge, Tennessee provided invaluable assistance in the calibration of our gamma spectroscopy system.

Nutrient and gas fluxes at the sediment-water interface of the eastern Chukchi Sea shelf

Souza, A.C., and K.H. Dunton

Afonso C. Souza and Ken H. Dunton
Marine Sciences Institute
The University of Texas at Austin, Port Aransas, TX 78373

Abstract

Net nitrogen (N_2), oxygen (O_2), nitrate (NO_3^-), and phosphate (PO_4^{-3}) benthic fluxes at the sediment-water interface of intact cores using continuous flow through technique and hydrographic properties including temperature (T) and salinity (S) were measured during the summer of 2010 on the shelf of the COMIDA CAB study area in the Chukchi Sea. The northeastern portion of the study area was dominated by cold (-1.68 ^oC) and relatively saline (S=33.72) waters while the southern half of the study area were comprised predominately of warm (8.33 ^oC) and less saline (S=29.88) waters. Benthic fluxes at stations 9 and 103 were intense where positive fluxes (from sediment into water column) of net N_2 ranged from 260 ± 25 to 73 ± 2.3 μmoles m^{-2} h^{-1}, and fluxes of NO_3^- (6.1 ± 2.2 to 1.7 ± 0.1 3 μmoles m^{-2} h^{-1}) and phosphate PO_4^{-3} (3.6 ± 0.5 to 1.0 ± 0.23 μmoles m^{-2} h^{-1}) occurred. Net oxygen fluxes into the sediment occurred at all four stations measured. Highest O_2 influx (601 ± 33 μmoles m^{-2} h^{-1}) was measured at station 103.

Introduction

The broad continental shelf of the Chukchi Sea is an important region for biogeochemical cycles in the Arctic Ocean. Heat, salinity, and nutrient advection affect primary productivity in the Chukchi Sea (Coachman and Aagaard, 1988; Weingartner et al., 2005), which is one of the most productive regions in the Arctic Ocean (Sakshaug, 2004). Shelf primary production can reach up to 2.5 g C m^{-2} day^{-1} (Gosselin et al., 1997) and benthic secondary standing stock ranges from 360 to 4000 g m^{-2} (Dunton et al., 2005; Grebmeier et al., 2006b). Benthic infaunal biomass and primary productivity display high spatial variability (Dunton et al., 2005; Grebmeier et al., 2006b), which is linked to water column characteristics such as temperature and nutrient availability (Springer and McRoy, 1993). Important factors driving spatial variability in biomass include the advection of nutrient-rich Pacific water (Codispoti et al., 2005; Walsh et al., 1989) in addition to the seasonality and structure of this Pacific water inflow (Woodgate et al., 2005).

Considering the progressive climate changes occurring in the arctic region, an important overarching goal of this research is to develop relevant mechanistic insights that can be used to predict biogeochemical changes in the Chukchi Sea. The main purpose of this study was to define the spatial variability of benthic biogeochemical processes, including net nutrient regeneration, oxygen (O_2) consumption, and nitrogen gas (N_2) fluxes measured at the sediment-water interface.

Methods

Sample collection

During the summer field season on board the *R/V Moana Wave* July-August 2010, seawater properties, including temperature (T) and salinity (S), were measured using a YSI-650-MDS Sonde, which has a resolution of 0.01 parameter units. The accuracy of measurements was ± 0.15 °C and ±0.001 mS cm^{-1}, respectively. Prior to deployment, the salinity probe was calibrated using conductivity/TDS standard (Ricca Chemical Co., part# 2248-32) 50,000 micromhos cm-1 (30.300 ppm) as NaCl.

Samples analyzed for N_2, O_2, NO_3^-, and PO_4^{-3} concentrations were collected in continuous flow experiments with intact sediment cores (An et al., 2001; Lin et al., 2011) collected using a HYPOX coring device (Gardner et al., 2009) at four stations (103, 9, 1015, and 48 - Figure 1). A water bath of circulating surface seawater maintained intact cores at a constant T ± 1°C for an incubation period of four days. Seawater stored in 20-L carboys was passed over the sediment in capped cores at a rate of 0.9 ml min^{-1}.

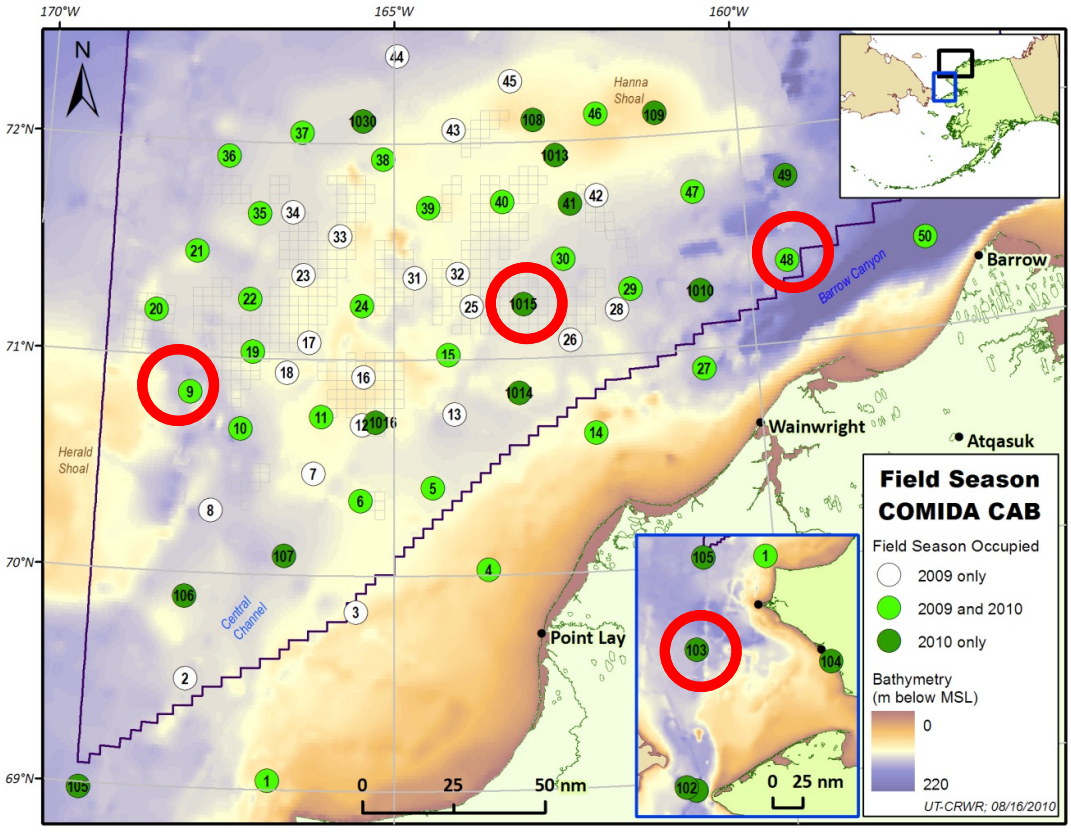

Figure 1: Maps showing sampling stations for 2009 and 2010 field surveys for the COMIDA Project. Lower inset map shows stations to the south of those shown on the larger map and upper inset map shows location of study area off the northwest coast of Alaska. Stations where benthic sediment fluxes were measured are circled in red.

Laboratory Methods

Fluxes were calculated by using the difference between concentrations of constituents in inflow and outflow samples (Gardner et al., 2006). Seawater samples were preserved with 50% $ZnCl_2$ w/v in capped 15-ml glass vials and stored in sealed 4-L containers submersed in water. Gases were analyzed upon return to The University of Texas Marine Science Institute (UTMSI) using a Membrane Inlet Mass Spectrometer (MIMS), (An et al., 2001). Nitrate and PO_4^{-3} concentrations were measured using a Latchat Quikchem 8000 Flow injection analysis system. The coefficients of variation in replicate NO_3^-, and PO_4^{-3} standard solutions were less than 0.02.

Results and Discussion

Hydrological properties

Temperature and S are considered conservative characteristics of seawater; therefore, T-S diagrams are a valuable approach to distinguish water masses of a region. Based on our T-S diagram (Figure 2), four different water types were involved in physical mixing in the study area.

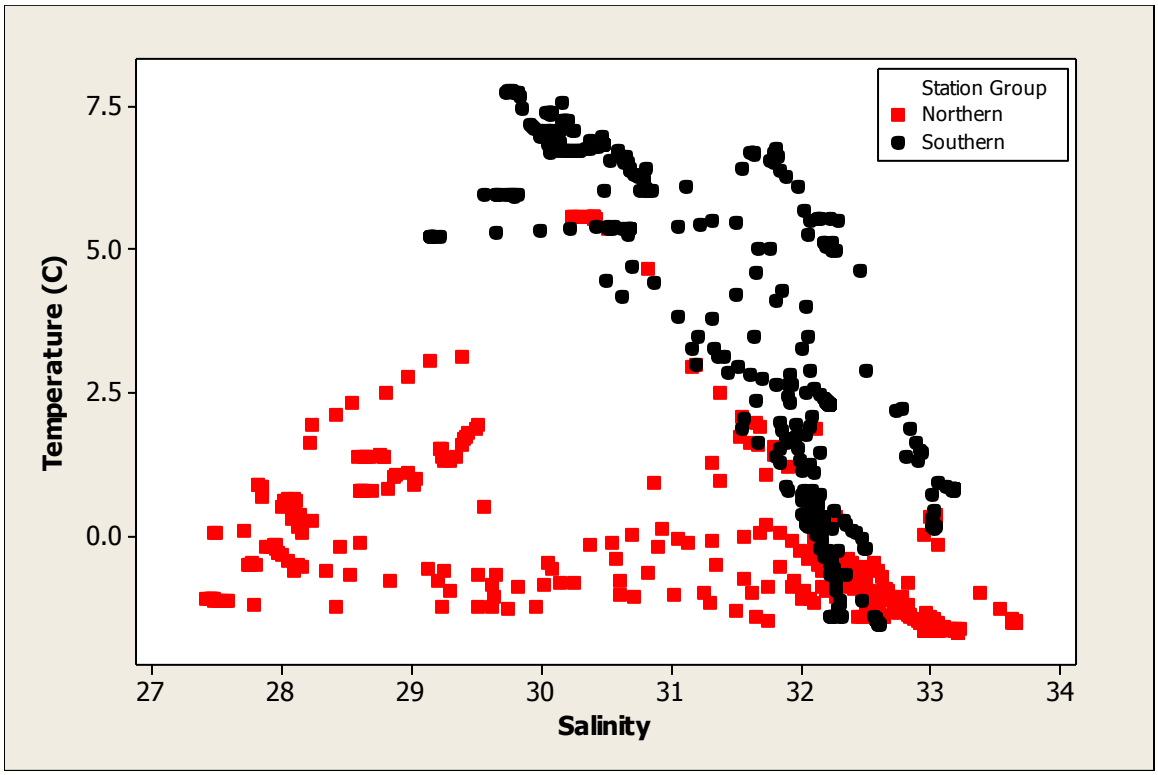

Figure 2: Temperature-salinity diagram of stations below ~71°N (red square, southern) and above ~71°N (black circle, northern). Approximate location of the mixing front was assumed ~71°N.

However, shelf sediments were overlain primarily by relatively warm and less saline waters in the southern region and by cold and relatively more saline waters in the northern region. The

presence of cold and salty waters T ≈ -1.8°C and S ≈ 33.8 during summer may have been resulted from either the production of brine caused by gradual ice formation in the shelf or from remnant winter-transformed Pacific water from the previous winter (Pickart et al., 2005; Weingartner et al., 1998).

Benthic fluxes

Net flux values determined by continuous flow of seawater over intact sediment cores are presented in μmol N m^{-2} h^{-1} (Table 1) for each respective station. Positive values (sediment → water) represent efflux and negative values (water → sediment) indicate influx or removal from the water column. N_2 production was higher at station 103 (73.2 ±2.3 μmoles N m^{-2} h^{-1}) and station 9 (260 ±25.0 μmoles N m^{-2} h^{-1}), which were influenced largely by the warm and less saline water, in contrast to station 1015 (8.2 ±6.5 μmoles N m^{-2} h^{-1}) and station 48 (24.2 ±9.9 μmoles N m^{-2} h^{-1}) that were overlain by the cold and hypersaline water. The efflux of NO_3^- into the overlying water (1.7 ±0.1 and 6.1 ±2.2 μmoles N m^{-2} h^{-1}) and the efflux of PO_4^{-3} (3.6 ±0.5 and 1.0 ±0.2 μmoles P m^{-2} h^{-1}) at stations 9 and 103, respectively, show that sediments at those stations act as a source of nutrients for the water column.

Table 1: Gas and nutrient fluxes at the sediment-water interface over the Chukchi Sea shelf. Negative values reflect fluxes into the sediment (water → sediment).

Stations	*Latitude*	*Longitude*	*Depth*	*Net N_2*	*O_2*	*NO_3^-*	*PO_4^{-3}*
	(dd)	*(dd)*	*(m)*	*(μmoles m^{-2} h^{-1})*			
48	71.377	-159.468	46	24.2 (9.9)	-268.7 (55.2)	-0.8 (0.2)	1.1 (0.1)
1015	70.840	-163.291	46	8.2 (6.5)	-209.5 (42.4)	0.4 (0.9)	-0.9 (0.3)
9	70.671	-167.083	45	260.1 (25.0)	-131.3 (18.6)	1.7 (0.1)	1.0 (0.2)
103	67.670	-168.958	43	73.2 (2.3)	-601.9 (33.1)	6.1 (2.2)	3.6 (0.5)

Ecological implications of nutrient fluxes

The efflux of NO_3^- from the sediments concomitant with an efflux of N_2 at stations 9 and 103 suggests that benthic NO_3^- production exceeds its consumption by denitrification. It is therefore possible to infer that benthic nitrification compensates for the N removal and maintains a supply of NO_3^- to benthic primary producers, if present, by oxidizing porewater ammonium. This proposed mechanism is extremely likely given that the depth of 1% light may reach 46 m under clear skies based on the light attenuation coefficient of around 0.1 measured at several stations, high benthic chlorophyll (Grebmeier et al., 2006b), and high porewater NH_4^+ concentrations (Devol et al., 1997) in the southern region of the COMIDA quadrat. In contrast, fluxes of nitrogen decreased significantly at station 1015 (0.4 μmoles N m^{-2} h^{-1}) and reversed direction into the sediment at station 48 (-0.8 μmoles N m^{-2} h^{-1}).

Dinitrogen flux values indicate a significant N loss in the northeastern shelf region. Considering the average flux of 4 stations, the overall estimate of N loss within the study region (ca. 1100 km $^{-2}$) during the 30-day cruise was about 0.24 Tg N, which is a substantial loss considering the nitrogen budget of the region. As most of the sediment efflux of nutrients is related to warmer and less saline water, the potential change of water mass dominance in response to changing climate patterns may alter rates of benthic primary productivity, which could then force a change in the abundance and diversity of benthic infauna present along the northern region of the shelf.

Summary and Conclusions

This work examined the distribution of gases N_2 and O_2 and nutrient fluxes NO_3^- and PO_4^{-3} at the sediment-water interface and their relationship to bottom water masses in the Chukchi Sea shelf during summer 2010. Two distinct hydrological features appear when examining the distribution of waters: warm and less saline waters in the southern region and cold and hypersaline saline waters dominating the northeastern shelf region. Benthic biogeochemical processes were distinguished spatially through the distribution of bottom water masses. At station 103 of the study area, net community nutrient, nitrogen gas flux, and oxygen consumption were high. There was an efflux of both N_2 and NO_3^- from the sediment into the overlying water. In contrast, low efflux of N_2, moderate O_2 consumption, and nutrient fluxes into the sediments were found at stations 48 and 1015 on the shelf region.

Acknowledgments

We are sincerely appreciative to Captain J. Seville and the crew of the *R/V Moana Wave* for their superb support of our research in summer 2010. We thank K. Aagaard for his valuable comments and suggestions which helped improve this report considerably. Study design, oversight, and funding were provided by the U.S. Department of the Interior, Bureau of Ocean Energy Management (BOEM) and Alaska OCS Region, Anchorage, AK under Contract M08PC20056 for the "COMIDA-CAB" program, under the highly effective leadership of D. Prentki, to whom we are very grateful. We also thank M. Macrander for supporting a collaborative study that provided funding from Shell Exploration and Production Company for ship operations.

Water Column Chlorophyll, Benthic Infauna and Sediment Markers

Grebmeier, J.M. and L.W. Cooper

Jacqueline M. Grebmeier and Lee W. Cooper
University of Maryland Center for Environmental Science
Chesapeake Biological Laboratory, Solomons, MD 20688

Abstract

Water column nutrients and chlorophyll (chl *a*), sediment markers (total organic carbon/nitrogen, sediment grain size, radioisotopes), infaunal benthic abundance and biomass, and epibenthic camera surveys were undertaken during the 2009 and 2010 COMIDA sampling effort. We found post-bloom conditions in the water column, with most chlorophyll settling to sub-surface maxima and the surface sediments, as nutrients were drawn down in surface waters for most stations. Higher chl *a* values were found in surface sediments in the offshore waters of the northern Chukchi Sea under Anadyr water compared to lower values in nearshore coastal water influenced by Alaska Coastal water. Surface sediment total organic carbon (TOC) content was highest in offshore waters of the northern Chukchi Sea and in the northeast section of the Chukchi Sea near upper Barrow Canyon, indicative of higher export production reaching the underlying sediments in these regions. Inshore stations in the COMIDA study area have higher C/N values, indicative of a more terrigenous signal; lower surface C/N values are observed offshore and to the north, which indicates higher quality organic matter, perhaps resulting from the higher chl *a* content of both the water column and surface sediments. Sediment community oxygen consumption (SCOC), an indicator of carbon supply to the benthos, was measured in 2010 and indicates the highest level of SCOC occurs in the southeast Chukchi Sea "hotspot" and sites in the northern portion of the study area, both areas where higher integrated chl *a* occurs. For both years of sampling, the dominant macrobenthic infaunal taxa by abundance were bivalves, polychaetes and amphipods. Notably the highest abundance of infauna occurred in a transect from off Wainwright to offshore locations in the north central Chukchi Sea. Echinoid sand dollars (*Echinarachnius parma*) were dominant by biomass in the nearshore Alaska Coastal water. For biomass (both g wet wt. and g C/m^2), bivalves, polychaetes and sipunculids were the dominant macroinfauna and highest values occurred offshore in the northern Chukchi Sea. Statistical evaluation indicates that water mass type (defined by salinity), station depth, sediment grain size and food quality (N content and C/N values) are the most significant environmental variables driving benthic macroinfaunal abundance and biomass values in the COMIDA region. Qualitative video imagery obtained of the epibenthos shows high biomass of echinoderms over large areas, as well as high diversity in inshore areas. Radionuclide findings for sedimentation rates are summarized in a separate sub-chapter. Finally, two graduate student M.S. projects are also investigating ostracod distributions relative to sea ice extent and the caloric value of invertebrates to help assess walrus diet requirements.

Introduction

The Chukchi Sea Offshore Monitoring in Drilling Area (COMIDA): Chemistry and Biology (CAB) project (http://www.comidacab.org/) is a Bureau of Ocean Energy Management (BOEM) research program in which our group collected water, sediment and benthic faunal data. Field sampling was accomplished in 21 July-12 August 2009 from the *R/V Alpha Helix* and 24 July-12 August 2010 from the *R/V Moana Wave*. Goals for our component of this open-water season sampling included evaluation of water column chlorophyll *a* and nutrients, chlorophyll *a* in surface sediments, sediment indicators (grain size, carbon and nitrogen content), downcore radioisotopic analyses to estimate sedimentation rates, benthic infaunal composition and biomass, and video analysis of epibenthic organisms. The BOEM sampling plan was designed as a robust, comprehensive effort to characterize Lease Area 193 biota and chemistry within the Chukchi Sea and to generate data that is comparable to current and past sampling efforts in the area. Oil companies that have leased exploration blocks in the Chukchi Sea Lease Sale 193 area (e.g. Shell, Conoco-Phillips and Statoil) also have developed comparable monitoring programs to assess pre-drilling baseline benthic and water column environmental conditions.

One of the important bases to our work are the recent reductions in seasonal arctic sea ice that have the potential to alter the current benthic-based food web to one more dominated by pelagic trophic transfers. The vulnerability of the ecosystem to environmental change is thought to be high, particularly as sea ice extent declines and seawater warms (Grebmeier et al., 2006b). The duration and extent of seasonal sea ice, seawater temperature, and water mass structure are critical controls on water column production, organic carbon cycling, and pelagic–benthic coupling. Because the productive areas in the Chukchi Sea are associated with short food chains and shallow depths, changes in lower trophic levels can rapidly impact walruses and other apex predators (Grebmeier et al., 2006b).

Benthic infaunal biomass reflects persistent, annual carbon deposition to the seafloor on the shallow Chukchi Sea continental shelf (Feder et al., 1994a; Feder et al., 1994b; Grebmeier, 1992; Grebmeier and Barry, 1991; Grebmeier and Barry, 2007; Grebmeier et al., 2006b; Grebmeier and McRoy, 1989; Grebmeier et al., 1988; Stoker, 1981). The northeast outer continental shelf of the Chukchi Sea and the head of Barrow Canyon are at the interface of the Chukchi and Beaufort Seas outer shelves and slope regions and are a key conduit for transformed Pacific water and associated organisms that transit to the deep Arctic Basin (Grebmeier and Harvey, 2005). It is likely that large-scale changes on the shelf, as influenced by environmental change in the Pacific inflow and ice dynamics, will impact higher trophic organisms. In addition to food supply and community composition, sediment grain size reflects local current speed. Sediment grain size is a key predictor of benthic faunal community composition; by comparison, organic carbon, which is positively correlated with the smaller silt and clay grain particles, is a key predictor of biomass (Grebmeier et al., 2006b; Grebmeier et al., 1995).

Bivalves, polychaetes, and sipunculids dominate the general infaunal community of the northern Chukchi Sea, where average infaunal benthic biomass is 5-15 g C m^{-2} (200-400 g wet wt. m^{-2}; Grebmeier et al. 2006a). This benthic community changes to a low biomass, foraminifera-dominated community on the upper slope (200-1000 m depth), with benthic biomass <5 g C m^{-2} (<200 g wet wt. m^{-2}), extending down into the Canada Basin (Grebmeier et al. 2006a). Notably,

the northeast Chukchi Sea, including upper Barrow Canyon, is a "hotspot" footprint for the entire Chukchi Sea, with a rich community of suspension feeding infauna and epifauna (e.g., bivalves, barnacles, basket stars, and tunicates) attached to rocks, cobble and mixed sediments, and suggests the presence of strong currents (Feder et al., 1994a; Feder et al., 1994b; Grebmeier et al., 2006b; MacGinitie, 1955). In areas with interspersed silt, clay, and gravel, the suspension-feeding mussel *Musculus sp.* is abundant, with individual station biomass up to ~150 g C m^{-2} (~4000 g wet wt m^{-2}; Grebmeier et al. 2006a). This benthic biomass maximum at the head of Barrow Canyon coincides with extremely high sediment oxygen uptake, an indicator of carbon supply to the benthos (Grebmeier et al., 2006b; Lepore et al., 2007; Moran et al., 2005).

In a separate distinct portion of our study component, M. S. student Lisa Wilt is evaluating the caloric content of both macroinfaunal and epifaunal benthic fauna in a study of walrus prey base in the Chukchi Sea. The goal of this study is to conduct a caloric analysis of the walrus prey field in the Chukchi Sea to look for spatial variation and changes over time using samples collected during the 2010 COMIDA cruise. Walrus are known to consume a wide variety of benthic invertebrates. In particular, stomach content surveys have concluded that bivalves, gastropods and polychaetes are the most frequently consumed prey items for walruses (Sheffield and Grebmeier, 2009). These values are being compared to previous estimates from the 1970s (Stoker, 1978) to evaluate potential changes over time. These data will be ultimately shared with cooperating marine mammal investigators to model food resource availability for walrus populations that use the COMIDA study area for foraging.

Material and Methods

Sample locations

We selected station sites in 2009 via two methods: 1) a general randomized tessellation stratified design (GRTS) in the core COMIDA area, and 2) a spatially-oriented, nearshore-to-offshore, south to north grid overlaying the GRTS design (Figure 1). This arrangement allowed for placing the core station sites in a spatial grid. Of the 30 GRTS stations, 10 were chosen as overlap stations to cross-calibrate and provide QA/QC between the UTMSI (University of Texas Marine Science Institute, labeled UTX in data reports) and CBL (Chesapeake Biological Laboratory) benthic labs (Figure 1). In addition to these COMIDA 2009 sites, additional locations in the Bering Strait and southeast Chukchi were also added for 2010.

For this report, we have separated the cruises by year, identified the station number and name for each year (Figs. 2 and 3) and also show a combined map (Figure 4) for comparison of tables and figures throughout the report. Data maps are provided by individual years as well as combined, depending on the discussion of the results. Individual station data, including station number, name, type, date, latitude, longitude, and depth are provided for COMIDA 2009 (Table 1) and COMIDA 2010 (Table 2). Note that during COMIDA 2010 a chronological station sequence number was added that allows both the station number and name to be linked between years.

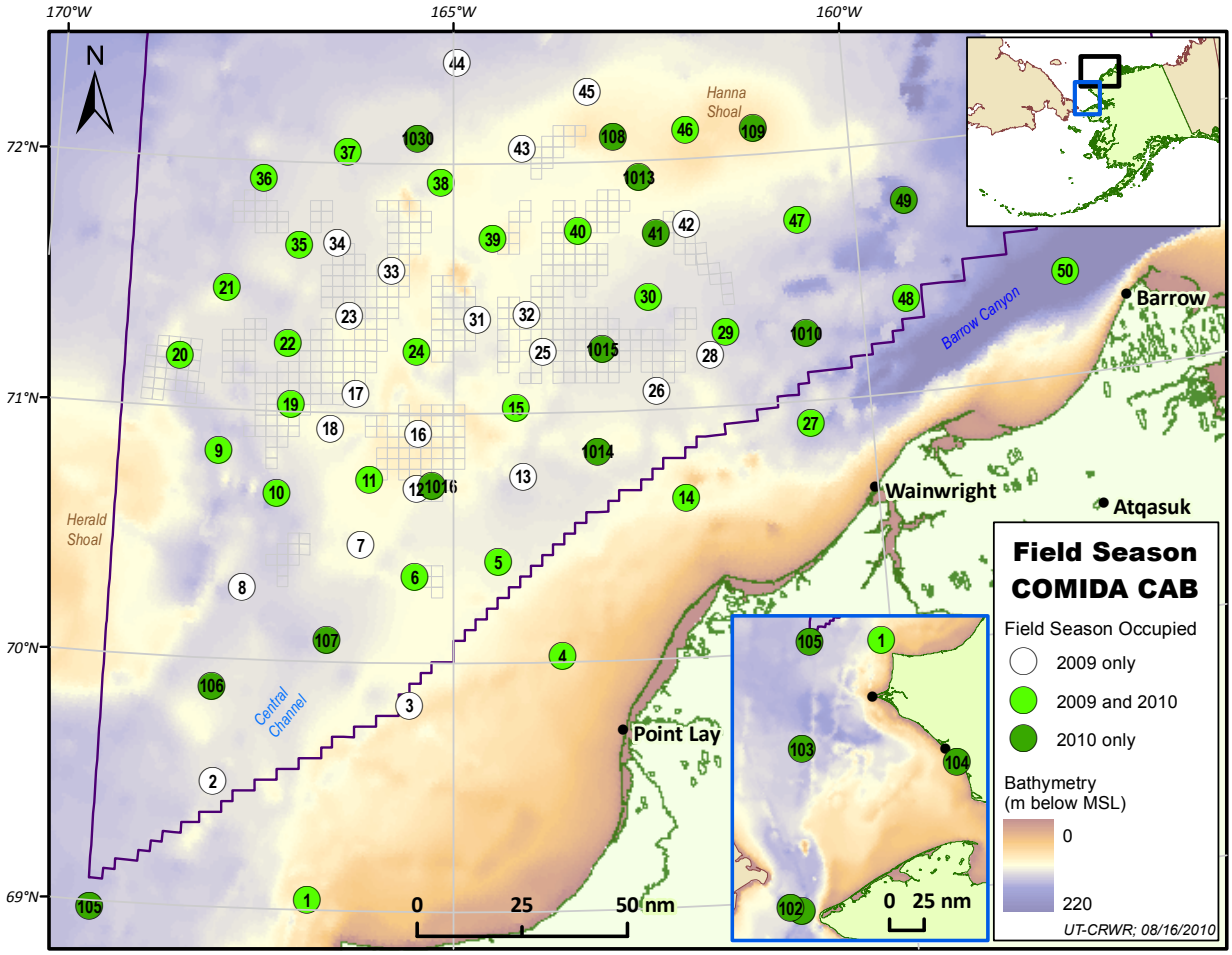

Figure 1. Location of COMIDA sampling stations in 2009 and 2010.

Methods

Water column

We collected data from both the water column and the benthos for chemical and biological evaluation. Water column samples were collected at the pumping stations each morning and were used for chlorophyll and nutrient analyses. These samples were collected throughout the water column at 2-6 different depths. Chlorophyll-a was extracted and processed on-board using a Turner fluorometer. Nutrient samples were filtered, frozen, and analyzed post-cruise for four nutrients (nitrate/nitrate, phosphate, ammonium and silicate) at CBL's Nutrient Analytical Services Laboratory in Solomons, MD. Temperature and salinity data were collected by other members of the COMIDA team and are discussed elsewhere in the report (see chapters authored by J. Trefry and K. Dunton).

Sediments

Surface sediment samples were collected at stations to assay for viable chlorophyll in sediments, total organic carbon, and sediment grain size. Two samples of the upper 1-cm of sediment were

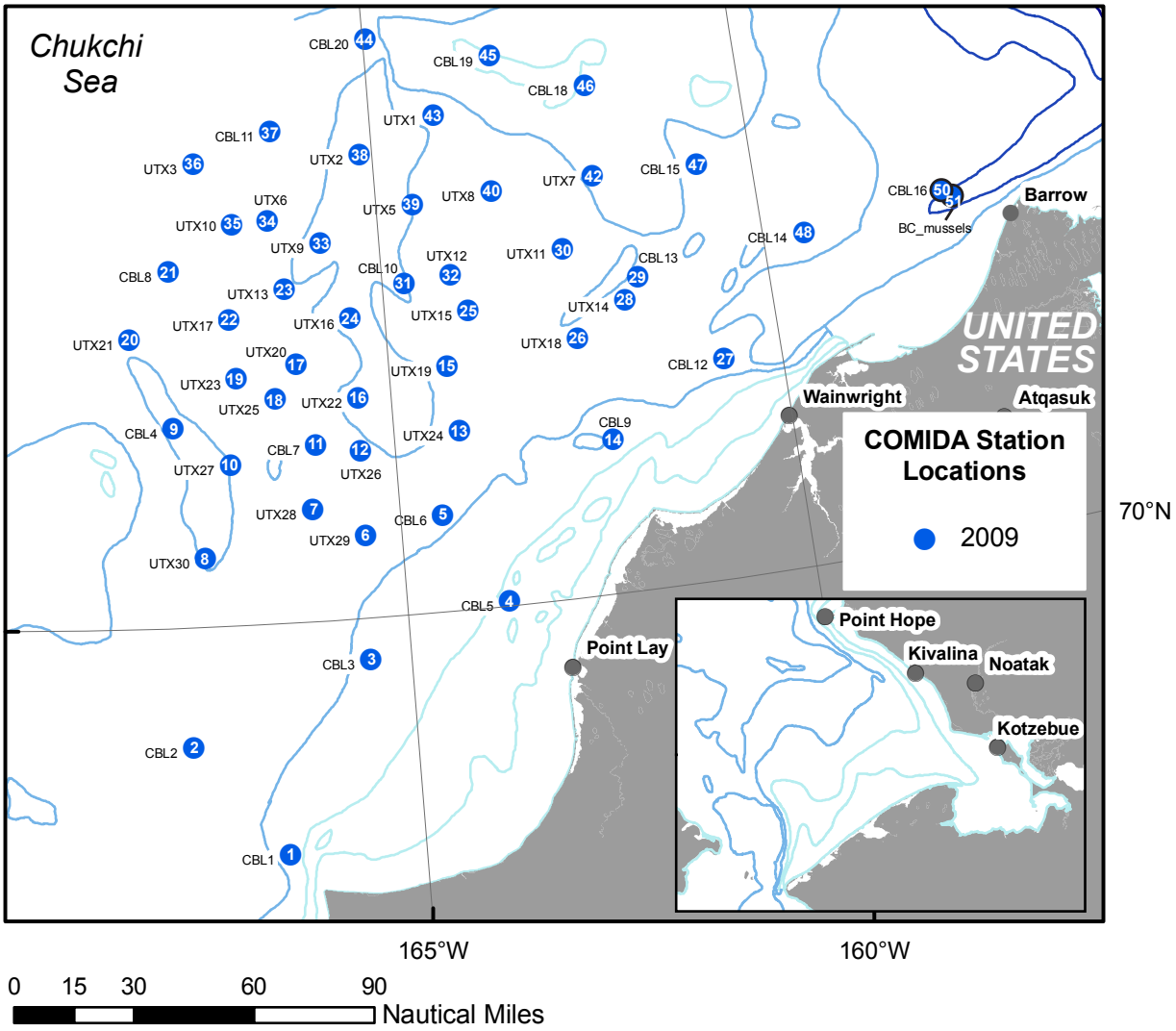

Figure 2. Station location for 2009 field surveys for the COMIDA project by station number (within symbol) and name.

removed from a 0.1 m^2 van Veen grab sample and analyzed for chlorophyll-a inventories. The upper layer of sediment was bagged, frozen, and analyzed for grain size and organic carbon content at CBL using standard procedures (Cooper et al., 2002). Surface sediment samples were also collected for a M.S. thesis project that is matching ostracod assemblages with sea ice distributions in cooperation with the US Geological Survey in Reston, Virginia.

Benthos

Two (UTX/CBL overlap stations) or four van Veen grab samples (CBL stations) were taken for quantitative biological samples and preserved in buffered seawater formalin. Sorting and determination of infaunal abundance and biomass for our CBL program occurred at UMCES CBL. Two grabs were taken at each UTX/CBL station in 2009 to provide quality assurance for taxonomic identifications between the University of Texas (independent analysis of two additional samples) and our University of Maryland lab. The van Veen samples were sieved using seawater on a 1 mm stainless steel screen to collect macrofauna, packaged and preserved with 10% buffered seawater formalin for post-cruise taxonomic identification, abundance and wet biomass determinations at CBL. Infauna were identified to the family level and wet weight biomass was converted to g carbon dry weight using methods of Grebmeier et al. (2006b; 1989a).

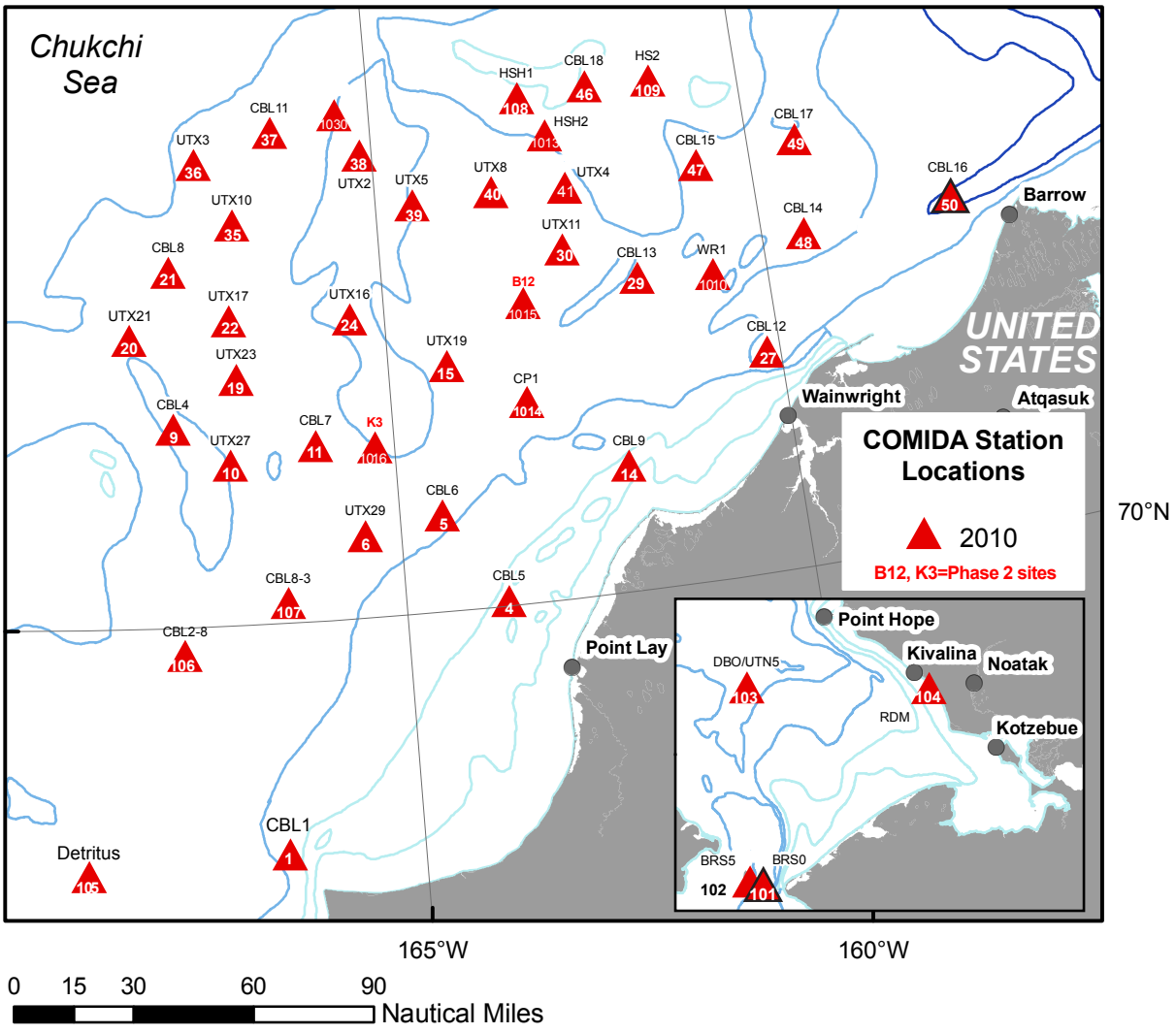

Figure 3. Station locations for 2010 field surveys for the COMIDA project by station number (within symbol) and name. Lower insert indicates stations sampled in the southern Chukchi Sea.

Subsamples of box cores and HAPS cores were collected for determinations of Pb-210 and Cs-137 in 2009 as a means to estimate sedimentation rates. Cores were sectioned, canned, and frozen and returned to CBL for radioisotope analyses (see Cooper sub-report submitted separately).

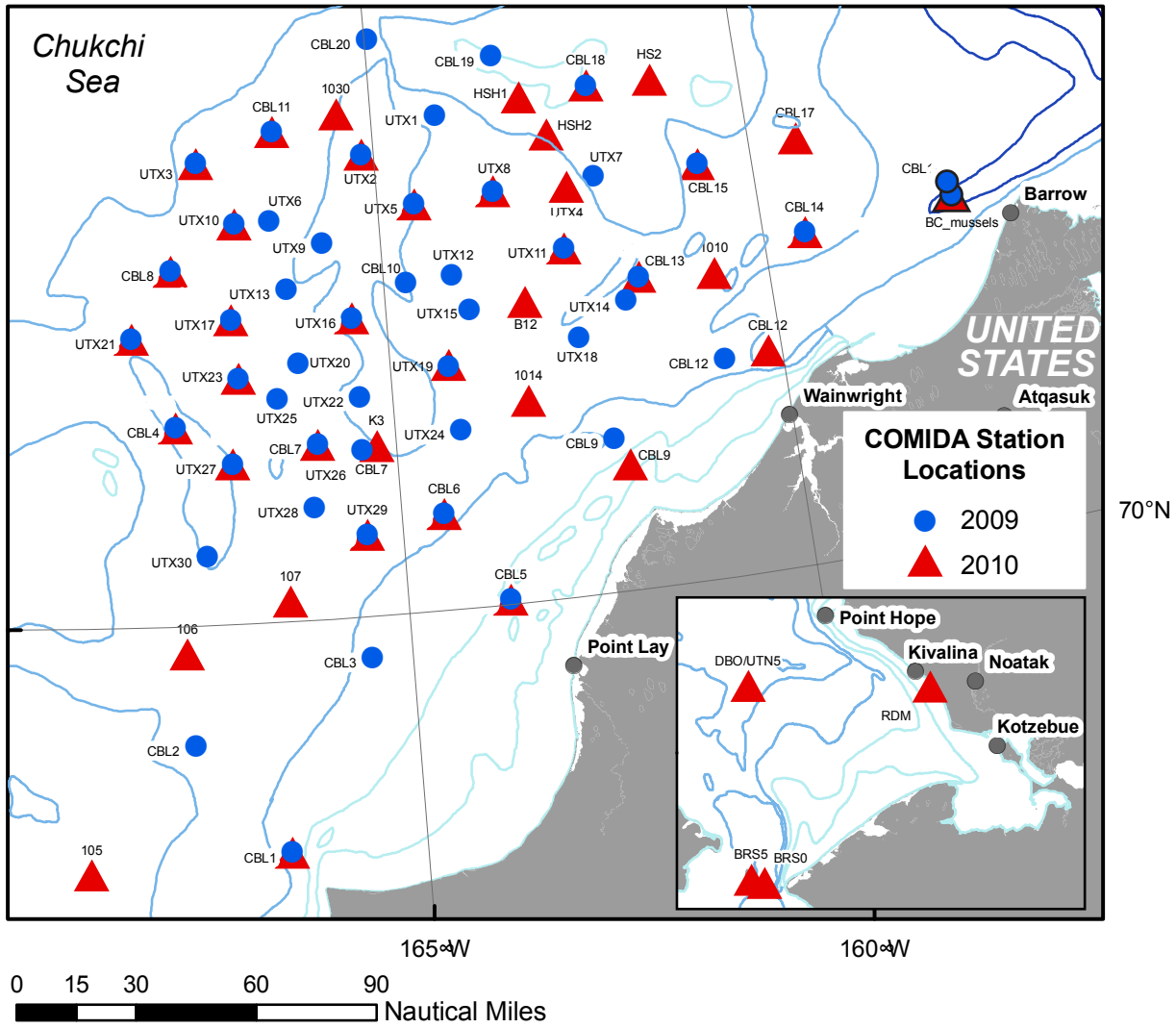

Figure 4. Map showing both COMIDA2009 and 2010 sampling stations by station names. Lower insert for stations sampled in the southern Chukchi Sea.

A HAPS benthic corer was also used to collect sediment cores for shipboard sediment oxygen uptake experiments during 2010 only, following the methods outlined in Grebmeier and Cooper (1995).

An underwater benthic video camera was used to qualitatively document the epibenthos and sediment habitat at each station in both 2009 and 2010. Standard recording was for 10 min, although in some cases fast bottom currents, ship drift, or large swells interfered with film quality and the recording was terminated. These videos were also used shipboard to assist the UAF epibenthic trawl team in planning their deployments.

Table 1. Station listing for COMIDA09 on the *R/V Alpha Helix* in 2009.

2009 Station Number	Station Name	Date Occupied	Station Type	Depth (m)	Latitude (°N)	Longitude (°W)
1	CBL1	7/27/09	CBL	38	69 02.380	166 35.608
2	CBL2	7/27/09	CBL	49	69 30.126	167 40.513
3	CBL3	7/28/09	CBL	41	69 49.747	165 29.974
4	CBL5	7/28/09	CBL	28	70 01.383	163 45.670
5	CBL6	7/28/09	CBL	44	70 24.285	164 28.940
6	UTX29	7/29/09	UTX random	46	70 20.706	165 27.024
7	UTX28	7/29/09	UTX random	46	70 28.122	166 05.168
8	UTX30	7/29/09	UTX random overlap	51	70 17.233	167 26.609
9	CBL4	7/29/09	CBL	58	70 49.881	167 47.204
10	UTX27	7/30/09	UTX random	54	70 40.275	167 04.990
11	CBL7	7/30/09	CBL	42	70 43.965	165 59.800
12	UTX26	7/30/09	UTX random	45	70 41.833	165 26.437
13	UTX24	7/31/09	UTX random overlap	51	70 44.803	164 10.534
14	CBL9	7/31/09	CBL	42	70 38.490	162 15.976
15	UTX19	7/31/09	UTX random	45	71 01.089	164 15.281
16	UTX22	8/1/09	UTX random	44	70 55.151	165 25.232
17	UTX20	8/1/09	UTX random overlap	45	71 04.636	166 10.708
18	UTX25	8/1/09	UTX random	45	70 56.115	166 28.442
19	UTX23	8/1/09	UTX random	47	71 01.669	166 57.162
28	UTX14	8/3/09	UTX random	49	71 12.492	161 53.392
29	CBL13	8/3/09	CBL	51	71 17.891	161 41.321
25	UTX15	8/3/09	UTX random overlap	45	71 14.549	163 55.317
26	UTX18	8/3/09	UTX random overlap	47	71 04.641	162 33.503
27	CBL12	8/4/09	CBL	52	70 54.512	160 44.450
24	UTX16	8/5/09	UTX random	44	71 14.952	165 26.871
23	UTX13	8/5/09	UTX random	46	71 23.228	166 16.588
22	UTX17	8/5/09	UTX random	48	71 16.328	167 00.865
20	UTX21	8/6/09	UTX random	51	71 12.399	168 18.676
21	CBL8	8/6/09	CBL	51	71 29.079	167 46.900
36	UTX3	8/6/09	UTX random	51	71 55.815	167 23.351
35	UTX10	8/6/09	UTX random	48	71 40.150	166 55.039
37	CBL11	8/7/09	CBL	48	72 02.744	166 20.404
34	UTX6	8/7/09	UTX random	47	71 40.587	166 26.627
33	UTX9	8/7/09	UTX random overlap	44	71 34.123	165 46.127
44	CBL20	8/8/09	CBL	51	72 24.238	164 57.482
43	UTX1	8/8/09	UTX random overlap	41	72 03.702	164 07.836
38	UTX2	8/8/09	UTX random	53	71 55.614	165 09.650
32	UTX5	8/9/09	UTX random	47	71 23.759	164 06.542
31	CBL10	8/9/09	CBL	45	71 22.732	164 42.710
39	UTX5	8/9/09	UTX random overlap	40	71 42.117	164 30.898
45	CBL19	8/10/09	CBL	42	72 16.942	163 17.333
46	CBL18	8/10/09	CBL	28	72 06.989	162 03.279
42	UTX9	8/10/09	UTX random	45	71 44.311	162 06.210
40	UTX8	8/10/09	UTX random overlap	41	71 43.527	163 27.370

2009 Station Number	Station Name	Date Occupied	Station Type	Depth (m)	Latitude (°N)	Longitude (°W)
30	UTX11	8/11/09	UTX random overlap	47	71 27.180	162 36.643
47	CBL15	8/11/09	CBL	48	71 43.642	160 43.097
48	CBL14	8/11/09	CBL	54	71 22.610	159 28.066
50	CBL16	8/12/09	CBL	130	71 24.741	157 29.495

Table 2. Station listing for COMIDA010 on the RV Moana Wave in 2010. Key: Random=r and Phase 2=Ph2.

2010 Station Number	Station Code	Station Name	Date Occupied	Station Type	Station Origin	Depth (m)	Latitude (°N)	Longitude (°W)
1	101	BRS0	7/25/10	new	2010add	40	65 41.399	168 38.399
2	102	BRS5	7/25/10	new	2010add	52	65 43.440	168 57.419
3	103	DBO-UTN5	7/26/10	new	2010add	51	67 40.223	168 57.467
4	104	Red Dog Mine	7/27/10	new	2010add	16	67 33.731	164 10.674
5	105	detritus	7/27/10	new	2010add	53	68 58.428	168 56.693
6	1	CBL1	7/28/10	CBL	2008	37	69 02.382	166 35.610
7	106	CBL2-8	7/28/10	new	2010add	48	69 53.112	167 44.237
8	107	CBL8-3	7/29/10	new	2010add	46	70 05.147	166 27.324
9	5	CBL6	7/29/10	CBL	2009r	42	70 24.287	164 28.937
10	4	CBL5	7/29/10	CBL	2008	26	70 01.386	163 45.671
11	6	UTX29	7/30/10	UTX	2009r	44	70 20.705	165 27.023
12	1016	K3	7/30/10	2009-2	2010add	42	70 42.611	165 15.162
13	11	CBL7	7/30/10	CBL	2008	40	70 43.967	165 59.802
14	19	UTX23	7/30/10	UTXr	2009r	46	71 01.667	166 57.162
15	10	UTX27	7/31/10	UTXr	09r	52	70 40.278	167 04.992
16	9	CBL4	7/31/10	CBL	2008	56	70 49.884	167 47.202
17	22	UTX17	7/31/10	UTXr	2009r	47	71 16.325	167 00.8634
18	24	UTX16	8/1/10	UTXr	2009r	42	71 14.952	165 26.873
19	15	UTX19	8/1/10	UTXr	2009r	43	71 01.278	164 15.300
20	1014	ICP1	8/1/10	new	2010add	45	70 50.399	163 17.459
21	50(51)	CBL16	8/2/10	CBL	08Plan	127	71 24.815	157 29.489
22	48	CBL14	8/3/10	CBL	09new	52	71 22.607	159 28.068
23	49	CBL17	8/4/10	CBL	09new	52	71 46.044	159 22.379
24	47	CBL15	8/4/10	CBL	09new	46	71 43.643	160 43.098
25	109	HS2	8/4/10	new	2010add	31	72 06.228	161 11.370
26	46	CBL18	8/5/10	CBL	2009	27	72 06.990	162 03.281
27	108	HSH1	8/5/10	new	2010add	38	72 06.035	162 58.524
28	1013	HS3	8/5/10	new	2010add	41	71 55.998	162 40.079
29	41	UTX4	8/5/10	UTX/CBL	2009r	42	71 42.419	162 28.919
30	30	UTX11	8/5/10	UTX/CBL	2009r	45	71 27.179	162 36.642

2010 Station Number	Station Code	Station Name	Date Occupied	Station Type	Station Origin	Depth (m)	Latitude (°N)	Longitude (°W)
31	40	UTX8	8/6/10	UTX/CBL	2009r	39	71 43.529	163 27.371
32	39	UTX5	8/6/10	UTX/CBL	2009r	38	71 42.119	164 30.900
33	38	UTX2	8/6/10	UTXr	2009r	41	71 55.613	165 09.648
34	1030	n/a	8/6/10	new	2010add	45	72 06.198	165 27.335
35	37	CBL11	8/7/10	CBL	09new	47	72 2.7414	166 20.405
36	36	UTX3	8/7/10	UTXr	2009r	50	71 55.817	167 23.351
37	35	UTX10	8/7/10	UTXr	2009r	47	71 40.151	166 55.037
38	21	CBL8	8/7/10	CBL	2008Plan	49	71 29.082	167 46.902
39	20	UTX21	8/8/10	UTXr	2009r	49	71 12.402	168 08.678
40	1010	WR1	8/10/10	new	2010add	53	71 16.169	160 42.941
41	29	CBL13	8/10/10	CBL	2008	49	71 17.891	161 41.321
42	1015	B12	8/11/10	2009-Ph2	2010add	45	71 15.047	163 11.808
43	14	CBL9	8/16/10	CBL	2008Plan	42	70 31.658	162 06.506
44	27	CBL12	8/16/10	CBL	2008	52	70 54.919	160 10.946

Infauna for the caloric study (Lisa Wilt, MS student) were collected using either a single or double van Veen grab and sieved through 1-mm screens. Additional epibenthic fauna were collected from benthic trawls undertaken by Brenda Konar's group. Animals large enough for caloric analysis were identified taxonomically (to phylum or class), frozen and transported back to CBL for post-cruise processing. Samples for caloric studies were prepared to reflect the portion of the animal that would typically be consumed by a predator such as a walrus. For example, worms and other soft bodied animals were used whole, while bivalves and gastropods were removed from their shells. These samples were dried in an oven at 80 °C until constant weight was achieved, and then ground into powder using a tissue grinder. Ground samples were pelletized using a pellet press and combusted in a Parr Bomb Calorimeter. Either a large or micro bomb was used depending upon the amount of sample available (1-3 g samples for large bomb, 0.1-0.5 g samples for the micro bomb). Replicates were conducted for each sample until a percent difference less than 2% in measured energy was achieved.

Data analysis of biotic and abiotic parameters

PRIMER statistics

Benthic infaunal communities and various environmental, or abiotic, variables were analyzed after the COMIDA2009 and COMIDA2010 cruises using the PRIMER statistical package (v.6, Clarke and Gorely, 2006). Some details on the configuration of the statistical tests performed are provided below.

From the benthic infauna samples, measures of abundance and gC biomass were computed and arrayed into biotic data matrices. Environmental data were similarly arrayed into data matrices. Exploratory analysis sought to find structural patterns within the benthic infaunal assemblages as influenced by simultaneously-measured environmental variables. Biotic variables arranged in the

abundance and biomass arrays underwent 4^{th}-root transformations to account for bias from super-abundant groups or groups with individuals of high mass.

Environmental data were evaluated after analysis in an expectation maximum likelihood algorithm to account for data that we were not able to collect at every site. Variables with too few samples to run through the algorithm were removed. Initial plots of the variables were used as a tool to identify variables with large skew and high co-linearity. Skew was then factored out through the log-transformation of the relevant variables. Resemblance matrices, also known as similarity matrices, were then computed for the biotic and environmental data. The resemblance metric, or measure of similarity used for the biotic data was the Bray-Curtis index while Euclidean distance was used for the environmental array.

From the biotic resemblance matrices, non-metric multi-dimensional scaling (NMMDS) plots were generated, along with dendrograms that provided the basis for cluster overlays for the NMMDS plots. Hierarchical clustering of the biotic arrays was based on the group average agglomerative clustering method. The clusters produced were validated using a randomization test of a similarity profile based on the resemblance matrix of a biotic array.

A number of exploratory statistical tests were employed to look for relationships between the arrays of biotic and abiotic variables. To establish that a relationship existed Mantel tests were run against the environmental and biotic data that then produced Spearman correlation coefficients. Bio-Env routines, which select combinations of variables of one data array that best correlates with variables of another array, identified environmental variables that best accounted for the structure observed in the biotic data arrays. The correlations computed were evaluated using a permutation test to determine level of statistical significance.

Data Analysis-Lisa Wilt caloric study

The caloric component of the study (M.S. student Lisa Wilt) used the open source statistical software R for analysis. Replicate energy values (caloric content) for each taxon at each station were averaged once a 2% difference level was achieved. Analysis of variance (ANOVA) was used for partitioning of variance into components causing potential variation in order to compare measured energy values and consequently to identify the potential drivers of spatial variation. The energy measured for each taxon was used as the response variable, and a number of explanatory variables were included in the ANOVA. Categories of animals (class) were used as an explanatory variable instead of strict taxonomic classifications which would otherwise increase the degrees of freedom and lead to overfitting the model. Depth was also considered, as it reflects upon the amount of primary production reaching the benthos, which is the major food source for macroinvertebrate infauna. Location descriptors including station and distance offshore were also used as explanatory variables. Homogeneity of variance and normality tests including Bartlett, network cross-validation, Anderson-Darling, Cramer-von Mises, Lilliefors, Pearson, and Shapiro Francia were used to test the ANOVA assumptions of homogeneity of variance and normality of residuals. To highlight which levels of the explanatory variables included in the model were significant, a Tukey Honestly Significant Difference test was performed on the final linear model.

These data will ultimately be used to assess food prey resources available to Pacific walrus that forage in the Bering and Chukchi Seas. We compared our new calculated caloric values for the Chukchi walrus prey field to those measured in the 1970s by Sam Stoker (Stoker, 1981); taxonomically, samples were grouped taxonomically by family. Normality (Anderson-Darling, Cramer-von Mises, Lilliefors, Pearson, and Shapiro Francia) and homogeneity of variance (Bartlett, Fligner) tests were applied to the paired differences between the data sets before a paired T-test was performed to test the null hypothesis that there is no difference between the means of the historic values and the newly calculated values.

Results and Discussion

Water column

Overall the nutrient and chlorophyll profiles indicate summer, post-production conditions in the COMIDA region in the central and northern Chukchi Sea for both 2009 (Figure 5) and 2010 (Figure 6). Chlorophyll values were low in the surface waters (<1 ug/L), with highest values at mid-depth or near the bottom of the water column (1-3 ug/L) in 2009.

In 2010, higher chl *a* levels occurred both at mid-depth and near-bottom in offshore sites, with values reaching 15-20 ug/L at some stations (Figure 6, e.g., stn 103/DBO-UTN5, 49-CBL 17). The earlier season ice retreat in 2010 may have allowed more water column chlorophyll production to occur, which settled downwards to the benthos, a characteristic common for the Chukchi Sea (Grebmeier, 2012; Grebmeier et al., 2006b; Hill and Cota, 2005). Coincidently, nutrient values were drawn down in surface waters for most stations in both years due to earlier season primary production, with highest values in bottom waters (Figures 5 and 6). We observed an overall pattern of lower chlorophyll values in the spatial integrated maps in 2009 (Figure 7a) compared to the noticeably higher integrated chl *a* values in 2010 (Figure 7b).

Sediments

The sediments of the Chukchi Sea are good indicators of export production of phytoplankton to the underlying sediments (Figure 8 a, b). Higher chl *a* values in surface sediments in the offshore waters of the northern Chukchi Sea occur under Anadyr water compared to lower values in nearshore coastal water influenced by Alaska Coastal water.

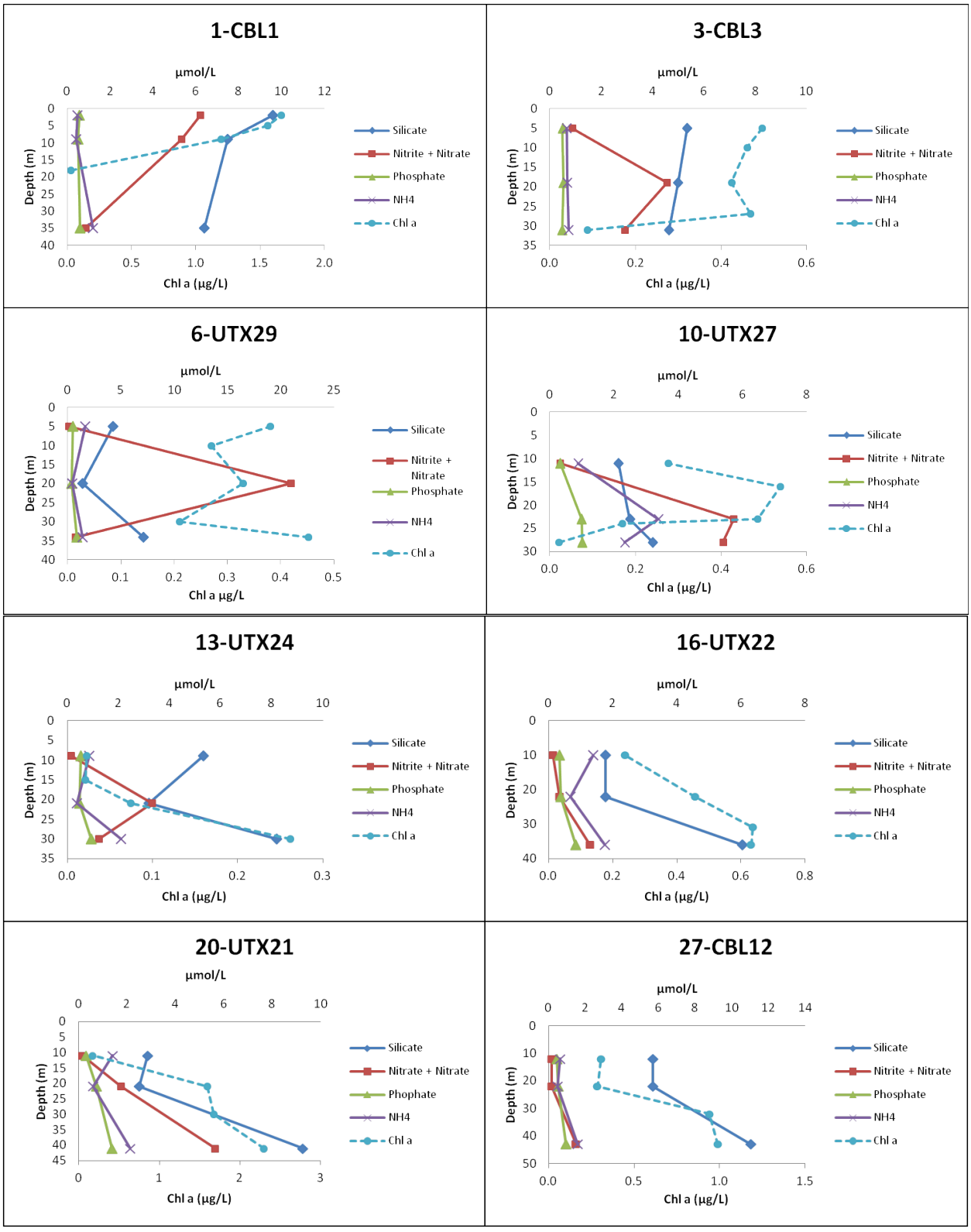
1-CBL1
µmol/L
Depth (m)
Chl a (µg/L)
3-CBL3
µmol/L
Depth (m)
Chl a (µg/L)
6-UTX29
µmol/L
Depth (m)
Chl a µg/L
10-UTX27
µmol/L
Depth (m)
Chl a (µg/L)
13-UTX24
µmol/L
Depth (m)
Chl a (µg/L)
16-UTX22
µmol/L
Depth (m)
Chl a (µg/L)
20-UTX21
µmol/L
Depth (m)
Chl a (µg/L)
27-CBL12
µmol/L
Depth (m)
Chl a (µg/L)
Silicate
Nitrite + Nitrate
Phosphate
NH4
Chl a

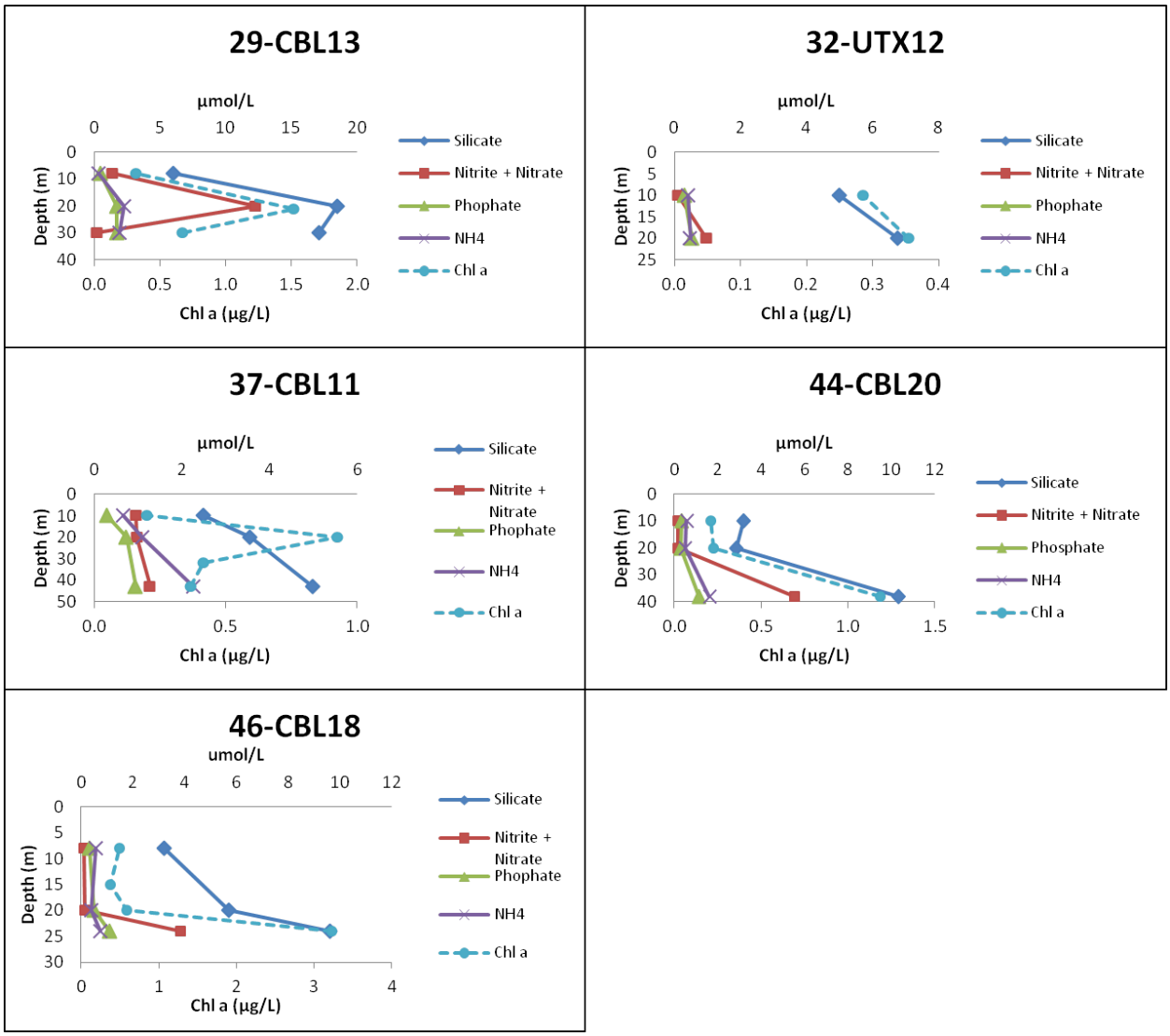

Figure 5. Water column nutrient levels nitrate/nitrite, phosphate, silicate, and ammonium at the daily process stations collected during COMIDA 2009.

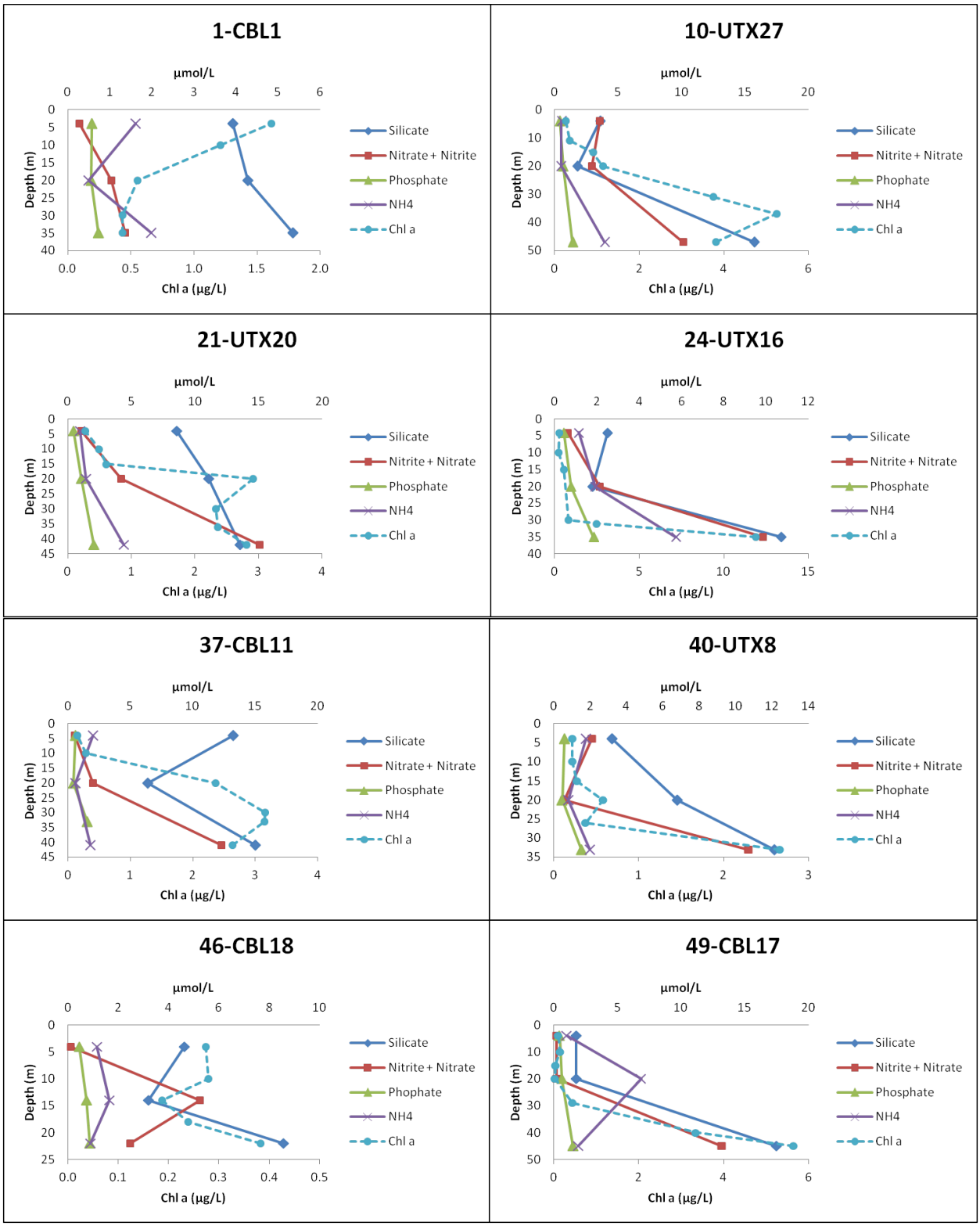
1-CBL1
µmol/L
Depth (m)
Chl a (µg/L)
Silicate
Nitrate + Nitrite
Phosphate
NH4
Chl a
10-UTX27
µmol/L
Depth (m)
Chl a (µg/L)
Silicate
Nitrite + Nitrate
Phophate
NH4
Chl a
21-UTX20
µmol/L
Depth (m)
Chl a (µg/L)
Silicate
Nitrite + Nitrate
Phosphate
NH4
Chl a
24-UTX16
µmol/L
Depth (m)
Chl a (µg/L)
Silicate
Nitrite + Nitrate
Phosphate
NH4
Chl a
37-CBL11
µmol/L
Depth (m)
Chl a (µg/L)
Silicate
Nitrate + Nitrate
Phosphate
NH4
Chl a
40-UTX8
µmol/L
Depth (m)
Chl a (µg/L)
Silicate
Nitrite + Nitrate
Phophate
NH4
Chl a
46-CBL18
µmol/L
Depth (m)
Chl a (µg/L)
Silicate
Nitrite + Nitrate
Phophate
NH4
Chl a
49-CBL17
µmol/L
Depth (m)
Chl a (µg/L)
Silicate
Nitrite + Nitrate
Phosphate
NH4
Chl a

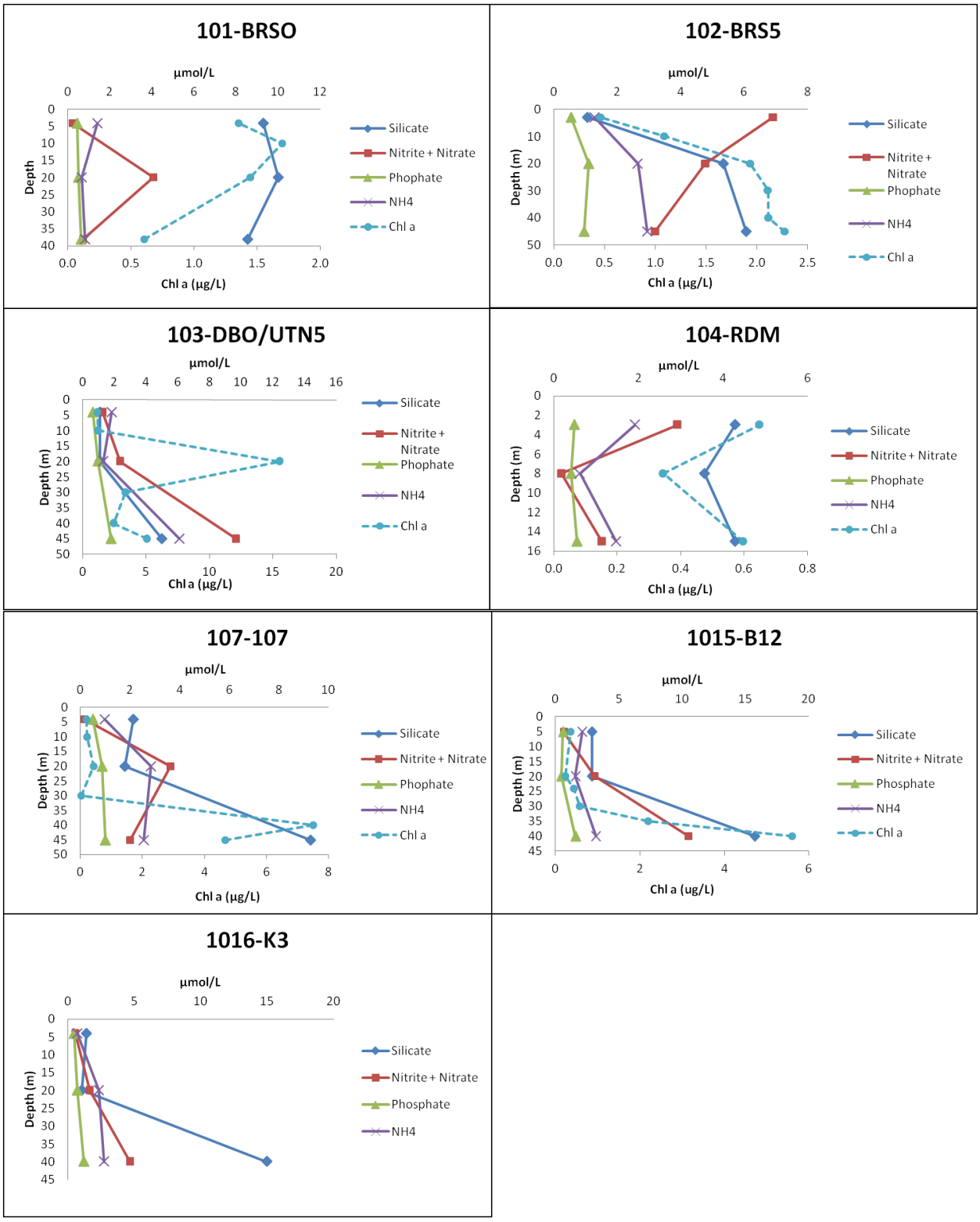

Figure 6. Water column nutrient levels nitrate/nitrite, phosphate, silicate, and ammonium at the daily process stations collected during COMIDA 2010.

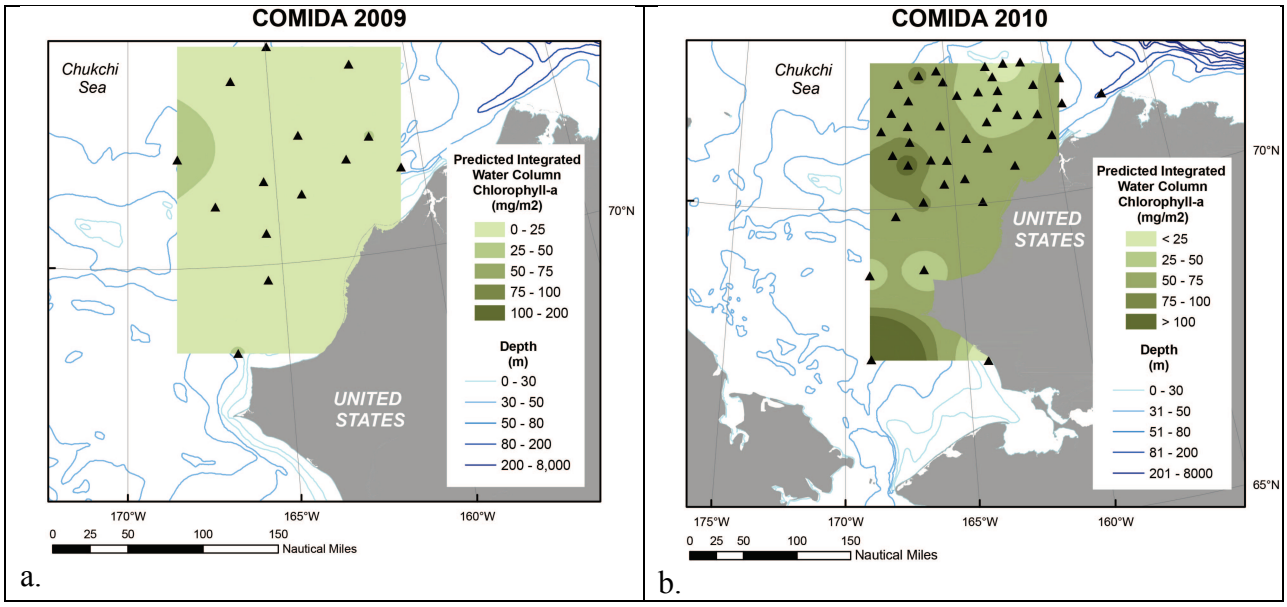

Figure 7. Spatial distribution of water column chlorophyll *a* during a. COMIDA09 and b. COMIDA10 on an integrated square meter basis.

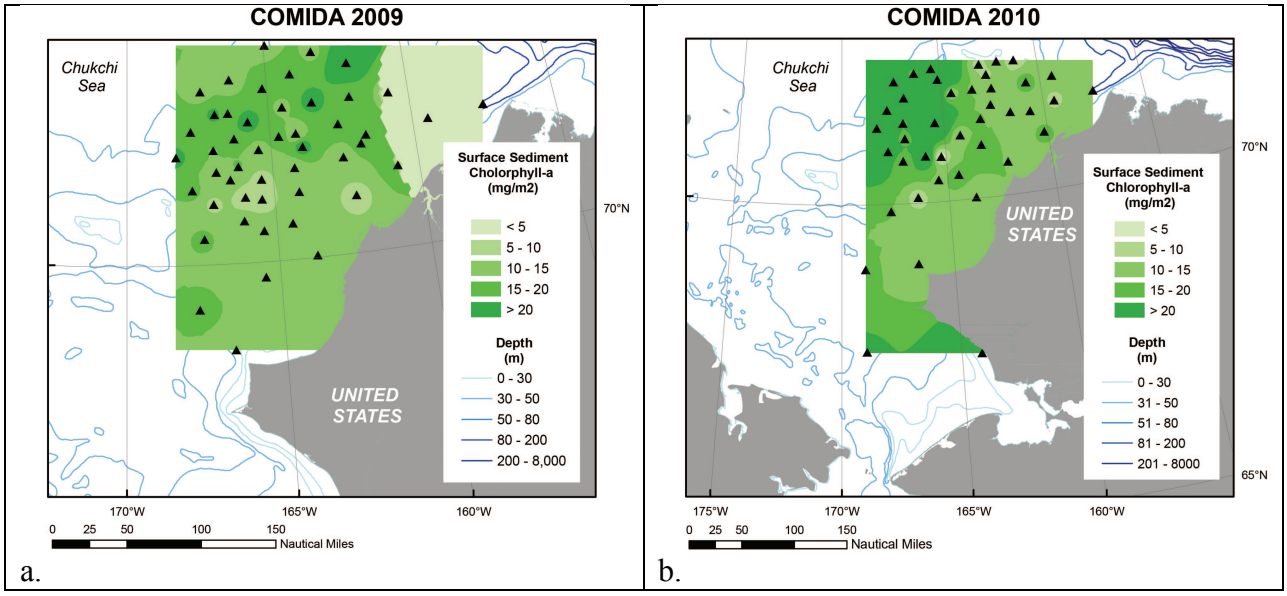

Figure 8. Spatial distribution of a. surface sediment chlorophyll a (chl *a*) during a. COMIDA09 and b. surface sediment chl *a* during COMIDA10.

Surface sediment total organic carbon (TOC) content is highest in offshore waters of the northern Chukchi Sea and in the northeast section of the Chukchi Sea near upper Barrow Canyon (Figure 9a, b). Similarly, the surface sediment silt and clay content (≥5 phi) indicates deposition in offshore waters in the northern Chukchi Sea as well as in the northeast sector near the head of Barrow Canyon (Figure 9c, d).

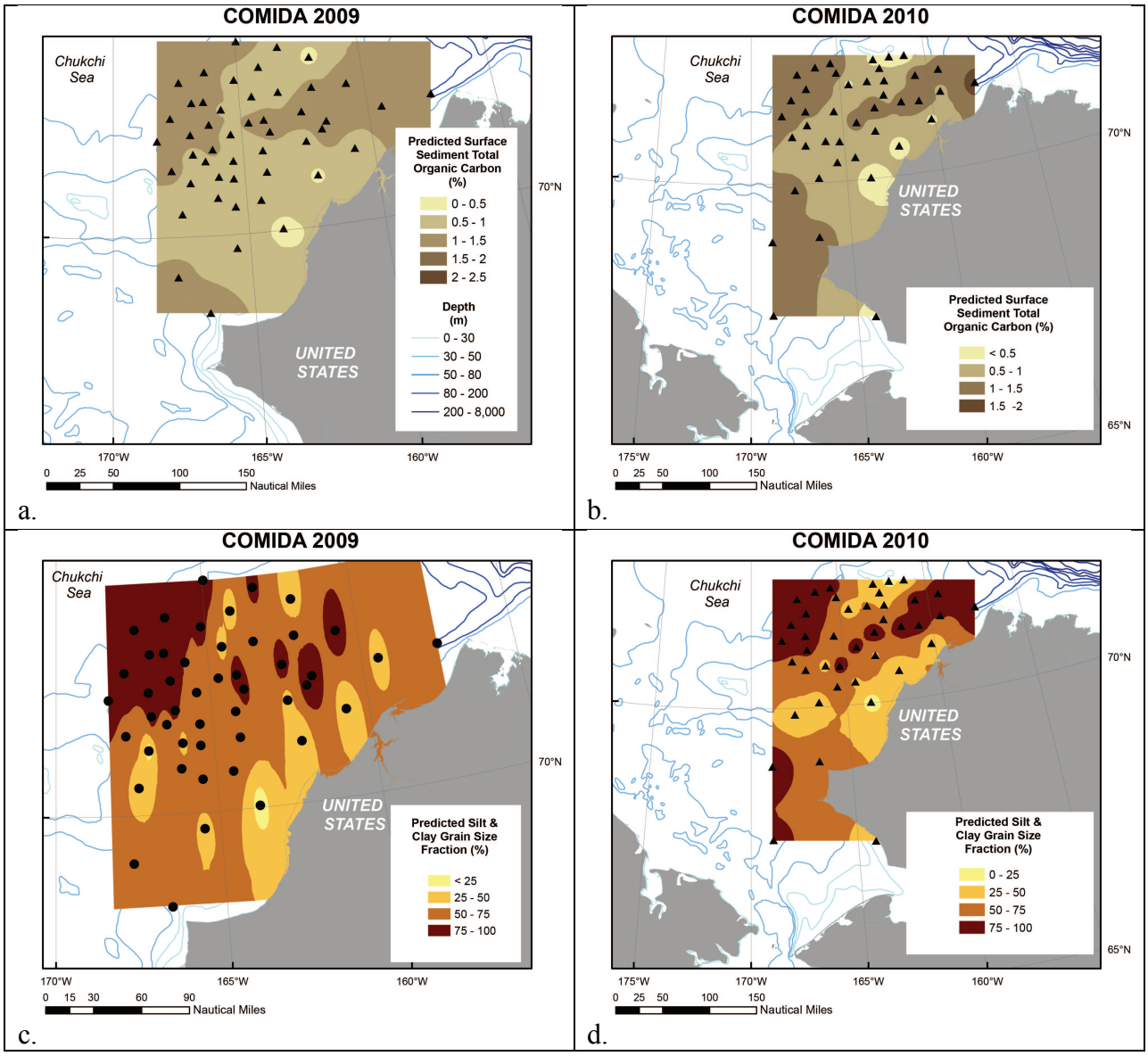

Figure 9. Distribution of total organic carbon (TOC) in a. 2009 and b. 2010 coincident with silt and clay contact (≥5phi) in c. 2009 and d. 2010.

The C/N ratios of surface sediments provide a qualitative indication of the lability of the phytodetritus and organic matter settling to the benthos. Stations in the southern COMIDA study region have higher C/N values, indicative of a more terrigenous signal (Figure 10). By comparison, sampling in the northcentral region of the Chukchi Seas in both years indicates higher quality organic matter, perhaps as a consequence of the higher chl *a* content in both the water and sediments (Figure 7b and Figure 8a,b). Comparison of the sediment C/N with stable C and N isotope analysis undertaken by the University of Texas (Dunton) component will help test the hypothesis of a more nutrient-rich carbon base in the northern Chukchi Sea, which could be related to a higher percentage of sea ice algal input to the total phytoplankton base descending to the benthos.

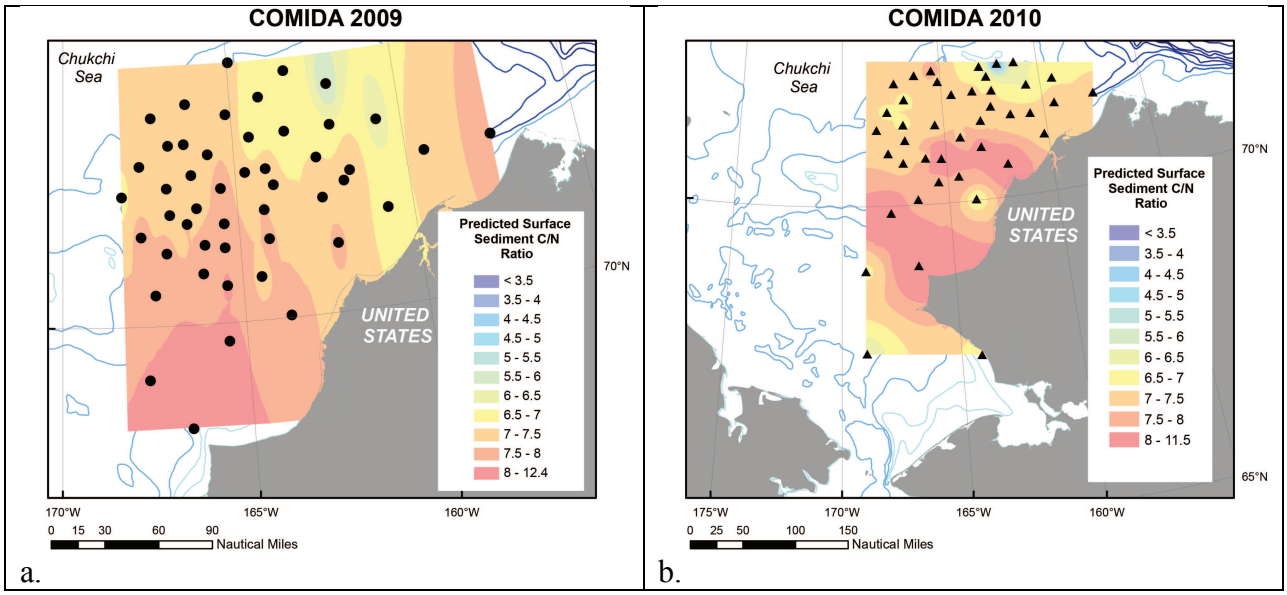

Figure 10. Distribution of surface sediment carbon/nitrogen content (C/N) in a. 2009 and b. 2010.

Sediment community oxygen consumption (SCOC) provides an indication of carbon supply to the benthos on shallow continental shelves like the Chukchi Sea (Figure 11a.). The limited sampling in 2010 indicates the highest level of SCOC (~30 mmol $O_2/m^2/d$) in the southeast Chukchi Sea "hotspot" [Distributed Biological Observatory (DBO) site UTN5] and sites in the northern Chukchi Sea (Figure 11b.), both regions of higher integrated chlorophyll *a* (Grebmeier et al., 2006b, Fig. 7b). The distribution of total biomass (gC/m^2) in the region also reflects the similar pattern of high benthic biomass in the southeastern Chukchi Sea and the northern portion of the Chukchi Sea (Figure 11 c., d.). The highest benthic biomass in the Chukchi Sea observed during the COMIDA field years was in upper Barrow Canyon (Figure 11d.), which is a similar finding to previous studies over the past decade (Fig. 11c, see Grebmeier, 2012).

For both years of sampling, the dominant macrobenthic infauna taxa by abundance are bivalves, polychaetes and amphipods across the COMIDA study area (Figure 12). For biomass (both g wet wt and g C/m^2), bivalves, polychaetes and sipunculids were the dominant macrofauna (Figure 13a and b, respectively). Notably echinoids (specifically sand dollars *Echinarachnius parma*) were dominant by biomass in the nearshore Alaska Coastal water. The highest biomass for the study area was observed at the head of Barrow Canyon at DBO site BC2, just off Barrow, Alaska (see Figure 3).

We divided benthic community composition by class because it is useful for categorizing the 6 major faunal types over the COMIDA study area for each year. The top three dominant families (by percentage of stations totals) for each station are identified in Table 3 and 4. Although the biomass figures and table present both g wet wt and gC values, for brevity we will discuss only biomass as gC dry weight as it more explicitly identifies the organic carbon content from an ecosystem perspective.

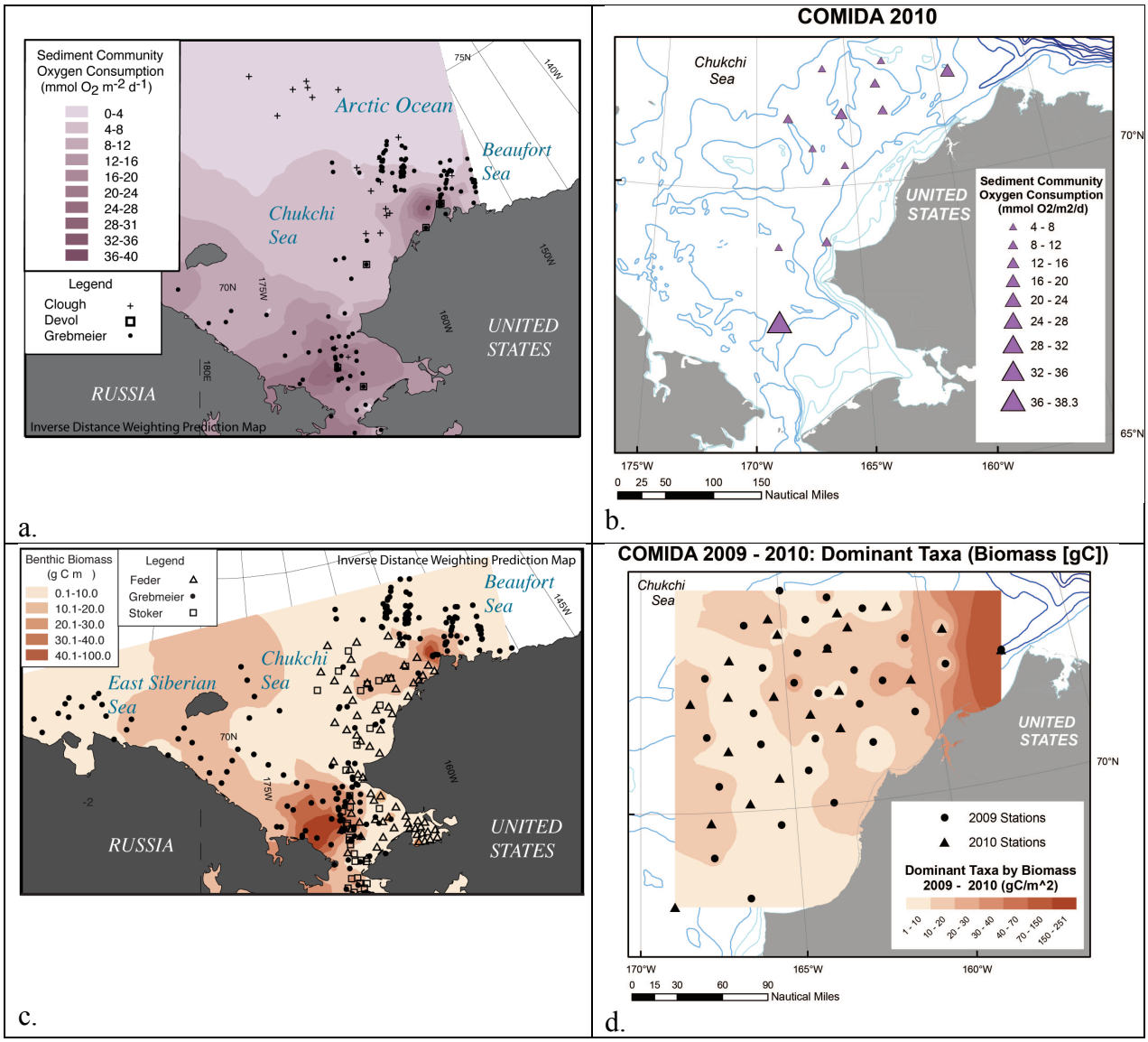

Figure 11. Distribution of a. sediment community oxygen consumption (SCOC) in the Chukchi Sea (modified from Grebmeier et al., 2006b) and b. SCOC collected during the 2010 COMIDA cruise. The bottom panel shows c. benthic biomass in the Chukchi Sea modified from Grebmeier et al. (2006b) and d. benthic biomass obtained in the COMIDA region in 2009 and 2010.

By abundance (individuals per square meter), the nearshore regions were dominated by nuculid and tellinid bivalves in both years, although mytelid mussels and cumaceans dominated the head of Barrow Canyon DBO hotspot (Figure 14a,b, Tables 3 and 4). Nuculanid and nuculid bivalves, capitellid, cirratulid, lubrinerid and oweniid polychaetes, phoxochephalid amphipods, and ostracods dominated the offshore areas. Notably the highest abundance occurred in a transect from off Wainwright to further offshore in the northcentral Chukchi Sea, dominated by ampeliscid and isaied amphipods and maldanid polychaetes in nearshore, shifting to nuculid and nuculanid bivalves and cirratulid polychaetes offshore. Also, areas around Hanna Shoal were dominated by sabellid polychaetes (a suspension feeder).

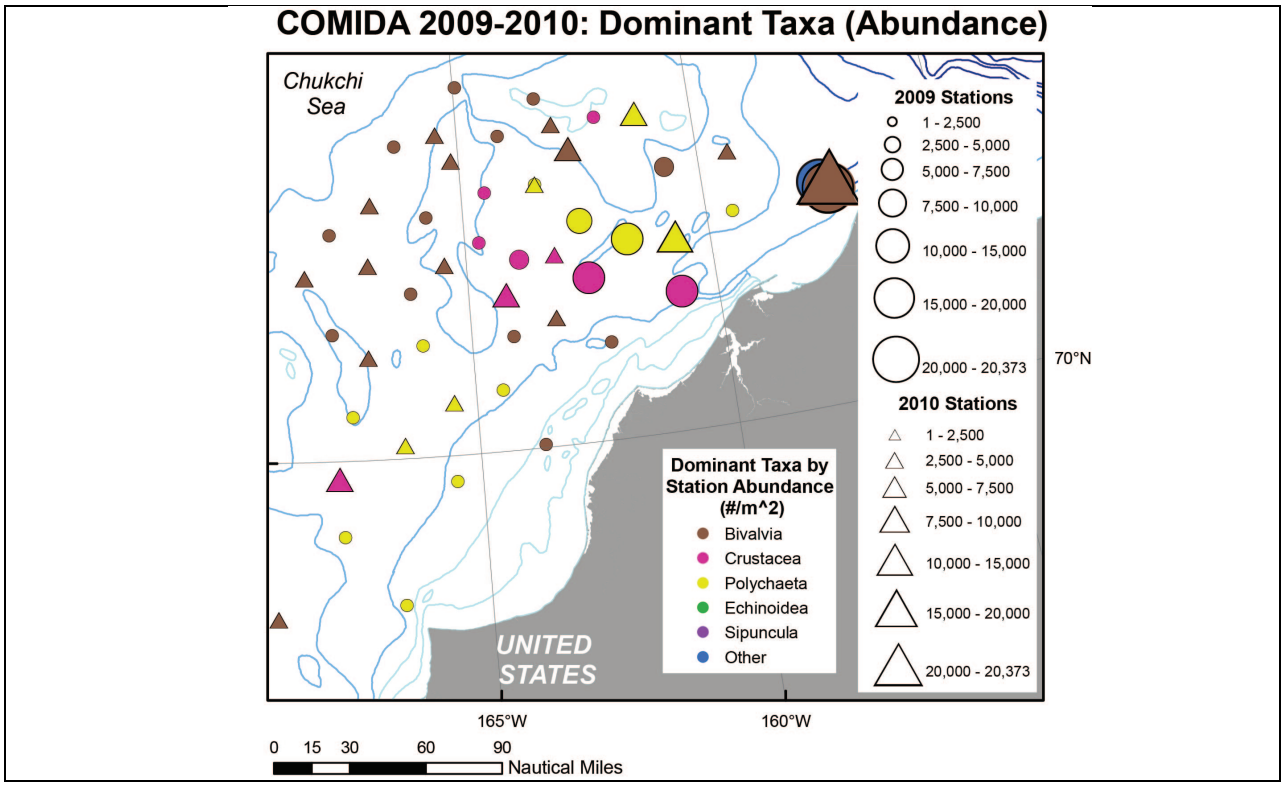

Figure 12. Distribution of dominant taxa by station macroinfaunal abundance for COMIDA09 and COMIDA10.

For biomass, the nearshore areas were dominanted by nephtyid and maldanid polychaetes, echinarachniid enchinoids (sand dollars), and ampeliscid ampipods (Figure 14a c, d, e, f, Tables 3 and 4). Moving offshore, nephtyid and maldanid polychaetes and sipunculids dominated biomass whereas the more offshore regions were dominated by nuculanid, nuculid and tellinid bivalves, and maldanid and nephtyid polychaetes. One station was dominated by ampeliscid amphipods in the central region, and pyurid tunicates dominated around some Hanna Shoal stations.

Results: Benthic macroinfauna

Clustering of the family macroinfaunal data identified seven major groupings at the 60% similarity level, along with 5 individual stations that didn't cluster with any other groups (Figures 17a,b and 18). Cluster group 1 of 3 stations was dominated by nuculanid bivalves and cirratulid polychaetes. Cluster group 2, composed of two stations west of Hanna Shoal, was also dominated by cirratulid polychaetes, but nuculid bivalves were the other dominant infauna. Cluster group 3 located south of Hanna Shoal was dominated by nuculid and nuculanid bivalves. Cluster group 4, one of the two largest cluster groups and found in the most offshore waters, was dominated by nuculid and nuculanid bivalves and maldanid, cirratulid, and capitellid polychaetes. Cluster group 5 along the southern portion of the Alaska coast was dominated by

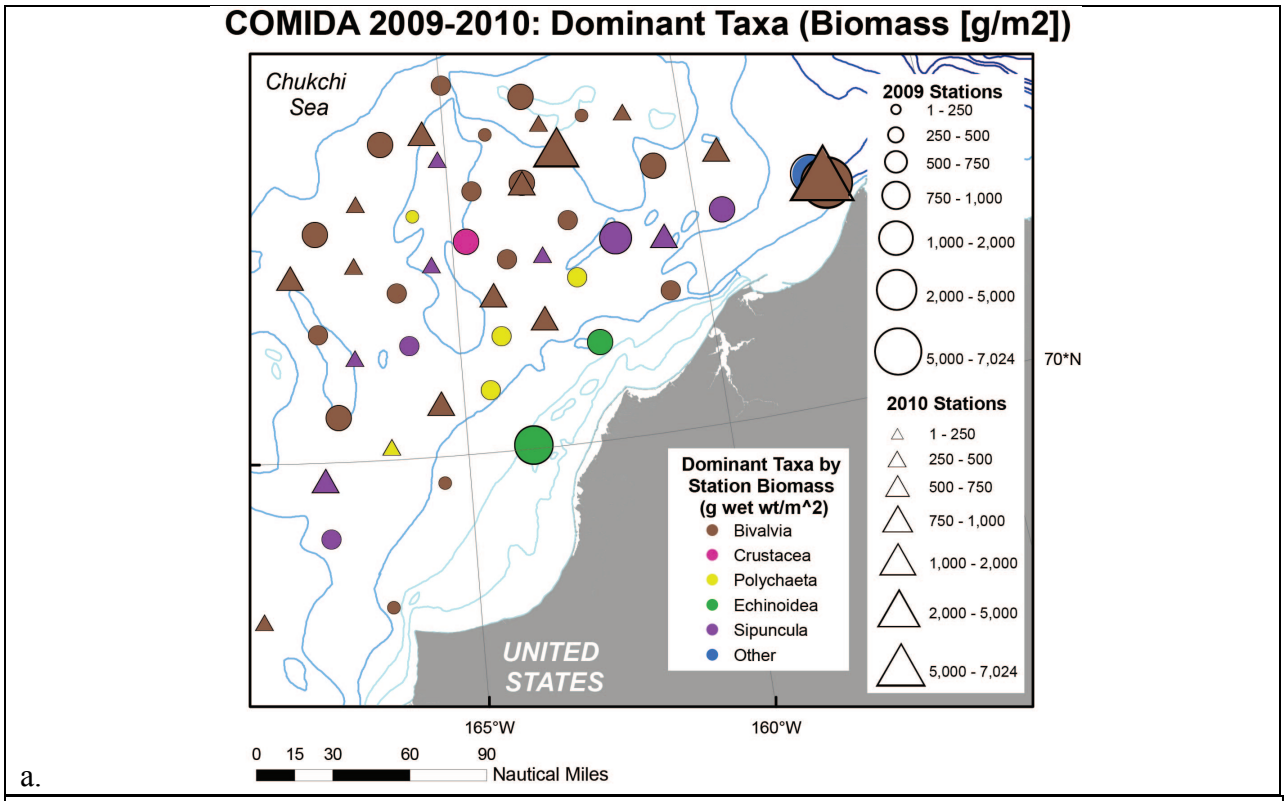

a.

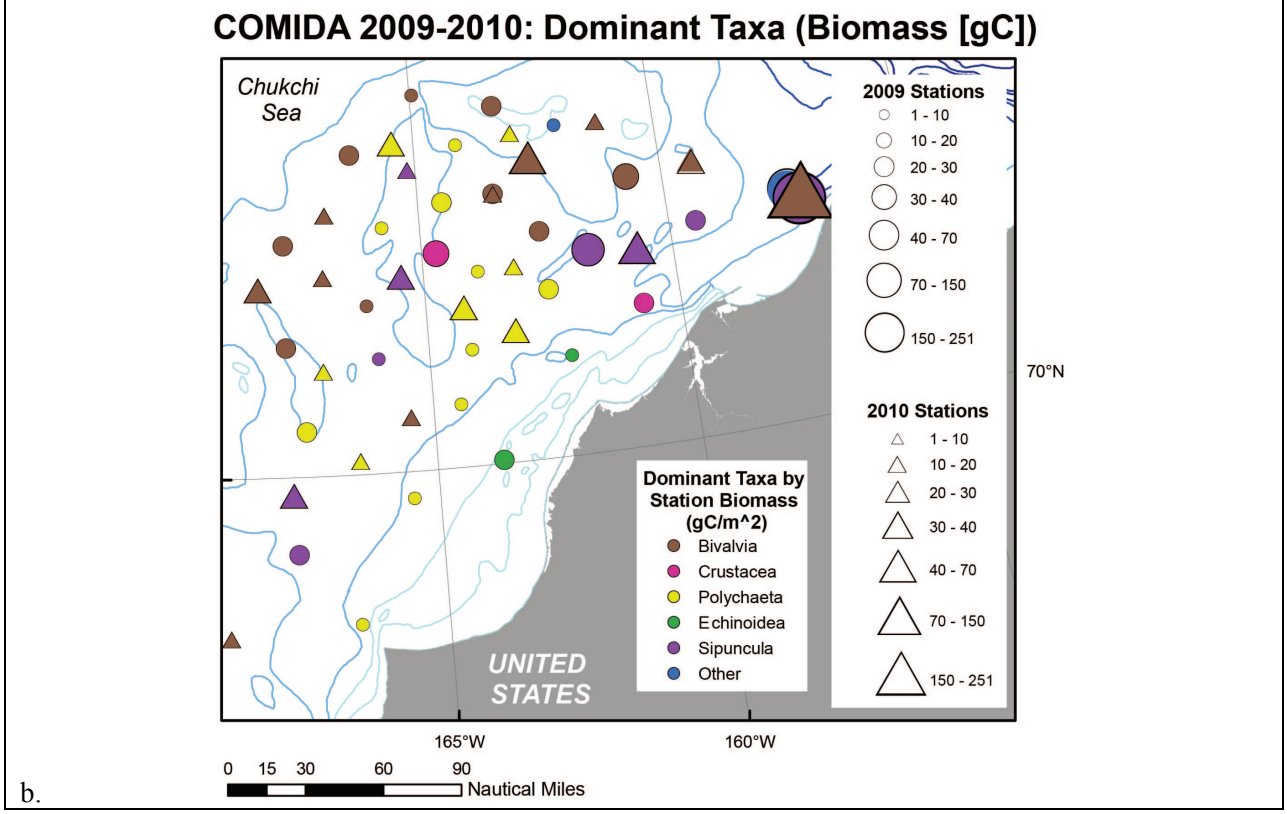

b.

Figure 13. Distributon of dominant macrobenthic fauna and station biomass by: a. wet weight biomass (g wet wt/m^2) and b. gram carbon dry weight (gC/m^2).

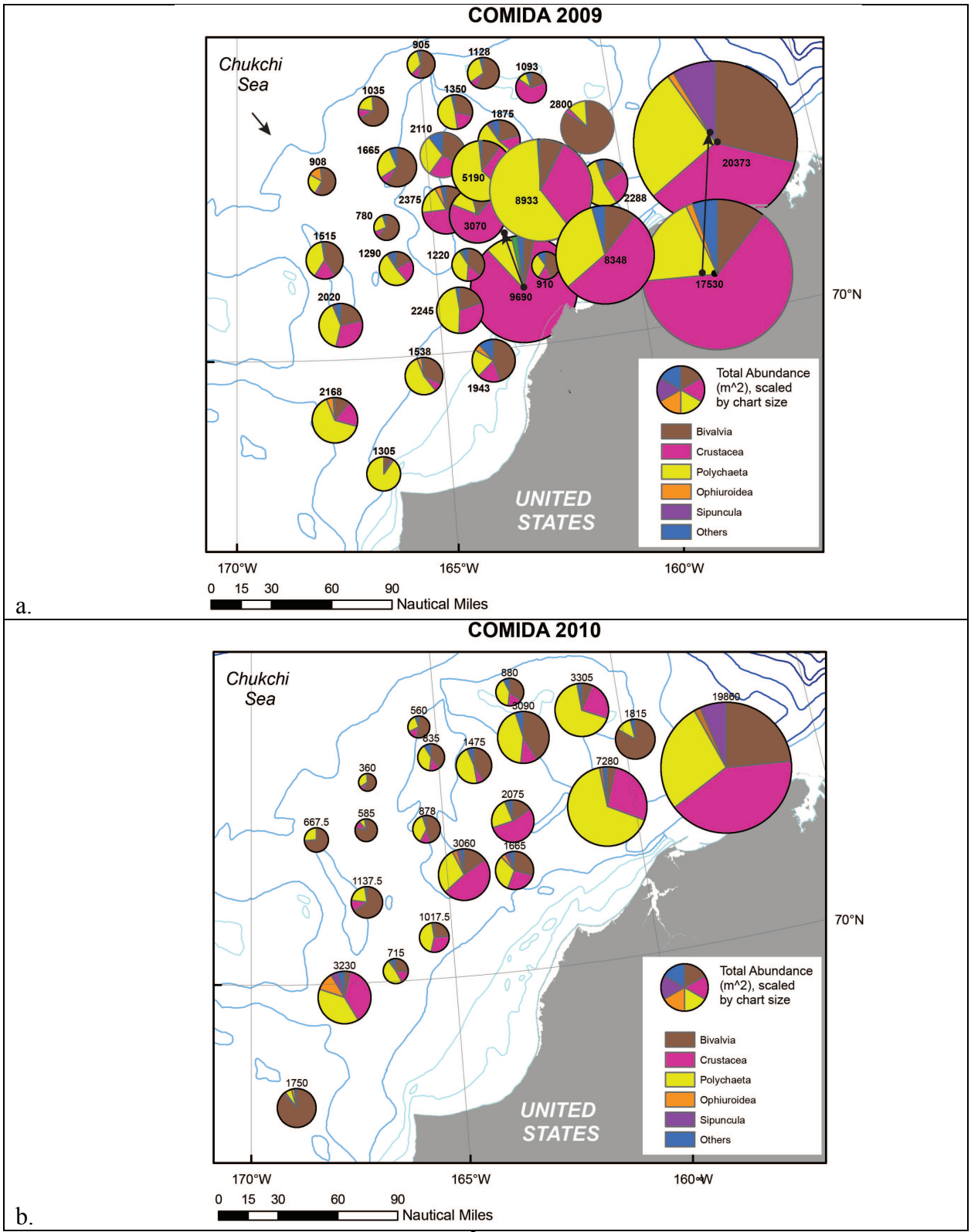

Figure 14. Distribution of abundance (no m^{-2}) of dominant taxa type during a. COMIDA2009 and b. COMIDA10. Total station abundance values provided numerically on the graph.

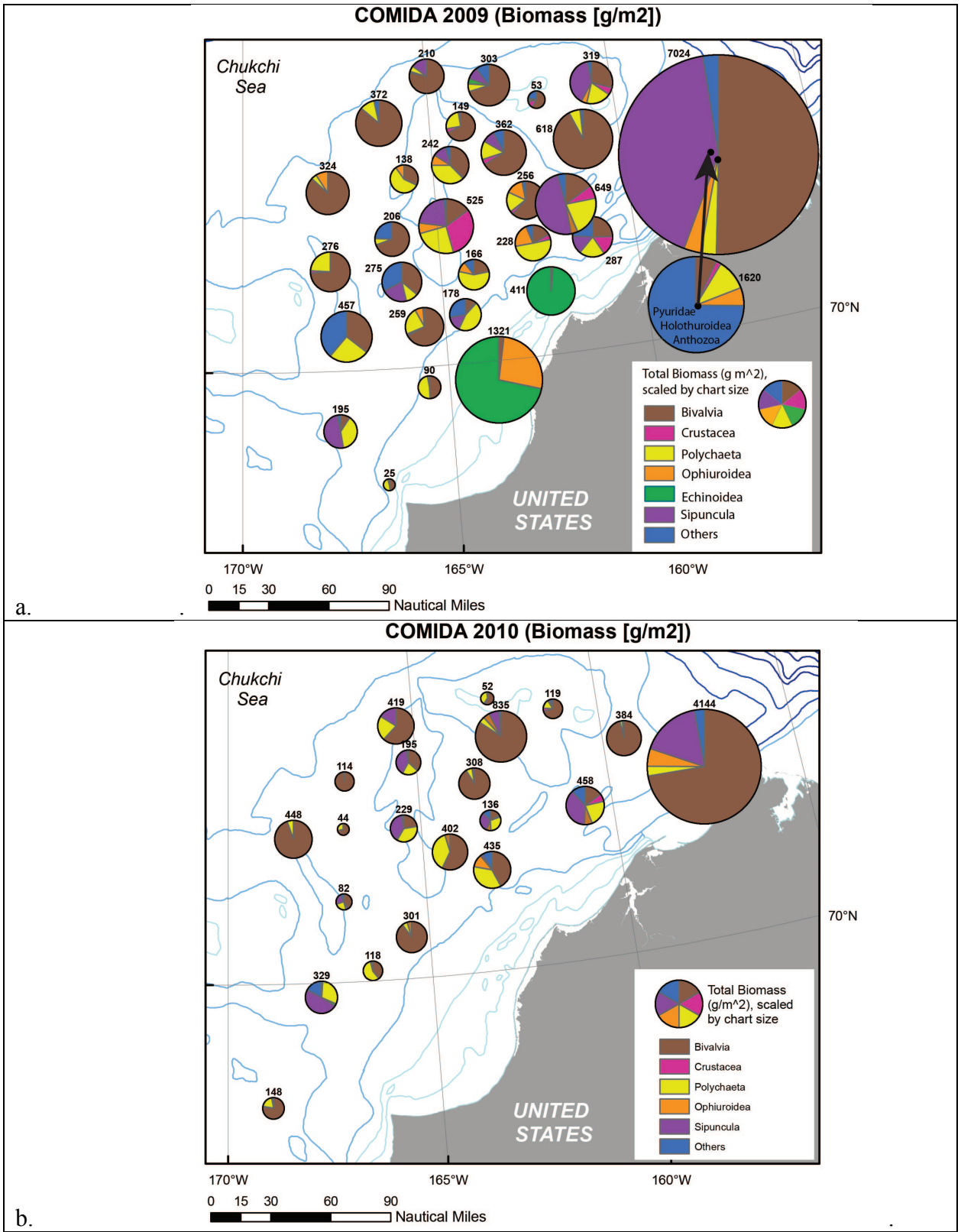

Figure 15. Distribution of benthic infaunal biomass (g wet wt/m^2) by dominant taxa type during (a) COMIDA2009 and (b) COMIDA2010. Note that when the "other" category >50%, the dominant fauna are listed. Total station abundance values are provided numerically on the graph.

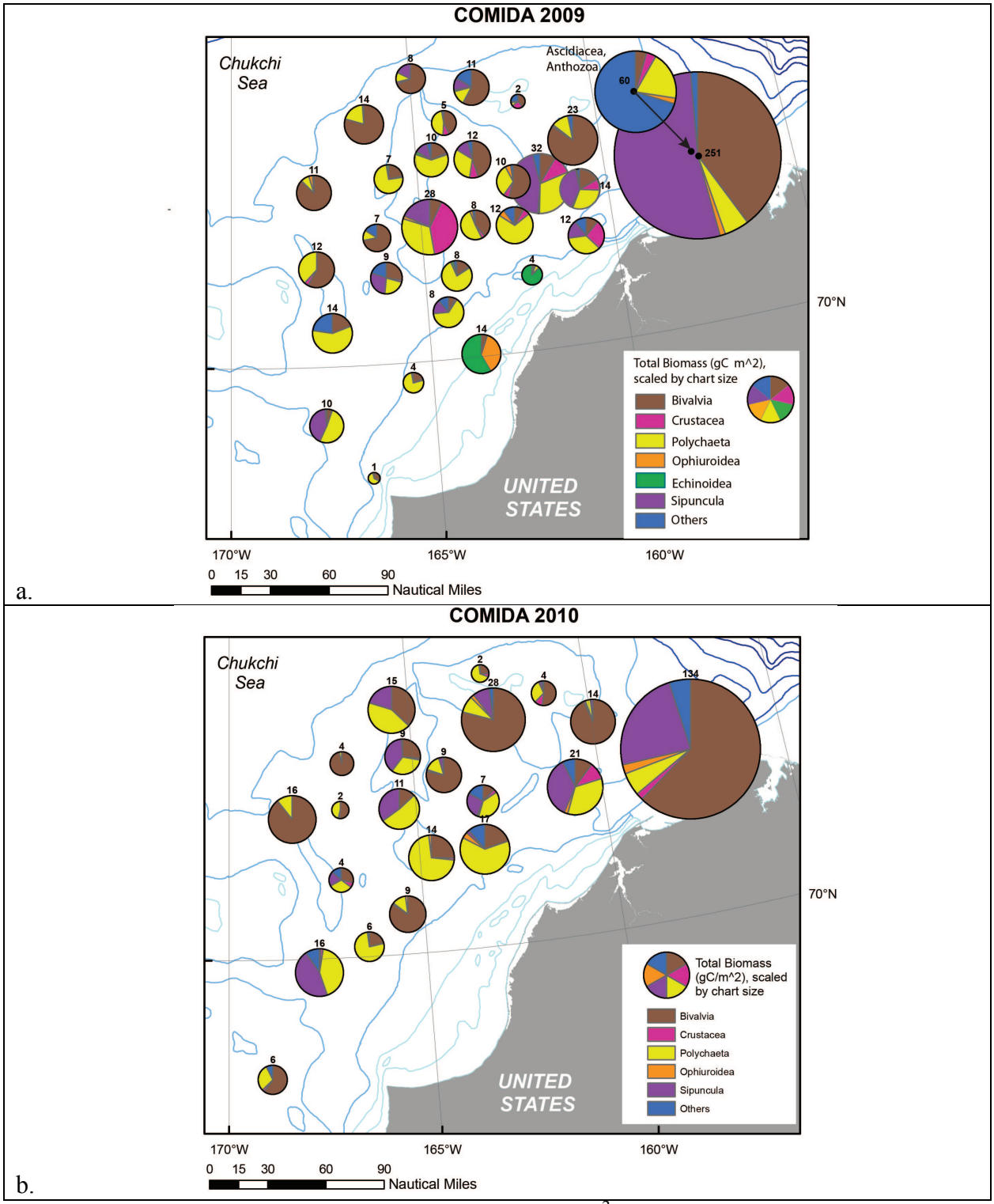

Figure 16. Distribution of benthic biomass (g C m^{-2}) by dominant taxa type during a. COMIDA2009 and b. COMIDA2010. Note that when the "other" category >50% (COMIDA2009), only the dominant fauna are listed. Total station biomass values are provided numerically on the graph.

Table 3. Summary of dominant infaunal abundance and biomass for COMIDA2009 and listing of the top 3 faunal types by percent of total station abundance and biomass (both wet weight (Wt, g/m^2) and carbon dry weight (gC/m^2).

Stn #	Stn. Name* *=2 grabs	Abundance (#/m²)	Biomass (g/m²)	Biomass (gC/m²)	Taxa (#)	Abundance: (#/m²)	%	Wet Wt Biomass: (g/m²)	%	Biomass: (gC/m²)	%
1	CBL1	1305	24.58	1.20	27	Cirratulidae	52.9	Nuculanidae	24.4	Nephtyidae	35.4
						Cossuridae	10.2	Nephtyidae	24	Nuculanidae	16.4
						Capitellidae	8.6	Tellinidae	15.7	Tellinidae	9.9
2	CBL2	2168	195.43	10.25	49	Maldanidae	34.7	Sipunculidae	48.2	Sipunculidae	41.4
						Capitellidae	11.2	Maldanidae	22.4	Maldanidae	29.9
						Lampropidae	8.4	Capitellidae	5.2	Capitellidae	6.8
3	CBL3	1538	90.44	3.83	40	Cirratulidae	19.7	Astartidae	43.5	Nephtyidae	51.9
						Nuculidae	10.9	Nephtyidae	30.6	Astartidae	15.4
						Nuculanidae	8.0	Maldanidae	5.5	Maldanidae	9.1
4	CBL5	1943	1321.26	13.62	48	Tellinidae	17.4	Echinarachniidae	70.2	Echinarachniidae	54.5
						Cardiidae	9.3	Amphiuridae	26.5	Amphiuridae	36
						Echinarachniidae	8.4	Synaptidae	1.2	Carditidae	2.8
5	CBL6	2245	177.98	8.43	49	Capitellidae	19.7	Maldanidae	34.3	Maldanidae	50.8
						Isaeidae	12.1	Molgulidae	20.9	Sipunculidae	14.8
						Cirratulidae	10.4	Sipunculidae	15.6	Molgulidae	6.2
8	UTX30*	2020	456.84	14.11	52	Capitellidae	11.9	Astartidae	32.9	Maldanidae	48.9
						Nuculidae	9.2	Maldanidae	21.3	Astartidae	16
						Cirratulidae	8.7	Ectoprocta	14.2	Rhodosomatidae	6.6
9	CBL4	1515	276.36	11.52	30	Nuculidae	26.6	Tellinidae	54.6	Tellinidae	40.6
						Capitellidae	14.5	Nuculidae	14.2	Nephtyidae	20.1
						Lysianassidae	12.7	Nephtyidae	11.7	Nuculidae	13.3

						Lysianassidae	12.7	Nephtyidae	11.7	Nuculidae	13.3
11	CBL7	1290	274.74	8.98	57	Cirratulidae	16.7	Sipunuclidae	20.8	Sipunculidae	28.6
						Capitellidae	12.6	Rhodosomatidae	12.9	Maldanidae	10.2
						Nuculidae	8.5	Styelidae	12.7	Mytilidae	9.9
13	UTX24*	1220	166.31	8.37	38	Nuculidae	26.2	Maldanidae	50.7	Maldanidae	70.5
						Maldanidae	8.6	Ophiuridae	10.6	Nuculanidae	6.9
						Cirratulidae	7.8	Nuculanidae	10.5	Tellinidae	3.9
14	CBL9	910	411.29	3.69	42	Cardiidae	17	Echinarachniidae	97.5	Echinarachniidae	86.9
						Astartidae	8.5	Lumbrinereidae	0.4	Lumbrinereidae	4.2
						Echinarachniidae	8.0	Veneridae	0.3	Ampeliscidae	1.6
17	UTX20*	780	206.30	6.86	31	Nuculidae	35.3	Nuculanidae	49	Nuculanidae	48.6
						Nuculanidae	19.2	Synaptidae	24.2	Nuculidae	21.3
						Cirratulidae	6.4	Nuculidae	18.2	Synaptidae	15.3
21	CBL8	908	323.54	10.85	31	Nuculanidae	27.5	Nuculanidae	60.1	Nuculanidae	59.1
						Ophiuridae	15.2	Nuculidae	15.4	Nuculidae	18
						Nuculidae	13.5	Tellinidae	10.6	Tellinidae	9.8
25	UTX15*	3070	259.38	7.82	46	Ostracoda	38.8	Astartidae	58.8	Maldanidae	42.7
						Phoxocephalidae	19.1	Maldanidae	18.4	Astartidae	29.2
						Leuconidae	4.6	Ophiuridae	7	Nuculidae	6
26	UTX18*	9690	228.16	12.28	54	Isaeidae	69.8	Maldanidae	34.1	Maldanidae	44.4
						Phoxocephalidae	5.5	Ophiuridae	21.2	Lumbrinereidae	16.2
						Ostracoda	3.3	Lumbrinereidae	9.4	Reineidae	9.9
27	CBL12	8348	287.58	11.71	73	Ampeliscidae	20.3	Astartidae	20.3	Ampeliscidae	17.7
						Isaeidae	15.8	Molgulidae	16.1	Sipunculidae	16.3

						Cirratulidae	7.7	Sipunculidae	14.7	Maldanidae	8.8
29	CBL13	8933	649.44	31.79	61	Maldanidae	45.9	Sipunculidae	48.5	Sipunculidae	44.6
						Ostracoda	7.8	Maldanidae	17	Maldanidae	24.3
						Diastylidae	6.4	Ampeliscidae	5.8	Ampelliscidae	8.1
30	UTX11*	5190	255.89	10.16	44	Oweniidae	18.9	Nuculidae	32.2	Nuculidae	31.6
						Ostracoda	13.5	Tellinidae	23.4	Tellinidae	18.3
						Lumbrinereidae	13.3	Ophiuridae	15.1	Lumbrinereidae	8.6
31	CBL10	2375	524.73	27.96	56	Ostracoda	16.6	Ampeliscidae	30	Ampeliscidae	38.4
						Phoxocephalidae	10.7	Sipunculidae	21.7	Maldanidae	27.2
						Nuculidae	7.6	Maldanidae	20.7	Sipunculidae	18.3
33	UTX9*	1665	137.87	7.39	34	Nuculidae	36.9	Maldanidae	49.4	Maldanidae	64.5
						Thyasiridae	13.2	Nuculidae	19.8	Nuculidae	14.4
						Polynoidae	6.0	Nuculanidae	9.8	Nuclanidae	6
37	CBL11	1035	372.22	13.70	33	Nuculanidae	30.2	Nuculanidae	68	Nuculanidae	61
						Nuculidae	26.6	Nuculidae	13.8	Nuculidae	14.7
						Tellinidae	7.2	Nephtyidae	5.8	Nephtyidae	11.4
39	UTX5*	2110	242.02	10.35	44	Phoxocephalidae	18.5	Astartidae	22	Magelonidae	27.6
						Nuculidae	10.9	Magelonidae	17.1	Maldanidae	21.2
						Anthozoa	5.7	Maldanidae	13	Sipunuclidae	12.1
40	UTX8*	1875	361.92	12.24	43	Lumbrinereidae	13.3	Astartidae	36.4	Astartidae	16.2
						Cirratulidae	9.9	Tellinidae	16.6	Tellinidae	15.2
						Orbiniidae	7.5	Nuculanidae	10	Lumbrinereidae	14.4
43	UTX1*	1350	148.60	5.35	37	Nuculidae	11.1	Astartidae	39.1	Maldanidae	25.5
						Cirratulidae	8.1	Tellinidae	17.4	Astartidae	16.3

						Ampeliscidae	7	Maldanidae	13.1	Tellinidae	14.9
44	CBL20	905	209.72	7.85	39	Nuculanidae	32	Nuculanidae	54.6	Nuculanidae	48.1
						Nuculidae	13.5	Tellinidae	18.9	Sipunculidae	18.1
						Lumbrinereidae	9.4	Sipunculidae	15	Tellinidae	15.7
45	CBL19	1128	302.63	11.40	36	Nuculidae	31.5	Nuculanidae	38	Nuculanidae	33.3
						Nuculanidae	14.2	Telllinidae	15	Reineidae	14
						Cirratulidae	7.8	Sipunculidae	9.3	Tellinidae	12.4
46	CBL18	1093	52.67	1.77	41	Amphipoda	38.4	Astartidae	25.5	Pyuridae	22.7
						Ampeliscidae	9.6	Veneridae	24	Veneridae	20
						Corophidae	8.5	Pyuridae	18.6	Amphipoda	12.8
47	CBL15	2800	617.77	22.50	37	Nuculidae	64.1	Nuculidae	38.5	Nuculidae	41.2
						Nuculanidae	13.6	Nuculanidae	28.4	Nuculanidae	25.7
						Cirratulidae	5.0	Tellinidae	16.2	Tellinidae	13.8
48	CBL14	2288	319.12	14.09	56	Lumbrinereidae	15	Sipunculidae	39	Sipunculidae	39.8
						Orbiniidae	12.5	Astartidae	10.9	Maldanidae	9.1
						Ampeliscidae	9.5	Maldanidae	5.7	Nephtyidae	7.9
50	CBL16	17530	1620.27	59.58	68	Diastylidae	24.4	Pyuridae	21.3	Anthozoa	28.5
						Phoxocephalidae	12.9	Holothuridea	18.6	Pyuridae	23.7
						Ostracoda	10.9	Anthozoa	17.2	Holothuroidea	10.6
51	BC_mussels	20373	7024.27	251.18	71	Mytilidae	20.8	Mytilidae	48.3	Sipunculidae	52.5
						Sipunculidae	8.6	Sipunculidae	41.7	Mytilidae	37.8
						Diastylidae	8.1	Ophiuridae	2.3	Nephtyidae	1.7

Table 4. Summary of dominant infaunal abundance and biomass for COMIDA2010 and listing of the top 3 faunal types by percent of total station abundance and biomass (both wet weight (Wt, g/m^2) and carbon dry weight (gC/m^2).

Stn #	Stn. Name *=2 grabs	Abundance (#/m²)	Biomass (g/m²)	Biomass (gC/m²)	Taxa (#)	Abundance (#/m²)	%	Wet Wt Biomass (g/m²)	%	Biomass (gC/m²)	%
6	UTX29	1017.5	301.34	9.08	38.0	Capitellidae	14.7	Tellinidae	32.6	Nuculanidae	35.7
						Cirratulidae	10.3	Nuculanidae	32.6	Tellinidae	33.5
						Nuculidae	9.8	Astartidae	20.1	Astartidae	10.0
10	UTX27	1137.5	82.56	4.11	34.0	Nuculidae	54.3	Sipunculidae	21.3	Maldanidae	26.5
						Nuculanidae	7.7	Maldanidae	18.9	Sipunculidae	19.3
						Capitellidae	5.7	Nuculanidae	16.0	Reineidae	12.3
15	UTX19	3060.0	401.68	14.41	59.0	Phoxocephalidae	19.4	Astartidae	54.1	Maldanidae	55.6
						Ostracoda	17.4	Maldanidae	28.5	Astartidae	22.6
						Nuculidae	8.6	Ophiuridae	4.9	Terebellidae	3.5
20	UTX21	667.5	460.24	16.01	20.0	Nuculanidae	53.2	Nuculanidae	84.0	Nuculanidae	79.7
						Nuculidae	15.4	Nuculidae	5.2	Nephtyidae	7.4
						Cirratulidae	6.0	Nephtyidae	3.6	Nuculidae	5.9
22	UTX17	585.0	45.78	2.06	22.0	Nuculidae	45.7	Nuculanidae	60.4	Nuculanidae	44.3
						Nuculanidae	27.8	Lumbrineridae	11.1	Lumbrineridae	23.0
						Phoxocephalidae	6.0	Nuculidae	7.7	Nuculidae	6.6
24	UTX16	877.5	229.36	11.24 .	44.0	Nuculidae	30.8	Sipunculidae	37.5	Sipunculidae	34.4
						Maldanidae	8.5	Maldanidae	18.4	Maldanidae	26.2
						Cirratulidae	7.1	Nephtyidae	8.2	Nephtyidae	12.0
35	UTX10	360.0	116.65	3.89	23.0	Nuculidae	25.0	Nuculanidae	88.1	Nuculanidae	87.2
						Nuculanidae	22.9	Nuculidae	3.2	Nuculidae	3.7
						Cirratulidae	9.0	Thraciidae	2.5	Thraciidae	2.1
38	UTX2	835.0	206.01	8.95	34.0	Nuculidae	22.5	Sipunculidae	36.2	Sipunculidae	37.6
						Nuculanidae	8.1	Nuculanidae	24.3	Maldanidae	24.2

						Cylichnidae	7.2	Maldanidae	15.0	Nuculanidae	18.4
40	UTX8*	1475.0	314.86	8.74	41.0	Cirratulidae	18.0	Astartidae	40.1	Tellinidae	28.0
						Nuculanidae	15.9	Tellinidae	25.1	Astartidae	21.7
						Lumbrineridae	11.2	Nuculanidae	16.0	Nuculanidae	19.1
49	CBL17	1815.0	384.49	13.72	31.0	Nuculidae	34.0	Nuculidae	38.5	Nuculidae	42.1
						Montacutidae	25.2	Nuculanidae	29.2	Nuculanidae	27.0
						Nuculanidae	9.8	Tellinidae	23.8	Tellinidae	20.6
50	CBL9(16)	19860.0	4149.15	134.47	73.0	Mytilidae	16.9	Mytilidae	69.0	Mytilidae	59.6
						Leuconidae	9.4	Sipunculidae	17.0	Sipunculidae	23.5
						Phoxocephalidae	7.7	Ophiuridae	4.8	Ophiuridae	2.1
105	Detritus	1750.0	147.60	5.83	20.0	Nuculanidae	47.7	Tellinidae	74.9	Tellinidae	58.8
						Nuculidae	29.1	Terebellidae	17.5	Terebellidae	27.1
						Tellinidae	7.4	Reineidae	3.1	Reineidae	7.2
106	CBL2-8*	3230.0	329.78	15.82	56.0	Phoxocephalidae	15.5	Sipunculidae	48.2	Sipunculidae	45.2
						Ophiuridae	11.3	Terebellidae	12.2	Terebellidae	15.5
						Cirratulidae	10.4	Maldanidae	10.5	Maldanidae	15.3
107	CBL8-3*	715.0	119.85	6.05	28.0	Maldanidae	14.7	Maldanidae	42.4	Maldanidae	58.9
						Nuculidae	13.3	Nuculanidae	18.8	Nuculanidae	12.3
						Capitellidae	11.2	Astartidae	11.6	Lumbrineridae	7.6
108	HSH1*	880.0	51.70	2.10	37.0	Nuculanidae	15.9	Astartidae	45.5	Maldanidae	31.0
						Nuculidae	8.5	Maldanidae	18.0	Astartidae	16.8
						Lumbrineridae	6.2	Tellinidae	8.3	Onuphidae	14.0
109	HS2*	3305.0	121.71	4.25	46.0	Sabellidae	30.6	Tellinidae	44.5	Tellinidae	39.5
						Cirratulidae	14.8	Astartidae	22.4	Astartidae	9.6
						Isaeidae	12.4	Orbiniidae	3.7	Ampeliscidae	7.0
1010	WR1*	7280.0	458.28	21.32	40.0	Maldanidae	54.5	Sipunculidae	37.5	Sipunculidae	36.2
						Haustoriidae	9.2	Maldanidae	18.9	Maldanidae	28.5

						Lumbrineridae	5.7	Carditidae	7.3	Ampeliscidae	7.5
1013	HSH2*	3090.0	852.88	28.23	47.0	Tellinidae	22.5	Tellinidae	52.1	Tellinidae	48.8
						Lumbrineridae	9.4	Nuculanidae	23.8	Nuculanidae	23.7
						Nuculanidae	9.2	Sipunculidae	6.1	Sipunculidae	8.3
1014	1CP1*	1665.0	434.81	17.02	41.0	Nuculidae	21.3	Astartidae	34.7	Maldanidae	60.0
						Maldanidae	14.1	Maldanidae	33.6	Astartidae	13.3
						Phoxocephalidae	8.1	Ophiuridae	11.3	Priapulidae	9.3
1015	B12*	2075.0	135.95	7.12	50.0	Ostracoda	16.4	Sipunculidae	30.6	Maldanidae	31.6
						Isaeidae	15.2	Maldanidae	23.7	Sipunculidae	26.3
						Phoxocephalidae	8.7	Nuculidae	13.0	Reineidae	16.0
1030	n/a*	560.0	419.77	15.27	25.0	Nuculidae	23.2	Astartidae	39.4	Nepthyidae	35.1
						Nuculanidae	21.4	Nephtyidae	17.7	Sipunculidae	20.1
						Sternaspidae	8.9	Sipunculidae	16.2	Astartidae	16.3

cardiidid and tellinid bivalves as well as amphipods. Cluster group 6 located NE near the coast was dominated by mytillid bivalves (mussels, head of Barrow Canyon), ampeliscid amphipods, diastyelid cumaceans, and maldanid and sabellid polychaetes. The other larger grouping of stations, Cluster group 7 that is located mid-shelf to the east of Cluster group 4, was dominated by nuculid and tellinid bivalves, capitellid, cirratulid, lumbrinereid, maldanid, and owenid polychaetes, isaeid and phoxochephalid amphipods and ostracod. The combined COMIDA 2009 and 2010 MDS plot also identified 7 groupings (Figure 18), although the overlap of some of the clustering groups is apparent (groups 2 and 4). Reducing the similarity clustering to 55% would reduce the number of cluster groups to 3 that would be differentiated by longitude and water type.

Environmental and biotic data

The Mantel test was used to evaluate any significant relationships between environmental data and biotic parameters. Results indicated that benthic abundance and biomass values are directly linked to environmental factors, which are key drivers for biotic variability (Table 5). Based upon this finding, we primarily utilized the converted gC biomass data because it is a more accurate indicator of carbon content for the benthic biomass because calcium carbonate is removed from the wet weight values.

Table 5. Mantel tests between environmental data and biotic data using nonparametric Spearman's rho statistics.

COMIDA2009	**Rho**	**p-value**
gC Biomass x Environmental	0.554	$p < 0.001$
Abundance x Environmental	0.530	$p < 0.001$
COMIDA2010		
gC Biomass x Environmental	0.268	$p = 0.021$
Abundance x Environmental	0.284	$p = 0.012$
COMIDA combined (both years)		
gC Biomass x Environmental*	0.471	$p < 0.001$
Abundance x Environmental*	0.47	$p < 0.001$

* indicates the full environmental data collected was used in the test.

To determine the most significant environmental drivers influencing benthic abundance and biomass we used the BIO_ENV routine in PRIMER. The BIO-ENV routine allowed for comparison of specific environmental data influencing benthic abundance and gC biomass using 17 parameters, including station latitude and longitude, depth, sediment chl *a*, sediment grain size, organic carbon and nitrogen content and bottom water temperature and salinity. The overall abundance of infauna for both COMID2009 and COMIDA2010 was most associated with the longitude of the station, depth, coarse grain size, organic nitrogen content of the sediment carbon, and bottom water salinity ($rho=0.542$, $p<0.01$). A composite view of these environmental associations can be summarized as follows: the highest benthic abundance stations were in offshore higher salinity Bering Sea water over deeper sites, characterized by coarse sediments with higher organic nitrogen contents in surface sediments. By comparison, the highest station benthic macroinfaunal biomass (gC m^{-2}) also occurred offshore (but at higher longitudes) in

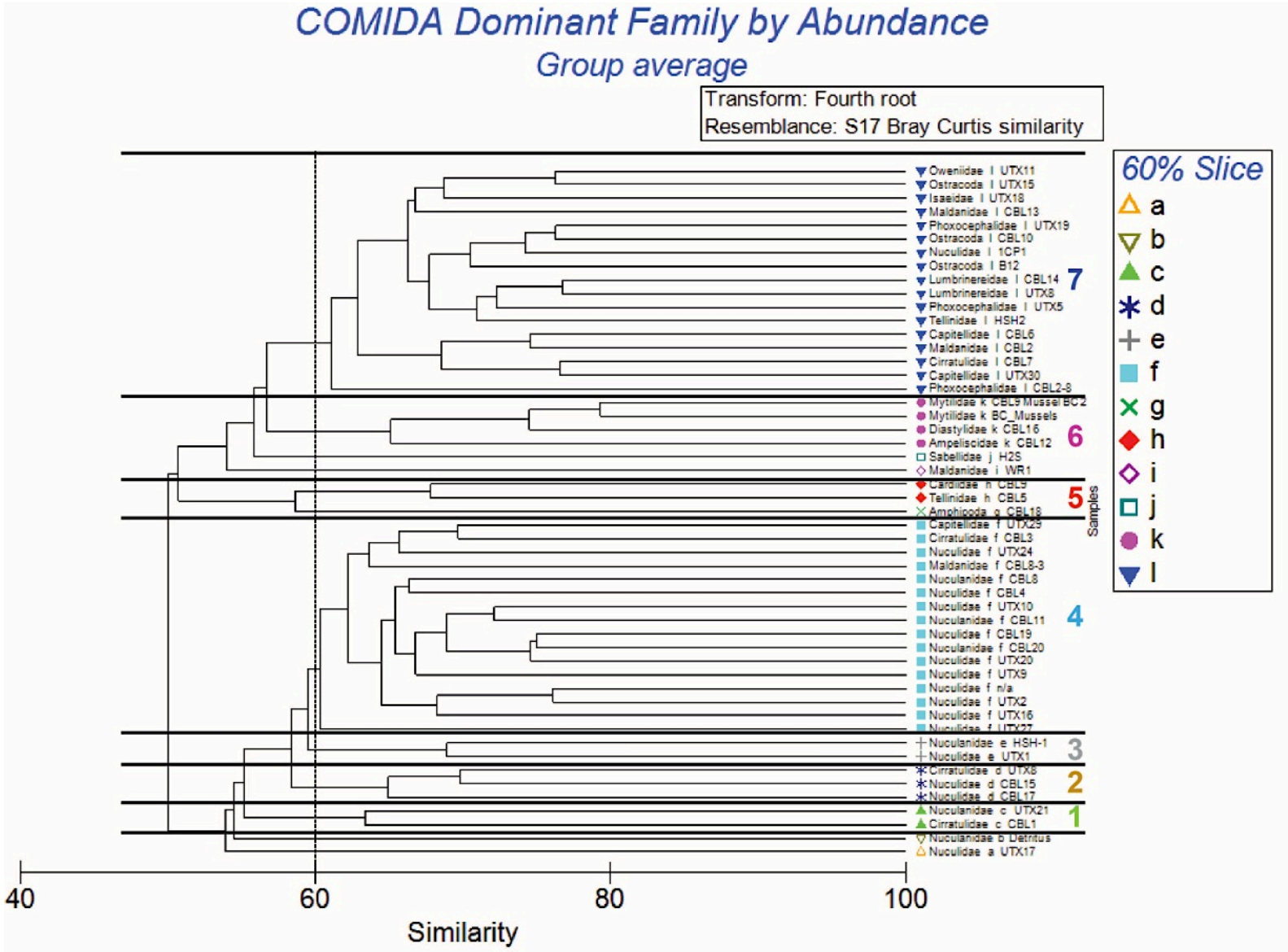

Figure 17. Similarity dendrogram for COMIDA2009 and COMIDA2010 stations, clustering by abundance with a 60% similarity threshold.

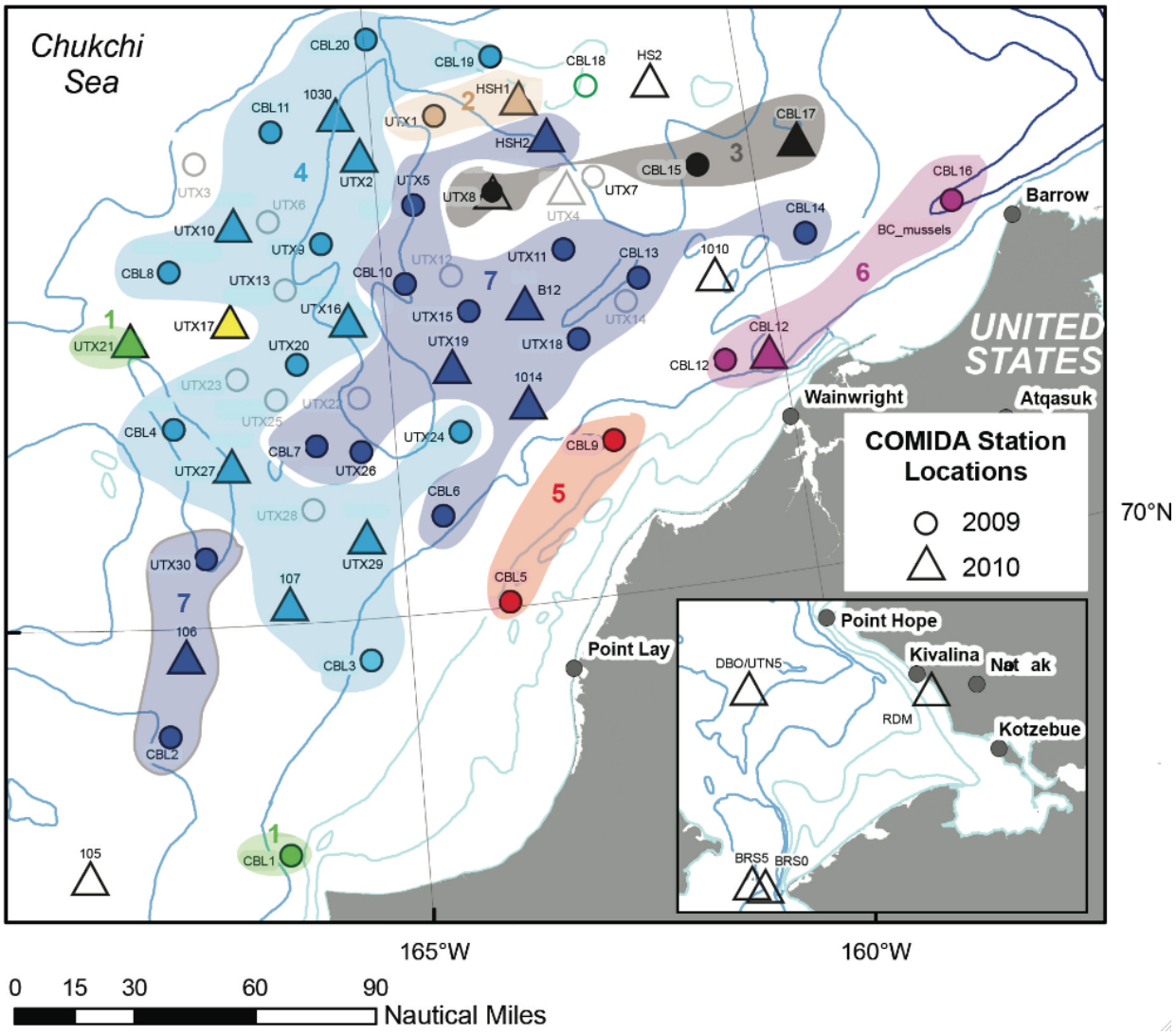

Figure 18. Spatial location of the 7 major clustering groups and associated stations identified through PRIMER analysis (see Figure 17 for dendrogram).

higher salinity water with relatively higher surface sediment C/N values (7-8, albeit with still labile carbon, see Figure 10) and coarse, sandy sediments.

These findings indicate that water mass type (defined by salinity), station depth, sediment grain size and food quality (N content and C/N values) are the most significant environmental variables driving benthic macroinfaunal abundance and biomass values. These findings support at larger composite, multi-decadal evaluation of factors influencing benthic macrofaunal abundance and biomass identified in Grebmeier et al. 2006 (2006a).

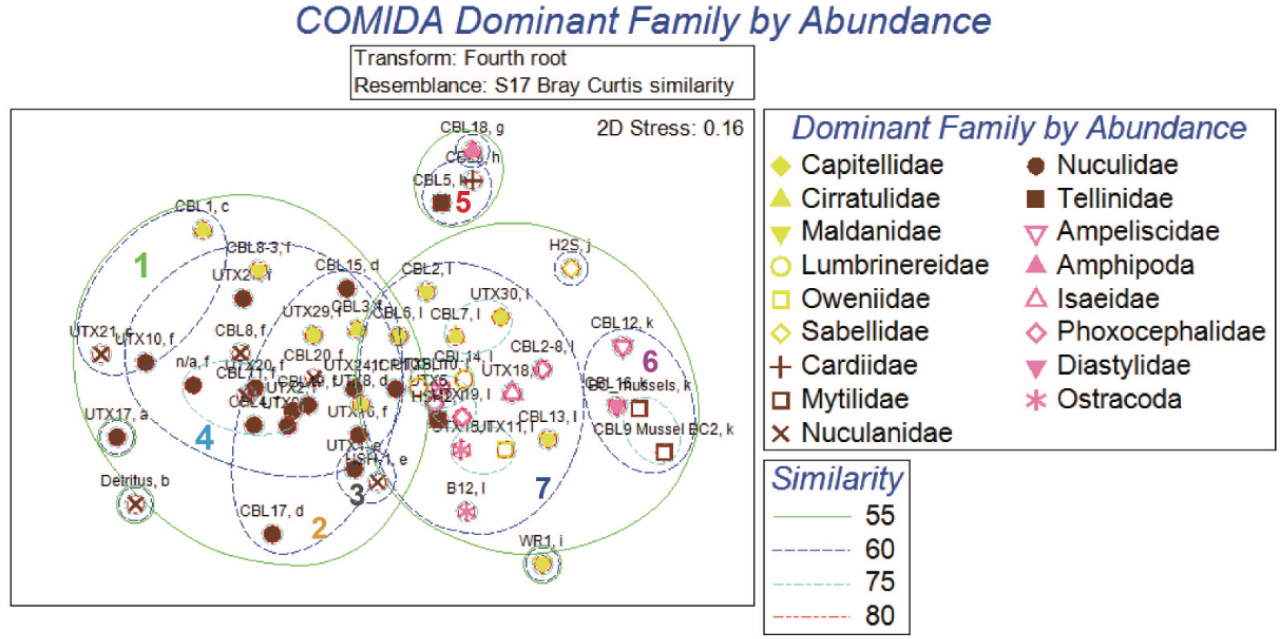

Figure 19. Multidimensional scaling (MDS) map of dominant families by abundance for the combined COMIDA2009 and COMIDA2010 field sampling periods. The highlighted colors #1-7 are tied to the cluster dendrogram shown in Figure 17 and spatial extent shown in Figure 18.

Table 6. Comparison of environmental data and biotic variables (abundance and biomass of macroinfauna) for combined years (COMIDA2009 & COMDIA2010) using the PRIMER Bio-Env routine. The 17 environmental parameters are: 1. Latitude, 2. Longitude, 3. Depth, 4. Sediment Chl *a*, 5. Sediment phi0, 6. Sediment phi1, 7. Sediment phi2, 8. Sediment phi3, 9. Sediment phi4, 10, Sediment 1-4phi (sand), 11 Sediment phi5 (silt&clay), 12 Sediment modal size, 13. Total organic carbon, 14. total organic nitrogen, 15. sediment carbon/nitrogen, 16. Bottom water temperature, 17. Bottom water salinity.

COMBINED COMIDA09 & COMDIA10	
Most Significant Environmental Variables x Abundance	Combined Abundance (no m^{-2}) Global Test
2 LON	Sample statistic (Rho): 0.542; $p < 0.01$
3 Depth	
6 phi1	Best results
14 TON	No.Vars Corr. Selections
17 Bottom Sal	5 0.542 2,3,6,14,17
b. Most Significant Environmental Variables x Biomass	Combined Biomass (gC m^{-2}) Global Test
2 LON	Sample statistic (Rho): 0.536 $p < 0.01$
15 C/N	
7 phi2	Best results
10 phi1-4	No.Vars Corr. Selections
17 Bottom Sal	5 0.536 2,7,10,15,17

Caloric content of benthic prey for walrus

Average caloric content for taxa over the study area ranged from 3578 cal/g for the tunicates to 5135 cal/g for the bivalves (Table 7). A plot of caloric content versus offshore zone suggests a trend of increasing caloric content from nearshore to offshore, although it was only marginally significant ($p = 0.7070$, $\alpha = 0.05$). Taxonomic classes were treated as separated categories and this proved to be a significant explanatory variable for energy content ($p = 2.806e\text{-}10$, $\alpha = 0.05$). When testing the model assumptions, the Bartlett and NCV HOV tests were positive ($p = 0.1207$ and $p = 0.6771$ respectively, $\alpha = 0.05$), as was the case with normality (AD: $p = 0.2546$, CVM: $P = 0.3253$, Lillie: $P = 0.2353$, Pearson: $p=0.4870$, and SF: $p = 0.1025$, $\alpha = 0.05$). Over the Chukchi study area, the bivalves were significantly more energy-rich than many of the other taxa, while the echinoderms and tunicates were significantly less energy dense.

Caloric content of benthic animals by class were found to be significantly higher than historical values determined by Sam Stoker in the 1980s (paired-t test, $p=0.0093$, $\alpha=0.05$; Stoker, 1978). This finding may be due to: 1) a longer open water growth season and enhanced algal blooms in the Chukchi as responses to sea ice decline, 2) seasonal differences in faunal collections, 3) level of faunal comparisons, and/or 4) technological differences in bomb calorimetry over the last thirty years. These new caloric content data suggest a possible trend of increasing caloric content for macroinvertebrates from nearshore to offshore areas.

Table 7. Average caloric content (cal/g) for various taxa (separated by class) collected during COMIDA2010.

Taxa by Class	Average energy density (cal/g)
Ascidian	3578.1
Echinoids	3680.9
Anthozoa	4029.1
Arthropoda	4591.7
Sipunculida	4953.7
Gastropoda	4995.1
Polychaeta	5024.4
Bivalvia	5135.3

The ANOVA analysis of spatial variation in the walrus prey field indicate that the soft tissue (bivalve, worm, gastropod) infauna are more energy dense than the chitin-synthesizing infauna (e.g. arthropods) is in agreement with other studies performed in temperate zone ecosystems.

Seafloor Video Survey of the Chukchi Sea

During our summer 2009 and 2010 cruises in the Chukchi Sea we recorded video footage of the seafloor at about 40 stations in each year (41 in 2009 and 36 in 2010). This video imagery was used at sea to determine whether and for how long to deploy the epibenthic trawl. We also used the video to capture broad scale patterns in epifaunal communities, which are important trophic links in marine ecosystems. We defined habitat types based on general abiotic characteristics and the dominant fauna observed at each station. In addition we quantified the density (#/m^2) of

brittle stars (*Ophiura* sp.) and sand dollars (*Echinarachnus parma*) at sites where they were overwhelmingly dominant (Figure 20a-c).

Our video footage documents a patchy array of epifaunal habitats within the Chukchi Sea with the majority of stations dominated by brittle stars and an assortment of mobile epifauna (e.g., crabs, gastropods). The dominant epibenthic habitat types observed were bioturbated silty sediment with brittle stars (Habitat #1) and bioturbated silty sediment with mobile epifauna (Habitat #3) and these two communities overlap at the study area scale in the Chukchi Sea (Figure 20 a,b). Sea cucumbers (Habitat #2) and diverse sessile epifauna (e.g., soft coral *Gersemia rubiformis*) are examples of other epibenthic fauna in the Chukchi Sea. In addition, we observed sand dollars inshore of the boundary between Bering Shelf-Anadyr Water (BSAW) and

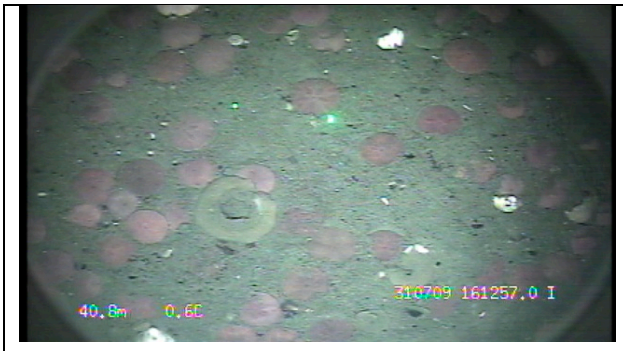

a.

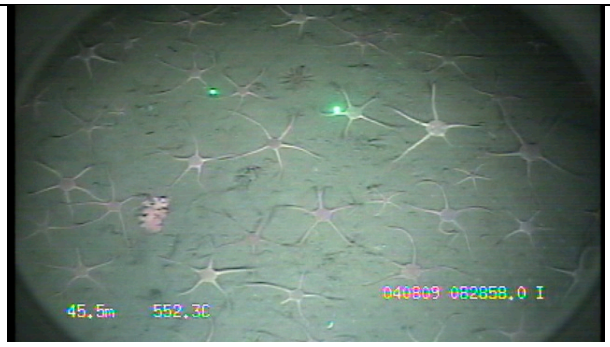

b.

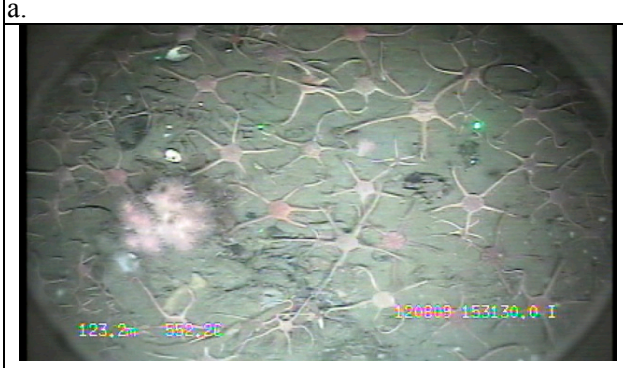

c.

Figure 20. Bottom camera images in the Chukchi Sea study are of a. sand dollars (*Echinarachnius parma*) at a station near the coast in Alaska Coastal water, b. brittle stars (*Ophiura sarsi* and *Ophiura* sp.) in offshore waters, and c. brittle stars (*Ophiura sarsi*) and soft corals (*Gersemia rubiformis*) in Barrow Canyon.

Alaska Coastal Water (ACW). We found a similar range of the dominant brittle stars, including *Ophiura sarsi, at* densities as observed in other studies (Ambrose et al., 2001). We also observed more biologically diverse and dense coral and sea anemone communities at near-shore sites and within Barrow Canyon. The exceptionally high density of brittle stars (nearly 3x greater than the next highest value station in the study area), provides further evidence that Barrow Canyon is a hot spot for biological activity (Grebmeier et al., 2006b; Mathis et al., 2009).

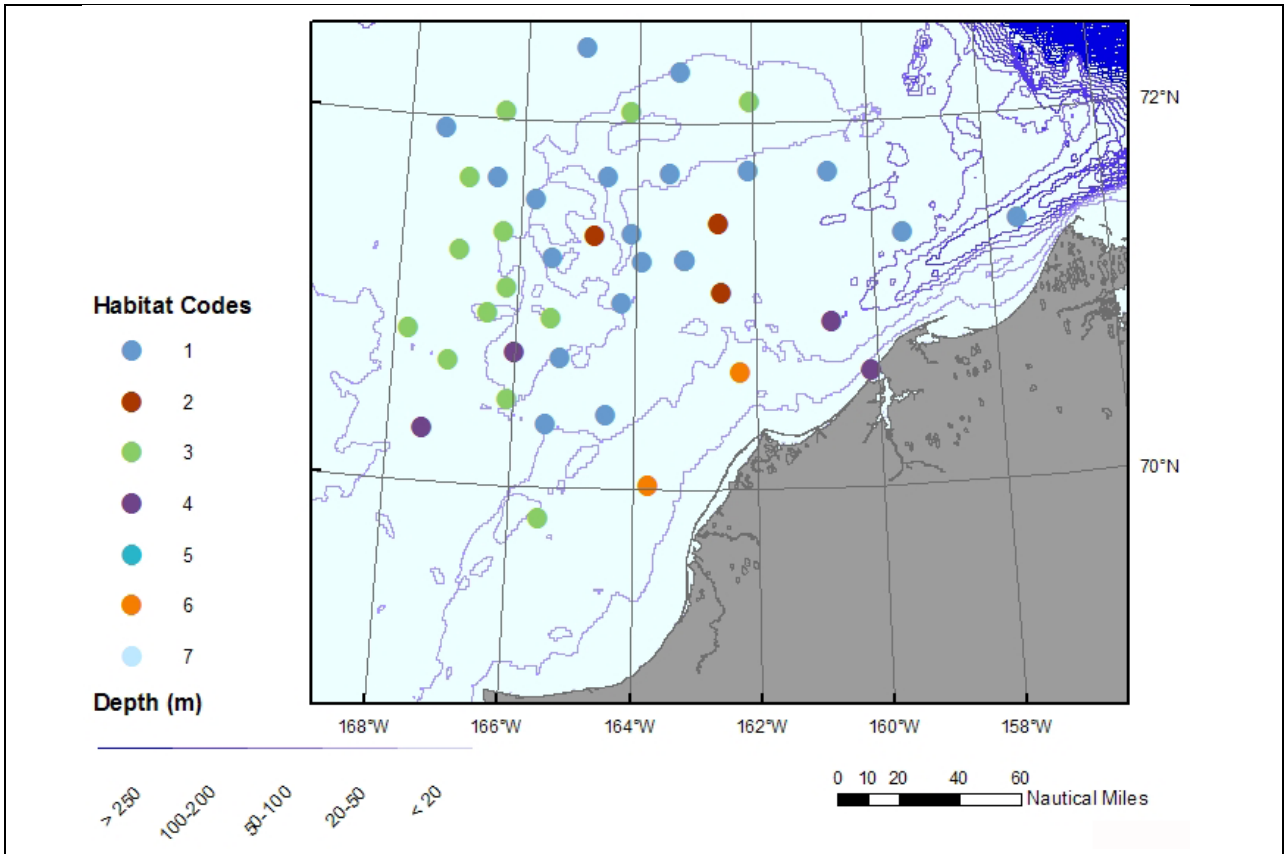

a.

HABITAT CODE	DESCRIPTION
1	bioturbated silty sediment and brittle stars
2	bioturbated silty sediment, brittle stars, and sea cucumbers
3	bioturbated silty sediment and mobile epifauna
4	bioturbated silty sediment, abundant and diverse sessile epifauna
5	mixed sandy sediment and sea stars
6	sand, sand dollars, and disciform bryozoans
7	mixed gravel over silt and hard/soft coral structure

b.

Figure 21. a. Distribution of habitat types in the COMIDA region in 2009 by habitat codes. These 7 habitat codes correspond to habitats defined from seafloor video from the Chukchi and Northern Bering Seas b., although habitat types '5' and '7' were not observed in our study area in the Chukchi Sea.

Future direction

Our immediate activities will include support for MS student Lisa Wilt on her walrus caloric prey base study, as well as continued work to determine sedimentation rates. We are cooperating with other COMIDA PIs in development of a special COMIDA CAB issue (Deep-Sea Research II) that will convey the results of the COMIDA CAB study to the scientific community, program managers and general public.

Acknowledgments

We thank the Bureau of Ocean Energy Management (BOEM), U.S. Department of Interior for funding support for this study and BOEM project manager Dick Prentki for his participation in COMIDA scientific discussions and field efforts. Linton Beaven, Marisa Guarinello, Christian Johnson, Arvind Shanmarthan, Regan Simpson and Stephanie Soques participated in the benthic sorting efforts, sediment analyses, field sampling, and data analyses during the course of the COMIDA project. Both Marisa Guarinello and Alynne Bayard assisted in the GIS analyses. We also extend our appreciation to Ken Dunton, John Trefry, Susan Schonberg and their COMIDA field assistants for data collection efforts at sea. Both Eric Hersh and Harish Sangireddy provided computer support for cruise operations and data cataloging both during and after the cruises. Finally, we thank Captain John Seville and the crews on the *R/V Alpha Helix* (2009) and *R/V Moana Wave* (2010) for their efforts at sea that helped make COMIDA a successful research program.

The distribution, abundance, and diversity of the benthic fauna of the northeastern Chukchi Sea

Schonberg, S.V. and K.H. Dunton

Susan V. Schonberg and Kenneth H. Dunton
Marine Science Institute
The University of Texas at Austin, Port Aransas, Texas 78373

Abstract

This report details the results of a benthic species inventory of 365 taxa from 142 individual van Veen grab samples. These samples were collected from 54 stations under the COMIDA project in summers 2009 and 2010. The inventory was dominated by the phyla Annelida (38%), Mollusca (22%), and Arthropoda (21%). Three dominant groups within these phyla (polychaetes, molluscs, amphipods) were analyzed for species composition and diversity. Species abundance distribution was also correlated to site-specific environmental conditions. The polychaete *Maldane sarsi* (205 n m^{-2}; 12.6%) represented the most abundant species followed by the taxa Nematoda (180 n m^{-2}; 11.1%) and the bivalve species *Ennucula tenuis* (114 n m^{-2}; 7.0%). The bivalve *Macoma calcarea* (57.8 gww m^{-2}; 14.6%) exhibited the highest overall biomass followed by the sipunculid *Golfingia margaritacea* (42.1 gww m^{-2}; 10.6%) and the bivalve *Nuculana pernula* (36.3 gww m^{-2}; 9.2%). The seven most abundant amphipod species and six most abundant bivalve species were collected in the highest concentrations at Station 103, located to the Southwest of Point Hope. High concentrations of these organisms were also documented at multiple stations situated west of Barrow Canyon and within the Barrow Canyon. Marine mammal aerial surveys have recorded large numbers of gray whales and walrus at these same locations (Bowhead whale aerial survey project – BWASP 2008-2010). The Biota and Environment matching (BEST) routine in PRIMER v6 was performed to determine which environmental factors had the greatest effect on species abundance distribution. The highest Spearman correlation ranking for all invertebrates (0.588) and polychaetes (0.594) indicated that longitude, bottom water salinity, and C/N exhibited the greatest influence on organismal distributions. Bivalve species abundance distribution was more closely correlated (0.530) to a combination of latitude, longitude, water depth, and C/N. Infaunal abundance and biomass were higher within known marine mammal foraging locations, and these areas generally contained mud substratum, high salinities and low C/N values.

Introduction

Background

According to a review by Sirenko and Gagaev (2007), various regions of the Chukchi Sea were first investigated in 1878 by the Swedish, followed by Canadians (1913), Norwegians (1922), and Russians (1929, 1932, 1933, 1935, 1938, 1946, and1976). In the late 1980^{s} and 1990^{s}, a joint Soviet-American expedition (BERPAC: Program for Long-Term Ecological Research of Ecosystems of the Bering and Chukchi Seas and the Pacific Ocean) sampled the southern Chukchi Sea. However, quantitative benthic data from the northeastern sector of the Chukchi Sea was non-existent until results from the MMS/Outer Continental Shelf Environmental Assessment Program (OCSEAP) surveys in the 1970s and 1980s were reported by Stoker (1978; 1981) and Feder et al. (1994a; 1994b). Additional information collected in 2002 and 2004 under the Western Arctic Shelf Basin Interactions (SBI) project (Grebmeier and Harvey, 2005) and the 2004-2011 RUSALCA (Russian-American Long-term Census of the Arctic; http://www.arctic.noaa.gov/aro/russian-american/) have also contributed to our knowledge of the Chukchi Sea. This program, COMIDA-CAB 2009 and 2010, is the first large-scale benthic survey focused on the northeastern Chukchi Sea since the OCSEAP surveys occurred 30-40 years ago (Figure 1). Additional small-scale benthic surveys in proximity to planned drill sites in the Chukchi Sea Lease Sale 193 area have been supported during summers 2009-2011 by private oil and gas companies (Shell and Conoco-Phillips). Exploratory drilling for oil was carried out at five locations between 1989 and 1992 (Figure 1). However, no additional activity occurred until the 2008 Chukchi Sea Lease Sale 193, which sparked renewed interest in the biological and physical attributes in this lease area which encompasses the historic well sites.

Dunton et al. (2005) synthesized historical benthic data from 1974-2004 and Grebmeier et al. (2006b) reviewed ecosystem dynamics in the northern Bering and Chukchi Seas. These investigations revealed a rich abundance of bottom fauna correlated with high pelagic primary production (Feder et al., 1994a; Feder et al., 1994b; Grebmeier et al., 2006b; Iken et al., 2010). The northeastern Chukchi Sea contains some of the highest faunal biomass reported in the Arctic (Dunton et al., 2005; Grebmeier and Dunton, 2000). Elevated nutrient levels in the seawater are upwelled onto the northern Bering Sea shelf and carried northward by currents to support the rich planktonic and benthic food web communities of the northeastern Chukchi Sea. Since pelagic fauna are unable to graze all of the primary production, large quantities of organic matter sink to the seafloor and are utilized by a rich and diverse benthic community. These prolific benthic communities provide an important food source for demersal fish, diving ducks, walruses, bearded seals and migrating whales (Grebmeier and Dunton, 2000).

Throughout the Arctic, major environmental changes are already occurring and projected to continue in response to sea ice shrinkage, increasing water temperatures, coastal erosion, species range shifts, ocean acidification, and pollutants (ACIA, 2004; CAFF, 2001). Over the last decade, the Arctic perennial ice cover has thinned and retreated significantly from the Chukchi Sea slope and adjacent southwestern Canada Basin (Stroeve et al., 2007). The loss of ice cover has increased subsurface light levels and water temperatures in regions previously known to exhibit sea ice cover throughout the summer season (Perovich et al., 2007). The impending loss of summer sea ice and anticipated increase in anthropogenic perturbations will likely alter

ecosystem function. In particular, Arctic ecosystems will likely exemplify large-scale changes in primary production, species distributions, and indigenous subsistence use (Bluhm et al., 2011). Although this study was funded to provide baseline information associated with gas and oil production, it is also quite timely for providing a snapshot of Chukchi Sea ecology in the midst of a changing climate.

The objectives of this project were to 1) create an inventory of infaunal species occurrence and 2) document the ecological diversity of benthic invertebrate communities inhabiting northeastern Chukchi Sea sediments. These results will serve as a baseline to assess future ecological change resulting from natural and/or anthropogenic sources.

Specifically, the purpose of this study is to:

- Develop a quantitative assessment of spatial patterns of infaunal abundance, biomass and diversity based on taxa identified to the lowest possible trophic level (usually species)

- Identify the environmental variables correlated with spatial patterns of infaunal abundance and diversity.

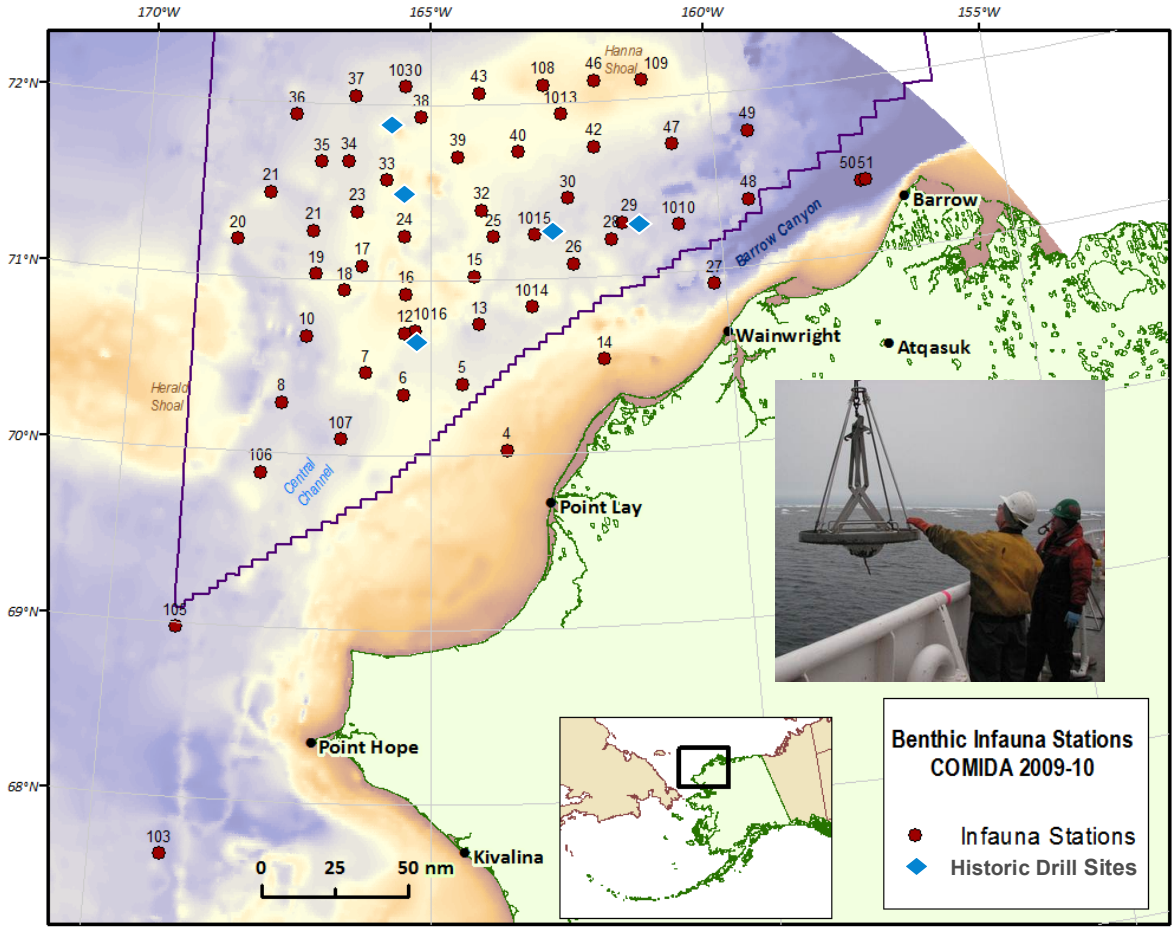

Figure 1. Sampling station locations where infaunal cores were collected by The University of Texas during 2009 and 2010 COMIDA field surveys. Blue diamonds indicate locations of historical drill sites from 1989-1992.

Methods

Study Area

The majority of COMIDA stations were positioned in the northeastern Chukchi Sea at the location of oil and gas lease sites. However, several additional stations were opportunistically sampled just north of the Bering Straits while in route from Nome, Alaska. The southern boundary of infaunal collections was located just north of the Bering Straits in the southeastern Chukchi Sea (67.7°N, -168.96°W; Station 103), and the northern boundary was located at Hanna Shoal (72.1°N, -162.06°W; Station 46) (Figure 1). A broad, shallow shelf extends from the northern Chukchi Sea south through the Bering Sea to the Aleutian Islands. Water depths in the study area ranged from 25 m near Hanna Shoal to 160 m in the Barrow Canyon. The mean water depth for all infaunal survey stations was 47 ± 1.9 m (mean ± SE).

Sample Collection - Benthic cores

Sampling for this study took place during July and August 2009 and 2010 using the vessels *R/V Alpha Helix* (2009) and *R/V Moana Wave* (2010). Sample stations were selected using a probability-based grid to create random locations within each grid cell of the study site. Benthic sampling at each station followed specific procedures, which included identifying the station (latitude and longitude) and maintaining the station location to within a 0.5 nautical mile (nm) radius of the original location. Photo documentation, station logs, and field notes were recorded at each station during the field survey.

During summer 2009, 29 stations were quantitatively sampled for infauna with a double van Veen grab (0.01 m^{-2}). Two replicate samples were taken at 10 locations that overlapped with J. Grebmeier (see companion paper to this volume) and four replicates were taken at the remaining 19 stations. In 2010, 25 stations were sampled with two replicates per station. At each station, a paired grab was used to insure that that the environmental samples (grain size, sediment Chl *a*, sediment carbon and nitrogen, etc.) from one grab of the pair was in close proximity to the biological samples obtained from the second grab. The environmental data are presented in companion papers (this volume, J. Trefry and L. Cooper). While shipboard, the sediments were sieved through a 1 mm mesh and infaunal samples were immediately sorted, identified, and preserved in 90% ethanol. Upon arrival to The University of Texas Marine Science Institute, all infaunal samples were reexamined. Amphipod specimens were sent to Ken Coyle at the University of Alaska, Fairbanks, mollusc samples were sent to Nora Foster in Fairbanks, Alaska and polychaete samples were sent to Leslie Harris at the Natural History Museum of Los Angeles County for identification verification. Samples were also blotted and measured for wet mass (including shells). No correction factor was applied for preservation effects. Taxa, including molluscs, crustaceans (except ostracods and harpacticoids), polychaetes, echinoderms and additional smaller groups, were identified to species level or the lowest taxa possible.

Statistical Analysis – PRIMER v6

An ecological analysis of infaunal species abundance data was performed using routines available in the PRIMER v6 software package (Clarke and Gorely, 2006; http://www.primer-e-

com). Several indices (species count, Margalef, Pielou, Shannon, Simpson and Hill) were calculated using the DIVERSE routine in PRIMER.

Principal Component Analysis (PCA), a parametric multivariate method, was used to assess relationships between physical variables (longitude, latitude, water depth, bottom temperature, pH, sediment Chl *a*, gravel, sand, mud, TOC, TON, C/N) characteristic of sample stations. Variables were log-transformed prior to analysis. Results are presented in a bivariate plot.

Relationships between macrofauna communities and environmental factors were investigated using the Biota-Environmental (BIO-ENV) in PRIMER. The BIO-ENV procedure is a multivariate method that matches biotic observations with environmental variables (Clarke and Warwick, 2001). Abundance was square root transformed prior to analysis.

Mapping Data – ArcMap 10

Values for infaunal species abundance, biomass, diversity (output from PRIMER), and environmental observations (water depth, bottom temperature, bottom pH, sediment Chl *a*, gravel & sand, mud, TOC, TON, C/N) were entered into ArcMap 10 (ESRI) to create a geographic image of values. These images were used to explore geographic trends and 'hotspots'.

Results and Discussion

Macrofauna - Inventory

A total of 365 taxa were identified from 142 van Veen grab samples (0.01 m^{-2}) collected from 54 stations in 2009 and 2010. Species occurrence was dominated by Annelida (38%), Mollusca (22%), Arthropoda (21%), Nematoda (11%), other phyla (5%), and Echinodermata (3%) (Figure 2 and the species list in the Appendix Table A-1). Within the Arthropoda, Malacostraca represent the most diverse class with 94 species (including 64 Amphipoda, 17 Cumacea, and 11 Decapoda, 1 Isopoda, 1 Tanaidacea), followed by Maxillopoda (2), and Pycnagonida (1). Gastropoda (41) and Bivalvia (39) were the most prevalent molluscs (Figure 3). All annelid species belonged to Polychaeta. The major echinoderm classes were comprised of Ophiuroidea (7 species), followed by Holothuroidea (3), Echinoidea (3), and Asteroidea (1). The remaining phyla included sipunculids, nemerteans, sponges, bryozoans, hydroids, ascideans, priapulids, actinaria, alcyonaria, brachiopods, and platyhelminthes.

The taxa ranking in either the top ten in abundance or biomass are listed in Table 1. Three bivalve species were among the most abundant and six bivalve species ranked in the top ten of biomass. Although the group Amphipoda was well represented by total number of species (64), only one species was represented in the top ten abundance list (*Pontoporeia femorata*). The most abundant species overall was the polychaete *Maldane sarsi* (205 n m^{-2}; 12.6%) followed by the taxa Nematoda (180 n m^{-2}; 11.1%) and the bivalve species *Ennucula tenuis* (114 n m^{-2}; 7.0%). The species with highest overall biomass was the bivalve *Macoma calcarea* (57.8 m gww^{-2}; 14.6%) followed by the sipunculid *Golfingia margaritacea* (42.1 gww m^{-2}; 10.6%) and

the bivalve *Nuculana pernula* (36.3 gww m^{-2}; 9.2%). The number m^{-2} represents the mean value of the taxa for all 52 sampling stations. The majority of Nematoda consisted of relatively large individuals collected at Barrow Canyon Station 50, and existed in high densities among the bissell threads of the mussel *Musculus discors*. The remaining five dominant species were common throughout the study area.

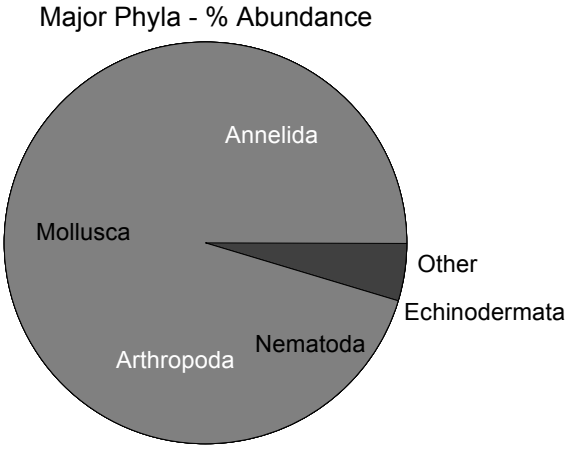

Figure 2. Percent abundance of major phyla of all samples collected in the study area.

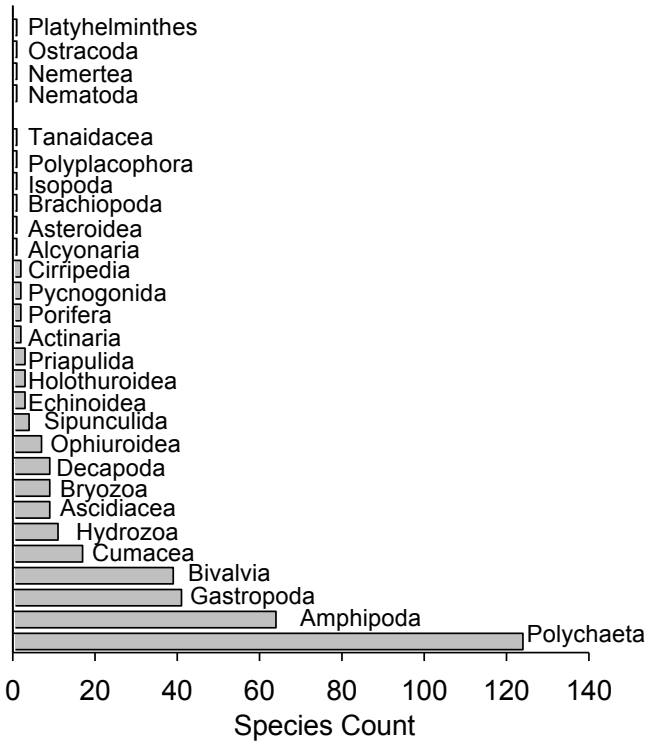

Figure 3. The number of species, by group, collected in the study area. The four taxa listed above the x-axis break were not identified to species.

Table 1. The top ten taxa by percent abundance and biomass. Three taxa in the % abundance list and one species in the % biomass list where collected in high numbers at only a few stations (see footnote). All others were widespread throughout the study area. The biomass is wet weight and includes shells.

Group	Taxa	% Abundance
Polychaete	*Maldane sarsi*	12.6
Nematoda	Nematoda[1]	11.1
Bivalve	*Ennucula tenuis*	7.0
Polychaete	*Owenia cf. assimilis*[2]	4.9
Polychaete	*Scoletoma sp.*	3.8
Bivalve	*Nuculana pernula*	3.3
Ostracoda	Ostracoda	3.2
Bivalve	*Musculus discors*[1]	2.7
Cumacea	*Brachydiastylis resima*	2.4
Amphipod	*Pontoporeia femorata*	2.4

Group	Taxa	% Biomass
Bivalve	*Macoma calcarea*	14.6
Sipunculid	*Golfingia margaritacea*	10.6
Bivalve	*Nuculana pernula*	9.2
Bivalve	*Astarte borealis*	9.0
Bivalve	*Musculus discors*[1]	7.6
Echinoderm	*Echinarachnius parma*[3]	6.0
Bivalve	*Ennucula tenuis*	5.8
Echinoderm	*Ophiura sarsi*	3.5
Polychaete	*Maldane sarsi*	3.2
Bivalve	*Cyclocardia crebricostata*	2.2

[1]Majority collected in Barrow Canyon (Sta 50)

[2]Majority collected west of Barrow Canyon (Sta 48, 30)

[3]All collected on west coast between Pt. Lay & Wainwright (Sta 4, 14)

Community Structure

The number of species collected at a station ranged from 102 species at Station 27, located at the southern end of Barrow Canyon, to 13 species at Station 37 (Overall project mean = 40 ± SE 2.4) (Table 2). Station total abundance values ranged from 14,390 n m^{-2} at Station 50 (Barrow Canyon) to 145 n m^{-2} at Station 37 (Overall project mean 1565 ± SE 329). Biomass was highest at Station 50 (3008 gww m^{-2}) and lowest at Station 105 (3.8 gww m^{-2}; Overall project mean 382 ± SE 66). Maximum, minimum, mean and SE values were calculated using PRIMER v6 and are listed for five diversity indices (Table 2).

The geographic locations of the seven most abundant species of amphipods were analyzed using ArcMap 10 (Figure 4). Large numbers of amphipods were collected at Station 103, located to

the Southwest of Point Hope, at stations located west of Barrow Canyon and within the Barrow Canyon. These were the same locations where large numbers of gray whales were observed during mammal aerial studies (Bowhead whale aerial survey project – BWASP 2008-2010), funded by BOEM and NOAA/NMML (per. comm. Sue Moore, NMML). Amphipod abundance exhibited a large range of values from 2930 n m^{-2} in Barrow Canyon (Station 50) to only 5 n m^{-2} at Stations 5 and 21.

The six most abundant species of bivalves were also plotted (Figure 5). Bivalves were most abundant to the west of Barrow Canyon in the Hanna Shoal area and within the Barrow Canyon. This same location was reported to contain large numbers of walrus observed during mammal aerial studies (BWASP 2008-2010; per. comm. Sue Moore, NMML). The station abundance of molluscs (bivalves, gastropods, polyplacophora) ranged from a minimum of 40 n m^{-2} at Station 37 to a maximum of 2690 n m^{-2} in the Barrow Canyon (Station 50). The mussel, *Musculus discors* comprised the majority of the individuals collected at Station 50. Overall average project abundance for molluscs was 348 n m^{-2} when including *Musculus* individuals from Station 50 and drops to 304 n m^{-2} when Station 50 is omitted. Feder et al. (1994a) reported an average of 227 n m^{-2} for the mollusc group in his study of the northeast Chukchi Sea.

Polychaete abundance values also exhibited a large range, from 4655 n m^{-2} at Station 30 to 55 n m^{-2} at Stations 4 and 37. Large numbers of the tube worms *Maldane* and *Owenia* were collected to the west of the Barrow Canyon (Figure 6). Leslie Harris, a polychaete taxonomist and curator at the Natural History Museum of Los Angeles County, studied a selection of polychaetes collected in summer 2010. She found that many of our most commonly collected polychaetes were incorrectly identified because they are currently undescribed species (Table 2 and Appendix A-2). Most current species identifications are Atlantic based. More Pacific Ocean or indigenous species may actually inhabit the Chukchi Sea than previously thought. This project will continue to provide polychaete samples for further taxonomic research.

Total station abundance (n m^{-2}) and Shannon diversity values are illustrated in Figures 7 and 8. Abundance values were large at Station 103 near Pt. Hope, and multiple stations located within the Hanna Shoal area and Barrow Canyon. This is a similar distribution pattern to amphipod abundance. High abundance does not necessarily mean that species diversity is also high. At some stations in the vicinity of Hanna Shoal, the abundance is high but the diversity is low due to either station dominance by only a few species of bivalves or polychaetes. At some stations in the western portion of the study site, both abundance and diversity were low. Shannon's Index: H' = SUM(Pi*Log(Pi)) assumes that individuals are randomly sampled from an independently large population. A Shannon diversity value usually lies between 1.5 and 3.5. Values above 3.0 indicate that the structure of habitat is stable and balanced; values under 1.0 indicate degradation of habitat structure (Turkmen and Kazanci, 2010). Shannon diversity is the most widely used index for comparing diversity between various habitats (Clarke and Warwick, 2001).

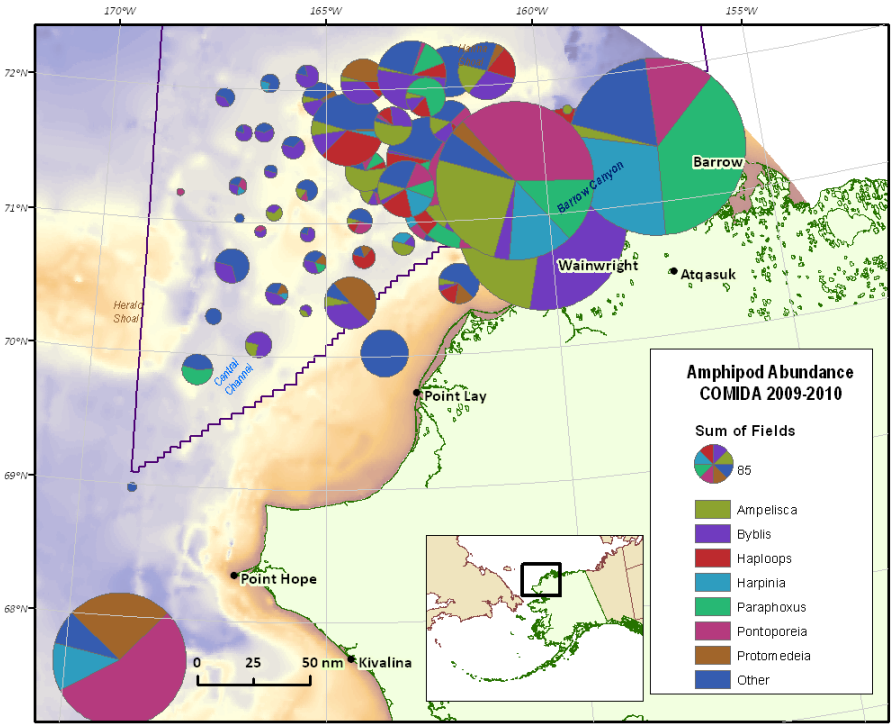

Figure 4. A map of amphipod abundance distribution by the seven dominant species. A total of 64 amphipod species were identified from the study area.

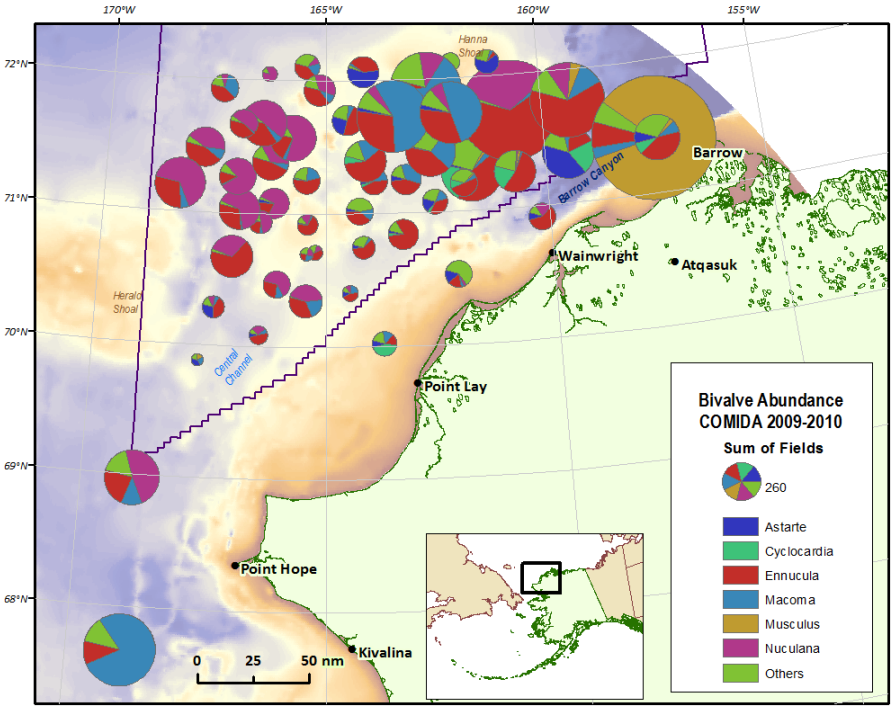

Figure 5. A map of bivalve abundance distribution by the six dominant species. A total of 39 bivalve species were identified from the study area.

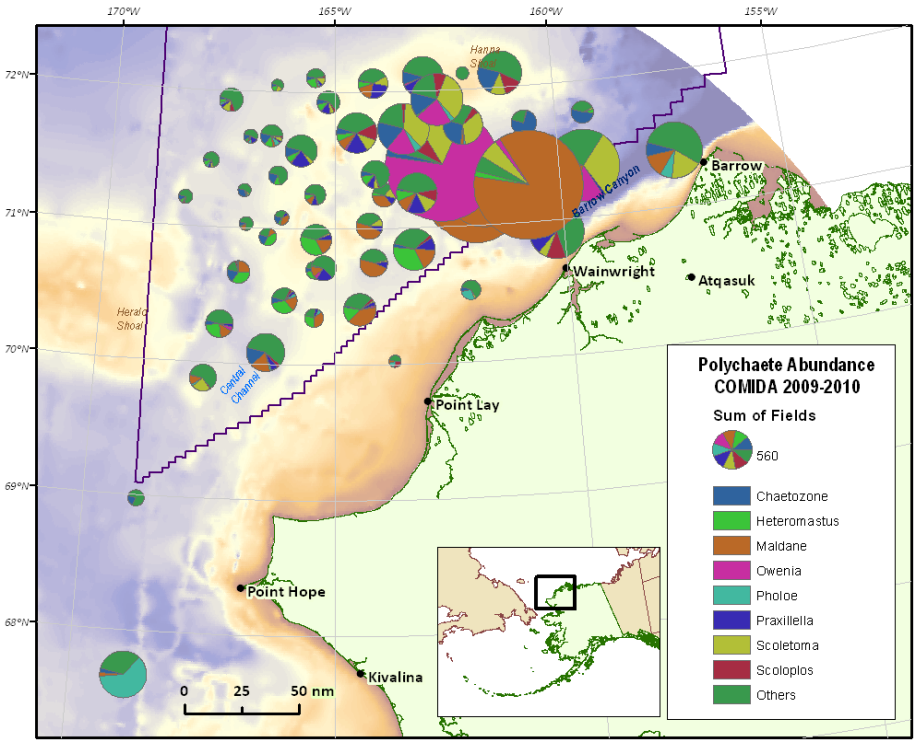

Figure 6. A map of polychaet abundance distribution by the eight dominant species. A total of 124 polychaete species were identified from the study area.

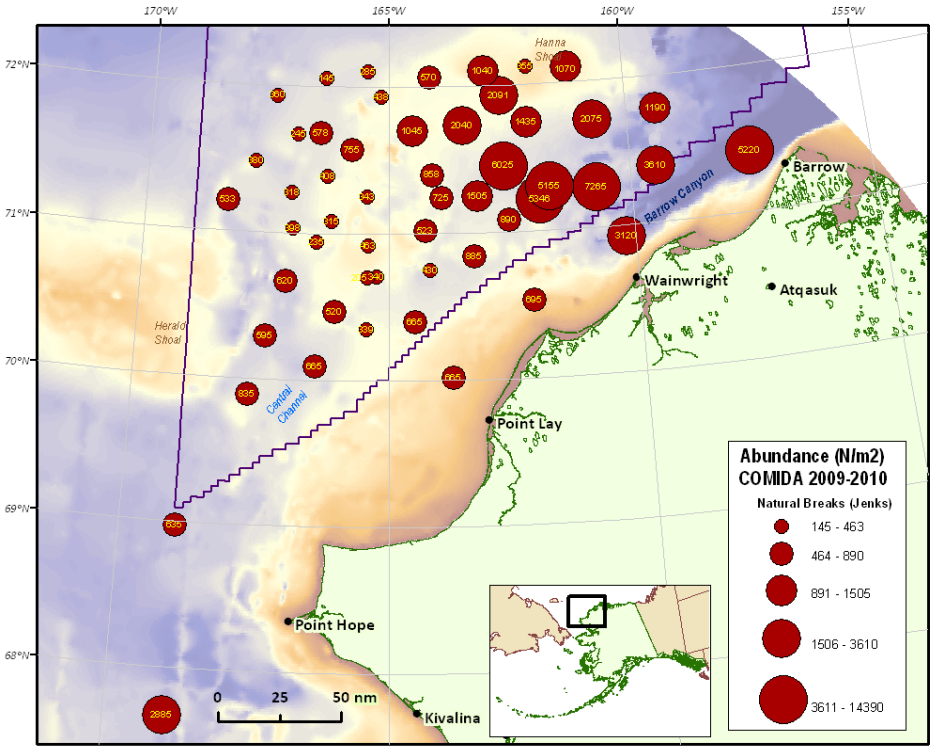

Figure 7. Mean infaunal abundance (n m^{-2}) at study stations.

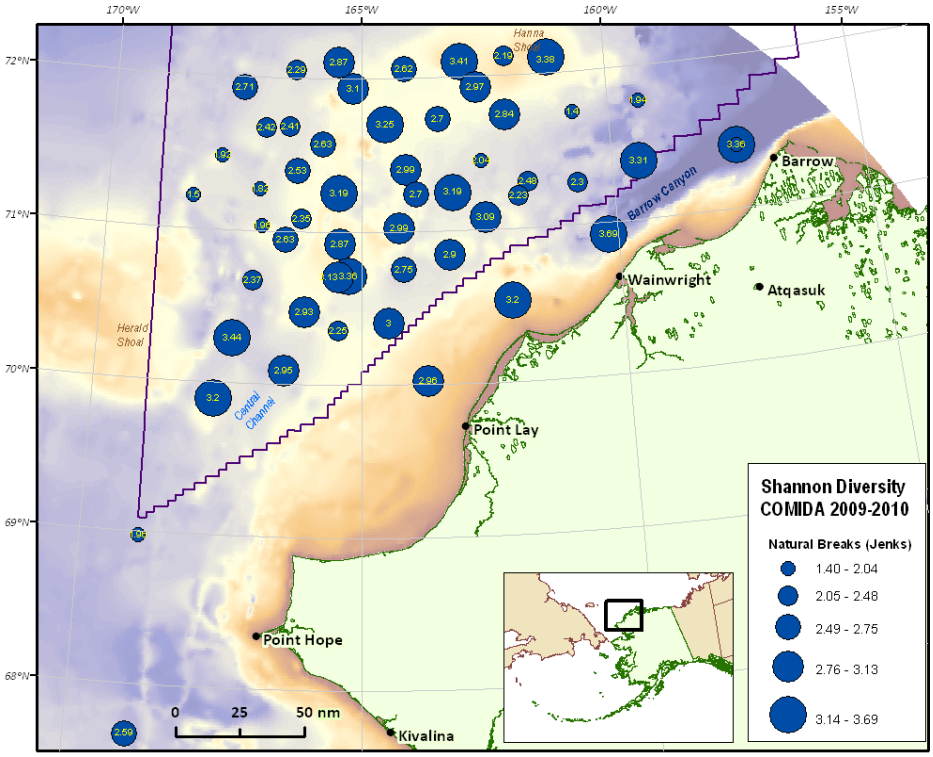

Figure 8. Mean Shannon diversity values calculated from species abundance at study stations.

Table 2. Polychaete identifications from samples collected from this study in the Chukchi Sea during summer 2010. Individual samples were studied by taxonomist Leslie Harris who provided the following changes and comments. See the Appendix Table A-2 for additional details.

PROBLEM POLYCHAETE IDENTIFICATIONS

Current identification	Old Identification	References for Re-identification
Ampharete finmarchia	Ampharete arctica	Holthe 1986; Jirkov, 1989; Jirkov, 2001
Aphelochaeta "tigrina", Aphelochaeta "marioni", Chaetozone sp. 1, Chaetozone sp. 2	Chaetozone setosa	Harris personal notes; C.A. Phillips, personal notes; Blake 1996
Arcteobia anticostiensis	Harmothoe imbricata	Uschakov, 1982
Barantolla sp.	Barantolla americana	Green 2002; Hutchings & Rainer 1981; Harris personal Notes
Brada?n. sp; Diplocirrus longisetosus	Flabelligera mastigophora	Jirkov & Filippova 2001; Salzar-Vallejo unpublished manuscript; Our, Bakke, & Kongsrus 2011
Bradabyssa	Brada granulata, Brada nuda, Brada villosa, Diplocirrus longisetosus	Salazar-Vallejo unpublished manuscript
Chone n. sp. 1	Chone sp, Sabellidae, Laonome kroyeri	Tovar-Hernandez 2007a, 2007b; Nishi et al. 2009
Chone n. sp. 2	Chone sp.	Tovar-Hernandez 2007a, 2007b; Nishi et al. 2009
Cistenides hyperborea	Cistenides granulata	Uschakov 1955; Jirkov 2001
Eteone longa/flava complex	Eteone longa	Pleijel 1993a
Eteone sp.	Eteone longa	Uschakov 1972; Pleijel 1993a; Wilson 1988; Pleijel 1993b
Euchone n. sp. 1	Euchone sp.	Tovar-Hernandez 2007a, 2007b; Nishi et al. 2009; Banse 1970, 1972; Cochrane 2000, 2003
Flabelliderma n. sp.	Flabelligera affinis	Salazar-Vallejo 2007
Glycinde wireni	Glycinde picta	Boggemann, 2005
Heteromastus sp.	Heteromastus filiformis	Hutchings & Rainer 1982
Nepthys pente Nephtys ciliata	Nephtys ciliata	Rainer, 1991
Ophelina n. sp.?	Ophelina sp.	Jirkov 2001; Rowe 2010; Parapar et al. 2011
Owenia cf. assimilis	Owenia fusiformis	Ford & Hutchings 2005; Koh & Bhaud 2003; Koh, Bhand, & Jirkov 2003.
Pholoe sp. D Harris	Pholoe minuta	Petersen 1998; Pettibone 1992; Harris, personal notes
Phyllodoce groenlandica	Anaitides groenlandica	Uschakov, 1972; Pleijel, 1993a; Pleijel, 1993b
Polyphysia crassa Scalibregma inflatum	Scalibregma inflatum	Worsfold, undated; Boggemann 1997
Scoletoma fragilis	Lumbrineris fragilis	Harris, personal notes; Budaeva 2005
Scoletoma minuta	Lumbrineris fragilis	Harris, personal notes; Budaeva 2005

PROBLEM POLYCHAETE IDENTIFICATIONS

Current identification	Old Identification	References for Re-identification
Scoletoma sp. 1	Lumbrineris fragilis	Harris, personal notes; Budaeva 2005
Scoletoma sp. 2	Lumbrineris fragilis	Harris, personal notes; Budaeva 2005
Sphaerodoropsis n.sp.?	Sphaerodoropsis minuta	Fauchald, 1974; Reuscher & Fiege, 2011
Sternaspis n. sp.?	Sternaspis scutata	Petersen 2000
Syllis "oerstedi"	Syllis sp., Syllis oerstedi	Licher 1999
Syllis sp. B	Syllis sp.	Licher 2000
Terebellides n. sp.?	Terebellides stroemi	Jirkov 1989; Jirkov 2001; Williams 1984; Garraffoni, Lana & Hutchings 2005
Travisia cf. forbesi	Travisia forbesii	Jirkov 2001; Rowe 2010; Kirkegaard 1996; Uschakov 1955

Linking physical variables with macrofauna

Northern-flowing currents carry nutrient rich Pacific Ocean water through the Bering Strait over the Chukchi shelf and into the Arctic Ocean. Grebmeier and Barry (1991) studied pelagic-benthic coupling in this area and found a direct relationship exists between water column primary production and benthic infaunal abundance and biomass. The area surrounding Hanna Shoal (yellow lines) and Barrow Canyon (purple line) in Figure 9 are areas of high infauna production.

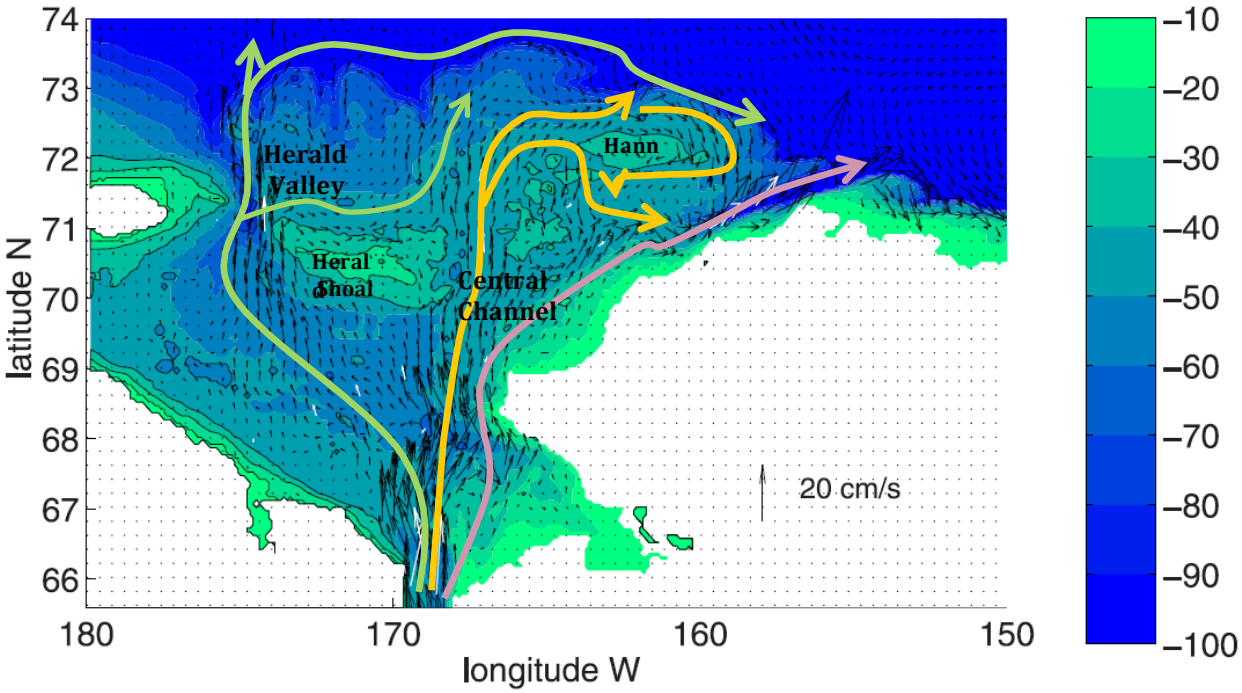

Figure 9. Annual mean horizontal velocity at 27.5 m depth as a function of bottom topography. Net flows are denoted by colored arrows. From Spall (2007) and Weingartner (pers. comm).

A set of physical data measurements were collected and incorporated into the Biota and Environment matching (BEST) routine to determine which environmental factors had the greatest effect on species abundance distribution (Table 3, Figure 11). The highest Spearman correlation ranking for all invertebrates (0.588) and polychaetes (0.594) indicated that longitude, bottom water salinity, and C/N presented the greatest environmental influence on organismal distributions (Figure 11). Bivalve species abundance distribution was more closely correlated (0.530) to a combination of latitude, longitude, water depth, and C/N. All reported Spearman correlation values had a significance level of 0.5%.

Table 3. Station maximum, minimum, mean and standard error (SE) values of environmental variables associated with 50 of the 54 infaunal stations collected in summers 2009 and 2010. Sonde data were collected by J. Trefry. Sediment samples were collected and analyzed by L. Cooper.

		Station			
Variable Name	**Variable Description**	**Max**	**Min**	**Mean**	**SE**
Water Depth	m, Sonde	130	25	46.79	1.89
Bottom Water Temperature	°C, Sonde	3.08	-1.69	-0.55	0.17
Bottom Water Salinity	‰, Sonde	33.32	23.20	32.35	0.19
pH	Sonde	8.17	7.35	7.70	0.03
Sediment chlorophyll *a*	mg m^{-2}	59.87	1.15	13.29	1.29
<0 phi gravel	%	57.99	0.00	3.88	1.50
1-4 phi sand	%	95.32	2.12	31.28	3.55
>5 phi mud	%	97.88	4.52	64.84	4.00
Sediment modal size phi		5.00	0.00	4.46	0.17
TOC	%	1.79	0.03	0.90	0.06
TON	%	0.25	0.01	0.13	0.01
C/N		9.33	3.00	7.21	0.13

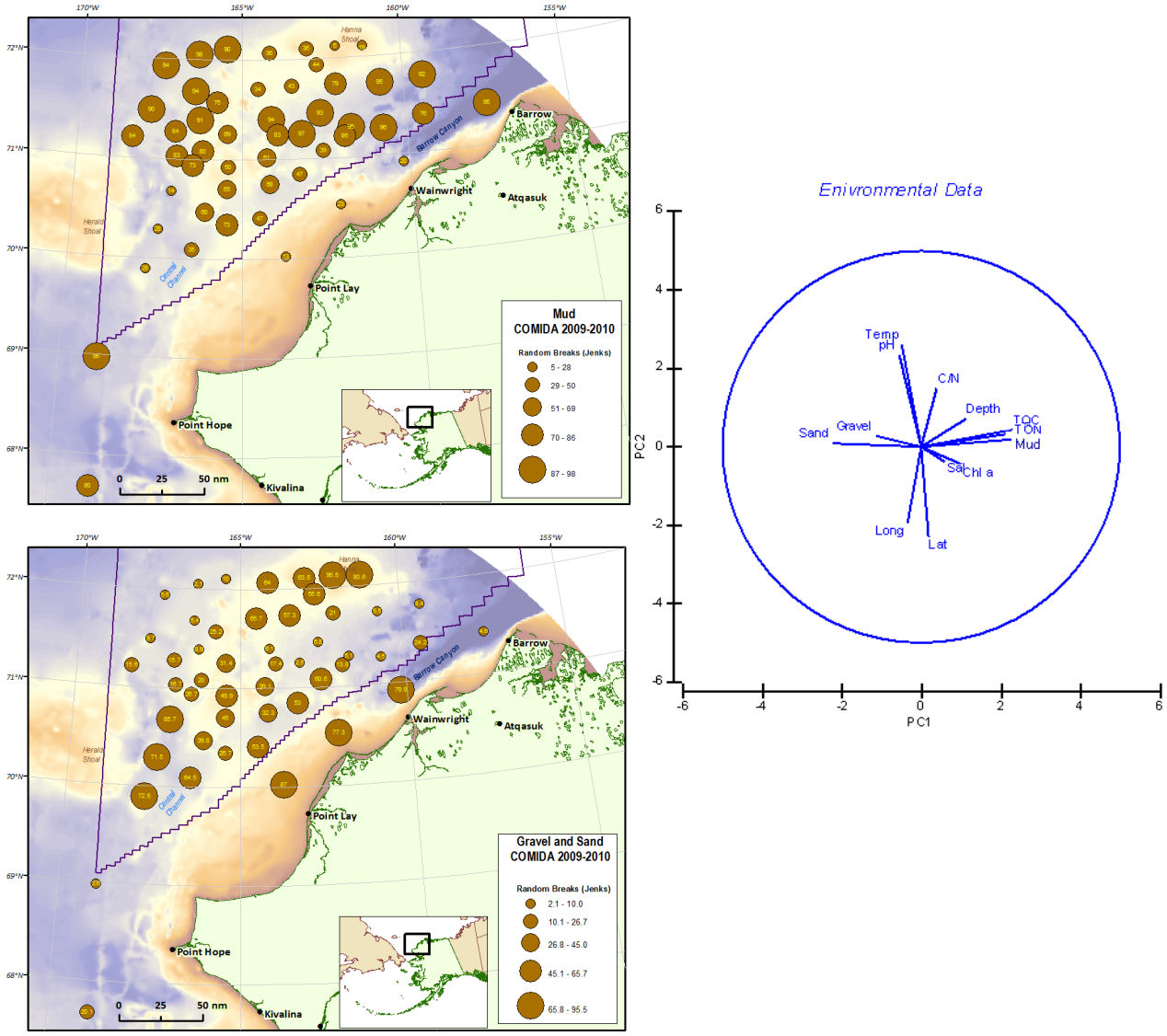

Figure 10. The maps show the distribution of mud sediments (≥5 phi; top panel), and gravel and sand (≤4 phi; bottom panel).

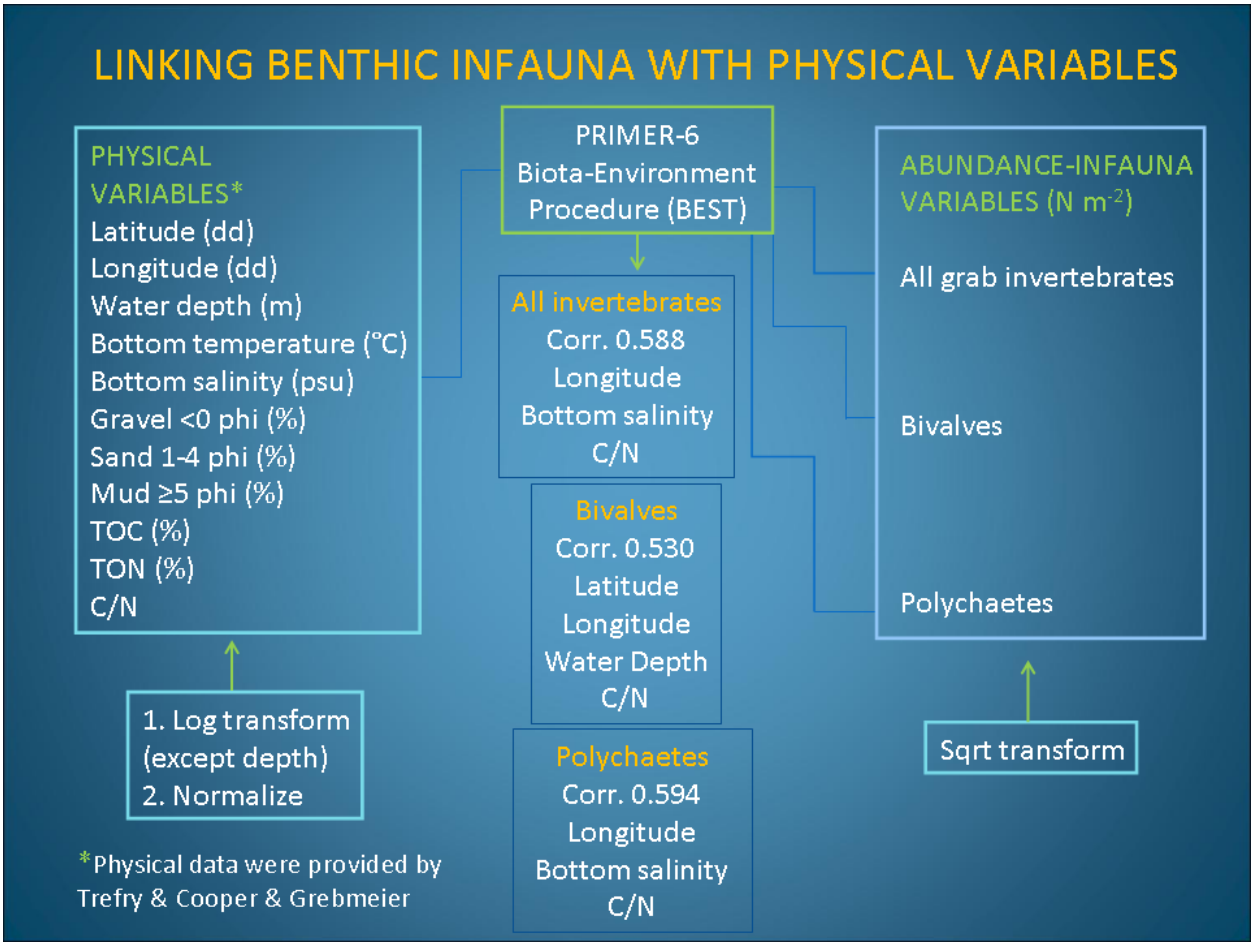

Figure 11. A schematic of variables and results of the Biota-Environment Procedure (BEST) routine used to determine which physical factors best explained species abundance distribution.

The water quality and sediment variables for all stations were merged and plotted using PRIMER's Principal Components Analysis (PCA) to determine how environmental parameters collected from the 50 distributed stations related to one another (Figure 10). Principal component analysis (PCA) is a mathematical procedure that uses an orthogonal transformation to convert a set of possibly correlated variable values into a set of values of linearly uncorrelated variables called principal components. The first principal component (PC1) accounts for as much of the variability in the data as possible, and the second component (PC2) contains the highest variance possible under the constraint that it be uncorrelated with the preceding components. The data were normalized prior to running the PCA function.

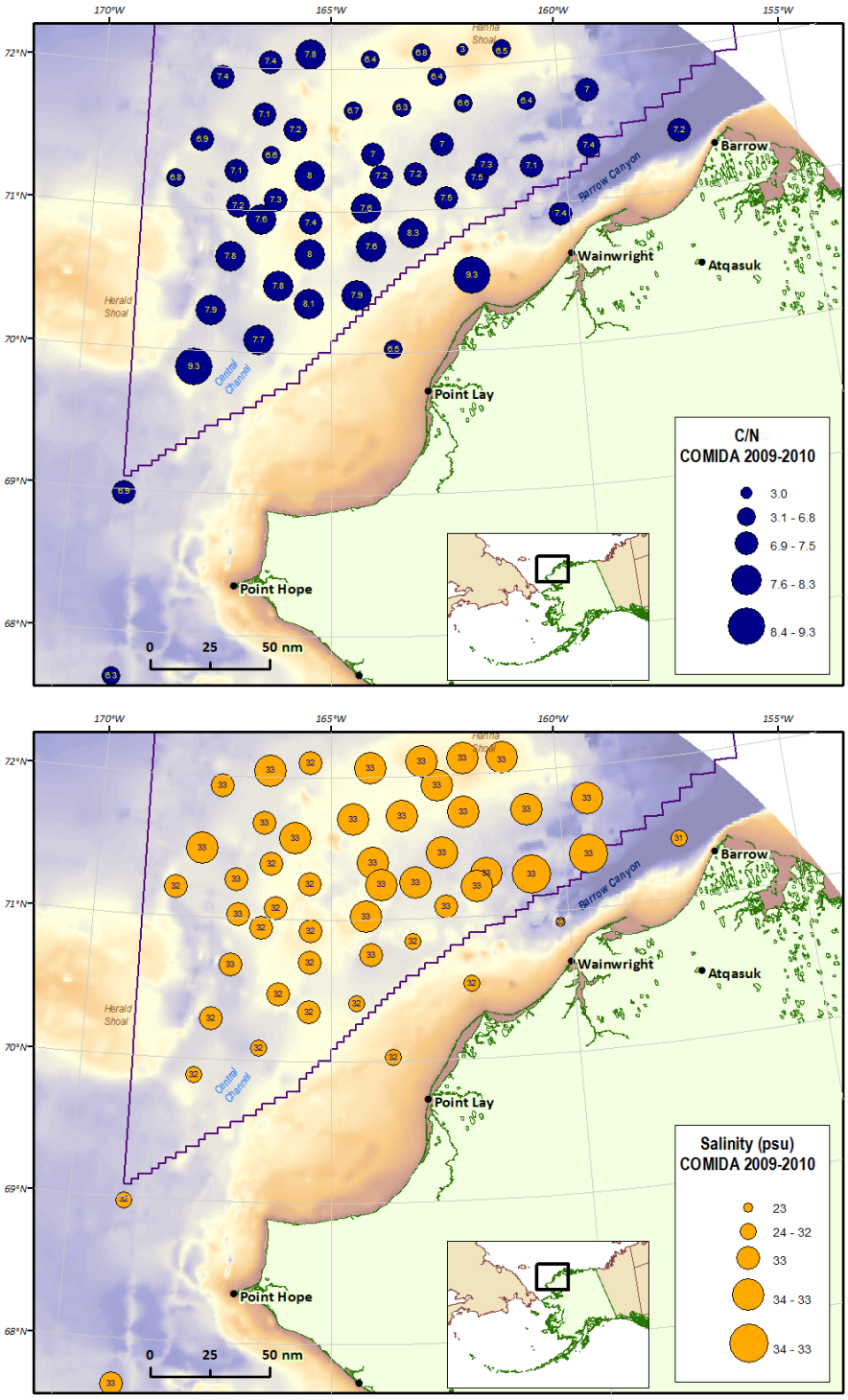

Figure 12. Plots of C/N and salinity (psu) station means. These two variables along with longitude, created the closest correlation with all species and polychaete abundance distribution.

Results on the PC1 axis show that stations with higher measurements of mud also have higher levels of TOC, TON, and to a lesser degree, higher Chl *a*, salinity and C/N values. Longer

vector lines represent a large variable influence. The PC2 axis showed that stations with lower latitude or longitude (in decimal degrees) have higher pH, and temperature. The substrate maps illustrate the geographic distributions of different substrate types within the study area. Infaunal species were most prolific within mud sediments with associated variables located on right side of the PC1 axis.

Physical attributes exhibited distributional trends. Water temperature decreased as latitude increased from a temperature of 3.1° C at the southernmost faunal station (Station 103) to -1.7° C around Hanna Shoals. pH values revealed a similar distributional pattern ranging from 8.2 to 7.4. Water salinity at bottom depths varied little (33.3 – 31.5 psu), with the exception of Station 27 in the nearshore Alaska Coastal Current waters (23.2 psu). Water salinities were generally higher west of Barrow Canyon and in the Hanna Shoal vicinity then in other parts of the study area (Figure 12). Saline waters occurred in the same locations where benthic infaunal abundance and biomass was elevated. C/N ratios of sediment POM ranged from 9.3 to 3.0 (Overall mean 7.2 ± SE 0.13). Higher C/N values represent organic matter with most degradation. The lowest C/N values (indicating freshest organic material) documented in this study were located in the Hanna Shoal region. Species abundance distribution was correlated to longitude because stations located in western portion of the study area had fewer individuals and less species than stations in the eastern sector of the study area (Hanna Shoal/Barrow Canyon).

Conclusions

The infaunal stations sampled during this study covered a large and varied extent of the Northeastern Chukchi benthos. A broad spectrum of species lived in high concentrations in areas surrounding Hanna Shoal and east to Barrow Canyon. The location of these communities appears to correlate with food availability, which is evident in the geographic distribution of POC, PON, Chl *a* and C/N values. These locations also exhibited similar bottom water salinities and mud substrates. A GIS map of C/N measurements showed that water flowing up from Bering Straits and through the Central Channel carried fresh organic matter north to the Chukchi Sea shelf and the vicinity of Hanna Shoal. Diversity was not necessarily tied to abundance and biomass because some stations contained high numbers of either a few polychaete or bivalve species.

Acknowledgments

We thank the Bureau of Ocean Energy Management (BOEM), U.S. Department of Interior for funding to support this study. We appreciate that Dick Prentki of BOEM was an integral part of the team, participating in the cruises and played an active role in project planning and scientific discussions. We thank Jackie Grebmeier for her expert leadership as Chief Scientist on the cruises. We thank Captain John Seville of both the *R/V Alpha Helix* and *R/V Moana Wave* and his crew for fearlessly sailing us around the Chukchi Sea. We thoroughly enjoyed all the COMIDA scientists as professionals and pals and thank them for the passion and teamwork that they brought to the project.

Epibenthic community variability in the Chukchi Sea

Ravelo, A.M., B. Konar, J.H. Trefry, and J.M. Grebmeier

Alexandra M. Ravelo and Brenda Konar
School of Fisheries and Ocean Sciences
University of Alaska Fairbanks, Fairbanks, Alaska 99775

John H. Trefry
Department of Marine and Environmental Systems
Florida Institute of Technology, Melbourne, Florida 32901

Jacqueline M. Grebmeier
Chesapeake Biological Laboratory,
University of Maryland, Solomons, MD 20688

Abstract

In the continental shelf of the Chukchi Sea, epibenthic organisms can occur in large numbers and high biomass. These organisms are key elements of the local food web, as well as important prey items for birds, fish and marine mammals. From an ecosystem perspective, they are known to be important for recycling and redistributing organic matter deposited from the pelagic zone as bioturbators and their role in organic carbon remineralization. Many representatives of the epibenthos have long life spans and slow growth rates, which accentuates the issues related to bioaccumulation of trace metals. In 2009 and 2010, biological and environmental data were collected in the Chukchi Sea in an area leased for oil exploration, with the purpose of characterizing the biota to monitor for potential changes due to anthropogenic disturbances. As a main objective, this analysis determined the epibenthic species composition, abundance, biomass, and characterized the patterns of community distribution as a part of a baseline data set for the study area. In our results, the epibenthic communities in the Northestern Chukchi shelf were dominated by crustaceans or echinoderms. Communities dominated by crustaceans had higher diversity and evenness index values compared to communities dominated by echinoderms. In this study, the assemblages had low correlation values to the environmental variables that were included in the analysis. However, assemblages dominated by different taxa followed a distinct pattern of distribution that matched the path of important water masses in the region. Completing our understanding of the epibenthic assemblages and the environmental variables that affect their distribution is fundamentally important considering the increasing economic interest in this area and its associated disturbance.

Introduction

Epibenthic organisms on the continental shelf of the Chukchi Sea can be found in high abundance and biomass. Several members of the benthic community constitute a key element in the Arctic food web, as prey of marine mammals, birds and fish (Bluhm and Gradinger, 2008). The Arctic epibenthic community structure is highly variable, with peaks in abundance of

specific groups, such as echinoderms and crustaceans, creating a mosaic or "patchiness" in the species distribution (Ambrose et al., 2001; Bluhm et al., 2009; Piepenburg, 2005). In this way, the Arctic benthos cannot be described as one typical assemblage. Distinct communities are determined by an array of environmental variables, such as water depth, water current, seafloor composition and food availability (Bluhm et al., 2009; Piepenburg, 2005). However, which factors define the epibenthic community variability and to what extent is still uncertain and a subject of debate in the literature (Bluhm et al., 2009). Despite the overwhelming presence of echinoderms (particularly ophiuroids), Arctic epibenthic communities compared at a global scale can have an intermediate species richness, only marginally lower than Antarctic communities (Piepenburg, 2005). The increasing economic interest in the Chukchi Sea has risen concern in regards to the negative effects that anthropogenic activities, such as offshore oil exploration, mineral extractions and fisheries (fish and shellfish) may cause to the stability and success of the epibenthic communities in this region (Bluhm et al., 2009; Grebmeier et al., 2006b). In addition, global warming and ocean acidification have the potential of creating acute changes in the habitat of Arctic benthic organisms (Bluhm et al., 2009; Fabry et al., 2008; Piepenburg, 2005). As a result, it is first necessary to complete our understanding of the epibenthic community composition and its relationship with the environmental processes that define its natural variability in order to conserve and manage this unique natural resource. Without this knowledge, tracking temporal changes the epibenthic communities undergo due to anthropogenic disturbances would be a great challenge.

The continental shelf of the central Chukchi Sea is relatively shallow, with water depth averaging 50 meters. Sediment composition has high percentages of fine sand, silt and clay; with minor proportions of gravel and sand in the outer continental shelf and relatively coarse sand and gravel substrate near shore (Naidu, 1988). The area is covered by ice seven to eight months of the year, causing light limitation, vertical stability of the water column and reduced nutrient supply (Dunbar, 1968). Compared to other Arctic regions, the Chukchi Sea is considered highly productive, with water column primary production values ranging from 80-90 g C m^{-2} y^{-1} in the northern shelf to 470 g C m^{-2} y^{-1} in the southern Chukchi Sea, with the lowest values of 20-70 g C m^{-2} y^{-1} recorded in coastal water (Sakshaug, 2004). The distinct water masses found in the region are defined by variations in salinity. Low salinity levels (<31.8) characterize the low nutrient Alaska Coastal Water (ACW), that flows northward along the coast. Bering Shelf Water (BSW) also flows northwards through the Bering Strait, and is characterized by high salinity and nutrient levels (Coachman et al., 1975). In general, input of high nutrient water originated in the Bering Sea and transported northward through the Bering Strait allows for a high seasonal primary production, which in conjunction with low grazing pressure, translates into high deposition of organic matter to the benthos (Grebmeier et al., 1988).

Many characteristics of the epibenthic communities in the Arctic make them especially important to benthic systems. In the Chukchi Sea, echinoderms were reported in dense assemblages (several hundred individuals per meter square) and high biomass, up to 30% higher than the highest values reported for echinoderms in the Barents Sea (Ambrose et al., 2001). These assemblages also showed higher respiration values compared to the Barents Sea, which marks the importance of the epibenthos for Chukchi Sea benthic respiration. In the same study, the epibenthos were responsible for up to 25% of the benthic respiration (Ambrose et al. 2001). Many members of the epifaunal community have great mobility that allows them to access and

redistribute organic carbon deposited from the pelagic zone, and also play an important role in the organic carbon remineralization (Piepenburg, 2005). Epibenthic organisms are also significant bioturbators and contributors to the total benthic energy turnover (Grebmeier and McRoy, 1989; Piepenburg et al., 1995). The Chukchi Sea is populated by many species of slow growth rates and long life spans. This characteristic has added importance due to the high levels of trace metals these organism can bioaccumulate throughout their life and subsequently transfer to higher trophic levels (Clarke, 1983). Epibenthic and benthic organisms have great importance in the diet of many Arctic marine mammals, either as an opportunistic resource (i.e. Bearded Seal) or a specific preference (walrus). With this in consideration, the potential for biomagnification of trace metals to higher trophic levels becomes an issue of great concern, especially for species with importance in the subsistence harvests of local human communities (Bluhm and Gradinger, 2008; Dehn et al., 2006).

Seasonal changes in salinity, solar irradiance and ice coverage that occur in the Chukchi Sea directly affect the primary production of the area. In the spring, light increases and sea ice melting creates stratification in the water column, which favors phytoplankton blooms in the ice edge zone. These marginal ice zone blooms occur before phytoplankton growth in the open ocean, adding up to 50% of the total primary production in Arctic waters (Sakshaug, 2004). Epibenthic organisms that inhabit this region endure a severe seasonal food limitation seven to eight months out of the year, which is reflected in the slow growth rates and long life spans of many of these Arctic benthic organisms (Clarke, 1983). The benthic community structure and biomass in the Chukchi Sea is strongly influenced by the carbon input from the water column and the quality of the organic carbon (Grebmeier et al., 1988). Many studies have highlighted the importance of the pelagic-benthic coupling as a major factor modifying the benthic communities in Arctic ecosystems (Grebmeier and McRoy, 1989; Piepenburg, 2005). In addition, many environmental variables such as sediment grain size, water depth, temperature, as well as sediment C/N ratios and surface primary production are of great importance in structuring benthic communities (Feder et al., 2005; Feder et al., 1981; Piepenburg, 2005). A more recent study of the epibenthos in the Chukchi Sea suggest benthic-pelagic coupling to be less important in determining the epibenthic community composition and having a more important role for macroinfauna (Bluhm et al., 2009). This study also highlights the need of further analysis in regards to environmental variables modifying the epibenthic community composition. Thus, many environmental variables used traditionally to explain epibenthic assemblages may be acting as proxies for different environmental factors (Bluhm et al., 2009).

In the Arctic Seas, the effects of climate change are amplified by the positive feedback associated with the high albedo of ice and snow (Manabe et al., 1991). The loss of perennial sea ice has been calculated to reach a rate of 9% per decade (Comiso, 2002). The changes are likely to result in altered productivity regimes, changes in quality and quantity of available food, and higher lithogenous sediment deposition levels (Renaud et al., 2007). The early retreat of sea ice would create a longer growing season favoring zooplankton populations and increasing the pelagic biota. As a consequence, this may diminish the amount of organic matter transported down the water column for feeding epibenthic organisms. Shifting from a sea ice algal-benthos regime to phytoplankton-zooplankton dominance could have a marked effect on benthic community composition (Grebmeier and Barry, 1991). Impacts of these climate related events on benthic community structure will likely have repercussions throughout the ecosystem.

Oil exploration in Alaska's Arctic waters started more than 40 years ago, mostly on the North Slope near Prudhoe Bay. The interest for oil exploration has extended to the Chukchi Sea in recent years, with the belief that this region holds over 30 billion barrels of oil and gas equivalent. If this area is opened to oil extraction, the chances of pollutant exposure for the epibenthic organisms will increase significantly. The effect of oil contamination has been well studied for fishes (Reynaud and Deschaux, 2006), marine mammals (Sprague et al., 1981; Suchanek, 1993) and benthic organisms (Suchanek, 1993). It is assumed that motile organisms, like many epibenthic taxa, would be the least affected of the benthic community. However, there is evidence that after the "Tampico Maru" wreck off the coast of Baja California in 1957, sea stars (*Pisaster* spp.) and sea urchins (*Strongylocentrotus* spp.) were eliminated from the area for several years (Nelson-Smith, 1973). Echinoderms may be specially sensitive to oil exposure due to the proportion of exposed epidermis in this group (Suchanek, 1993). Molluscs exposed to oil contamination showed an increase in energy expenditure and a decrease in feeding rates, leaving less energy for growth and reproduction (Suchanek, 1993). In addition, exposure to oil at high latitudes has a greater effect on organisms due to the increased persistence of hydrocarbons at low temperature (Rice et al., 1980). In 2009 and 2010, biological and environmental data were collected in the Chukchi Sea in an area leased for oil exploration, with the purpose of characterizing the biota to monitor for potential changes due to anthropogenic disturbances. As a main objective, this analysis determined the epibenthic species composition, abundance, biomass, and characterized the patterns of community distribution as a part of a baseline data set for the study area. We hypothesized that the epibenthic communities would be distributed in patches dominated by distinct taxonomic groups and that the zonation patterns of the communities would be determined by discrete environmental characteristics. To explore these hypotheses, our analysis identified the taxa that best represented the epifaunal community in terms of abundance and biomass. Also, the distributions of the most representative taxa and community assemblages throughout the study area were analyzed and the combination of environmental variables that had the highest correlation to the epibenthic community distribution was determined.

Materials and Methods

The data used for these analyses were generated by the Chukchi Sea Offshore Monitoring In Drilling Area Chemical And Benthos (COMIDA CAB) Program, an area corresponding to the Lease Sale 193. Stations extended from 69° 02' to 72° 24' latitude N and ranged in water depths between 23 and 58 m. All sites were determined via two methods: 1) a general randomized tessellation stratified design (GRTS) in the core COMIDA area, and 2) a spatially oriented, nearshore-to-offshore, south to north grid overlaying the GRTS design. This arrangement allowed the location of the core station sites in a spatial grid. Data were collected on two summer cruises (end of July to mid-August) of 2009 and 2010. Biological data were collected using one epibenthic trawl at the 53 stations (Figure 1).

The epibenthic trawl used in this study was a 3.05 meter plumb-staff beam trawl with a 7 mm mesh and a 4 mm codend liner, modified with a lead-filled line and six inch sections of chain seized to the footrope every six inches (Gunderson and Ellis, 1986). This trawl was towed for 2

to 5 minutes on the sea floor while the vessel was moving at 1 to 1.5 knots. A rigid 3 m pipe forward of the net held the mouth open for an effective swath of 2.26 m, allowing for adequate quantifications of trawl effort by area swept (the calculated area of seafloor trawled was 262 m²). The vertical opening of the net was approximately 1.2 m. A typical beam trawl catch ranged from 40 to 100 kg in the codend. This trawl design is very effective at collecting epibenthic organisms >4 mm. After the trawl was brought on board, catches were cleaned and organisms sorted to the lowest taxonomic level (in most cases to genus). All groups were individually counted and their damp biomass determined. Voucher specimens were fixed in 10% buffered formalin for further taxonomic identification.

Environmental variables were collected by the COMIDA CAB team. Vertical profiles of salinity, temperature, dissolved oxygen, turbidity, chlorophyll a and pH were obtained at each trawled station using a YSI SONDE 6600 (details in Trefry et al., this report). Sediments were collected using 0.1 m² van Veen Grabs for total organic carbon, grain size and sediment chlorophyll analyses (details in Grebmeier and Cooper, this report).

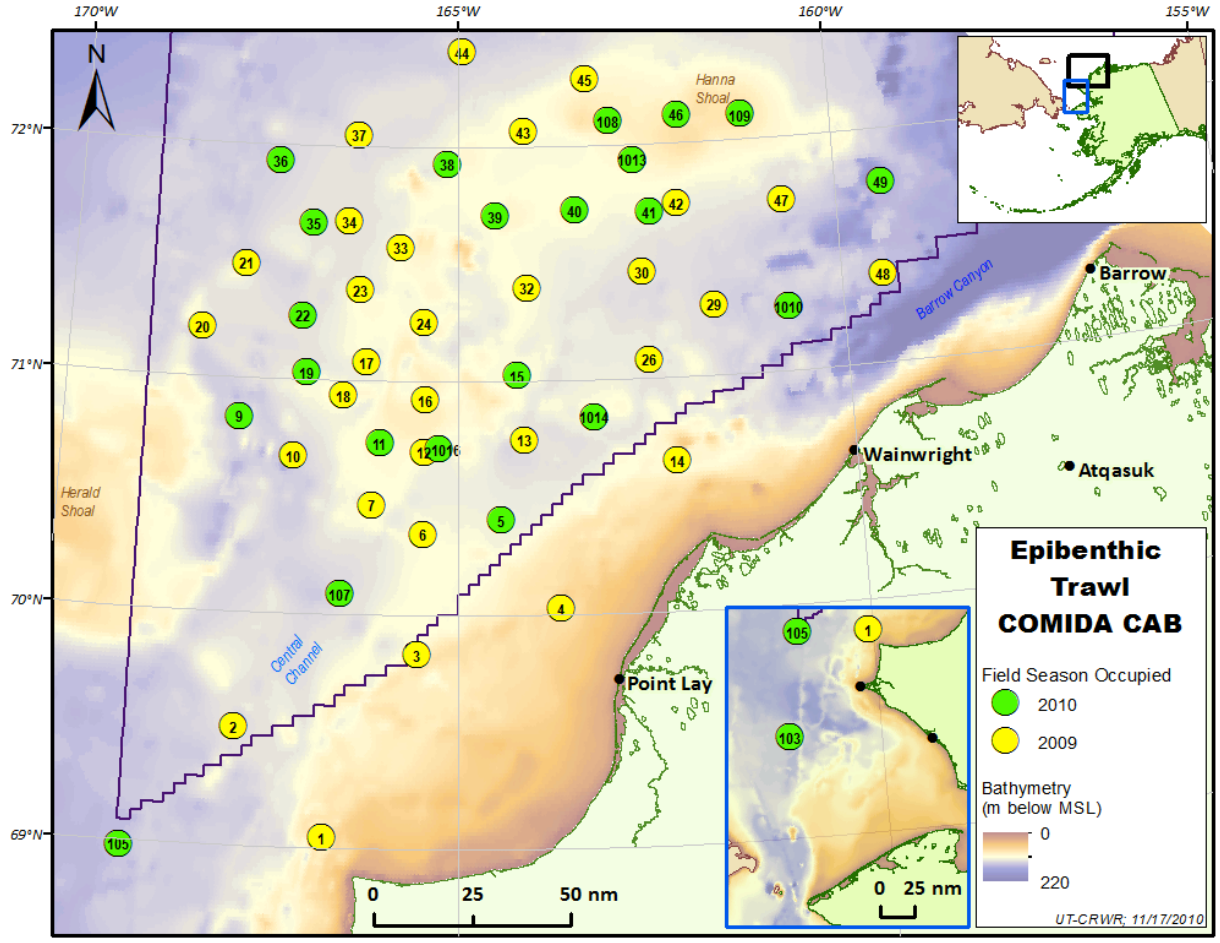

Figure 1. Epibenthic stations sampled in 2009 and 2010 in the Chukchi Sea. In the top right corner insert, the main study area is outlined by a black box and the blue box includes stations sampled in the upstream Bering Strait/SE Chukchi region, seen in detail in the insert at the bottom right.

Data Analysis

Abundance and biomass data were standardized to 2.5 minutes of tow time and to relative percentage per trawl. When necessary to meet normality, data were transformed to square root values. To determine the taxa that best represented the epifaunal community across all stations, a BVST procedure in the PRIMER v.6 package (Clarke and Gorely, 2006) was used for abundance and biomass, using Bray-Curtis resemblance matrix and Spearman rank correlation. Cluster analysis for abundance was used to group stations by similarity (group average from Bray-Curtis resemblance matrix). An MDS (Multi-dimensional scaling) plot was used to better visualize the grouping of stations by similarity. Simpson's diversity, Pielou's evenness and Margalef's richness indices were calculated from untransformed abundance data for groups of stations and independent stations, using the DIVERSE routine in PRIMER. Similarity Percentages Test (SIMPER) in PRIMER through Bray-Curtis similarity matrix was used to determine the levels of similarity within clusters, dissimilarity between clusters and the role of individual taxa in contributing to the separation between groups of samples. To identify the group of environmental variables that best correlated to the epibenthic community, the BIO-ENV routine in PRIMER selected a list of variables from a set of transformed and normalized environmental parameters (Eucledean distance resemblance matrix). The environmental variables that were included in these analyses were latitude, longitude and depth (as indirect determinants of community structure), bottom water salinity, temperature, dissolved oxygen, turbidity and pH (for bottom water characteristics) and sediment grain size. Also, mean sediment chlorophyll *a*, total organic carbon (TOC), total organic nitrogen (TON) and carbon to nitrogen ratio (C/N) were analyzed as indicators of food supply and quality. Some variables were excluded from the analysis due to high autocorrelation including TON and sediment grain sizes 1 phi, 3 phi and 1-4 phi.

Results

From the 53 stations a total of 44 taxa in six phyla with 499,294 individuals were counted, ranging from 157 individuals at Station 10 to 114,684 individuals at Station 1010 (mean across all stations 9,421 ± 20,858 s.d.; Figure 2a). Counts included four cnidarians, 11 echinoderms, 21 molluscs, five crustaceans, one pycnogonid, and two ascidiaceans. The number of taxa present in each trawl varied from six at Station 109 to 25 at Stations 1014 and 5 (mean 16 ± 4 s.d.). Across all stations, ophiuroids represented 73% of the total abundance, *Ocnus* spp. 14%, shrimp 4%, *Echinarachnius* spp. 3% and *Chionoecetes opilio* 2%. Biomass for all stations combined was 928.2 kg, ranging from 0.232 kg at Station 46 to 134.78 kg at Station 1010 (mean 17.51 kg ± 26.38 s.d.) (Figure 2b). Across all stations for biomass, ophiuroids accounted for 39%, *Chionoecetes opilio* 14%, *Ocnus* spp. 13%, *Echinarachnius* spp. 9% and *Pagurus* spp. 4%.

Overall, the six taxa that best represented the community structure for abundance included *Chionoecetes opilio*, ophiuroids, *Pagurus* spp., shrimp, *Echinarachnius* spp., and *Cryptonatica* spp. (BEST Primer-e, Spearman correlation value of 0.958). For biomass, the six best taxa were *Chionoecetes opilio*, ophiuroids, *Pagurus* spp., shrimp, *Gorgonocephalus* spp., and *Cryptonatica* spp.; with the alternative of *Neptunea* spp. as a substitute to *Cryptonatica* spp. (BEST Primer-e, Spearman correlation value of 0. 924 with *Cryptonatica* spp. and 0.922 *Neptunea* spp.; Figure 3, a & b).

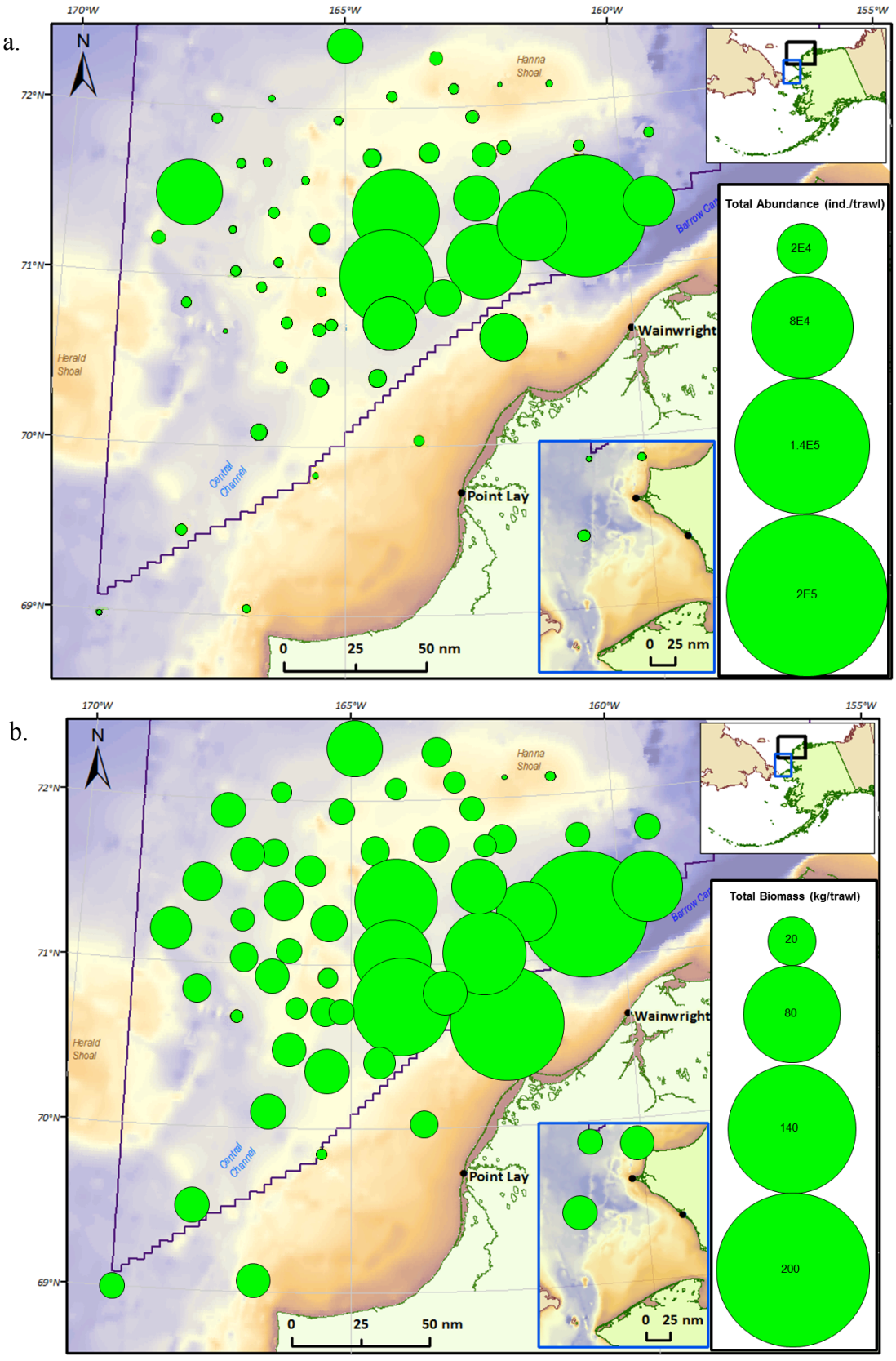

Figure 2. Map of all stations, bubble size reflects a) the total abundance (number of individuals) and b) biomass (kg) for each station.

(a)

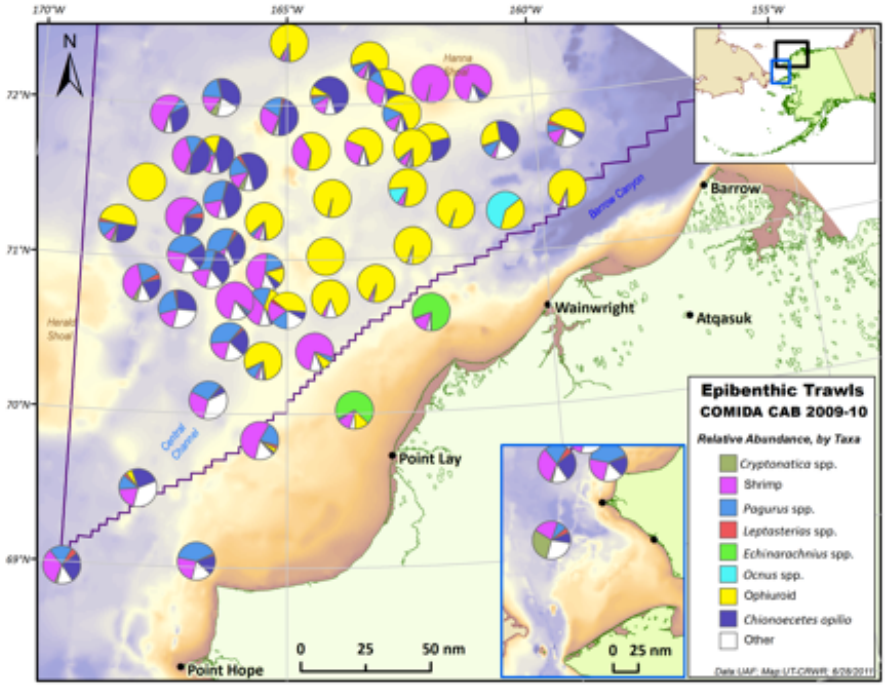

(b)

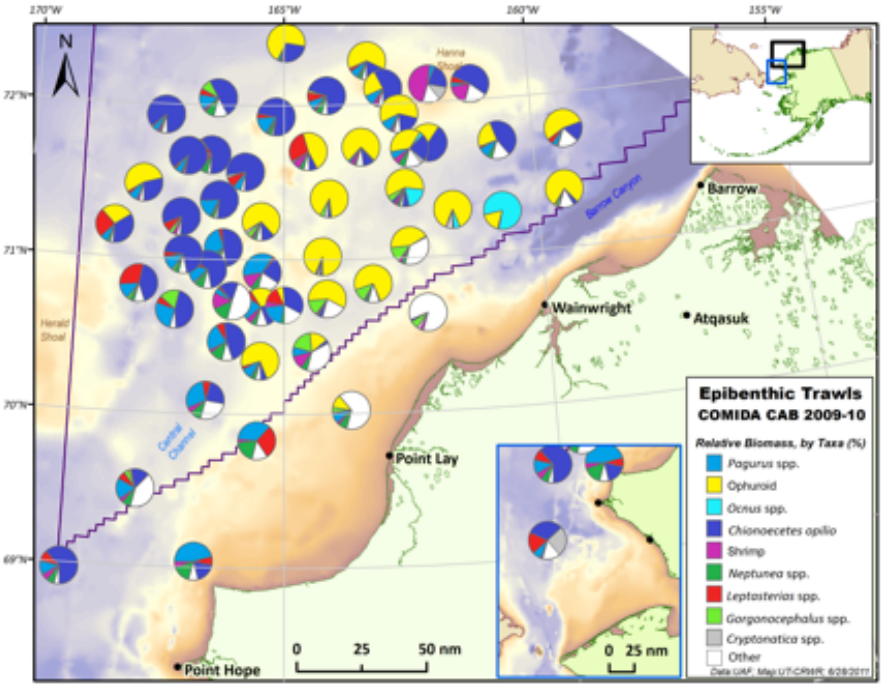

Figure 3: Maps show a) relative abundance and b) biomass for taxa selected by the BEST analysis, including taxa of high abundance or biomass that were not selected as important in the community composition, i.e. *Ocnus* spp. and *Leptasterias* spp.

A cluster analysis for abundance at the 55% similarity level identified four clusters and two independent stations (103 and 1010), which did not join any group (Figure 4a). SIMPER analysis, showed within group similarity to vary from 63% to 78% (70% average) (Table 2), dissimilarity between pairs of groups ranged from 50% to 90% (68% average) (Table 3). Ordination of stations in an MDS plot with a stress level of 0.12 showed no overlap of groups at the 55% similarity level (Figure 4b). Analysis of variance between cluster groups for diversity indices measures were calculated at a 95% confidence level. Margalef's richness index resulted in no significant difference between groups of stations and was not included for further analysis. A pairwised comparison of means at a 0.05 significance level revealed significant differences between Group 4 and all other groups for Simpson's index; also, statistical differences were observed between Groups 2, 3 and 4 for Pielou's index.

Overall, station clusters grouped in a geographic distribution with few stations of Group 2 located within the area of Group 4, and stations in Group 3 were divided in two separate areas (Figure 4c). Group 1 formed by two stations of coastal location, had a mean abundance of 9,417 individuals per trawl and biomass of 58.46 kg per trawl (Table 1). This group was highly dominated by *Echinarachnius* spp. in abundance (69% and 80% of total trawl abundance) and biomass (55% and 75% of the total trawl weight; Figure 3), however, diversity indices (Simpson and Pielou's) were intermediate in relation to other groups and independent stations (Table 3). Stations in Group 2 were located easterly and south of Hanna Shoal, with the exception of Stations 21 and 44, the first located in the far west of the study area and the second located north of Hanna Shoal (Figure 4c). The mean abundance and biomass in this group amounted to 22,123 individuals per trawl and 29.88 kg per trawl (Table 1). High abundance and biomass of ophiuroids characterized stations in Group 2 (Figure 3). Simpson index had intermediate values and Pielou's evenness index was the lowest of all groups (Table 1). Group 3 accounted for four stations, two on Hanna Shoal and the other two placed south between Herald Shoal and the coast (Figure 4c). These stations are characterized by the high abundance of shrimp present in relation to all other taxa found across stations (Figure 3a). The mean abundance for this group amounted to 1,047 individuals per trawl and the mean biomass was 3.42 kg per trawl. Intermediate Pielou's evenness and the lowest Simpson's indices were calculated for Group 3 (Table 1). The largest Group included most of its stations west of 165° longitude with eight stations following the western and southern limit of Hanna Shoal (Figure 4c). Stations in this group were dominated by the crustaceans *Chionoecetes opilio*, *Pagurus* spp., and shrimp (Figure 3). These stations had the highest average evenness and diversity index of all groups. The mean abundance and biomass of these stations was 11,621 individuals per trawl and 7.14 kg per trawl (Table 1). The independent Station 103 was the southernmost station with 1,164 individuals per trawl and 10.08 kg per trawl, the gastropod *Cryptonatica* spp. accounted for 30% of the trawl abundance and 26% of the trawls biomass (Figure 3). This station also had intermediate diversity and low evenness indices values. Station 1010 was also segregated from all groups. It had the highest abundance and biomass of all stations (114,864 individuals per trawl; 134.78 kg per trawl) (Figure 2, Table 1). This station was highly dominated by *Ocnus* spp., which had a biomass of 109 kg (81% of the trawls total biomass) and abundance of 68,304 individuals (60% of the trawls abundance) (Figure 3). This station had the highest diversity and evenness values (Table 1).

a.

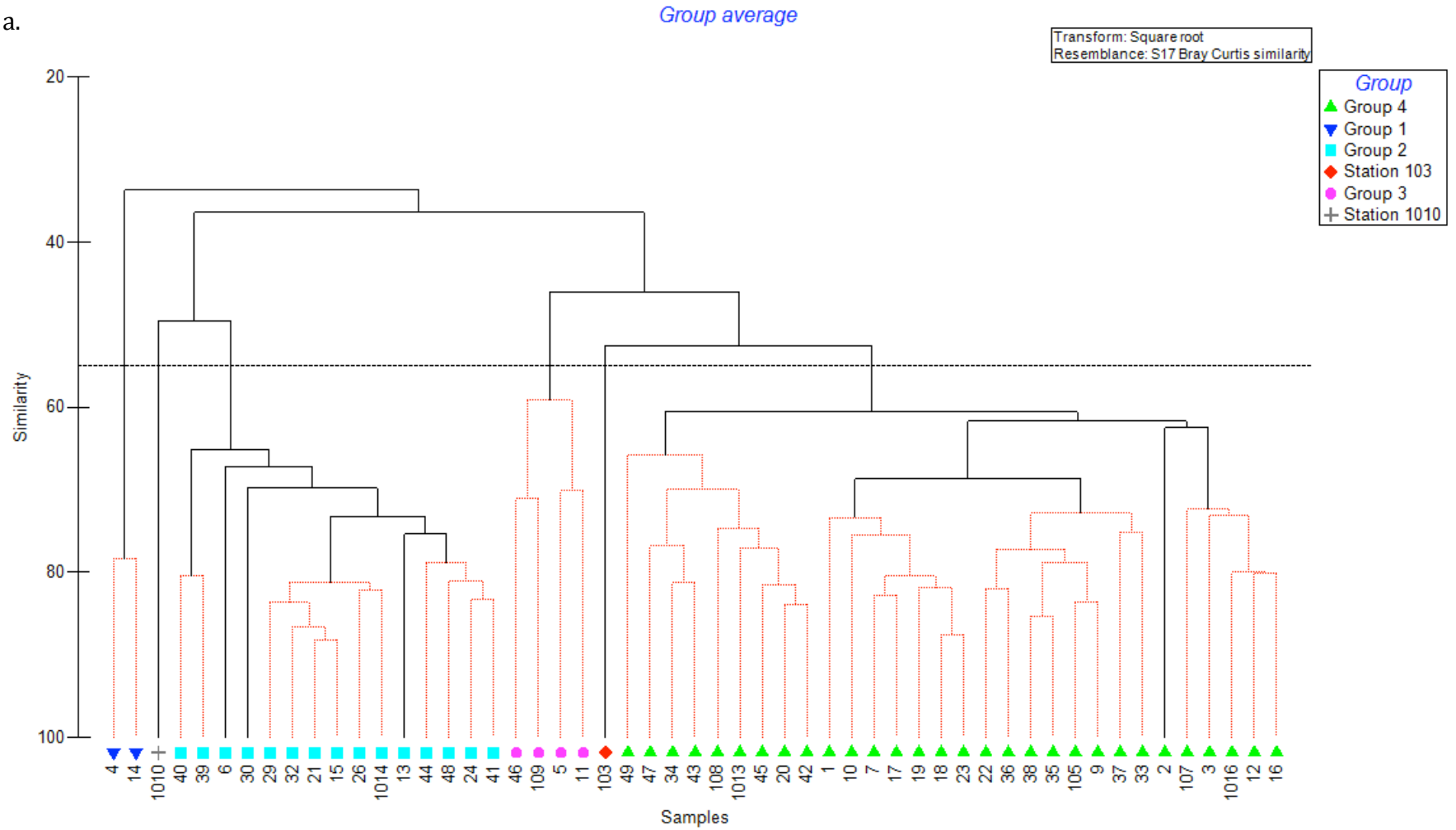

Figure 4. Caption on following page.

b)

b.

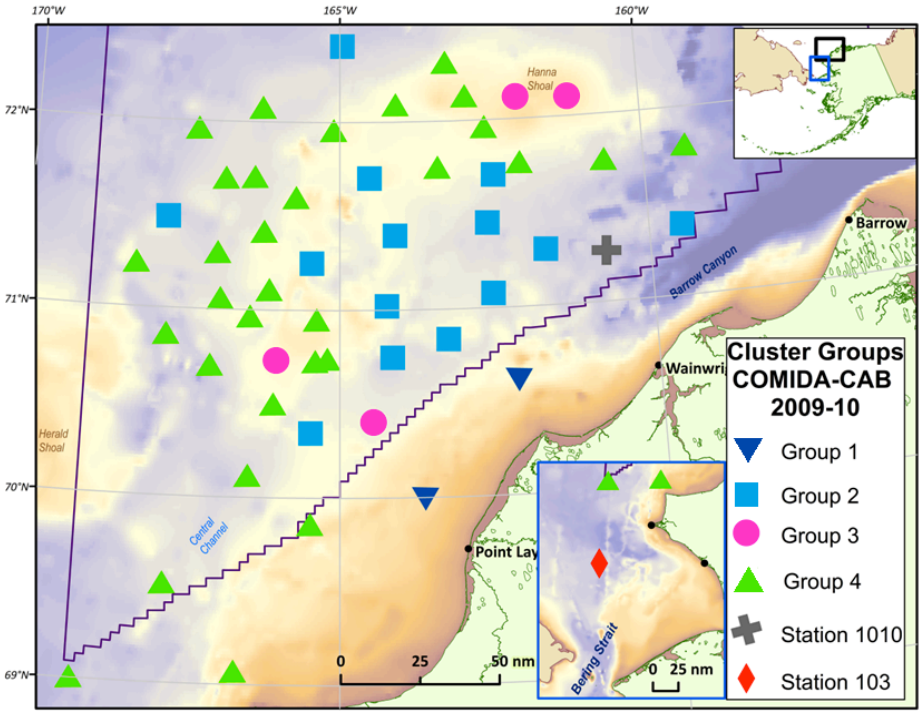

c.

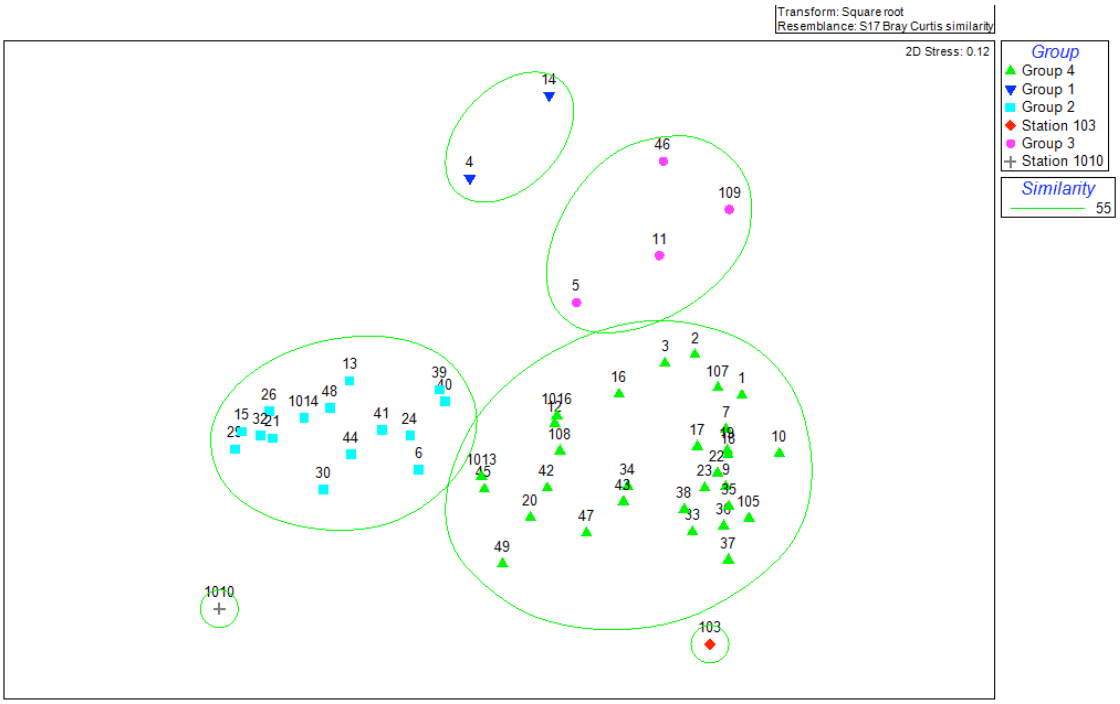

Figure 4. Station groups, symbols represent the cluster groups at 55% similarity and are constant for all figures. a) (Previous page) Station clusters from the relative percentage per trawl of abundance (square-root-transformed, Bray-Curtis similarity), dotted line shows the 55% similarity level. b) MDS of abundance, station groups are outlined by the 55% similarity level and 0.12 stress level. c) Map shows the spatial distribution of cluster groups and independent stations.

Similarity analysis within groups of stations included shrimp in the top two contributors of the similarity for all groups, and alone contributing 68% of the similarity in Group 3. In Group 2, ophiuroids contributed 67% of the similarity among stations, *Echinarachnius* spp. contributed to 50% in Group 1, and the similarity among stations in Group 4 was divided almost evenly among shrimp, *Chionoecetes opilio* and *Pagurus* spp. (approximately 20% each; Table 2). The presence of *Cryptonatica* spp. at Station 103 aided in the dissimilarity between this station and all other groups (including Station 1010), with an average contribution of 15 %. In the case of Station 1010, *Ocnus* spp. added on average 26% of the dissimilarity among all other groups and Station 103 (Table 3).

Table 1: Mean abundance (number of individuals per trawl) and biomass (kg per trawl) of station groups and totals for independent Stations 103 and 1010. In parenthesis s.d. refers to standard deviation. Diversity indices: 1-λ (Simpson's dominance index) and J' (Pielou's evenness index).

Group/ Station	Number of taxa	Abundance (s.d.)	Biomass (s.d.)	1-λ (s.d.)	J' (s.d.)
1	16	9,417 (8,4730	58.45 (52)	0.61 (0.03)	0.44 (0.06)
2	37	22,123 (20,695)	29.88 (18)	0.63 (0.04)	0.33 (0.07)
3	27	1,047 (918)	3.42 (3)	0.57 (0.04)	0.42 (0.07)
4	42	11,621 (592)	7.14 (3)	0.68 (0.02)	0.54 (0.04)
103	13	1,164	10.08	0.6222	0.3735
1010	16	114,864	134.78	0.7066	0.6362

Table 2: Percent similarity among samples within cluster groups, with percent contribution of each taxa up to approximately 80%. In parenthesis s.d. refers to standard deviation. Contrib.: Percent Contribution. Cum.: Percent Cumulative.

	Av. Abundance (% in trawl)	Av. % similarity (s.d.)	Contrib. (%)	Cum. (%)
Group 1 - Av. similarity: 78%				
Echinarachnius spp.	8.61	39.2	50.06	50.06
shrimp	3.56	15.98	20.4	70.46
Hyas spp.	1.53	6.7	8.56	79.02
Chionoecetes opilio	0.99	4.61	5.89	84.91
Group 2 - Av. similarity: 72%				
ophiuroid	9.28	48.49 (5.24)	67.19	67.19
shrimp	2.08	6.78 (2.5)	9.4	76.59
Chionoecetes opilio	0.95	3.26 (1.83)	4.51	81.1
Group 3 - Av. similarity: 63%				
shrimp	9.11	42.86 (5.2)	68.02	68.02
Pagurus spp.	1.45	4.97 (3.78)	7.89	75.92

Chionoecetes opilio	1.48	4.76 (3.6)	7.55	83.47
Group 4 - Av. similarity: 65%				
shrimp	4.68	13.76 (3.32)	21.17	21.17
Chionoecetes opilio	4.74	13.62 (2.35)	20.95	42.12
Pagurus spp.	4.24	12.85 (4.59)	19.77	61.89
Leptasterias spp.	1.35	3.73 (2.03)	5.73	67.63
ophiuroid	2.62	3.54 (0.54)	5.45	73.08
Neptunea spp.	1.26	3.45 (2.61)	5.31	78.39
Colus spp.	1.07	2.56 (1.64)	3.93	82.32

Table 3: Dissimilarity between station groups and independent Stations 103 and 1010, determined by taxa with approximately 50% contribution. In parenthesis s.d. refers to standard deviation. Contrib.: Percent Contribution. Cum.: Percent Cumulative.

	Av. abundance (% in trawl)		Av. % Dissimilarity (s.d.)	Contrib. (%)	Cum. (%)
Groups 1 & 2 - Av. dissimilarity = 67%	**Group 1**	**Group 2**			
Echinarachnius spp.	8.61	0.07	21.61 (8.06)	32.05	32.05
ophiuroid	2.04	9.28	18.51 (3.42)	27.46	59.51
Groups 1 & 3 - Av. dissimilarity = 63%	**Group 1**	**Group 3**			
Echinarachnius spp.	8.61	0	20.78 (6.13)	33.15	33.15
shrimp	3.56	9.11	13.51 (4.44)	21.55	54.7
Groups 1 & 4 - Av. dissimilarity = 65%	**Group 1**	**Group 4**			
Echinarachnius spp.	8.61	0.03	17.57 (10.67)	26.82	26.82
Chionoecetes opilio	0.99	4.74	7.73 (2.14)	11.8	38.62
Pagurus spp.	0.96	4.24	6.68 (2.8)	10.2	48.83
ophiuroid	2.04	2.62	5.42 (1.28)	8.28	57.1
Groups 1 & Station 103 - Av. dissimilarity = 72%	**Group 1**	**Station 103**			
Echinarachnius spp.	8.61	0	16.95 (11.18)	23.58	23.58
Cryptonatica spp.	0	5.44	10.71 (26.27)	14.89	38.47
Stomphia spp.	0.12	3.32	6.28 (70.29)	8.74	47.2
anemone	0	3.13	6.15 (26.27)	8.56	55.76

Groups 1 & Station 1010 - Av. dissimilarity = 81%	**Group 1**	**Station 1010**			
Echinarachnius spp.	8.61	0	22.78 (9.76)	28.06	28.06
Ocnus spp.	0	7.71	20.37 (19.57)	25.1	53.16
Groups 2 & 3 - Av. dissimilarity = 67%	**Group 2**	**Group 3**			
ophiuroid	9.28	1.08	21.5 (3.4)	32.09	32.09
shrimp	2.08	9.11	18.51 (2.9)	27.62	59.72
Groups 2 & 4 - Av. dissimilarity = 61%	**Group 2**	**Group 4**			
ophiuroid	9.28	2.62	14.49 (2.1)	23.6	23.6
Chionoecetes opilio	0.95	4.74	8.31 (2.03)	13.54	37.14
Pagurus spp.	0.86	4.24	7.34 (2.43)	11.95	49.1
shrimp	2.08	4.68	6.44 (1.65)	10.49	59.58
Groups 2 & Station 103 - Av. dissimilarity = 75%	**Group 2**	**Station 103**			
ophiuroid	9.28	0	19.3 (7.32)	25.61	25.61
Cryptonatica spp.	0.36	5.44	10.55 (8.58)	14	39.61
Stomphia spp.	0.03	3.32	6.8 (12.14)	9.03	48.64
anemone	0.06	3.13	6.37 (11.19)	8.45	57.09
Groups 2 & Station 1010 - Av. dissimilarity = 50%	**Group 2**	**Station 1010**			
Ocnus spp.	0.45	7.71	20.67 (5.51)	40.98	40.98
ophiuroid	9.28	6.3	8.6 (3.29)	17.04	58.02
Groups 3 & 4 - Av. dissimilarity = 54%	**Group 3**	**Group 4**			
shrimp	9.11	4.68	9.24 (2.53)	17.18	17.18
Chionoecetes opilio	1.48	4.74	6.92 (1.78)	12.87	30.05
Pagurus spp.	1.45	4.24	5.86 (2.06)	10.9	40.95
ophiuroid	1.08	2.62	5.28 (1.02)	9.82	50.77
Groups Station 3 & 103 - Av. dissimilarity = 60%	**Group 3**	**Station 103**			
Cryptonatica spp.	0.34	5.44	10.15 (8.04)	16.87	16.87
shrimp	9.11	4.64	8.99 (4.19)	14.94	31.81
Stomphia spp.	0.26	3.32	6.13 (4.44)	10.2	42.01
anemone	0.09	3.13	6.08 (6.01)	10.11	52.12
Groups 3 & Station 1010 - Av. dissimilarity = 85%	**Group 3**	**Station 1010**			
shrimp	9.11	0.67	22.98 (4.33)	27.07	27.07

Ocnus spp.	0	7.71	20.83 (5.75)	24.54	51.61
Groups 4 & Station 103 - Av. dissimilarity = 47%	**Group 4**	**Station 103**			
Cryptonatica spp.	0.79	5.44	8.06 (6.5)	16.98	16.98
Stomphia spp.	0.22	3.32	5.39 (7.48)	11.36	28.35
anemone	0.04	3.13	5.38 (13.13)	11.33	39.68
ophiuroid	2.62	0	4.53 (0.87)	9.55	49.23
Chionoecetes opilio	4.74	3.03	3.69 (1.77)	7.77	57.00
Groups 4 & Station 1010 - Av. dissimilarity = 80%	**Group 4**	**Station 1010**			
Ocnus spp.	0.04	7.71	17.22 (13.45)	21.63	21.63
Chionoecetes opilio	4.74	0.22	10.23 (2.52)	12.84	34.47
Pagurus spp.	4.24	0.17	9.11 (3.72)	11.44	45.91
ophiuroid	2.62	6.3	9.11 (1.62)	11.43	57.34
Groups Station 103 & Station 1010 - Av. dissimilarity = 90%	**Station 103**	**Station 1010**			
Ocnus spp.	0	7.71	16.6	18.37	18.37
ophiuroid	0	6.3	13.56	15.01	33.38
Cryptonatica spp.	5.44	0.2	11.28	12.48	45.86
shrimp	4.64	0.67	8.56	9.47	55.33

The seven environmental variables that best explained the community in terms of abundance were longitude, sediment grain size >5 phi, oxygen, sediment grain size 2 phi, temperature, water depth, and TOC. The correlation coefficient for this set of variables was moderate at 0.428; with the alternative of pH replacing temperature and a correlation coefficient of 0.425 (Table 4). Similar variables were selected by the BIO-ENV analysis that matched with biomass. In this case five variables were selected, also with a moderate correlation coefficient of 0.476, these included longitude, sediment grain size >5 phi, oxygen, sediment grain size 2 phi and pH. The alternative of temperature instead of pH yielded a correlation coefficient of 0.475 (Table 5). It should be noted that longitude and grain size may be a proxy for water depth, topography, or other factors related to water mass movement. Recent oceanographic data (Weingartner unpub data) may suggest that water masses in this area are associated with trends found in benthic community structure, although this has not been yet tested.

Table 4: Combination of variables that best explain the community similarity matrix based on relative abundance per trawl. Correlation coefficients appear in parenthesis.

Number of variables	Best variable combination	Second best variable combination
1	Longitude (0.332)	TOC (0.236)
2	Longitude, Sediment Grain Size >5 phi (0.413)	Longitude, TOC (0.379)
3	Longitude, Sediment Grain Size >5 phi, Oxygen (0.406)	Longitude, Sediment Grain Size >5 phi, water Depth (0.403)
4	Longitude, Sediment Grain Size >5 phi, Oxygen, Sediment grain size 2 phi (0.413)	Longitude, Sediment Grain Size >5 phi, Oxygen, TOC (0.411)
5	Longitude, Sediment Grain Size >5 phi, Oxygen, Sediment grain size 2 phi, Temperature (0.421)	Longitude, Sediment Grain Size >5 phi, Oxygen, Sediment grain size 2 phi, pH (0.420)
6	Longitude, Sediment Grain Size >5 phi, Oxygen, Sediment grain size 2 phi, Water Depth, pH (0.425)	Longitude, Sediment Grain Size >5 phi, Oxygen, Sediment grain size 2 phi, Temperature, Water Depth (0.424)
7	Longitude, Sediment Grain Size >5 phi, Oxygen, Sediment grain size 2 phi, Temperature, Water Depth, TOC (0.428)	Longitude, Sediment Grain Size >5 phi, Oxygen, Sediment grain size 2 phi, pH, Water depth, TOC (0.425)

Table 5: Combination of variables that best explain the community similarity matrix based on relative biomass per trawl. Correlation coefficients appear in parenthesis.

Number of variables	Best variable combination	Second best variable combination
1	Longitude (0.300)	Sediment Grain Size >5 phi (0.297)
2	Longitude, Sediment Grain Size >5 phi (0.426)	Longitude, Sediment Grain Size 2 phi (0.398)
3	Longitude, Sediment Grain Size >5 phi, Oxygen (0.437)	Longitude, Sediment Grain Size 2 phi, Oxygen (0.431)
4	Longitude, Sediment Grain Size >5 phi, Oxygen, Sediment grain size 2 phi (0.461)	Longitude, Sediment Grain Size >5 phi, Oxygen, TOC (0.442)
5	Longitude, Sediment Grain Size >5 phi, Oxygen, Sediment grain size 2 phi, pH (0.476)	Longitude, Sediment Grain Size >5 phi, Oxygen, Sediment grain size 2 phi, Temperature (0.475)

Discussion

Communities included in this analysis were dominated in abundance and biomass by echinoderms or crustaceans; however, these two groups appeared to have an inverse relationship in their distribution. Stations dominated by echinoderms (mainly ophiuroids, *Ocnus* spp. and *Echinarachnius* spp.) had low abundance and biomass values of crustaceans, and at stations where crustaceans (mainly *Chionoecetes opilio*, shrimp and various hermit crab species, *Pagurus* spp.) where dominant echinoderms were scarce. Ophiuroids were the most abundant of all taxa (365,644 individuals) and had the highest biomass (362.86 kg) across stations. Their distribution was not homogeneous throughout the study area. From the 53 stations sampled, ophiuroids were present at 42 stations, with a range in abundance from 1 to 66,432 individuals in a trawl. The dominance of ophiuroids was concentrated in the central eastern stations with a couple of stations on the far west side of the study area. This dominance ranged from 50% to 97% of the trawl's abundance (Figure 3). On the western side of the study area, ophiuroid abundance was greatly reduced, ranging from 0.1% to 48% individuals in each trawl. This extreme pattern of abundance did not correspond to any depth range or visual substrate characteristic. Many studies have described the overwhelming abundance of ophiuroids in the Arctic shelves (Ambrose et al., 2001; Bluhm et al., 2009; Piepenburg et al., 1996; Piepenburg and Schmid, 1996a, 1997). This study supports this previous knowledge and also confirms the extreme variability in the distribution of these assemblages dominated by ophiuroids.

The second most abundant echinoderm in this study was the sea cucumber *Ocnus* spp., present at nine stations with great variability among sites. In the majority of stations, the number of individuals was very low (1 to 24 individuals per trawl), and showed peaks in abundance at stations 29, 30 and 1010 (with 688, 2332 and 68304 individuals per trawl). This organism's distribution didn't follow a discernable pattern. However, seven of the nine stations where *Ocnus* spp. was present were adjacent to one another. Many holothurians, including ones common in the Antarctic, brood their young (Pawson, 1983). *Ocnus sacculus* has three pouches to carry their young and have been found with embryos of the same stage of development, which would infer one common breeding period (Pawson, 1983). This breeding synchronization and restricted dispersal capacity is reflected in the large abundance and close proximity of stations where *Ocnus* spp. was present in our study area.

Within the dominant crustaceans, shrimp were present at all stations and had the highest abundance, ranging from 26 to 2,490 individuals in a trawl. Shrimp dominated the community at four stations (75% to 97% of the trawls abundance). These stations did not correspond to a particular depth range, substrate characteristic, or geographic location. Furthermore, the shrimp dominated stations were not exclusively ones with the highest abundance of these taxa across stations. The extensive distribution and occasional high abundance of shrimp could be attributed to characteristics of these taxa. Shrimp are mobile omnivores, capable of exploiting water column resources, such as pelagic organisms, as well as being transported in the water column by turbulence (Feder et al., 2011; Feder et al., 2005). In the same way, *Chionoecetes opilio* were present in every station in varying abundance and biomass. The distribution of stations dominated by *C. opilio* followed a south-north orientation on the western side of the study area.

Clusters

Cluster analysis at a 55% similarity level resulted in four clusters and two independent stations. The same cluster analysis showed a greater number of smaller clusters of statistical significance (SIMPROF test in Primer) at higher similarity levels (average 76%) in addition to six independent stations. Despite the slightly higher average similarity within clusters, the average dissimilarity between the smaller cluster groups was reduced significantly to an average of 34%. The dominant taxa in the smaller clusters selected by the SIMPROF test were the same as the dominant taxa of the clusters at the 55% similarity that included the former, which means that the assemblages of the smaller clusters were explained by the same taxa as the larger clusters. With this logic, we considered for this analysis the 55% similarity level cut off to be an adequate level of segregation among cluster groups. In concordance with our hypotheses, cluster analysis determined two main groups of stations, Groups 2 and 4 (Figure 4). The stations belonging to these groups had a very distinct geographic distribution and were dominated by different taxa. Two smaller clusters, Group 1 (with two stations) and 3 (with four stations), had similarity levels among stations of up to 78% and 63%, respectively. Within Group 1, Station 14 had an absence of molluscs and was grouped with Station 4 as a result of the high abundance of *Echinarachnius* spp.. The biomass of *Echinarachnius* spp. amounted to 55% and 75% of the total catch at Stations 4 and 14, respectively. Based on visual observations of the sediment from the van Veen grabs and sediments in the trawl, the stations corresponding to Group 1 had a high proportion of sand. Also, the two sites were located nearshore in shallow water (depth <40 m) under the influence of the ACC. These data agree with those collected in the same area by Feder et al. (1994) for which they suggest the strong effect of the ACC in particle entrainment and associated particulate organic matter favors the presence of suspension-feeder sand dollars (Feder et al., 1994a). The similarity among stations in Group 2 was 72%, with ophiuroids alone accounting for nearly 50% of the similarity. In Group 4, the similarity among stations amounted to 65%. *Chionoecetes opilio*, *Pagurus* spp., and shrimp were the most representative taxa, with the contribution of these to the total similarity of the group divided almost equally between the three.

Environmental analysis

The link between the environmental variables included in this analysis and the community data resulted in a moderate correlation. The highest correlation with epibenthic abundance was 0.428, and with biomass, was 0.476. In these analyses, three water mass characteristics, oxygen, temperature and pH, were selected as important in structuring the epibenthic community. However, these variables both appeared later in the selection of the BIO-ENV analyses and also did not create a significant increase in the correlation value with abundance or biomass. The variation of the values measured for salinity and temperature among stations was very low. This explains how, in our results, temperature showed a low contribution and salinity was not selected as important in explaining the variability in epibenthic communities. One possibility for the limited difference in these values could be the narrow window in time these data were collected, which resulted in a failure in capturing the true temporal variability that the bottom water undergoes throughout the year (Weingartner personal communication). We hypothesized that a discreet list of environmental variables would explain the community assemblages, our results showed two main variables, longitude and sediment grain size >5 phi, adding the highest values to the correlation coefficient. The only variable selected as a representative of food supply and

quality was TOC; however, this variable showed a low contribution to the correlation coefficient for biomass and abundance.

Water masses characterize the marine physical environment, they affect the distribution of food and dispersion of the planktonic larvae of benthic species. Therefore, the different water masses may play an important role in the composition and abundance of benthic communities (Feder et al., 1994b; Stewart et al., 1985). Of the three water masses that affect the northeastern Chukchi Sea shelf, two main ones, the Bering Shelf Waters and Alaska Coastal Waters, have been well described and studied (Coachman et al., 1975; Walsh et al., 1989). Both water masses move northward through the Bering Strait. One branch eastward through Hope Valley and Herald Valley, denominated Bering Sea water, is characterized by high salinity, rich nutrient and carbon waters (Coachman et al., 1975). The Alaska Coastal Current (ACC) is described as a low salinity, low nutrient and carbon depleted water that runs along the coast from Cape Lisburne up to Barrow Canyon (Walsh et al., 1989). A third branch traveling east of Herald Shoal (referred to as Central Channel), first described by Coachman et al. (1975), was rediscovered not long ago. This branch on an annual average could be responsible for approximately 25% of the mean Bering Strait transport (Weingartner et al., 2005). The Central Channel water moves north and to the east of Herald Shoal, then continues in a slow flow up to Hanna Shoal, moving eastward and merging with the Alaskan Coastal Water close to Barrow Canyon (Coachman et al., 1975; Weingartner et al., 2005; Winsor and Chapman, 2004). This northeastward drift of nutrient and carbon rich waters could support high benthic standing stocks despite a relatively low annual primary production (Feder et al., 1994b). Despite the low correlation of epibenthic assemblages and the environmental variables included in this analysis, the geographical distribution of the main cluster groups coincided with the trajectory of water masses in the region. The variable selected first in the BIO-ENV analysis for abundance and biomass was longitude with correlation values of 0.332 and 0.300, respectively. Most likely, longitude is acting as a proxy for the effect of the different water currents and is reflected in the south-north trajectory over the sample stations. Stations in Group 4 start from off the coast of Cape Lisburne (at the 69° N parallel) and extend along the Central Channel following the east flank of Herald Shoal. Further north, stations follow the west and south flanks of Hanna Shoal. This distribution matches the description of Winsor and Chapman (2004) of the branch of Bering Sea Water that flows through the Central Channel mixed with water that flows northward offshore of Cape Lisburne and around the southern limit of Hanna Shoal (Weingartner et al., 2005; Winsor and Chapman, 2004).

Communities in Group 4 also had the highest diversity and were dominated by crustaceans. The stations with highest biomass coincide with the water pathways carrying nutrients and carbon from the central shelf into Barrow Canyon (Weingartner et al., 2005). However, variability in ice cover and the formation of winter polynyas mainly caused by changes in wind direction and advection of heat and salt through the Bering Strait, create changes in the flow pattern of water masses off the coast of the northeastern shelf (Spall, 2007; Weingartner et al., 1998). With extended ice cover and smaller winter polynyas, the flow of Bering Shelf water through this area becomes more passive and reduces the ventilation of water towards Barrow Canyon (Weingartner et al., 2005). The stations corresponding to Group 2 could be affected by the persistence of water in the area, due to the variability in dense water formation (Weingartner

personal communication). The extended flushing time of the water in this area would allow longer time for POC deposition to the benthos, favoring benthic deposit feeders like ophiuroids.

Conclusion

In general, there was an increase in the total biomass of stations from south to north, as well as a decrease from east to west. The location of these higher abundance stations matches the location of stations with higher benthic carbon biomass in another study (Feder et al., 1994b). In that study, the bottom water characteristics of the high biomass stations corresponded to typical BSW, which is associated with higher nutrient values (Feder et al., 1994b). Stations in cluster Group 4 had the highest mean diversity values, which could be explained by the path of the Central Channel water mass and the enhanced primary production associated with this water mass due to nutrients transported and the seasonal increase of ice-edge zones (Weingartner et al., 2005). The stations in Group 2 had the lowest diversity, however, the high biomass of these stations and the overwhelming dominance by ophiuroids indicated high food availability. The flow of water in this area is affected by wind direction and seasonality, which could create great variability in the quality and abundance of organic matter and favor the dominance of taxa capable of enduring changing conditions. Sediment characteristics are important for epifaunal community composition (Ambrose et al., 2001; Feder et al., 1994a; Mayer and Piepenburg, 1996). In this study, sediment grain size measurements used for the environmental correlation did not reflect a tight correlation with community assemblages. Similar to another study, our analysis of the distribution of *Echinarachnius* spp. corresponded to an area of sandy sediments (Ambrose et al., 2001). Using seabed categories (number and size of stones) and traits (presence of sponge spiculae and shell hash) is ecologically a more accurate measurement for large epibenthos than sediment grain size (Mayer and Piepenburg, 1996).

To better understand the effect that anthropogenic disturbances have on the epibenthic communities of lease area 193, it is necessary to make the distinction between the different aspects of variability in the epibenthic community in the Chukchi Sea. In the area included in this analysis, there were marked differences in the total biomass recorded for each station, with the highest biomass values corresponding to the northeastern area. Community assemblages also varied in diversity values. Stations in the center of the study area had the lowest diversity and stations following the trajectory of the Central Channel had the highest diversity index values. Moreover, there was a marked variability in the dominating taxa across stations. Ophiuroids, crustaceans (*Chionoecetes opilio*, shrimp and *Pagurus* spp.), sand dollars, and sea cucumbers appeared as dominant groups. The variability in the communities was determined by the flow and trajectory of water masses, sediment characteristics, and possibly variability in food quality and quantity. The taxa that form a community have specific requirements for their success. To determine the factors that are affecting the community, it is necessary to both measure environmental variables in the correct scale (i.e. seabed categories vs sediment grain size) and account for the variability and fluctuations that many of the influencing factor may have (i.e. temporal changes in water current direction and dense water formation). Considering the complexity of the variability in the epibenthic assemblages in the Chukchi Sea, the effect of disturbances could be fundamentally different from one area to the next, even within adjacent areas. The impact on an area that supports a community with large biomass, but highly dominated by few taxa, would be more severe than for communities with higher diversity and

evenness, especially if the dominant taxa were eliminated from the area. The former communities would be less capable of recovering from disturbance.

Acknowledgements

We would like to acknowledge the Bureau of Ocean Energy Management (BOEM), U.S. Department of Interior for funding to support this study, with especial thanks to Dick Prentki, for his support, experience and love for birds. We thank Ken Dunton for his role as lead scientist of the COMIDA Project, and the entire COMIDA crew, for it was a pleasure working with them. We thank the captain John Seville and his crews on the *R/V Alpha Helix* and *R/V Moana Wave* for making this project possible and their great seamanship. Very special thanks to Martin Schuster for his most valuable help on deck, cheerful attitude and great music selection; Eric Hersh for his technical support and extreme patience in creating most of the maps here presented; Susan Schonberg for her help in identifying many of the organisms collected. We are also very grateful to Tom Weingartner and Katrin Iken from University of Alaska Fairbanks, for sharing their time and extensive knowledge.

Influence of environmental parameters on the size frequencies of key epibenthic organisms in the Chukchi Sea.

Konar, B., A. Ravelo, J. Grebmeier, and J.H. Trefry

Brenda Konar and Alexandra Ravelo
School of Fisheries and Ocean Sciences
University of Alaska Fairbanks, Fairbanks Alaska 99775

Jackie Grebmeier
Chesapeake Biological Laboratory,
University of Maryland, Solomons, MD 20688

John H. Trefry
Department of Marine and Environmental Systems
Florida Institute of Technology, Melbourne, Florida 32901

Abstract

Epibenthic communities play a key role in ecosystem functioning in the Chukchi Sea. Communities, however, are patchily distributed in groups and are influenced by various environmental parameters. Along with distribution, one aspect of these epibenthic communities that may be influenced by the environment is body size. Size can in turn influence the physiology, survival, and competition of a species. This study presents size frequency distributions of the dominant epifaunal organisms in the Chukchi Sea, including male, female and gravid *Chionoecetes* and *Hyas* crabs, the gastropods *Plicifusus, Colus*, *Cryptonatica*, and *Neptunea*, and the echinoderms *Gorgonocephalus, Leptasterias,* and *Echinarachnius.* The size frequencies of these epibenthic organisms were then related to some key environmental parameters. It was found that some taxa had very restricted sizes while others had a wide range of sizes. It also was found that size distributions of particular organisms were influenced by specific environmental parameters, including longitude, dissolved oxygen, sediment grain size 2 and 5 phi, and percent total organic carbon. This study demonstrated that size frequency may be another variable that can be used to examine the status of a population

Introduction

Epifaunal communities are extremely important in many marine systems, including the Arctic. They often contain the bulk of the biogenic biomass (Schwinghamer, 1981) and are pivotal in ecosystem functioning. It has been shown that a significant portion of the energy in the Arctic passes through the epibenthos (Piepenburg et al., 1995; Piepenburg and Schmid, 1996b; Piepenburg and Schmid, 1997). Epibenthic organisms are often bioturbators (Graf, 1992; Grebmeier and McRoy, 1989), interact trophically with infaunal organisms, demersal fish, and

marine mammals (Feder and Jewett, 1981; Jewett and Feder, 1980; Jewett and Feder, 1981), and contribute to total benthic energy turnover (Piepenburg et al., 1996).

The Chukchi Sea in the Alaska Arctic has an extremely productive epifaunal community and has among the highest biomass values in the world (25 to 60 g C m^{-2}; (Grebmeier et al., 2006b; Grebmeier et al., 1988). Many epibenthic taxa are highly mobile and contribute to the redistribution and remineralization of the organic carbon reaching the seafloor (Piepenburg, 2000; Piepenburg et al., 1997; Piepenburg et al., 1995; Piepenburg et al., 1996; Piepenburg and Schmid, 1996a; Piepenburg and Schmid, 1996b). In the Chukchi Sea, these taxa include echinoderms (primarily seastars) for biomass and crustaceans for abundance (Bluhm et al., 2009; Feder et al., 2005). Crustaceans are of particular significance because if, in the future, larger snow crab *Chionoecetes opilio* move into this area, there may be a fishery potential in this region. Also included in the mobile grouping are molluscs, which are the most species-rich taxon in the Chukchi Sea (Bluhm et al., 2009; Feder et al., 2005; Frost et al., 1983), and particularly abundant with highest biomass near the coast (Feder et al., 1994). Of all the mollusks found in this region, gastropods make up the greatest epifaunal portion for abundance and biomass (Feder et al., 1994a). Dominant gastropod taxa include the largely carnivorous and scavenger families Buccinidae and Naticidae (Bluhm et al., 2009). While these two families are more abundant in the nearshore, *Neptunea* (within the Naticidae) are common throughout the Chukchi Sea (Feder et al., 1994a).

Benthic biomass is generally controlled by the supply of food raining down on the seafloor, especially in areas where there is tight benthic-pelagic coupling, such as the Chukchi Sea (Graf, 1989; Grebmeier and Barry, 1991). Along with food, there are other important environmental drivers that can correlate with and perhaps structure the distribution and biomass of Chukchi Sea communities. These can include water depth, water mass, currents, pelagic primary productivity, carbon flux, latitude, sediment grain size, bottom water temperature and salinity, and distribution of predators (Bluhm et al., 2009; Feder et al., 1994a; Grebmeier et al., 2006b; Lee et al., 2007; Stoker, 1981). For the data set used in this study, longitude, dissolved oxygen, sediment grain size 2 and 5 phi, and percent total organic carbon were found to correlate with community distribution (Primer-e, BIO-ENV Procedure, Ravelo et al. this report). Although these were the correlated drivers, it should be noted that this does not imply a cause-and-effect relationship. For example, one study found that latititude was an important driver in determining epifaunal distribution, however, this same study also pointed out that this may just reflect other related conditions that vary with latitude such as bottom temperature, primary productivity distribution, distance from shore, and current regime (Stoker, 1981).

Body size influences many aspects of the biology of a species, including physiology, survival, competition, and others (Calder, 1984; Peters, 1983), however, little is known about if and how size frequency distributions vary with their environment. In a freshwater stream system, the size frequency distributions of invertebrate assemblages did not vary along a nutrient gradient or among substrate categories, despite clear differences in taxonomic composition among sites (Bourassa and Morin, 1995). In one study on marine bivalves, no difference was seen in size frequency distributions with latitude although differences were found with species richness (Roy et al., 2000). In another study, small differences in grain size (coarse, medium, and fine sand) did not influence size frequency distributions of the seastar *Oreaster reticulatus*, but mean size

was inversely related to density (Scheibling, 1980). Although the few studies that have examined size frequency distributions of benthic organisms have not found any significant trends, these studies have only examined one to two environmental parameters.

Although there has been much research in the Chukchi Sea spanning back to 1878 (for review see Sirenko and Gagaev, 2007), little information exists on epifaunal size frequency distributions. One of the goals of the research described below was to present the size frequency distributions of the dominant epifaunal organisms currently inhabiting the Chukchi Sea. The organisms chosen were ones that were important in determining community structure as far as biomass and abundance (based on a Primer-e BEST analysis, Ravelo et al. this report). Another goal of this report was to take these basic size frequency distributions and relate them to the environmental parameters that were correlated with community structure (based on Primer-e BIO-ENV analysis, Ravelo et al. this report). With these data, we then asked whether size distributions of the various dominant organisms in the Chukchi Sea are influenced by the environmental parameters that correlated with community structure as far as biomass and abundance.

Methods

Sampling was completed in 2009 and 2010 at 53 stations within the Chukchi Sea (Figure 1). For a description of the station selection, see Ravelo et al., this report. Bottom invertebrate communities were sampled using an epibenthic 3.05 m plumb-staff beam trawl with a 7 mm mesh and a 4 mm codend liner. One beam trawl was deployed at each station for approximately 2.5 minutes at 1.5 knots. Water depths ranged from 28 to 50 m with a mean of 42.3 ± 0.85 s.e. m.

All trawls were sieved through a 4 mm sieve to remove soft sediments. They were then sorted on deck and all taxa were weighed and counted. In addition to these basic measurements, crabs, gastropods, and echinoderms were measured to obtain size frequencies. For crabs, carapaces were separated into males and females and widths were measured using calipers to the nearest mm. For gastropods, the shell was measured with calipers from the apex to the lowest whorl. For echinoderms, the central disk of each basket star, the longest arm of each seastar, and the disc diameter of each sand dollar were all measured using calipers. For the snow crab, *Chionoecetes*, size of gravid females was determined in 2009 and 2010. For the lyre crab, *Hyas*, gravid females were only measured in 2010. For the purpose of this report, the size frequency distributions for the taxa that best described community structure as far as biomass and abundance were examined (based on Primer-e BEST analysis, Ravelo et al. this report). For biomass, these taxa included the crab *Chionoecetes,* the gastropods *Plicifusus, Colus*, and *Cryptonatica*, and the echinoderms *Gorgonocephalus* and *Leptasterias.* For abundance, these taxa included *Chionoecetes*, *Crypotnatica*, and the sand dollar, *Echinarachnius.* The other true crab in this area, *Hyas*, was also examined as it was fairly abundant and widespread. The gastropod *Neptunea* was examined as it is an ecologically important predator/scavenger in the system and fairly widespread throughout the study area (Dunton et al. this report and Ravelo et al. this report).

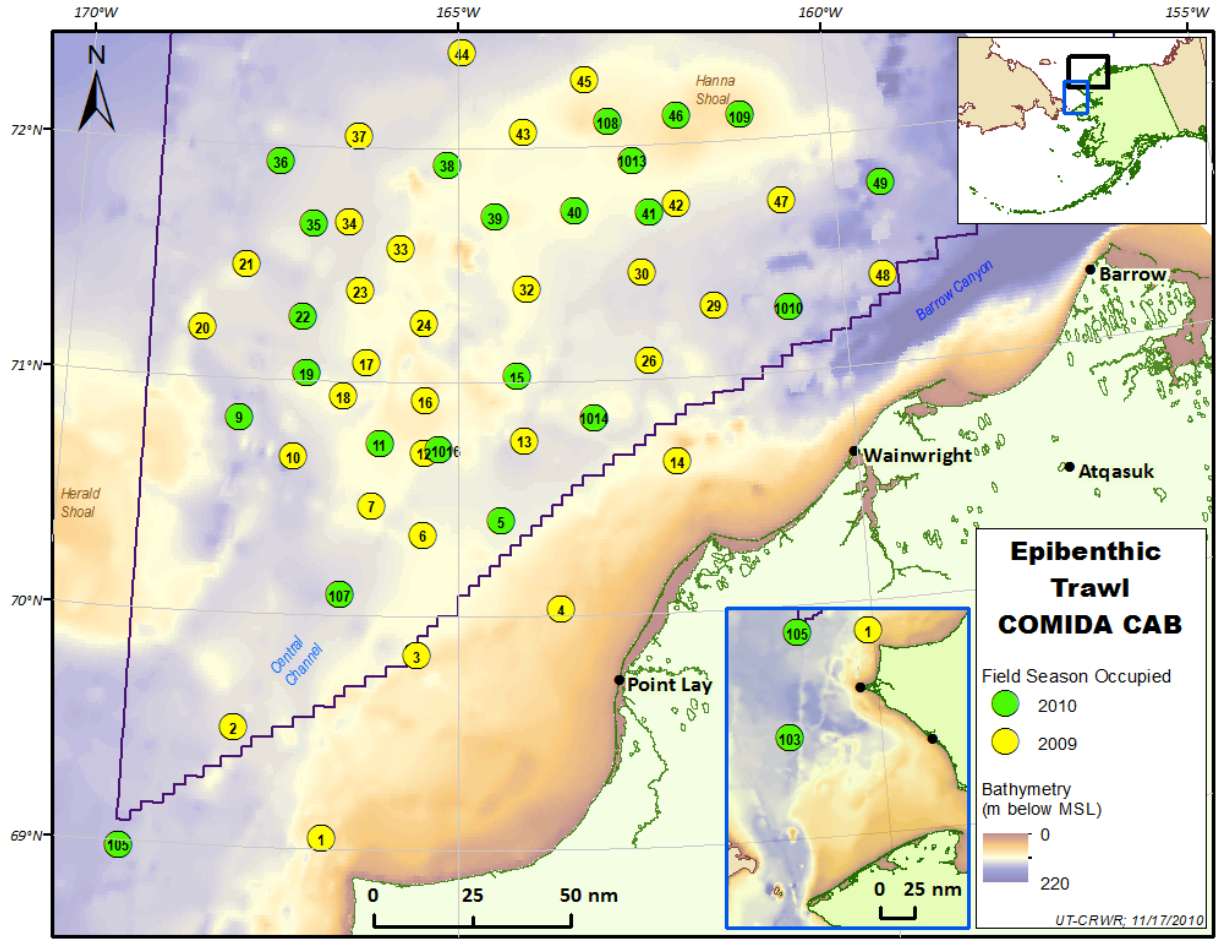

Figure 1. Map showing stations that were trawled and where size frequency data were taken in 2009 and 2010. Insert on top right corner shows the two general study regions, with the black square designating the Chukchi Sea area and the blue square designating the region by the Bering Strait.

In addition to overall study area size frequencies, we used environmental parameters that were correlated to community structure across the study area (based on Primer-e BIO-ENV analysis, Ravelo et al. this report) to complete Linear Least Squares Regressions (Systat 13). These regressions were performed between the parameters and each of the taxa to determine which parameters were influencing the size distributions of the various taxa. These parameters included longitude, dissolved oxygen, sediment grain size 2 and 5 phi, and percent total organic carbon. Vertical profiles of dissolved oxygen were obtained at each trawled station using a YSI SONDE 6600 (details in Trefry et al., this report). Sediments were collected using 0.1 m² van Veen grabs for total organic carbon and grain size analyses (details in Grebmeier and Cooper, this report). Taxa included in these analyses were the crabs *Chionoecetes* and *Hyas*, the gastropods *Plicifusus, Colus*, *Cryptonatica*, and *Neptunea*, and the echinoderms *Gorgonocephalus* and *Leptasterias*. *Echinarachnius* was excluded from these analyses as it was only found at four stations.

Results

The snow crab, *Chionoecetes* is one of the most dominant (for abundance and biomass) epifaunal organisms in the Chukchi Sea and was found at all 53 of the trawled stations. In this region, female size distribution was more bimodally distributed than were the males (Figure 2). Although males were more abundant (4084 males were measured in this study versus 2919 females), females were larger with a mean of 36.4 ± 0.19 mm (width of carapace) than the males with a mean of 32.6 ± 0.16 s.e. mm. Gravid females (n = 257) were found at 19 trawled stations with an average size of 51.8 ± 0.32 s.e. mm and ranging from 36 to 65 mm (Figure 2).

Hyas, the other true crab found in this region, was found at 38 of the 53 stations. While males and females were approximately the same size (26.4 ± 0.51 s.e. mm for females and 26.8 ± 0.69 s.e. mm for males), the size distribution for males was more widely spread ranging from 57 to 79 mm (Figure 3). Males and females were fairly equally abundant through the study area with 405 males and 373 females. Sizes of gravid females ranged between 34 and 52 mm, which were much smaller than the gravid *Chionoecetes*. Gravid *Hyas* were only found at five stations (n = 19).

The gastropods that were deemed important in this region (for high abundance, biomass or ecological importance) were *Plicifusus, Colus*, *Cryptonatica,* and *Neptunea*. *Plicifusus*, which was found at 24 stations, was the second largest of the gastropods with a mean of 43.7 ± 0.94 s.e. mm (n = 226; Figure 4). The size range for this taxon was 14 to 84 mm. *Colus*, the third largest gastropod taxa, was found at 40 stations (n = 326). *Colus* showed a bimodal distribution, with sizes ranging from 12 to 65 mm, and a mean of 33.8 ± 0.63 s.e. mm (Figure 4). *Cryptonatica,* found at 36 stations, was one of the more abundant gastropods (n = 777). The size range for this taxon was smaller than the previously mentioned gastropods, ranging from 6 to 48 mm, with a mean of 20.6 ± 0.28 s.e. mm (Figure 4). *Neptunea* was the largest of the gastropods in this study and also very abundant (n = 631), found at 46 of the 53 trawled stations (Figure 4). The size range for this taxon ranged from 11 to 128 mm, with an average size of 49.7 ± 0.88 s.e. mm (Figure 4). Large individuals of this taxon were found throughout the region but were rare.

The dominant echinoderms determining community structure in this region were *Gorgonocephalus, Leptasterias,* and *Echinarachnius*. *Gorgonocephalus* was found at 18 stations and had a mean central body disk size of 23.2 ± 0.89 s.e. mm (n = 282; Figure 5). Although some basket stars were large (maximum central body disk size in the study area was 65 mm), most were smaller than 16 mm. *Leptasterias* was very common, found at 46 of the 53 stations (n = 743). Although most of these stars were smaller than 46 mm, their size range was 2 to 154 mm, with a mean of 42.2 ± 1.0 s.e. mm (Figure 5). *Echinarachnius* was found at only four stations, fewer stations than the other community structuring echinoderms, however at these stations, they dominated for abundance and biomass (n = 1385). The size distribution of these sand dollars was very limited, with individuals ranging from 20 to 50 mm with a mean size of 32.4 ± 0.09 s.e. mm (Figure 5).

All environmental parameters examined were correlated with the size frequencies for most of the taxa in the study (Table 1). Specifically, longitude was the most correlated parameter with all of the taxa, followed by total organic carbon. Together, these were most correlated of all the taxa

except female *Chionoecetes* (which was not correlated with total organic carbon). In addition to these, dissolved oxygen was correlated with all taxa except for *Neptunea* and *Gorgonocephalus*. Lastly, at least one of the two grain sizes was correlated with all taxa except for *Colus* and *Leptasterias*.

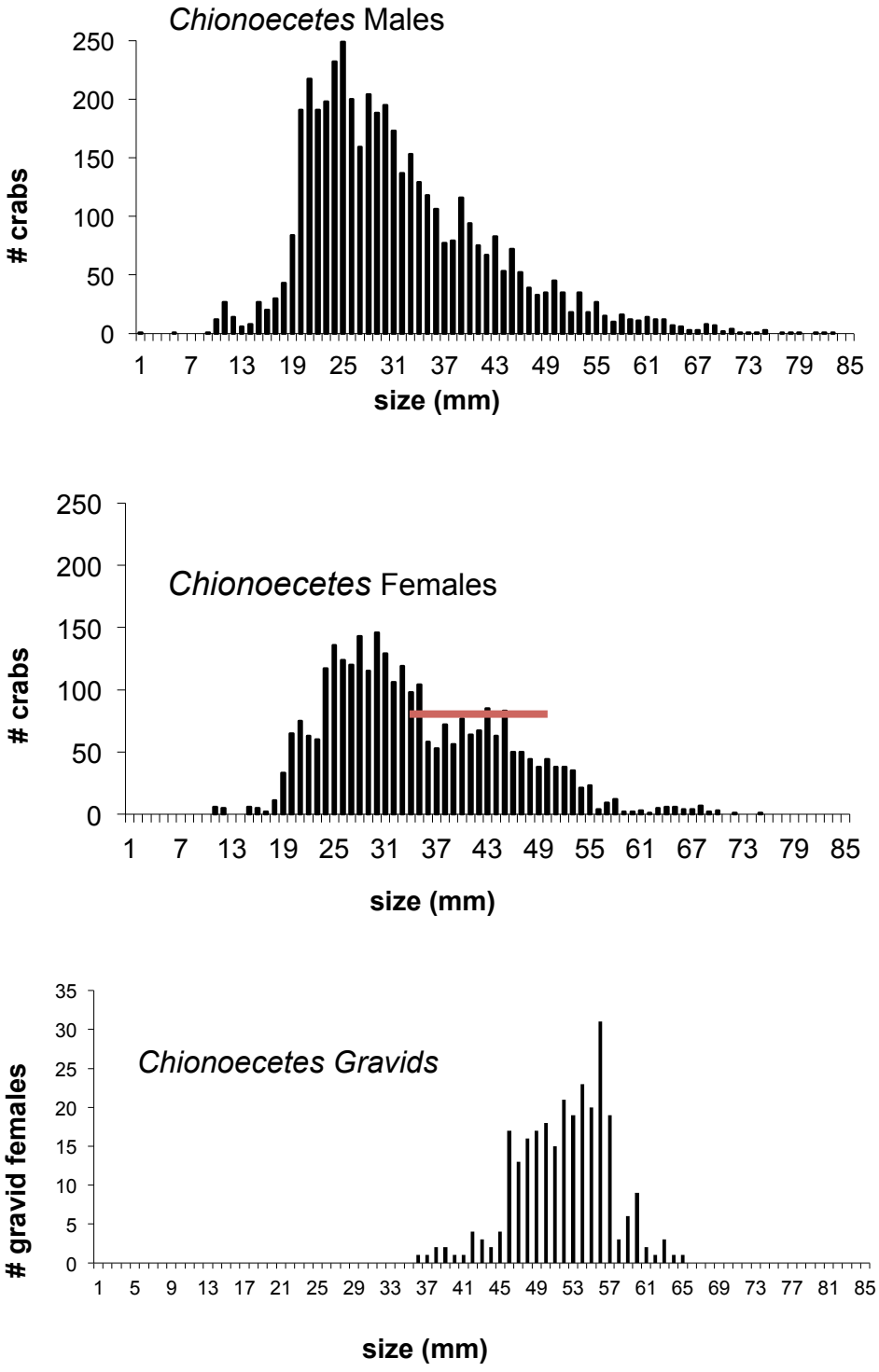

Figure 2. Size frequency histograms of male (n = 4464) and female (n = 2919) *Chionoecetes*, and gravid females (n = 257). Bar on female graph refers to the range where females were gravid.

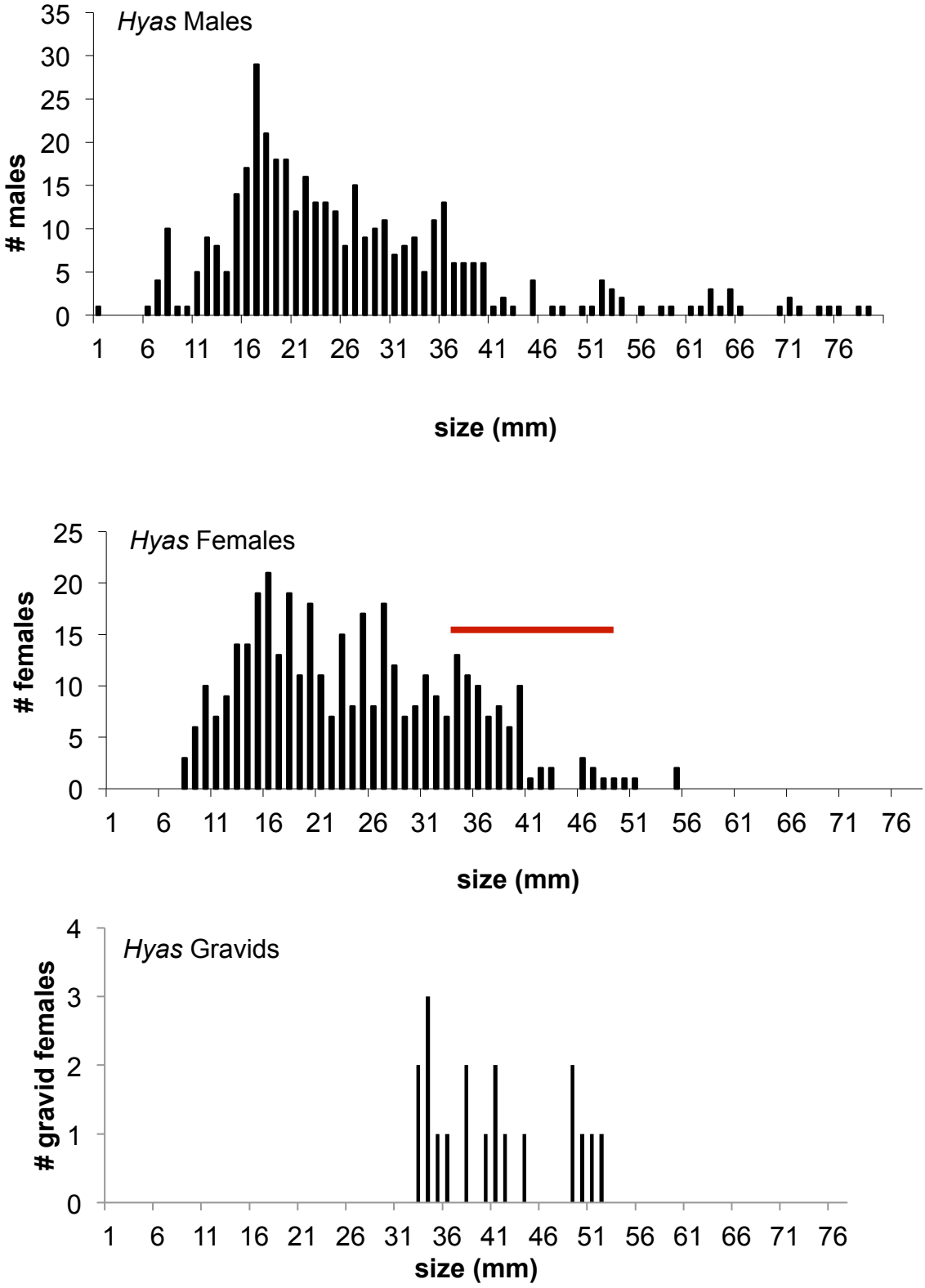

Figure 3. Size frequency histograms of male (n = 405) and female (n = 373) *Hyas*, and gravid females (n = 19). Bar on female graph refers to the range where females were gravid.

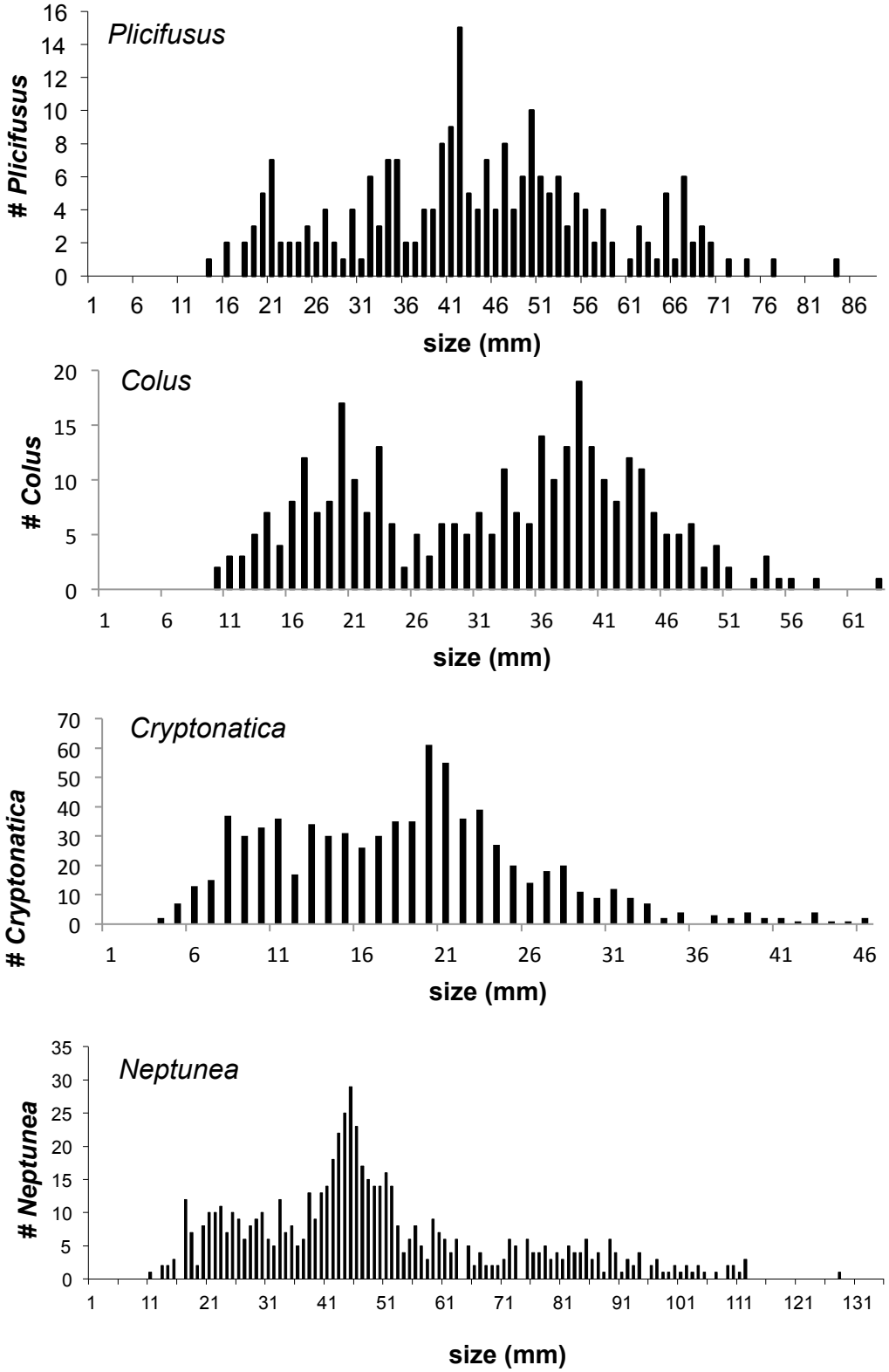

Figure 4. Size frequency histograms of *Plicifusus* (n = 226), *Colus* (n = 326), *Cryptonatica* (n = 777), and *Neptunea* (n = 631).

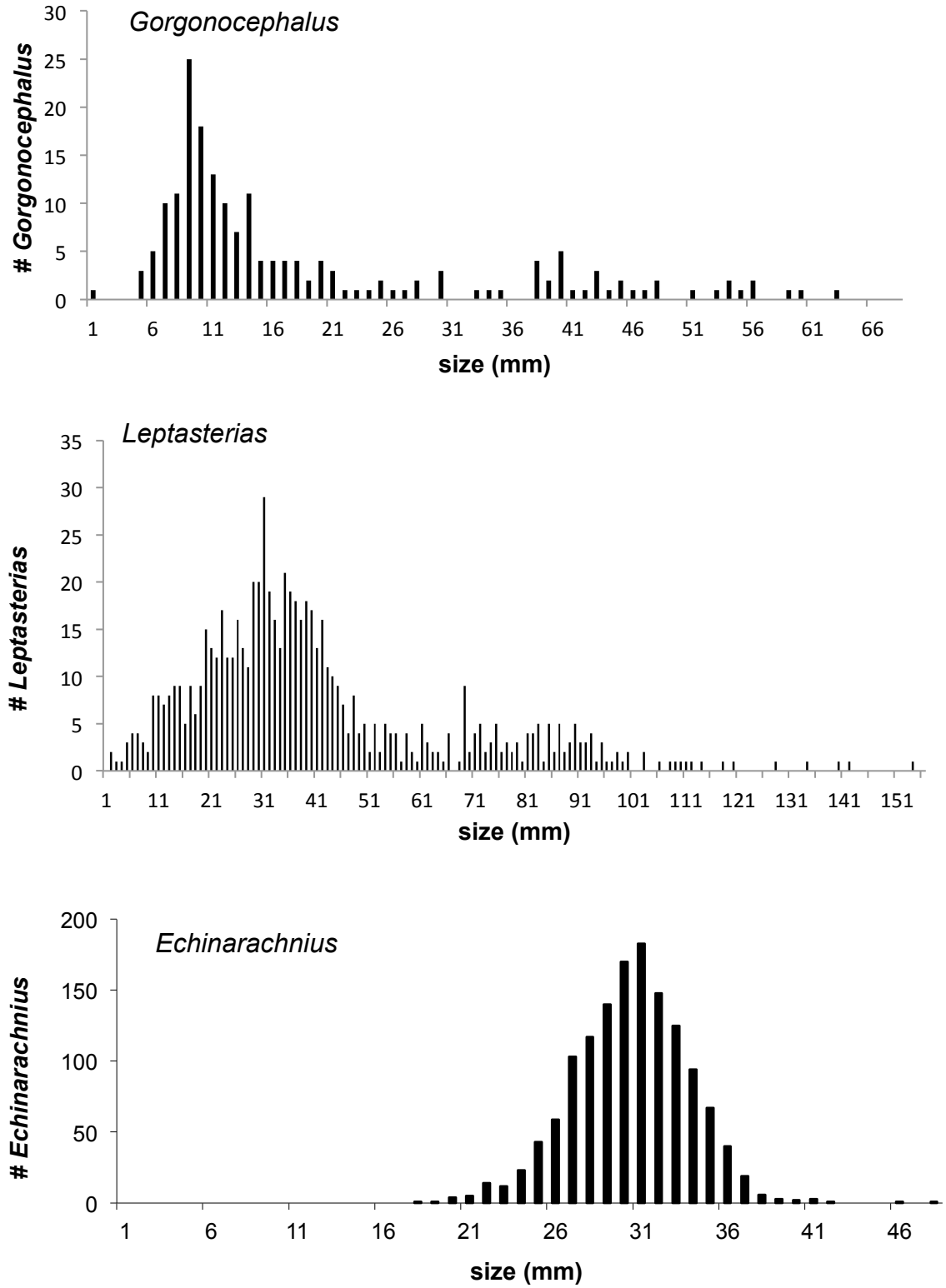

Figure 5. Size frequency histograms of *Gorgonocephalus* (n = 283), *Leptasterias* (n = 743), and *Echinarachnius* (n = 1385).

Table 1. Linear least squares regression for five environmental variables (longitude, total organic carbon, dissolved oxygen, sediment grain size: 2 phi, and sediment grain size: 5 phi) with the target taxa.

Chionoecetes Males					
Effect	Coefficient	Standard Error	Std. Coeff.	t	p-value
Constant	-163.806	11.769	0	-13.919	0
Longitude	1.389	0.07	0.3	19.944	0
Total Organic Carbon	-2.244	1.018	-0.071	-2.203	0.028
Dissolved Oxygen	-0.361	0.027	-0.244	-13.55	0
Sediment grain size, 2 phi	0.218	0.077	0.056	2.834	0.005
Sediment grain size, 5 phi	0.039	0.015	0.077	2.621	0.009
Chionoecetes Females					
Effect	Coefficient	Standard Error	Std. Coeff.	t	p-value
Constant	-167.387	15.301	0	-10.94	0
Longitude	1.318	0.089	0.274	14.746	0
Dissolved Oxygen	-0.196	0.028	-0.141	-7.107	0
Sediment grain size, 5 phi	0.04	0.01	0.076	3.821	0
Hyas Males					
Effect	Coefficient	Standard Error	Std. Coeff.	t	p-value
Constant	-385.962	57.713	0	-6.688	0
Longitude	2.224	0.325	0.363	6.854	0
Total Organic Carbon	23.77	3.051	0.598	7.791	0
Dissolved Oxygen	0.42	0.149	0.136	2.813	0.005
Sediment grain size, 2 phi	0.558	0.116	0.313	4.818	0
Sediment grain size, 5 phi	-0.249	0.07	-0.33	-3.574	0
Hyas Females					
Effect	Coefficient	Standard Error	Std. Coeff.	t	p-value
Constant	-314.375	40.947	0	-7.678	0
Longitude	1.827	0.231	0.442	7.909	0
Total Organic Carbon	6.544	1.832	0.239	3.572	0
Dissolved Oxygen	0.332	0.105	0.162	3.156	0.002
Sediment grain size, 2 phi	0.65	0.062	0.619	10.457	0
Plicifusus					
Effect	Coefficient	Standard Error	Std. Coeff.	t	p-value
Constant	-453.718	116.121	0	-3.907	0
Longitude	2.787	0.713	0.293	3.908	0
Total Organic Carbon	14.069	8.773	0.219	1.604	0.11
Dissolved Oxygen	0.571	0.257	0.151	2.218	0.028
Sediment grain size, 5 phi	-0.451	0.114	-0.526	-3.94	0
Colus					
Effect	Coefficient	Standard Error	Std. Coeff.	t	p-value
Constant	-125.664	68.584	0	-1.832	0.068
Longitude	0.712	0.401	0.113	1.774	0.077
Total Organic Carbon	14.656	2.377	0.436	6.167	0

Dissolved Oxygen	0.303	0.111	0.188	2.73	0.007
Cryptonatica					
Effect	Coefficient	Standard Error	Std. Coeff.	t	p-value
Constant	-110.996	22.545	0	-4.923	0
Longitude	0.763	0.136	0.303	5.596	0
Total Organic Carbon	7.519	2.575	0.302	2.92	0.004
Dissolved Oxygen	0.082	0.054	0.063	1.535	0.125
Sediment grain size, 2 phi	-0.591	0.209	-0.165	-2.834	0.005
Sediment grain size, 5 phi	-0.132	0.043	-0.29	-3.06	0.002
Neptunea					
Effect	Coefficient	Standard Error	Std. Coeff.	t	p-value
Constant	-200.434	71.363	0	-2.809	0.005
Longitude	1.602	0.434	0.143	3.689	0
Total Organic Carbon	17.464	3.854	0.267	4.531	
Sediment grain size, 5 phi	-0.459	0.061	-0.437	-7.465	0
Gorgonocephalus					
Effect	Coefficient	Standard Error	Std. Coeff.	t	p-value
Constant	24.9	215.476	0	0.116	0.908
Longitude	-0.062	1.315	-0.003	-0.047	0.963
Total Organic Carbon	36.65	11.106	0.494	3.3	0.001
Sediment grain size, 2 phi	0.915	0.27	0.277	3.394	0.001
Sediment grain size, 5 phi	-0.377	0.142	-0.39	-2.648	0.009
Leptasterias					
Effect	Coefficient	Standard Error	Std. Coeff.	t	p-value
Constant	-477.774	65.25	0	-7.322	0
Longitude	2.946	0.395	0.281	7.46	0
Total Organic Carbon	-9.044	3.583	-0.119	-2.524	0.012
Dissolved Oxygen	0.449	0.199	0.106	2.258	0.024

Discussion

This paper presents size frequency data for the dominant epibenthic organisms in the Chukchi Sea. This is a first attempt at analyzing these types of data for this region. We have shown that some organisms are very abundant with a wide range of sizes (i.e. *Chionoecetes*, *Neptunea*, and *Leptasterias)*, while others have a much more restricted size range (i.e. *Cryptonatica* and *Echinarachnius*). We also demonstrate that some taxa have rare, but very large individuals (i.e. male and female *Chionoecetes*, male *Hyas*, *Neptunea*, *Gorgonocephalus*, and *Leptasterias*). Lastly, we suggest that some environmental variables, namely longitude, dissolved oxygen, sediment grain size 2 and 5 phi, and percent total organic carbon, may be correlated with the size distribution of some members of the epibenthic community. Obviously, longitude is a proxy for some biological or environmental variable (perhaps water masses); however, determination of this proxy was beyond the scope of this project.

One of the dominant and most widely spread organisms examined in this study was *Chionoecetes*. Although small individuals were common, large individuals were also found. An ample food supply may be contributing to the success of this group in the study area. This genus feeds on ophiuroids in the southeastern Bering Sea (Feder and Jewett, 1980; Feder and Jewett, 1981) and ophuroids also are very abundant in the Chukchi Sea (Ravelo et al. this report). Similarly, these crabs can prey on the common infauna in this area (Feder et al., 1994a). For example, in one study in 1990, 61% of the *Chionoecetes* in the southeastern Chukchi Sea fed on small bivalves (Feder et al., 1994a). Other studies from the Chukchi Sea have reported smaller *Chionoecetes* carapace sizes at more northern stations (Barber et al., 1997; Feder et al., 2005; Paul et al., 1997). It has been speculated that this may be due to physiology constraining them in colder waters (Bluhm et al., 2009; Frederich et al., 2000). This study found that while longitude did influence size in both the crab genera, other environmental parameters also appeared to play a role (i.e. total organic carbon, dissolved oxygen, and sediment grain sizes).

Another prominent and long-lived group in the Arctic is the molluscs (Chia, 1970; Dunbar, 1968). Since they are long-lived, the larger species as adults, represent a carbon sink that mainly contributes carbon to the system via gamete production and death (Feder and Jewett, 1981). This is particularly true of the gastropods. The broad distribution of large gastropods, primarily *Neptunea* (as was seen in this study) can probably be attributed to their mobility and opportunistic feeding behavior (Feder, 1967; MacIntosh and Somerton, 1981; Pearce and Thorson, 1967). Neptunid and buccinid snails feed on polychaetes and bivalves (MacIntosh and Somerton, 1981; Pearce and Thorson, 1967). Unlike the large individuals, small mollusks (especially smaller species and juveniles) probably represent a food resource for bottom-feeding predators in the Chukchi Sea (Feder et al., 1994a). In general, gastropods are the most species-rich taxa in this area (Bluhm et al., 2009; Feder et al., 2005; Frost et al., 1983; this study).

Echinoderms were also prominent in this study. Seastars are particularly important in ecosystem functioning because of their large predatory role (Himmelman and Dutil, 1991; Ross et al., 2002). For example, the common seastar in this study, *Leptasterias* feeds on the gastropod *Buccinum* (Himmelman and Dutil, 1991). *Leptasterias* in the Chukchi Sea have a very wide size range but it is probably the large ones that are preying on other species and affecting ecosystem functioning.

Another group of echinoderms that are particularly important include the sand dollars. They were very abundant but patchily distributed in the study region. Interestingly, this genus did not have a large size range distribution. At one inshore station in 1998, *Echinarachnius* covered the bottom with nearly 100% cover as seen in video transects (Ambrose et al., 2001). This was also seen in the current study at the stations where they were present. These types of high abundances are common and are similar to those reported at lower latitudes (Birkeland and Chia, 1971; Highsmith, 1982). The sand dollars in 1998 had an average disc diameter size of 30 mm and showed a normally distributed size frequency. These 1998 results are remarkably similar to what was found in this study, with *Echinarachnius* having a normal distribution and a mean size of approximately 32 mm. Since this is only a comparison of two points in time (1998 and 2009/2010), we cannot be sure that changes in sizes have not occurred between these two times.

The Chukchi Sea has been undergoing biological and physical changes over the last few decades (Stroeve et al., 2005; Woodgate et al., 2006). Current climate changes occurring in the arctic may be transforming the Chukchi Sea into an extension of the Bering Sea (Grebmeier et al., 2006c). The vulnerability of this region to environmental change is high due to a deline in sea ice extent and seawater warming (Grebmeier et al., 2006b). This could result in warmer Bering Sea organisms moving north and invading and competing with organisms in the Chukchi Sea (Grebmeier et al., 2006c). However, thus far no dramatic changes in community composition have been found among benthic samplings that spanned 20 years (Feder et al., 2007; Grebmeier et al., 1988), except for an increase in epifaunal predators (Feder et al., 2005). These changes could also result in the short food chain turning from a benthic-based (benthic communities being supported by carbon raining down to them) to pelagic-based ecosystem (one where zooplankton grazing and the microbial loop in the water column are high), thus limiting the carbon export that is supporting the benthic communities (Piepenburg, 2005). The ramifications of these changes have been discussed in the literature but include severe impacts on marine mammals and others (Grebmeier et al., 2006c; Piepenburg, 2005). How these changes may affect individual population parameters, such as size frequencies, is unclear. The data presented in this paper provides a baseline from which future comparisons can be made.

Acknowledgments

Many thanks go to the Bureau of Ocean Energy Management (BOEM), U.S. Department of Interior for funding of this study, particularly Dick Prentki for his continued support and enthusiastic assistance for the COMIDA Project. Thanks also go to Ken Dunton for and Dana Sjostrom for their overall support and guidance and to David Maidment, Eric Hersh and Harish Sangireddy for their assistance with data management. Appreciation also goes to Captain John Seville and his crews on the *R/V Alpha Helix* and *R/V Moana Wave*. A huge thank you goes to Martin Schuster for his hard work and long hours during the cruises to help get the trawls processed. Lastly, we would like to thank the rest of the COMIDA team for making this such a great group with which to work.

Trophodynamics of the Northeastern Chukchi Sea Food Webs Based on Stable ^{13}C and ^{15}N Isotopic Ratios

McTigue, N.D, S.V. Schonberg, and K.H. Dunton

Nathan D. McTigue, Susan V. Schonberg, and Kenneth H. Dunton
Marine Science Institute
The University of Texas at Austin, Port Aransas, Texas 78373

Abstract

Although previous research has shown the shallow shelf of the Chukchi Sea supports rich and diverse benthic fauna communities, the trophic structure of the northeastern Chukchi Sea (Lease Area 193) has not been investigated in species-level detail. Baseline trophic structure was established from stable nitrogen isotope analyses of organisms sampled during the COMIDA project. We found that benthic communities consisted of four trophic levels. Gastropods occupied the top trophic positions, with *Plicifusus kroeyeri* having the most enriched $\delta^{15}N$ value (17.09±0.29‰), along with cephalopods, fish, priapulids, crabs, and seastars. Omnivorous polychaetes, sipunculids, and ophiuroids characterized the third trophic level, while herbivorous bivalves, hydrozoans, byrozoans, and amphipods at the second trophic level. Particulate organic matter (POM) was collected from 13 stations and had mean stable carbon and nitrogen values of -24.26‰ and 5.40‰, respectively. Phytoplankton had stable isotope values that were similar to that of POM ($\delta^{13}C$ = -23.96±0.40, $\delta^{15}N$ = 7.74±0.34). Both represent the carbon end-member of the pelagic system. Amphipods, holothurians, echinoids, forams, and pycnogonids showed marked fidelity to phytoplankton, while second trophic level organisms (e.g. ($\delta^{13}C$ ascidians, sponges, bivalves, hydrozoans, isopods) exhibited relatively high $\delta^{13}C$ values, suggesting assimilation of a ^{13}C enriched carbon source, which we believe is benthic microalgae. Sipunculids (*Golfingia margaritacea*) derived 87% of its body carbon from benthic microalgae while most other taxa derived intermediate amounts of carbon from this source (e.g. bivalves assimilated 46% benthic microalgae carbon). Zooplankton were also ^{13}C-enriched, suggesting that their diet may include a benthic microalgal carbon subsidy. Sediments had mean stable isotopic values that fell near that of water column endmembers ($\delta^{13}C$ = -23.23±0.09, $\delta^{15}N$ = 7.15±0.10), and were replete with porewater ammonium (range 49 to 535 μM; average 154 μM). Mean light attenuation (k = 0.99) showed that most of the study area receives adequate downwelling irradiance to fuel photosynthesis for benthic primary producers. The Chukchi Sea food web clearly assimilates pelagic-produced carbon and a benthic ^{13}C-enriched source that provides energy to the highest trophic level organisms. The pathways of carbon flow provide a model for the linkages of potential contaminant flow through the biological component of the Chukchi Sea ecosystem.

Introduction

The Arctic Ocean differs markedly from the rest of the world's oceans. It displays notably shallow bathymetry in the shelves surrounding its basin (Carmack and Wassmann, 2006). A disproportionate amount (25%) of the world's continental shelves (defined as areas shallower than 200 m) are within the Arctic Mediterranean (Menard and Smith, 1966). The Chukchi Sea spans 620,000 km^2 of this area with mean depth of 58 m. The Chukchi Sea, situated directly north of the 70 km wide and 70 m deep Bering Strait, represents one of two gateways that connect the Arctic Ocean to the global ocean (Dayton, 1990).

In general, the seasonal advance and retreat of sea ice coincides with the extreme absence and presence of sunlight. The Chukchi Sea receives approximately 0.83±0.66 Sv of water advected northerly through the Bering Strait annually. This water moves at a speed of 20-50 cm s^{-1} in spring and summer and at 5-15 cm s^{-1} in fall and winter (Roach et al., 1995). Water transport can vary between 2 Sv northward and 0.2 Sv southward and is strongly correlated with surface atmospheric pressure (Coachman et al., 1975). The northward delivery of relatively warm water through the Bering Strait directly impacts the seasonal ice coverage in the Arctic. In spring, the flux of heat induces ice melt and break-up. The continuous flow during autumn months prevents a hard freeze of water in the Strait until November (Coachman et al., 1975; Walsh et al., 1989). The sea ice dictates light penetration of the water column, and therefore, primary production.

Despite a brief photosynthetic season, arctic marine systems are not biological deserts (Gosselin et al., 1997). The strong advection of biogenic matter (i.e. particulate organic matter or POM) from the Bering Strait in concert with high pelagic primary production during the photosynthetic season, forms a tight pelagic-benthic coupling that is intimately related to benthic fauna (Carmack and Wassmann, 2006). A spring bloom of phytoplankton usually follows the receding ice edge as open water is formed, and it quickly depletes nutrients that have accumulated over winter. The short, though relatively productive, spring bloom is directly related to the 120-day duration of photosynthetically available radiation (PAR) (Sakshaug and Slagstad, 1991). Regions of high water column primary production in the Chukchi Sea correlate strongly with benthic biomass (Grebmeier et al., 1988). Water mass characteristics, food supply, and benthic processes are strongly coupled at a regional scale (Grebmeier et al., 1989b; Grebmeier and McRoy, 1989; Grebmeier et al., 1988). The initial, large pulse of pelagic-produced carbon is mostly ungrazed by zooplankton; thus, water column primary production is tightly coupled with benthic secondary production (Coyle and Cooney, 1988).

The benthic shelf food webs are important for the cycling of organic carbon and transfer of energy in the Arctic (Grebmeier et al., 2006b). Food webs describe both energy flow between organisms and the trophic assemblage in the community. Energy must pass from primary producers through low trophic levels to sustain higher trophic level consumers (e.g. marine mammals and birds) that are important for cultural and subsistence hunting practices of native Alaskan communities (Highsmith, 2006; Lovvorn et al., 2003). Several carbon sources (e.g. phytoplankton, POM, microphytobenthos, ice algae, terrestrial organic matter, and microbial carbon and derivatives) are potentially available for consumers and may be preferentially selected by certain organisms. Other indiscriminate feeders may consume any available carbon sources local to their habitat. As the arctic ecosystems currently experience the most pronounced

climate change effects globally (ACIA, 2005; IPCC, 2007), it is crucial to investigate the roles of various carbon sources and how their availability and abundance affects consumer diversity and abundance.

The fate of potential anthropogenic contamination related to oil and natural gas exploration and extraction are of particular interest since high concentrations of volatile organic compounds, polycyclic aromatic hydrocarbons (PAHs), or heavy metals associated with the drilling process may impair an organism's endocrine, reproductive, and nervous systems (Walker et al., 2006). Trophic transfer occurs when a contaminant is moved from a lower trophic level to a higher one during biological processes (e.g. heterotrophy). In this way, many contaminants are concentrated, or biomagnified, as trophic level increases (Rasmussen et al., 1990). Biomagnification can lead to the detrimental concentration of toxins in organisms, especially apex predators, that may be harvested for human consumption. Previous studies have shown a reasonably strong relationship between stable carbon and nitrogen isotope ratios and contaminants so that one may eventually become a predictor of the other (Fisk et al., 2001; Fisk et al., 2003; Hobson et al., 2002). For this reason, the carbon pathways elucidated by stable isotope analyses can model the potential pathways of contaminant transfer through a food web.

Stable isotope analyses can be used to track the transfer of assimilated carbon among organisms and identify the ultimate sources of carbon that are critical components of consumer diets. Stable isotope analysis is a reliable proxy to measure food web dynamics because of the consistent, stepwise fractionation or enrichment exhibited by carbon and nitrogen atoms during biological processing (Fry and Sherr, 1984). The ratio of ^{13}C atoms to ^{12}C atoms (or $\delta^{13}C$) fractionates as little as 0-1‰ per trophic step (DeNiro and Epstein, 1978; Post, 2002; Vander Zanden and Rasmussen, 2001). Stable carbon isotopes are, therefore, a tracer of ultimate carbon from its origin to any level of consumer. Stable nitrogen values ($\delta^{15}N$) of organisms, however, become enriched by 3-4‰ per trophic transfer (DeNiro and Epstein, 1978; Post, 2002; Vander Zanden and Rasmussen, 2001). Consequently, $\delta^{15}N$ values are used to model species' trophic position in a community. Although a standard deviation of ~1‰ occurs within averaged marine and freshwater realms globally, the trophic enrichment per trophic level is consistent within a system (Post, 2002). For this reason, it is crucial to determine the isotopic enrichments within a particular system to properly study the trophodynamics that operate therein. This approach is advantageous to use in the Chukchi Sea system because it not only incorporates a long-term average food web position for organisms, but also distinguishes between food source assimilation versus mere ingestion.

The main questions we sought to answer during COMIDA-CAB concerned food web dynamics of the Chukchi Sea benthic fauna and included: (1) What is the baseline trophic structure of benthic consumers in the ecosystem prior to oil and gas exploration and development? (2) What are the ultimate carbon sources in the Chukchi Sea for organisms to assimilate? (3) Is carbon produced in the water column ultimately assimilated by the benthic food web? (4) How does energy (or contaminants) move through the food web to higher trophic levels? We hypothesize that: (1) the pelagic food web is tightly coupled so that zooplankton assimilate phytoplankton carbon; (2) the bulk organic matter in sediments is ultimately of pelagic origin; (3) pelagic primary production is assimilated by benthic fauna; (4) multiple and isotopically-distinct ultimate carbon sources are assimilated by the benthic food web.

Methods

Study Area

The COMIDA study area is located in the eastern Chukchi Sea with study sites roughly between the Alaska coastline and 169°W, ranging as far south as the Bering Strait and as far north as 72.4°N (Figure 1). Except for one station at Barrow Canyon (station 50, 130 m), station depths range from 15-55 m (Table 1). Mean station depth was 42 m excluding the Barrow Canyon station.

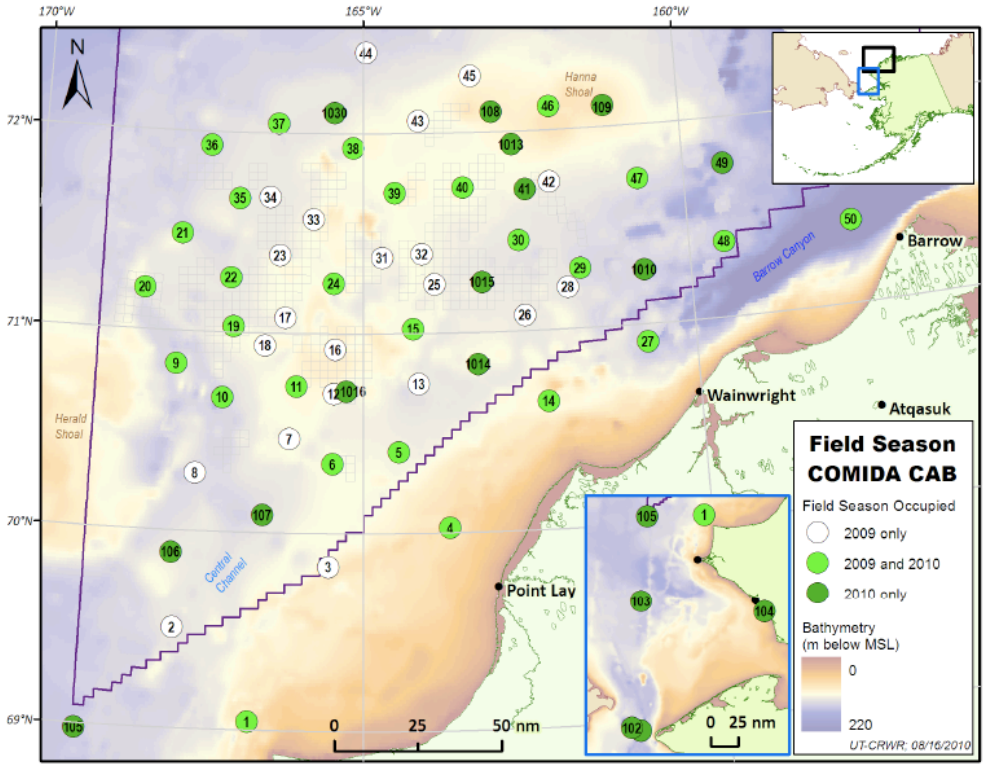

Figure 1. Stations occupied in 2009 only during COMIDA cruise are shown in white circles. Stations re-occupied in 2010 are in light green circles. Stations new to 2010 are shown in dark green.

Sample Collection

Samples were collected between 27 July and 12 August 2009 and 25 July and 16 August 2010 aboard the vessels *R/V Alpha Helix* and *R/V Moana Wave*, respectively. Various mechanisms were employed to collect the appropriate samples required for this research.

Hydrography

Hydrographic parameters of depth, temperature, salinity and *in situ* chlorophyll *a* were measured using a YSI Data Sonde 6690 (YSI, Yellow Springs, OH). Conductivity was calibrated with Ricca Chemical Company (Arlington, TX) standards at 10,000 and 50,000 microsiemens. The optical *in situ* fluorescence chlorophyll probe was calibrated at 0 μg/L with DI water. Temperature and depth was factory calibrated.

Light Measurements (PAR)

PAR data were collected using a spherical quantum sensor connected to a LI-1000 datalogger (LI-COR Inc., Lincoln, NE, USA) during cloudless conditions. The sensor was lowered on a lowering frame, and measurements were recorded from surface, 5, and 10 m. Care was taken during deployment to avoid shading the sensor by the vessel.

Particulate Organic Matter

A peristaltic pump attached to weighted, metered Tygon tubing was used to collect water at specific depths for POM collection. Water depths were verified by a HOBO pressure datalogger (Pocasset, MA) attached to the Tygon tubing. Water was filtered through 25 mm GF/F filters (Whatman, Buckinghamshire, UK) that were previously combusted at 900°C for 24 hours to remove trace organic material and pre-weighed. Filters were then dried at 60°C and stored in opaque vials for transport to University of Texas Marine Science Institute (UTMSI) for stable isotope preparation and analysis.

Phytoplankton and Zooplankton

Vertical tows of 20 μm and 335 μm mesh plankton nets (Sea Gear, Melbourne, FL) were used to collect phytoplankton and zooplankton, respectively. Prior to filtration, concentrated phytoplankton was homogenized and zooplankton were sorted by taxonomy (e.g. ctenophores, copepods, chaetagnaths, etc.). All plankton were filtered through 25 mm GF/F filters that were previously combusted at 900°C for 24 hours. Phytoplankton and zooplankton filters were dried at 60°C and stored for transport to UTMSI for stable isotope preparation and analysis.

Benthic Fauna

A van Veen grab (0.1 m^2) was used to collect surface sediments. Grab samples were sieved through 1000 μm mesh and washed with ambient seawater to clean infauna from extraneous organic matter and sediment. Benthic epifauna were collected using a 3.05 m plumb-staff beam trawl with a 7 mm mesh and a 4 mm cod-end liner. Epifauna were washed with ambient seawater to remove extraneous organic matter and sediment. Faunal organisms were keyed to lowest taxonomic level, usually species, in the field. When possible, muscle tissue was extracted from the organism (e.g. gastropods, bivalves, large arthropods, and fish). Small organisms were kept whole. Tissues were dried at 60°C in aluminum trays in the shipboard drying oven, then stored for transport to UTMSI for stable isotope preparation and analysis.

Sediments

One small core (2 cm diameter, 20 cm depth) of sediment was extracted per site from undisturbed surface sediment via the van Veen grab for porewater ammonium concentration analysis. Sediment cores were placed in pre-labeled Whirl-paks (Nasco, USA), immediately frozen in darkness, and then stored for transport to UTMSI for analysis.

Another aliquot of undisturbed surface sediment (1.4 cm diameter, 2 cm depth) was taken per site from the van Veen grab for stable carbon and nitrogen isotope analysis of organic matter in surface sediments. Sediment aliquots were placed in pre-labeled Falcon tubes (BD, USA) and immediately frozen in darkness. Sediment was transported to UTMSI for stable isotope preparation and analysis.

Sample Analyses

Stable Isotope Analysis

Faunal tissues were subsampled so that the portion of one sample for stable carbon isotope analysis was soaked in 1 *N* HCl until bubbling stopped, rinsed in deionized water, and dried at 60°C. The portion used for stable nitrogen isotope analysis was not subjected to acidification. All tissues were manually homogenized with a mortar and pestle.

Filtered samples (i.e. POM, phytoplankton, zooplankton) for stable carbon isotope analysis were acidified in H_2PO_4 for 24 hours prior to analysis. Replicate samples for stable nitrogen isotope analysis were not subjected to acidification.

Sediments were subsampled so that one portion of the aliquot, prior to stable carbon isotope analysis, was soaked in 1 *N* HCl until bubbling stopped, rinsed with deionized water, and dried at 60°C. The portion of the aliquot measured for stable nitrogen isotopes was not subjected to acidification.

All samples were analyzed on an automated system for coupled $\delta^{13}C$ and $\delta^{15}N$ measurements using a Finnegan MAT Delta Plus mass spectrometer attached to an elemental analyzer (CE Instruments, NC 2500). Samples were combusted at 1020°C and injected into the mass spectrometer with continuous flow. Isotopic ratios are denoted in standard δ notation relative to carbon and nitrogen standards, PDB and atmospheric N_2, respectively, where

$$\delta X = [(R_{sample}/R_{standard})\text{-}1] \times 1000. \quad (1)$$

X is either ^{13}C or ^{15}N of the sample and R is the corresponding ratio $^{13}C/^{12}C$ or $^{15}N/^{14}N$.

Trophic level is calculated using $\delta^{15}N$ enrichments between consumer and food source. The equation

$$TL = [(\delta^{15}N_{consumer} - \delta^{15}N_{POM})/3.4] + 1 \quad (2)$$

was used to determine trophic level of consumers. The trophic enrichment factor of 3.4 was chosen based on the $\delta^{15}N$ enrichment of the suspension feeding holothuroidian *Ocnus glacialis* ($\delta^{15}N$=11.71±0.56‰, $\delta^{13}C$=-23.67±0.16‰) and amphipod *Ampelisca macrocephala* ($\delta^{15}N$=10.98±0.32‰, $\delta^{13}C$=-22.54±0.39‰) to phytoplankton ($\delta^{15}N$=7.74±0.34‰, $\delta^{13}C$=-23.96±0.40‰). Both *O. glacialis* and *A. macrocephala* have $\delta^{13}C$ values signifying high dependence on phytoplankton carbon. The mean $\delta^{15}N$ value of all individuals of these two species is ~3.4‰ more enriched than the phytoplankton value. This enrichment factor represents an estimated enrichment factor applied to all consumers in the Chukchi Sea, and this value agrees with other enrichment factors reported for the Chukchi Sea (Hobson et al., 2002; Hobson and Welch, 1992; Iken et al., 2010).

Porewater Ammonium (NH_4^+) Concentration Analysis

Sediment cores were thawed and centrifuged at 5000 rpm for 20 min to separate porewater from sediment. Porewater was decanted and prepared for analysis using the phenolhypochlorite (or indophenol blue) method (Solórzano, 1969). Samples were read against a blank on the Shimandzu UV-2401PC spectrophotometer at 640 nm.

Results

Hydrography

The Chukchi Sea showed variation in bottom temperatures in both 2009 and 2010 (Table 1). The southernmost stations and those nearest the Alaska coast showed relative warm bottom temperatures (e.g. stations 104, 101, 1, 103, 2, 102, and 103). Although the mean bottom temperature for both years was ~0 °C, many station bottom temperatures were colder, especially northern stations deeper than 35 m.

Table 1. Physiochemical parameters measured in near-bottom depths (within 1 m of sea floor) for each station within the COMIDA study area for 2009 and 2010. ND = no data (probe malfunction). *Denotes sensor depth. Actual depth in parentheses.

Station Number	Date Occupied	Latitude (°N)	Longitude (°W)	Depth (m)	Salinity (psu)	Temperature (°C)	Chlorophyll *a* (ug/L)
1	27-Jul-2009	69.0360	166.5860	36	31.2	4.62	1.6
2	27-Jul-2009	69.5059	167.6895	46	31.8	2.43	0.6
5	28-Jul-2009	70.4053	164.4870	43	32.4	-0.17	0.8
4	28-Jul-2009	70.0228	163.7583	27	32.3	-0.23	1.0
3	28-Jul-2009	69.8279	165.5000	39	32.5	1.96	1.6
9	29-Jul-2009	70.8360	167.7840	55	32.7	-1.74	2.9
6	29-Jul-2009	70.3456	165.4600	44	32.3	1.07	1.1
7	29-Jul-2009	70.4689	166.0870	45	32.3	1.08	0.9
8	29-Jul-2009	70.2855	167.4410	48	32.4	-0.19	1.5
10	30-Jul-2009	70.6702	167.0880	52	32.4	-0.28	1.9
11	30-Jul-2009	70.7333	166.0080	41	32.3	0.68	0.9

12	30-Jul-2009	70.6976	165.4430	43	32.4	0.64	0.9
13	31-Jul-2009	70.7491	164.1910	47	32.6	-1.06	1.8
14	31-Jul-2009	70.6415	162.2640	40	32.1	0.35	0.7
15	31-Jul-2009	71.0213	164.2550	42	32.6	-1.67	8.0
19	1-Aug-2009	71.0280	166.9550	45	32.4	0.26	1.5
18	1-Aug-2009	70.9368	166.4760	43	32.3	0.64	1.3
17	1-Aug-2009	71.0739	166.1880	43	32.3	0.74	1.0
16	1-Aug-2009	70.9181	165.4200	42	32.3	0.67	1.7
28	3-Aug-2009	71.2092	161.9120	35	32.7	-1.61	ND
29	3-Aug-2009	70.9058	160.7333	49	32.9	-1.68	2.4
26	3-Aug-2009	71.0778	162.5670	45	32.5	-1.57	6.6
25	3-Aug-2009	71.2425	163.9930	44	32.6	-1.69	4.3
27	4-Aug-2009	71.3978	164.7000	50	32.3	-0.48	1.3
22	5-Aug-2009	71.2706	167.0190	46	32.3	0.88	1.0
23	5-Aug-2009	71.3933	166.2710	44	32.4	0.26	1.4
24	5-Aug-2009	71.2431	165.4450	42	32.4	0.45	0.8
20	6-Aug-2009	71.2077	168.3250	48	32.6	-0.99	3.3
21	6-Aug-2009	71.4857	167.7860	45	32.7	-1.29	1.5
35	6-Aug-2009	71.6696	166.9170	45	32.5	-0.36	1.5
36	6-Aug-2009	71.9300	167.3940	48	32.6	-1.29	2.0
33	7-Aug-2009	71.5702	165.7700	42	32.8	-1.64	1.9
37	7-Aug-2009	72.0463	166.3490	47	32.2	0.24	1.2
34	7-Aug-2009	71.6781	166.4560	45	32.5	-0.49	1.4
43	8-Aug-2009	72.0650	164.1230	39	32.8	-1.49	1.5
44	8-Aug-2009	72.4206	164.9880	49	32.7	-1.33	2.7
39	9-Aug-2009	71.7033	164.5110	38	32.8	-1.7	2.0
31	9-Aug-2009	71.3107	161.6500	43	32.9	-1.72	2.5
32	9-Aug-2009	71.4412	165.0860	44	32.9	-1.70	2.8
40	10-Aug-2009	71.7272	163.4640	38	32.6	-1.58	1.7
45	10-Aug-2009	72.2824	163.2900	40	32.6	-1.39	ND
46	10-Aug-2009	72.1166	162.0480	25	32.6	-0.68	ND
42	10-Aug-2009	71.7402	162.1100	43	32.8	-1.61	ND
48	11-Aug-2009	71.3749	159.4700	52	32.7	-1.72	ND
47	11-Aug-2009	71.7281	160.7320	46	32.6	-1.76	ND
30	11-Aug-2009	71.4519	162.6140	44	32.6	-1.48	ND
50	12-Aug-2009	71.4640	157.2150	37* (130)	32.6	-1.26	ND
B-site	13-Aug-2009	71.2512	163.1952	45	32.7	-1.67	ND
K-site	14-Aug-2009	70.7114	165.2491	43	32.0	1.73	ND
C-site	15-Aug-2009	71.4192	165.5402	ND	ND	ND	ND
103	25-Jul-2010	67.6704	168.9578	47	32.5	3.08	2.4
102	25-Jul-2010	65.7240	168.9570	31	31.9	2.33	1.9
101	25-Jul-2010	65.6900	168.6400	39	30.3	6.88	0.9
105	27-Jul-2010	68.9738	168.9449	50	31.6	2.32	0.7

104	27-Jul-2010	67.5622	164.1779	15	30.6	7.38	ND
106	28-Jul-2010	69.8852	167.7373	47	32.0	-0.02	ND
1	28-Jul-2010	69.0397	166.5935	35	30.0	6.03	0.8
107	29-Jul-2010	70.0858	166.4554	36	31.9	0.14	3.9
5	29-Jul-2010	70.4048	164.4823	41	32.1	0.2	2.2
4	29-Jul-2010	70.0231	163.7612	26	32.2	0.86	4.0
19	30-Jul-2010	71.0278	166.9527	44	32.2	0.26	2.2
11	30-Jul-2010	70.7328	165.9967	40	32.0	0.53	1.4
6	30-Jul-2010	70.3451	165.4504	44	32.2	-0.22	2.6
1016	30-Jul-2010	70.7102	165.2527	42	32.2	0.22	1.7
9	31-Jul-2010	70.8314	167.7867	48	32.5	-1.47	ND
10	31-Jul-2010	70.6713	167.0832	52	32.5	-0.42	1.6
22	31-Jul-2010	71.2721	167.0144	46	32.3	-0.8	1.6
24	1-Aug-2010	71.2492	165.4479	42	30.6	-1.41	3.0
15	1-Aug-2010	71.0213	164.2550	42	32.6	-1.53	2.4
1014	1-Aug-2010	70.8400	163.2910	44	32.1	0.19	0.4
48	3-Aug-2010	71.3768	159.4678	51	33.6	-1.52	3.1
50	3-Aug-2010	71.4136	157.4915	60* (130)	32.8	-0.87	1.3
109	4-Aug-2010	72.1038	161.1895	31	33.1	-1.64	0.8
47	4-Aug-2010	71.7274	160.7183	45	33.2	-1.66	4.4
49	4-Aug-2010	71.7674	159.3730	50	33.2	-1.65	3.0
108	5-Aug-2010	72.1006	162.9754	37	33.0	-1.66	5.2
1013	5-Aug-2010	71.9333	162.6680	39	33.0	-1.55	3.2
30	5-Aug-2010	71.4530	162.6108	43	32.9	-1.7	2.1
41	5-Aug-2010	71.7070	162.4820	41	33.0	-1.62	0.8
46	5-Aug-2010	72.1165	162.0547	25	33.2	-1.6	6.0
1030	6-Aug-2010	72.1033	165.4556	45	32.6	-1.39	1.0
38	6-Aug-2010	71.9269	165.1608	35	32.4	-1.01	0.6
39	6-Aug-2010	71.7020	164.5150	37	32.8	-1.57	0.6
40	6-Aug-2010	71.7255	163.4562	39	33.0	-1.69	0.7
21	7-Aug-2010	71.4847	167.7817	48	32.7	-1.72	0.8
36	7-Aug-2010	71.9303	167.3892	48	32.8	-1.76	1.6
35	7-Aug-2010	71.6692	166.9173	45	32.6	-1.6	0.9
37	7-Aug-2010	72.0457	166.3401	46	32.8	-1.68	1.2
20	8-Aug-2010	71.2067	168.3113	47	32.6	-1.68	0.8
29	10-Aug-2010	71.2982	161.6887	22	32.1	-1.14	0.0
1010	10-Aug-2010	71.2695	160.7157	52	33.3	-1.41	0.5
1015	11-Aug-2010	71.2508	163.1968	45	30.8	-1.67	1.8
14	16-Aug-2010	70.5276	162.1084	40	31.8	1.37	2.1
27	16-Aug-2010	70.9153	160.1824	52	32.2	-0.78	1.3

Salinity in the Chukchi Sea ranged from 30.0 to 33.6 psu. Stations in the northeast of the study area exhibited the highest salinities (>33 psu). The stations with the lowest bottom salinity, including stations 1015, 24, 104, and 101, were somewhat scattered. Notably, the two stations in the Bering Strait, station 101 on the east and station 102 on the west, display drastically different hydrography. Station 101 had a bottom temperature of 6.88 °C and a salinity of 30.3 psu, whereas station 102 had a bottom temperature of 2.33 °C and salinity of 31.9 psu.

Chlorophyll *a* ranged from below detection limit (i.e. 0 μg L^{-1}) to 8.0 μg L^{-1}. The range surrounded a mean value of 1.9 μg L^{-1}. Bottom chlorophyll *a* does not appear to be a function of geography since stations with highest chlorophyll *a* values are scattered among those with the lowest. For example in 2009, the stations with lowest values (stations 2, 14, 5, and 24) were near those with the highest values (stations 25, 26, and 15). In 2010 a similar spatial trend occurred where stations with lowest values (e.g. stations 29, 1014, 1010, 108) were scattered among stations with high bottom chlorophyll *a* values (stations 46, 1013, 4, 107). Notably in 2010, some of the highest observed values occurred near Hanna Shoal (e.g. stations 108, 46, 1013).

PAR values at the surface of station 14 at 0930 hours were 700 μmol photons m^{-2} s^{-1}, whereas PAR was 1300 μmol photons m^{-2} s^{-1} at station 27 at 1400 hours. Light attenuation (*k*) at station 14 was 0.12, at station 27 was 0.11, and at station 38 was 0.7.

Particulate Organic Matter

Stable nitrogen isotope values of POM ranged between 0.47 and 11.49‰ (Table 2). The low end of the range reflects possible nitrogen fixation or microbial fractionation of nitrogen while the highly enriched values reflect second trophic level organisms. The value of 11.49‰ is abnormally high, as most POM values were clustered around the mean value of 5.12‰. In this instance, second trophic level organisms (e.g. zooplankton) may have been inadvertently captured in the sample. Stable nitrogen isotopic signatures often varied throughout the water column, with both extremely depleted and extremely enriched values in the near-bottom water column. However, bottom values were not significantly different from surface values (Student's *t*-Test for paired samples, $p > 0.05$).

Stable carbon isotopic values of POM ranged from -26.17 to -20.96‰ (Table 2). The mean $\delta^{13}C$ POM value of -24.19‰ is similar to that of phytoplankton in the Chukchi Sea. As with $\delta^{15}N$ values, $\delta^{13}C$ values often varied throughout the water column at each station. At Stations 1, 6, 10, 13, 16, 20, 27, 32, 37, 44, and 46, stable carbon isotopes were significantly more enriched at the near-bottom compared to near-surface depths (Student's *t*-Test for paired samples, $p < 0.003$). For Station 10, POM from 23 m was used instead of 28 m.

Table 2. Particulate organic matter stable nitrogen and carbon isotope values. ND = no data (machine analytical error). Data represent 2009 samples. Values are mean ± standard error when $n > 1$.

Station	Depth (m)	$\delta^{15}N$ (‰)	$\delta^{13}C$ (‰)
1	2	6.14±0.60	-24.23±0.05
	5	5.53±0.66	-24.55±0.02
	18	2.21±0.69	-24.19±0.09
	35	0.47±0.39	-23.69±0.27
3	5	4.98±0.25	-24.23±1.44
	10	6.37±0.25	-24.72±1.29
	19	4.95±0.75	-25.62±0.19
	27	2.07±3.41	-25.22±0.10
	31	5.43±0.79	-25.38±0.25
6	5	1.63±6.39	-25.40±0.04
	10	5.55±0.25	-25.62±0.31
	20	3.08±0.79	-24.85±0.23
	30	1.71±1.26	-24.14±0.11
	34	2.84±0.11	-22.93±0.43
10	11	2.44	-24.99±0.17
	16	5.40±1.36	-24.69±0.47
	23	3.61±0.63	-24.15±0.09
	28	3.51±0.36	ND
13	9	6.15±0.80	-25.94±0.14
	15	3.55±1.22	-26.17±0.14
	21	4.40±0.71	-25.71±0.09
	30	2.75±1.07	-24.42±0.01
16	10	7.71±2.21	-25.49±0.21
	22	6.36±1.16	-25.41±0.05
	31	3.99±0.65	-23.79±0.02
	36	3.80±0.03	-23.79±0.22
20	11	6.97±0.52	-24.56±0.20
	21	8.11±0.75	-23.38±0.15
	30	5.79±0.38	-22.89±0.01
	41	8.57±1.41	-22.17±0.12
27	12	5.63±0.76	-25.56±0.03

	22	5.60±1.37	-25.50±0.05
	32	2.60±0.25	-23.97±0.33
	43	2.41±0.16	-23.35±0.09
29	8	6.00±0.79	-22.12±0.06
	21	11.49±0.11	-20.96±0.12
	30	5.69±0.02	-22.04±0.05
32	10	6.40±4.53	-23.72±0.02
	20	7.97±0.45	-23.83±0.14
	30	9.08±1.28	-21.79±0.56
37	10	5.28±0.70	-25.14±0.15
	20	2.81±0.17	-25.10±0.28
	32	1.89±0.77	-22.64±0.30
	43	3.28±2.30	-23.95±1.41
44	10	ND	-25.73±0.12
	20	5.06±0.43	-24.29±0.10
	38	3.16±0.40	-23.13±0.18
46	8	7.85±1.05	-24.21±0.10
	15	8.85±0.57	-24.06±0.16
	20	7.48±0.43	-23.66±0.05
	24	9.17±0.47	-22.26±0.19

Phytoplankton and Zooplankton

Phytoplankton stable nitrogen isotopic values range from 5.62 to 10.12‰ with a mean value of 7.74‰ (Table 3). Stable carbon isotopic values range from -26.39 to -21.17‰.

Table 3. Replicate phytoplankton stable nitrogen and carbon isotope values for COMIDA stations from 2009 expressed as mean ± standard error. For all stations, n = 2, except for station 30 where n= 1.

Station	$\delta^{15}N$ (‰)	$\delta^{13}C$ (‰)
1	9.49±0.35	-21.17±0.48
3	8.88±0.14	-26.39±0.01
6	7.42±0.02	-25.67±0.19
10	7.32±0.67	-25.13±0.80
13	7.74±0.73	-23.89±0.14
16	7.59±0.22	-24.57±0.10
27	6.62±0.43	-24.73±0.04
29	7.71±0.37	-22.53±0.12
30	5.62	-22.24
33	6.72±0.15	-24.27±0.09
37	10.12	-23.54±1.02
46	8.20±0.07	-23.34±0.04
50	7.19±0.02	-24.01±0.12

The mean $\delta^{13}C$ value of phytoplankton from all stations was -23.96‰. There was substantial overlap in isotopic values of POM and phytoplankton. Food sources present in the water column (i.e. POM and phytoplankton) have similar stable isotope values and represent a pelagic production end-member for consumers.

Zooplankton were sorted into major taxonomic categories prior to stable isotopic analysis (Table 4**)**. Stable $\delta^{15}N$ and $\delta^{13}C$ in pteropods ranged from 8.85 to 13.87‰ and from -25.64 to -21.87‰ with mean values of 11.57±0.54‰ and -23.20±0.51‰, respectively. For mysids, this range was 9.95 to 14.31‰ and between -23.39 to -18.00‰, with mean values of 11.74±0.69‰ and -20.90±0.69‰ for nitrogen and carbon, respectively. Copepods ranged from 9.24 to 12.34‰ and -23.35 to -19.66‰, with mean values of 10.93±0.18‰ and -21.67±0.29‰.

Table 4. Zooplankton stable isotope values expressed as mean ± standard error when $n > 1$. Samples from 2009 represented. ND = no data (machine analytical error).

Group	Station	$\delta^{15}N$ (‰)	$\delta^{13}C$ (‰)
Pteropod	6	12.17±0.60	-23.41±0.40
	20	10.06	-22.56
	37	8.95	-22.54
	44	10.91	-22.77
Mysid	6	12.31±1.07	-20.53±0.30
	30	9.95	-18.00
	44	12.41	-22.82
	50	10.55	-23.39
Copepod	3	10.62±0.28	-22.43±0.16
	6	10.63±0.91	-20.90±0.44
	10	11.29±0.16	-22.24±0.19
	13	10.77	-23.35
	16	10.33±0.40	ND
	20	11.05	-20.25
	25	11.72	-19.66
	29	11.34±0.07	-21.35±1.83
	30	11.72	-21.25
	37	10.88	-23.33
Ctenophore	1	10.12±2.43	-22.16±0.42
	3	12.19	-22.70
	10	13.04	-22.81
	13	6.82±1.29	-22.67
	16	10.04	-21.83
	27	10.23	-21.14
	37	8.04	-20.54
	44	8.04	-22.59
Chaetognath	3	13.04±0.47	-21.41±0.39
	13	12.73	-21.07
	37	13.79	-21.12

Ctenophores were also collected during zooplankton vertical tows. Ctenophores ranged from 5.53 to 13.04‰ in stable nitrogen isotopic values. Stable carbon isotope values ranged from -23.98 to -20.54‰. The mean stable isotopic value of all ctenophores was 9.82±0.75‰ for nitrogen and -22.05±0.29‰ for carbon.

Predatory chaetognaths were found in zooplankton tows at stations 3, 13, and 37. Their stable nitrogen values ranged from 12.57 to 13.79‰ and their stable carbon isotopic values ranged from -21.80 to -21.01. The mean chaetognath stable isotopic values for all specimens analyzed

were 13.15±0.23‰ and -21.25±0.14‰. Chaetognaths are a full trophic level higher than the rest of the analyzed zooplankton based upon a ~3.4‰ trophic enrichment. The $\delta^{13}C$ value of chaetognaths had a narrow range and suggests they strictly feed on prey with $\delta^{13}C$ values approximately -23 to -22‰, which encompasses most other zooplankton.

Sediment Stable Isotopes

Stable isotopes of organic matter in surface sediments did not significantly vary between 2009 and 2010 (Table 5). Ranges of stable nitrogen values were similar between 2009 and 2010. The mean sediment $\delta^{15}N$ value for 2009 was 7.15‰ (ranging from 5.11‰ to 8.47‰), and the mean sediment $\delta^{15}N$ value for 2010 was 7.70‰ (ranging from 6.27‰ to 9.08‰).

In 2009, the mean sediment $\delta^{13}C$ value was -23.23±0.09‰ (ranging from -25.67 to -22.25‰). Comparably, the mean sediment $\delta^{13}C$ value for 2010 was -23.32±0.16‰ (ranging from -26.20 to -22.29‰).

Molar C:N ratios were also measured for sediments in the COMIDA study area. C:N ratios ranged from 4.46 to 13.09 with a mean value of 9.28 for the stations occupied in 2009. In the following year, C:N ratios ranged from 5.02 to 16.30 with mean value of 10.13.

When comparing stations occupied both during 2009 and 2010, there is no significant difference between stable carbon isotope values or C:N ratios (Student's *t*-Test for paired samples, p=0.60 and p = 0.19, respectively). However, stable nitrogen isotope values significantly differed between years (Student's *t*-Test for paired samples, $p<0.001$).

Table 5. Sediment stable isotope values from COMIDA stations occupied in 2009 and 2010. Blank values indicate stations not occupied. ND = no data (machine analytical error).

Station	2009			2010		
	$\delta^{15}N$ (‰)	$\delta^{13}C$ (‰)	Molar C:N	$\delta^{15}N$ (‰)	$\delta^{13}C$ (‰)	Molar C:N
1	5.64	-24.71	12.56	6.27	-24.67	16.30
2	7.46	-23.31	9.36			
3	7.27	-23.46	9.96			
4	7.00	-25.67	8.63	ND	-24.94	
5	6.64	-23.68	8.35	7.91	-23.73	8.13
6	7.05	-23.48	8.99	7.31	-23.46	10.10
7	7.01	-23.27	11.24			
8	8.07	-23.16	10.04			
9	7.48	-22.99	8.65	7.59	-22.95	8.52
10	6.68	-23.34	9.94	6.59	-23.04	10.37
11	6.82	-23.07	10.04	7.94	-23.05	11.77
12	7.43	-23.47	7.64			
13	7.83	-23.38	12.45			
14	8.47	-24.70	9.63	ND	-24.78	
15	6.48	-23.19	7.80	7.35	-23.19	9.75

16	7.03	-23.33	7.45			
17	5.11	-23.02	13.09			
18	6.89	-22.81	10.23			
19	7.80	-22.80	10.42	8.25	-23.59	12.42
20	7.99	-22.63	10.04	8.36	-22.48	9.85
21	7.39	-22.72	9.39	8.10	-22.72	9.67
22	7.51	-23.01	9.42	7.28	-22.74	9.64
23	6.60	-22.89	9.09			
24	6.80	-22.95	7.69	7.73	-23.23	9.98
25	6.80	-23.02	9.40			
26	5.61	-23.48	8.40	ND	-24.22	
27	6.42	-24.28	4.46			
28	7.25	-23.46	9.76			
29	7.45	-22.91	8.90	7.35	-23.36	9.56
30	7.49	ND	8.00	8.23	-23.15	11.57
31	6.87	-22.65	9.45			
32	7.45	-23.01	8.77			
33	7.11	-22.91	8.74			
34	7.79	-22.74	8.77			
35	6.67	-22.63	9.02	7.73	-22.49	10.11
36	7.71	-22.25	9.15	7.90	-22.52	9.63
37	7.17	-23.04	10.87	8.40	-23.06	5.02
38	6.35	-22.85	9.28	7.10	-22.43	14.57
39	6.53	-23.43	7.18	ND	-23.33	
40	8.29	-22.69	7.61	8.75	-22.86	9.14
42	8.24	-22.87	9.26	7.51	-22.80	9.10
43	6.74	-23.27	8.63			
44	7.68	-22.60	8.72			
45	6.11	-22.79	10.14			
46	8.26	-22.92	8.04	ND	-25.14	
47	7.88	-23.10	8.99	8.19	-22.51	10.73
48	7.45	-23.37	11.48	8.18	-22.94	7.55
49				7.86	-22.67	8.69
50	7.38	-24.45	10.41	6.99	-24.13	10.82
103				7.93	-22.29	8.58
105				9.08	-22.36	9.23
106				8.04	-23.32	12.62
107				ND	-23.49	
108				ND	-22.94	
109				ND	-23.45	
1010				7.94	-23.21	10.12
1013				8.36	-22.76	10.23
1014				7.48	-23.63	11.75

1015	7.87	-23.05	10.57
1016	ND	-26.20	
1030	8.25	-22.62	9.68

Sediment Porewater Ammonium

Porewater ammonium (NH_4^+) concentrations in the Chukchi Sea sediments differed significantly between 2009 and 2010 (Student's t-test, $p < 0.0000001$). In 2009 concentrations ranged from 112-535 μM, while in 2010 they were much lower and ranged from 49-234 μM (Table 6). The average concentration in 2009 was 191 μM, while the average in 2010 was 108 μM. Comparing stations occupied in both years shows a stark difference in concentrations (Student's t-test for paired samples, $p < 0.0001$).

Benthic Fauna

The stable nitrogen isotopic values of the benthic fauna determine the trophic structure in the COMIDA study area (Figure 2). The benthic consumers are categorized into four trophic levels (i.e. TL 2, 3, and 4). Herbivorous primary consumers fall into the second trophic level. This consists of filter/suspension feeders and interface deposit feeders. Porifera (sponges) and Echinarachniidae (sand dollars) posses the lowest measured $\delta^{15}N$ values. Bivalvia (bivalves), Ascidiacea (tunicates), Amphipoda (amphipods), Bryozoa (bryozoans), Isopoda (isopods), and Hydrozoa (hydroids) make up the majority of the second trophic level with $\delta^{15}N$ values very similar to one another (Table 7).

The third trophic level consists largely of omnivores. Ophiuroidea (brittle stars and basket stars), nemerteans, and omnivorous polychaete species are mobile benthic feeders that consume both algal material and detrital organismal tissue. Basket stars, Anthozoa (anemones and soft corals), forams, and holothurians (sea cucumbers) filter zooplankton from the water column, explaining their enriched $\delta^{15}N$ value. The one sipunculid species (*Golfingia margaritacea*) and the omnivorous polychaetes are mostly deposit feeders that consume organic matter within the sediments.

In the fourth trophic level, representing the benthic predators in the Chukchi Sea, are asteroids (sea stars), polychaetes, and gastropods. The whelks *Neptunea heros* and *Plicifusus kroeyeri*, and the nudibranch *Tritonia diomedea* are the species with the highest $\delta^{15}N$ values in the entire food web. These gastropods are exclusive predators. Decapoda (crabs), priapulids, fish (bering sea flounder and arctic cod), and cephalpods also compose the fourth trophic level of predatory scavengers.

Table 6. Sediment porewater ammonium values compared from all sites occupied in 2009 and 2010. Blank values indicate stations not occupied. ND = no data (machine analytical error).

Sediment Porewater Ammonium (μM)					
Station	2009	2010	Station	2009	2010
1	262	195	32	190	
2	213		33	169	
3	236		34	160	
4	349	116	35	190	83
5	132	84	36	262	132
6	129	72	37	173	97
7	200		38	163	100
8	133		39	156	100
9	221	100	40	202	78
10	147	89	41	112	82
11	193	118	43	158	
12	137		44	210	
13	170		45	269	
14	379	86	46	147	
15	184	75	47	175	81
16	125		48	134	86
17	174		50	149	234
18	145		103		207
19	180	81	104		
20	174	153	105		187
21	187	122	106		99
22	226	98	107		95
23	217		108		132
24	178	63	109		61
25	137		1010		113
26	167		1013		93
27	143	49	1014		104
28	179		1015		156
29	151	141	1016		54
30	535	107	1030		121
31	169				

The $\delta^{13}C$ values of the benthic fauna range from -26.01‰ (*Ampelisca macrocephala*) to -15.59‰ (*G. margaritacea*). The range of phytoplankton $\delta^{13}C$ values (-26.39 to -21.17‰) overlapped the depleted end of the fauna; however, the ^{13}C-enriched value of *G. margaritacea* and others enriched species fall outside of plausible phytoplankton values. Clear evidence shows that a ^{13}C-enriched carbon source is assimilated by benthic fauna. Although several potential 13C-enriched carbon sources potentially exist in the Chukchi Sea benthos, we use the literature

value of benthic microalgae as a second potential carbon source. Dubois et al. (2007) report a value of -17.0±1.0‰ for benthic microalgae, which also falls within the range reported by Grippo et al. (2011) of -18.7 to -15.9‰. The mean $\delta^{13}C$ value for all *G. margaritacea* sampled fell within the range of literature values of benthic microalgae. Microbial carbon, microbial by-products, and the meiofaunal food web are potential end-members for the system, although not discussed here. Since benthic microalgae are observed as a ^{13}C-enriched carbon source to marine food webs in other studies, the ^{13}C-enriched carbon source observed in the Chukchi Sea is hereafter referred to as benthic microalgae. This nomenclature, however, does not preclude the possibility of the microbial food web interacting with and becoming assimilated by the benthic food web in the Chukchi Sea.

The distribution of benthic fauna was contained by the two end-members (Figure 3). Holothurians, forams, sand dollars, pycnogonids (sea spiders), and amphipods had values very similar to POM.

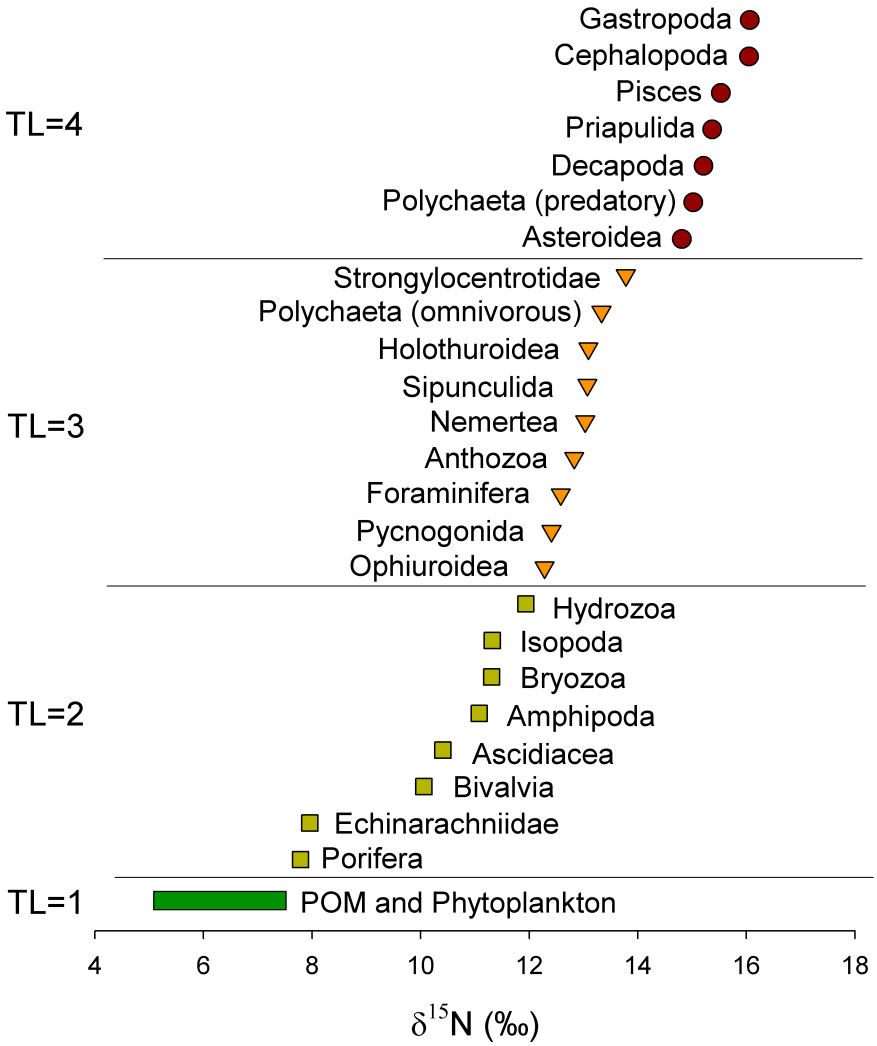

Figure 2. Trophic structure of the northeast Chukchi Sea as delineated using Equation 2.

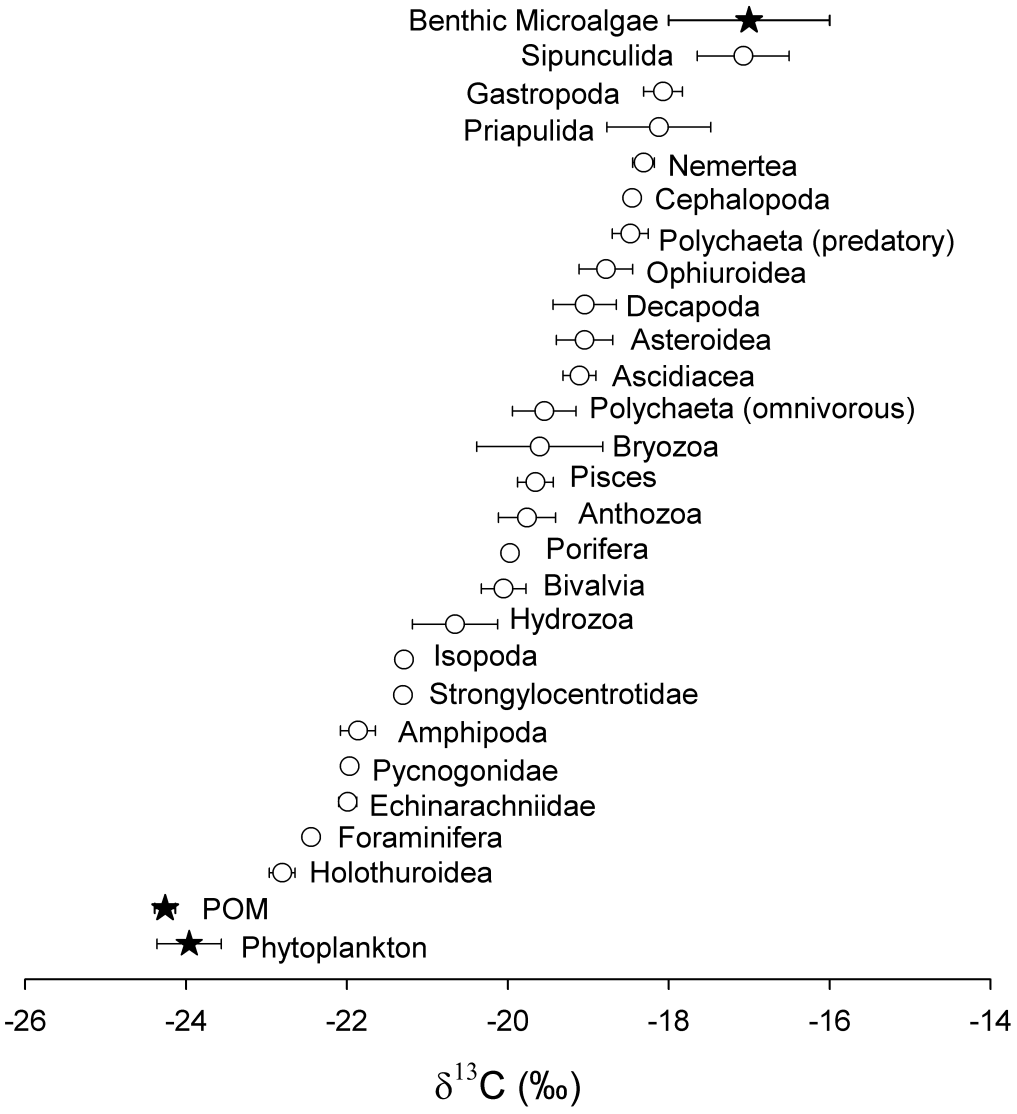

Figure 3. The distribution of organism $\delta^{13}C$ values plotted between ultimate carbon sources, benthic microalgae, phytoplankton, and POM.

Other taxonomic groups such as sipunculids, gastropods, priapulids, and nemerteans had $\delta^{13}C$ values very near benthic microalgae. The vast majority of mean $\delta^{13}C$ values of taxonomic groups of consumers were intermediate of the two end-members. The progressive enrichments of $\delta^{13}C$ for these taxa do not follow the enrichments of $\delta^{15}N$ measured for trophic level determination (see Figure 2). In other words, enriched $\delta^{13}C$ values are not merely trophic enrichments. For example, sipunculids had the most enriched $\delta^{13}C$ value, yet possessed only a moderately enriched $\delta^{15}N$ value as a third trophic level organism. Bryozoans had a $\delta^{13}C$ value more enriched than Pisces, even though it had a relatively depleted $\delta^{15}N$ value compared to the fourth trophic level organisms. These findings suggest that two carbon sources are indeed assimilated by benthic fauna.

The benthic fauna were plotted on a stable isotope bi-plot (Figure 4). A linear regression was plotted through the cluster of organisms to determine linearity. The regression has weak correlation ($r^2 = 0.27$) showing much scatter around the regression line. If the entire food web used one ultimate source of carbon, then the stable isotope values of the organisms would regress tightly around the single line.

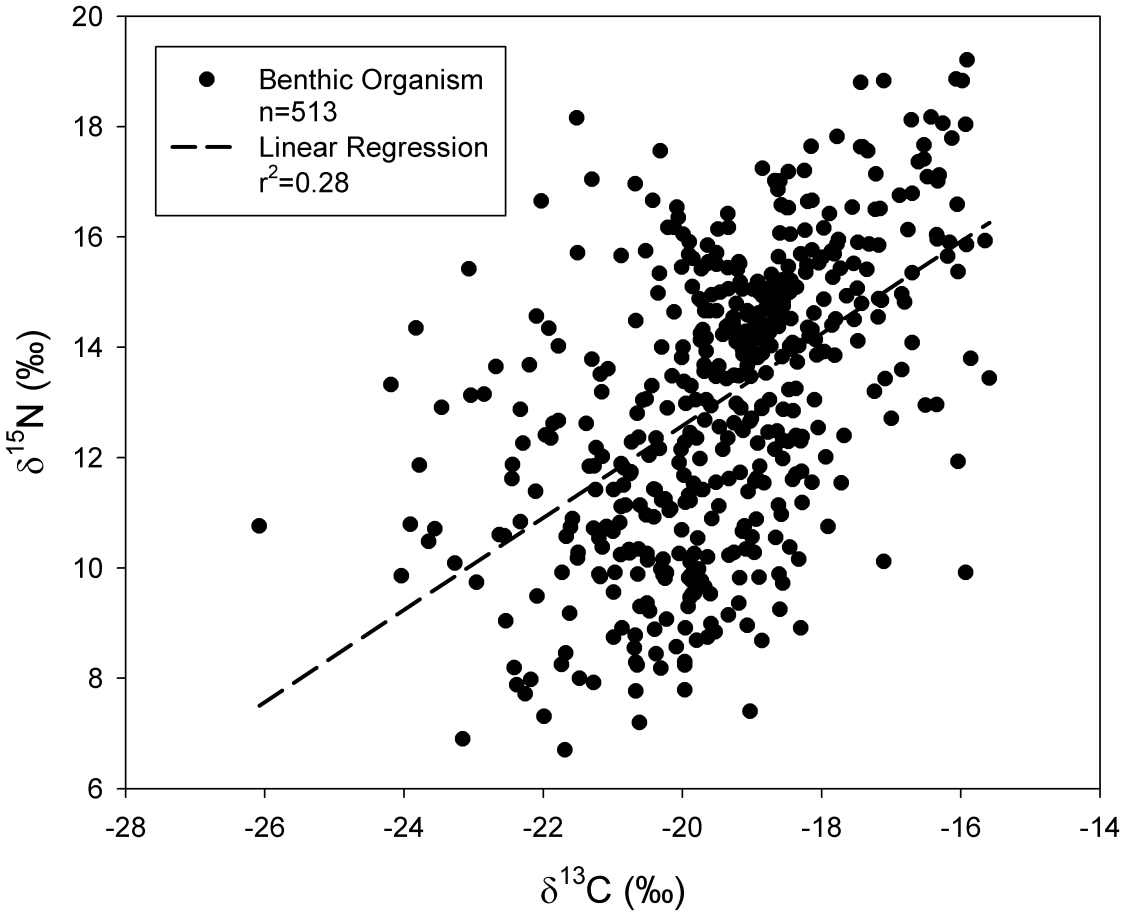

Figure 4. Bi-plot of $\delta^{13}C$ vs. $\delta^{15}N$ values for benthic consumers collected in the northern Chukchi Sea. The linear regression ($y = 0.83 + 29.3$) shows a weak correlation ($r^2 = 0.28$) between the two axes suggesting that multiple, isotopically distinct carbon sources are assimilated by consumers.

Table 7. Stable nitrogen and carbon isotope values (expressed as mean ±s tandard error when *n*>1) for benthic food web components in the COMIDA study area. Trophic level (TL) was derived from Equation 2.

Taxonomic group or species	*n*	$\delta^{15}N$ (‰)	TL	$\delta^{13}C$ (‰)	Molar C:N
POM	85	5.40±0.22		-24.26±0.13	
Phytoplankton	25	7.74±0.34		-23.96±0.40	
Sediment	80	7.41±0.08		-23.26±0.09	
FORAMINIFERA					
Benthic Foraminfera	2	12.57±0.71	3.2	-22.44	4.02
PORIFERA					
Unidentified sponge	1	7.79	1.8	-19.97	4.69
CNIDARIA					
Octocorallia					
Gersemia rubiformis	7	11.99±0.30	3.0	-20.45±0.24	8.04
Hexacorallia					
Tealia sp.	2	15.73±1.46	4.1	-19.06±0.39	4.81
Hydrozoa					
Hydroid sp.	9	12.05±0.47	3.1	-20.85±0.17	7.25
Sertularia sp.	6	11.76±0.30	3.0	-20.46±0.16	5.50
NEMERTEA					
Nemertea sp.	2	13.03±0.88	3.4	-18.31±0.35	4.72
SIPUNCULIDA					
Golfingia margaritacea	12	13.07±0.21	3.4	-17.07±0.31	3.96
PRIAPULIDA					
Priapulus caudatus	2	15.37±0.52	4.0	-18.12±0.64	4.51
ANNELIDA					
Polychaeta (omnivorous)					
Axiothella cantenata	9	12.61±0.11	3.2	-18.94±0.18	4.82
Maldane sarsi	40	14.38±0.09	3.7	-18.95±0.08	4.59
Nicolea zostericola	2	12.77±0.09	3.3	-21.00±1.32	4.94
Nicomache lumbricalis	1	13.05	3.4	-19.66	3.12
Onuphis parva	7	11.94±0.35	3.0	-18.59±0.20	4.83
Pectinaria granulata	3	12.86±0.55	3.3	-20.37±0.26	4.25
Praxillella gracilis	6	13.09±0.49	3.4	-18.60±0.39	4.52

Praxillella praetermissa	6	13.47±0.29	3.5	-19.11±0.38	4.92
Sternaspis scutata	11	11.77±0.80	3.0	-19.49±0.40	4.37
Terebellides stroemi	3	11.55±0.35	2.9	-20.71±0.78	5.64
Polychaeta (predatory)					
Harmothoe imbricata	9	14.61±0.25	3.8	-18.37±0.39	5.26
Lumbrineris fragilis	8	14.84±0.37	3.9	-18.67±0.14	4.57
Nephtys ciliata	22	15.27±0.24	4.0	-18.04±0.24	4.76
Phyllodoce groenlandica	2	14.60±0.06	3.8	-18.81±0.17	4.87
MOLLUSCA					
Bivalvia					
Astarte borealis	7	11.65±0.41	2.9	-19.81±0.31	4.76
Astarte montagui	2	12.10±0.05	3.1	-20.40±0.07	4.88
Clinocardium ciliatum	3	10.97±0.15	2.7	-19.07±0.24	3.82
Cyclocardia crebricostata	5	11.03±0.73	2.7	-19.83±0.29	5.00
Ennucula tenuis	44	9.494±0.12	2.3	-20.04±0.11	5.27
Liocyma fluctuosa	2	12.65±0.64	3.2	-20.79±0.35	5.19
Macoma calcarea	10	9.822±0.73	2.4	-20.64±0.37	6.03
Macoma moesta	4	9.499±0.53	2.3	-20.35±0.45	5.39
Musculus discors	2	10.56±0.67	2.6	-20.74±0.44	5.43
Musculus niger	1	11.60	2.9	-18.42	4.09
Mya truncata	1	9.18	2.2	-21.62	5.49
Nuculana pernula	6	10.48±0.26	2.6	-20.06±0.40	4.84
Serripes groenlandica	4	10.67±0.47	2.7	-19.50±0.53	4.03
Yoldia hyperborea	6	9.139±0.48	2.2	-19.37±0.30	4.85
Gastropoda					
Buccinum sp.	3	15.49±1.17	4.1	-18.05±0.40	4.26
Euspira pallida	7	12.64±0.29	3.2	-19.62±0.50	4.80
Neptunea heros	37	16.40±0.24	4.3	-17.30±0.21	4.25
Plicifusus kroeyeri	9	17.09±0.29	4.5	-16.86±0.21	4.26
Tritonia diomedea	4	16.96±0.11	4.5	-18.48±0.10	4.36
Cephalopoda					
Octopusidae	1	16.05	4.2	-18.45	4.06
ARTHROPODA					
Pycnogonida					
Pycnogonid sp.	1	12.41	3.2	-21.97	4.02
Amphipoda					
Ampelisca macrocephala	13	10.89±0.32	2.7	-22.54±0.38	6.99
Metopa sp.	1	13.51	3.5	-21.18	8.54
Isopoda					
Synidotea bicuspida	3	11.32±0.32	2.8	-21.29±0.02	11.09
Decapoda					

Chionoecetes opilio	28	15.39±0.17	4.0	-18.65±0.13	4.69
Hyas coarcticus	4	15.82±0.17	4.2	-18.63±0.28	4.26
Pagurus rathbuni	5	13.67±0.16	3.5	-19.84±0.75	3.60
ECHINODERMATA					
Asteroidea					
Leptasterias polaris	4	14.80±0.46	3.9	-19.04±0.89	7.01
Ophiuroidea					
Gorgonocephalus eucnemis	5	13.50±0.70	3.5	-18.84±0.57	18.03
Ophiura sarsii	19	11.95±0.47	3.0	-18.71±0.27	24.73
Echinoidea					
Echinarachniidae					
Echinarachnius parma	13	7.96±0.32	1.9	-21.98±0.15	50.22
Strongylocentrotidae					
Strongylocentrotus sp.	1	13.78	3.6	-21.30	4.93
Holothuroidea					
Ocnus glacialis	7	11.70±0.55	3.0	-23.67±0.15	10.68
Psolus chitonoides	10	14.04±0.86	3.6	-21.93±0.15	16.96
BRYOZOA					
Alcyonidium gelatinosum	4	10.28±0.28	2.5	-20.35±0.37	7.97
Carbasea carbasea	10	12.16±0.42	3.1	-20.31±0.25	9.28
Eucratea loricata	4	10.53±0.13	2.6	-19.82±0.76	8.42
Securiflustra securifrons	2	10.62±0.70	2.6	-17.92±1.99	5.98
TUNICATA					
Ascidiacea					
Boltenia ovifera	4	10.08±0.36	2.5	-20.40±0.16	11.16
Molgula griffithsii	4	10.34±0.58	2.6	-20.87±0.04	9.42
Pelonaia corrugata	1	11.93	3.0	-16.04	13.28
VERTEBRATA					
Pisces					
Boreogadus saida	29	15.63±0.14	4.1	-19.98±0.16	4.29
Hippoglossoides robustus	4	14.78±0.17	3.9	-19.32±0.08	3.50

Discussion

Water Column

The dramatic differences in temperature and salinity at stations 101 and 102 demonstrate the influence of the two principal pathways in which Pacific water moves through the Bering Strait and flows into the Chukchi Sea, namely the Anadyr water (AW) in the west, and the Alaska coastal water (ACW) in the east (Coachman et al., 1975). Areas under AW influence exhibit high pelagic primary production (Hill and Cota, 2005; Springer et al., 1996; Walsh et al., 1989) since high concentrations of nutrients are upwelled from the deep Gulf of Anadyr and advected northward (Codispoti et al., 2005; Walsh et al., 1989). Opposite the AW, the ACW exhibits far lower water column nutrients (Hansell et al., 1989) and water column production (Walsh et al., 1989). The effects of differing water mass characteristics (i.e. nutrients and primary production) are reflected in benthic fauna biomass (Dunton et al., 2005; Grebmeier et al., 2006b). Iken et al. (2010) showed that although food web length and relative proportions of trophic levels were similar between food webs compared in ACW and AW, the food web within the more productive AW possessed higher faunal biomass, especially those taxa able to capitalize on abundant, fresh production.

Bottom values of chlorophyll *a* are indicative of abundant food resources for benthic suspension feeders but do not appear strongly correlated to the water masses. The identity of the chlorophyll *a* is undetermined, but may be senesced phytoplankton, chlorophyll pigments suspended from sediments, or a mixture of both. The synoptic sampling employed only shows a snapshot of the standing stock and does not indicate the origin of the chlorophyll *a* (i.e. phytoplankton, etc.), if the pigment-containing cells were viable, or if the standing stock observed was long-lasting or ephemeral. Small-scale bottom currents may play a role in the amount of chlorophyll *a* measured at each site.

The suspension of sediments and settled particles by bottom currents is likely responsible for the enrichment of organic matter in the near-bottom POM. The ^{13}C-enriched organic matter in the water column is assimilated by benthic fauna, and has implications on food web dynamics for the Chukchi Sea (see Food Web Dynamics section).

Zooplankton $\delta^{13}C$ values range from very near phytoplankton to values far more ^{13}C-enriched. Some discrepancies arise when comparing the values of zooplankton with values of phytoplankton from the same station, under the assumption that zooplankton consume phytoplankton. Pteropods at station 6 have average $\delta^{13}C$ values of -23.41±0.40‰. Assuming a conservatively high ^{13}C enrichment of 1‰, these pteropods' food source likely had a $\delta^{13}C$ value of -24.81‰. Phytoplankton at station 6 have a mean $\delta^{13}C$ value of -25.67±0.19‰, another 1‰ more enriched than the predicted food source value if only one trophic step from phytoplankton. The pteropods at station 6 have a mean $\delta^{15}N$ value of 12.17±0.60‰, approximately two trophic levels higher than phytoplankton at 7.42±0.02‰. These pteropods appear to be secondary consumers of phytoplankton carbon.

Mysids and copepods at station 6 also exhibit anomalous isotope values compared to their assumed food source. Mysids have a $\delta^{13}C$ value of -20.53±0.30‰ and copepods have a $\delta^{13}C$

value of -20.90±0.44‰. Both of these values are approximately 4‰ more enriched than phytoplankton. Despite the relatively enriched $\delta^{15}N$ value of mysids, neither mysids nor copepods appear solely to consume phytoplankton. Mysids collected at station 30 are ~4‰ more enriched than the phytoplankton collected. The copepods collected at station 3 and 10 are more than 1‰ enriched compared to phytoplankton even though their $\delta^{15}N$ values suggest they are primary consumers. Ctenophores at stations 3, 10, 16, 27, and 37 are more enriched than phytoplankton values measured at those same stations. Throughout the COMIDA study area, there are examples of zooplankton that are not consuming phytoplankton based on isotope values. In all instances, where stable isotope values of zooplankton do not coincide with phytoplankton values, the zooplankton are more enriched in ^{13}C than phytoplankton. Values less enriched in ^{13}C than phytoplankton (<-28‰) would indicate that terrestrial carbon is assimilated into the food web. However, there is no evidence for the presence of terrestrial carbon in the COMIDA study area; the stable isotope signals are exclusively marine. There is clear evidence, however, that a carbon source more enriched in ^{13}C than phytoplankton is being assimilated into the pelagic food web. We hypothesize that this source is not pelagic, but suspended benthic carbon accessible for zooplankters and benthic suspension feeders alike.

Sediments

Stable C and N Isotopic Ratios of Bulk Organic Matter

Sediment organic nitrogen in 2009 was less enriched in ^{15}N than in 2010, possibly due to a stronger presence of nitrogen-fixing microorganisms in overall COMIDA study area sediments. Since some POM depth profiles show the depletion of $\delta^{15}N$ close to the sediments, some of this organic material likely resides or settles in the sediments. The lack of significant changes in stable carbon isotope values suggests that the ultimate sources of organic carbon in the sediments do not change interannually. The broadly overlapping C:N ratios of sediments also suggest that the amount of carbon and nitrogen in the sediments did not change dramatically between years. The processes that deliver and cycle organic matter of the Chukchi Sea sediments did not significantly change in one year.

The variable sediment C:N ratios (range of 4.46 to 16.30) suggests that throughout the Chukchi Sea sediments varied from fresh organic material to more refractory materials. Ratios < 7 represent freshly deposited marine algal material (Redfield et al. 1963), whereas sediments with ratios > 7 contain more refractory materials, possibly already processed by benthic macro- and microfauna. It does not appear in our study area, dominated by Bering Sea-Anadyr water, that terrestrial materials dominate the sediments since C:N ratios typical of terrestrial plant material (> 20) were not measured (Scheffer and Schachtschnabel 1984). Further evidence for the lack of allochthonous terrestrial matter transport to our study site is found in the stable carbon isotope ratios of the organic material present in the sediments. The vast majority of Chukchi Sea sediments possessed $\delta^{13}C$ values more enriched than -24‰, converse to the terrestrial C_3 plant stable carbon isotope signature of -28‰ to -26‰ (Fry 2006).

We tested the hypothesis that the ultimate source of carbon in the sediments originates from pelagic primary production by comparing the stable carbon isotopes of phytoplankton and sediment organic carbon. Only stations at which both phytoplankton and sediments were

collected are used for the comparison (i.e. stations 1, 3, 6, 10, 13, 16, 27, 29, 33, 37, and 46). If the stable carbon isotope value of sediment organic matter falls within the standard error of phytoplankton stable isotopes, then we can deduce the sediment organic matter ultimately originated via pelagic fixation. Only at station 37 does the sediment $\delta^{13}C$ value fall within the standard error of phytoplankton. This is attributed to the large standard error of stable carbon isotopic value measured in the phytoplankton at station 37. At ten of the eleven stations examined, the sediment $\delta^{13}C$ values fall outside of the standard error. Furthermore, the sediment values are consistently more enriched in ^{13}C than phytoplankton with the exceptions of stations 1 and 29 where the sediments were less enriched. This stark discrepancy is strong evidence for multiple ultimate carbon sources with different $\delta^{13}C$ values existing in the COMIDA study area.

Porewater Ammonium Concentrations

The concentrations measured in 2009 and 2010 were markedly high compared to another coastal Arctic system in Greenland where concentrations were <60 μM (Rysgaard et al., 1998). High porewater NH_4^+ is indicative of high rates of remineralization in the sediments. This also suggests replete amounts of organic matter and oxygen are available throughout summer if benthic biota (e.g. macrofauna, meiofauna, microfauna, etc.) are responsible for the remineralization processes. With such a large source of inorganic nitrogen available, benthic nutrients may contribute to the primary production on the shallow shelf.

Benthic Fauna

Food Web Dynamics

A weak linear regression of a stable isotope bi-plot (Figure 4) is an indication that the fauna assimilate multiple carbon sources with distinct stable carbon isotopic values (Fanelli et al., 2009). POM and phytoplankton both have $\delta^{13}C$ values of approximately -24‰. An enrichment line with a slope of ~3 (i.e. an enrichment of 3‰ on the y-axis for every 1‰ enrichment on the x-axis) contains the ^{13}C-depleted side of the scatterplot. Hypothetically, a ^{13}C-enriched carbon source exists to contain the ^{13}C-enriched side of the plot.

Further evidence for the assimilation of multiple carbon sources is examined in a species-level resolution food web bi-plot (Figure 5). The isotopic values for phytoplankton are known in the COMIDA study area, and it is apparent that certain second trophic level organisms like the suspension feeding sea cucumber *Ocnus glacialis* and amphipod *Ampelisca macrocephala* obtain most of their carbon from phytoplankton, as these two organisms exhibit very little enrichment in $\delta^{13}C$ value despite having $\delta^{15}N$ values ~3.4‰ (one trophic level) more enriched than phytoplankton. The suspension/deposit feeding bivalve *Astarte borealis* does not fall near *O. glacialis* or *A. macrocephala* in isotopic space (i.e. does not possess similar stable carbon and nitrogen values). When comparing all other bivalve species analyzed from the COMIDA study area, a distinct dichotomy exists between second trophic level *O. glacialis* and *A. macrocephala* and second trophic level bivalves. All bivalve species fall relatively close together in isotopic space, indicating that their ultimate carbon source is similar to one another. Furthermore, there is a decoupling between feeding modes, described as the morphological features that the organism

uses to capture food, and trophic guild, described as the trophic level and ultimate carbon source of the organism. Despite *A. macrocephala* and *A. borealis* using the same feeding mode, they fall into different trophic guilds since their isotope values do not overlap.

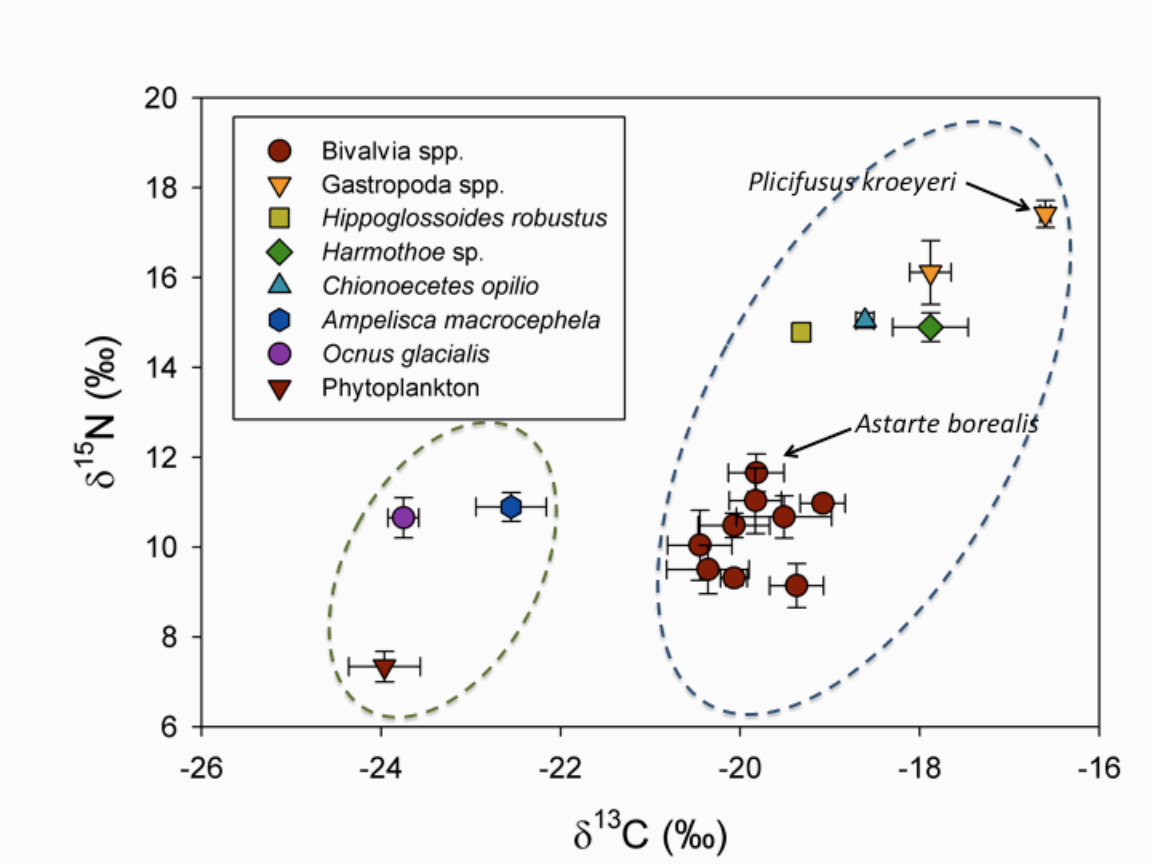

Figure 5. The stable isotopic bi-plot depicts two major pathways of carbon assimilation. Ovals contain groups of organisms that either assimilate phytoplankton and POM (left oval) or benthic microalgae (right oval) as a carbon source.

Importantly, higher trophic level organisms possess ^{13}C-enriched signatures similar to the bivalves. Predatory gastropods and predatory polychaetes, three crab species, and two fish species have $\delta^{13}C$ values that cannot trace back to phytoplankton as the sole, ultimate carbon source, assuming 0-1‰ enrichment per trophic level. The ^{13}C-enriched benthic carbon source is assimilated by primary and secondary consumers, and is likely assimilated by the highest trophic level organisms in the Chukchi Sea, such as birds and marine mammals.

The percentage of body carbon derived from benthic microalgae is determined using the mixing equation after McConnaughey and McRoy (1979) and Dunton and Schell (1987)

$$\% \text{ Benthic Microalgae} = [(\delta^{13}C_{animal} - \delta^{13}C_{POM} - I)/(\delta^{13}C_{benthic\ microalgae} - \delta^{13}C_{POM})] \times 100 \quad (3)$$

where I is an added term to compensate for the small but significant post-photosynthetic enrichments of ^{13}C per trophic step. The term standardizes $\delta^{13}C$ values so that trophic enrichments do not bias the mixing equation. $I = (TL_{organism} - 1) \times 1.15$, since the suspension-

feeding second trophic level amphipod *A. macrocephala* and sea cucumber *O. glacialis* have a mean $\delta^{13}C$ value 1.15‰ more enriched than the mean value of POM. This is a conservative estimate of ^{13}C enrichment and may underestimate the dependence of benthic fauna on benthic microalgae carbon.

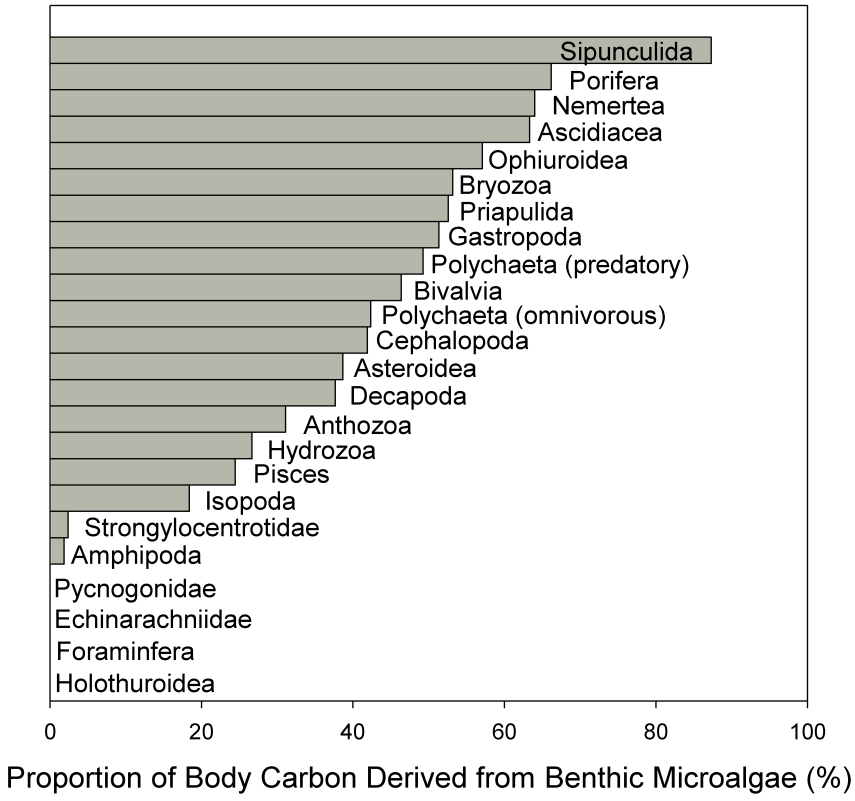

Figure 6. The assimilation of benthic microalgae by benthic organisms as calculated using Equation 3 (see text for details). Post-photosynthetic fractionation was accounted for during each calculation. No bar indicates a proportion of 0%.

The proportion of body carbon derived from benthic microalgae for benthic fauna ranged from 0 to 87% (Figure 6). Both species of holothurians (*O. glacialis* and *Psolus chitonoides*) derive 0% of their ultimate carbon from benthic microalgae despite occupying different trophic levels. Forams, sand dollars, and pycnogonids also derive 0% carbon from benthic microalgae. Despite *A. macrocephala* assimilating 0%, *Metopa* sp. amphipods assimilate a small fraction of benthic microalgae carbon, hence amphipods assimilating 2% benthic microalgal carbon. Sipunculids (*G. margaritacea*) assimilated the highest percentage of benthic microalgae carbon at 87%. The Porifera species, the lowest trophic level organism, derived 66% of its ultimate carbon from benthic microalgae. Other second trophic level organisms like ascidians and bivalves also assimilate high proportions of benthic microalgae carbon at 63% and 46%, respectively. Gastropods assimilate 51% benthic microalgae carbon, which aligns with their primary food source of bivalves. The two Pisces species assimilate only 24% of their carbon from benthic

microalgae showing a relatively high dependence on pelagic production, likely through consuming zooplankton.

Trophic guilds

When the benthic organisms within the COMIDA study area are plotted by their mean $\delta^{15}N$ and $\delta^{13}C$ values, there is a separation of organisms into clusters (Figure 7). There is a group of organisms (denoted by green shapes) that reflect phytoplankton, POM, and sediment based on assumed trophic enrichments of 3.4‰ for $\delta^{15}N$ and 1‰ for $\delta^{13}C$. This group consists of second trophic level organisms comprised of amphipods, sand dollars, and isopods, and the third trophic level organisms comprised of Pycnogonida, forams, and holothurians. These organisms exhibit different feeding modes (e.g. amphipods are suspension feeders while sand dollars are surface deposit feeders), but occupy similar isotopic space. Despite differences in morphological adaptations to obtain food, they are similar in the trophic guild they occupy. Their ultimate carbon source is likely pelagic in origin considering the mean isotopic values of phytoplankton and POM. Groups of organisms within this guild are considered part of the Pelagic Production Guild (PP Guild).

A cluster of organisms within the same trophic levels as the PP Guild ($\delta^{15}N$ = 7-13‰) possesses more ^{13}C-enriched values (Figure 7). These organisms display values too enriched to assimilate exclusively phytoplankton, POM, or sediments. Interestingly, most of these organisms are suspension feeders (e.g. ascidians, bivalves, bryozoans, hydrozoans, anthozoans, and poriferans). They share the same feeding mode as the groups of organisms in the PP Guild. Omnivorous polychaetes and some bivalve species are deposit feeders, sharing the same feeding mode as *E. parma* in the PP Guild. For these reasons, feeding mode is not indicative of trophic function in the Chukchi Sea. Furthermore, this provides strong evidence for a ^{13}C-enriched carbon source to exist in the Chukchi Sea that is available for benthic consumers. These consumers are referred to as the Enriched Carbon Guild (EC Guild).

The fourth trophic guild consists of predominantly of epibenthic and benthic predators. Not only are their $\delta^{15}N$ values similar, which places them all in the same trophic level, but also their $\delta^{13}C$ values are similar, meaning they assimilate the same ultimate carbon source. The organisms in this trophic guild display predator or scavenger feeding modes, occupy the fourth trophic level, and possess enriched carbon values giving them the classification of High-trophic, Enriched-carbon Guild (HE Guild). With the exception of Pisces species (*Boreogadus saida* and *Hippoglossoides robustus*), the trophic guild does not appear to assimilate any carbon from phytoplankton or POM. Their enriched $\delta^{13}C$ values must be attributed to an enriched carbon source available to benthic primary consumers. Asteroids, consisting of one species of seastar *Leptasterias polaris*, and the one species of Priapulida, are characterized by large variation around their mean values, especially in the $\delta^{13}C$ direction (x-axis). This variation tells us that these species may indiscriminately consume and assimilate multiple ultimate carbon sources. This trend is ubiquitous throughout the food web exhibited in all trophic guilds (e.g. ascidians, nemerteans, anthozoans, and holothurians).

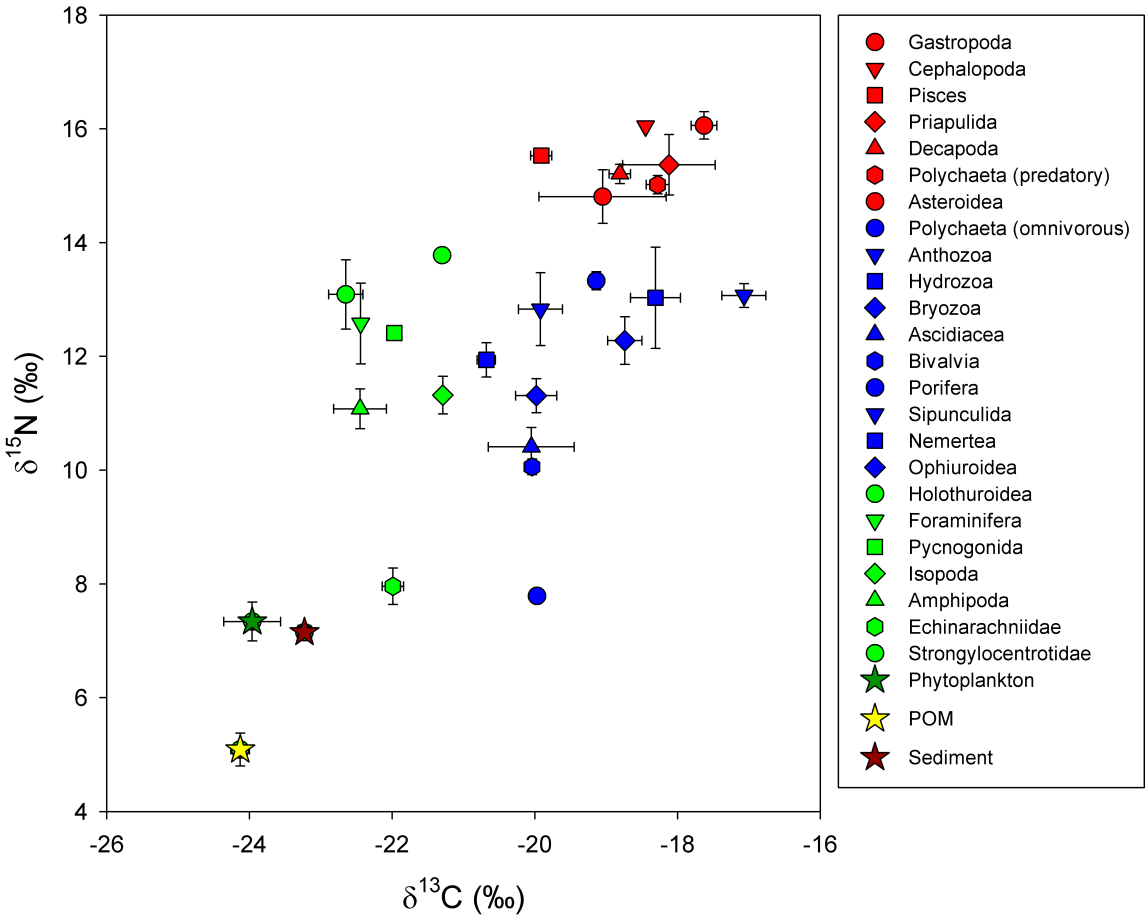

Figure 7. Taxonomic separation of benthic organisms common to the Chukchi Sea plotted as a function of $\delta^{13}C$ and $\delta^{15}N$ values. Consumers fall into specific guilds based on trophic level and ultimate carbon source requirements. The Pelagic Production Guild is color-coded green, the Enriched Carbon Guild is blue, and the High-trophic Enriched-carbon Guild is red (see Discussion-Trophic Guilds for description of each guild). Ultimate carbon sources measured during the COMIDA project are shown as stars.

Based on this isotopic evidence, a major pathway of energy transfer occurs from the EC Guild to the HE Guild, which contains organisms such as the arctic cod (*Boreogadus saida*) and the snow crab (*Chionoecetes opilio*). The identity of the enriched carbon source is extremely important to definitively determine. One opportunistic sampling opportunity that occurred during the COMIDA cruises occurred when numerous *E. parma* were placed in a holding container. Soon a green substance leeched from the surface of the organisms noticeably dying the water dark green. This water was filtered and run for stable isotopes. The $\delta^{13}C$ value of this substance was -19.35±0.32‰, which fills the missing gap in the food web as an enriched carbon source. Unfortunately, the stable nitrogen values from these samples were extremely noisy and unreliable. Attempts to identify living cells through light microscopy were unsuccessful. However, we do hypothesize that benthic microalgae are the most probable source of ^{13}C-

enriched carbon in the Chukchi Sea since other work has shown benthic microalgae exist on arctic shelf sea floors (e.g. Horner and Schrader, 1982; von Quillfeldt et al., 2003). Benthic microalgae are enriched in ^{13}C compared to phytoplankton due to a boundary layer effect (Doi et al., 2010; France, 1995; Hecky and Hesslein, 1995). Benthic microalgae may also contribute to the sediment chlorophyll values observed in the Chukchi Sea (see Grebmeier and Cooper, this report).

The conceptual food web of the northeastern Chukchi Sea has two end-members that provide energy (carbon) for benthic consumers (Figure 8). Energy moves from pelagic carbon, one of the two end-members, to zooplankton, amphipods, holothurians, sand dollars, isopods, and forams. These groups rely little on benthic microalgae carbon (see Figure 6), and therefore, assimilate almost exclusively pelagic carbon. Pisces ascertains most of its carbon from these groups, although some carbon is obtained from other groups that rely on benthic microalgae carbon. Bivalves, bryozoans, hydrozoans, Porifera, and ascidians obtain a major portion of their carbon from benthic microalgae; however, they do have a connection to pelagic carbon. Carbon from these organisms is transferred to the benthic predators gastropods, cephalopoda, priapulids, decapods, and polychaetes. Third trophic level omnivores sipunculids, ophiuroids, and polychaetes obtain carbon from both primary producers and primary consumers. As indiscriminant feeders, they assimilate both benthic microalgae and pelagic carbon. Both pelagic carbon and benthic algal carbon plays an important role as carbon sources for the benthic food web.

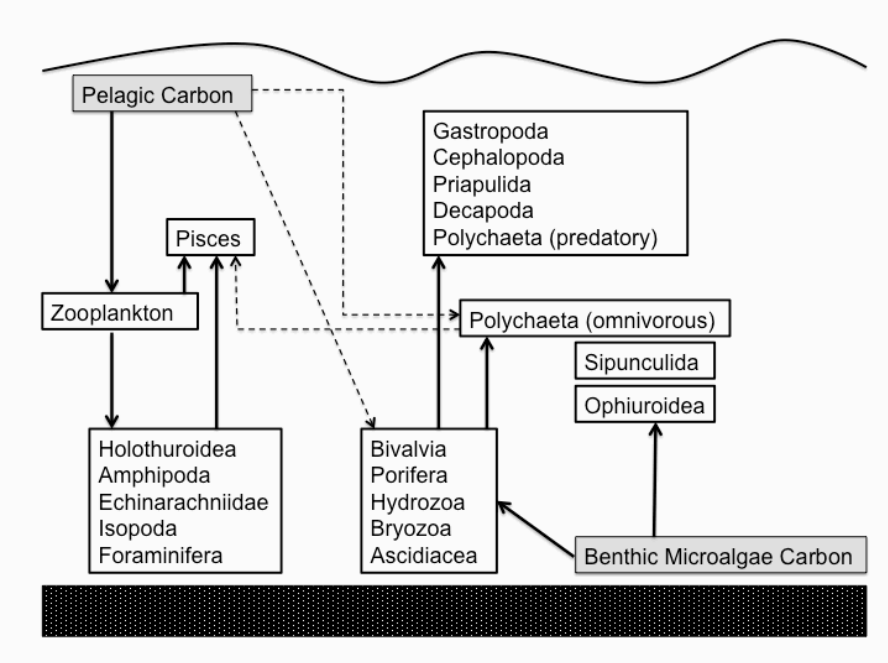

Figure 8. Conceptual food web incorporates benthic taxa from the Chukchi Sea. Solid arrows represent pathways of energy flow from ultimate carbon sources (grey boxes). Dashed arrows represent weaker connections of energy flow.

Trophic Pathways for Contaminants

Contaminants associated with oil and natural gas exploration and extraction have several possible pathways to move through the Chukchi Sea ecosystem. Seasonally varying physical factors (e.g. currents, winds, sea ice, etc.) mediate the pathways that largely dictate biological processing of contaminants (Macdonald et al., 2005). Ultimately, when contaminants reach the biota in the Chukchi Sea, primary producers, such as phytoplankton, serve as the first trophic link of contaminant introduction into the food web.

When contaminants enter the food web via primary producers, organic contaminant biomagnification factors are very consistent with food chain transfer (Borga et al., 2001); the contaminants move on similar pathways as energy moves in the food web. Since the stable carbon and nitrogen isotope analyses employed during this work has elucidated the pathways that energy (carbon) is transferred (Figure 8), we can deduce the likely pathways of contaminants once assimilated by the food web (Figure 9).

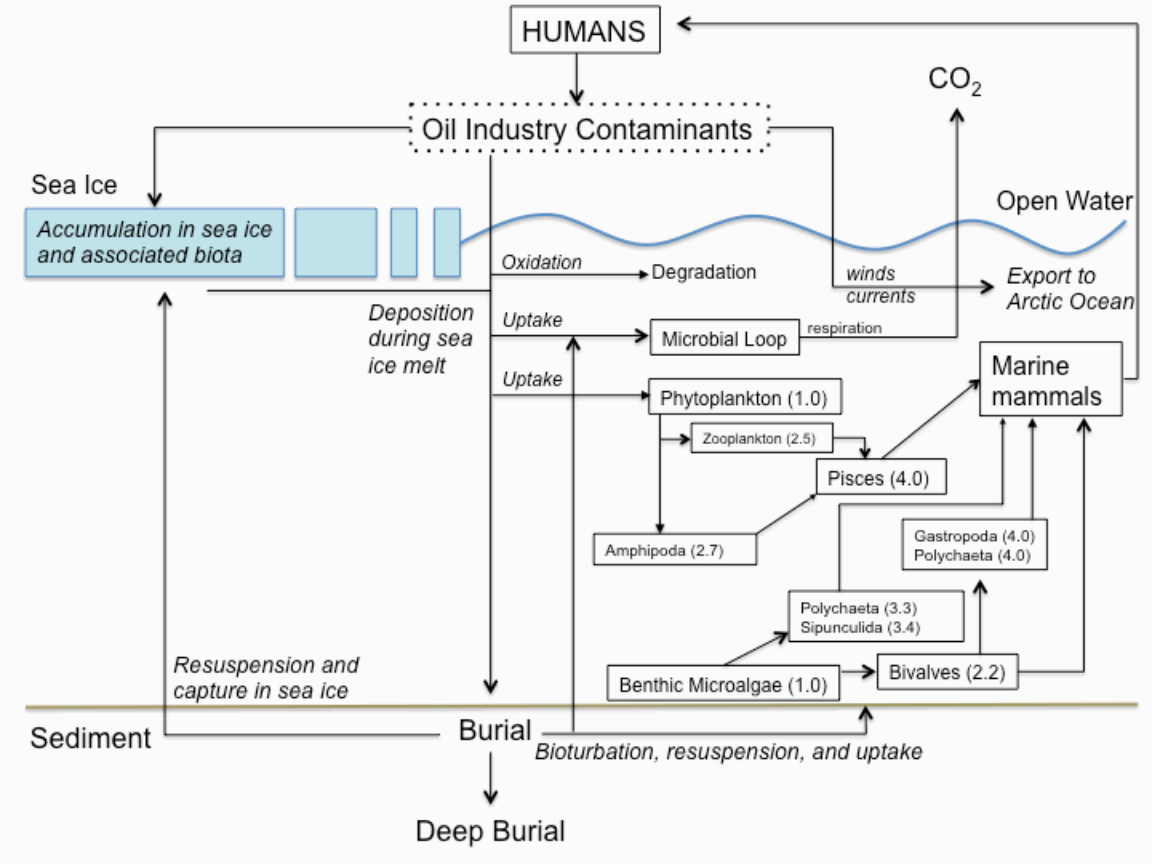

Figure 9. Simplified schematic of potential pathways for an anthropogenic contaminant exposed to the Chukchi Sea ecosystem. Average trophic level contained in parentheses after each taxonomic group name.

Though not a focus in the COMIDA project, other pathways for contaminants include uptake by the microbial loop, which leads to subsequent metabolism, respiration, and export from the system. Most contaminants ultimately undergo rapid deposition to the sediments for burial if not subjected to microbial processes or physical export (e.g. winds, currents, etc.). Once in the benthos, the fate of these contaminants is likely resuspension by bottom currents or bioturbation. Contaminants can also be assimilated by deposit feeding worms and mollusks, providing another avenue for transfer to higher trophic levels. Gut contents analyses have found various benthic consumers, including bivalves, sipunculids, polychaetes, priapulids, and gastropods, in the stomachs of the walrus *Odobenus rosmarus* (Fisher and Stewart, 1997).

Phytoplankton carbon pathways are directly linked to zooplankton and the benthic omnivorous amphipods. Zooplankton and amphipods are consumed by various fish species in the Chukchi Sea, including arctic cod. Arctic cod are an important carbon source for the ringed seal, *Phoca hispida*, which is a primary prey species for polar bears and harvested by native populations of subsistence hunters (Holst et al., 2001).

The effects of biomagnification are more severe with the consumption of high trophic level organisms compared to lower trophic level organisms since contaminants can increase by a factor of 10^5 to 10^9 from water to apex predator (Fisk et al., 2001; Muir et al., 1999). *O. rosmarus* that consume primarily bivalves (TL 2.2) will obtain far lower (potentially orders of magnitude less) biomagnified contaminants than one consuming higher trophic level organisms like predatory polychaetes (TL 3.9), sipunculids (3.4), and gastropods (4.0). Biomagnification of contaminants is complex since it operates within biological processes that can change based on the physical operators surrounding it (Macdonald et al., 2005). Because polar environments are exceptionally sensitive to physical changes (e.g. climate change), and physical changes impact biological processing, the 'box and arrow' schematic is not as rigid as it implies. Our isotopic data provide some insight to these trophodynamic complexities, since these tracers have proven excellent predictors of contaminant flow through the food web (e.g. Fisk et al., 2001). This model, despite its plasticity of vectors, demonstrates that humans, as the apex predator in the Chukchi Sea, are at highest risk of the effects of contaminant biomagnification.

Trophodynamic Implications

The shallow expanse of the Chukchi Sea supports high benthic invertebrate biomass (Bluhm et al., 2009; Grebmeier et al., 1989b; Grebmeier et al., 1988). Locally produced phytoplankton and POM advected from the Bering Sea provide previously-identified carbon sources for benthic fauna; however, isotopic analyses of benthic invertebrates show that a ^{13}C-enriched, distinctly non-pelagic carbon source is important to secondary production. Benthic diatoms may fulfill this role, as microphytobenthic communities are prolific elsewhere around the globe. Using stable isotope evidence, Abrantes and Sheaves (2009) demonstrated that the microphytobenthos play an important role as an ultimate carbon source to piscivores in a tropical Australian estuary, whereas Dubois et al. (2007) determined microphytobenthic contribution to oyster ultimate carbon sources using similar methods in the temperate estuaries of France. At 191m, some of the deepest communities of productive, obligate benthic diatoms on the continental slope east of North Carolina, USA are reported to receive a mere 0.028% of mid-day surface irradiance (McGee et al., 2008). The microphytobenthos have also been described in Antarctic waters in

concentrations of 60-360 mg chl *a* m^{-2} at depths of 40 m measured in the austral summer (Dayton et al., 1986).

Benthic microalgae in nearshore (~5m) arctic ecosystems near Barrow, Alaska, USA, exist at concentrations between 130-360 mg chl *a* m^{-2} and represent 76% of combined pelagic and benthic production (Matheke and Horner, 1974). Even in deeper shelf areas (20-30 m), benthic microalgae account for notable concentrations of chlorophyll *a* (92-186 mg chl *a* m^{-2}) and represent equal rates of production to integrated water column production (Glud et al., 2002). Conversely, other studies found extremely low benthic production rates despite photopigments (chlorophyll *a*) present in surface sediments (Horner and Schrader, 1982; Kuznetsov, 2002). Grebmeier and Cooper (this report) show that the northeast Chukchi Sea sediments in 2009 and 2010 contained between ~0 to ~60 mg chl *a* m^{-2}. Such results suggest that a mosaic of living, photosynthesizing benthic microalgae and senesced, non-living algal cells exists on the arctic sea floor.

On average, at least 25% of arctic shelf area receives more than 1% of surface downwelling irradiance during the summer months (Gattuso et al., 2006). Photosynthetically active radiation was measured at stations 14, 27, and 38 during cloudless conditions. The mean extinction coefficient *k* for these stations was 0.99. Assuming surface irradiances of 1300 µmol photons m^{-2} s^{-1}, a value we measured for cloudless summer conditions, >1% surface irradiance occurs to a depth of 47 m. Even at 50 m, PAR is 9 µmol photons m^{-2} s^{-1}. Kuhl et al. (2001) report that benthic microalgae in arctic sediments, adapted for low light conditions, require 2-30 µmol photons m^{-2} s^{-1}. The deepest recorded viable (cells containing intact chloroplasts) benthic microalgae receive a mere 0.1% of surface irradiance at 0.04 µmol photons m^{-2} s^{-1} (Cahoon, 1999). Living benthic diatoms have been observed to survive, at least temporarily, in 0.03% surface irradiance or 0.1 µmol photons m^{-2} s^{-1} at 191 m (McGee et al., 2008). The observed amount of PAR in the Chukchi Sea falls within and above previously measured amounts of light necessary for the survival of benthic microalgae.

Ice algae represent another source of potential carbon for benthic consumers. These primary producers are ^{13}C-enriched since the brine channels within the sea ice in which they dwell contain a closed pool of inorganic carbon (Gradinger, 2009; Hobson et al., 1995). Sea ice was scarce in the northeastern Chukchi Sea during the COMIDA cruises in 2009 and 2010, and subsequently, ice algae were not collected. Hobson et al. (2002) report ice algae stable carbon and nitrogen values in the North Water Polynya of -17.7±0.2‰ and 5.1±0.3‰, respectively, and McMahon et al. (2006) report stable carbon isotope values as enriched as -15.7±0.5‰ in the Svalbard archipelago. Ice algae are not considered a potential carbon source to benthic consumers for this study since it is rapidly consumed upon deposition (McMahon et al., 2006; Sun et al., 2007) and unlikely present in late summer months when our sampling was conducted. The stable isotopic values of organisms do incorporate the average diet within the isotopic turnover window. One estimate of isotopic turnover for organismal tissue is ~20 days, as measured in Arctic amphipods (Kaufman et al., 2008). Arctic bivalves show marked changes of $\delta^{13}C$ in tissues after a dietary change four weeks prior (McMahon et al., 2006). If the isotopic ratios measured in our samples reflect what was assimilated no less than four weeks prior, our samples represent food resources from late June and early July. Ice derived material can reach the sediments within six weeks of ice retreat (Cooper et al., 2005), so samples reflect organic

matter that began sinking in mid-May. This rough timeline suggests that our samples cannot exhibit a signature from ice algae, which begins sinking in April, unless ice algae remain on the Chukchi sediments for at least a month.

Speculations on the connections between ice algae, the high concentrations of chlorophyll *a* in sediments, and benthic microalgae are not novel (e.g. Horner and Schrader, 1982; Matheke and Horner, 1974; von Quillfeldt et al., 2003; Wulff et al., 2009). The relationship between ice algae and benthic microalgae is poorly understood and, indeed, complicates food web dynamics in polar shelves. Evidence, including isotopic analysis of benthic faunal communities presented here, suggests there is some ^{13}C-enriched primary producer that can receive sufficient downwelling light and utilize a benthic source of nutrients (e.g. porewater NH_4^+) to survive on the sediments (see sediment nutrient efflux rates in Souza and Dunton, this report). The ^{13}C-enriched carbon source provides an important and widely assimilated ultimate carbon source for the benthic fauna in the Chukchi Sea. Furthermore, this enriched carbon source supplies vital energy for the highest trophic level marine mammals like the bearded seal, *Eringnathus barbatus* ($\delta^{13}C$ = -16.6±0.3‰), and the walrus, *Odobenus rosmarus* ($\delta^{13}C$ = -17.8±0.1‰) based on its enriched $\delta^{13}C$ value (Hobson et al., 2002).

Conclusions

The baseline trophic structure for the COMIDA study area, Lease area 193, shows the existence of four trophic levels within the benthos. The highest trophic level organisms are mollusks, specifically the predacious gastropods. Stable isotope analyses for the study area reveal a food web that is not tied to a single carbon source; instead the food web is scattered among isotopic space suggesting the rich and diverse benthic fauna assimilate multiple carbon sources. It appears that phytoplankton and POM are a pelagic end-member of the food web with $\delta^{13}C$ values near -24‰. Another, more enriched carbon source must exist near enriched portion of the food web. A likely source for the ^{13}C-enriched carbon that is assimilated into the food web is benthic microalgae. There is a strong need to identify all the potential end-members (taxonomically and isotopically) in an ecosystem to fully understand the food web dynamics that govern the energy flow from primary producers to high trophic level consumers. Compound-specific stable isotope analysis (CSIA) is another method that can potentially trace the flow of specific compounds from different end-members through the food web. Since samples did not undergo lipid extraction prior to processing for stable carbon isotopic ratios, values may actually be more enriched than reported since lipids exhibit a lower ^{13}C:^{12}C ratio than proteins and carbohydrates. Mathematical corrections can be applied to the isotope dataset, although great effort was made to take muscle tissue from organisms when possible. Lastly, microbial processing of benthic organic matter was not measured in this study. Some evidence (e.g. Sun et al., 2009) has been found to support the hypothesis that benthic food webs often exhibit higher trophic enrichments due to the microbial respiration of ^{12}C in organic matter prior to macrofauna consumption.

In this food web study, we have identified that the organic matter within the sediments may not entirely be of pelagic origin. POM in the near-bottom water column may also reflect ^{13}C-enriched organic carbon, possibly suspended from the sediments themselves. Second trophic level zooplankton show discrepancies in their isotopic values that allude they are not sole

phytoplankton consumers. The three trophic guilds that the benthic fauna fall into based on their stable carbon and nitrogen isotope values shows a strong connection between the lower trophic level organisms that assimilate the enriched carbon and higher trophic level organisms. Any disruption to the natural cycle of sea ice dynamics or activities that lead to increased turbidity or sedimentation on the Chukchi Sea shelf can potentially alter the amount of primary production that takes place in the water column and benthos. The benthic fauna in the Chukchi Sea shelf ecosystem ultimately rely on multiple sources of carbon, regardless of whether it is phytoplankton, sea ice, or benthic microalgae.

Acknowledgements

We thank the Bureau of Ocean Energy Management (BOEM), U.S. Department of the Interior for funding this study. We are most grateful to Captain John Seville and the crews of the *R/V Alpha Helix* and *R/V Moana Wave* for skillfully and safely guiding us through the Chukchi Sea. Their cooperation and willingness to help our scientific endeavors and to facilitate our sampling effort is sincerely appreciated. We thank Kim Jackson, Patty Garlough, and Travis Bartholomew (UTMSI) for the meticulous work associated with stable isotope analysis, and also Norma Haubenstock (University of Alaska-Fairbanks) for quickly processing samples at her facility. Finally, the success of this project would not be possible without the enthusiastic support of Dick Prentki (BOEM).

A Chain-of-Custody Approach to Managing Arctic Marine Observations Data

Hersh, E.S., H. Sangireddy, and D.R. Maidment

Eric S. Hersh, Harish Sangireddy, and David R. Maidment
Center for Research in Water Resources
The University of Texas at Austin, Austin, Texas 78758

Abstract

The Chukchi Sea Offshore Monitoring in Drilling Area – Chemical and Benthos (COMIDA CAB) project is a robust, comprehensive effort to characterize the lease area biota and chemistry and to conduct a baseline assessment of the continental shelf ecosystem. Particular focus is on ship-based physical, chemical, and biological sampling of the benthos and on the development of a workable food web model. As can be expected from such a multi-disciplinary effort, data management is an important and potentially challenging task and the COMIDA CAB project includes a dedicated, ship-board data manager to provide real-time, field-based data services and Geographic Information System (GIS) support. Project data management is accomplished via the Observations Data Model relational database schema from a National Science Foundation-supported cyberinfrastructure project for the hydrologic sciences, used extensively for storing observations of the physical, chemical, and biological components of the water environment. But actively managing data during the project isn't enough, as an interdisciplinary project of this magnitude and scope produces a wealth of information and represents a significant research investment. Effective project data management must include public outreach, data sharing, and data archiving both during and after the life of the project. As such, a secure, web-based system was developed for observational data storage (via the Integrated Rule-Oriented Data System grid software), geographic data storage (via the ArcGIS Online community), document sharing, and public outreach. This paper includes discussion of COMIDA CAB back-end and front-end project data infrastructure and presents both a novel chain-of-custody approach to data tracking and a new template for improved data archiving.

Introduction

The Arctic Ocean is changing. Temperatures are warming and the minimum sea ice extent is retreating (Pachauri and Reisinger, 2007). Changes in the presence and condition of sea ice are stressing some ice-dependent species such as polar bears (CFR, 2010). On shore, the yield of the Prudhoe Bay oil field has diminished and the Trans-Alaska Pipeline is operating below capacity (API, 2009). America's continued thirst for oil and gas has led to an increased desire to explore new offshore sources, including the outer continental shelf regions of the Chukchi and Beaufort Seas off the northwest and north coasts of Alaska. In 2008, the Minerals Management Service (now the Bureau of Ocean Energy Management, Regulation and Enforcement) generated $2.6 billion in high bids for 488 blocks under Lease Sale 193 (MMS, 2008a, b). The Chukchi Sea Offshore Monitoring in Drilling Area: Chemical and Benthos (COMIDA CAB) project was initiated in 2008 to be a robust, comprehensive effort to characterize the lease area biota and

chemistry, to conduct a baseline assessment of the continental shelf ecosystem via ship-based physical, chemical, and biological sampling of the benthos, and to develop a workable food web model.

The COMIDA CAB effort involves seven Principal Investigators hailing from four universities and one Contracting Office Representative. Over two field seasons aboard the *R/V Alpha Helix* (summer 2009) and the *R/V Moana Wave* (summer 2010) in the northeastern Chukchi Sea, the project team collected diverse observational data from multiple instruments and sensors, in varying sample media, across varying spatial and temporal scales, in the broad disciplines of physical, chemical, and biological oceanography. In all, a total of 48 stations were occupied in 2009 and 44 in 2010 including 27 stations which were reoccupied for quality control and time series comparative purposes (Figure 1).

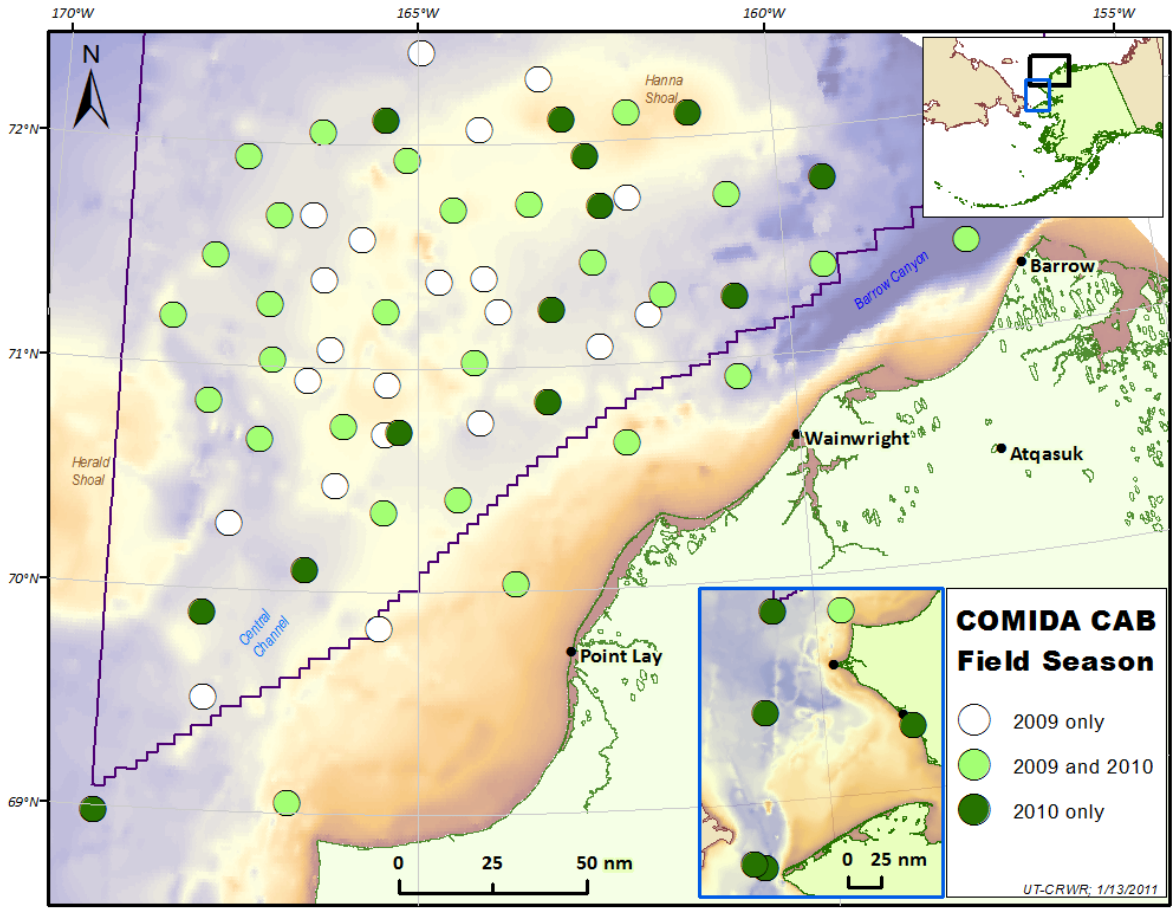

Figure 1. Stations occupied during the 2009 and 2010 COMIDA CAB field seasons in the northeastern Chukchi Sea, Alaska.

As can be expected from such a multi-disciplinary effort, data management is an important and potentially challenging task. The COMIDA CAB project includes a dedicated, ship-board data manager to provide real-time, field-based data services and Geographic Information System (GIS) support. Project data management is accomplished via the SQL/Server relational

database and the Observations Data Model (ODM) relational database schema. The ODM originates from the Consortium of Universities for the Advancement of Hydrologic Science – Hydrologic Information System (CUAHSI HIS), a National Science Foundation-supported cyberinfrastructure project for the hydrologic sciences, used extensively for storing observations of the physical, chemical, and biological components of the water environment (Horsburgh et al., 2008; Maidment, 2009).

Actively managing data during the project isn't enough as an interdisciplinary project of this magnitude and scope produces a wealth of information and represents a significant research investment. Effective project data management must include public outreach, data sharing, and data archiving both during and after the life of the project. As such, a secure, web-based system was developed for observational data storage (via the Integrated Rule-Oriented Data System (iRODS), geographic data storage (via the ArcGIS Online community), document sharing, and public outreach (Rajasekar et al., 2009; Rajasekar et al., 2006).

Thus, the objectives of this chapter are, broadly: to present an approach to making observations of the ocean environment, to put forth a methodology for organizing and storing these observations, and to offer various avenues for communicating scientific results.

Literature and Technology Review

Cyberinfrastructure

The term *infrastructure* has been used since the 1920s to refer collectively to the roads, power grids, telephone systems, bridges, rail lines, and similar public works that are required for an industrial economy to function. Although good infrastructure is often taken for granted and noticed only when it stops functioning, it is among the most complex and expensive thing that society creates. The newer term *cyberinfrastructure* refers to infrastructure based upon distributed computer, information and communication technology. "If *infrastructure* is required for an *industrial economy*, then we could say that *cyberinfrastructure* is required for a *knowledge economy* (Atkins et al., 2003).

Geographic Information Systems

A Geographic Information System "integrates hardware, software, and data for capturing, managing, analyzing, and displaying all forms of geographically referenced information" (ESRI, 2011). Geographic data are typically static in time, complex in space, and are organized in standardized formats such as geodatabases. Geographic Information Systems were first conceptualized in the 1960s and now sustain a mature commercial market (Foresman, 1998).

The most common building block for geographic data today is the proprietary geodatabase from ESRI. Introduced in 1999 as part of the ArcGIS 8.0 release, a geodatabase is a collection of geographic elements stored within a SQL Server relational database structure. A geodatabase is comprised of: (1) feature datasets, collections of feature classes of vector-based geographic data with the topology and network objects supporting them; (2) tables of attributes; (3) relationships

linking the tables and feature classes; (4) raster data for continuous geographic phenomena; and (5) metadata (Arctur and Zeiler, 2004).

Data models provide the underlying structure to both Geographic Information Systems and Hydrologic Information Systems. Data models are a formal method of describing the behavior of real-world entities, "sets of concepts describing a simplification of reality expressed in database structures such as tables and relationships, and they provide standardized frameworks for users to store information and serve as the basis for applications" (Arctur and Zeiler, 2004). Geographic data models are a special case of data model where spatial database structures are used and stored in a spatial database (a.k.a. geodatabase) to describe geospatial phenomena using Geographic Information Systems. Put more simply, data models define objects of interest and identify relationships and geographic data models do this in a spatial context. In a GIS, geography is dominant and variable and time are subordinate; in an HIS, variable is dominant and geography and time are subordinate. That is to say, geography is the central focus of a GIS data model and the observation itself is the central focus of an HIS data model.

ESRI supports and maintains 34 data models in fields ranging from agriculture to defense to petroleum (ESRI, 2010). Arc Hydro is the data model for surface water resources, combining geospatial and temporal data within an ESRI geodatabase schema in order to support hydrologic analysis and modeling (Maidment, 2002). A related data model has been developed to support observations in the ocean realm, Arc Marine. Arc Marine includes similar representations of vector, raster, and time series data as Arc Hydro but adds additional support for limited three-dimensional geographic data from model mesh volumes and also the unique feature of storing observations data collected from a moving track (ESRI, 2010; Wright et al., 2007). Streamflow data and other similar surface water observations are made at a fixed point location, as are plenty of marine observations- buoys, ADCPs, hydrophones, tidal gauges. However, it is not uncommon for marine data to come from a mobile sampling platform such as a ship, drifter, autonomous underwater vehicle, or even a tagged animal, so Arc Marine's schema has the capacity to store the observations themselves as well as the track and its attributes (Wright et al., 2007).

Hydrologic Information Systems

A Hydrologic Information System is "a services-oriented architecture for water information" consisting of a repository of hydrologic time series data (HIS Server), a national water metadata catalog (HIS Central), and a desktop appliance for hydrologic data access (Hydro Desktop) (Maidment, 2009). Water observations data are typically dynamic in time (time series), simple in space (sampling and gaging points), lacking in standardized formats, and potentially stored in relational databases.

The CUAHSI Hydrologic Information System is built around a normalized data storage schema called the Observations Data Model (ODM). The ODM provides a consistent relational database format for storing point observations data and their supporting metadata in a manner which exposes each single measurement as a unique record and which addresses many of the syntactic and semantic differences between heterogeneous data sets (Horsburgh et al., 2008). The ODM logical data model consists of a series of tables for the data and metadata relating to observation

values, monitoring site locations, variables, data qualifiers, data sources, data collection methods, value grouping, and categorical data, along with a compiled series catalog to facilitate indexing and searching (Figure 2).

Managing Marine Observations Data

Biological oceanographers have a number of large-scale, well-received data archives, notably the National Oceanographic Data Center (NODC) and National Center for Atmospheric Research Earth Observing Laboratory (NCAR EOL), but these archives store datasets; very few databases and/or data models exist for biological observations in the marine environment. Both the NODC and NCAR EOL archives includes a wealth of researcher-submitted data for a wide range of physical, chemical, and biologic oceanographic observations, however, data are welcomed in any native physical format or structure and are archived as such; no efforts toward synthesis or integration are evident (NCAR-EOL, 2011; NODC, 2011).

Data from the Western Arctic Shelf-Basin Interactions (SBI) project of the National Science Foundation are an example of project data stored in the EOL archive; a brief investigation of the SBI data archive yields various data provided in txt, pdf, gif, and xls file formats with access via html and ftp; no standardization appears evident (SBI, 2008). There are some nascent efforts toward developing cyberinfrastructure for the ocean realm, however. One such effort is the Ocean Biogeographic Information System – Spatial Ecological Analysis of Marine Megavertebrate Animal Populations, or OBIS-SEAMAP. This project seeks to develop a geodatabase of sea turtle, marine mammal, and seabird global distribution and abundance data (Halpin et al., 2006).

Observing the Ocean Environment

Basemap Development

The study area extends from approximately 65º to 72º N and from 169º to 157º W. A basemap was developed for the study area based on bathymetric data from the NOAA National Geophysical Data Center. The ETOPO1 1-Arc Minute Global Relief Model integrates land topography and ocean bathymetry from numerous global and regional data sets (Amante and Eakins, 2008). Coastlines, cities, and political boundaries were added for spatial orientation and oil and gas wells, Lease Sale 193 information, existing moorings, and previous sampling locations were added to provide a context of former and current energy development activities and scientific studies.

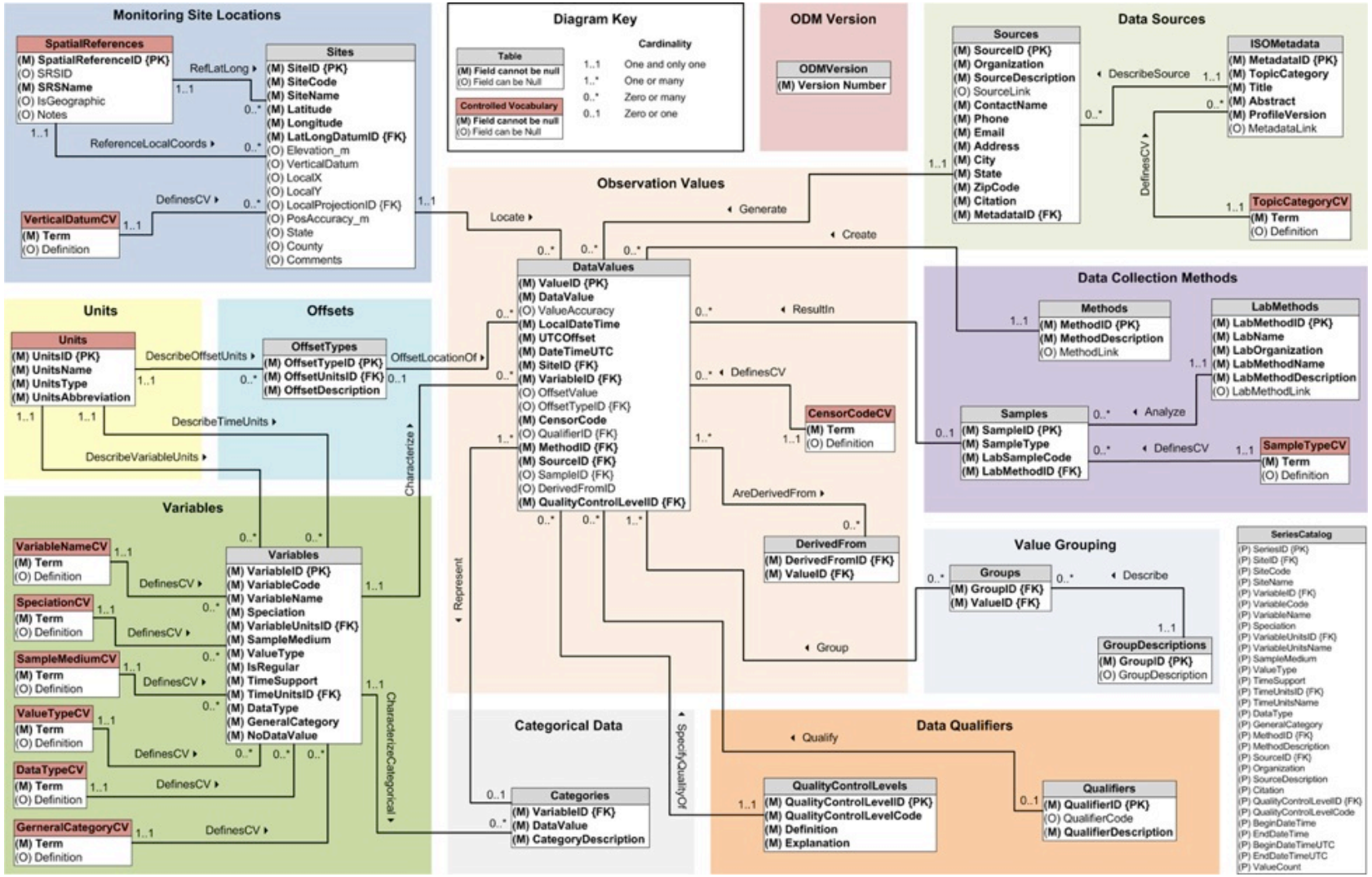

Figure 2. CUAHSI Observations Data Model schema.

Sampling Design

Station locations were determined via two methods for random yet even distribution: (1) a general randomized tessellation stratified design (GRTS) in the core project area, and (2) a spatially-oriented, nearshore-to-offshore, south to north grid overlaying the GRTS design. This arrangement allowed for putting the core station sites in a spatial grid. Of the 30 GRTS stations, 10 were chosen as overlap stations to cross-calibrate and provide QA/QC based on replicate benthic samples. The GRTS design was based on the approach employed by the US Environmental Protection Agency's Environmental Monitoring and Assessment Program (White et al., 1992). The grid stations were positioned to provide insight into upstream and downstream conditions with a select number outside the lease area as control sites. Twenty-seven stations were sampled in both field seasons to initiate a time-series of benthic and water column parameters and for quality control purposes.

Data Collection

Observations were made of the water column, sediments, epibenthos and benthos. During the 2009 field effort, 270 sampling events occurred totaling 142 hours of sampling time with events such as: epibenthic trawls, data sondes, light meters, discrete-depth water column pumping, double van Veen grabs, single van Veen grabs, HAPS sediment cores, box cores, phytoplankton nets, zooplankton nets, and benthic camera deployment. Project data collected includes physical, chemical, and biological observations and the associated geographic data plus video and still imagery. An example of the diverse data collected is shown in

Table 1.

Table 1. Examples of the types of data collected in various sample media.

Water Column	Epibenthos	Sediment
Surface & subsurface PAR	Community composition	Hydrocarbons
Chlorophyll a	Abundance, biomass, population size structure	19 anthropogenic metals
POC & POM	Organic contaminants	Cesium and lead dating
Zooplankton	Nutrients, stable isotopes	TOC, POC, nutrients
Phytoplankton	Caloric content	Sediment chlorophyll
Hydrographic profiles	Oxygen consumption	Benthic infauna
Turbidity, TSS, nutrients	Nutrient flux experiments	Biomarkers
Trace metals	Qualitative video habitat survey	Grain size distribution
Fish toxicology		Oxygen uptake experiments
Birds & marine mammals		

Appendix 1

Concentrations (**ng g^{-1} wt**) of individual polycyclic aromatic hydrocarbons (PAHs) in surface sediments (0-1 cm) from the Chukchi shef collected during COMIDA09 and COMIDA10

Station Code	**1**	**2**	**3**	**4**	**5**	**6**	**7**	**8**	**9**	**10**	**11**	**12**	**13**	**14**	**15**	**16**	**17**	**19**
Latitude (N)	69°02.380'	69°30.126'	69°49.747'	70°01.383'	70°24.285'	70°20.706'	70°28.122'	70°17.233'	70°49.881'	70°40.275'	70°43.965'	70°41.833'	70°44.803'	70°38.490'	71°01.089'	70°55.151'	71°04.636'	71°01.669'
Longitude (W)	166°35.608'	167°40.513'	165°29.974'	163°45.670'	164°28.940'	165°27.024'	166°05.168'	167°26.609'	167°47.204'	167°04.990'	165°59.800'	165°26.437'	164°10.534'	162°15.976'	164°15.281'	165°25.232'	166°10.708'	166°57.162'
2-Methylnapthalene	86.3	15.0	9.1	0.0	5.7	14.1	0.0	1.2	2.9	9.7	1.0	3.8	17.5	1.0	4.4	8.0	15.4	14.2
1-Methylnapthalene	62.9	9.9	8.3	0.0	7.0	10.4	1.8	2.9	5.3	7.4	2.4	4.8	13.2	2.7	5.5	5.8	11.6	9.5
Biphenyl	19.4	5.9	5.2	1.1	1.5	5.1	3.6	5.0	7.7	4.5	4.0	4.9	6.5	3.6	6.3	3.1	6.4	6.3
2,7-Dimethylnapthalene	29.4	3.1	7.5	1.8	9.0	2.2	9.1	14.5	33.9	1.6	7.9	9.7	2.9	4.8	11.3	1.2	2.5	2.0
1,3-Dimethylnapthalene	27.7	16.8	4.8	0.3	4.3	11.3	0.0	0.0	0.0	12.6	0.0	0.0	20.2	0.0	0.0	3.4	26.4	13.2
1,6-Dimethylnapthalene	66.7	12.4	14.6	1.8	12.3	12.3	8.1	9.5	10.9	9.4	7.4	9.5	14.6	7.3	11.4	5.9	12.7	11.2
1,5-Dimethylnapthalene	63.5	11.1	12.3	1.5	10.1	10.2	7.1	8.8	9.7	7.0	6.0	7.9	12.2	5.6	9.0	5.6	10.2	9.1
1,4-Dimethylnapthalene	31.9	6.0	6.7	1.0	5.7	4.8	4.0	4.0	4.4	4.4	3.8	4.3	6.7	3.3	5.3	2.1	6.0	5.2
1,2-Dimethylnapthalene	14.8	0.0	2.5	0.4	2.5	2.6	1.9	2.9	7.3	0.0	1.9	1.4	2.6	1.2	2.1	1.9	2.7	2.2
1,8-Dimethylnapthalene	12.7	2.4	2.8	0.3	2.3	2.1	1.9	1.9	2.1	1.6	1.6	1.8	2.6	1.3	2.1	1.0	2.3	2.0
Fluorene	5.1	2.3	2.5	0.6	1.9	1.5	1.5	2.3	3.7	1.0	1.6	1.2	2.2	1.2	2.3	0.7	2.1	1.9
2,3,5-Trimethylnapthalene	25.4	3.4	5.2	0.8	4.5	3.9	3.8	4.9	6.4	3.5	2.8	3.1	4.8	2.3	3.7	1.8	4.0	4.1
1-Methylfluorene	13.7	4.0	4.6	5.2	10.8	2.7	13.3	13.7	16.7	4.0	5.3	8.0	5.2	5.9	12.4	1.7	11.2	12.2
1,4,5,8-Tetramethylnapthalene	19.4	3.3	3.9	3.1	7.1	2.7	7.6	7.1	11.4	3.3	3.8	5.2	4.5	3.9	8.1	1.6	8.6	8.4
Dibenzothiophene	19.1	4.5	5.4	9.1	18.6	3.5	23.6	22.1	30.9	6.6	9.8	14.3	7.4	11.9	22.6	1.9	21.3	26.2
Phenanthrene	129.5	21.1	39.5	43.8	88.0	13.1	115.2	118.7	167.7	23.1	53.2	56.1	35.2	46.6	96.3	5.6	87.4	94.1
2-Methyldibenzothiophene	56.6	7.5	10.5	32.0	62.7	6.1	84.3	89.3	104.9	13.5	29.1	45.3	16.0	35.1	79.2	4.6	72.3	74.1
4-Methyldibenzothiophene	34.2	2.3	7.8	22.3	37.7	1.9	51.5	46.8	62.4	3.6	17.8	26.3	3.7	21.8	46.4	1.2	22.4	23.0
2-Methylphenanthrene	74.1	10.5	17.5	40.1	71.8	9.2	80.8	87.7	115.0	16.2	39.4	42.6	18.5	38.8	86.8	6.0	79.5	87.8
2-Methylanthracene	97.6	13.2	25.6	53.8	93.6	11.2	101.8	116.3	152.4	17.6	52.0	54.9	20.6	47.5	105.2	8.0	86.8	83.8
1-Methylanthracene	110.3	13.0	20.3	65.6	111.6	12.1	126.7	151.2	179.9	24.0	53.9	72.4	28.9	63.8	144.0	9.0	135.0	144.3
1-Methylphenanthrene	86.5	9.8	17.9	50.3	84.2	10.3	89.8	110.1	130.3	17.0	39.9	51.2	19.7	43.2	99.6	7.2	88.3	97.3
3,6-Dimethylphenanthrene	14.8	11.9	0.0	7.0	13.0	10.0	15.3	23.2	34.7	20.0	5.2	-1.6	22.2	1.3	11.4	7.8	133.0	128.3
9,10-Dimethylanthracene	14.1	6.2	2.3	8.3	13.3	5.1	14.5	22.1	29.4	10.0	9.1	4.9	10.6	4.1	12.4	4.2	69.0	69.6
Fluoranthene	27.0	2.2	13.1	8.8	22.5	0.0	22.0	20.1	37.2	1.1	22.4	12.2	2.0	9.2	20.7	0.0	8.5	8.3
Pyrene	51.3	14.9	17.4	21.5	46.9	4.7	53.4	49.6	62.9	8.9	27.8	25.1	11.6	21.5	61.3	2.4	44.3	48.8
Retene	43.5	6.1	8.4	1.9	10.1	8.1	6.7	14.8	14.0	8.1	6.5	4.6	8.5	8.2	8.4	4.0	10.1	9.0
Benzo[b]fluorene	10.6	2.6	2.8	1.7	4.8	2.3	4.4	4.1	6.5	2.1	3.3	2.4	2.9	8.7	5.8	1.5	5.2	5.3
Benz[a]anthracene	6.5	1.3	1.6	0.3	1.6	1.5	1.0	1.3	2.0	1.2	1.3	1.2	1.7	1.1	1.5	0.8	1.5	1.3
Chrysene	6.5	2.5	2.9	0.9	3.4	3.0	2.3	2.4	3.3	2.2	2.4	2.7	3.6	2.1	3.4	1.9	3.4	3.1
Napthacene/Benz[b]anthracene	12.6	4.0	3.4	0.7	4.1	4.1	2.7	3.0	4.1	3.0	2.7	2.7	5.2	2.6	3.6	2.3	3.4	3.7
4-Methylchrysene	3.6	2.1	1.1	0.2	1.0	2.0	0.7	0.8	1.0	1.3	0.7	0.8	2.4	0.6	1.2	1.0	1.9	1.9
Benzo[a]pyrene	14.3	5.0	4.4	0.8	6.3	6.0	4.0	4.1	5.1	4.6	4.7	4.2	7.5	3.6	5.9	4.3	5.7	5.5
Perylene	46.7	47.3	22.5	3.1	36.0	42.1	28.4	35.7	36.6	41.7	29.1	33.9	57.0	19.7	48.1	31.5	50.6	50.3
TOTAL PAH (ng g^{-1} wt)	**1338.4**	**283.4**	**314.2**	**390.2**	**816.0**	**241.9**	**892.9**	**1002.1**	**1302.8**	**295.7**	**460.0**	**521.8**	**400.8**	**435.6**	**947.4**	**148.9**	**1051.7**	**1067.3**
TOTAL Parent PAHs (ng g^{-1} wt)	348.5	113.5	120.6	92.4	235.6	86.9	262.2	268.4	367.7	100.0	162.3	160.9	142.7	131.8	277.7	55.9	239.8	254.8
TOTAL Alkyl-PAHs (ng g^{-1} wt)	989.9	169.9	193.6	297.8	580.5	155.0	630.7	733.7	935.1	195.7	297.6	360.9	258.1	303.8	669.7	93.0	811.9	812.4

Appendix 1

Concentrations (**ng g^{-1} wt**) of individual polycyclic aromatic hydrocarbons (PAHs) in surface sediments (0-1 cm) from the Chukchi shef collected during COMIDA09 and COMIDA10 (continued)

Station Code	**20**	**21**	**22**	**23**	**24**	**25**	**26**	**27**	**28**	**29**	**30**	**31**	**32**	**34**	**35**	**36**	**37**	**38**
Latitude (N)	71°12.399'	71°29.079'	71°16.328'	71°23.228'	71°14.952'	71°14.549'	71°04.641'	70°54.512'	71°12.492'	71°17.891'	71°27.180'	71°22.732'	71°23.759'	71°40.587'	71°40.150'	71°55.815'	72°02.744'	71°55.614'
Longitude (W)	168°18.676'	167°46.900'	167°00.865'	166°16.588'	165°26.871'	163°55.317'	162°33.503'	160°44.450'	161°53.392'	161°41.321'	162°36.643'	164°42.710'	164°06.542'	166°26.627'	166°55.039'	167°23.351'	166°20.404'	165°09.650'
2-Methylnapthalene	17.3	16.0	13.2	14.8	9.0	12.8	14.4	10.4	25.4	1.8	16.5	13.3	9.1	16.4	14.0	12.9	10.5	10.8
1-Methylnapthalene	12.5	10.6	9.0	11.4	6.6	8.6	10.5	8.2	21.1	2.0	12.9	10.8	7.5	12.8	10.8	9.8	8.3	8.3
Biphenyl	7.3	8.7	7.4	6.3	3.4	5.6	8.4	4.9	10.4	3.3	9.8	4.4	3.4	7.3	6.1	6.1	4.3	4.5
2,7-Dimethylnapthalene	4.9	2.1	2.3	1.7	1.7	2.2	2.6	1.8	4.2	1.4	2.9	1.9	1.5	2.7	2.3	2.1	1.7	1.6
1,3-Dimethylnapthalene	62.3	32.6	16.7	20.3	27.6	15.9	20.3	16.5	41.1	15.0	72.5	21.6	17.0	24.7	36.0	14.0	19.0	9.7
1,6-Dimethylnapthalene	15.7	13.9	12.8	14.0	7.4	11.9	14.5	9.6	22.9	10.7	15.4	11.1	8.1	14.2	12.4	10.6	9.2	8.6
1,5-Dimethylnapthalene	14.4	12.1	11.6	10.1	7.1	8.7	11.3	6.9	19.4	10.9	14.9	10.6	8.0	12.1	10.6	9.3	9.4	7.8
1,4-Dimethylnapthalene	5.3	6.3	4.9	6.6	3.5	5.8	6.5	4.4	11.0	4.4	7.1	3.7	2.5	5.6	5.1	4.6	2.9	3.4
1,2-Dimethylnapthalene	12.5	4.1	3.1	2.3	2.5	0.0	2.6	2.7	6.8	5.0	7.4	4.1	3.8	3.2	4.0	2.8	4.6	2.7
1,8-Dimethylnapthalene	2.9	2.7	2.5	1.3	1.2	2.2	2.4	1.9	4.2	2.8	2.7	1.8	1.4	2.6	2.3	2.0	2.3	1.7
Fluorene	4.0	2.8	1.9	2.5	1.4	2.3	4.0	1.2	4.0	2.8	2.8	2.7	2.1	3.6	3.1	2.6	2.4	1.7
2,3,5-Trimethylnapthalene	5.6	5.5	4.4	4.3	2.4	3.5	5.6	2.2	7.3	3.7	5.0	3.5	3.2	4.7	3.8	4.0	3.3	2.7
1-Methylfluorene	7.5	20.1	14.0	12.0	4.4	9.1	29.9	6.8	14.0	6.8	11.9	4.9	4.8	6.3	6.5	7.1	5.1	5.4
1,4,5,8-Tetramethylnapthalene	4.9	13.6	9.5	9.2	3.6	6.8	18.6	4.7	10.5	5.0	8.3	3.6	3.3	4.9	5.0	5.5	3.9	4.1
Dibenzothiophene	8.4	39.1	26.1	25.1	7.9	17.6	52.5	12.5	24.5	10.6	22.3	7.2	4.8	11.2	13.5	12.7	6.4	9.4
Phenanthrene	39.4	146.5	116.4	85.3	28.8	77.6	251.3	54.2	112.4	44.5	93.4	35.6	24.5	51.4	57.8	58.3	24.0	37.7
2-Methyldibenzothiophene	15.5	116.7	91.0	78.6	24.6	57.4	233.7	49.3	84.6	23.2	76.3	19.8	12.3	35.3	41.3	45.7	14.8	33.2
4-Methyldibenzothiophene	10.4	37.2	28.5	25.5	6.6	19.4	77.0	15.1	23.8	6.5	21.8	5.8	4.6	10.6	14.5	16.3	4.3	11.7
2-Methylphenanthrene	16.8	130.7	94.9	74.1	23.3	68.2	238.6	45.4	85.0	23.0	79.6	23.3	13.2	38.7	44.6	45.5	13.6	35.4
2-Methylanthracene	20.3	164.3	113.5	78.1	28.4	72.8	307.1	51.4	106.7	30.7	97.6	29.7	18.5	47.9	56.3	57.1	19.1	47.0
1-Methylanthracene	22.8	200.7	151.7	116.6	42.6	117.6	412.5	76.9	148.4	39.5	133.6	41.8	24.2	66.2	78.9	81.5	25.8	65.5
1-Methylphenanthrene	17.7	143.3	119.5	82.9	27.0	73.2	305.3	51.0	101.8	29.5	95.7	31.2	19.4	49.1	57.9	58.8	19.7	48.8
3,6-Dimethylphenanthrene	17.6	177.4	136.2	112.7	41.2	129.8	417.4	86.9	126.4	32.6	132.9	33.1	22.5	57.4	77.0	68.7	27.7	56.1
9,10-Dimethylanthracene	8.8	88.2	66.3	55.0	16.9	67.1	197.8	38.6	59.7	16.4	65.8	17.0	11.3	26.9	39.7	34.9	14.6	27.5
Fluoranthene	8.7	10.9	13.1	8.1	1.3	10.4	36.1	7.9	11.6	3.7	13.0	3.8	3.2	6.1	6.4	5.9	4.7	3.1
Pyrene	26.8	60.0	67.0	38.7	13.4	52.8	180.5	34.9	46.2	12.8	57.5	14.9	9.9	20.9	26.4	23.5	12.2	19.5
Retene	6.4	11.4	10.7	9.1	6.1	9.5	20.3	7.9	15.2	10.7	11.4	7.9	7.3	10.8	4.9	8.6	2.9	6.6
Benzo[b]fluorene	2.6	5.8	6.9	5.3	2.4	6.5	18.0	5.3	8.2	4.9	7.1	3.4	2.8	4.2	10.3	3.4	3.8	2.7
Benz[a]anthracene	1.3	1.7	1.5	1.7	1.0	1.4	2.0	1.2	3.4	1.7	1.9	1.6	0.6	1.8	1.8	1.3	1.0	0.9
Chrysene	2.2	3.4	3.8	3.3	2.3	3.1	5.9	3.3	6.7	5.5	4.2	3.4	2.6	4.0	3.7	2.3	3.0	2.0
Napthacene/Benz[b]anthracene	3.9	4.4	3.6	4.0	2.5	4.1	3.9	3.2	7.3	5.5	4.9	4.7	3.3	5.1	4.6	2.7	3.9	2.1
4-Methylchrysene	1.5	2.1	1.9	2.4	1.4	2.3	3.9	1.9	4.0	2.6	2.5	2.1	1.7	2.7	2.3	1.8	1.2	1.5
Benzo[a]pyrene	5.7	7.0	5.8	5.5	4.2	5.0	5.1	4.7	11.4	10.6	6.9	8.1	5.4	9.2	7.2	6.0	5.9	5.1
Perylene	49.0	66.3	50.0	54.4	36.3	41.1	35.5	27.6	74.8	71.4	55.3	70.8	49.8	82.1	67.1	54.3	57.6	46.3
TOTAL PAH (ng g^{-1} wt)	**463.1**	**1568.3**	**1221.2**	**983.3**	**399.9**	**932.4**	**2956.2**	**661.6**	**1264.2**	**461.6**	**1174.0**	**462.7**	**317.7**	**662.9**	**738.3**	**682.5**	**353.2**	**534.8**
TOTAL Parent PAHs (ng g^{-1} wt)	159.3	356.7	303.3	240.2	104.8	227.5	603.1	161.0	320.8	177.3	279.0	160.4	112.5	207.0	208.1	179.1	129.3	134.9
TOTAL Alkyl-PAHs (ng g^{-1} wt)	303.7	1211.7	917.9	743.1	295.1	704.9	2353.0	500.7	943.4	284.3	895.0	302.3	205.1	455.9	530.2	503.4	224.0	399.9

Appendix 1

Concentrations (**ng g^{-1} wt**) of individual polycyclic aromatic hydrocarbons (PAHs) in surface sediments (0-1 cm) from the Chukchi shef collected during COMIDA09 and COMIDA10 (continued)

Station Code	**39**	**40**	**42**	**43**	**44**	**45**	**47**	**48**	**103**	**105**	**106**	**107**	**1013**	**1014**	**1015**	**1016**
Latitude (N)	71°42.117'	71°43.527'	71°44.311'	72°03.702'	72°24.238'	72°16.942'	71°43.642'	71°22.610'	67°40.134'	68°58.256'	69°53.671'	69°53.671'	71°55.598'	70°50.239'	71°15.284'	70°42.360'
Longitude (W)	164°30.898'	163°27.370'	162°06.210'	164°07.836'	164°57.482'	163°17.333'	160°43.097'	159°28.066'	168°57.280'	168°56.416'	167°44.142'	166°27.194'	162°40.476'	163°17.275'	163°11.484'	165°15.090'
2-Methylnapthalene	5.5	8.6	0.9	6.4	1.0	1.9	15.3	18.5	75.4	73.9	107.1	29.8	29.5	47.4	85.5	291.8
1-Methylnapthalene	3.9	6.2	0.5	4.7	0.8	1.6	11.7	14.1	45.8	44.9	62.2	19.1	19.0	29.9	52.8	167.0
Biphenyl	2.7	4.1	2.0	3.1	3.5	1.7	7.1	7.2	5.1	5.0	2.2	3.0	3.5	4.5	9.2	6.9
2,7-Dimethylnapthalene	0.8	1.1	0.7	1.0	1.4	0.7	2.4	2.8	1.5	1.5	1.4	1.2	1.0	1.7	7.6	4.3
1,3-Dimethylnapthalene	6.1	17.8	7.5	4.8	26.3	4.4	32.6	21.8	55.1	54.0	4.5	8.8	10.4	13.2	33.8	15.9
1,6-Dimethylnapthalene	4.3	7.0	4.5	5.3	7.0	4.1	12.8	15.6	6.1	6.0	6.9	7.6	6.3	8.7	35.2	16.3
1,5-Dimethylnapthalene	3.7	6.4	4.9	4.4	8.6	4.7	11.3	13.1	4.6	4.5	4.3	5.5	4.1	6.2	23.6	7.9
1,4-Dimethylnapthalene	2.2	2.8	1.6	1.9	2.5	1.4	5.3	6.1	1.6	1.6	1.8	3.0	1.9	3.6	15.7	4.4
1,2-Dimethylnapthalene	0.8	2.4	2.0	1.2	4.0	1.7	4.7	3.8	1.9	1.8	0.6	1.1	0.9	1.4	3.5	1.5
1,8-Dimethylnapthalene	0.9	1.3	1.3	1.0	2.1	1.6	2.1	2.8	0.9	0.8	0.9	1.2	0.9	1.5	7.0	1.9
Fluorene	1.0	1.6	2.1	1.2	2.5	1.1	3.0	3.4	2.2	2.1	0.0	1.8	3.2	2.6	7.8	2.2
2,3,5-Trimethylnapthalene	1.5	2.2	2.2	1.7	3.4	1.7	3.9	4.2	1.4	1.3	2.5	2.7	1.4	2.3	9.6	1.5
1-Methylfluorene	3.7	4.2	7.0	3.3	14.1	3.6	6.9	4.6	1.7	1.6	1.8	0.8	0.6	1.5	3.7	5.8
1,4,5,8-Tetramethylnapthalene	2.4	3.1	4.3	2.3	8.5	2.4	5.2	3.6	1.2	1.2	2.9	1.3	0.9	1.4	9.1	4.3
Dibenzothiophene	5.5	7.2	10.3	5.1	21.5	4.7	10.3	6.0	4.1	4.0	3.9	2.3	3.2	3.4	4.8	11.7
Phenanthrene	23.7	28.6	45.8	19.9	82.4	18.5	52.6	33.3	32.8	32.2	7.0	25.0	48.3	36.0	55.9	68.7
2-Methyldibenzothiophene	21.5	23.6	26.4	17.0	58.1	12.2	37.9	15.8	10.9	10.7	17.5	3.4	3.6	6.1	5.1	41.8
4-Methyldibenzothiophene	6.6	7.5	7.7	5.3	16.8	3.7	12.3	4.8	3.5	3.4	5.4	0.9	1.0	1.7	1.2	12.6
2-Methylphenanthrene	23.5	24.9	23.1	18.8	61.5	10.9	40.7	19.5	13.3	13.0	19.2	7.0	9.2	9.8	13.7	47.9
2-Methylanthracene	28.9	31.6	33.1	23.4	80.3	16.8	52.7	25.5	17.2	16.9	21.9	8.3	10.8	11.4	14.7	56.0
1-Methylanthracene	42.8	45.1	44.4	35.0	106.0	20.7	74.4	33.6	17.7	17.3	35.0	7.6	8.5	11.7	16.6	82.5
1-Methylphenanthrene	30.0	33.2	32.9	25.3	76.6	16.3	53.7	25.1	15.4	15.1	24.1	5.4	5.3	8.2	12.5	55.4
3,6-Dimethylphenanthrene	45.8	41.9	45.3	39.4	96.6	20.3	75.9	94.5	22.0	21.6	42.2	8.0	9.2	10.3	15.7	89.8
9,10-Dimethylanthracene	22.3	20.3	21.4	17.9	47.4	9.8	36.0	45.1	12.2	11.9	20.2	3.7	4.4	4.9	8.5	40.2
Fluoranthene	3.1	1.9	6.1	2.6	8.6	0.0	9.7	27.6	1.4	1.4	0.0	0.9	15.3	7.6	11.5	6.2
Pyrene	19.9	15.8	14.8	16.8	31.0	6.4	34.5	49.1	6.8	6.7	7.4	2.0	6.2	5.7	9.2	27.4
Retene	4.0	4.8	6.7	4.8	9.0	3.9	9.9	29.2	2.1	2.0	4.9	4.6	3.4	5.4	6.6	5.6
Benzo[b]fluorene	1.5	2.2	2.3	2.0	9.0	1.5	5.0	13.3	1.2	1.2	1.7	1.5	1.5	1.8	4.8	3.3
Benz[a]anthracene	0.6	0.9	0.8	0.7	0.9	0.3	1.8	5.1	0.5	0.5	0.6	0.8	0.7	0.9	1.7	0.9
Chrysene	1.4	2.2	2.9	1.6	3.2	1.3	4.5	14.3	1.0	1.0	0.4	1.8	1.8	2.1	4.2	1.3
Napthacene/Benz[b]anthracene	1.7	2.6	2.9	2.3	4.2	2.8	5.5	14.3	1.4	1.4	0.7	1.9	1.8	2.0	3.8	0.9
4-Methylchrysene	0.9	1.8	1.4	1.0	2.0	1.0	2.9	8.8	0.5	0.5	0.4	0.7	0.9	1.3	2.6	1.3
Benzo[a]pyrene	2.6	5.1	4.8	3.7	8.0	2.7	10.6	9.3	2.4	2.3	1.0	3.3	3.3	4.0	11.5	5.5
Perylene	23.5	40.7	38.8	32.1	77.6	28.9	78.3	59.5	28.1	27.5	5.5	25.5	26.0	23.9	42.7	219.3
TOTAL PAH (ng g^{-1} wt)	**349.2**	**410.8**	**413.4**	**317.3**	**886.5**	**215.3**	**733.9**	**655.3**	**398.6**	**390.7**	**418.2**	**201.7**	**247.9**	**284.1**	**551.5**	**1309.9**
TOTAL Parent PAHs (ng g^{-1} wt)	87.1	112.9	133.5	91.1	252.3	69.9	223.0	242.3	86.8	85.1	30.5	69.8	114.9	94.6	167.1	354.2
TOTAL Alkyl-PAHs (ng g^{-1} wt)	262.0	297.9	279.9	226.1	634.1	145.3	510.8	413.0	311.8	305.6	387.7	131.9	133.0	189.5	384.4	955.7

Appendix 2

Concentrations (**ng g^{-1} wt**) of individual aliphatic n-alkanes in surface sediments (0-1 cm) from the Chukchi shef collected during COMIDA09 and COMIDA10

Station Code	Latitude (N)	Longitude (W)	C15-n	C16-n	C17-n	C18-n	C19-n	C20-n	C21-n	C22-n	C23-n	C24-n	C25-n	C26-n	C27-n	C28-n	C29-n	C30-n	C31-n	C32-n	C33-n	**TOTAL n-Alkanes (ng g^{-1})**	TOTAL Short-chain (C_{15-C22}) n-Alkanes (ng g^{-1})	TOTAL Long-chain (C_{23-C33}) n-Alkanes (ng g^{-1})
1	69°02.380'	166°35.608'	0.20	0.45	0.44	0.37	0.51	0.42	0.35	0.00	0.68	0.02	0.54	0.02	0.81	0.00	0.75	0.21	1.01	0.10	0.55	**7.43**	2.74	4.69
2	69°30.126'	167°40.513'	0.08	0.40	0.16	0.11	0.09	0.01	0.26	0.17	0.59	0.00	0.82	0.05	0.93	0.00	0.64	0.05	0.73	0.11	0.25	**5.46**	1.29	4.17
3	69°49.747'	165°29.974'	0.11	0.68	0.12	0.02	0.00	0.00	0.09	0.00	0.27	0.00	0.17	0.00	0.34	0.00	0.39	0.25	0.49	0.11	0.36	**3.39**	1.01	2.37
4	70°01.383'	163°45.670'	0.05	0.38	0.51	0.55	0.54	0.60	0.15	0.40	0.13	0.15	0.00	0.00	0.00	0.12	0.00	0.13	0.04	0.06	0.06	**3.85**	3.17	0.68
5	70°24.285'	164°28.940'	0.14	0.47	0.49	0.52	0.62	0.54	0.24	0.01	0.41	0.00	0.28	0.00	0.46	0.14	0.52	0.18	0.76	0.06	0.57	**6.41**	3.03	3.37
6	70°20.706'	165°27.024'	0.00	0.00	0.00	0.07	0.21	0.07	0.45	0.29	0.88	0.00	1.15	0.10	1.45	0.00	1.01	0.05	1.05	0.12	0.30	**7.21**	1.10	6.11
7	70°28.122'	166°05.168'	0.06	0.27	0.25	0.27	0.41	0.23	0.11	0.04	0.30	0.00	0.10	0.00	0.15	0.00	0.24	0.09	0.47	0.06	0.35	**3.43**	1.66	1.77
8	70°17.233'	167°26.609'	0.09	0.43	0.34	0.35	0.55	0.34	0.22	0.09	0.50	0.01	0.34	0.00	0.41	0.00	0.37	0.13	0.57	0.05	0.35	**5.12**	2.40	2.72
9	70°49.881'	167°47.204'	0.16	0.51	1.12	1.13	1.55	0.78	0.75	1.10	1.08	1.06	1.00	0.56	1.31	0.08	1.21	0.82	1.51	0.41	0.85	**16.98**	7.11	9.87
10	70°40.275'	167°04.990'	0.00	0.00	0.12	0.11	0.20	0.08	0.36	0.22	0.68	0.00	1.13	0.46	1.19	0.14	0.68	0.06	0.67	0.09	0.20	**6.41**	1.10	5.31
11	70°43.965'	165°59.800'	0.10	0.51	0.37	0.40	0.53	0.38	0.23	0.22	0.59	0.15	0.57	0.32	0.73	0.32	0.83	0.63	0.89	0.35	0.60	**8.73**	2.74	5.98
12	70°41.833'	165°26.437'	0.09	0.41	0.45	0.48	0.69	0.55	0.42	0.19	0.74	0.21	0.67	0.08	0.96	0.00	0.83	0.15	0.98	0.08	0.59	**8.59**	3.28	5.30
13	70°44.803'	164°10.534'	0.00	0.09	0.23	0.17	0.32	0.14	0.44	0.24	0.72	0.00	0.84	0.00	0.90	0.00	0.66	0.02	0.76	0.10	0.26	**5.86**	1.63	4.23
14	70°38.490'	162°15.976'	0.00	0.19	0.09	0.00	0.18	0.03	0.10	0.00	0.28	0.00	0.15	0.00	0.09	0.00	0.15	0.10	0.21	0.02	0.18	**1.78**	0.59	1.18
15	71°01.089'	164°15.281'	0.00	0.29	0.27	0.42	0.85	0.65	0.42	0.00	0.73	0.02	0.56	0.09	0.77	0.03	0.73	0.30	0.84	0.12	0.52	**7.61**	2.90	4.71
16	70°55.151'	165°25.232'	0.06	0.07	0.13	0.05	0.12	0.00	0.17	0.09	0.32	0.00	0.47	0.00	0.28	0.00	0.21	0.00	0.32	0.06	0.14	**2.48**	0.67	1.80
17	71°04.636'	166°10.708'	0.10	0.15	0.30	0.39	0.62	0.38	0.40	0.32	0.71	0.00	0.87	0.03	0.87	0.00	0.63	0.00	0.73	0.07	0.33	**6.90**	2.66	4.24
19	71°01.669'	166°57.162'	0.00	0.00	0.33	0.59	0.67	0.52	0.48	0.48	0.88	0.00	0.99	0.04	1.09	0.00	0.83	0.03	0.98	0.10	0.50	**8.51**	3.08	5.43
20	71°12.399'	168°18.676'	0.26	1.47	0.37	0.42	0.29	0.16	0.40	0.33	0.84	0.17	1.38	0.22	1.79	0.00	0.95	0.05	0.99	0.11	0.34	**10.55**	3.70	6.85
21	71°29.079'	167°46.900'	0.11	0.16	0.45	0.62	0.83	0.61	0.55	0.48	0.91	0.11	1.11	0.09	1.33	0.00	1.06	0.04	1.25	0.11	0.52	**10.34**	3.81	6.53
22	71°16.328'	167°00.865'	0.00	0.10	0.34	0.59	0.93	0.74	0.55	0.51	0.77	0.08	0.95	0.09	1.17	0.00	0.95	0.03	1.12	0.11	0.41	**9.44**	3.76	5.68
23	71°23.228'	166°16.588'	0.00	0.12	0.36	0.45	0.75	0.48	0.56	0.52	1.02	0.00	1.32	0.20	1.77	0.06	1.48	0.14	1.69	0.15	0.59	**11.64**	3.23	8.41
24	71°14.952'	165°26.871'	0.00	0.06	0.04	0.10	0.13	0.19	0.12	0.24	0.23	0.07	0.33	0.00	0.60	0.00	0.54	0.08	0.72	0.04	0.33	**3.82**	0.88	2.93
25	71°14.549'	163°55.317'	0.05	0.12	0.33	0.48	0.81	0.58	0.46	0.42	0.72	0.00	0.88	0.11	1.06	0.00	0.88	0.08	1.02	0.10	0.38	**8.47**	3.24	5.23
26	71°04.641'	162°33.503'	0.08	0.23	0.75	1.55	3.09	2.74	1.04	0.82	0.69	0.00	0.74	0.01	0.61	0.00	0.59	0.02	0.72	0.07	0.27	**14.02**	10.31	3.71
27	70°54.512'	160°44.450'	0.00	0.08	0.26	0.38	0.65	0.48	0.36	0.26	0.44	0.00	0.46	0.00	0.36	0.00	0.34	0.00	0.42	0.06	0.15	**4.70**	2.48	2.22
28	71°12.492'	161°53.392'	0.00	0.09	0.42	0.54	1.10	0.55	0.68	0.54	1.15	0.00	1.39	0.18	1.78	0.06	1.45	0.10	1.56	0.13	0.71	**12.42**	3.92	8.50
29	71°17.891'	161°41.321'	0.08	0.16	0.33	0.38	0.67	0.49	0.80	0.69	1.30	0.49	1.22	0.19	1.72	0.06	1.35	0.07	1.57	0.06	0.71	**12.32**	3.59	8.73
30	71°27.180'	162°36.643'	0.00	0.11	0.41	0.59	1.13	0.79	0.68	0.56	0.96	0.00	1.19	0.12	1.45	0.03	1.15	0.11	1.35	0.14	0.53	**11.30**	4.27	7.03
31	71°22.732'	164°42.710'	0.00	0.08	0.18	0.33	0.46	0.47	0.60	0.59	0.94	0.45	1.03	0.29	1.53	0.13	1.07	0.14	1.02	0.09	0.40	**9.77**	2.71	7.06
32	71°23.759'	164°06.542'	0.06	0.11	0.18	0.30	0.47	0.37	0.57	0.50	0.87	0.35	0.78	0.05	1.05	0.00	0.71	0.00	0.84	0.02	0.40	**7.62**	2.57	5.06
34	71°40.587'	166°26.627'	0.00	0.08	0.21	0.41	0.52	0.52	0.64	0.64	1.01	0.42	1.03	0.15	1.66	0.00	1.18	0.03	1.26	0.04	0.52	**10.34**	3.02	7.32
35	71°40.150'	166°55.039'	0.10	0.20	0.26	0.41	0.62	0.53	0.65	0.61	0.97	0.37	1.03	0.14	1.66	0.01	1.28	0.03	1.51	0.06	0.61	**11.03**	3.37	7.66
36	71°55.815'	167°23.351'	0.00	0.08	0.20	0.38	0.56	0.53	0.53	0.55	0.75	0.28	0.75	0.05	1.15	0.00	0.93	0.02	1.10	0.03	0.47	**8.37**	2.84	5.53
37	72°02.744'	166°20.404'	0.09	0.87	0.27	0.44	0.37	0.31	0.46	0.43	0.71	0.27	0.69	0.00	1.06	0.00	0.77	0.00	0.78	0.00	0.27	**7.79**	3.24	4.55
38	71°55.614'	165°09.650'	0.00	0.09	0.16	0.32	0.42	0.40	0.41	0.41	0.56	0.22	0.55	0.03	0.90	0.00	0.75	0.08	0.90	0.04	0.40	**6.62**	2.20	4.43
39	71°42.117'	164°30.898'	0.00	0.05	0.12	0.23	0.35	0.31	0.23	0.25	0.30	0.15	0.24	0.00	0.44	0.00	0.44	0.07	0.64	0.05	0.30	**4.19**	1.55	2.64
40	71°43.527'	163°27.370'	0.04	0.11	0.16	0.27	0.48	0.34	0.37	0.37	0.54	0.29	0.56	0.05	0.83	0.03	0.77	0.18	1.04	0.12	0.41	**6.95**	2.13	4.82
42	71°44.311'	162°06.210'	0.00	0.10	0.15	0.33	0.52	0.40	0.49	0.50	0.55	0.19	0.46	0.00	0.65	0.00	0.50	0.00	0.66	0.01	0.30	**5.79**	2.48	3.31
43	72°03.702'	164°07.836'	0.05	0.11	0.16	0.11	0.36	0.32	0.25	0.42	0.36	0.15	0.25	0.06	0.41	0.00	0.41	0.02	0.51	0.01	0.25	**4.20**	1.77	2.43
44	72°24.238'	164°57.482'	0.00	0.08	0.27	0.40	0.51	0.43	0.48	0.53	0.76	0.37	0.78	0.15	1.14	0.00	0.86	0.00	0.93	0.01	0.48	**8.19**	2.70	5.49
45	72°16.942'	163°17.333'	0.05	0.09	0.12	0.18	0.24	0.22	0.29	0.31	0.38	0.13	0.26	0.00	0.39	0.00	0.32	0.00	0.55	0.00	0.26	**3.78**	1.50	2.28
47	71°43.642'	160°43.097'	0.12	0.13	0.25	0.39	0.67	0.51	0.50	0.52	0.77	0.34	0.79	0.07	1.21	0.00	1.03	0.01	1.18	0.04	0.53	**9.08**	3.10	5.98
48	71°22.610'	159°28.066'	0.10	0.16	0.22	0.32	0.62	0.44	0.55	0.51	0.78	0.29	0.69	0.04	1.14	0.00	1.03	0.04	1.16	0.04	0.52	**8.65**	2.93	5.72
103	67°40.134'	168°57.280'	0.00	0.24	0.18	0.09	0.17	0.15	0.31	0.28	0.54	0.25	0.70	0.29	1.14	0.25	0.87	0.15	0.91	0.09	0.47	**7.06**	1.41	5.65
105	68°58.256'	168°56.416'	0.00	0.18	0.14	0.09	0.18	0.16	0.47	0.47	1.02	0.38	1.21	0.36	2.05	0.28	1.33	0.13	1.15	0.07	0.55	**10.24**	1.69	8.54
106	69°53.671'	167°44.142'	0.48	1.10	0.74	1.03	0.93	0.75	0.45	0.39	0.53	0.23	0.57	0.22	0.77	0.14	0.55	0.07	0.42	0.06	0.20	**9.64**	5.88	3.76
107	69°53.671'	166°27.194'	0.04	0.19	0.02	0.09	0.10	0.09	0.20	0.21	0.45	0.15	0.46	0.13	0.59	0.07	0.33	0.04	0.25	0.02	0.16	**3.60**	0.95	2.65
1013	71°55.598'	162°40.476'	0.05	0.16	0.04	0.07	0.06	0.07	0.13	0.19	0.34	0.14	0.45	0.19	0.57	0.13	0.45	0.09	0.40	0.04	0.21	**3.77**	0.78	2.99
1014	70°50.239'	163°17.275'	0.07	0.23	0.04	0.11	0.13	0.10	0.20	0.23	0.36	0.16	0.43	0.21	0.57	0.20	0.50	0.13	0.45	0.06	0.22	**4.38**	1.10	3.28
1015	71°15.284'	163°11.484'	0.14	0.52	0.12	0.23	0.18	0.14	0.26	0.27	0.54	0.28	0.69	0.33	1.07	0.30	0.93	0.19	0.73	0.08	0.29	**7.30**	1.86	5.44
1016	70°42.360'	165°15.090'	0.08	0.28	0.12	0.20	0.18	0.15	0.11	0.14	0.14	0.06	0.25	0.10	0.55	0.17	0.77	0.11	0.34	0.03	0.10	**3.89**	1.25	2.63

Appendix 3

Concentrations of individual **PAHs (ng g^{-1} wt)** in a sediment core from Station 37 on the Chukchi Sea shelf

Depth of sediment (cm)	**0 to 1**	**1 to 2**	**3 to 4**	**5 to 6**	**7 to 8**	**9 to 10**	**12 to 14**	**16 to 18**	**18 to 20**
2-Methylnapthalene	10.5	8.9	10.3	12.6	16.4	11.9	11.5	17.2	12.2
1-Methylnapthalene	8.3	6.6	7.4	9.5	12.2	9.0	8.7	12.6	10.4
Biphenyl	4.3	3.3	3.8	4.7	5.2	4.6	4.5	4.9	4.6
2,7-Dimethylnapthalene	1.7	0.8	0.9	1.5	1.9	1.4	1.6	1.8	1.0
1,3-Dimethylnapthalene	19.0	6.7	12.3	14.9	21.4	17.6	15.7	18.9	15.3
1,6-Dimethylnapthalene	9.2	6.4	8.1	10.0	11.0	9.2	9.0	11.0	9.7
1,5-Dimethylnapthalene	9.4	5.4	6.8	8.4	8.9	7.7	7.5	9.1	8.1
1,4-Dimethylnapthalene	2.9	2.8	3.3	4.3	5.0	4.0	4.1	4.3	4.3
1,2-Dimethylnapthalene	4.6	1.6	1.6	2.0	2.4	1.9	1.5	2.4	2.0
1,8-Dimethylnapthalene	2.3	1.2	1.4	1.6	1.8	1.5	1.5	1.9	1.6
Fluorene	2.4	0.9	1.1	1.3	1.8	1.1	1.3	1.5	1.1
2,3,5-Trimethylnapthalene	3.3	1.7	2.2	2.6	3.1	2.2	2.4	3.3	2.8
1-Methylfluorene	5.1	1.1	1.7	1.8	6.7	1.8	1.7	7.4	2.1
1,4,5,8-Tetramethylnapthalene	3.9	1.2	1.7	2.0	4.8	1.8	1.7	5.4	2.0
Dibenzothiophene	6.4	1.4	2.1	2.1	11.2	2.1	1.7	13.0	2.5
Phenanthrene	24.0	3.6	7.7	8.1	44.8	8.5	7.3	54.8	9.0
2-Methyldibenzothiophene	14.8	2.0	4.3	3.0	39.6	4.6	1.9	51.3	5.7
4-Methyldibenzothiophene	4.3	0.4	1.1	0.7	13.5	1.2	0.3	16.2	1.5
2-Methylphenanthrene	13.6	3.3	6.8	7.5	49.0	7.5	4.2	59.1	8.6
2-Methylanthracene	19.1	4.2	8.7	9.5	61.5	9.5	6.3	76.0	11.0
1-Methylanthracene	25.8	5.0	10.1	8.8	89.2	9.8	5.7	106.5	13.7
1-Methylphenanthrene	19.7	3.6	8.1	9.0	66.7	7.2	4.4	74.4	9.9
3,6-Dimethylphenanthrene	27.7	4.0	9.8	7.9	125.5	10.8	6.1	164.4	18.7
9,10-Dimethylanthracene	14.6	2.5	5.6	4.7	60.1	5.4	3.2	72.8	9.9
Fluoranthene	4.7	0.0	1.1	0.9	12.7	2.3	3.3	14.6	1.9
Pyrene	12.2	2.5	5.2	4.6	50.6	6.0	5.2	66.4	11.0
Retene	2.9	3.6	5.3	5.8	10.9	6.0	6.3	13.4	7.2
Benzo[b]fluorene	3.8	1.3	1.9	2.1	6.8	2.2	6.4	7.2	3.0
Benz[a]anthracene	1.0	1.0	1.1	1.4	1.4	1.2	1.4	1.6	1.6
Chrysene	3.0	1.7	2.5	2.5	3.7	2.4	3.1	4.8	4.3
Napthacene/Benz[b]anthracene	3.9	2.5	3.2	3.7	3.6	3.0	3.5	3.7	3.9
4-Methylchrysene	1.2	1.5	1.9	2.0	2.1	2.0	1.6	2.3	2.7
Benzo[a]pyrene	5.9	3.7	5.6	5.8	5.7	6.1	6.5	6.7	7.4
Perylene	57.6	33.7	49.5	54.1	54.7	57.1	63.4	63.5	72.1
TOTAL PAH (ng g^{-1} wt)	**353.2**	**129.9**	**204.2**	**221.3**	**815.9**	**230.5**	**214.3**	**974.6**	**282.5**
TOTAL Parent PAHs (ng g^{-1} wt)	129.3	55.6	84.8	91.3	202.1	96.5	107.6	242.7	122.4
TOTAL Alkyl-PAHs (ng g^{-1} wt)	224.0	74.3	119.4	130.1	613.8	134.0	106.8	731.8	160.2

Concentrations of **n-alkanes (mg g^{-1} wt)** in a sediment core from Station 37 on the Chukchi Sea shelf

Depth of sediment (cm)	**0 to 1**	**1 to 2**	**3 to 4**	**5 to 6**	**7 to 8**	**9 to 10**	**12 to 14**	**16 to 18**	**18 to 20**
C15-n	0.09	0.09	0.00	0.07	0.04	0.06	0.04	0.00	0.00
C16-n	0.87	0.14	0.08	0.10	0.08	0.08	0.07	0.14	0.07
C17-n	0.27	0.25	0.21	0.22	0.19	0.18	0.19	0.36	0.14
C18-n	0.44	0.11	0.21	0.11	0.36	0.12	0.13	0.26	0.07
C19-n	0.37	0.17	0.22	0.21	0.63	0.16	0.16	0.53	0.10
C20-n	0.31	0.21	0.13	0.17	0.62	0.18	0.18	0.73	0.17
C21-n	0.46	0.23	0.23	0.27	0.66	0.28	0.33	0.67	0.26
C22-n	0.43	0.93	0.12	0.16	0.41	0.17	0.27	0.37	0.21
C23-n	0.71	1.73	0.60	0.57	0.76	0.61	0.71	0.65	0.73
C24-n	0.27	1.46	0.14	0.05	0.21	0.02	0.25	0.02	0.28
C25-n	0.69	2.51	1.01	0.82	1.07	0.87	0.95	0.86	1.08
C26-n	0.00	1.97	0.39	0.20	0.36	0.20	0.36	0.24	0.63
C27-n	1.06	3.80	2.53	2.06	2.29	2.02	1.81	2.15	2.05
C28-n	0.00	1.55	0.00	0.00	0.01	0.00	0.05	0.00	0.14
C29-n	0.77	2.63	1.82	1.07	1.38	1.26	1.03	1.57	0.97
C30-n	0.00	1.21	0.05	0.00	0.00	0.00	0.04	0.00	0.02
C31-n	0.78	2.15	1.86	0.89	1.15	1.31	1.04	1.51	0.93
C32-n	0.00	0.78	0.04	0.00	0.00	0.01	0.04	0.02	0.03
C33-n	0.27	1.00	0.66	0.32	0.45	0.48	0.42	0.52	0.29
TOTAL n-Alkane (mg g^{-1} wt)	**7.79**	**22.92**	**10.29**	**7.29**	**10.67**	**8.02**	**8.07**	**10.61**	**8.17**
TOTAL Short-chain ($C_{15\text{-}C22}$) n-Alkane (mg g^{-1} wt)	3.24	2.13	1.21	1.29	3.00	1.23	1.37	3.06	1.01
TOTAL Long-chain ($C_{23\text{-}C33}$) n-Alkane (mg g^{-1} wt)	4.55	20.79	9.09	6.00	7.67	6.79	6.69	7.55	7.16

Appendix 3

Concentrations of individual **PAHs (ng g^{-1} wt)** in a sediment core from Station 40 on the Chukchi Sea shelf

Depth of sediment (cm)	**0 to 1**	**2 to 3**	**4 to 5**	**6 to 7**	**8 to 9**	**9 to 10**
2-Methylnapthalene	32.6	6.3	5.5	8.6	6.6	9.6
1-Methylnapthalene	21.7	4.4	4.0	6.3	4.9	7.4
Biphenyl	7.0	3.1	2.3	3.5	2.4	4.0
2,7-Dimethylnapthalene	1.4	0.4	0.5	0.6	0.9	0.8
1,3-Dimethylnapthalene	25.3	5.1	7.6	8.8	9.1	13.1
1,6-Dimethylnapthalene	12.7	4.9	4.1	6.9	5.3	7.6
1,5-Dimethylnapthalene	9.9	4.0	3.3	5.7	4.2	6.1
1,4-Dimethylnapthalene	5.5	2.1	1.8	2.7	2.3	2.9
1,2-Dimethylnapthalene	2.6	1.0	1.0	1.4	1.2	1.7
1,8-Dimethylnapthalene	2.2	0.8	0.7	1.2	1.0	1.3
Fluorene	3.7	0.8	0.6	1.1	0.7	1.2
2,3,5-Trimethylnapthalene	4.9	1.2	1.0	1.6	1.1	1.6
1-Methylfluorene	23.9	0.8	0.7	1.2	0.8	1.2
1,4,5,8-Tetramethylnapthalene	14.7	0.9	0.7	1.2	0.9	1.3
Dibenzothiophene	46.6	1.0	0.8	1.6	0.9	1.6
Phenanthrene	204.1	3.2	4.0	7.5	2.4	7.9
2-Methyldibenzothiophene	181.5	1.6	1.6	2.8	1.4	2.2
4-Methyldibenzothiophene	56.5	0.4	0.4	0.7	0.3	0.5
2-Methylphenanthrene	200.9	2.9	2.2	4.4	2.9	3.8
2-Methylanthracene	252.8	4.2	3.7	6.4	3.3	4.6
1-Methylanthracene	368.5	4.2	3.9	7.9	3.8	4.4
1-Methylphenanthrene	251.7	3.3	3.5	4.8	2.6	3.9
3,6-Dimethylphenanthrene	518.1	4.4	4.1	7.5	4.3	7.0
9,10-Dimethylanthracene	246.3	2.7	2.6	4.0	2.3	3.8
Fluoranthene	36.3	1.2	0.8	4.0	1.1	4.2
Pyrene	146.2	2.7	2.5	5.1	2.8	4.9
Retene	16.8	3.0	2.7	4.5	3.0	4.9
Benzo[b]fluorene	12.5	1.2	1.0	1.8	1.2	1.9
Benz[a]anthracene	1.3	0.6	0.7	1.0	0.7	1.0
Chrysene	3.4	1.6	1.1	2.2	1.4	2.2
Napthacene/Benz[b]anthracene	3.6	1.7	1.7	2.7	2.0	2.9
4-Methylchrysene	3.6	0.9	0.9	1.3	1.2	1.4
Benzo[a]pyrene	6.7	3.5	3.0	5.7	3.9	6.3
Perylene	50.5	31.1	26.1	48.6	31.4	55.4
TOTAL PAH (ng g^{-1} wt)	**2776.0**	**111.1**	**101.4**	**175.4**	**114.2**	**184.7**
TOTAL Parent PAHs (ng g^{-1} wt)	521.9	51.7	44.9	84.9	50.9	93.4
TOTAL Alkyl-PAHs (ng g^{-1} wt)	2254.1	59.4	56.6	90.5	63.3	91.3

Concentrations of **n-alkanes (mg g^{-1} wt)** in a sediment core from Station 40 on the Chukchi Sea shelf

Depth of sediment (cm)	**0 to 1**	**2 to 3**	**4 to 5**	**6 to 7**	**8 to 9**	**9 to 10**
C15-n	0.05	0.00	0.00	0.00	0.00	0.00
C16-n	0.14	0.07	0.07	0.07	0.07	0.00
C17-n	0.43	0.18	0.18	0.19	0.16	0.19
C18-n	0.76	0.16	0.13	0.15	0.08	0.13
C19-n	1.20	0.20	0.16	0.14	0.10	0.20
C20-n	0.84	0.21	0.14	0.18	0.12	0.20
C21-n	0.62	0.23	0.12	0.20	0.14	0.18
C22-n	0.27	0.14	0.03	0.11	0.06	0.11
C23-n	0.44	0.16	0.00	0.20	0.11	0.17
C24-n	0.08	0.00	0.00	0.00	0.00	0.00
C25-n	0.42	0.00	0.00	0.00	0.00	0.00
C26-n	0.00	0.00	0.00	0.00	0.00	0.00
C27-n	1.39	0.12	0.00	0.23	0.27	0.26
C28-n	0.17	0.00	0.00	0.00	0.00	0.00
C29-n	1.31	0.35	0.21	0.37	0.49	0.44
C30-n	0.45	0.13	0.11	0.13	0.18	0.14
C31-n	1.26	0.55	0.41	0.47	0.67	0.62
C32-n	0.20	0.08	0.05	0.08	0.08	0.07
C33-n	0.45	0.29	0.21	0.22	0.27	0.28
TOTAL n-Alkane (mg g^{-1} wt)	**10.47**	**2.86**	**1.82**	**2.74**	**2.78**	**2.98**
TOTAL Short-chain ($C_{15\text{-}C22}$) n-Alkane (mg g^{-1} wt)	4.31	1.18	0.83	1.04	0.72	1.00
TOTAL Long-chain ($C_{23\text{-}C33}$) n-Alkane (mg g^{-1} wt)	6.17	1.69	0.99	1.70	2.07	1.99

Appendix 3

Concentrations of individual **PAHs (ng g^{-1} wt)** in a sediment core from Station 1016 on the Chukchi Sea shelf

Depth of sediment (cm)	**0 to 1**	**2 to 3**	**4 to 5**	**6 to 7**	**8 to 9**	**10 to 12**
2-Methylnapthalene	291.8	29.9	20.5	43.5	16.9	21.9
1-Methylnapthalene	167.0	19.7	14.8	32.4	12.6	16.1
Biphenyl	6.9	5.1	4.9	6.5	5.0	5.1
2,7-Dimethylnapthalene	4.3	3.0	2.0	3.0	1.6	1.9
1,3-Dimethylnapthalene	15.9	10.3	11.7	17.7	11.6	10.7
1,6-Dimethylnapthalene	16.3	16.3	14.2	25.0	12.6	14.4
1,5-Dimethylnapthalene	7.9	13.5	12.4	21.6	10.6	11.9
1,4-Dimethylnapthalene	4.4	6.1	6.4	10.8	5.4	5.9
1,2-Dimethylnapthalene	1.5	3.0	3.0	5.3	2.7	2.9
1,8-Dimethylnapthalene	1.9	2.9	2.7	5.1	2.3	2.7
Fluorene	2.2	2.3	1.8	3.2	1.6	1.9
2,3,5-Trimethylnapthalene	1.5	3.6	3.8	5.2	3.8	3.5
1-Methylfluorene	5.8	3.2	2.8	3.4	2.1	1.9
1,4,5,8-Tetramethylnapthalene	4.3	3.1	2.5	3.8	2.5	2.6
Dibenzothiophene	11.7	2.9	2.9	5.5	2.2	2.2
Phenanthrene	68.7	14.3	14.2	17.3	8.5	9.5
2-Methyldibenzothiophene	41.8	6.4	6.8	6.2	2.5	2.9
4-Methyldibenzothiophene	12.6	1.6	2.0	2.3	0.6	0.8
2-Methylphenanthrene	47.9	9.1	11.3	8.5	5.6	5.7
2-Methylanthracene	56.0	10.7	12.1	10.2	6.4	7.2
1-Methylanthracene	82.5	14.1	15.3	12.6	6.7	7.5
1-Methylphenanthrene	55.4	10.5	12.7	9.7	6.0	5.8
3,6-Dimethylphenanthrene	89.8	17.8	18.2	13.6	7.5	8.2
9,10-Dimethylanthracene	40.2	9.3	9.1	7.4	4.6	4.6
Fluoranthene	6.2	1.8	1.9	2.9	2.0	1.4
Pyrene	27.4	6.4	7.7	6.2	5.6	4.8
Retene	5.6	7.6	9.4	9.3	9.9	8.1
Benzo[b]fluorene	3.3	2.9	3.0	3.6	3.0	2.8
Benz[a]anthracene	0.9	1.4	1.7	2.0	1.8	1.5
Chrysene	1.3	3.1	3.6	4.6	4.2	3.6
Napthacene/Benz[b]anthracene	0.9	3.6	4.6	4.9	4.2	3.8
4-Methylchrysene	1.3	2.0	2.1	2.6	2.5	2.1
Benzo[a]pyrene	5.5	6.1	7.2	9.4	8.9	6.6
Perylene	219.3	37.4	58.1	63.0	77.0	51.2
TOTAL PAH (ng g^{-1} wt)	**1309.9**	**291.1**	**307.5**	**388.0**	**260.9**	**243.6**
TOTAL Parent PAHs (ng g^{-1} wt)	354.2	87.2	111.7	129.0	123.9	94.2
TOTAL Alkyl-PAHs (ng g^{-1} wt)	955.7	203.8	195.8	259.0	137.0	149.3

Concentrations of **n-alkanes (mg g^{-1} wt)** in a sediment core from Station 1016 on the Chukchi Sea shelf

Depth of sediment (cm)	**0 to 1**	**2 to 3**	**4 to 5**	**6 to 7**	**8 to 9**	**10 to 12**
C15-n	0.08	0.07	0.09	0.09	0.00	0.08
C16-n	0.28	0.12	0.11	0.11	0.10	0.08
C17-n	0.12	0.31	0.28	0.25	0.31	0.21
C18-n	0.20	0.11	0.20	0.08	0.17	0.09
C19-n	0.18	0.17	0.20	0.16	0.18	0.17
C20-n	0.15	0.15	0.17	0.13	0.17	0.14
C21-n	0.11	0.23	0.26	0.23	0.26	0.25
C22-n	0.14	0.18	0.13	0.12	0.16	0.17
C23-n	0.14	0.39	0.37	0.27	0.45	0.40
C24-n	0.06	0.06	0.00	0.00	0.00	0.00
C25-n	0.25	0.20	0.17	0.03	0.33	0.07
C26-n	0.10	0.00	0.00	0.00	0.00	0.00
C27-n	0.55	0.88	0.93	0.48	1.08	0.52
C28-n	0.17	0.07	0.00	0.00	0.00	0.00
C29-n	0.77	0.88	0.90	0.49	0.98	0.71
C30-n	0.11	0.30	0.17	0.11	0.21	0.14
C31-n	0.34	0.86	0.94	0.39	0.71	0.78
C32-n	0.03	0.15	0.09	0.03	0.08	0.05
C33-n	0.10	0.34	0.37	0.09	0.17	0.12
TOTAL n-Alkane (mg g^{-1} wt)	**3.89**	**5.47**	**5.36**	**3.07**	**5.37**	**4.00**
TOTAL Short-chain (C_{15-C22}) n-Alkane (mg g^{-1} wt)	1.25	1.33	1.43	1.18	1.36	1.21
TOTAL Long-chain (C_{23-C33}) n-Alkane (mg g^{-1} wt)	2.63	4.14	3.93	1.89	4.01	2.79

Appendix 4

Concentrations of individual **PAHs (ng g^{-1} wet wt)** in Neptunea foot muscle collected from Station 7

Size class (cm)	**< 5**	**5 to 8**	**> 8**
2-Methylnapthalene	1.43	0.56	0.74
1-Methylnapthalene	0.68	0.30	0.41
Biphenyl	0.52	0.46	0.34
2,7-Dimethylnapthalene	0.00	0.00	0.17
1,3-Dimethylnapthalene	0.00	0.00	0.14
1,6-Dimethylnapthalene	0.72	0.37	0.40
1,5-Dimethylnapthalene	0.65	0.39	0.32
1,4-Dimethylnapthalene	0.49	0.44	0.32
1,2-Dimethylnapthalene	0.00	0.00	0.00
1,8-Dimethylnapthalene	0.23	0.00	0.00
Fluorene	0.67	0.00	0.29
2,3,5-Trimethylnapthalene	0.00	0.00	0.00
1-Methylfluorene	0.12	0.00	0.06
1,4,5,8-Tetramethylnapthalene	0.00	0.00	0.00
Dibenzothiophene	0.23	0.02	0.14
Phenanthrene	0.18	0.00	0.00
2-Methyldibenzothiophene	0.12	0.08	0.14
4-Methyldibenzothiophene	0.00	0.00	0.00
2-Methylphenanthrene	0.14	0.01	0.05
2-Methylanthracene	0.27	0.00	0.11
1-Methylanthracene	0.33	0.08	0.11
1-Methylphenanthrene	0.49	0.24	0.20
3,6-Dimethylphenanthrene	0.50	0.33	0.24
9,10-Dimethylanthracene	0.29	0.00	0.21
Fluoranthene	0.00	0.00	0.00
Pyrene	2.66	1.01	0.08
Retene	0.00	0.00	0.00
Benzo[b]fluorene	0.00	0.00	0.00
Benz[a]anthracene	0.00	0.00	0.00
Chrysene	0.00	0.00	0.00
Napthacene/Benz[b]anthracene	0.00	0.00	0.00
4-Methylchrysene	0.00	0.00	0.00
Benzo[a]pyrene	0.00	0.90	0.00
Perylene	0.00	0.00	0.00
TOTAL PAH (ng g^{-1} wt)	**10.70**	**5.17**	**4.47**
TOTAL Parent PAHs (ng g^{-1} wt)	4.26	2.39	0.85
TOTAL Alkyl-PAHs (ng g^{-1} wt)	6.44	2.78	3.62

Concentrations of **n-alkanes (μg g^{-1} wet wt)** in Neptunea foot muscle collected from Station 7

Size class (cm)	**< 5**	**5 to 8**	**> 8**
C15-n	0.00	0.00	0.00
C16-n	0.00	0.00	0.00
C17-n	0.00	0.00	0.00
C18-n	0.00	0.00	0.00
C19-n	0.05	0.00	0.04
C20-n	0.09	0.04	0.07
C21-n	0.03	0.02	0.09
C22-n	0.01	0.03	0.11
C23-n	0.00	0.04	0.25
C24-n	0.00	0.08	0.45
C25-n	0.00	0.04	0.55
C26-n	0.00	0.06	0.65
C27-n	0.00	0.09	0.70
C28-n	0.00	0.14	0.70
C29-n	0.00	0.15	0.52
C30-n	0.16	0.21	0.66
C31-n	0.09	0.14	0.00
C32-n	0.12	0.12	0.27
C33-n	0.10	0.10	0.14
TOTAL n-Alkane (μg g^{-1} wt)	**0.66**	**1.25**	**5.20**
TOTAL Short-chain (C_{15-C22}) n-Alkane (μg g^{-1} wt)	0.18	0.08	0.31
TOTAL Long-chain (C_{23-C33}) n-Alkane (μg g^{-1} wt)	0.48	1.16	4.89

Appendix 5

Validation of internal reference compounds for polycyclic aromatic hydrocarbon (PAH) analysis

Internal reference standards	**Acenaphthene-d10**	**Phenathrene-d10**	**Benz(a)anthracene-d12**	**Benzo(a)pyrene-d12**
PAHs assigned for quantification	2-Methylnapthalene	Fluorene	3,6-Dimethylphenanthrene	Benzo[a]pyrene
	1-Methylnapthalene	2,3,5-Trimethylnapthalene	9,10-Dimethylanthracene	Perylene
	Biphenyl	1-Methylfluorene	Fluoranthene	
	2,7-Dimethylnapthalene	1,4,5,8-Tetramethylnapthalene	Pyrene	
	1,3-Dimethylnapthalene	Dibenzothiophene	Retene	
	1,6-Dimethylnapthalene	Phenanthrene	Benzo[b]fluorene	
	1,5-Dimethylnapthalene	2-Methyldibenzothiophene	Benz[a]anthracene	
	1,4-Dimethylnapthalene	4-Methyldibenzothiophene	Chrysene	
	1,2-Dimethylnapthalene	2-Methylphenanthrene	Napthacene	
	1,8-Dimethylnapthalene	2-Methylanthracene	4-Methylchrysene	
		1-Methylanthracene		
		1-Methylphenanthrene		
Standard addition (ng) ***w/o*** extraction	100	100	100	100
Standard addition (ng) ***with*** extraction	100	100	100	100
GCMS base peak area response of standard addition ***w/o*** extraction	473500	782763	939150	640119
GCMS base peak area response of standard addition ***with*** extraction	482977	774047	956796	531481
% Recovery	**102**	**99**	**102**	**83**

Validation of internal reference compounds for n-alkane analysis

Internal reference standard	**n-Octadecane-d38**
n-Alkanes assigned for quantification	C15-n
	C16-n
	C17-n
	C18-n
	C19-n
	C20-n
	C21-n
	C22-n
	C23-n
	C24-n
	C25-n
	C26-n
	C27-n
	C28-n
	C29-n
	C30-n
	C31-n
	C32-n
	C33-n
Standard addition (ng) ***w/o*** extraction	530
Standard addition (ng) ***with*** extraction	1766
Avg GC base peak area response of standard addition ***w/o*** extraction and HPLC fractionation	34.0418
Avg GC base peak area response of standard addition ***with*** extraction and HPLC fractionation	10.3744
% Recovery	**9.1**

Appendix 6

Polycyclic aromatic hydrocarbons (PAHs) in ship and procedureal blanks (**ng**) from COMIDA09 and COMIDA10

	R/V Alpha Helix Lab Air Blank	R/V Alpha Helix Deck Air Blank	R/V Moana Wave Lab Air Blank	R/V Moana Wave Deck Air Blank	Procedural Blank 09-1	Procedural Blank 09-2	Procedural Blank 09-3	Procedural Blank 10-1
2-Methylnapthalene	0.73	0.91	0.73	0.83	16.77	1.27	0.37	2.66
1-Methylnapthalene	0.47	0.64	0.40	0.56	8.78	0.63	0.50	1.79
Biphenyl	0.24	0.38	0.36	0.83	0.00	0.88	0.31	0.00
2,7-Dimethylnapthalene	0.18	0.20	0.00	0.56	0.00	0.38	0.18	0.00
1,3-Dimethylnapthalene	0.37	0.71	0.18	0.19	0.00	0.74	0.14	0.39
1,6-Dimethylnapthalene	0.62	0.72	0.24	0.34	0.00	0.52	0.15	1.11
1,5-Dimethylnapthalene	0.37	0.43	0.51	0.52	0.00	0.56	0.25	1.37
1,4-Dimethylnapthalene	0.25	0.30	0.32	0.33	0.00	0.18	0.00	1.37
1,2-Dimethylnapthalene	0.00	0.10	0.00	0.26	0.00	0.12	0.00	0.75
1,8-Dimethylnapthalene	0.13	0.15	0.11	0.13	0.00	0.10	0.00	0.31
Fluorene	1.18	1.43	1.27	1.06	0.26	0.73	0.43	3.23
2,3,5-Trimethylnapthalene	0.10	0.14	0.09	0.00	0.00	0.08	0.04	0.00
1-Methylfluorene	0.15	0.15	0.24	0.31	0.51	0.13	0.09	1.69
1,4,5,8-Tetramethylnapthalene	0.08	0.10	0.11	0.00	0.53	0.10	0.00	0.36
Dibenzothiophene	0.85	1.00	1.00	0.80	0.87	0.32	0.22	2.74
Phenanthrene	19.09	23.01	20.52	17.95	20.56	8.54	5.30	52.72
2-Methyldibenzothiophene	0.44	0.46	0.33	0.34	2.20	0.42	0.12	1.51
4-Methyldibenzothiophene	0.13	0.18	0.11	0.00	0.68	0.00	0.00	0.44
2-Methylphenanthrene	1.51	1.73	1.50	1.40	13.52	2.22	0.58	4.27
2-Methylanthracene	2.14	2.37	2.27	1.67	20.72	3.68	0.88	5.37
1-Methylanthracene	0.96	1.11	1.03	0.75	13.50	1.96	0.56	4.07
1-Methylphenanthrene	0.84	0.97	0.99	0.64	9.70	1.35	0.41	4.50
3,6-Dimethylphenanthrene	1.54	2.10	1.76	1.67	38.59	3.85	1.63	4.87
9,10-Dimethylanthracene	0.77	1.08	0.75	0.67	19.02	1.84	0.80	1.91
Fluoranthene	10.01	11.82	11.01	9.89	20.14	3.18	2.01	52.71
Pyrene	3.71	3.82	3.34	3.27	10.67	1.86	0.93	18.44
Retene	0.26	0.27	0.20	0.33	3.69	0.53	0.16	0.96
Benzo[b]fluorene	0.14	0.18	0.10	0.00	2.58	0.34	0.12	0.00
Benz[a]anthracene	0.00	0.00	0.00	0.00	0.00	0.00	0.00	0.00
Chrysene	0.00	0.00	0.00	0.00	0.00	0.06	0.00	0.00
Napthacene/Benz[b]anthracene	0.00	0.00	0.00	0.00	0.00	0.09	0.00	0.00
4-Methylchrysene	0.00	0.00	0.00	0.00	0.00	0.00	0.00	0.00
Benzo[a]pyrene	0.28	0.00	0.00	0.00	0.00	0.00	0.00	0.00
Perylene	0.00	0.00	0.00	0.00	0.00	0.00	0.00	0.00
TOTAL PAH (ng)	**47.54**	**56.47**	**49.49**	**45.32**	**203.31**	**36.67**	**16.21**	**169.53**

Aliphatic n-alkanes in ship and procedureal blanks (**ng**) from COMIDA09 and COMIDA10

	R/V Alpha Helix Lab Air Blank	R/V Alpha Helix Deck Air Blank	R/V Moana Wave Lab Air Blank	R/V Moana Wave Deck Air Blank	Procedural Blank 09-1	Procedural Blank 09-2	Procedural Blank 09-3	Procedural Blank 10-1
C15-n	0.00	0.00	0.00	0.00	0.00	0.00	0.00	0.00
C16-n	0.00	0.00	0.00	0.00	0.00	0.00	0.00	0.00
C17-n	0.00	0.00	0.00	0.00	1.07	0.00	0.00	0.27
C18-n	0.00	0.00	0.00	0.00	2.44	0.40	0.00	0.19
C19-n	0.00	0.00	0.00	0.00	1.64	0.39	0.00	0.15
C20-n	0.00	0.00	0.00	0.00	2.69	0.72	0.00	0.20
C21-n	0.17	0.00	0.00	0.00	0.92	0.27	0.00	0.11
C22-n	0.67	0.31	0.34	0.23	2.82	0.99	0.33	0.26
C23-n	0.94	0.28	0.00	0.00	0.60	0.69	0.00	0.16
C24-n	1.12	0.27	0.42	0.26	1.93	1.38	0.00	0.20
C25-n	1.45	0.94	0.33	0.00	0.43	1.07	0.00	0.11
C26-n	1.69	1.19	0.34	0.00	0.63	1.17	0.43	0.12
C27-n	1.70	1.36	0.35	0.00	0.27	1.15	0.32	0.10
C28-n	1.55	1.24	0.34	0.00	0.21	0.86	0.00	0.09
C29-n	1.27	0.92	0.36	0.00	0.17	0.62	0.00	0.00
C30-n	1.00	0.67	0.33	0.00	0.92	0.61	0.00	0.09
C31-n	0.73	0.42	0.00	0.00	1.07	0.78	0.00	0.08
C32-n	0.50	0.27	0.33	0.00	0.52	0.42	0.00	0.08
C33-n	0.33	0.23	0.00	0.00	0.00	0.54	0.00	0.08
TOTAL n-alkane (ng)	**13.11**	**8.10**	**3.15**	**0.49**	**18.32**	**12.06**	**1.08**	**2.28**

Organizing and Storing Ocean Observations Data

Data Management Workflow

It is the goal of the COMIDA CAB project team and a requirement of the BOEM contracting procedure that all project data be preserved in the public domain. However, adequate data and metadata management can be a cumbersome and time-consuming task for project scientists unfamiliar with best practices for good data stewardship. In recognition of these dual interests, a data management workflow was developed for the COMIDA CAB project seeking to minimize the burden to project Principal Investigators yet providing sufficiently described data such that it may be discovered, accessed, and used by others in the future. The workflow is described below and is depicted in Figure 3.

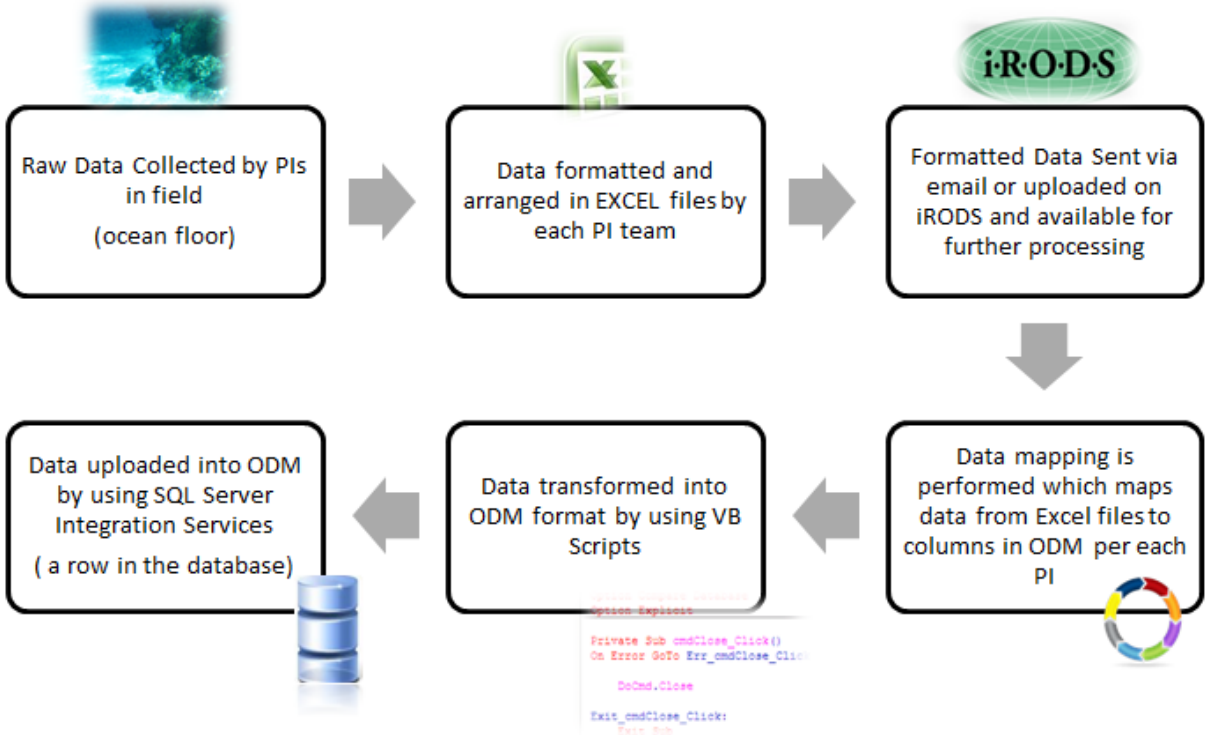

Figure 3. The COMIDA CAB project data management workflow.

Data are collected by PIs while aboard the research vessel or from samples brought back to the laboratory. Data are recorded by PIs in their native, traditional format in Microsoft Excel, a widely used platform which requires no specialized database knowledge. Data spreadsheets are uploaded to a secure online document-sharing system, in this case the iRODS database, which has been created for the project team and is password-protected. This security is afforded since, according to contract requirements, access to preliminary project data is currently limited to project participants and is provided via a log-in interface. Once data have been quality-

controlled and approved for release, project data and analytical products will become publicly-available. Once uploaded to iRODS, notification of such is given to the data management team.

At this point, the data team 'takes over' management of the data. However, a chain-of-custody is established at the data handoff and this custody signature persists throughout the data workflow, from loading the database all the way through to archiving; the chain-of-custody is described further below. Customized scripts are developed using Visual Basic which establish a 'template' for each PIs data format. These templates serve to map the PIs data to the ODM data model, from the PIs personal terminology to a standardized ontology of variables and controlled vocabularies for metadata. Since templates are developed for each PI and each data type, repeat and/or revised submissions may be loaded simply and efficiently into the project database; this feature is convenient since the project included two years of field sampling with many similar observations made year-to-year. Finally, data are loaded into the ODM using SQL/Server Integration Services (SSIS). This data management workflow may be characterized as an Extract-Transform-Load procedure: data are extracted from diverse file formats, transformed into a standardized data structure, and loaded into the project database.

Chain-of-Custody Tracking

The importance of establishing data provenance is widely acknowledged, for quality control and quality assurance purposes, for questions of clarification and of collaboration, for discovering errors or making revisions, and for providing appropriate credit and citation for data use. Each data value stored in the COMIDA CAB project database is treated as an individual entity. As such, each data value has associated metadata describing the source of that value – who was the data collector/provider, what organization do they represent, and how can they be contacted. This type of provenance-tracking is in use in many data systems today, although admittedly not frequently enough, and might be considered the current best-practice.

The COMIDA CAB project team has taken the chain-of-custody approach one step further, however. Since this is a large project with diverse and complex project data, quality assurance and quality control assume increased importance. To aid project PIs in data validation and to allow for individual researchers to 'track' their input data as it moves through the data management workflow process, each data value maintains as metadata the name of the Excel file that in which it was originally provided. Since the ultimate data archiving will include the 'raw' Excel files in addition to the SQL/Server project database, each data kernel may be traced back to its file of origin and to the PI who provided it.

This enhanced chain-of-custody tracking affords the opportunity for each PI to review their data as it is represented within the complete project database. As such, PIs can be confident that their own data has been represented faithfully and accurately within the database. Similarly, queries may be performed on the data by individual PI and/or by Excel file of origin.

Communicating Results

Web-Based Data Access

The COMIDA CAB project is federally-funded; this means that the United States taxpayer owns the project results and data. Furthermore, access to the complete project results will hopefully be beneficial to the multiple PIs, to other scientists, to regulators, and to stakeholders in the Chukchi Sea and its environs. As such, a project website was established as the primary project outreach platform, http://www.comidacab.org (Figure 4).

The website includes tabs for: (1) Home – providing a brief project overview plus recent updates; (2) Maps – linked to the ArcGIS Online community for sharing geographic data; (3) Data – linked to the Integrated Rule-Oriented Data System (iRODS) on the Corral Server of the Texas Advanced Computing Center (TACC); and (4) About – the COMIDA CAB project team.

Data Archiving

In addition to these project-specific outreach efforts, the project data will be archived externally at the National Oceanographic Data Center (NODC), which has as its mission the provision of scientific stewardship of marine data and information and represents the world's largest holding of publicly-accessible oceanographic data. As such, NODC serves as the national repository for information specific to the oceanographic discipline (NODC, 2011).

Figure 4. The comidacab.org homepage.

Based on discussions with NODC data officials, the COMIDA CAB project team will submit a data package to the NODC upon approval for public data release (scheduled to be September 23, 2012). The package will consist of: (1) original PI data files as Microsoft Excel; (2) ASCII files output from the project SQL/Server database along with a blank database schema (as XML or UML); (3) shapefiles and rasters of project geographic data; and (4) the project report. It is believed that this submission package represents the most complete description available of the project results and affords the greatest flexibility for others to find, access, and ultimately use the project data from the NODC archive. It is hoped that this novel submission package template will serve as a model for others submitting data to NODC to better leverage this valuable public resource for understanding and protecting our oceans.

Acknowledgments

The authors wish to thank the Bureau of Ocean Energy Management (BOEM) for supporting this study (M08PC20056); the efforts of Dick Prentki of BOEM are especially acknowledged. Also thanks to Captain John Seville and the crews of the R/V Alpha Helix and R/V Moana Wave for two safe and productive field seasons.

References (all chapters)

Aagaard, K., 1984. Current, CTD, and pressure measurements in possible dispersal regions of the Chukchi Sea, final report. OCS Study MMS-84-0069. USDOC, NOAA and USDOI, MMS, Anchorage, AK, pp. 255-333.

Abrantes, K., Sheaves, M., 2009. Food web structure in a near-pristine mangrove area of the Australian Wet Tropics. Estuarine Coastal and Shelf Science 82, 597-607.

ACIA, 2004. Impacts of a warming Arctic : Arctic Climate Impact Assessment. Cambridge University Press, Cambridge, U.K.

ACIA, 2005. Arctic Climate Impact Assessment - Scientific Report. Cambridge University Press, Cambridge.

Amante, C., Eakins, B.W., 2008. ETOPO1 1 Arc-Minute Global Relief Model: Procedures, Data Sources and Analysis. . National Geophysical Data Center, NOAA, USDOC, Boulder, CO.

Ambrose, W.G., Clough, L.M., Tilney, P.R., Beer, L., 2001. Role of echinoderms in benthic remineralization in the Chukchi Sea. Mar. Biol. 139, 937-949.

An, S.M., Gardner, W.S., Kana, T., 2001. Simultaneous measurement of denitrification and nitrogen fixation using isotope pairing with membrane inlet mass spectrometry analysis. Appl. Environ. Microbiol. 67, 1171-1178.

API, 2009. American Petroleum Institute. History of Northern Alaska Petroleum Development.

Arctur, D., Zeiler, M., 2004. Designing Geodatabases: Case Studies in GIS Data Modeling. ESRI Press, Redlands, CA.

Are, F., Reimnitz, E., Grigoriev, M., Hubberten, H.W., Rachold, V., 2008. The influence of cryogenic processes on the erosional arctic shoreface. J. Coast. Res. 24, 110-121.

Ariya, P.A., Dastoor, A.P., Amyot, M., Schroeder, W.H., Barrie, L., Anlauf, K., Raofie, F., Ryzhkov, A., Davignon, D., Lalonde, J., Steffen, A., 2004. The Arctic: a sink for mercury. Tellus B 56, 397-403.

Arukwe, A., Goksoyr, A., 1997. Changes in three hepatic cytochrome P450 subfamilies during a reproductive cycle in Turbot (Scophthalmus maximus L). J Exp Zool 277, 313-325.

Arukwe, A., Nordtug, T., Kortner, T.M., Mortensen, A.S., Brakstad, O.G., 2008. Modulation of steroidogenesis and xenobiotic biotransformation responses in zebrafish (Danio rerio) exposed to water-soluble fraction of crude oil. Environ. Res. 107, 362-370.

Atkins, D.E., Droegemeier, K.K., Feldman, S.I., Garcia-Molina, H., Klein, M.L., Messerschmitt, D.G., Messina, P., Ostriker, J.P., Wright, M.H., 2003. Revolutionizing Science and Engineering through Cyberinfrastructure: Report of the National Science Foundation Blue-Ribbon Advisory Panel on Cyberinfrastructure. http://www.nsf.gov/od/oci/reports/atkins.pdf.

Barber, W.E., Smith, R.L., Vallarino, M., Meyer, R.M., 1997. Demersal fish assemblages of the northeastern Chukchi Sea, Alaska. Fishery Bulletin Washington D C 95, 195-209.

Baskaran, M., Naidu, A.S., 1995. Pb-210-Derived Chronology and the Fluxes of Pb-210 and Cs-137 Isotopes into Continental-Shelf Sediments, East-Chukchi-Sea, Alaskan Arctic. Geochim. Cosmochim. Acta 59, 4435-4448.

Becker, S., Halsall, C.J., Tych, W., Hung, H., Attewell, S., Blanchard, P., Li, H., Fellin, P., Stern, G., Billeck, B., Friesen, S., 2006. Resolving the long-term trends of polycyclic aromatic hydrocarbons in the Canadian Arctic atmosphere. Environ. Sci. Technol. 40, 3217-3222.

Belicka, L.L., Harvey, H.R., 2009. The sequestration of terrestrial organic carbon in Arctic Ocean sediments: A comparison of methods and implications for regional carbon budgets. Geochim. Cosmochim. Acta 73, 6231-6248.
Belicka, L.L., Macdonald, R.W., Harvey, H.R., 2002. Sources and transport of organic carbon to shelf, slope, and basin surface sediments of the Arctic Ocean. Deep-Sea Research Part I-Oceanographic Research Papers 49, 1463-1483.
Belicka, L.L., Macdonald, R.W., Yunker, M.B., Harvey, H.R., 2004. The role of depositional regime on carbon transport and preservation in Arctic Ocean sediments. Mar. Chem. 86, 65-88.
Bendel, V., Fouquet, Y., Auzende, J.M., Lagabrielle, Y., Grimaud, D., Urabe, T., 1993. The white-lady hydrothermal field, north Fiji Back-Arc Basin, Southwest Pacific Economic Geology and the Bulletin of the Society of Economic Geologists 88, 2237-2249.
Benedetti, M., Regoli, F., Martuccio, G., Fattorini, D., Canapa, A., Barucca, M., Nigro, M., 2007. Oxidative and modulatory effects of trace metals on metabolism of polycyclic aromatic hydrocarbons in the Antarctic fish *Trematomus bernacchiile*. Aquat. Toxicol. 85, 167-175.
Bianchi, G., Avato, P., Scarpa, O., Murelli, C., Audisio, G., Rossini, A., 1989. Composition and Structure of Maize Epicuticular Wax Esters. Phytochemistry 28, 165-171.
Birkeland, C., Chia, F.-S., 1971. Recruitment risk, growth, age and predation in two populations of sand dollars, *Dendraster excentricus* (Eschscholtz). J. Exp. Mar. Biol. Ecol. 6, 265-278.
Bloom, N., 1989. Determination of Picogram Levels of Methylmercury by Aqueous Phase Ethylation, Followed by Cryogenic Gas-Chromatography with Cold Vapor Atomic Fluorescence Detection. Can. J. Fish. Aquat. Sci. 46, 1131-1140.
Bloom, N.S., Crecelius, E.A., 1983. Determination of Mercury in Seawater at Sub-Nanogram Per Liter Levels. Mar. Chem. 14, 49-59.
Bluhm, B., Ambrose Jr, W.G., Bergmann, M., Clough, L., Gebruk, A.V., Hasemann, C., Iken, K., Klages, M., MacDonald, I.R., Renaud, P., Schewe, I., Soltwedel, T., Wlodarska-Kowalczuk, M., 2011. Diversity of the arctic deep-sea benthos. Marine Biodiversity 41, 87-107.
Bluhm, B.A., Gradinger, R., 2008. Regional variability in food availability for arctic marine mammals. Ecol. Appl. 18, S77-S96.
Bluhm, B.A., Iken, K., Mincks Hardy, S., Sirenko, B.I., Holladay, B.A., 2009. Community structure of epibenthic megafauna in the Chukchi Sea. Aquatic Biology 7, 269-293.
Boehm, P.D., LeBlanc, L., Trefry, J.H., Marajh-Wittemore, P., Brown, J., Sohutzberg, A., Kick, A., 1990. Monitoring hydrocarbons and trace metals in Beaufort Sea sediments and organisms, final report. OCS Study MMS 90-0054. USDOI, Minerals Management Service, Anchorage, AK.
Boehm, P.D., Steinhauer, M.S., Crecelius, E.A., Neff, J.M., Tuckfield, T., 1987. Analysis of trace metals and hydrocarbons from outer continental shelf (OCS) activities, final report. OCS Study MMS 87-0072. USDOI, Minerals Management Service, Anchorage, AK.
BOEMRE, 2011. Bureau of Ocean Energy Management, Regulation, and Enforcement (BOEMRE) Alaska OCS Region. Chukchi Sea Planning Area: Oil and Gas Lease Sale 193 in Chukchi Sea, Alaska, Revised Draft Supplemental Environmental Impact Statement. OCS EIS/EA BOEMRE 2010-034. U.S. Department of Interior BOEMRE, Anchorage, AK.

Boothe, P.N., Knauer, G.A., 1972. Possible Importance of Fecal Material in Biological Amplification of Trace and Heavy-Metals. Limnol. Oceanogr. 17, 270-274.
Borga, K., Gabrielsen, G.W., Skaare, J.U., 2001. Biomagnification of organochlorines along a Barents Sea food chain. Environ. Pollut. 113, 187-198.
Boucsein, B., Stein, R., 2000. Particulate organic matter in surface sediments of the Laptev Sea (Arctic Ocean): application of maceral analysis as organic-carbon-source indicator. Mar. Geol. 162, 573-586.
Bourassa, N., Morin, A., 1995. Relationships between Size Structure of Invertebrate Assemblages and Trophy and Substrate Composition in Streams. J. N. Am. Benthol. Soc. 14, 393-403.
Brabets, T., Wang, B., Meade, R.H., 2000. Environmental and hydrologic overview of the Yukon River Basin, Alaska and Canada. . U.S. Geological Survey Water Resources Investigations Report, pp. 99-4204.
Bradstreet, M.S.W., Cross, W.E., 1982. Trophic Relationships at High Arctic Ice Edges. Arctic 35, 1-12.
Bradstreet, M.S.W., Finley, K.J., Sekerak, A.D., Griffiths, W.B., Evans, C.R., Fabijan, M.F., Stallard, H.E., 1986. Aspects of the biology of Arctic cod (*Boreogadus saida*) and its importance in Arctic marine food chains. Canadian Technical Report of Fisheries and Aquatic Sciences 1491, 193.
Brown, J.S., Trefry, J.H., Cook, L.L., Boehm, P.D., 2004. ANIMIDA Task 2: Hydrocarbon and metal characterization of sediments, bivalves and amphipods in the ANIMIDA study area, final report. OCS Study MMS 2004-024. USDOI, Minerals Management Service, Anchorage, AK.
Brown, J.S., Trefry, J.H., Cook, L.L., Boehm, P.D., 2010. Continuation of the Arctic nearshore impact monitoring in the development area (cANIMIDA): synthesis, 1999-2007, final report. OCS Study BOEMRE 2010-032. USDOI, Bureau of Ocean Energy Management, Regulation, and Enforcement, Anchorage, Alaska.
Bruland, K.W., Bertine, K., Koide, M., Goldberg, E.D., 1974. History of Metal Pollution in Southern-California Coastal Zone. Environ. Sci. Technol. 8, 425-432.
CAFF, 2001. CAFF (Conservation of Arctic Flora & Fauna) Arctic Flora and Fauna: Status Conservation Edita Helsinki.
Cahoon, L.B., 1999. The role of benthic microalgae in neritic ecosystems, Oceanography and Marine Biology, Vol 37, pp. 47-86.
Calder, W.A., 1984. Size, function, and life history. Harvard University Press, Cambridge, Mass.
Campbell, L.M., Norstrom, R.J., Hobson, K.A., Muir, D.C.G., Backus, S., Fisk, A.T., 2005. Mercury and other trace elements in a pelagic Arctic marine food web (Northwater Polynya, Baffin Bay). Sci. Total Environ. 351, 247-263.
Cardona-Marek, T., Knott, K.K., Meyer, B.E., O'Hara, T.M., 2009. Mercury Concentrations in Southern Beaufort Sea Polar Bears: Variation Based on Stable Isotopes of Carbon and Nitrogen. Environ. Toxicol. Chem. 28, 1416-1424.
Carmack, E., Wassmann, P., 2006. Food webs and physical-biological coupling on pan-Arctic shelves: Unifying concepts and comprehensive perspectives. Prog Oceanogr 71, 446-477.
Cassini, A., Favero, M., Albergoni, V., 1993. Comparative-Studies of Antioxidant Enzymes in Red-Blooded and White-Blooded Antarctic Teleost Fish - Pagothenia-Bernacchii and Chionodraco-Hamatus. Comp Biochem Phys C 106, 333-336.

CFR, 2010. Code of Federal Regulations. Endangered and Threatened Wildlife and Plants; Designation of Critical Habitat for the Polar Bear (*Ursus maritimus*) in the United States. Title 50, Part 17. . U.S. Department of the Interior Fish and Wildlife Service.
Chan, H.M., 1988. Accumulation and Tolerance to Cadmium, Copper, Lead and Zinc by the Green Mussel Perna-Viridis. Mar. Ecol.-Prog. Ser. 48, 295-303.
Chen, C.Y., Dionne, M., Mayes, B.M., Ward, D.M., Sturup, S., Jackson, B.P., 2009. Mercury Bioavailability and Bioaccumulation in Estuarine Food Webs in the Gulf of Maine. Environ. Sci. Technol. 43, 1804-1810.
Chia, F.-S., 1970. Reproduction of Arctic marine invertebrates. Mar. Pollut. Bull. 1, 78-79.
Chow, T.J., Earl, J.L., Reeds, J.H., Hansen, N., Orphan, V., 1978. Barium Content of Marine-Sediments near Drilling Sites - Potential Pollutant Indicator. Mar. Pollut. Bull. 9, 97-99.
Clarke, A., 1983. Life in cold water: the physiological ecology of polar marine ectoderms. Oceanographic Marine Biological Annual Review 21, 341-453.
Clarke, K.R., Gorely, R.N., 2006. PRIMER v. 6: User manual/tutorial, PRIMER-E, Plymouth, UK.
Clarke, K.R., Warwick, R.M., 2001. PRIMER-E, Change in Marine Communities: An Approach to Statistical Analysis and Interpretation, 2nd Ed., Plymouth, UK, p. 172 pp.
Coachman, L.K., Aagaard, K., 1988. Transports through Bering strait: Annual and interannual variability. J. Geophys. Res. 93, 15,535-515,539.
Coachman, L.K., Aagaard, K., Tripp, R.B., 1975. Bering Strait: The regional physical oceanography. University of Washington Press, Seattle.
Codispoti, L.A., Flagg, C., Kelly, V., Swift, J.H., 2005. Hydrographic conditions during the 2002 SBI process experiments. Deep Sea Research Part II: Topical Studies in Oceanography 52, 3199-3226.
Comiso, J.C., 2002. A rapidly declining perennial sea ice cover in the Arctic. Geophysical Research Letters 29, 17-11.
Cooper, L.W., Grebmeier, J.M., Larsen, I.L., Dolvin, S., Reed, A.J., 1998. Inventories and distribution of radiocessium in arctic marine sediments: Influence of biological and physical processes. Chem. Ecol. 15, 27-46.
Cooper, L.W., Grebmeier, J.M., Larsen, I.L., Egorov, V.G., Theodorakis, C., Kelly, H.P., Lovvorn, J.R., 2002. Seasonal variation in sedimentation of organic materials in the St. Lawrence Island polynya region, Bering Sea. Mar. Ecol. Prog. Ser. 226, 13-26.
Cooper, L.W., Grebmeier, J.M., Larsen, I.L., Solis, C., Olsen, C.R., 1995. Evidence for re-distribution of ^{137}Cs in Alaskan tundra, lake, and marine sediments. Sci. Total Environ. 161, 295-306.
Cooper, L.W., Larsen, I.L., Grebmeier, J.M., Moran, S.B., 2005. Detection of rapid deposition of sea ice-rafted material to the Arctic Ocean benthos using the cosmogenic tracer 7Be. Deep Sea Research Part II: Topical Studies in Oceanography 52, 3452-3461.
Coyle, K.O., Cooney, R.T., 1988. Estimating carbon flux to pelagic grazers in the ice-edge zone of the eastern Bering Sea. Mar. Biol. 98, 299-306.
Craig, P.C., Griffiths, W.B., Haldorson, L., Mcelderry, H., 1982. Ecological-Studies of Arctic Cod (*Boreogadus saida*) in Beaufort Sea Coastal Waters, Alaska. Canadian Journal of Fisheries and Aquatic Sciences 39, 395-406.
Cranwell, P.A., Eglinton, G., Robinson, N., 1987. Lipids of Aquatic Organisms as Potential Contributors to Lacustrine Sediments .2. Org. Geochem. 11, 513-527.

Creager, J.S., McManus, D.A., 1965. Pleistocene drainage patterns on the floor of the Chukchi Sea. Mar. Geol. 3, 279-290.
Curtis, L.R., Garzon, C.B., Arkoosh, M., Collier, T., Myers, M.S., Buzitis, J., Hahn, M.E., 2011. Reduced cytochrome P4501A activity and recovery from oxidative stress during subchronic benzo[a]pyrene and benzo[e]pyrene treatment of rainbow trout. Toxicol. Appl. Pharmacol. 254, 1-7.
Cutshall, N.H., Larsen, I.L., Olsen, C.R., 1983. Direct analysis of 210Pb in sediment: self-absorption corrections. Nuclear Instrument Methods 206, 309-312.
Dayton, P.K., 1990. 12 Polar Benthos. Polar Oceanography Part B, 631-685.
Dayton, P.K., Watson, D., Palmisano, A., Barry, J.P., Oliver, J.S., Rivera, D., 1986. Distribution patterns of benthic microalgal standing stock at McMurdo Sound, Antarctia. Polar Biol. 6, 207-213.
Dehn, L.A., Follmann, E.H., Thomas, D.L., Sheffield, G.G., Rosa, C., Duffy, L.K., O'Hara, T.M., 2006. Trophic relationships in an Arctic food web and implications for trace metal transfer. Science of the Total Environment 362, 103-123.
DeNiro, M., Epstein, S., 1978. Influence of diet on distribution of carbon isotopes in animals. Geochim Cosmochim Ac 42, 495-506.
Devol, A.H., Codispoti, L.A., Christensen, J.P., 1997. Summer and winter denitrification rates in western Arctic shelf sediments. Cont. Shelf Res. 17, 1029-.
Doi, H., Kikuchi, E., Shikano, S., Takagi, S., 2010. Differences in nitrogen and carbon stable isotopes between planktonic and benthic microalgae. Limnology 11, 185-192.
Dubois, S., Orvain, F., Marin-Leal, J.C., Ropert, M., Lefebvre, S., 2007. Small-scale spatial variability of food partitioning between cultivated oysters and associated suspension-feeding species, as revealed by stable isotopes. Marine Ecology-Progress Series 336, 151-160.
Dunbar, M.J., 1968. Ecological development in polar regions; a study in evolution. Concepts of modern biology series, viii, 119 p.
Dunton, K.H., Goodall, J.L., Schonberg, S.V., Grebmeier, J.M., Maidment, D.R., 2005. Multi-decadal synthesis of benthic-pelagic coupling in the western arctic: Role of cross-shelf advective processes. Deep Sea Research Part II: Topical Studies in Oceanography 52, 3462-3477.
Dunton, K.H., Schell, D.M., 1987. Dependence of Consumers on Macroalgal (Laminaria-Solidungula) Carbon in an Arctic Kelp Community - Delta-C-13 Evidence. Mar. Biol. 93, 615-625.
Eggens, M.L., Galgani, F., 1992. Ethoxyresorufin-O-Deethylase (Erod) Activity in Flatfish - Fast Determination with a Fluorescence Plate-Reader. Mar. Environ. Res. 33, 213-221.
Eicken, H., Gradinger, R., Gaylord, A., Mahoney, A., Rigor, I., Melling, H., 2005. Sediment transport by sea ice in the Chukchi and Beaufort Seas: Increasing importance due to changing ice conditions? Deep Sea Research Part II: Topical Studies in Oceanography 52, 3281-3302.
ESRI, 2010. ArcGIS Resource Center: Data Models. http://resources.arcgis.com/content/data-models.
ESRI, 2011. What is GIS? http://www.esri.com/what-is-gis/index.html.
Fabry, V.J., Seibel, B.A., Feely, R.A., Orr, J.C., 2008. Impacts of ocean acidification on marine fauna and ecosystem processes. ICES Journal of Marine Science: Journal du Conseil 65, 414-432.

Fanelli, E., Cartes, J.E., Badalamenti, F., Rumolo, P., Sprovieri, M., 2009. Trophodynamics of suprabenthic fauna on coastal muddy bottoms of the southern Tyrrhenian Sea (western Mediterranean). Journal of Sea Research 61, 174-187.
Farmer, J.G., Lovell, M.A., 1986. Natural Enrichment of Arsenic in Loch Lomond Sediments. Geochim. Cosmochim. Acta 50, 2059-2067.
Feder, H.M., 1967. Organisms responsive to predatory sea stars. Sarsia 29, 371-394.
Feder, H.M., Foster, N.R., Jewett, S.C., Weingartner, T.J., Baxter, R., 1994a. Mollusks in the northeastern Chukchi Sea. Arctic 47, 145-163.
Feder, H.M., Iken, K., Blanchard, A.L., Jewett, S.C., Schonberg, S., 2011. Benthic food web structure in the southeastern Chukchi Sea: an assessment using 13 C and 15 N analyses. Polar Biology 34, 1-12.
Feder, H.M., Jewett, S.C., 1980. A survey of the epifaunal invertebrates of the southeastern Bering Sea with notes on the feeding biology of selected species. University of Alaska, Institute of Marine Science, Fairbanks, Alaska.
Feder, H.M., Jewett, S.C., 1981. Feeding interactions in the eastern Bering Sea with emphasis on the benthos, in: Hood, D.W., Calder, J.A. (Eds.), The Eastern Bering Sea Shelf: Oceanography and Resources. University of Washington Press, Seattle, pp. 1229-1261.
Feder, H.M., Jewett, S.C., Blanchard, A., 2005. Southeastern chukchi sea (Alaska) epibenthos. Polar Biol. 28, 402-421.
Feder, H.M., Jewett, S.C., Blanchard, A.L., 2007. Southeastern Chukchi Sea (Alaska) macrobenthos. Polar Biol. 30, 261-275.
Feder, H.M., Jewett, S.C., University of Alaska Fairbanks. Institute of Marine Science, 1981. Distribution, abundance, community structure and trophic relationships of the nearshore epibenthos of the Kodiak continental shelf. Institute of Marine Science, University of Alaska, Fairbanks.
Feder, H.M., Naidu, A.S., Jewett, S.C., Hameedi, J.M., Johnson, W.R., Whitledge, T.E., 1994b. The northeastern Chukchi Sea: Benthos-environmental interactions. Mar. Ecol. Prog. Ser. 111, 171-190.
Feely, R.A., 1981. Distribution and elemental composition of suspended matter in Alaskan coastal waters. National Oceanic and Atmospheric Administration, Environmental Research Laboratories, Pacific Marine Environmental Laboratory, Seattle, Washington.
Field, L.J., MacDonald, D.D., Norton, S.B., Ingersoll, C.G., Severn, C.G., Smorong, D., Lindskoog, R., 2002. Predicting amphipod toxicity from sediment chemistry using logistic regression models. Environ. Toxicol. Chem. 21, 1993-2005.
Field, L.J., MacDonald, D.D., Norton, S.B., Severn, C.G., Ingersoll, C.G., 1999. Evaluating sediment chemistry and toxicity data using logistic regression modeling. Environ. Toxicol. Chem. 18, 1311-1322.
Fisher, K.I., Stewart, R.E.A., 1997. Summer foods of Atlantic walrus, Odobenus rosmarus rosmarus, in northern Foxe basin, northwest territories. Canadian Journal of Zoology-Revue Canadienne De Zoologie 75, 1166-1175.
Fisk, A.T., Hobson, K.A., Norstrom, R.J., 2001. Influence of chemical and biological factors on trophic transfer of persistent organic pollutants in the northwater polynya marine food web. Environ. Sci. Technol. 35, 732-738.
Fisk, A.T., Hoekstra, P.F., Gagnon, J.M., Duffe, J., Norstrom, R.J., Hobson, K.A., Kwan, M., Muir, D.C.G., 2003. Influence of habitat, trophic ecology and lipids on, and spatial trends

of, organochlorine contaminants in Arctic marine invertebrates. Marine Ecology-Progress Series 262, 201-214.
Fitzgerald, W.F., Engstrom, D.R., Mason, R.P., Nater, E.A., 1998. The case for atmospheric mercury contamination in remote areas. Environ. Sci. Technol. 32, 1-7.
Fitzgerald, W.F., Lamborg, C.H., Hammerschmidt, C.R., 2007. Marine biogeochemical cycling of mercury. Chem Rev 107, 641-662.
Folk, R.L., 1974. Petrology of sedimentary rocks Hemphill Publishing Co, Austin, Texas.
Foresman, T.W., 1998. History of Geographic Information Systems: Perspectives from the Pioneers. Prentice Hall PTR.
France, R.L., 1995. Carbon-13 enrichment in benthic compared to planktonic algae: foodweb implications. Mar. Ecol. Prog. Ser. 124, 307-312.
Frederich, M., Sartoris, F.J., Arntz, W.E., Portner, H.O., 2000. Haemolymph Mg2+ regulation in decapod crustaceans: Physiological correlates and ecological consequences in polar areas. J. Exp. Biol. 203, 1383-1393.
French, B.L., Reichert, W.L., Hom, T., Nishimoto, M., Sanborn, H.R., Stein, J.E., 1996. Accumulation and dose-response of hepatic DNA adducts in English sole (Pleuronectes vetulus) exposed to a gradient of contaminated sediments. Aquat. Toxicol. 36, 1-16.
Frost, K.J., Lowry, L.F., United States. National Marine Fisheries Service, United States. National Oceanic and Atmospheric Administration, 1983. Demersal fishes and invertebrates traweled in the northeastern Chukchi and western Beaufort Seas, 1976-77. National Oceanic and Atmospheric Administration, National Marine Fisheries Service, [Seattle, Wash.].
Fry, B., Sherr, E.B., 1984. $\delta^{13}C$ measurements as indicators of carbon flow in marine and freshwater ecosystems. Contributions in Marine Science 27, 13-47.
Gardner, W.S., McCarthy, M.J., An, S.M., Sobolev, D., Sell, K.S., Brock, D., 2006. Nitrogen fixation and dissimilatory nitrate reduction to ammonium (DNRA) support nitrogen dynamics in Texas estuaries. Limnol. Oceanogr. 51, 558-568.
Gardner, W.S., McCarthy, M.J., Carini, S.A., Souza, A.C., Lijun, H., McNeal, K.S., Puckett, M.K., Pennington, J., 2009. Collection of intact sediment cores with overlying water to study nitrogen- and oxygen-dynamics in regions with seasonal hypoxia. Cont. Shelf Res. 29, 2207-2213.
Gattuso, J.P., Gentili, B., Duarte, C.M., Kleypas, J.A., Middelburg, J.J., Antoine, D., 2006. Light availability in the coastal ocean: impact on the distribution of benthic photosynthetic organisms and their contribution to primary production. Biogeosciences 3, 489-513.
Gautier, D.L., Bird, K.J., Charpentier, R.R., Grantz, A., Houseknecht, D.W., Klett, T.R., Moore, T.E., Pitman, J.K., Schenk, C.J., Schuenemeyer, J.H., Sorensen, K., Tennyson, M.E., Valin, Z.C., Wandrey, C.J., 2009. Assessment of Undiscovered Oil and Gas in the Arctic. Science 324, 1175-1179.
George, S.G., Christiansen, J.S., Killie, B., Wright, J., 1995. Dietary Crude-Oil Exposure during Sexual-Maturation Induces Hepatic Mixed-Function Oxygenase (Cyp1a) Activity at Very-Low Environmental Temperatures in Polar Cod Boreogadus-Saida. Mar. Ecol.-Prog. Ser. 122, 307-312.
Giger, W., Schaffner, C., Wakeham, S.G., 1980. Aliphatic and Olefinic Hydrocarbons in Recent Sediments of Greifensee, Switzerland. Geochim. Cosmochim. Acta 44, 119-129.
Gillespie, J.G., Smith, R.L., Barbour, E., Barber, W.E., 1997. Distribution, abundance, and growth of Arctic cod in the Northeastern Chukchi Sea, in: Reynolds, J. (Ed.), Fish

Ecology in Arctic North America. American Fisheries Society Symposium, Bethesda, MD, pp. 81–89.
Glud, R.N., Kuhl, M., Wenzhofer, F., Rysgaard, S., 2002. Benthic diatoms of a high Arctic fjord (Young Sound, NE Greenland): importance for ecosystem primary production. Marine Ecology-Progress Series 238, 15-29.
Gobeil, C., MacDonald, R.W., Sundby, B., 1997. Diagenetic separation of cadmium and manganese in suboxic continental margin sediments. Geochim. Cosmochim. Acta 61, 4647-4654.
Goñi, M.A., Yunker, M.B., Macdonald, R.W., Eglinton, T.I., 2000. Distribution and sources of organic biomarkers in arctic sediments from the Mackenzie River and Beaufort Shelf. Mar. Chem. 71, 23-51.
Gosselin, M., Levasseur, M., Wheeler, P.A., Horner, R.A., Booth, B.C., 1997. New measurements of phytoplankton and ice algal production in the Arctic Ocean. Deep-Sea Res. Part II-Top. Stud. Oceanogr. 44, 1623-1644.
Gradinger, R., 2009. Sea-ice algae: Major contributors to primary production and algal biomass in the Chukchi and Beaufort Seas during May/June 2002, Deep-Sea Research Part II, pp. 1201-1212.
Graf, G., 1989. Benthic Pelagic Coupling in a Deep-Sea Benthic Community. Nature 341, 437-439.
Graf, G., 1992. Benthic-Pelagic Coupling: A Benthic View. Oceanogrpahy Marine Biology Annual 30, 149-190.
Grantz, A., Dinter, D.A., Hill, E.R., Hunter, R.E., May, S.D., McMullen, R.H., Philips, R.L., 1982. Geologic framework, hydrocarbon potential and environmental conditions for exploration and development of proposed oil and gas lease sale 85 in the central and northern Chukchi Sea - A Summary Report. U.S. Geological Survey Open-File Report, p. 1053.
Grebmeier, J.M., 1992. Benthic processes on the shallow continental shelf, in: Nagel, P.A. (Ed.), Results of the Third Joint US-USSR Bering & Chukchi Sea Expedition (BERPAC), Summer 1988. US Fish and Wildlife Service, Washington, DC, pp. 243-251.
Grebmeier, J.M., 2012. Shifting Patterns of Life in the Pacific Arctic and Sub-Arctic Seas. Annual Review of Marine Science 4, 63-78.
Grebmeier, J.M., Barry, J.P., 1991. The influence of oceanographic processes on pelagic-benthic coupling in polar regions: A benthic perspective. J. Mar. Syst. 2, 495-518.
Grebmeier, J.M., Barry, J.P., 2007. Benthic Processes in Polynyas, in: Barber, W.O.S.a.D. (Ed.), Polynyas: Windows to the World. Elsevier, Amsterdam, pp. 363-390.
Grebmeier, J.M., Cooper, L.W., 1995. Influence of the St. Lawrence Island Polynya upon the Bering Sea Benthos. Journal of Geophysical Research 100, 4439-4460.
Grebmeier, J.M., Cooper, L.W., Feder, H.M., Sirenko, B.I., 2006a. Ecosystem dynamics of the Pacific-influenced Northern Bering and Chukchi Seas in the Amerasian Arctic. Progress in Oceanography 71, 331-361.
Grebmeier, J.M., Cooper, L.W., Feder, H.M., Sirenko, B.I., 2006b. Ecosystem dynamics of the Pacific-influenced northern Bering, Chukchi, and East Siberian Seas. Prog. Oceanogr. 71, 331-361.
Grebmeier, J.M., Dunton, K.H., 2000. Benthic processes in the Northern Bering/Chukchi Seas: Status and Global Change, in: Huntington, H.P. (Ed.), Impacts of Changes in Sea Ice and

Other Environmental Parameters in the Arctic, Marine Mammal Commission Workshop, Girdwood, Alaska, 15-17 February 2000, pp. 80-93.
Grebmeier, J.M., Feder, H.M., McRoy, C.P., 1989a. Pelagic-benthic coupling on the shelf of the northern Bering and Chukchi Seas. II. Benthic communitv structure. Marine Ecology Progress Series 51, 253-268.
Grebmeier, J.M., Feder, H.M., McRoy, C.P., 1989b. Pelagic-benthic coupling on the shelf of the northern Bering and Chukchi Seas. II. Benthic community structure. Mar. Ecol. Prog. Ser. 51, 253-268.
Grebmeier, J.M., Harvey, R.H., 2005. The Western Arctic Shelf-Basin Interactions (SBI) project: An overview. Deep Sea Research Part II: Topical Studies in Oceanography 52, 3109-3115.
Grebmeier, J.M., McRoy, C.P., 1989. Pelagic-benthic coupling on the shelf of the northern Bering and Chukchi Seas. III. Benthic food supply and carbon cycling. Marine Ecology - Progress Series 53, 79-91.
Grebmeier, J.M., McRoy, C.P., Feder, H.M., 1988. Pelagic-Benthic Coupling on the Shelf of the Northern Bering and Chukchi Seas .1. Food-Supply Source and Benthic Biomass. Mar. Ecol.-Prog. Ser. 48, 57-67.
Grebmeier, J.M., Moore, S.E., Overland, J.E., Frey, K.E., Gradinger, R., 2010. Biological response to recent Pacific Arctic sea ice retreats. Trans. AGU (EOS) 91, 161-168.
Grebmeier, J.M., Overland, J.E., Moore, S.E., Farley, E.V., Carmack, E.C., Cooper, L.W., Frey, K.E., Helle, J.H., McLaughlin, F.A., McNutt, S.L., 2006c. A major ecosystem shift in the northern Bering Sea. Science 311, 1461-1464.
Grebmeier, J.M., Smith, W.O., Jr., Conover, R.B., 1995. Biological Processes on Arctic Continental Shelves: Ice-Ocean-Biotic Interactions, in: Smith, W.O., Jr., Grebmeier, J.M. (Eds.), Arctic Oceanography: Marginal Ice Zones and Continental Shelves, Washington, DC, pp. 231-261.
Grippo, M.A., Fleeger, J.W., Dubois, S.F., Condrey, R., 2011. Spatial variation in basal resources supporting benthic food webs revealed for the inner continental shelf. Limnology and Oceanography 56, 841-856.
Guay, C.K., Falkner, K., 1997. Barium as a tracer of Arctic halocline and river waters. Deep-Sea Res II 44, 1543-1569.
Gunderson, D.R., Ellis, I.E., 1986. Development of a Plumb Staff Beam Trawl for Sampling Demersal Fauna. Fisheries Research 4, 35-41.
Halbach, P., Blum, N., Munch, U., Pluger, W., Garbe-Schonberg, D., Zimmer, M., 1998. Formation and decay of a modern massive sulfide deposit in the Indian ocean. Miner Deposita 33, 302-309.
Halpin, P.N., Read, A.J., Best, B.D., Hyrenbach, K.D., Fujioka, E., Coyne, M.S., Crowder, L.B., Freeman, S.A., Spoerri, C., 2006. OBIS-SEAMAP: developing a biogeographic research data commons for the ecological studies of marine mammals, seabirds, and sea turtles. Mar. Ecol.-Prog. Ser. 316, 239-246.
Halsall, C.J., Barrie, L.A., Fellin, P., Muir, D.C.G., Billeck, B.N., Lockhart, L., Rovinsky, F.Y., Kononov, E.Y., Pastukhov, B., 1997. Spatial and temporal variation of polycyclic aromatic hydrocarbons in the Arctic atmosphere. Environ. Sci. Technol. 31, 3593-3599.
Hammerschmidt, C.R., Fitzgerald, W.F., Lamborg, C.H., Balcom, P.H., Visscher, P.T., 2004. Biogeochemistry of methylmercury in sediments of Long Island Sound. Mar. Chem. 90, 31-52.

Hansell, D.A., Goering, J.J., Walsh, J.J., McRoy, C.P., Coachman, L.K., Whitledge, T.E., 1989. Summer phytoplankton production and transport along the shelf break in the Bering Sea. Cont. Shelf. Res. 9, 1085-1104.

Hartl, M.G.J., van Pelt, F.N.A.M., Kilemade, M., Sheehan, D., Mothersill, C., O'Halloran, J., O'Brien, N.M., 2007. Hepatic biomarkers of sediment-associated pollution in juvenile turbot, Scophthalmus maximus L. Mar. Environ. Res. 64, 191-208.

Hecky, R.E., Hesslein, R.H., 1995. Contributions of benthic algae to lake food webs as revealed by stable isotope analysis. Journal of the North American Benthological Society 14, 631-653.

Highsmith, R.C., 1982. Induced Settlement and Metamorphosis of Sand Dollar (*Dendraster excentricus*) Larvae in Predator-Free Sites - Adult Sand Dollar Beds. Ecology 63, 329-337.

Highsmith, R.C., Coyle, K.O., Bluhm, B.A., Konar, B., 2006. Gray Whales in the Bering and Chukchi Seas, in: Estes, J.A., DeMaster, D.P., Doak, D.F., Williams, T.M., Brownell, R.L. (Ed.), Whales, Whaling and Ocean Ecosystems. University of California Press, Berkeley, pp. 303-313.

Hill, V., Cota, G., 2005. Spatial patterns of primary production on the shelf, slope and basin of the Western Arctic in 2002. Deep Sea Research Part II: Topical Studies in Oceanography 52, 3344-3354.

Himmelman, J.H., Dutil, C., 1991. Distribution, Population-Structure and Feeding of Subtidal Seastars in the Northern Gulf of St-Lawrence. Mar. Ecol.-Prog. Ser. 76, 61-72.

Hobson, K.A., Ambrose, W.G., Jr., Renaud, P.E., 1995. Sources of primary production, benthic-pelagic coupling, and trophic relationships within the Northeast Water Polynya: insights from $\delta^{13}C$ and $\delta^{15}N$ analysis. Mar. Ecol. Prog. Ser. 64(1-3), 1-10.

Hobson, K.A., Fisk, A.T., Karnovsky, N., Holst, M., Gagnon, J.-M., Fortier, M., 2002. A stable isotope ($\delta^{13}C$, $\delta^{15}N$) model for the North Water food web: implications for evaluating trophodynamics and the flow of energy and contaminants. Deep Sea Research II 49, 5131-5150.

Hobson, K.A., Welch, H.E., 1992. Determination Of Trophic Relationships Within A High Arctic Marine Food Web Using Delta-C-13 And Delta-N-15 Analysis. Mar Ecol-Prog Ser 84, 9-18.

Holst, M., Stirling, I., Hobson, K.A., 2001. Diet of ringed seals (Phoca hispida) on the east and west sides of the North Water Polynya, northern Baffin Bay. Marine Mammal Science 17, 888-908.

Hop, H., Graham, M., Trudeau, V.L., 1995. Spawning Energetics of Arctic Cod (Boreogadus-Saida) in Relation to Seasonal Development of the Ovary and Plasma Sex Steroid-Levels. Can. J. Fish. Aquat. Sci. 52, 541-550.

Hopkins, D.M., 1967. The Bering Land Bridge. Stanford University Press, Stanford, Calif.,.

Horner, R., Schrader, G.C., 1982. Relative contributions of ice algae, phytoplankton and benthic microalgae to primary production in nearshore regions of the Beaufort Sea. Arctic 35, 485-503.

Horsburgh, J.S., Tarboton, D.G., Maidment, D.R., Zaslavsky, I., 2008. A relational model for environmental and water resources data. Water Resour Res 44.

Iken, K., Bluhm, B., Dunton, K., 2010. Benthic food-web structure under differing water mass properties in the southern Chukchi Sea. Deep-Sea Research Part Ii-Topical Studies in Oceanography 57, 71-85.

IPCC, 2007. Climate change 2007 - The Physical Science Basis (Working Group I. Contribution to the Fourth Assessment Report of the IPCC), Cambridge.
Jaeger, I., Hop, H., Gabrielsen, G.W., 2009. Biomagnification of mercury in selected species from an Arctic marine food web in Svalbard. Sci. Total Environ. 407, 4744-4751.
Jewett, S.C., Feder, H.M., 1980. Autumn food of adult starry flounder *Platichthys stellatus* from the NE Bering Sea and the SE Chukchi Sea. Journal of Cons. Int. Explor. Mer. 39, 7-14.
Jewett, S.C., Feder, H.M., 1981. Epifaunal invertebrates of the continental shelf of the eastern Bering Sea and Chukchi Seas, in: Hood, D.W., Calder, J.A. (Eds.), The Eastern Bering Sea Shelf: Oceanography and Resources. University of Washington Press, Seattle, pp. 1131-1154.
Jones, M.C., Yu, Z.C., 2010. Rapid deglacial and early Holocene expansion of peatlands in Alaska. Proceedings of the National Academy of Sciences of the United States of America 107, 7347-7352.
Jonsson, H., Sundt, R.C., Aas, E., Sanni, S., 2010. The Arctic is no longer put on ice: Evaluation of Polar cod (*Boreogadus saida*) as a monitoring species of oil pollution in cold waters. Mar. Pollut. Bull. 60, 390-395.
Kalkreuth, W., Keuser, C., Fowler, M., Li, M., Mcintyre, D., Puttmann, W., Richardson, R., 1998. The petrology, organic geochemistry and palynology of Tertiary age Eureka Sound Group coals, Arctic Canada. Org. Geochem. 29, 799-809.
Kanneworff, E., Nicolaisen, W., 1973. The "HAPS:" A frame supported bottom corer. Ophelia Supplement 10, 119-129.
Kaufman, M.R., Gradinger, R.R., Bluhm, B.A., O'Brien, D.M., 2008. Using stable isotopes to assess carbon and nitrogen turnover in the Arctic sympagic amphipod Onisimus litoralis. Oecologia 158, 11-22.
Kawamura, K., Suzuki, I., Fujii, Y., Watanabe, O., 1994. Ice Core Record of Polycyclic Aromatic-Hydrocarbons over the Past 400 Years. Naturwissenschaften 81, 502-505.
Knoblauch, C., Jorgensen, B.B., 1999. Effect of temperature on sulphate reduction, growth rate and growth yield in five psychrophilic sulphate-reducing bacteria from Arctic sediments. Environ. Microbiol. 1, 457-467.
Kuhl, M., Glud, R.N., Borum, J., Roberts, R., Rysgaard, S., 2001. Photosynthetic performance of surface-associated algae below sea ice as measured with a pulse-amplitude-modulated (PAM) fluorometer and O-2 microsensors. Marine Ecology-Progress Series 223, 1-14.
Kuznetsov, L.L., 2002. Production of phytocenoses and transformation of nutrients in ecosystem of the Barents Sea. Shirshov Institute of Ocenaography, Moscow.
Laurier, F.J.G., Mason, R.P., Gill, G.A., Whalin, L., 2004. Mercury distributions in the North Pacific Ocean - 20 years of observations. Mar. Chem. 90, 3-19.
Lavoie, R.A., Hebert, C.E., Rail, J.F., Braune, B.M., Yumvihoze, E., Hill, L.G., Lean, D.R.S., 2010. Trophic structure and mercury distribution in a Gulf of St. Lawrence (Canada) food web using stable isotope analysis. Sci. Total Environ. 408, 5529-5539.
Lee, S.H., Whitledge, T.E., Kang, S.H., 2007. Recent carbon and nitrogen uptake rates of phytoplankton in Bering Strait and the Chukchi Sea. Cont. Shelf Res. 27, 2231-2249.
Leitch, D.R., Stern, G.A., Carrie, J., Lean, D., Macdonald, R.W., Wang, F.Y., 2007. The delivery of mercury to the Beaufort Sea of the Arctic Ocean by the Mackenzie River. Sci. Total Environ. 373, 178-195.
Lepore, K., Moran, S.B., Grebmeier, J.M., Cooper, L.W., Lalande, C., Maslowski, W., Hill, V., Bates, N.R., Hansell, D.A., Mathis, J.T., Kelly, R.P., 2007. Seasonal and interannual

changes in particulate organic carbon export and deposition in the Chukchi Sea. Journal of Geophysical Research-Oceans 112.
Lin, X., McCarthy, M.J., Carini, S.A., Gardner, W.S., 2011. Net, actual, and potential sediment-water interface NH(4)(+) fluxes in the northern Gulf of Mexico (NGOMEX): Evidence for NH(4)(+) limitation of microbial dynamics. Cont. Shelf Res. 31, 120-128.
Livingstone, D.R., 2003. Oxidative stress in aquatic organisms in relation to pollution and aquaculture. Rev. Med. Vet. 154, 427-430.
Livingstone, D.R., Archibald, S., Chipman, J.K., Marsh, J.W., 1992. Antioxidant Enzymes in Liver of Dab *Limanda limanda* from the North-Sea. Mar. Ecol.-Prog. Ser. 91, 97-104.
Long, E.R., Macdonald, D.D., Smith, S.L., Calder, F.D., 1995. Incidence of Adverse Biological Effects within Ranges of Chemical Concentrations in Marine and Estuarine Sediments. Environ. Manage. 19, 81-97.
Long, E.R., Morgan, L.G., 1990. The potential for biological effects of sediment-sorbed contaminants tested in the National Status and Trends Program, NOAA technical memorandum NOS OMA ; 52. U.S. Dept. of Commerce, National Oceanic and Atmospheric Administration, National Ocean Service, Seattle, Wash., pp. United States. National Ocean Service, National Status and Trends Program (U.S.),.
Lovvorn, J.R., Richman, S.E., Grebmeier, J.M., Cooper, L.W., 2003. Diet and body condition of spectacled elders wintering in pack ice of the Bering Sea. Polar Biol. 26, 259-267.
Lowry, F.L., Frost, K.J., 1981. Feeding and trophic relationships of phocid seals and walruses in the eastern Bering Sea, in: Hood, D.W., Calder, F.D. (Eds.), The Eastern Bering Sea Shelf: Oceanography and Resources. University of Washington Press, Seattle, WA, pp. 813-824.
Luengen, A.C., Flegal, A.R., 2009. Role of phytoplankton in mercury cycling in the San Francisco Bay estuary. Limnol. Oceanogr. 54, 23-40.
MacDonald, D.D., Carr, R.S., Calder, F.D., Long, E.R., Ingersoll, C.G., 1996. Development and evaluation of sediment quality guidelines for Florida coastal waters. Ecotoxicology 5, 253-278.
Macdonald, R.W., Harner, T., Fyfe, J., 2005. Recent climate change in the Arctic and its impact on contaminant pathways and interpretation of temporal trend data. Science Of The Total Environment 342, 5-86.
Macdonald, R.W., Solomon, S.M., Cranston, R.E., Welch, H.E., Yunker, M.B., Gobeil, C., 1998. A sediment and organic carbon budget for the Canadian Beaufort Shelf. Mar. Geol. 144, 255-273.
MacGinitie, G.E., 1955. Distribution and ecology of the marine invertebrates of Point Barrow, Alaska. Smithsonian Institution, Washington.
MacIntosh, R.A., Somerton, D.A., 1981. Large marine gastropods of the eastern Bering Sea, in: Hood, D.W., Calder, J.A. (Eds.), The Eastern Bering Sea Shelf : oceanography and resources. U.S. Dept. of Commerce, National Oceanic and Atmospheric Administration, Distributed by the University of Washington Press, Rockville, Maryland, pp. 1215-1228.
Maidment, D.R., 2002. Arc Hydro: GIS for Water Resources. ESRI Press, Redlands, CA.
Maidment, D.R., 2009. CUAHSI Hydrologic Information System: 2009 Status Report. http://his.cuahsi.org/documents/HISOverview2009.pdf.
Malins, D.C., 1977. Biotransformation of petroleum hydrocarbons in marine organisms indigenous to the Arctic and Sub-Arctic, in: Wollie, D.A. (Ed.), Fate and Effects of

Petroleum Hydrocarbons in Marine Organisms and Ecosystems. Pergamon, New York, pp. 47-59.
Manabe, S., Stouffer, R., Spelman, M., Bryan, K., 1991. Transient responses of a coupled ocean-atmosphere model to gradual changes of atmospheric CO2. Part I. Annual mean response. Journal of Climate 4, 785-818.
Martinez-Gomez, C., Vethaak, A.D., Hylland, K., Burgeot, T., Kohler, A., Lyons, B.P., Thain, J., Gubbins, M.J., Davies, I.M., 2010. A guide to toxicity assessment and monitoring effects at lower levels of biological organization following marine oil spills in European waters. ICES J. Mar. Sci. 67, 1105-1118.
Masclet, P., Hoyau, V., 1994. Evidence for the Presence of Polycyclic Aromatic-Hydrocarbons in the Polar Atmosphere and in Polar Ice. Analusis 22, M31-M33.
Mason, R.P., Lawrence, A.L., 1999. Concentration, distribution, and bioavailability of mercury and methylmercury in sediments of Baltimore Harbor and Chesapeake Bay, Maryland, USA. Environ. Toxicol. Chem. 18, 2438-2447.
Matheke, G.E.M., Horner, R., 1974. Primary productivity of the benthic microalgae in the Chukchi Sea near Barrow, Alaska. J. Fish. Res. Bd. Canada 31, 1779-1786.
Mathis, J.T., Bates, N.R., Hansell, D.A., Babila, T., 2009. Net community production in the northeastern Chukchi Sea. Deep-Sea Res. Part II-Top. Stud. Oceanogr. 56, 1213-1222.
Mayer, M., Piepenburg, D., 1996. Epibenthic community patterns on the continental slope off East Greenland at 75° N. Marine Ecology-Progress Series 143, 151-164.
McConnaughey, T., McRoy, C.P., 1979. C-13 Label Identifies Eelgrass (Zostera-Marina) Carbon in an Alaskan Estuarine Food Web. Mar. Biol. 53, 263-269.
McCord, J.M., Fridovich, I., 1969. Superoxide Dismutase an Enzymic Function for Erythrocuprein (Hemocuprein). J. Biol. Chem. 244, 6049-&.
McGee, D., Laws, R.A., Cahoon, L.B., 2008. Live benthic diatoms from the upper continental slope: extending the limits of marine primary production. Marine Ecology-Progress Series 356, 103-112.
McMahon, K.W., Ambrose, W.G., Johnson, B.J., Sun, M.Y., Lopez, G.R., Clough, L.M., Carroll, M.L., 2006. Benthic community response to ice algae and phytoplankton in Ny Alesund, Svalbard. Mar. Ecol.-Prog. Ser. 310, 1-14.
McManus, D.A., Kelley, J.C., Creager, J.S., 1969. Continental Shelf Sedimentation in an Arctic Environment. Geol Soc Am Bull 80, 1961.
Menard, H., Smith, S., 1966. Hypsometry of Ocean Basin Provinces. J Geophys Res 71, 4305-4325.
Meyers, P.A., Ishiwatari, R., 1993. Lacustrine Organic Geochemistry - an Overview of Indicators of Organic-Matter Sources and Diagenesis in Lake-Sediments. Org. Geochem. 20, 867-900.
Milner, N.J., 1982. The Accumulation of Zinc by O-Group Plaice, Pleuronectes-Platessa (L), from High-Concentrations in Sea-Water and Food. J. Fish Biol. 21, 325-336.
Mitchelmore, C.L., Chipman, J.K., 1998a. Detection of DNA strand breaks in brown trout (Salmo trutta) hepatocytes and blood cells using the single cell gel electrophoresis (comet) assay. Aquat. Toxicol. 41, 161-182.
Mitchelmore, C.L., Chipman, J.K., 1998b. DNA strand breakage in aquatic organisms and the potential value of the comet assay in environmental monitoring. Mutat. Res.-Fundam. Mol. Mech. Mutag. 399, 135-147.

MMS, 2006. Minerals Management Services (MMS) Alaska OCS Region: Undiscovered oil and gas resources Alaska Federal Offshore 2006 National Assessment. Department of the Interior, MMS, Anchorage, AK.
MMS, 2008a. Final Notice of Sale (FNOS) Outer Continental Shelf (OCS), Oil and Gas Lease Sale 193, Chukchi Sea. 73 Federal Register 1, pp. 209-213.
MMS, 2008b. MMS Chukchi Sea Lease Sale 193 Breaks Energy Records With $2.6 Billion in High Bids. http://www.alaska.boemre.gov/latenews/newsrel/News Releases 2008/News Release - 193 results _2_.pdf, News Release.
Moran, S.B., Kelly, R.P., Hagstrom, K., Smith, J.N., Grebmeier, J.M., Cooper, L.W., Cota, G.F., Walsh, J.J., Bates, N.R., Hansell, D.A., 2005. Seasonal changes in POC export flux in the Chukchi Sea and implications for water column-benthic coupling in Arctic shelves. Deep Sea Research Part II: Topical Studies in Oceanography 52, 3427-3451.
Muhaya, B.B.M., Leermakers, M., Baeyens, W., 1997. Total mercury and methylmercury in sediments and in the polychaete *Nereis diversicolor* at Groot Buitenschoor (Scheldt estuary, Belgium). Water Air Soil Poll 94, 109-123.
Muir, D., Braune, B., DeMarch, B., Norstrom, R., Wagemann, R., Lockhart, L., Hargrave, B., Bright, D., Addison, R., Payne, J., Reimer, K., 1999. Spatial and temporal trends and effects of contaminants in the Canadian Arctic marine ecosystem: a review. Science Of The Total Environment 230, 83-144.
Mull, C.G., 1995. Preliminary evaluation of the hydrocarbon source rock potential of the Tingmerkpuk sandstone (Neocomian) and related rocks, northwestern De Long Mountains, Brooks Range, Alaska. Public Data File 95-30. State of Alaska, Dept. of Natural Resources, Div.of Geological and Geophysical Surveys, Fairbanks, AK.
Nacci, D.E., Cayula, S., Jackim, E., 1996. Detection of DNA damage in individual cells from marine organisms using the single cell gel assay. Aquat. Toxicol. 35, 197-210.
Nahrgang, J., Camus, L., Carls, M.G., Gonzalez, P., Jonsson, M., Taban, I.C., Bechmann, R.K., Christiansen, J.S., Hop, H., 2010a. Biomarker responses in polar cod (*Boreogadus saida*) exposed to the water soluble fraction of crude oil. Aquat. Toxicol. 97, 234-242.
Nahrgang, J., Camus, L., Gonzalez, P., Goksoyr, A., Christiansen, J.S., Hop, H., 2009. PAH biomarker responses in polar cod (*Boreogadus saida*) exposed to benzo(a)pyrene. Aquat. Toxicol. 94, 309-319.
Nahrgang, J., Jonsson, M., Camus, L., 2010b. EROD activity in liver and gills of polar cod (*Boreogadus saida*) exposed to waterborne and dietary crude oil. Mar. Environ. Res. 70, 120-123.
Naidu, A., 1988. Marine surficial sediments, Bering, Chukchi, and Beaufort Seas Strategic Assessment: Data Atlas NOAA, US Department of Commerce, Rockville, Maryland.
Naidu, A.S., Blanchard, A., Kelley, J.J., Goering, J.J., Hameed, M.J., Baskaran, M., 1997. Heavy metals in Chukchi Sea sediments as compared to selected circum-arctic shelves. Mar. Pollut. Bull. 35, 260-269.
Naidu, A.S., Creager, J.S., Mowatt, T.C., 1982. Clay Mineral Dispersal Patterns in the North Bering and Chukchi Seas. Mar. Geol. 47, 1-15.
Naidu, A.S., Goering, J.J., Kelley, J.J., Venkatesan, M.I., 2001. Historical changes in trace metals and hydrocarbons in the inner shelf sediments, Beaufort Sea: Prior and subsequent to petroleum-related industrial developments, final report. OCS Study MMS 2001-061. University of Alaska Coastal Marine Institute, University of Alaska Fairbanks and USDOI, MMS, Alaska OCS Region.

Naidu, A.S., Kelley, J.J., Goering, J.J., Venkatesan, M.I., 2003. Trace metals and hydrocarbons in sediments of Elson Lagoon (Barrow, Northwest Arctic Alaska) as related to the Prudhoe Bay Industrial Region, final report. OSC Study MMS 2003-057
. University of Alaska Costal Marine Institute, University of Alaska Fairbanks and USDOI, MMS, Alaska OCS Region.
Nakashima, S., Sturgeon, R.E., Willie, S.N., Berman, S.S., 1988. Determination of Trace-Elements in Sea-Water by Graphite-Furnace Atomic-Absorption Spectrometry after Preconcentration by Tetrahydroborate Reductive Precipitation. Anal. Chim. Acta 207, 291-299.
NCAR-EOL, 2011. National Center for Atmospheric Research Earth Observing Laboratory, http://www.eol.ucar.edu/.
Neff, J.M., 2002a. Bioaccumulation in marine organisms : effect of contaminants from oil well produced water. Elsevier, Amsterdam Boston.
Neff, J.M., 2002b. Polycyclic aromatic hydrocarbons in the ocean, Bioaccumulation in marine organisms : effect of contaminants from oil well produced water. Elsevier, Amsterdam Boston, pp. 241-313.
Neff, J.M., Boehm, P.D., Kropp, R., Stubblefield, W.A., Page, D.S., 2003. Monitoring recovery of Prince William Sound, Alaska, following the Exxon Valdez oil spill: Bioavailability of PAH in offshore sediments, Proceedings of the 2003 International Oil Spill Conference. , American Petroleum Institute, Washington, DC.
Neff, J.M., Durell, G.S., Trefry, J.H., Brown, J.S., 2010. Environmental studies in the Chukchi Sea 2008: Chemical Characterization, Report to ConocoPhillips Alaska.
Nelson-Smith, A., 1973. Oil pollution and marine ecology. Plenum Press, New York.
NODC, 2011. National Oceanographic Data Center, http://www.nodc.noaa.gov/.
NRC, 2003. National Research Council. Oil in the Sea: Inputs, fates, and effects., Washington, DC.
O'Connor, T.P., 2004. The sediment quality guideline, ERL, is not a chemical concentration at the threshold of sediment toxicity. Mar. Pollut. Bull. 49, 383-385.
Olsvik, P.A., Lie, K.K., Goksoyr, A., Midtun, T., Frantzen, S., Maage, A., 2009. Are Atlantic Cod in Store Lungegrdsvann, a Seawater Recipient in Bergen, Affected by Environmental Contaminants? A qRT-PCR Survey. J Toxicol Env Heal A 72, 140-154.
Oremland, R.S., Culbertson, C.W., Winfrey, M.R., 1991. Methylmercury Decomposition in Sediments and Bacterial Cultures - Involvement of Methanogens and Sulfate Reducers in Oxidative Demethylation. Appl. Environ. Microbiol. 57, 130-137.
Ortiz, J.D., Polyak, L., Grebmeier, J.M., Darby, D., Eberl, D.D., Naidu, S., Nof, D., 2009. Provenance of Holocene sediment on the Chukchi-Alaskan margin based on combined diffuse spectral reflectance and quantitative X-Ray Diffraction analysis. Global Planet. Change 68, 71-84.
Oudot, J., Fusey, P., Vanpraet, M., Feral, J.P., Gaill, F., 1981. Hydrocarbon Weathering in Seashore Invertebrates and Sediments over a 2-Year Period Following the Amoco-Cadiz Oil-Spill - Influence of Microbial-Metabolism. Environ Pollut A 26, 93-110.
Outridge, P.M., Macdonald, R.W., Wang, F., Stern, G.A., Dastoor, A.P., 2008. A mass balance inventory of mercury in the Arctic Ocean. Environ Chem 5, 89-111.
Pachauri, R.K., Reisinger, A., 2007. Climate Change 2007: Synthesis Report. Contribution of Working Groups I, II and III to the Fourth Assessment Report of the Intergovernmental Panel on Climate Change. . PICC, Geneva, Switzerland.

Pacyna, J., 2005. AMAP Assessent 2002: heavy metals in the Arctic. Oslo: Arctic Monitoring and Assessment Program, 5-10.
Patton, G.W., Walla, M.D., Bidleman, T.F., Barrie, L.A., 1991. Polycyclic Aromatic and Organochlorine Compounds in the Atmosphere of Northern Ellesmere-Island, Canada. Journal of Geophysical Research-Atmospheres 96, 10867-10877.
Paul, J.M., Paul, A.J., Barber, W.E., 1997. Reproductive biology and distribution of the snow crab from the northeastern Chukchi Sea, in: Reynolds, J.B. (Ed.), American Fisheries Society Symposium; Fish ecology in arctic North America, pp. 287-294.
Pawson, D.L., 1983. *Ocnus sacculus* new species (Echinodermata: Holothuroidea), a brood-protecting holothurian from southeastern New Zealand. New Zealand Journal of Marine and Freshwater Research 17, 227-230.
Pearce, J.B., Thorson, G., 1967. The feeding and reproductive biology fo the red whelk, *Neptunea antiqua* (L.) (Gastropods, Prosobrnachia). Ophelia 4, 227-213.
Perovich, D.K., Light, B., Eicken, H., Jones, K.F., Runciman, K., Nghiem, S.V., 2007. Increasing solar heating of the Arctic Ocean and adjacent seas, 1979-2005: Attribution and role in the ice-albedo feedback. Geophys. Res. Lett. 34.
Peters, R.H., 1983. The ecological implications of body size. Cambridge University Press, Cambridge Cambridgeshire ; New York.
Phillips, R.L., 1984. Nearshore marine geologic investigations, Icy Cape to Wainwright, northeast Chukchi Sea [microform] / by R. Lawrence Phillips and Thomas E. Reiss. U.S. Dept. of the Interior, Geological Survey, [Reston, Va.?] :.
Pickart, R.S., Weingartner, T.J., Pratt, L.J., Zimmermann, S., Torres, D.J., 2005. Flow of winter-transformed Pacific water into the Western Arctic. Deep Sea Research Part II: Topical Studies in Oceanography 52, 3175-3198.
Piepenburg, D., 2000. Arctic brittle stars (echinodermata: ophiuroidea). Oceanogr Mar Biol 38, 189-256.
Piepenburg, D., 2005. Recent research on Arctic benthos: common notions need to be revised. Polar Biol. 28, 733-755.
Piepenburg, D., Ambrose, W.G., Brandt, A., Renaud, P.E., Ahrens, M.J., Jensen, P., 1997. Benthic community patterns reflect water column processes in the Northeast Water polynya (Greenland). J. Mar. Syst. 10, 467-482.
Piepenburg, D., Blackburn, T.H., Vondorrien, C.F., Gutt, J., Hall, P.O.J., Hulth, S., Kendall, M.A., Opalinski, K.W., Rachor, E., Schmid, M.K., 1995. Partitioning of Benthic Community Respiration in the Arctic (Northwestern Barents Sea). Mar. Ecol.-Prog. Ser. 118, 199-213.
Piepenburg, D., Chernova, N.V., vonDorrien, C.F., Gutt, J., Neyelov, A.V., Rachor, E., Saldanha, L., Schmid, M.K., 1996. Megabenthic commmunities in the waters around Svalbard. Polar Biol. 16, 431-446.
Piepenburg, D., Schmid, M.K., 1996a. Brittle star fauna (Echinodermata: Ophiuroidea) of the Arctic northwestern Barents Sea: Composition, abundance, biomass and spatial distribution. Polar Biol. 16, 383-392.
Piepenburg, D., Schmid, M.K., 1996b. Distribution, abundance, biomass, and mineralization potential of the epibenthic megafauna of the Northeast Greenland shelf. Marine Biology Berlin 125, 321-332.

Piepenburg, D., Schmid, M.K., 1997. A photographic survey of the epibenthic megafauna of the Arctic Laptev Sea shelf: Distribution, abundance, and estimates of biomass and organic carbon demand. Mar. Ecol.-Prog. Ser. 147, 63-75.

Pirtle-Levy, R., Grebmeier, J.M., Cooper, L.W., Larsen, I.L., 2009. Seasonal variation of chlorophyll a in Arctic sediments implies long persistence of plant pigments. Deep-Sea Research 56, 1326–1338.

Ponomarenko, V.P., 1968. Some data on the distribution and migration of polar cod in the seas of the Soviet Arctic. ICES Rapp P-V Re'un 158, 131-134.

Post, D., 2002. Using stable isotopes to estimate trophic position: Models, methods, and assumptions. Ecology 83, 703-718.

Rajasekar, A., Wan, M., Moore, R.M., 2009. Event Processing in Policy Oriented Data Grids. Proceedings of Intelligent Event Processing AAAI Spring Symposium, Stanford, California, pp. 61-66.

Rajasekar, A., Wan, M., Moore, R.M., Schroeder, W., 2006. A Prototype Rule-based Distributed Data Management System., HPDC workshop on "Next Generation Distributed Data Management", Paris, France.

Rasmussen, J.B., Rowan, D.J., Lean, D.R.S., Carey, J.H., 1990. Food-Chain Structure in Ontario Lakes Determines PCB Levels In Lake Trout (*Salvelinus-Namaycush*) and Other Pelagic Fish. Canadian Journal Of Fisheries And Aquatic Sciences 47, 2030-2038.

Renaud, P.E., Morata, N., Ambrose, W.G., Bowie, J.J., Chiuchiolo, A., 2007. Carbon cycling by seafloor communities on the eastern Beaufort Sea shelf. Journal of Experimental Marine Biology and Ecology 349, 248-260.

Reynaud, S., Deschaux, P., 2006. The effects of polycyclic aromatic hydrocarbons on the immune system of fish: A review. Aquat Toxicol 77, 229-238.

Rice, S., Korn, S., Karinen, J., 1980. Lethal and sublethal effects on selected Alaskan marine species after acute and long-term exposure to oil and oil components. NOAA/ERL Outer Continental Shelf Environmental Assessment Program, Final Reports of Principal Investigators 3, 1-12.

Roach, A.T., Aagaard, K., Pease, C.H., Salo, S.A., Weingartner, T., Pavlov, V., Kulakov, M., 1995. Direct measurements of transport and water properties through the Bering Strait. Journal of Geophysical Research 100, 18,443-418,457.

Robins, C.R., Bailey, R.M., Bond, C.E., Brooker, J.R., Lachner, E.A., Lea, R.N., Scott, W.B., 1980. A list of common and scientific names of fishes from the United States and Canada, 4th Edition, 5th ed. American Fisheries Society, Bethesda, MD.

Ross, D.J., Johnson, C.R., Hewitt, C.L., 2002. Impact of introduced seastars Asterias amurensis on survivorship of juvenile commercial bivalves Fulvia tenuicostata. Mar. Ecol.-Prog. Ser. 241, 99-112.

Roy, K., Jablonski, D., Martien, K.K., 2000. Invariant size-frequency distributions along a latitudinal gradient in marine bivalves. Proceedings of the National Academy of Sciences of the United States of America 97, 13150-13155.

Roy, L.A., Schlenk, D., Steinert, S., Bay, S.M., Greenstein, D., Sapozhnikova, Y., Bawardi, O., Leifer, I., 2003. Biochemical effects of petroleum exposure in hornyhead turbot (*Pleuronichthys verticalis*) exposed to a gradient of sediments collected from a natural petroleum seep in CA, USA. Aquat. Toxicol. 65, 159-169.

Rysgaard, S., Thamdrup, B., Risgaard-Petersen, N., Fossing, H., Berg, P., Christensen, P.B., Dalsgaard, T., 1998. Seasonal carbon and nutrient mineralization in a high-Arctic coastal

marine sediment, Young Sound, Northeast Greenland. Mar. Ecol.-Prog. Ser. 175, 261-276.
Sakshaug, E., 2004. Primary and secondary production in the Arctic Seas, in: Stein, R., Macdonald, R.W. (Eds.), The Organic Carbon Cycle in the Arctic Ocean. Springer, New York, pp. 57-81.
Sakshaug, E., Slagstad, D., 1991. Light and Productivity of Phytoplankton in Polar Marine Ecosystems - a Physiological View. Polar Res. 10, 69-85.
Salomons, W., Förstner, U., 1984. Metals in the hydrocycle. Springer-Verlag.
SBI, 2008. Shelf Basin Interaction, SBI Data Archive. http://www.eol.ucar.edu/projects/sbi/cruise_summary_info.html.
Scheibling, R.E., 1980. Abundance, spatial-distribution, and size structure of populations of *Oreaster reticulatus* (Echinodermata, Asteroidea) on sand bottoms. Mar. Biol. 57, 95-105.
Schropp, S.J., Lewis, F.G., Windom, H.L., Ryan, J.D., Calder, F.D., Burney, L.C., 1990. Interpretation of Metal Concentrations in Estuarine Sediments of Florida Using Aluminum as a Reference Element. Estuaries 13, 227-235.
Schubert, C.J., Calvert, S.E., 2001. Nitrogen and carbon isotopic composition of marine and terrestrial organic matter in Arctic Ocean sediments: implications for nutrient utilization and organic matter composition. Deep-Sea Research Part I-Oceanographic Research Papers 48, 789-810.
Schwinghamer, P., 1981. Characteristic Size Distributions of Integral Benthic Communities. Can. J. Fish. Aquat. Sci. 38, 1255-1263.
Sheffield, G., Grebmeier, J.M., 2009. Pacific walrus (Odobenus rosmarus divergens): Differential prey digestion and diet. Mar. Mamm. Sci. 25, 761-777.
Sinex, S.A., Cantillo, A.Y., Helz, G.R., 1980. Accuracy of Acid-Extraction Methods for Trace-Metals in Sediments. Anal Chem 52, 2342-2346.
Sirenko, B.I., Gagaev, S.Y., 2007. Unusual abundance of macrobenthos and biological invasions in the Chukchi Sea. Russ J Mar Biol 33, 355-364.
Solomon, S.M., 2005. Spatial and temporal variability of shoreline change in the Beaufort-Mackenzie region, northwest territories, Canada. Geo-Mar. Lett. 25, 127-137.
Solórzano, L., 1969. Determination of Ammonia in Natural Waters by Phenolhypochlorite Method. Limnology and Oceanography 14, 799-801.
Spall, M.A., 2007. Circulation and water mass transformation in a model of the Chukchi Sea. Journal of Geophysical Research-Oceans 112.
Speers-Roesch, B., Ballantyne, J.S., 2005. Activities of antioxidant enzymes and cytochrome c oxidase in liver. of Arctic and temperate teleosts. Comp Biochem Phys A 140, 487-494.
Sprague, J.B., Vandermeulen, J.H., Wells, P.G., 1981. Oil and Dispersants in Canadian Seas - Recommendations from a Research Appraisal. Mar Pollut Bull 12, 45-46.
Springer, A.M., McRoy, C.P., 1993. The paradox of pelagic food webs in the northern Bering Sea III. Patterns of primary production. Cont. Shelf Res. 13, 575-600.
Springer, A.M., McRoy, C.P., Flint, M.V., 1996. The Bering Sea Green Belt: Shelf-edge processes and ecosystem production. Fish. Oceanogr. 5, 205-223.
Starczak, V.R., Fuller, C.M., Butman, C.A., 1992. Effects of Barite on Aspects of the Ecology of the Polychaete Mediomastus-Ambiseta. Mar. Ecol.-Prog. Ser. 85, 269-282.
Stegeman, J.J., Hahn, M.E., 1994. Biochemistry and molecular biology of monooxygenases: Current directions in forms, functions, and regulation of cytochrome P450 in aquatic

species, in: Malins, D.C., Ostrander, G.K. (Eds.), Aquatic Toxicology: Molecular, Biochemical and Cellular Perspectives. Lewis Publishers, Boca Raton, FL, pp. 87-206.
Stegeman, J.J., Pajor, A.M., Thomas, P., 1982. Influence of estradiol and testosterone on cytochrome-P-450 and monooxygenase activity in immature Brook Trout, *Salvelinus fontinalis*. Biochem. Pharmacol. 31, 3979-3989.
Stein, R., Nam, S.I., Schubert, C., Vogt, C., Futterer, D., Heinemeier, J., 1994. The Last Deglaciation Event in the Eastern Central Arctic-Ocean. Science 264, 692-696.
Steinhauer, M.S., Boehm, P.D., 1992. The composition and distribution of saturated and aromatic hydrocarbons in nearshore sediments, river sediments, and coastal peat of the Alaskan Beaufort Sea: Implications for detecting anthropogenic hydrocarbon inputs. Mar. Environ. Res. 33, 223-253.
Stewart, P.L., Pocklington, P., Cunjak, R.A., 1985. Distribution, abundance and diversity of benthic macroinvertebrates on the Canadian continental shelf and slope of Southern Davis Strait and Ungava Bay. Arctic 38, 281-291.
Stoker, S.W., 1978. Benthic invertebrate macrofauna of the eastern continental shelf of the Bering/Chukchi Seas. University of Alaska Fairbanks.
Stoker, S.W., 1981. Benthic invertebrate macrofauna of the eastern Bering/Chukchi continental shelf, in: Hood, D.W., Calder, J.A. (Eds.), The Eastern Bering Sea Shelf: Oceanography and Resources. University of Washington Press, Seattle, pp. 1069-1091.
Stroeve, J., Holland, M.M., Meier, W., Scambos, T., Serreze, M., 2007. Arctic sea ice decline: Faster than forecast. Geophys. Res. Lett. 34.
Stroeve, J.C., Serreze, M.C., Fetterer, F., Arbetter, T., Meier, W., Maslanik, J., Knowles, K., 2005. Tracking the Arctic's shrinking ice cover: Another extreme September minimum in 2004. Geophys. Res. Lett. 32, L04501, doi:10.1029/2004GL021810.
Suchanek, T.H., 1993. Oil Impacts on Marine Invertebrate Populations and Communities. Am Zool 33, 510-523.
Sun, M.-Y., Carroll, M.L., Ambrose, W.G., Clough, L.M., Zou, L., Lopez, G.R., 2007. Rapid consumption of phytoplankton and ice algae by Arctic soft-sediment benthic communities: Evidence using natural and C-13-labeled food materials. J Mar Res 65, 561-588.
Sun, M.-Y., Clough, L.M., Carroll, M.L., Dai, J., Jr, W.G.A., Lopez, G.R., 2009. Different responses of two common Arctic macrobenthic species (Macoma balthica and Monoporeia affinis) to phytoplankton and ice algae: Will climate change impacts be species specific?, Journal of Experimental Marine Biology and Ecology, pp. 110-121.
Szakacs, O., Lasztity, A., Horvath, Z., 1980. Breakdown of Organic Mercury-Compounds by Hydrochloric Acid-Permanganate or Bromine Monochloride Solution for the Determination of Mercury by Cold-Vapor Atomic-Absorption Spectrometry. Anal. Chim. Acta 121, 219-224.
Taylor, K.A., Harvey, H.R., 2011. Bacterial hopanoids as tracers of organic carbon sources and processing across the western Arctic continental shelf. Org. Geochem. 42, 487-497.
Thain, J.E., Vethaak, A.D., Hylland, K., 2008. Contaminants in marine ecosystems: developing an integrated indicator framework using biological-effect techniques. ICES J. Mar. Sci. 65, 1508-1514.
Thomann, R.V., Mahony, J.D., Mueller, R., 1995. Steady-State Model of Biota Sediment Accumulation Factor for Metals in 2 Marine Bivalves. Environ. Toxicol. Chem. 14, 1989-1998.

Tolosa, I., de Mora, S., 2004. Isolation of neutral and acidic lipid biomarker classes for compound-specific-carbon isotope analysis by means of solvent extraction and normal-phase high-performance liquid chromatography. J. Chromatogr. 1045, 71-84.
Tomil, L.J., Grantz, A., 1976. Origin of a Bergfield at Hanna Shoal, northeastern Chukchi Sea, and its influence on the sedimentary environment. AIDJEX (Arctic Ice Dynamics Joint Experiment) Bulletin 34, 1-42.
Trefry, J.H., Metz, S., Trocine, R.P., Nelsen, T.A., 1985. A Decline in Lead Transport by the Mississippi River. Science 230, 439-441.
Trefry, J.H., Presley, B.J., 1976. Heavy-Metals in Sediments from San Antonio Bay and Northwest Gulf of Mexico. Environmental Geology 1, 283-294.
Trefry, J.H., Presley, B.J., 1982. Manganese Fluxes from Mississippi Delta Sediments. Geochim. Cosmochim. Acta 46, 1715-1726.
Trefry, J.H., Rember, R.D., Trocine, R.P., Brown, J.S., 2003. Trace metals in sediments near offshore oil exploration and production sites in the Alaskan Arctic. Environmental Geology 45, 149-160.
Trefry, J.H., Trocine, R.P., McElvaine, M.L., Rember, R.D., Hawkins, L.T., 2007. Total mercury and methylmercury in sediments near offshore drilling sites in the Gulf of Mexico. Environmental Geology 53, 375-385.
Trefry, J.H., Trocine, R.P., Naito, K.L., Metz, S., 1996. Assessing the potential for enhanced bioaccumulation of heavy metals from produced water discharges to the Gulf of Mexico. Envir Sci R 52, 339-354.
Tuo, J.C., Simoneit, B.R.T., Wang, X.B., Chen, J.F., 2003. Aliphatic and diterpenoid hydrocarbons and their individual carbon isotope compositions in coals from the Liaohe Basin, China. Org. Geochem. 34, 1615-1625.
Turkmen, G., Kazanci, N., 2010. Applications of various diversity indices to benthic macroinvertebrate assemblages in streams of a natural park in Turkey. Unpublished report. Hacettepe University, Turkey.
van der Oost, R., Beyer, J., Vermeulen, N.P.E., 2003. Fish bioaccumulation and biomarkers in environmental risk assessment: a review. Environ. Toxicol. Pharmacol. 13, 57-149.
Vander Zanden, M., Rasmussen, J., 2001. Variation in delta N-15 and delta C-13 trophic fractionation: Implications for aquatic food web studies. Limnol Oceanogr 46, 2061-2066.
von Quillfeldt, C.H., Ambrose, W.G., Clough, L.M., 2003. High number of diatom species in first-year ice from the Chukchi Sea. Polar Biol. 26, 806-818.
Vonk, J.E., Gustafsson, O., van Dongen, B.E., 2008. Lipid biomarker investigation of the origin and diagenetic state of sub-arctic terrestrial organic matter presently exported into the northern Bothnian Bay. Mar. Chem. 112, 1-10.
Wainwright, P.F., Humphrey, B., 1984. Analysis of sediment data from the Beaufort Shorebase Monitoring Program, 1982-1984.
Wakeham, S., Farrington, J., 1980. Hydrocarbons in contemporary aquatic sediments, in: Baker, R.A. (Ed.), Contaminants and Sediments, Volume 1. Ann Arbor Science.
Wakeham, S.G., 1990. Algal and Bacterial Hydrocarbons in Particulate Matter and Interfacial Sediment of the Cariaco Trench. Geochim. Cosmochim. Acta 54, 1325-1336.
Walker, C.H., Hopkin, S.P., Sibly, R.M., Peakall, D.B., 2006. Principles of Ecotoxicology, 3 ed. CRC Press, Boca Raton.

Walsh, J.J., McRoy, C.P., Coachman, L.K., Goering, J.J., Nihoul, J.J., Whitledge, T.E., Blackburn, T.H., Parker, P.L., Wirick, C.D., Shuert, P.G., Grebmeier, J.M., Springer, A.M., Tripp, R.D., Hansell, D.A., Djenidi, S., Deleersnijder, E., Henricksen, K., Lund, B.A., Andersen, P., Müller-Karger, F.E., Dean, K., 1989. Carbon and nitrogen cycling within the Bering/Chukchi Seas: Source regions for organic matter effecting AOU demands of the Arctic Ocean. Prog. Oceanogr. 22, 277-359.

Wang, W.X., Ke, C.H., 2002. Dominance of dietary intake of cadmium and zinc by two marine predatory gastropods. Aquat. Toxicol. 56, 153-165.

Wedepohl, K.H., 1995. The Composition of the Continental-Crust. Geochim. Cosmochim. Acta 59, 1217-1232.

Weingartner, T., Aagaard, K., Woodgate, R., Danielson, S., Sasaki, Y., Cavalieri, D., 2005. Circulation on the north central Chukchi Sea shelf. Deep Sea Research Part II: Topical Studies in Oceanography 52, 3150-3174.

Weingartner, T.J., Cavalieri, D.J., Aagaard, K., Sasaki, Y., 1998. Circulation, dense water formation, and outflow on the northeast Chukchi shelf. Journal of Geophysical Research 103, 7647-7661.

Welch, H.E., Muir, D.C.G., Billeck, B.N., Lockhart, W.L., Brunskill, G.J., Kling, H.J., Olson, M.P., Lemoine, R.M., 1991. Brown Snow - a Long-Range Transport Event in the Canadian Arctic. Environ. Sci. Technol. 25, 280-286.

White, D., Kimerling, J., Overton, S., 1992. Cartographic and geometric components of a global sampling design for environmental monitoring. Cartography and Geographic Information Systems.

White, S.L., Rainbow, P.S., 1982. Regulation and Accumulation of Copper, Zinc and Cadmium by the Shrimp Palaemon-Elegans. Mar. Ecol.-Prog. Ser. 8, 95-101.

Whyte, J.J., Tillitt, D.E., Jung, R.E., Schmitt, C.J., 2000. Ethoxyresorufin-O-deethylase (EROD) activity in fish as a biomarker of chemical exposure. Crit. Rev. Toxicol. 30, 347-570.

Willis, J.N., Sunda, W.G., 1984. Relative Contributions of Food and Water in the Accumulation of Zinc by 2 Species of Marine Fish. Mar. Biol. 80, 273-279.

Winsor, P., Chapman, D.C., 2004. Pathways of Pacific Water across the Chukchi Sea: A numerical model study. Journal of Geophysical Research-Oceans 109, 109, C03002, doi:03010.01029/02003JC001962.

Woodgate, R.A., Aagaard, K., Weingartner, T.J., 2005. A year in the physical oceanography of the Chukchi Sea: Moored measurements from autumn 1990-1991. Deep Sea Research Part II: Topical Studies in Oceanography 52, 3116-3149.

Woodgate, R.A., Aagaard, K., Weingartner, T.J., 2006. Interannual changes in the Bering Strait fluxes of volume, heat and freshwater between 1991 and 2004. Geophys. Res. Lett 33, L15609, doi:15610.11029/12006GL026931, 022006

Wright, D.J., Blongewicz, M.J., Halpin, P.N., Breman, J., 2007. Arc Marine: GIS for a Blue Planet. ESRI Press, Redlands, CA.

Wulff, A., Iken, K., Quartino, M.L., Al-Handal, A., Wiencke, C., Clayton, M.N., 2009. Biodiversity, biogeography and zonation of marine benthic micro- and macroalgae in the Arctic and Antarctic. Botanica Marina 52, 491-507.

Xiao, L., Zhu, L., Lin, X., Wang, Y., Wang, J., Xie, M., Ju, J., Maubacher, R., Schwalb, A., 2008. Environmental changes reflected by n-alkanes of lake core in Nam Co on the Tibetan Plateau since 8.4 kaBP. Chin. Sci. Bull. 53, 3051-3057.

Yamamoto, M., Okino, T., Sugisaki, S., Sakamoto, T., 2008. Late Pleistocene changes in terrestrial biomarkers in sediments from the central Arctic Ocean. Org. Geochem. 39, 754-763.

Young, M.L., 1977. Roles of Food and Direct Uptake from Water in Accumulation of Zinc and Iron in Tissues of Dogwhelk, Nucella-Lapillus (L). J. Exp. Mar. Biol. Ecol. 30, 315-325.

Yunker, M.B., Backus, S.M., Graf Pannatier, E., Jeffries, D.S., Macdonald, R.W., 2002. Sources and significance of alkane and PAH hydrocarbons in Canadian arctic rivers. Estuar Coast Shelf S 55, 1-31.

Yunker, M.B., Belicka, L.L., Harvey, H.R., Macdonald, R.W., 2005. Tracing the inputs and fate of marine and terrigenous organic matter in Arctic Ocean sediments: A multivariate analysis of lipid biomarkers. Deep Sea Research Part II: Topical Studies in Oceanography 52, 3478-3508.

Yunker, M.B., MacDonald, R.W., 1995. Composition and origins of polycyclic aromatic hydrocarbons in the Mackenzie River and on the Beaufort Sea shelf. Arctic 48, 118-129.

Yunker, M.B., Macdonald, R.W., Cretney, W.J., Fowler, B.R., Mclaughlin, F.A., 1993. Alkane, Terpene, and Polycyclic Aromatic Hydrocarbon Geochemistry of the Mackenzie River and Mackenzie Shelf - Riverine Contributions to Beaufort Sea Coastal Sediment. Geochim. Cosmochim. Acta 57, 3041-3061.

Yunker, M.B., Macdonald, R.W., Snowdon, L.R., Fowler, B.R., 2011. Alkane and PAH biomarkers as tracers of terrigenous organic carbon in Arctic Ocean sediments. Org. Geochem. 42, 1109-1146.

Yunker, M.B., Snowdon, L.R., MacDonald, R.W., Smith, J.N., Fowler, M.G., Skibo, D.N., McLaughlin, F.A., Danyushevskaya, A.I., Petrova, V.I., Ivanov, G.I., 1996. Polycyclic aromatic hydrocarbon composition and potential sources for sediment samples from the Beaufort and Barents Seas. Environmental Science and Technology 30, 1310-1320.

Appendix 1

Concentrations (**ng g^{-1} wt**) of individual polycyclic aromatic hydrocarbons (PAHs) in surface sediments (0-1 cm) from the Chukchi shef collected during COMIDA09 and COMIDA10

Station Code	**1**	**2**	**3**	**4**	**5**	**6**	**7**	**8**	**9**	**10**	**11**	**12**	**13**	**14**	**15**	**16**	**17**	**19**
Latitude (N)	69°02.380'	69°30.126'	69°49.747'	70°01.383'	70°24.285'	70°20.706'	70°28.122'	70°17.233'	70°49.881'	70°40.275'	70°43.965'	70°41.833'	70°44.803'	70°38.490'	71°01.089'	70°55.151'	71°04.636'	71°01.669'
Longitude (W)	166°35.608'	167°40.513'	165°29.974'	163°45.670'	164°28.940'	165°27.024'	166°05.168'	167°26.609'	167°47.204'	167°04.990'	165°59.800'	165°26.437'	164°10.534'	162°15.976'	164°15.281'	165°25.232'	166°10.708'	166°57.162'
2-Methylnapthalene	86.3	15.0	9.1	0.0	5.7	14.1	0.0	1.2	2.9	9.7	1.0	3.8	17.5	1.0	4.4	8.0	15.4	14.2
1-Methylnapthalene	62.9	9.9	8.3	0.0	7.0	10.4	1.8	2.9	5.3	7.4	2.4	4.8	13.2	2.7	5.5	5.8	11.6	9.5
Biphenyl	19.4	5.9	5.2	1.1	1.5	5.1	3.6	5.0	7.7	4.5	4.0	4.9	6.5	3.6	6.3	3.1	6.4	6.3
2,7-Dimethylnapthalene	29.4	3.1	7.5	1.8	9.0	2.2	9.1	14.5	33.9	1.6	7.9	9.7	2.9	4.8	11.3	1.2	2.5	2.0
1,3-Dimethylnapthalene	27.7	16.8	4.8	0.3	4.3	11.3	0.0	0.0	0.0	12.6	0.0	0.0	20.2	0.0	0.0	3.4	26.4	13.2
1,6-Dimethylnapthalene	66.7	12.4	14.6	1.8	12.3	12.3	8.1	9.5	10.9	9.4	7.4	9.5	14.6	7.3	11.4	5.9	12.7	11.2
1,5-Dimethylnapthalene	63.5	11.1	12.3	1.5	10.1	10.2	7.1	8.8	9.7	7.0	6.0	7.9	12.2	5.6	9.0	5.6	10.2	9.1
1,4-Dimethylnapthalene	31.9	6.0	6.7	1.0	5.7	4.8	4.0	4.0	4.4	4.4	3.8	4.3	6.7	3.3	5.3	2.1	6.0	5.2
1,2-Dimethylnapthalene	14.8	0.0	2.5	0.4	2.5	2.6	1.9	2.9	7.3	0.0	1.9	1.4	2.6	1.2	2.1	1.9	2.7	2.2
1,8-Dimethylnapthalene	12.7	2.4	2.8	0.3	2.3	2.1	1.9	1.9	2.1	1.6	1.6	1.8	2.6	1.3	2.1	1.0	2.3	2.0
Fluorene	5.1	2.3	2.5	0.6	1.9	1.5	1.5	2.3	3.7	1.0	1.6	1.2	2.2	1.2	2.3	0.7	2.1	1.9
2,3,5-Trimethylnapthalene	25.4	3.4	5.2	0.8	4.5	3.9	3.8	4.9	6.4	3.5	2.8	3.1	4.8	2.3	3.7	1.8	4.0	4.1
1-Methylfluorene	13.7	4.0	4.6	5.2	10.8	2.7	13.3	13.7	16.7	4.0	5.3	8.0	5.2	5.9	12.4	1.7	11.2	12.2
1,4,5,8-Tetramethylnapthalene	19.4	3.3	3.9	3.1	7.1	2.7	7.6	7.1	11.4	3.3	3.8	5.2	4.5	3.9	8.1	1.6	8.6	8.4
Dibenzothiophene	19.1	4.5	5.4	9.1	18.6	3.5	23.6	22.1	30.9	6.6	9.8	14.3	7.4	11.9	22.6	1.9	21.3	26.2
Phenanthrene	129.5	21.1	39.5	43.8	88.0	13.1	115.2	118.7	167.7	23.1	53.2	56.1	35.2	46.6	96.3	5.6	87.4	94.1
2-Methyldibenzothiophene	56.6	7.5	10.5	32.0	62.7	6.1	84.3	89.3	104.9	13.5	29.1	45.3	16.0	35.1	79.2	4.6	72.3	74.1
4-Methyldibenzothiophene	34.2	2.3	7.8	22.3	37.7	1.9	51.5	46.8	62.4	3.6	17.8	26.3	3.7	21.8	46.4	1.2	22.4	23.0
2-Methylphenanthrene	74.1	10.5	17.5	40.1	71.8	9.2	80.8	87.7	115.0	16.2	39.4	42.6	18.5	38.8	86.8	6.0	79.5	87.8
2-Methylanthracene	97.6	13.2	25.6	53.8	93.6	11.2	101.8	116.3	152.4	17.6	52.0	54.9	20.6	47.5	105.2	8.0	86.8	83.8
1-Methylanthracene	110.3	13.0	20.3	65.6	111.6	12.1	126.7	151.2	179.9	24.0	53.9	72.4	28.9	63.8	144.0	9.0	135.0	144.3
1-Methylphenanthrene	86.5	9.8	17.9	50.3	84.2	10.3	89.8	110.1	130.3	17.0	39.9	51.2	19.7	43.2	99.6	7.2	88.3	97.3
3,6-Dimethylphenanthrene	14.8	11.9	0.0	7.0	13.0	10.0	15.3	23.2	34.7	20.0	5.2	-1.6	22.2	1.3	11.4	7.8	133.0	128.3
9,10-Dimethylanthracene	14.1	6.2	2.3	8.3	13.3	5.1	14.5	22.1	29.4	10.0	9.1	4.9	10.6	4.1	12.4	4.2	69.0	69.6
Fluoranthene	27.0	2.2	13.1	8.8	22.5	0.0	22.0	20.1	37.2	1.1	22.4	12.2	2.0	9.2	20.7	0.0	8.5	8.3
Pyrene	51.3	14.9	17.4	21.5	46.9	4.7	53.4	49.6	62.9	8.9	27.8	25.1	11.6	21.5	61.3	2.4	44.3	48.8
Retene	43.5	6.1	8.4	1.9	10.1	8.1	6.7	14.8	14.0	8.1	6.5	4.6	8.5	8.2	8.4	4.0	10.1	9.0
Benzo[b]fluorene	10.6	2.6	2.8	1.7	4.8	2.3	4.4	4.1	6.5	2.1	3.3	2.4	2.9	8.7	5.8	1.5	5.2	5.3
Benz[a]anthracene	6.5	1.3	1.6	0.3	1.6	1.5	1.0	1.3	2.0	1.2	1.3	1.2	1.7	1.1	1.5	0.8	1.5	1.3
Chrysene	6.5	2.5	2.9	0.9	3.4	3.0	2.3	2.4	3.3	2.2	2.4	2.7	3.6	2.1	3.4	1.9	3.4	3.1
Napthacene/Benz[b]anthracene	12.6	4.0	3.4	0.7	4.1	4.1	2.7	3.0	4.1	3.0	2.7	2.7	5.2	2.6	3.6	2.3	3.4	3.7
4-Methylchrysene	3.6	2.1	1.1	0.2	1.0	2.0	0.7	0.8	1.0	1.3	0.7	0.8	2.4	0.6	1.2	1.0	1.9	1.9
Benzo[a]pyrene	14.3	5.0	4.4	0.8	6.3	6.0	4.0	4.1	5.1	4.6	4.7	4.2	7.5	3.6	5.9	4.3	5.7	5.5
Perylene	46.7	47.3	22.5	3.1	36.0	42.1	28.4	35.7	36.6	41.7	29.1	33.9	57.0	19.7	48.1	31.5	50.6	50.3
TOTAL PAH (ng g^{-1} wt)	**1338.4**	**283.4**	**314.2**	**390.2**	**816.0**	**241.9**	**892.9**	**1002.1**	**1302.8**	**295.7**	**460.0**	**521.8**	**400.8**	**435.6**	**947.4**	**148.9**	**1051.7**	**1067.3**
TOTAL Parent PAHs (ng g^{-1} wt)	348.5	113.5	120.6	92.4	235.6	86.9	262.2	268.4	367.7	100.0	162.3	160.9	142.7	131.8	277.7	55.9	239.8	254.8
TOTAL Alkyl-PAHs (ng g^{-1} wt)	989.9	169.9	193.6	297.8	580.5	155.0	630.7	733.7	935.1	195.7	297.6	360.9	258.1	303.8	669.7	93.0	811.9	812.4

Appendix 1

Concentrations (**ng g^{-1} wt**) of individual polycyclic aromatic hydrocarbons (PAHs) in surface sediments (0-1 cm) from the Chukchi shef collected during COMIDA09 and COMIDA10 (continued)

Station Code	**20**	**21**	**22**	**23**	**24**	**25**	**26**	**27**	**28**	**29**	**30**	**31**	**32**	**34**	**35**	**36**	**37**	**38**
Latitude (N)	71°12.399'	71°29.079'	71°16.328'	71°23.228'	71°14.952'	71°14.549'	71°04.641'	70°54.512'	71°12.492'	71°17.891'	71°27.180'	71°22.732'	71°23.759'	71°40.587'	71°40.150'	71°55.815'	72°02.744'	71°55.614'
Longitude (W)	168°18.676'	167°46.900'	167°00.865'	166°16.588'	165°26.871'	163°55.317'	162°33.503'	160°44.450'	161°53.392'	161°41.321'	162°36.643'	164°42.710'	164°06.542'	166°26.627'	166°55.039'	167°23.351'	166°20.404'	165°09.650'
2-Methylnapthalene	17.3	16.0	13.2	14.8	9.0	12.8	14.4	10.4	25.4	1.8	16.5	13.3	9.1	16.4	14.0	12.9	10.5	10.8
1-Methylnapthalene	12.5	10.6	9.0	11.4	6.6	8.6	10.5	8.2	21.1	2.0	12.9	10.8	7.5	12.8	10.8	9.8	8.3	8.3
Biphenyl	7.3	8.7	7.4	6.3	3.4	5.6	8.4	4.9	10.4	3.3	9.8	4.4	3.4	7.3	6.1	6.1	4.3	4.5
2,7-Dimethylnapthalene	4.9	2.1	2.3	1.7	1.7	2.2	2.6	1.8	4.2	1.4	2.9	1.9	1.5	2.7	2.3	2.1	1.7	1.6
1,3-Dimethylnapthalene	62.3	32.6	16.7	20.3	27.6	15.9	20.3	16.5	41.1	15.0	72.5	21.6	17.0	24.7	36.0	14.0	19.0	9.7
1,6-Dimethylnapthalene	15.7	13.9	12.8	14.0	7.4	11.9	14.5	9.6	22.9	10.7	15.4	11.1	8.1	14.2	12.4	10.6	9.2	8.6
1,5-Dimethylnapthalene	14.4	12.1	11.6	10.1	7.1	8.7	11.3	6.9	19.4	10.9	14.9	10.6	8.0	12.1	10.6	9.3	9.4	7.8
1,4-Dimethylnapthalene	5.3	6.3	4.9	6.6	3.5	5.8	6.5	4.4	11.0	4.4	7.1	3.7	2.5	5.6	5.1	4.6	2.9	3.4
1,2-Dimethylnapthalene	12.5	4.1	3.1	2.3	2.5	0.0	2.6	2.7	6.8	5.0	7.4	4.1	3.8	3.2	4.0	2.8	4.6	2.7
1,8-Dimethylnapthalene	2.9	2.7	2.5	1.3	1.2	2.2	2.4	1.9	4.2	2.8	2.7	1.8	1.4	2.6	2.3	2.0	2.3	1.7
Fluorene	4.0	2.8	1.9	2.5	1.4	2.3	4.0	1.2	4.0	2.8	2.8	2.7	2.1	3.6	3.1	2.6	2.4	1.7
2,3,5-Trimethylnapthalene	5.6	5.5	4.4	4.3	2.4	3.5	5.6	2.2	7.3	3.7	5.0	3.5	3.2	4.7	3.8	4.0	3.3	2.7
1-Methylfluorene	7.5	20.1	14.0	12.0	4.4	9.1	29.9	6.8	14.0	6.8	11.9	4.9	4.8	6.3	6.5	7.1	5.1	5.4
1,4,5,8-Tetramethylnapthalene	4.9	13.6	9.5	9.2	3.6	6.8	18.6	4.7	10.5	5.0	8.3	3.6	3.3	4.9	5.0	5.5	3.9	4.1
Dibenzothiophene	8.4	39.1	26.1	25.1	7.9	17.6	52.5	12.5	24.5	10.6	22.3	7.2	4.8	11.2	13.5	12.7	6.4	9.4
Phenanthrene	39.4	146.5	116.4	85.3	28.8	77.6	251.3	54.2	112.4	44.5	93.4	35.6	24.5	51.4	57.8	58.3	24.0	37.7
2-Methyldibenzothiophene	15.5	116.7	91.0	78.6	24.6	57.4	233.7	49.3	84.6	23.2	76.3	19.8	12.3	35.3	41.3	45.7	14.8	33.2
4-Methyldibenzothiophene	10.4	37.2	28.5	25.5	6.6	19.4	77.0	15.1	23.8	6.5	21.8	5.8	4.6	10.6	14.5	16.3	4.3	11.7
2-Methylphenanthrene	16.8	130.7	94.9	74.1	23.3	68.2	238.6	45.4	85.0	23.0	79.6	23.3	13.2	38.7	44.6	45.5	13.6	35.4
2-Methylanthracene	20.3	164.3	113.5	78.1	28.4	72.8	307.1	51.4	106.7	30.7	97.6	29.7	18.5	47.9	56.3	57.1	19.1	47.0
1-Methylanthracene	22.8	200.7	151.7	116.6	42.6	117.6	412.5	76.9	148.4	39.5	133.6	41.8	24.2	66.2	78.9	81.5	25.8	65.5
1-Methylphenanthrene	17.7	143.3	119.5	82.9	27.0	73.2	305.3	51.0	101.8	29.5	95.7	31.2	19.4	49.1	57.9	58.8	19.7	48.8
3,6-Dimethylphenanthrene	17.6	177.4	136.2	112.7	41.2	129.8	417.4	86.9	126.4	32.6	132.9	33.1	22.5	57.4	77.0	68.7	27.7	56.1
9,10-Dimethylanthracene	8.8	88.2	66.3	55.0	16.9	67.1	197.8	38.6	59.7	16.4	65.8	17.0	11.3	26.9	39.7	34.9	14.6	27.5
Fluoranthene	8.7	10.9	13.1	8.1	1.3	10.4	36.1	7.9	11.6	3.7	13.0	3.8	3.2	6.1	6.4	5.9	4.7	3.1
Pyrene	26.8	60.0	67.0	38.7	13.4	52.8	180.5	34.9	46.2	12.8	57.5	14.9	9.9	20.9	26.4	23.5	12.2	19.5
Retene	6.4	11.4	10.7	9.1	6.1	9.5	20.3	7.9	15.2	10.7	11.4	7.9	7.3	10.8	4.9	8.6	2.9	6.6
Benzo[b]fluorene	2.6	5.8	6.9	5.3	2.4	6.5	18.0	5.3	8.2	4.9	7.1	3.4	2.8	4.2	10.3	3.4	3.8	2.7
Benz[a]anthracene	1.3	1.7	1.5	1.7	1.0	1.4	2.0	1.2	3.4	1.7	1.9	1.6	0.6	1.8	1.8	1.3	1.0	0.9
Chrysene	2.2	3.4	3.8	3.3	2.3	3.1	5.9	3.3	6.7	5.5	4.2	3.4	2.6	4.0	3.7	2.3	3.0	2.0
Napthacene/Benz[b]anthracene	3.9	4.4	3.6	4.0	2.5	4.1	3.9	3.2	7.3	5.5	4.9	4.7	3.3	5.1	4.6	2.7	3.9	2.1
4-Methylchrysene	1.5	2.1	1.9	2.4	1.4	2.3	3.9	1.9	4.0	2.6	2.5	2.1	1.7	2.7	2.3	1.8	1.2	1.5
Benzo[a]pyrene	5.7	7.0	5.8	5.5	4.2	5.0	5.1	4.7	11.4	10.6	6.9	8.1	5.4	9.2	7.2	6.0	5.9	5.1
Perylene	49.0	66.3	50.0	54.4	36.3	41.1	35.5	27.6	74.8	71.4	55.3	70.8	49.8	82.1	67.1	54.3	57.6	46.3
TOTAL PAH (ng g^{-1} wt)	**463.1**	**1568.3**	**1221.2**	**983.3**	**399.9**	**932.4**	**2956.2**	**661.6**	**1264.2**	**461.6**	**1174.0**	**462.7**	**317.7**	**662.9**	**738.3**	**682.5**	**353.2**	**534.8**
TOTAL Parent PAHs (ng g^{-1} wt)	159.3	356.7	303.3	240.2	104.8	227.5	603.1	161.0	320.8	177.3	279.0	160.4	112.5	207.0	208.1	179.1	129.3	134.9
TOTAL Alkyl-PAHs (ng g^{-1} wt)	303.7	1211.7	917.9	743.1	295.1	704.9	2353.0	500.7	943.4	284.3	895.0	302.3	205.1	455.9	530.2	503.4	224.0	399.9

Appendix 1

Concentrations (**ng g^{-1} wt**) of individual polycyclic aromatic hydrocarbons (PAHs) in surface sediments (0-1 cm) from the Chukchi shef collected during COMIDA09 and COMIDA10 (continued)

Station Code	**39**	**40**	**42**	**43**	**44**	**45**	**47**	**48**	**103**	**105**	**106**	**107**	**1013**	**1014**	**1015**	**1016**
Latitude (N)	71°42.117'	71°43.527'	71°44.311'	72°03.702'	72°24.238'	72°16.942'	71°43.642'	71°22.610'	67°40.134'	68°58.256'	69°53.671'	69°53.671'	71°55.598'	70°50.239'	71°15.284'	70°42.360'
Longitude (W)	164°30.898'	163°27.370'	162°06.210'	164°07.836'	164°57.482'	163°17.333'	160°43.097'	159°28.066'	168°57.280'	168°56.416'	167°44.142'	166°27.194'	162°40.476'	163°17.275'	163°11.484'	165°15.090'
2-Methylnapthalene	5.5	8.6	0.9	6.4	1.0	1.9	15.3	18.5	75.4	73.9	107.1	29.8	29.5	47.4	85.5	291.8
1-Methylnapthalene	3.9	6.2	0.5	4.7	0.8	1.6	11.7	14.1	45.8	44.9	62.2	19.1	19.0	29.9	52.8	167.0
Biphenyl	2.7	4.1	2.0	3.1	3.5	1.7	7.1	7.2	5.1	5.0	2.2	3.0	3.5	4.5	9.2	6.9
2,7-Dimethylnapthalene	0.8	1.1	0.7	1.0	1.4	0.7	2.4	2.8	1.5	1.5	1.4	1.2	1.0	1.7	7.6	4.3
1,3-Dimethylnapthalene	6.1	17.8	7.5	4.8	26.3	4.4	32.6	21.8	55.1	54.0	4.5	8.8	10.4	13.2	33.8	15.9
1,6-Dimethylnapthalene	4.3	7.0	4.5	5.3	7.0	4.1	12.8	15.6	6.1	6.0	6.9	7.6	6.3	8.7	35.2	16.3
1,5-Dimethylnapthalene	3.7	6.4	4.9	4.4	8.6	4.7	11.3	13.1	4.6	4.5	4.3	5.5	4.1	6.2	23.6	7.9
1,4-Dimethylnapthalene	2.2	2.8	1.6	1.9	2.5	1.4	5.3	6.1	1.6	1.6	1.8	3.0	1.9	3.6	15.7	4.4
1,2-Dimethylnapthalene	0.8	2.4	2.0	1.2	4.0	1.7	4.7	3.8	1.9	1.8	0.6	1.1	0.9	1.4	3.5	1.5
1,8-Dimethylnapthalene	0.9	1.3	1.3	1.0	2.1	1.6	2.1	2.8	0.9	0.8	0.9	1.2	0.9	1.5	7.0	1.9
Fluorene	1.0	1.6	2.1	1.2	2.5	1.1	3.0	3.4	2.2	2.1	0.0	1.8	3.2	2.6	7.8	2.2
2,3,5-Trimethylnapthalene	1.5	2.2	2.2	1.7	3.4	1.7	3.9	4.2	1.4	1.3	2.5	2.7	1.4	2.3	9.6	1.5
1-Methylfluorene	3.7	4.2	7.0	3.3	14.1	3.6	6.9	4.6	1.7	1.6	1.8	0.8	0.6	1.5	3.7	5.8
1,4,5,8-Tetramethylnapthalene	2.4	3.1	4.3	2.3	8.5	2.4	5.2	3.6	1.2	1.2	2.9	1.3	0.9	1.4	9.1	4.3
Dibenzothiophene	5.5	7.2	10.3	5.1	21.5	4.7	10.3	6.0	4.1	4.0	3.9	2.3	3.2	3.4	4.8	11.7
Phenanthrene	23.7	28.6	45.8	19.9	82.4	18.5	52.6	33.3	32.8	32.2	7.0	25.0	48.3	36.0	55.9	68.7
2-Methyldibenzothiophene	21.5	23.6	26.4	17.0	58.1	12.2	37.9	15.8	10.9	10.7	17.5	3.4	3.6	6.1	5.1	41.8
4-Methyldibenzothiophene	6.6	7.5	7.7	5.3	16.8	3.7	12.3	4.8	3.5	3.4	5.4	0.9	1.0	1.7	1.2	12.6
2-Methylphenanthrene	23.5	24.9	23.1	18.8	61.5	10.9	40.7	19.5	13.3	13.0	19.2	7.0	9.2	9.8	13.7	47.9
2-Methylanthracene	28.9	31.6	33.1	23.4	80.3	16.8	52.7	25.5	17.2	16.9	21.9	8.3	10.8	11.4	14.7	56.0
1-Methylanthracene	42.8	45.1	44.4	35.0	106.0	20.7	74.4	33.6	17.7	17.3	35.0	7.6	8.5	11.7	16.6	82.5
1-Methylphenanthrene	30.0	33.2	32.9	25.3	76.6	16.3	53.7	25.1	15.4	15.1	24.1	5.4	5.3	8.2	12.5	55.4
3,6-Dimethylphenanthrene	45.8	41.9	45.3	39.4	96.6	20.3	75.9	94.5	22.0	21.6	42.2	8.0	9.2	10.3	15.7	89.8
9,10-Dimethylanthracene	22.3	20.3	21.4	17.9	47.4	9.8	36.0	45.1	12.2	11.9	20.2	3.7	4.4	4.9	8.5	40.2
Fluoranthene	3.1	1.9	6.1	2.6	8.6	0.0	9.7	27.6	1.4	1.4	0.0	0.9	15.3	7.6	11.5	6.2
Pyrene	19.9	15.8	14.8	16.8	31.0	6.4	34.5	49.1	6.8	6.7	7.4	2.0	6.2	5.7	9.2	27.4
Retene	4.0	4.8	6.7	4.8	9.0	3.9	9.9	29.2	2.1	2.0	4.9	4.6	3.4	5.4	6.6	5.6
Benzo[b]fluorene	1.5	2.2	2.3	2.0	9.0	1.5	5.0	13.3	1.2	1.2	1.7	1.5	1.5	1.8	4.8	3.3
Benz[a]anthracene	0.6	0.9	0.8	0.7	0.9	0.3	1.8	5.1	0.5	0.5	0.6	0.8	0.7	0.9	1.7	0.9
Chrysene	1.4	2.2	2.9	1.6	3.2	1.3	4.5	14.3	1.0	1.0	0.4	1.8	1.8	2.1	4.2	1.3
Napthacene/Benz[b]anthracene	1.7	2.6	2.9	2.3	4.2	2.8	5.5	14.3	1.4	1.4	0.7	1.9	1.8	2.0	3.8	0.9
4-Methylchrysene	0.9	1.8	1.4	1.0	2.0	1.0	2.9	8.8	0.5	0.5	0.4	0.7	0.9	1.3	2.6	1.3
Benzo[a]pyrene	2.6	5.1	4.8	3.7	8.0	2.7	10.6	9.3	2.4	2.3	1.0	3.3	3.3	4.0	11.5	5.5
Perylene	23.5	40.7	38.8	32.1	77.6	28.9	78.3	59.5	28.1	27.5	5.5	25.5	26.0	23.9	42.7	219.3
TOTAL PAH (ng g^{-1} wt)	**349.2**	**410.8**	**413.4**	**317.3**	**886.5**	**215.3**	**733.9**	**655.3**	**398.6**	**390.7**	**418.2**	**201.7**	**247.9**	**284.1**	**551.5**	**1309.9**
TOTAL Parent PAHs (ng g^{-1} wt)	87.1	112.9	133.5	91.1	252.3	69.9	223.0	242.3	86.8	85.1	30.5	69.8	114.9	94.6	167.1	354.2
TOTAL Alkyl-PAHs (ng g^{-1} wt)	262.0	297.9	279.9	226.1	634.1	145.3	510.8	413.0	311.8	305.6	387.7	131.9	133.0	189.5	384.4	955.7

Appendix 2

Concentrations (**ng g^{-1} wt**) of individual aliphatic n-alkanes in surface sediments (0-1 cm) from the Chukchi shef collected during COMIDA09 and COMIDA10

Station Code	Latitude (N)	Longitude (W)	C15-n	C16-n	C17-n	C18-n	C19-n	C20-n	C21-n	C22-n	C23-n	C24-n	C25-n	C26-n	C27-n	C28-n	C29-n	C30-n	C31-n	C32-n	C33-n	**TOTAL n-Alkanes (ng g^{-1})**	TOTAL Short-chain (C_{15-C22}) n-Alkanes (ng g^{-1})	TOTAL Long-chain (C_{23-C33}) n-Alkanes (ng g^{-1})
1	69°02.380'	166°35.608'	0.20	0.45	0.44	0.37	0.51	0.42	0.35	0.00	0.68	0.02	0.54	0.02	0.81	0.00	0.75	0.21	1.01	0.10	0.55	**7.43**	2.74	4.69
2	69°30.126'	167°40.513'	0.08	0.40	0.16	0.11	0.09	0.01	0.26	0.17	0.59	0.00	0.82	0.05	0.93	0.00	0.64	0.05	0.73	0.11	0.25	**5.46**	1.29	4.17
3	69°49.747'	165°29.974'	0.11	0.68	0.12	0.02	0.00	0.00	0.09	0.00	0.27	0.00	0.17	0.00	0.34	0.00	0.39	0.25	0.49	0.11	0.36	**3.39**	1.01	2.37
4	70°01.383'	163°45.670'	0.05	0.38	0.51	0.55	0.54	0.60	0.15	0.40	0.13	0.15	0.00	0.00	0.00	0.12	0.00	0.13	0.04	0.06	0.06	**3.85**	3.17	0.68
5	70°24.285'	164°28.940'	0.14	0.47	0.49	0.52	0.62	0.54	0.24	0.01	0.41	0.00	0.28	0.00	0.46	0.14	0.52	0.18	0.76	0.06	0.57	**6.41**	3.03	3.37
6	70°20.706'	165°27.024'	0.00	0.00	0.00	0.07	0.21	0.07	0.45	0.29	0.88	0.00	1.15	0.10	1.45	0.00	1.01	0.05	1.05	0.12	0.30	**7.21**	1.10	6.11
7	70°28.122'	166°05.168'	0.06	0.27	0.25	0.27	0.41	0.23	0.11	0.04	0.30	0.00	0.10	0.00	0.15	0.00	0.24	0.09	0.47	0.06	0.35	**3.43**	1.66	1.77
8	70°17.233'	167°26.609'	0.09	0.43	0.34	0.35	0.55	0.34	0.22	0.09	0.50	0.01	0.34	0.00	0.41	0.00	0.37	0.13	0.57	0.05	0.35	**5.12**	2.40	2.72
9	70°49.881'	167°47.204'	0.16	0.51	1.12	1.13	1.55	0.78	0.75	1.10	1.08	1.06	1.00	0.56	1.31	0.08	1.21	0.82	1.51	0.41	0.85	**16.98**	7.11	9.87
10	70°40.275'	167°04.990'	0.00	0.00	0.12	0.11	0.20	0.08	0.36	0.22	0.68	0.00	1.13	0.46	1.19	0.14	0.68	0.06	0.67	0.09	0.20	**6.41**	1.10	5.31
11	70°43.965'	165°59.800'	0.10	0.51	0.37	0.40	0.53	0.38	0.23	0.22	0.59	0.15	0.57	0.32	0.73	0.32	0.83	0.63	0.89	0.35	0.60	**8.73**	2.74	5.98
12	70°41.833'	165°26.437'	0.09	0.41	0.45	0.48	0.69	0.55	0.42	0.19	0.74	0.21	0.67	0.08	0.96	0.00	0.83	0.15	0.98	0.08	0.59	**8.59**	3.28	5.30
13	70°44.803'	164°10.534'	0.00	0.09	0.23	0.17	0.32	0.14	0.44	0.24	0.72	0.00	0.84	0.00	0.90	0.00	0.66	0.02	0.76	0.10	0.26	**5.86**	1.63	4.23
14	70°38.490'	162°15.976'	0.00	0.19	0.09	0.00	0.18	0.03	0.10	0.00	0.28	0.00	0.15	0.00	0.09	0.00	0.15	0.10	0.21	0.02	0.18	**1.78**	0.59	1.18
15	71°01.089'	164°15.281'	0.00	0.29	0.27	0.42	0.85	0.65	0.42	0.00	0.73	0.02	0.56	0.09	0.77	0.03	0.73	0.30	0.84	0.12	0.52	**7.61**	2.90	4.71
16	70°55.151'	165°25.232'	0.06	0.07	0.13	0.05	0.12	0.00	0.17	0.09	0.32	0.00	0.47	0.00	0.28	0.00	0.21	0.00	0.32	0.06	0.14	**2.48**	0.67	1.80
17	71°04.636'	166°10.708'	0.10	0.15	0.30	0.39	0.62	0.38	0.40	0.32	0.71	0.00	0.87	0.03	0.87	0.00	0.63	0.00	0.73	0.07	0.33	**6.90**	2.66	4.24
19	71°01.669'	166°57.162'	0.00	0.00	0.33	0.59	0.67	0.52	0.48	0.48	0.88	0.00	0.99	0.04	1.09	0.00	0.83	0.03	0.98	0.10	0.50	**8.51**	3.08	5.43
20	71°12.399'	168°18.676'	0.26	1.47	0.37	0.42	0.29	0.16	0.40	0.33	0.84	0.17	1.38	0.22	1.79	0.00	0.95	0.05	0.99	0.11	0.34	**10.55**	3.70	6.85
21	71°29.079'	167°46.900'	0.11	0.16	0.45	0.62	0.83	0.61	0.55	0.48	0.91	0.11	1.11	0.09	1.33	0.00	1.06	0.04	1.25	0.11	0.52	**10.34**	3.81	6.53
22	71°16.328'	167°00.865'	0.00	0.10	0.34	0.59	0.93	0.74	0.55	0.51	0.77	0.08	0.95	0.09	1.17	0.00	0.95	0.03	1.12	0.11	0.41	**9.44**	3.76	5.68
23	71°23.228'	166°16.588'	0.00	0.12	0.36	0.45	0.75	0.48	0.56	0.52	1.02	0.00	1.32	0.20	1.77	0.06	1.48	0.14	1.69	0.15	0.59	**11.64**	3.23	8.41
24	71°14.952'	165°26.871'	0.00	0.06	0.04	0.10	0.13	0.19	0.12	0.24	0.23	0.07	0.33	0.00	0.60	0.00	0.54	0.08	0.72	0.04	0.33	**3.82**	0.88	2.93
25	71°14.549'	163°55.317'	0.05	0.12	0.33	0.48	0.81	0.58	0.46	0.42	0.72	0.00	0.88	0.11	1.06	0.00	0.88	0.08	1.02	0.10	0.38	**8.47**	3.24	5.23
26	71°04.641'	162°33.503'	0.08	0.23	0.75	1.55	3.09	2.74	1.04	0.82	0.69	0.00	0.74	0.01	0.61	0.00	0.59	0.02	0.72	0.07	0.27	**14.02**	10.31	3.71
27	70°54.512'	160°44.450'	0.00	0.08	0.26	0.38	0.65	0.48	0.36	0.26	0.44	0.00	0.46	0.00	0.36	0.00	0.34	0.00	0.42	0.06	0.15	**4.70**	2.48	2.22
28	71°12.492'	161°53.392'	0.00	0.09	0.42	0.54	1.10	0.55	0.68	0.54	1.15	0.00	1.39	0.18	1.78	0.06	1.45	0.10	1.56	0.13	0.71	**12.42**	3.92	8.50
29	71°17.891'	161°41.321'	0.08	0.16	0.33	0.38	0.67	0.49	0.80	0.69	1.30	0.49	1.22	0.19	1.72	0.06	1.35	0.07	1.57	0.06	0.71	**12.32**	3.59	8.73
30	71°27.180'	162°36.643'	0.00	0.11	0.41	0.59	1.13	0.79	0.68	0.56	0.96	0.00	1.19	0.12	1.45	0.03	1.15	0.11	1.35	0.14	0.53	**11.30**	4.27	7.03
31	71°22.732'	164°42.710'	0.00	0.08	0.18	0.33	0.46	0.47	0.60	0.59	0.94	0.45	1.03	0.29	1.53	0.13	1.07	0.14	1.02	0.09	0.40	**9.77**	2.71	7.06
32	71°23.759'	164°06.542'	0.06	0.11	0.18	0.30	0.47	0.37	0.57	0.50	0.87	0.35	0.78	0.05	1.05	0.00	0.71	0.00	0.84	0.02	0.40	**7.62**	2.57	5.06
34	71°40.587'	166°26.627'	0.00	0.08	0.21	0.41	0.52	0.52	0.64	0.64	1.01	0.42	1.03	0.15	1.66	0.00	1.18	0.03	1.26	0.04	0.52	**10.34**	3.02	7.32
35	71°40.150'	166°55.039'	0.10	0.20	0.26	0.41	0.62	0.53	0.65	0.61	0.97	0.37	1.03	0.14	1.66	0.01	1.28	0.03	1.51	0.06	0.61	**11.03**	3.37	7.66
36	71°55.815'	167°23.351'	0.00	0.08	0.20	0.38	0.56	0.53	0.53	0.55	0.75	0.28	0.75	0.05	1.15	0.00	0.93	0.02	1.10	0.03	0.47	**8.37**	2.84	5.53
37	72°02.744'	166°20.404'	0.09	0.87	0.27	0.44	0.37	0.31	0.46	0.43	0.71	0.27	0.69	0.00	1.06	0.00	0.77	0.00	0.78	0.00	0.27	**7.79**	3.24	4.55
38	71°55.614'	165°09.650'	0.00	0.09	0.16	0.32	0.42	0.40	0.41	0.41	0.56	0.22	0.55	0.03	0.90	0.00	0.75	0.08	0.90	0.04	0.40	**6.62**	2.20	4.43
39	71°42.117'	164°30.898'	0.00	0.05	0.12	0.23	0.35	0.31	0.23	0.25	0.30	0.15	0.24	0.00	0.44	0.00	0.44	0.07	0.64	0.05	0.30	**4.19**	1.55	2.64
40	71°43.527'	163°27.370'	0.04	0.11	0.16	0.27	0.48	0.34	0.37	0.37	0.54	0.29	0.56	0.05	0.83	0.03	0.77	0.18	1.04	0.12	0.41	**6.95**	2.13	4.82
42	71°44.311'	162°06.210'	0.00	0.10	0.15	0.33	0.52	0.40	0.49	0.50	0.55	0.19	0.46	0.00	0.65	0.00	0.50	0.00	0.66	0.01	0.30	**5.79**	2.48	3.31
43	72°03.702'	164°07.836'	0.05	0.11	0.16	0.11	0.36	0.32	0.25	0.42	0.36	0.15	0.25	0.06	0.41	0.00	0.41	0.02	0.51	0.01	0.25	**4.20**	1.77	2.43
44	72°24.238'	164°57.482'	0.00	0.08	0.27	0.40	0.51	0.43	0.48	0.53	0.76	0.37	0.78	0.15	1.14	0.00	0.86	0.00	0.93	0.01	0.48	**8.19**	2.70	5.49
45	72°16.942'	163°17.333'	0.05	0.09	0.12	0.18	0.24	0.22	0.29	0.31	0.38	0.13	0.26	0.00	0.39	0.00	0.32	0.00	0.55	0.00	0.26	**3.78**	1.50	2.28
47	71°43.642'	160°43.097'	0.12	0.13	0.25	0.39	0.67	0.51	0.50	0.52	0.77	0.34	0.79	0.07	1.21	0.00	1.03	0.01	1.18	0.04	0.53	**9.08**	3.10	5.98
48	71°22.610'	159°28.066'	0.10	0.16	0.22	0.32	0.62	0.44	0.55	0.51	0.78	0.29	0.69	0.04	1.14	0.00	1.03	0.04	1.16	0.04	0.52	**8.65**	2.93	5.72
103	67°40.134'	168°57.280'	0.00	0.24	0.18	0.09	0.17	0.15	0.31	0.28	0.54	0.25	0.70	0.29	1.14	0.25	0.87	0.15	0.91	0.09	0.47	**7.06**	1.41	5.65
105	68°58.256'	168°56.416'	0.00	0.18	0.14	0.09	0.18	0.16	0.47	0.47	1.02	0.38	1.21	0.36	2.05	0.28	1.33	0.13	1.15	0.07	0.55	**10.24**	1.69	8.54
106	69°53.671'	167°44.142'	0.48	1.10	0.74	1.03	0.93	0.75	0.45	0.39	0.53	0.23	0.57	0.22	0.77	0.14	0.55	0.07	0.42	0.06	0.20	**9.64**	5.88	3.76
107	69°53.671'	166°27.194'	0.04	0.19	0.02	0.09	0.10	0.09	0.20	0.21	0.45	0.15	0.46	0.13	0.59	0.07	0.33	0.04	0.25	0.02	0.16	**3.60**	0.95	2.65
1013	71°55.598'	162°40.476'	0.05	0.16	0.04	0.07	0.06	0.07	0.13	0.19	0.34	0.14	0.45	0.19	0.57	0.13	0.45	0.09	0.40	0.04	0.21	**3.77**	0.78	2.99
1014	70°50.239'	163°17.275'	0.07	0.23	0.04	0.11	0.13	0.10	0.20	0.23	0.36	0.16	0.43	0.21	0.57	0.20	0.50	0.13	0.45	0.06	0.22	**4.38**	1.10	3.28
1015	71°15.284'	163°11.484'	0.14	0.52	0.12	0.23	0.18	0.14	0.26	0.27	0.54	0.28	0.69	0.33	1.07	0.30	0.93	0.19	0.73	0.08	0.29	**7.30**	1.86	5.44
1016	70°42.360'	165°15.090'	0.08	0.28	0.12	0.20	0.18	0.15	0.11	0.14	0.14	0.06	0.25	0.10	0.55	0.17	0.77	0.11	0.34	0.03	0.10	**3.89**	1.25	2.63

Appendix 3

Concentrations of individual **PAHs (ng g^{-1} wt)** in a sediment core from Station 37 on the Chukchi Sea shelf

Depth of sediment (cm)	**0 to 1**	**1 to 2**	**3 to 4**	**5 to 6**	**7 to 8**	**9 to 10**	**12 to 14**	**16 to 18**	**18 to 20**
2-Methylnapthalene	10.5	8.9	10.3	12.6	16.4	11.9	11.5	17.2	12.2
1-Methylnapthalene	8.3	6.6	7.4	9.5	12.2	9.0	8.7	12.6	10.4
Biphenyl	4.3	3.3	3.8	4.7	5.2	4.6	4.5	4.9	4.6
2,7-Dimethylnapthalene	1.7	0.8	0.9	1.5	1.9	1.4	1.6	1.8	1.0
1,3-Dimethylnapthalene	19.0	6.7	12.3	14.9	21.4	17.6	15.7	18.9	15.3
1,6-Dimethylnapthalene	9.2	6.4	8.1	10.0	11.0	9.2	9.0	11.0	9.7
1,5-Dimethylnapthalene	9.4	5.4	6.8	8.4	8.9	7.7	7.5	9.1	8.1
1,4-Dimethylnapthalene	2.9	2.8	3.3	4.3	5.0	4.0	4.1	4.3	4.3
1,2-Dimethylnapthalene	4.6	1.6	1.6	2.0	2.4	1.9	1.5	2.4	2.0
1,8-Dimethylnapthalene	2.3	1.2	1.4	1.6	1.8	1.5	1.5	1.9	1.6
Fluorene	2.4	0.9	1.1	1.3	1.8	1.1	1.3	1.5	1.1
2,3,5-Trimethylnapthalene	3.3	1.7	2.2	2.6	3.1	2.2	2.4	3.3	2.8
1-Methylfluorene	5.1	1.1	1.7	1.8	6.7	1.8	1.7	7.4	2.1
1,4,5,8-Tetramethylnapthalene	3.9	1.2	1.7	2.0	4.8	1.8	1.7	5.4	2.0
Dibenzothiophene	6.4	1.4	2.1	2.1	11.2	2.1	1.7	13.0	2.5
Phenanthrene	24.0	3.6	7.7	8.1	44.8	8.5	7.3	54.8	9.0
2-Methyldibenzothiophene	14.8	2.0	4.3	3.0	39.6	4.6	1.9	51.3	5.7
4-Methyldibenzothiophene	4.3	0.4	1.1	0.7	13.5	1.2	0.3	16.2	1.5
2-Methylphenanthrene	13.6	3.3	6.8	7.5	49.0	7.5	4.2	59.1	8.6
2-Methylanthracene	19.1	4.2	8.7	9.5	61.5	9.5	6.3	76.0	11.0
1-Methylanthracene	25.8	5.0	10.1	8.8	89.2	9.8	5.7	106.5	13.7
1-Methylphenanthrene	19.7	3.6	8.1	9.0	66.7	7.2	4.4	74.4	9.9
3,6-Dimethylphenanthrene	27.7	4.0	9.8	7.9	125.5	10.8	6.1	164.4	18.7
9,10-Dimethylanthracene	14.6	2.5	5.6	4.7	60.1	5.4	3.2	72.8	9.9
Fluoranthene	4.7	0.0	1.1	0.9	12.7	2.3	3.3	14.6	1.9
Pyrene	12.2	2.5	5.2	4.6	50.6	6.0	5.2	66.4	11.0
Retene	2.9	3.6	5.3	5.8	10.9	6.0	6.3	13.4	7.2
Benzo[b]fluorene	3.8	1.3	1.9	2.1	6.8	2.2	6.4	7.2	3.0
Benz[a]anthracene	1.0	1.0	1.1	1.4	1.4	1.2	1.4	1.6	1.6
Chrysene	3.0	1.7	2.5	2.5	3.7	2.4	3.1	4.8	4.3
Napthacene/Benz[b]anthracene	3.9	2.5	3.2	3.7	3.6	3.0	3.5	3.7	3.9
4-Methylchrysene	1.2	1.5	1.9	2.0	2.1	2.0	1.6	2.3	2.7
Benzo[a]pyrene	5.9	3.7	5.6	5.8	5.7	6.1	6.5	6.7	7.4
Perylene	57.6	33.7	49.5	54.1	54.7	57.1	63.4	63.5	72.1
TOTAL PAH (ng g^{-1} wt)	**353.2**	**129.9**	**204.2**	**221.3**	**815.9**	**230.5**	**214.3**	**974.6**	**282.5**
TOTAL Parent PAHs (ng g^{-1} wt)	129.3	55.6	84.8	91.3	202.1	96.5	107.6	242.7	122.4
TOTAL Alkyl-PAHs (ng g^{-1} wt)	224.0	74.3	119.4	130.1	613.8	134.0	106.8	731.8	160.2

Concentrations of **n-alkanes (mg g^{-1} wt)** in a sediment core from Station 37 on the Chukchi Sea shelf

Depth of sediment (cm)	**0 to 1**	**1 to 2**	**3 to 4**	**5 to 6**	**7 to 8**	**9 to 10**	**12 to 14**	**16 to 18**	**18 to 20**
C15-n	0.09	0.09	0.00	0.07	0.04	0.06	0.04	0.00	0.00
C16-n	0.87	0.14	0.08	0.10	0.08	0.08	0.07	0.14	0.07
C17-n	0.27	0.25	0.21	0.22	0.19	0.18	0.19	0.36	0.14
C18-n	0.44	0.11	0.21	0.11	0.36	0.12	0.13	0.26	0.07
C19-n	0.37	0.17	0.22	0.21	0.63	0.16	0.16	0.53	0.10
C20-n	0.31	0.21	0.13	0.17	0.62	0.18	0.18	0.73	0.17
C21-n	0.46	0.23	0.23	0.27	0.66	0.28	0.33	0.67	0.26
C22-n	0.43	0.93	0.12	0.16	0.41	0.17	0.27	0.37	0.21
C23-n	0.71	1.73	0.60	0.57	0.76	0.61	0.71	0.65	0.73
C24-n	0.27	1.46	0.14	0.05	0.21	0.02	0.25	0.02	0.28
C25-n	0.69	2.51	1.01	0.82	1.07	0.87	0.95	0.86	1.08
C26-n	0.00	1.97	0.39	0.20	0.36	0.20	0.36	0.24	0.63
C27-n	1.06	3.80	2.53	2.06	2.29	2.02	1.81	2.15	2.05
C28-n	0.00	1.55	0.00	0.00	0.01	0.00	0.05	0.00	0.14
C29-n	0.77	2.63	1.82	1.07	1.38	1.26	1.03	1.57	0.97
C30-n	0.00	1.21	0.05	0.00	0.00	0.00	0.04	0.00	0.02
C31-n	0.78	2.15	1.86	0.89	1.15	1.31	1.04	1.51	0.93
C32-n	0.00	0.78	0.04	0.00	0.00	0.01	0.04	0.02	0.03
C33-n	0.27	1.00	0.66	0.32	0.45	0.48	0.42	0.52	0.29
TOTAL n-Alkane (mg g^{-1} wt)	**7.79**	**22.92**	**10.29**	**7.29**	**10.67**	**8.02**	**8.07**	**10.61**	**8.17**
TOTAL Short-chain ($C_{15\text{-}C22}$) n-Alkane (mg g^{-1} wt)	3.24	2.13	1.21	1.29	3.00	1.23	1.37	3.06	1.01
TOTAL Long-chain ($C_{23\text{-}C33}$) n-Alkane (mg g^{-1} wt)	4.55	20.79	9.09	6.00	7.67	6.79	6.69	7.55	7.16

Appendix 3

Concentrations of individual **PAHs (ng g^{-1} wt)** in a sediment core from Station 40 on the Chukchi Sea shelf

Depth of sediment (cm)	**0 to 1**	**2 to 3**	**4 to 5**	**6 to 7**	**8 to 9**	**9 to 10**
2-Methylnapthalene	32.6	6.3	5.5	8.6	6.6	9.6
1-Methylnapthalene	21.7	4.4	4.0	6.3	4.9	7.4
Biphenyl	7.0	3.1	2.3	3.5	2.4	4.0
2,7-Dimethylnapthalene	1.4	0.4	0.5	0.6	0.9	0.8
1,3-Dimethylnapthalene	25.3	5.1	7.6	8.8	9.1	13.1
1,6-Dimethylnapthalene	12.7	4.9	4.1	6.9	5.3	7.6
1,5-Dimethylnapthalene	9.9	4.0	3.3	5.7	4.2	6.1
1,4-Dimethylnapthalene	5.5	2.1	1.8	2.7	2.3	2.9
1,2-Dimethylnapthalene	2.6	1.0	1.0	1.4	1.2	1.7
1,8-Dimethylnapthalene	2.2	0.8	0.7	1.2	1.0	1.3
Fluorene	3.7	0.8	0.6	1.1	0.7	1.2
2,3,5-Trimethylnapthalene	4.9	1.2	1.0	1.6	1.1	1.6
1-Methylfluorene	23.9	0.8	0.7	1.2	0.8	1.2
1,4,5,8-Tetramethylnapthalene	14.7	0.9	0.7	1.2	0.9	1.3
Dibenzothiophene	46.6	1.0	0.8	1.6	0.9	1.6
Phenanthrene	204.1	3.2	4.0	7.5	2.4	7.9
2-Methyldibenzothiophene	181.5	1.6	1.6	2.8	1.4	2.2
4-Methyldibenzothiophene	56.5	0.4	0.4	0.7	0.3	0.5
2-Methylphenanthrene	200.9	2.9	2.2	4.4	2.9	3.8
2-Methylanthracene	252.8	4.2	3.7	6.4	3.3	4.6
1-Methylanthracene	368.5	4.2	3.9	7.9	3.8	4.4
1-Methylphenanthrene	251.7	3.3	3.5	4.8	2.6	3.9
3,6-Dimethylphenanthrene	518.1	4.4	4.1	7.5	4.3	7.0
9,10-Dimethylanthracene	246.3	2.7	2.6	4.0	2.3	3.8
Fluoranthene	36.3	1.2	0.8	4.0	1.1	4.2
Pyrene	146.2	2.7	2.5	5.1	2.8	4.9
Retene	16.8	3.0	2.7	4.5	3.0	4.9
Benzo[b]fluorene	12.5	1.2	1.0	1.8	1.2	1.9
Benz[a]anthracene	1.3	0.6	0.7	1.0	0.7	1.0
Chrysene	3.4	1.6	1.1	2.2	1.4	2.2
Napthacene/Benz[b]anthracene	3.6	1.7	1.7	2.7	2.0	2.9
4-Methylchrysene	3.6	0.9	0.9	1.3	1.2	1.4
Benzo[a]pyrene	6.7	3.5	3.0	5.7	3.9	6.3
Perylene	50.5	31.1	26.1	48.6	31.4	55.4
TOTAL PAH (ng g^{-1} wt)	**2776.0**	**111.1**	**101.4**	**175.4**	**114.2**	**184.7**
TOTAL Parent PAHs (ng g^{-1} wt)	521.9	51.7	44.9	84.9	50.9	93.4
TOTAL Alkyl-PAHs (ng g^{-1} wt)	2254.1	59.4	56.6	90.5	63.3	91.3

Concentrations of **n-alkanes (mg g^{-1} wt)** in a sediment core from Station 40 on the Chukchi Sea shelf

Depth of sediment (cm)	**0 to 1**	**2 to 3**	**4 to 5**	**6 to 7**	**8 to 9**	**9 to 10**
C15-n	0.05	0.00	0.00	0.00	0.00	0.00
C16-n	0.14	0.07	0.07	0.07	0.07	0.00
C17-n	0.43	0.18	0.18	0.19	0.16	0.19
C18-n	0.76	0.16	0.13	0.15	0.08	0.13
C19-n	1.20	0.20	0.16	0.14	0.10	0.20
C20-n	0.84	0.21	0.14	0.18	0.12	0.20
C21-n	0.62	0.23	0.12	0.20	0.14	0.18
C22-n	0.27	0.14	0.03	0.11	0.06	0.11
C23-n	0.44	0.16	0.00	0.20	0.11	0.17
C24-n	0.08	0.00	0.00	0.00	0.00	0.00
C25-n	0.42	0.00	0.00	0.00	0.00	0.00
C26-n	0.00	0.00	0.00	0.00	0.00	0.00
C27-n	1.39	0.12	0.00	0.23	0.27	0.26
C28-n	0.17	0.00	0.00	0.00	0.00	0.00
C29-n	1.31	0.35	0.21	0.37	0.49	0.44
C30-n	0.45	0.13	0.11	0.13	0.18	0.14
C31-n	1.26	0.55	0.41	0.47	0.67	0.62
C32-n	0.20	0.08	0.05	0.08	0.08	0.07
C33-n	0.45	0.29	0.21	0.22	0.27	0.28
TOTAL n-Alkane (mg g^{-1} wt)	**10.47**	**2.86**	**1.82**	**2.74**	**2.78**	**2.98**
TOTAL Short-chain ($C_{15\text{-}C22}$) n-Alkane (mg g^{-1} wt)	4.31	1.18	0.83	1.04	0.72	1.00
TOTAL Long-chain ($C_{23\text{-}C33}$) n-Alkane (mg g^{-1} wt)	6.17	1.69	0.99	1.70	2.07	1.99

Appendix 3

Concentrations of individual **PAHs (ng g^{-1} wt)** in a sediment core from Station 1016 on the Chukchi Sea shelf

Depth of sediment (cm)	**0 to 1**	**2 to 3**	**4 to 5**	**6 to 7**	**8 to 9**	**10 to 12**
2-Methylnapthalene	291.8	29.9	20.5	43.5	16.9	21.9
1-Methylnapthalene	167.0	19.7	14.8	32.4	12.6	16.1
Biphenyl	6.9	5.1	4.9	6.5	5.0	5.1
2,7-Dimethylnapthalene	4.3	3.0	2.0	3.0	1.6	1.9
1,3-Dimethylnapthalene	15.9	10.3	11.7	17.7	11.6	10.7
1,6-Dimethylnapthalene	16.3	16.3	14.2	25.0	12.6	14.4
1,5-Dimethylnapthalene	7.9	13.5	12.4	21.6	10.6	11.9
1,4-Dimethylnapthalene	4.4	6.1	6.4	10.8	5.4	5.9
1,2-Dimethylnapthalene	1.5	3.0	3.0	5.3	2.7	2.9
1,8-Dimethylnapthalene	1.9	2.9	2.7	5.1	2.3	2.7
Fluorene	2.2	2.3	1.8	3.2	1.6	1.9
2,3,5-Trimethylnapthalene	1.5	3.6	3.8	5.2	3.8	3.5
1-Methylfluorene	5.8	3.2	2.8	3.4	2.1	1.9
1,4,5,8-Tetramethylnapthalene	4.3	3.1	2.5	3.8	2.5	2.6
Dibenzothiophene	11.7	2.9	2.9	5.5	2.2	2.2
Phenanthrene	68.7	14.3	14.2	17.3	8.5	9.5
2-Methyldibenzothiophene	41.8	6.4	6.8	6.2	2.5	2.9
4-Methyldibenzothiophene	12.6	1.6	2.0	2.3	0.6	0.8
2-Methylphenanthrene	47.9	9.1	11.3	8.5	5.6	5.7
2-Methylanthracene	56.0	10.7	12.1	10.2	6.4	7.2
1-Methylanthracene	82.5	14.1	15.3	12.6	6.7	7.5
1-Methylphenanthrene	55.4	10.5	12.7	9.7	6.0	5.8
3,6-Dimethylphenanthrene	89.8	17.8	18.2	13.6	7.5	8.2
9,10-Dimethylanthracene	40.2	9.3	9.1	7.4	4.6	4.6
Fluoranthene	6.2	1.8	1.9	2.9	2.0	1.4
Pyrene	27.4	6.4	7.7	6.2	5.6	4.8
Retene	5.6	7.6	9.4	9.3	9.9	8.1
Benzo[b]fluorene	3.3	2.9	3.0	3.6	3.0	2.8
Benz[a]anthracene	0.9	1.4	1.7	2.0	1.8	1.5
Chrysene	1.3	3.1	3.6	4.6	4.2	3.6
Napthacene/Benz[b]anthracene	0.9	3.6	4.6	4.9	4.2	3.8
4-Methylchrysene	1.3	2.0	2.1	2.6	2.5	2.1
Benzo[a]pyrene	5.5	6.1	7.2	9.4	8.9	6.6
Perylene	219.3	37.4	58.1	63.0	77.0	51.2
TOTAL PAH (ng g^{-1} wt)	**1309.9**	**291.1**	**307.5**	**388.0**	**260.9**	**243.6**
TOTAL Parent PAHs (ng g^{-1} wt)	354.2	87.2	111.7	129.0	123.9	94.2
TOTAL Alkyl-PAHs (ng g^{-1} wt)	955.7	203.8	195.8	259.0	137.0	149.3

Concentrations of **n-alkanes (mg g^{-1} wt)** in a sediment core from Station 1016 on the Chukchi Sea shelf

Depth of sediment (cm)	**0 to 1**	**2 to 3**	**4 to 5**	**6 to 7**	**8 to 9**	**10 to 12**
C15-n	0.08	0.07	0.09	0.09	0.00	0.08
C16-n	0.28	0.12	0.11	0.11	0.10	0.08
C17-n	0.12	0.31	0.28	0.25	0.31	0.21
C18-n	0.20	0.11	0.20	0.08	0.17	0.09
C19-n	0.18	0.17	0.20	0.16	0.18	0.17
C20-n	0.15	0.15	0.17	0.13	0.17	0.14
C21-n	0.11	0.23	0.26	0.23	0.26	0.25
C22-n	0.14	0.18	0.13	0.12	0.16	0.17
C23-n	0.14	0.39	0.37	0.27	0.45	0.40
C24-n	0.06	0.06	0.00	0.00	0.00	0.00
C25-n	0.25	0.20	0.17	0.03	0.33	0.07
C26-n	0.10	0.00	0.00	0.00	0.00	0.00
C27-n	0.55	0.88	0.93	0.48	1.08	0.52
C28-n	0.17	0.07	0.00	0.00	0.00	0.00
C29-n	0.77	0.88	0.90	0.49	0.98	0.71
C30-n	0.11	0.30	0.17	0.11	0.21	0.14
C31-n	0.34	0.86	0.94	0.39	0.71	0.78
C32-n	0.03	0.15	0.09	0.03	0.08	0.05
C33-n	0.10	0.34	0.37	0.09	0.17	0.12
TOTAL n-Alkane (mg g^{-1} wt)	**3.89**	**5.47**	**5.36**	**3.07**	**5.37**	**4.00**
TOTAL Short-chain (C_{15-C22}) n-Alkane (mg g^{-1} wt)	1.25	1.33	1.43	1.18	1.36	1.21
TOTAL Long-chain (C_{23-C33}) n-Alkane (mg g^{-1} wt)	2.63	4.14	3.93	1.89	4.01	2.79

Appendix 4

Concentrations of individual **PAHs (ng g^{-1} wet wt)** in Neptunea foot muscle collected from Station 7

Size class (cm)	**< 5**	**5 to 8**	**> 8**
2-Methylnapthalene	1.43	0.56	0.74
1-Methylnapthalene	0.68	0.30	0.41
Biphenyl	0.52	0.46	0.34
2,7-Dimethylnapthalene	0.00	0.00	0.17
1,3-Dimethylnapthalene	0.00	0.00	0.14
1,6-Dimethylnapthalene	0.72	0.37	0.40
1,5-Dimethylnapthalene	0.65	0.39	0.32
1,4-Dimethylnapthalene	0.49	0.44	0.32
1,2-Dimethylnapthalene	0.00	0.00	0.00
1,8-Dimethylnapthalene	0.23	0.00	0.00
Fluorene	0.67	0.00	0.29
2,3,5-Trimethylnapthalene	0.00	0.00	0.00
1-Methylfluorene	0.12	0.00	0.06
1,4,5,8-Tetramethylnapthalene	0.00	0.00	0.00
Dibenzothiophene	0.23	0.02	0.14
Phenanthrene	0.18	0.00	0.00
2-Methyldibenzothiophene	0.12	0.08	0.14
4-Methyldibenzothiophene	0.00	0.00	0.00
2-Methylphenanthrene	0.14	0.01	0.05
2-Methylanthracene	0.27	0.00	0.11
1-Methylanthracene	0.33	0.08	0.11
1-Methylphenanthrene	0.49	0.24	0.20
3,6-Dimethylphenanthrene	0.50	0.33	0.24
9,10-Dimethylanthracene	0.29	0.00	0.21
Fluoranthene	0.00	0.00	0.00
Pyrene	2.66	1.01	0.08
Retene	0.00	0.00	0.00
Benzo[b]fluorene	0.00	0.00	0.00
Benz[a]anthracene	0.00	0.00	0.00
Chrysene	0.00	0.00	0.00
Napthacene/Benz[b]anthracene	0.00	0.00	0.00
4-Methylchrysene	0.00	0.00	0.00
Benzo[a]pyrene	0.00	0.90	0.00
Perylene	0.00	0.00	0.00
TOTAL PAH (ng g^{-1} wt)	**10.70**	**5.17**	**4.47**
TOTAL Parent PAHs (ng g^{-1} wt)	4.26	2.39	0.85
TOTAL Alkyl-PAHs (ng g^{-1} wt)	6.44	2.78	3.62

Concentrations of **n-alkanes (μg g^{-1} wet wt)** in Neptunea foot muscle collected from Station 7

Size class (cm)	**< 5**	**5 to 8**	**> 8**
C15-n	0.00	0.00	0.00
C16-n	0.00	0.00	0.00
C17-n	0.00	0.00	0.00
C18-n	0.00	0.00	0.00
C19-n	0.05	0.00	0.04
C20-n	0.09	0.04	0.07
C21-n	0.03	0.02	0.09
C22-n	0.01	0.03	0.11
C23-n	0.00	0.04	0.25
C24-n	0.00	0.08	0.45
C25-n	0.00	0.04	0.55
C26-n	0.00	0.06	0.65
C27-n	0.00	0.09	0.70
C28-n	0.00	0.14	0.70
C29-n	0.00	0.15	0.52
C30-n	0.16	0.21	0.66
C31-n	0.09	0.14	0.00
C32-n	0.12	0.12	0.27
C33-n	0.10	0.10	0.14
TOTAL n-Alkane (μg g^{-1} wt)	**0.66**	**1.25**	**5.20**
TOTAL Short-chain (C_{15-C22}) n-Alkane (μg g^{-1} wt)	0.18	0.08	0.31
TOTAL Long-chain (C_{23-C33}) n-Alkane (μg g^{-1} wt)	0.48	1.16	4.89

Appendix 5

Validation of internal reference compounds for polycyclic aromatic hydrocarbon (PAH) analysis

Internal reference standards	**Acenaphthene-d10**	**Phenathrene-d10**	**Benz(a)anthracene-d12**	**Benzo(a)pyrene-d12**
PAHs assigned for quantification	2-Methylnapthalene	Fluorene	3,6-Dimethylphenanthrene	Benzo[a]pyrene
	1-Methylnapthalene	2,3,5-Trimethylnapthalene	9,10-Dimethylanthracene	Perylene
	Biphenyl	1-Methylfluorene	Fluoranthene	
	2,7-Dimethylnapthalene	1,4,5,8-Tetramethylnapthalene	Pyrene	
	1,3-Dimethylnapthalene	Dibenzothiophene	Retene	
	1,6-Dimethylnapthalene	Phenanthrene	Benzo[b]fluorene	
	1,5-Dimethylnapthalene	2-Methyldibenzothiophene	Benz[a]anthracene	
	1,4-Dimethylnapthalene	4-Methyldibenzothiophene	Chrysene	
	1,2-Dimethylnapthalene	2-Methylphenanthrene	Napthacene	
	1,8-Dimethylnapthalene	2-Methylanthracene	4-Methylchrysene	
		1-Methylanthracene		
		1-Methylphenanthrene		
Standard addition (ng) ***w/o*** extraction	100	100	100	100
Standard addition (ng) ***with*** extraction	100	100	100	100
GCMS base peak area response of standard addition ***w/o*** extraction	473500	782763	939150	640119
GCMS base peak area response of standard addition ***with*** extraction	482977	774047	956796	531481
% Recovery	**102**	**99**	**102**	**83**

Validation of internal reference compounds for n-alkane analysis

Internal reference standard	**n-Octadecane-d38**
n-Alkanes assigned for quantification	C15-n
	C16-n
	C17-n
	C18-n
	C19-n
	C20-n
	C21-n
	C22-n
	C23-n
	C24-n
	C25-n
	C26-n
	C27-n
	C28-n
	C29-n
	C30-n
	C31-n
	C32-n
	C33-n
Standard addition (ng) ***w/o*** extraction	530
Standard addition (ng) ***with*** extraction	1766
Avg GC base peak area response of standard addition ***w/o*** extraction and HPLC fractionation	34.0418
Avg GC base peak area response of standard addition ***with*** extraction and HPLC fractionation	10.3744
% Recovery	**9.1**

Appendix 6

Polycyclic aromatic hydrocarbons (PAHs) in ship and procedureal blanks (**ng**) from COMIDA09 and COMIDA10

	R/V Alpha Helix Lab Air Blank	R/V Alpha Helix Deck Air Blank	R/V Moana Wave Lab Air Blank	R/V Moana Wave Deck Air Blank	Procedural Blank 09-1	Procedural Blank 09-2	Procedural Blank 09-3	Procedural Blank 10-1
2-Methylnapthalene	0.73	0.91	0.73	0.83	16.77	1.27	0.37	2.66
1-Methylnapthalene	0.47	0.64	0.40	0.56	8.78	0.63	0.50	1.79
Biphenyl	0.24	0.38	0.36	0.83	0.00	0.88	0.31	0.00
2,7-Dimethylnapthalene	0.18	0.20	0.00	0.56	0.00	0.38	0.18	0.00
1,3-Dimethylnapthalene	0.37	0.71	0.18	0.19	0.00	0.74	0.14	0.39
1,6-Dimethylnapthalene	0.62	0.72	0.24	0.34	0.00	0.52	0.15	1.11
1,5-Dimethylnapthalene	0.37	0.43	0.51	0.52	0.00	0.56	0.25	1.37
1,4-Dimethylnapthalene	0.25	0.30	0.32	0.33	0.00	0.18	0.00	1.37
1,2-Dimethylnapthalene	0.00	0.10	0.00	0.26	0.00	0.12	0.00	0.75
1,8-Dimethylnapthalene	0.13	0.15	0.11	0.13	0.00	0.10	0.00	0.31
Fluorene	1.18	1.43	1.27	1.06	0.26	0.73	0.43	3.23
2,3,5-Trimethylnapthalene	0.10	0.14	0.09	0.00	0.00	0.08	0.04	0.00
1-Methylfluorene	0.15	0.15	0.24	0.31	0.51	0.13	0.09	1.69
1,4,5,8-Tetramethylnapthalene	0.08	0.10	0.11	0.00	0.53	0.10	0.00	0.36
Dibenzothiophene	0.85	1.00	1.00	0.80	0.87	0.32	0.22	2.74
Phenanthrene	19.09	23.01	20.52	17.95	20.56	8.54	5.30	52.72
2-Methyldibenzothiophene	0.44	0.46	0.33	0.34	2.20	0.42	0.12	1.51
4-Methyldibenzothiophene	0.13	0.18	0.11	0.00	0.68	0.00	0.00	0.44
2-Methylphenanthrene	1.51	1.73	1.50	1.40	13.52	2.22	0.58	4.27
2-Methylanthracene	2.14	2.37	2.27	1.67	20.72	3.68	0.88	5.37
1-Methylanthracene	0.96	1.11	1.03	0.75	13.50	1.96	0.56	4.07
1-Methylphenanthrene	0.84	0.97	0.99	0.64	9.70	1.35	0.41	4.50
3,6-Dimethylphenanthrene	1.54	2.10	1.76	1.67	38.59	3.85	1.63	4.87
9,10-Dimethylanthracene	0.77	1.08	0.75	0.67	19.02	1.84	0.80	1.91
Fluoranthene	10.01	11.82	11.01	9.89	20.14	3.18	2.01	52.71
Pyrene	3.71	3.82	3.34	3.27	10.67	1.86	0.93	18.44
Retene	0.26	0.27	0.20	0.33	3.69	0.53	0.16	0.96
Benzo[b]fluorene	0.14	0.18	0.10	0.00	2.58	0.34	0.12	0.00
Benz[a]anthracene	0.00	0.00	0.00	0.00	0.00	0.00	0.00	0.00
Chrysene	0.00	0.00	0.00	0.00	0.00	0.06	0.00	0.00
Napthacene/Benz[b]anthracene	0.00	0.00	0.00	0.00	0.00	0.09	0.00	0.00
4-Methylchrysene	0.00	0.00	0.00	0.00	0.00	0.00	0.00	0.00
Benzo[a]pyrene	0.28	0.00	0.00	0.00	0.00	0.00	0.00	0.00
Perylene	0.00	0.00	0.00	0.00	0.00	0.00	0.00	0.00
TOTAL PAH (ng)	**47.54**	**56.47**	**49.49**	**45.32**	**203.31**	**36.67**	**16.21**	**169.53**

Aliphatic n-alkanes in ship and procedureal blanks (**ng**) from COMIDA09 and COMIDA10

	R/V Alpha Helix Lab Air Blank	R/V Alpha Helix Deck Air Blank	R/V Moana Wave Lab Air Blank	R/V Moana Wave Deck Air Blank	Procedural Blank 09-1	Procedural Blank 09-2	Procedural Blank 09-3	Procedural Blank 10-1
C15-n	0.00	0.00	0.00	0.00	0.00	0.00	0.00	0.00
C16-n	0.00	0.00	0.00	0.00	0.00	0.00	0.00	0.00
C17-n	0.00	0.00	0.00	0.00	1.07	0.00	0.00	0.27
C18-n	0.00	0.00	0.00	0.00	2.44	0.40	0.00	0.19
C19-n	0.00	0.00	0.00	0.00	1.64	0.39	0.00	0.15
C20-n	0.00	0.00	0.00	0.00	2.69	0.72	0.00	0.20
C21-n	0.17	0.00	0.00	0.00	0.92	0.27	0.00	0.11
C22-n	0.67	0.31	0.34	0.23	2.82	0.99	0.33	0.26
C23-n	0.94	0.28	0.00	0.00	0.60	0.69	0.00	0.16
C24-n	1.12	0.27	0.42	0.26	1.93	1.38	0.00	0.20
C25-n	1.45	0.94	0.33	0.00	0.43	1.07	0.00	0.11
C26-n	1.69	1.19	0.34	0.00	0.63	1.17	0.43	0.12
C27-n	1.70	1.36	0.35	0.00	0.27	1.15	0.32	0.10
C28-n	1.55	1.24	0.34	0.00	0.21	0.86	0.00	0.09
C29-n	1.27	0.92	0.36	0.00	0.17	0.62	0.00	0.00
C30-n	1.00	0.67	0.33	0.00	0.92	0.61	0.00	0.09
C31-n	0.73	0.42	0.00	0.00	1.07	0.78	0.00	0.08
C32-n	0.50	0.27	0.33	0.00	0.52	0.42	0.00	0.08
C33-n	0.33	0.23	0.00	0.00	0.00	0.54	0.00	0.08
TOTAL n-alkane (ng)	**13.11**	**8.10**	**3.15**	**0.49**	**18.32**	**12.06**	**1.08**	**2.28**

Table A-2. A table of polychaete re-identifications with references and comments to support the changes by Leslie Harris, a polychaete taxonomist and curator at the Natural History Museum of Los Angeles County. She studied a selection of polychaetes collected on this project in summer 2010.

Problem identifications

Current identification	Old Identification	References for Re-identification	Leslie Harris Comments
Ampharete arctica	Ampharete finmarchica	Holthe 1986; Jirkov, 1989; Jirkov, 2001	A. arctica has been synonymized under A. finmarchica.
Aphelochaeta "tigrina", Aphelochaeta "marioni", Chaetozone sp. 1, Chaetozone sp. 2	Chaetozone setosa	Harris personal notes; C.A. Phillips, personal notes; Blake 1996	Specimens were examined by cirratulid specialist C.A.Phillips and found to consist of 4 distinct species, 2 of which appear to be undescribed. The other 2 seem to be described however the specimens were incomplete & lacking some characters necessary for confirmation. Quotation marks were used to denote the uncertainty of the latter 2 identifications. The geographic range of true C. setosa was recently restricted to Northern Europe in the area between the North Sea, Irish Sea, and Svalbard (Chambers et al 2007).
Arcteobia anticostiensis	Harmothoe imbricata	Uschakov, 1982	Easy to mistake for H. imbricata as this species also has ventro-lateral anterior eyes under the cephalic peaks. The areolated "half moon" pigment pattern is fairly distinctive as is the presence of 2 types of notosetae - short, blunt-tipped and long with capillary tips. Harmothoe only has 1 type o notosetae.
Barantolla sp.	Barantolla americana	Green 2002; Hutchings & Rainer 1981; Harris personal Notes	COMIDA material was compared to the types of B. americana Hartman 1963. There were differences in stain pattern & chaetal dentition between the types & the Chukchi worms plus significant differences among the Chukchi specimens so they were left as "Barantolla sp." pending further work. It is possible that Arctic records of B. americana represent an undescribed species.

Brada ?n. sp; Diplocirrus longisetosus	Flabelligera mastigophora	Jirkov & Filippova 2001; Salzar-Vallejo unpublished manuscript; Our, Bakke, & Kongsrus 2011	Some of these specimens turned out to be D. longisetosus; after consultation with Dr. Salazar-Vallejo the others were thought to be an undescribed species of Brada
Bradabyssa	Brada granulata, Brada nuda, Brada villosa, Diplocirrus longisetosus	Salazar-Vallejo unpublished manuscript	These particular specimens belong to the genus Bradabyssa Hartman 1967 as redefined by Dr. Sergio Salazar-Vallejo who is in the process of revising all genera & species in the family Flabelligeridae. They appear to belong to different species as well and will be sent to Dr. Salazar-Vallejo for re-identification.
Chone n. sp. 1	Chone sp, Sabellidae, Laonome kroyeri	Tovar-Hernandez 2007a, 2007b; Nishi et al. 2009	Does not match any described species and is probably undescribed (Dr. Mariana Tovar-Hernandez, personal communication)
Chone n. sp. 2	Chone sp	Tovar-Hernandez 2007a, 2007b; Nishi et al. 2009	Does not match any described species and is probably undescribed (Dr. Mariana Tovar-Hernandez, personal communication)
Cistenides hyperborea	Cistenides granulata	Uschakov 1955; Jirkov 2001	According to Uschakov (1955) C. granulata has 7-10 pairs of flabellum while C. hyperborea has 10-15. I counted 12 setae on each side.
Eteone longa/flava complex	Eteone longa	Pleijel 1993a	Falls into the E. longa/flava complex as discussed in Pleijel 1993a
Eteone sp.	Eteone longa	Uschakov 1972; Pleijel 1993a; Wilson 1988; Pleijel 1993b	Did not match any of the species described for the temperate-boreal North Pacific and Arctic regions in English-language literature.
Euchone n. sp. 1	Euchone sp.	Tovar-Hernandez 2007a, 2007b; Nishi et al. 2009; Banse 1970, 1972; Cochrane 2000, 2003	A small species, easily mis-identified as Chone. Appears to be an undescribed species.
Flabelliderma n. sp.	Flabelligera affinis	Salazar-Vallejo 2007	Distinctly different from F. affinis. Will be sent to Dr. Salazar-Vallejo for identification.
Glycinde wireni	Glycinde picta	Boggemann, 2005	According to Boggemann, 2005, 2 species of Glycinde have been found in the Chukchi Sea: G armigera & G. wireni Arwidsson 1899, both of which are easily distinguished from G. picta by the absence of ventral micrognaths (jaw pieces).

Heteromastus sp.	Heteromastus filiformis	Hutchings & Rainer 1982	The original type locality of H. filiformis is Mediterranean France; a neotype was erected by Hutchings & Rainer (1982) from Alexandria, Egypt. They regarded it as a cosmopolitan species. The Chukchi specimens did not quite match their re-description and given the difference in habitat (Arctic versus warm-temperate) I am reluctant to call them filiformis without direct comparison to verified specimens.
Nepthys pente	Nephtys ciliata	Rainer, 1991.	Keys to ciliata in Uschakov, 1955; keys to pente in Rainer, 1991. Pente found from Greenland to Murman coast, Labrador, North Sea. Rainer says pente "…has frequenty been identified as N. ciliata and may have a wider distribution….".
Ophelina n. sp.?	Ophelina sp.	Jirkov 2001; Rowe 2010; Parapar et al. 2011	May be new species or described in a non-English language publication.
Owenia cf. assimilis	Owenia fusiformis	Ford & Hutchings 2005; Koh & Bhaud 2003; Koh, Bhand, & Jirkov 2003.	Described from Norway, so this is a possible range extension for O. assimilis if the identification is correct. Specimens need to be compared to type or topotype material of O. assimilis.
Pholoe sp. D Harris	Pholoe minuta	Petersen 1998; Pettibone 1992; Harris, personal notes	Pholoe minuta, described from Greenland, is a strongly pigmented species which has erroneously been reported from many different regions. These specimens do not appear to be minuta nor do they match any of the NE Pacific species (P. glabra Hartman, courtneyae Blake, sp. A-B-C Harris) that I have encountered. P. assimilis Orsted has also been reported from the Chukchi Sea (MacDonald et al 2009) but I have no way of knowing if these specimens are the same species as their's or if they identified their P. assimils correctly as there isn't a good current description.
Phyllodoce groenlandica	Anaitides groenlandica	Uschakov, 1972; Pleijel, 1993a; Pleijel, 1993b	Species identified correctly; since the publication of Uschakov the genera Phyllodoce & Anaitides were synonymized.

Polyphysia crassa	Scalibregma inflatum	Worsfold, undated; Boggemann 1997	Scalibregma inflatum is nearly always orange or dark yellow in color & has dorsal & ventral cirri in the posterior body region. This animal is white & lacks dorsal & ventral cirri in the posterior. Normally P. crassa looks more maggot like but this specimen is elongated, giving it a typical S. inflatum shape which is misleading. It was the white color that made me take a closer look for the presence of parapodial cirri.
Scoletoma fragilis	Lumbrineris fragilis	Harris, personal notes; Budaeva 2005	The genus Lumbrineris has been split into several genera based on setal & jaw structure.
Scoletoma minuta	Lumbrineris fragilis	Harris, personal notes; Budaeva 2005	Misidentification.
Scoletoma sp. 1	Lumbrineris fragilis	Harris, personal notes; Budaeva 2005	Differs from S. fragilis in species-specific characters, e.g., arrangement of setae & number of teeth on jaw pieces.
Scoletoma sp. 2	Lumbrineris fragilis	Harris, personal notes; Budaeva 2005	Differs from S. fragilis in species-specific characters, e.g., arrangement of setae & number of teeth on jaw pieces.
Sphaerodoropsis n.sp.?	Sphaerodoropsis minuta	Fauchald, 1974; Reuscher & Fiege, 2011	S. minuta has 2 postsetal parapodial lobes & the ventrum is covered by small papilae; this has no postsetal lobes & no papillae on the ventrum. It did not key out in Fauchald, 1974. Using the updated species key in Reuscher & Fiege, 2011, it keyed out to S. polypapillata Hartmann-Schroder & Rosenfeldt, 1988, but does not match that Antarctic species. Probably an undescribed species.
Sternaspis n. sp.?	Sternaspis scutata	Petersen 2000	Petersen (2000) gives detailed descriptions of S. fossor (Maine), cf. fossor (California) and S. scutata (Mediterrean) and these specimens do not match any of the three. According to Petersen there are about 15 valid species many of which had been previously considered to be synonyms of S. scutata. Sendall (2006) examined all extant type material & topotype material in his revision. these specimens do not appear to match any the species he redescribes.

Syllis "oerstedi"	Syllis sp., Syllis oerstedi	Licher 1999	Syllis oerstedi is now considered a nomen dubium without an adequate description (Licher, 1999). The type cannot be found so the species cannot be redefined. Ramos, San Martin & Sikorski (2010) apparently feel it's valid & intend to establish a type & redefine the species but that hasn't been done yet. As it keys out to S. oerstedi in Uschakov 1955 I have left the specimens as "oerstedi" pending the redescription.
Syllis sp. B	Syllis sp.	Licher 2000	Does not key out to any known Syllis for the area; more work is needed to confirm if it is undescribed or not.
Terebellides n. sp.?	Terebellides stroemi	Jirkov 1989; Jirkov 2001; Williams 1984; Garraffoni, Lana & Hutchings 2005	T.stroemi was previously considered to be a cosmopolitan species. Starting with Williams (1984) authors have shown that it consists of many morphologically distinct species. The Chukchi specimens do not match any described species known for the region.
Travisia cf. forbesi	Travisia forbesii	Jirkov 2001; Rowe 2010; Kirkegaard 1996; Uschakov 1955	Several authors have suggested that T. forbesi is one of the "cosmopolitan" species which may prove to consist of multiple species. The discrepancies between descriptions in various references such as Kirkegaard 1996 & Uschakov 1955 may result from such a mix up of species.

APPENDIX

Table A-1. List, by Group, of taxa collected from the Chukchi Sea during 2009 and 2010. N Sum is the total number of individuals m^{-2} collected from 142 van Veen grabs at 54 stations. N Sum as % is the percentage of the overall abundance sum contributed by the listed taxa.

Group	Family	Species Name	N SUM	N SUM as
ALC	Nephtheidae	Gersemia rubiformis	30.00	0.04
AMP	Pontoporeiidae	Pontoporeia femorata	2055.83	2.43
AMP	Phoxocephalidae	Paraphoxus sp.	1468.33	1.74
AMP	Ampeliscidae	Byblis gaimardi	1098.33	1.30
AMP	Ampeliscidae	Byblis sp.	652.50	0.77
AMP	Phoxocephalidae	Harpinia serrata	645.00	0.76
AMP	Ampeliscidae	Ampelisca birulai	525.00	0.62
AMP	Ampeliscidae	Ampelisca macrocephala	457.50	0.54
AMP	Corophiidae	Protomedeia sp.	375.00	0.44
AMP	Photidae	Photis sp.	370.00	0.44
AMP	Melitidae	Melita quadrispinosa	290.00	0.34
AMP	Phoxocephalidae	Phoxocephalidae	282.50	0.33
AMP	Uristidae	Anonyx sp.	276.67	0.33
AMP	Corophiidae	Protomedeia fasciata	260.00	0.31
AMP	Ampeliscidae	Ampelisca eschrichii	254.17	0.30
AMP	Ampeliscidae	Haploops sp.	229.17	0.27
AMP	Phoxocephalidae	Harpinia sp.	190.00	0.22
AMP	Lysianassidae	Orchomene sp.	190.00	0.22
AMP	Ampeliscidae	Ampelisca sp.	182.50	0.22
AMP	Ampeliscidae	Haploops laevis	160.00	0.19
AMP	Photidae	Photis vinogradovi	140.00	0.17
AMP	Ampeliscidae	Haploops tubicola	132.50	0.16
AMP	Corophiidae	Corophium sp.	130.00	0.15
AMP	Lysianassidae	Lysianassidae	126.67	0.15
AMP	Oedicerotidae	Oedicerotidae	117.50	0.14
AMP	Pontoporeiidae	Pontoporeia sp.	117.50	0.14
AMP	Ischyroceridae	Ischyrocerus sp.	112.50	0.13
AMP	Lysianassidae	Hippomedon sp.	85.00	0.10
AMP	Photidae	Photis spasskii	80.00	0.09
AMP	Stenothoidae	Stenothoidae	70.00	0.08
AMP	Ampeliscidae	Byblis robustus	65.00	0.08
AMP	Maeridae	Maera sp.	60.00	0.07
AMP	Unciolidae	Unciola leucopis	60.00	0.07
AMP	Priscillinidae	Priscillina armata	55.00	0.07
AMP	Podoceridae	Podoceridae	50.00	0.06
AMP	Phoxocephalidae	Harpinia salebrosa	45.00	0.05
AMP	Corophiidae	Lembos arctica	45.00	0.05
AMP	Maeridae	Maera loveni	45.00	0.05
AMP	Phoxocephalidae	Harpinia kabjakovae	40.00	0.05
AMP	Ischyroceridae	Ischyrocerus latipes	33.33	0.04
AMP	Centropagidae	Guernea sp.	30.00	0.04
AMP	Caprellidae	Caprella sp.	25.00	0.03
AMP	Melitidae	Melita sp.	25.00	0.03
AMP	Synopiidae	Synopiidae	25.00	0.03

AMP	Haustoriidae	Haustorius sp.	20.00	0.02
AMP	Nebaliidae	Nebalia sp.	20.00	0.02
AMP	Pleustidae	Pleustidae	15.00	0.02
AMP	Photidae	Podoceropsis sp.	15.00	0.02
AMP	Lysianassidae	Socarnes bidenticulatus	15.00	0.02
AMP	Oedicerotidae	Arrhis luthkei	10.00	0.01
AMP	Phoxocephalidae	Grandiphoxus sp.	10.00	0.01
AMP	Melitidae	Melita dentata	10.00	0.01
AMP	Oedicerotidae	Monoculodes diamesus	10.00	0.01
AMP	Uristidae	Onisimus krassini	10.00	0.01
AMP	Oedicerotidae	Paroediceros sp.	10.00	0.01
AMP	Photidae	Photidae	10.00	0.01
AMP	Oedicerotidae	Aceroides latipes	5.00	0.01
AMP	Oedicerotidae	Arrhis sp.	5.00	0.01
AMP	Ischyroceridae	Ischyroceridae	5.00	0.01
AMP	Oedicerotidae	Monoculodes schneideri	5.00	0.01
AMP	Oedicerotidae	Monoculodes sp.	5.00	0.01
AMP	Uristidae	Onisimus sp.	5.00	0.01
AMP	Synopiidae	Syrrhoe crenulata	5.00	0.01
AMP	Liljeborgiidae	Liljeborgia fissicornis	2.50	0.00
AMP	Unicolidae	Unicola sp.	2.50	0.00
ANE	Actinaria	Actinaria	280.00	0.33
ANE	Hormathiidae	Hormathia sp.	25.00	0.03
ASC	Molgulidae	Mogula sp.	77.50	0.09
ASC	Molgulidae	Eugyra pedunculata	60.00	0.07
ASC	Styelidae	Dendrodoa sp.	40.00	0.05
ASC	Styelidae	Pelonaia corrugata	35.00	0.04
ASC	Ascidian	Ascidian	32.50	0.04
ASC	Corellidae	Chelyosoma macleayanum	17.50	0.02
ASC	Pyuridae	Halocynthia aurantium	5.00	0.01
ASC	Styelidae	Styela rustica	5.00	0.01
ASC	Styelidae	Styela sp.	5.00	0.01
AST	Asteridae	Asteridae	60.00	0.07
BIV	Nuculidae	Ennucula tenuis	5925.83	7.01
BIV	Nuculanidae	Nuculana pernula	2825.00	3.34
BIV	Mytilidae	Musculus discors	2280.00	2.70
BIV	Tellinidae	Macoma calcarea	1910.42	2.26
BIV	Tellinidae	Macoma moesta	785.00	0.93
BIV	Yoldiidae	Yoldia hyperborea	542.50	0.64
BIV	Carditidae	Cyclocardia crebricostata	435.83	0.52
BIV	Tellinidae	Macoma sp.	410.00	0.48
BIV	Thyasiridae	Thyasira flexuosa	385.00	0.46
BIV	Astartidae	Astarte borealis	375.00	0.44
BIV	Montacutidae	Montacuta spitzbergensis	369.17	0.44
BIV	Nuculanidae	Nuculana sp.	275.00	0.33
BIV	Veneridae	Liocyma fluctuosa	257.50	0.30
BIV	Astartidae	Astarte montagui	225.00	0.27
BIV	Lasaeidae	Rochefortia tumida	105.00	0.12
BIV	Montacutidae	Mysella planata	95.00	0.11
BIV	Yoldiidae	Yoldia myalis	95.00	0.11

BIV	Cardiidae	Serripes groenlandicus	82.50	0.10
BIV	Thyasiridae	Axinopsida serricata	52.50	0.06
BIV	Periplomatidae	Periploma aleutica	37.50	0.04
BIV	Thraciidae	Thracia sp.	37.50	0.04
BIV	Mytilidae	Musculus niger	35.00	0.04
BIV	Hiatellidae	Hiatella arctica	32.50	0.04
BIV	Mytilidae	Crenella decussata	25.00	0.03
BIV	Conidae	Curtitoma incisula	20.00	0.02
BIV	Astartidae	Astarte sp.	15.00	0.02
BIV	Cardiidae	Cardiidae	15.00	0.02
BIV	Tellinidae	Macoma torelli	15.00	0.02
BIV	Mytilidae	Musculus glacialis	15.00	0.02
BIV	Mytilidae	Musculus sp.	15.00	0.02
BIV	Myidae	Mya sp.	15.00	0.02
BIV	Cardiidae	Clinocardium ciliatum	12.50	0.01
BIV	Astartidae	Astarte elliptica	10.00	0.01
BIV	Lyonsiidae	Lyonsia arenosa	10.00	0.01
BIV	Pandoridae	Pandora glacialis	7.50	0.01
BIV	Lasaeidae	Lasaeidae	5.00	0.01
BIV	Mytilidae	Musulus niger	5.00	0.01
BIV	Yoldiidae	Yoldia sp.	5.00	0.01
BIV	Mytilidae	Musculus corrugatus	2.50	0.00
BRA	Brachiopoda	Brachiopoda	50.00	0.06
BRY	Alcyonidiidae	Alcyonidium disciforme	150.00	0.18
BRY	Alcyonidiidae	Alcyonidium gelatinosum	72.50	0.09
BRY	Eucrateidae	Eucratea loricata	56.67	0.07
BRY	Bryozoa	Bryozoa	45.00	0.05
BRY	Flustridae	Carbasea carbasea	12.50	0.01
BRY	Vesiculariidae	Bowerbankia sp.	5.00	0.01
BRY	Bugulidae	Dendrobeania murrayana	5.00	0.01
BRY	Flustridae	Securiflustra securifrons	5.00	0.01
BRY	Flustridae	Securiflustra truncata	5.00	0.01
CHI	Ischnochitonidae	Ischnochiton albus	12.50	0.01
CIR	Balanidae	Balanus crenatus	147.50	0.17
CIR	Balanidae	Balanus sp.	20.00	0.02
CRU	Oregoniidae	Hyas coarctacus	17.50	0.02
CRU	Paguridae	Pagurus rathbuni	12.50	0.01
CRU	Pandalidae	Pandalus sp.	12.50	0.01
CRU	Paguridae	Pagurus sp.	10.00	0.01
CRU	Oregoniidae	Chionoecetes opilio	5.00	0.01
CRU	Hippolytidae	Lebbeus sp.	5.00	0.01
CRU	Paguridae	Pagurus trigonocheirus	5.00	0.01
CRU	Decapod	Decapod	2.50	0.00
CRU	Pandalidae	Pandalus borealis	2.50	0.00
CUM	Diastylidae	Brachydiastylis resima	2063.33	2.44
CUM	Leuconidae	Leucon sp.	320.00	0.38
CUM	Leuconidae	Leucon nasica	267.50	0.32
CUM	Leuconidae	Eudorellopsis integra	115.00	0.14
CUM	Leuconidae	Eudorella sp.	105.00	0.12
CUM	Leuconidae	Leucon nasicoides	77.50	0.09

CUM	Leuconidae	Eudorella emarginata	35.00	0.04
CUM	Leuconidae	Eudorellopsis sp.	35.00	0.04
CUM	Diastylidae	Diastylis rathkei	15.00	0.02
CUM	Diastylidae	Diastylis sp.	10.00	0.01
CUM	Diastylidae	Diastylis spinulosa	6.67	0.01
CUM	Cumacea	Cumacea	5.00	0.01
CUM	Diastylidae	Diastylis dalli	5.00	0.01
CUM	Lambropidae	Lamprops sp.	5.00	0.01
CUM	Diastylidae	Leptostylis sp.	5.00	0.01
CUM	Leuconidae	Leuconidae	5.00	0.01
CUM	Nannastacidae	Nannastacidae	5.00	0.01
ECH	Echinarachniidae	Echinarachnius parma	220.00	0.26
ECH	Echiuridae	Echiurus echiurus alascanus	40.00	0.05
ECH	Strongylocentrotidae	Strongylocentrotus droebachiensis	5.00	0.01
FOR	Foraminifera	Foraminifera	210.00	0.25
GAS	Cylichnidae	Cylichna alba	132.50	0.16
GAS	Solariellidae	Solariella obscura	107.50	0.13
GAS	Turritellidae	Tachyrhynchus erosus	87.50	0.10
GAS	Conidae	Oenopota sp.	86.67	0.10
GAS	Naticidae	Cryptonatica affinis	70.00	0.08
GAS	Naticidae	Euspira pallida	60.00	0.07
GAS	Cancellariidae	Admete viridula	50.00	0.06
GAS	Solariellidae	Solariella varicosa	50.00	0.06
GAS	Cylichnidae	Cylichna occulta	38.33	0.05
GAS	Retusidae	Retusa obtusa	37.50	0.04
GAS	Turridae	Nodotoma impressa	30.00	0.04
GAS	Turritellidae	Tachyrhynchus sp.	30.00	0.04
GAS	Conidae	Obesotoma tenuilirata	25.00	0.03
GAS	Lepetidae	Lepeta caeca	20.00	0.02
GAS	Cancellariidae	Admete sp.	15.00	0.02
GAS	Buccinidae	Buccinidae	15.00	0.02
GAS	Solariellidae	Solariellidae	15.00	0.02
GAS	Turritellidae	Tachyrhynchus reticulatus	15.00	0.02
GAS	Conidae	Curtitoma novajasemijensis	12.50	0.01
GAS	Muricidae	Boreotrophon beringi	10.00	0.01
GAS	Muricidae	Boreotrophon truncatus	10.00	0.01
GAS	Buccinidae	Buccinum angulosum	10.00	0.01
GAS	Buccinidae	Colus hallii	10.00	0.01
GAS	Daphniidae	Daphnia minuta	10.00	0.01
GAS	Buccinidae	Neptunea heros	10.00	0.01
GAS	Conidae	Oenopota impressa	10.00	0.01
GAS	Cancellariidae	Admete regina	5.00	0.01
GAS	Buccinidae	Buccinum ciliatum	5.00	0.01
GAS	Buccinidae	Buccinum scalariforme	5.00	0.01
GAS	Gastropoda	Gastropoda	5.00	0.01
GAS	Mangeliidae	Granotoma krausei	5.00	0.01
GAS	Littorinidae	Lacuna glacialis	5.00	0.01
GAS	Turbinidae	Margarites sp.	5.00	0.01
GAS	Buccinidae	Neptunea communis	5.00	0.01
GAS	Conidae	Obesotoma simplex	5.00	0.01

GAS	Conidae	Oenopota elegans	5.00	0.01
GAS	Conidae	Oenopota viridula	5.00	0.01
GAS	Buccinidae	Plicifusus kroyeri	5.00	0.01
GAS	Mangeliidae	Propebela nobilis	5.00	0.01
GAS	Buccinidae	Buccinum sp.	2.50	0.00
GAS	Conidae	Curtitoma lawrenciana	2.50	0.00
HOL	Cucumariidae	Ocnus glacialis	460.00	0.54
HOL	Psolidae	Psolus sp.	32.50	0.04
HOL	Cucumariidae	Cucumaria sp.	5.00	0.01
HYD	Hydrozoa	Hydrozoa	67.50	0.08
HYD	Sertulariidae	Sertularia cupressoides	30.00	0.04
HYD	Sertulariidae	Abietinaria abietina	20.00	0.02
HYD	Lafoeidae	Grammaria sp.	20.00	0.02
HYD	Campanulariidae	Obelia longissima	15.00	0.02
HYD	Sertulariidae	Sertularia sp.	12.50	0.01
HYD	Bonneviellidae	Bonneviella sp.	10.00	0.01
HYD	Lafoeidae	Lafoeina sp.	5.00	0.01
HYD	Sertulariidae	Abietinaria sp.	2.50	0.00
HYD	Sertulariidae	Thuiaria sp.	2.50	0.00
HYD	Stylasteridae	Distichopora borealis	20.00	0.02
ISO	Idoteidae	Synidotea sp.	20.00	0.02
NEA	Nematoda	Nematoda	9360.83	11.07
NEM	Nemertea	Nemertea	469.17	0.55
OPH	Ophiuridae	Ophiura sarsi	1255.00	1.48
OPH	Amphiuridae	Amphiodia craterodmeta	222.50	0.26
OPH	Amphiuridae	Amphiura sundevalli	87.50	0.10
OPH	Ophiuridae	Ophiuridae	42.50	0.05
OPH	Amphiuridae	Amphiura sp.	30.00	0.04
OPH	Ophiuridae	Ophiura sp.	12.50	0.01
OPH	Ophiuridae	Ophiocten sericeum	10.00	0.01
OPH	Ophiuridae	Stegophiura nodosa	10.00	0.01
OST	Ostracoda	Ostracoda	2735.00	3.24
PLA	Platyhelminthes	Platyhelminthes	10.00	0.01
POL	Maldanidae	Maldane sarsi	10656.67	12.60
POL	Oweniidae	Owenia cf. assimilis	4100.00	4.85
POL	Lumbrineridae	Scoletoma sp	3187.50	3.77
POL	Cirratulidae	Chaetozone sp.	1410.00	1.67
POL	Capitellidae	Heteromastus sp.	1388.33	1.64
POL	Orbiniidae	Scoloplos armiger alaskensis	1168.33	1.38
POL	Maldanidae	Praxillella praetermissa	887.50	1.05
POL	Pholoidae	Pholoe sp. D Harris	852.50	1.01
POL	Capitellidae	Barantolla sp.	665.00	0.79
POL	Nephtyidae	Nephtys ciliata	617.50	0.73
POL	Sternaspidae	Sternaspis sp.	546.67	0.65
POL	Trichobranchidae	Terebellides n.sp.	497.50	0.59
POL	Onuphidae	Paradiopatra striata	435.83	0.52
POL	Cirratulidae	Chaetozone sp. 1	310.00	0.37
POL	Terebellidae	Laphania boecki	298.33	0.35
POL	Goniadidae	Glycinde wireni	295.00	0.35
POL	Polynoidae	Arcteobia anticostiensis	241.67	0.29

POL	Lumbrineridae	Scoletoma sp. 2	225.00	0.27
POL	Ampharetidae	Ampharete finmarchica	217.50	0.26
POL	Maldanidae	Nicomache lumbricalis	200.00	0.24
POL	Lumbrineridae	Scoletoma fragilis	170.00	0.20
POL	Ampharetidae	Lysippe labiata	160.00	0.19
POL	Opheliidae	Travisia cf. forbesi	155.00	0.18
POL	Maldanidae	Axiothella cantenata	142.50	0.17
POL	Flabelligeridae	Brada ?n. sp.	135.00	0.16
POL	Flabelligeridae	Bradabyssa sp.	117.50	0.14
POL	Ampharetidae	Ampharete acutifrons	112.50	0.13
POL	Pectinariidae	Cistenides hyperborea	112.50	0.13
POL	Phyllodocidae	Phyllodoce groenlandica	109.17	0.13
POL	Syllidae	Syllis sp.	107.50	0.13
POL	Lumbrineridae	Scoletoma sp. 1	100.00	0.12
POL	Sabellidae	Euchone n.sp 1	90.00	0.11
POL	Sabellidae	Sabellidae	90.00	0.11
POL	Phyllodocidae	Eteone longa/flava complex	82.50	0.10
POL	Sabellidae	Chone n.sp. 2	80.00	0.09
POL	Cirratulidae	Chaetozone sp. 2	70.00	0.08
POL	Spionidae	Prionospio sp.	67.50	0.08
POL	Syllidae	Syllis fasciata	65.00	0.08
POL	Terebellidae	Terebellidae	62.50	0.07
POL	Ampharetidae	Ampharete sp.	60.00	0.07
POL	Polynoidae	Enipo sp.	60.00	0.07
POL	Polynoidae	Gattyana cirrosa	60.00	0.07
POL	Maldanidae	Rhodine glacilior	60.00	0.07
POL	Magelonidae	Magelona pacifica	57.50	0.07
POL	Cirratulidae	Cirratulidae	50.00	0.06
POL	Polynoidae	Polynoidae	50.00	0.06
POL	Terebellidae	Terebellinae	50.00	0.06
POL	Polynoidae	Enipo tamarae	47.50	0.06
POL	Maldanidae	Praxillella sp.	45.00	0.05
POL	Spionidae	Prionospio cirrifera	42.50	0.05
POL	Paraonidae	Levinsenia gracilis	40.00	0.05
POL	Nephtyidae	Micronephthys ?minuta	40.00	0.05
POL	Maldanidae	Praxillella gracilis	40.00	0.05
POL	Syllidae	Syllis oerstedi	40.00	0.05
POL	Polynoidae	Gattyana sp.	35.00	0.04
POL	Polynoidae	Harmothoe imbricata	35.00	0.04
POL	Scalibregmatidae	Scalibregma inflatum	35.00	0.04
POL	Terebellidae	Artacama proboscidea	30.00	0.04
POL	Cirratulidae	Cirratulus cirratus	30.00	0.04
POL	Polynoidae	Enipo tarasovi	30.00	0.04
POL	Nereididae	Nereis zonata	30.00	0.04
POL	Sphaerodoridae	Sphaerodorum gracilis	30.00	0.04
POL	Terebellidae	Proclea emmi	27.50	0.03
POL	Sabellidae	Chone n.sp. 1	25.00	0.03
POL	Orbiniidae	Leitoscoloplos sp.	25.00	0.03
POL	Nephtyidae	Nephtys sp.	25.00	0.03
POL	Terebellidae	Nicolea zostericola	25.00	0.03

POL	Opheliidae	Ophelina n. sp.	25.00	0.03
POL	Terebellidae	Polycirrus sp.	25.00	0.03
POL	Flabelligeridae	Diplocirrus longisetosus	22.50	0.03
POL	Polynoidae	Eunoe sp.	22.50	0.03
POL	Cirratulidae	Aphelochaeta "tigrina"	20.00	0.02
POL	Flabelligeridae	Flabelligeridae	20.00	0.02
POL	Terebellidae	Lanassa nordenskioldi	20.00	0.02
POL	Ampharetidae	Lysippides sp.	20.00	0.02
POL	Maldanidae	Petaloproctus tenuis	20.00	0.02
POL	Polychaeta	Polychaeta	20.00	0.02
POL	Polynoidae	Bylgides sarsi	17.50	0.02
POL	Spionidae	Prionospio malmgreni	17.50	0.02
POL	Terebellidae	Thelepus cincinnatus	17.50	0.02
POL	Phyllodocidae	Eteone sp.	15.00	0.02
POL	Terebellidae	Lanassa sp.	15.00	0.02
POL	Spionidae	Marenzelleria wireni	15.00	0.02
POL	Nephtyidae	Nephtys longosetosa	15.00	0.02
POL	Nephtyidae	Nephtys pente	15.00	0.02
POL	Lumbrineridae	Scoletoma minuta	15.00	0.02
POL	Cirratulidae	Aphelochaeta sp. 1	10.00	0.01
POL	Terebellidae	Artacama conifera	10.00	0.01
POL	Polynoidae	Gattyana amondseni	10.00	0.01
POL	Terebellidae	Lanassa venusta	10.00	0.01
POL	Lumbrineridae	Lumbrineridae	10.00	0.01
POL	Opheliidae	Ophelina n. acuminata	10.00	0.01
POL	Paraonidae	Paraonidae	10.00	0.01
POL	Sphaerodoridae	Sphaerodoropsis n.sp.	10.00	0.01
POL	Syllidae	Syllidae	10.00	0.01
POL	Sabellidae	Euchone analis	7.50	0.01
POL	Maldanidae	Nicomache sp.	7.50	0.01
POL	Spionidae	Spionidae	7.50	0.01
POL	Spionidae	Spiophanes bombyx	7.50	0.01
POL	Polynoidae	Eunoe barbata	6.67	0.01
POL	Cirratulidae	Aphelochaeta "marioni"	5.00	0.01
POL	Spionidae	Boccardia sp.	5.00	0.01
POL	Polynoidae	Bylgides badia	5.00	0.01
POL	Polynoidae	Bylgides sp.	5.00	0.01
POL	Oenonidae	Drilonereis sp.	5.00	0.01
POL	Polynoidae	Enipo torelli	5.00	0.01
POL	Sabellidae	Euchone sp.	5.00	0.01
POL	Polynoidae	Eunoe nodosa	5.00	0.01
POL	Flabelligeridae	Flabelliderma n.sp.	5.00	0.01
POL	Oweniidae	Galathowenia oculata	5.00	0.01
POL	Spionidae	Laonice cirrata	5.00	0.01
POL	Maldanidae	Nicomache minor	5.00	0.01
POL	Orbiniidae	Orbiniidae	5.00	0.01
POL	Terebellidae	Polycirrinae	5.00	0.01
POL	Spionidae	Polydora sp.	5.00	0.01
POL	Scalibregmatidae	Polyphysia crassa	5.00	0.01
POL	Maldanidae	Praxillella affinis	5.00	0.01

POL	Spionidae	Spio filicornis	5.00	0.01
POL	Nephtyidae	Aglaophamus malmgreni	2.50	0.00
POL	Paraonidae	Aricidea suecica	2.50	0.00
POL	Capitellidae	Capitella capitata	2.50	0.00
POL	Polynoidae	Eunoe depressa	2.50	0.00
POL	Flabelligeridae	Flabelligera affinis	2.50	0.00
POL	Sabellidae	Potamilla neglecta	2.50	0.00
POR	Porifera	Porifera	15.00	0.02
POR	Halichondriidae	Halichondria panicea	5.00	0.01
PRI	Priapulidae	Priapulus caudatus	252.50	0.30
PRI	Priapulidae	Halicryptus spinulosus	35.00	0.04
PRI	Priapulidae	Priapulidae	17.50	0.02
PYC	Nymphonidae	Nymphon sp.	10.00	0.01
PYC	Pycnogonidae	Pycnogonidae	5.00	0.01
SIP	Gollfingiidae	Golfingia margaritacea	1219.17	1.44
SIP	Phascolionidae	Phascolion strombi	292.50	0.35
SIP	Sipunculida	Sipunculida	47.50	0.06
SIP	Golfingiidae	Golfingia vulgaris	30.00	0.04
TAN	Leptognathiidae	Leptognathia gracilis	55.00	0.07
UNK	Unknown	Unknown	50.00	0.06

APPENDIX

Table A-1. List, by Group, of taxa collected from the Chukchi Sea during 2009 and 2010. N Sum is the total number of individuals m^{-2} collected from 142 van Veen grabs at 54 stations. N Sum as % is the percentage of the overall abundance sum contributed by the listed taxa.

Group	Family	Species Name	N SUM	N SUM as
ALC	Nephtheidae	Gersemia rubiformis	30.00	0.04
AMP	Pontoporeiidae	Pontoporeia femorata	2055.83	2.43
AMP	Phoxocephalidae	Paraphoxus sp.	1468.33	1.74
AMP	Ampeliscidae	Byblis gaimardi	1098.33	1.30
AMP	Ampeliscidae	Byblis sp.	652.50	0.77
AMP	Phoxocephalidae	Harpinia serrata	645.00	0.76
AMP	Ampeliscidae	Ampelisca birulai	525.00	0.62
AMP	Ampeliscidae	Ampelisca macrocephala	457.50	0.54
AMP	Corophiidae	Protomedeia sp.	375.00	0.44
AMP	Photidae	Photis sp.	370.00	0.44
AMP	Melitidae	Melita quadrispinosa	290.00	0.34
AMP	Phoxocephalidae	Phoxocephalidae	282.50	0.33
AMP	Uristidae	Anonyx sp.	276.67	0.33
AMP	Corophiidae	Protomedeia fasciata	260.00	0.31
AMP	Ampeliscidae	Ampelisca eschrichii	254.17	0.30
AMP	Ampeliscidae	Haploops sp.	229.17	0.27
AMP	Phoxocephalidae	Harpinia sp.	190.00	0.22
AMP	Lysianassidae	Orchomene sp.	190.00	0.22
AMP	Ampeliscidae	Ampelisca sp.	182.50	0.22
AMP	Ampeliscidae	Haploops laevis	160.00	0.19
AMP	Photidae	Photis vinogradovi	140.00	0.17
AMP	Ampeliscidae	Haploops tubicola	132.50	0.16
AMP	Corophiidae	Corophium sp.	130.00	0.15
AMP	Lysianassidae	Lysianassidae	126.67	0.15
AMP	Oedicerotidae	Oedicerotidae	117.50	0.14
AMP	Pontoporeiidae	Pontoporeia sp.	117.50	0.14
AMP	Ischyroceridae	Ischyrocerus sp.	112.50	0.13
AMP	Lysianassidae	Hippomedon sp.	85.00	0.10
AMP	Photidae	Photis spasskii	80.00	0.09
AMP	Stenothoidae	Stenothoidae	70.00	0.08
AMP	Ampeliscidae	Byblis robustus	65.00	0.08
AMP	Maeridae	Maera sp.	60.00	0.07
AMP	Unciolidae	Unciola leucopis	60.00	0.07
AMP	Priscillinidae	Priscillina armata	55.00	0.07
AMP	Podoceridae	Podoceridae	50.00	0.06
AMP	Phoxocephalidae	Harpinia salebrosa	45.00	0.05
AMP	Corophiidae	Lembos arctica	45.00	0.05
AMP	Maeridae	Maera loveni	45.00	0.05
AMP	Phoxocephalidae	Harpinia kabjakovae	40.00	0.05
AMP	Ischyroceridae	Ischyrocerus latipes	33.33	0.04
AMP	Centropagidae	Guernea sp.	30.00	0.04
AMP	Caprellidae	Caprella sp.	25.00	0.03
AMP	Melitidae	Melita sp.	25.00	0.03
AMP	Synopiidae	Synopiidae	25.00	0.03

AMP	Haustoriidae	Haustorius sp.	20.00	0.02
AMP	Nebaliidae	Nebalia sp.	20.00	0.02
AMP	Pleustidae	Pleustidae	15.00	0.02
AMP	Photidae	Podoceropsis sp.	15.00	0.02
AMP	Lysianassidae	Socarnes bidenticulatus	15.00	0.02
AMP	Oedicerotidae	Arrhis luthkei	10.00	0.01
AMP	Phoxocephalidae	Grandiphoxus sp.	10.00	0.01
AMP	Melitidae	Melita dentata	10.00	0.01
AMP	Oedicerotidae	Monoculodes diamesus	10.00	0.01
AMP	Uristidae	Onisimus krassini	10.00	0.01
AMP	Oedicerotidae	Paroediceros sp.	10.00	0.01
AMP	Photidae	Photidae	10.00	0.01
AMP	Oedicerotidae	Aceroides latipes	5.00	0.01
AMP	Oedicerotidae	Arrhis sp.	5.00	0.01
AMP	Ischyroceridae	Ischyroceridae	5.00	0.01
AMP	Oedicerotidae	Monoculodes schneideri	5.00	0.01
AMP	Oedicerotidae	Monoculodes sp.	5.00	0.01
AMP	Uristidae	Onisimus sp.	5.00	0.01
AMP	Synopiidae	Syrrhoe crenulata	5.00	0.01
AMP	Liljeborgiidae	Liljeborgia fissicornis	2.50	0.00
AMP	Unicolidae	Unicola sp.	2.50	0.00
ANE	Actinaria	Actinaria	280.00	0.33
ANE	Hormathiidae	Hormathia sp.	25.00	0.03
ASC	Molgulidae	Mogula sp.	77.50	0.09
ASC	Molgulidae	Eugyra pedunculata	60.00	0.07
ASC	Styelidae	Dendrodoa sp.	40.00	0.05
ASC	Styelidae	Pelonaia corrugata	35.00	0.04
ASC	Ascidian	Ascidian	32.50	0.04
ASC	Corellidae	Chelyosoma macleayanum	17.50	0.02
ASC	Pyuridae	Halocynthia aurantium	5.00	0.01
ASC	Styelidae	Styela rustica	5.00	0.01
ASC	Styelidae	Styela sp.	5.00	0.01
AST	Asteridae	Asteridae	60.00	0.07
BIV	Nuculidae	Ennucula tenuis	5925.83	7.01
BIV	Nuculanidae	Nuculana pernula	2825.00	3.34
BIV	Mytilidae	Musculus discors	2280.00	2.70
BIV	Tellinidae	Macoma calcarea	1910.42	2.26
BIV	Tellinidae	Macoma moesta	785.00	0.93
BIV	Yoldiidae	Yoldia hyperborea	542.50	0.64
BIV	Carditidae	Cyclocardia crebricostata	435.83	0.52
BIV	Tellinidae	Macoma sp.	410.00	0.48
BIV	Thyasiridae	Thyasira flexuosa	385.00	0.46
BIV	Astartidae	Astarte borealis	375.00	0.44
BIV	Montacutidae	Montacuta spitzbergensis	369.17	0.44
BIV	Nuculanidae	Nuculana sp.	275.00	0.33
BIV	Veneridae	Liocyma fluctuosa	257.50	0.30
BIV	Astartidae	Astarte montagui	225.00	0.27
BIV	Lasaeidae	Rochefortia tumida	105.00	0.12
BIV	Montacutidae	Mysella planata	95.00	0.11
BIV	Yoldiidae	Yoldia myalis	95.00	0.11

BIV	Cardiidae	Serripes groenlandicus	82.50	0.10
BIV	Thyasiridae	Axinopsida serricata	52.50	0.06
BIV	Periplomatidae	Periploma aleutica	37.50	0.04
BIV	Thraciidae	Thracia sp.	37.50	0.04
BIV	Mytilidae	Musculus niger	35.00	0.04
BIV	Hiatellidae	Hiatella arctica	32.50	0.04
BIV	Mytilidae	Crenella decussata	25.00	0.03
BIV	Conidae	Curtitoma incisula	20.00	0.02
BIV	Astartidae	Astarte sp.	15.00	0.02
BIV	Cardiidae	Cardiidae	15.00	0.02
BIV	Tellinidae	Macoma torelli	15.00	0.02
BIV	Mytilidae	Musculus glacialis	15.00	0.02
BIV	Mytilidae	Musculus sp.	15.00	0.02
BIV	Myidae	Mya sp.	15.00	0.02
BIV	Cardiidae	Clinocardium ciliatum	12.50	0.01
BIV	Astartidae	Astarte elliptica	10.00	0.01
BIV	Lyonsiidae	Lyonsia arenosa	10.00	0.01
BIV	Pandoridae	Pandora glacialis	7.50	0.01
BIV	Lasaeidae	Lasaeidae	5.00	0.01
BIV	Mytilidae	Musulus niger	5.00	0.01
BIV	Yoldiidae	Yoldia sp.	5.00	0.01
BIV	Mytilidae	Musculus corrugatus	2.50	0.00
BRA	Brachiopoda	Brachiopoda	50.00	0.06
BRY	Alcyonidiidae	Alcyonidium disciforme	150.00	0.18
BRY	Alcyonidiidae	Alcyonidium gelatinosum	72.50	0.09
BRY	Eucrateidae	Eucratea loricata	56.67	0.07
BRY	Bryozoa	Bryozoa	45.00	0.05
BRY	Flustridae	Carbasea carbasea	12.50	0.01
BRY	Vesiculariidae	Bowerbankia sp.	5.00	0.01
BRY	Bugulidae	Dendrobeania murrayana	5.00	0.01
BRY	Flustridae	Securiflustra securifrons	5.00	0.01
BRY	Flustridae	Securiflustra truncata	5.00	0.01
CHI	Ischnochitonidae	Ischnochiton albus	12.50	0.01
CIR	Balanidae	Balanus crenatus	147.50	0.17
CIR	Balanidae	Balanus sp.	20.00	0.02
CRU	Oregoniidae	Hyas coarctacus	17.50	0.02
CRU	Paguridae	Pagurus rathbuni	12.50	0.01
CRU	Pandalidae	Pandalus sp.	12.50	0.01
CRU	Paguridae	Pagurus sp.	10.00	0.01
CRU	Oregoniidae	Chionoecetes opilio	5.00	0.01
CRU	Hippolytidae	Lebbeus sp.	5.00	0.01
CRU	Paguridae	Pagurus trigonocheirus	5.00	0.01
CRU	Decapod	Decapod	2.50	0.00
CRU	Pandalidae	Pandalus borealis	2.50	0.00
CUM	Diastylidae	Brachydiastylis resima	2063.33	2.44
CUM	Leuconidae	Leucon sp.	320.00	0.38
CUM	Leuconidae	Leucon nasica	267.50	0.32
CUM	Leuconidae	Eudorellopsis integra	115.00	0.14
CUM	Leuconidae	Eudorella sp.	105.00	0.12
CUM	Leuconidae	Leucon nasicoides	77.50	0.09

CUM	Leuconidae	Eudorella emarginata	35.00	0.04
CUM	Leuconidae	Eudorellopsis sp.	35.00	0.04
CUM	Diastylidae	Diastylis rathkei	15.00	0.02
CUM	Diastylidae	Diastylis sp.	10.00	0.01
CUM	Diastylidae	Diastylis spinulosa	6.67	0.01
CUM	Cumacea	Cumacea	5.00	0.01
CUM	Diastylidae	Diastylis dalli	5.00	0.01
CUM	Lambropidae	Lamprops sp.	5.00	0.01
CUM	Diastylidae	Leptostylis sp.	5.00	0.01
CUM	Leuconidae	Leuconidae	5.00	0.01
CUM	Nannastacidae	Nannastacidae	5.00	0.01
ECH	Echinarachniidae	Echinarachnius parma	220.00	0.26
ECH	Echiuridae	Echiurus echiurus alascanus	40.00	0.05
ECH	Strongylocentrotidae	Strongylocentrotus droebachiensis	5.00	0.01
FOR	Foraminifera	Foraminifera	210.00	0.25
GAS	Cylichnidae	Cylichna alba	132.50	0.16
GAS	Solariellidae	Solariella obscura	107.50	0.13
GAS	Turritellidae	Tachyrhynchus erosus	87.50	0.10
GAS	Conidae	Oenopota sp.	86.67	0.10
GAS	Naticidae	Cryptonatica affinis	70.00	0.08
GAS	Naticidae	Euspira pallida	60.00	0.07
GAS	Cancellariidae	Admete viridula	50.00	0.06
GAS	Solariellidae	Solariella varicosa	50.00	0.06
GAS	Cylichnidae	Cylichna occulta	38.33	0.05
GAS	Retusidae	Retusa obtusa	37.50	0.04
GAS	Turridae	Nodotoma impressa	30.00	0.04
GAS	Turritellidae	Tachyrhynchus sp.	30.00	0.04
GAS	Conidae	Obesotoma tenuilirata	25.00	0.03
GAS	Lepetidae	Lepeta caeca	20.00	0.02
GAS	Cancellariidae	Admete sp.	15.00	0.02
GAS	Buccinidae	Buccinidae	15.00	0.02
GAS	Solariellidae	Solariellidae	15.00	0.02
GAS	Turritellidae	Tachyrhynchus reticulatus	15.00	0.02
GAS	Conidae	Curtitoma novajasemijensis	12.50	0.01
GAS	Muricidae	Boreotrophon beringi	10.00	0.01
GAS	Muricidae	Boreotrophon truncatus	10.00	0.01
GAS	Buccinidae	Buccinum angulosum	10.00	0.01
GAS	Buccinidae	Colus hallii	10.00	0.01
GAS	Daphniidae	Daphnia minuta	10.00	0.01
GAS	Buccinidae	Neptunea heros	10.00	0.01
GAS	Conidae	Oenopota impressa	10.00	0.01
GAS	Cancellariidae	Admete regina	5.00	0.01
GAS	Buccinidae	Buccinum ciliatum	5.00	0.01
GAS	Buccinidae	Buccinum scalariforme	5.00	0.01
GAS	Gastropoda	Gastropoda	5.00	0.01
GAS	Mangeliidae	Granotoma krausei	5.00	0.01
GAS	Littorinidae	Lacuna glacialis	5.00	0.01
GAS	Turbinidae	Margarites sp.	5.00	0.01
GAS	Buccinidae	Neptunea communis	5.00	0.01
GAS	Conidae	Obesotoma simplex	5.00	0.01

GAS	Conidae	Oenopota elegans	5.00	0.01
GAS	Conidae	Oenopota viridula	5.00	0.01
GAS	Buccinidae	Plicifusus kroyeri	5.00	0.01
GAS	Mangeliidae	Propebela nobilis	5.00	0.01
GAS	Buccinidae	Buccinum sp.	2.50	0.00
GAS	Conidae	Curtitoma lawrenciana	2.50	0.00
HOL	Cucumariidae	Ocnus glacialis	460.00	0.54
HOL	Psolidae	Psolus sp.	32.50	0.04
HOL	Cucumariidae	Cucumaria sp.	5.00	0.01
HYD	Hydrozoa	Hydrozoa	67.50	0.08
HYD	Sertulariidae	Sertularia cupressoides	30.00	0.04
HYD	Sertulariidae	Abietinaria abietina	20.00	0.02
HYD	Lafoeidae	Grammaria sp.	20.00	0.02
HYD	Campanulariidae	Obelia longissima	15.00	0.02
HYD	Sertulariidae	Sertularia sp.	12.50	0.01
HYD	Bonneviellidae	Bonneviella sp.	10.00	0.01
HYD	Lafoeidae	Lafoeina sp.	5.00	0.01
HYD	Sertulariidae	Abietinaria sp.	2.50	0.00
HYD	Sertulariidae	Thuiaria sp.	2.50	0.00
HYD	Stylasteridae	Distichopora borealis	20.00	0.02
ISO	Idoteidae	Synidotea sp.	20.00	0.02
NEA	Nematoda	Nematoda	9360.83	11.07
NEM	Nemertea	Nemertea	469.17	0.55
OPH	Ophiuridae	Ophiura sarsi	1255.00	1.48
OPH	Amphiuridae	Amphiodia craterodmeta	222.50	0.26
OPH	Amphiuridae	Amphiura sundevalli	87.50	0.10
OPH	Ophiuridae	Ophiuridae	42.50	0.05
OPH	Amphiuridae	Amphiura sp.	30.00	0.04
OPH	Ophiuridae	Ophiura sp.	12.50	0.01
OPH	Ophiuridae	Ophiocten sericeum	10.00	0.01
OPH	Ophiuridae	Stegophiura nodosa	10.00	0.01
OST	Ostracoda	Ostracoda	2735.00	3.24
PLA	Platyhelminthes	Platyhelminthes	10.00	0.01
POL	Maldanidae	Maldane sarsi	10656.67	12.60
POL	Oweniidae	Owenia cf. assimilis	4100.00	4.85
POL	Lumbrineridae	Scoletoma sp	3187.50	3.77
POL	Cirratulidae	Chaetozone sp.	1410.00	1.67
POL	Capitellidae	Heteromastus sp.	1388.33	1.64
POL	Orbiniidae	Scoloplos armiger alaskensis	1168.33	1.38
POL	Maldanidae	Praxillella praetermissa	887.50	1.05
POL	Pholoidae	Pholoe sp. D Harris	852.50	1.01
POL	Capitellidae	Barantolla sp.	665.00	0.79
POL	Nephtyidae	Nephtys ciliata	617.50	0.73
POL	Sternaspidae	Sternaspis sp.	546.67	0.65
POL	Trichobranchidae	Terebellides n.sp.	497.50	0.59
POL	Onuphidae	Paradiopatra striata	435.83	0.52
POL	Cirratulidae	Chaetozone sp. 1	310.00	0.37
POL	Terebellidae	Laphania boecki	298.33	0.35
POL	Goniadidae	Glycinde wireni	295.00	0.35
POL	Polynoidae	Arcteobia anticostiensis	241.67	0.29

POL	Lumbrineridae	Scoletoma sp. 2	225.00	0.27
POL	Ampharetidae	Ampharete finmarchica	217.50	0.26
POL	Maldanidae	Nicomache lumbricalis	200.00	0.24
POL	Lumbrineridae	Scoletoma fragilis	170.00	0.20
POL	Ampharetidae	Lysippe labiata	160.00	0.19
POL	Opheliidae	Travisia cf. forbesi	155.00	0.18
POL	Maldanidae	Axiothella cantenata	142.50	0.17
POL	Flabelligeridae	Brada ?n. sp.	135.00	0.16
POL	Flabelligeridae	Bradabyssa sp.	117.50	0.14
POL	Ampharetidae	Ampharete acutifrons	112.50	0.13
POL	Pectinariidae	Cistenides hyperborea	112.50	0.13
POL	Phyllodocidae	Phyllodoce groenlandica	109.17	0.13
POL	Syllidae	Syllis sp.	107.50	0.13
POL	Lumbrineridae	Scoletoma sp. 1	100.00	0.12
POL	Sabellidae	Euchone n.sp 1	90.00	0.11
POL	Sabellidae	Sabellidae	90.00	0.11
POL	Phyllodocidae	Eteone longa/flava complex	82.50	0.10
POL	Sabellidae	Chone n.sp. 2	80.00	0.09
POL	Cirratulidae	Chaetozone sp. 2	70.00	0.08
POL	Spionidae	Prionospio sp.	67.50	0.08
POL	Syllidae	Syllis fasciata	65.00	0.08
POL	Terebellidae	Terebellidae	62.50	0.07
POL	Ampharetidae	Ampharete sp.	60.00	0.07
POL	Polynoidae	Enipo sp.	60.00	0.07
POL	Polynoidae	Gattyana cirrosa	60.00	0.07
POL	Maldanidae	Rhodine glacilior	60.00	0.07
POL	Magelonidae	Magelona pacifica	57.50	0.07
POL	Cirratulidae	Cirratulidae	50.00	0.06
POL	Polynoidae	Polynoidae	50.00	0.06
POL	Terebellidae	Terebellinae	50.00	0.06
POL	Polynoidae	Enipo tamarae	47.50	0.06
POL	Maldanidae	Praxillella sp.	45.00	0.05
POL	Spionidae	Prionospio cirrifera	42.50	0.05
POL	Paraonidae	Levinsenia gracilis	40.00	0.05
POL	Nephtyidae	Micronephthys ?minuta	40.00	0.05
POL	Maldanidae	Praxillella gracilis	40.00	0.05
POL	Syllidae	Syllis oerstedi	40.00	0.05
POL	Polynoidae	Gattyana sp.	35.00	0.04
POL	Polynoidae	Harmothoe imbricata	35.00	0.04
POL	Scalibregmatidae	Scalibregma inflatum	35.00	0.04
POL	Terebellidae	Artacama proboscidea	30.00	0.04
POL	Cirratulidae	Cirratulus cirratus	30.00	0.04
POL	Polynoidae	Enipo tarasovi	30.00	0.04
POL	Nereididae	Nereis zonata	30.00	0.04
POL	Sphaerodoridae	Sphaerodorum gracilis	30.00	0.04
POL	Terebellidae	Proclea emmi	27.50	0.03
POL	Sabellidae	Chone n.sp. 1	25.00	0.03
POL	Orbiniidae	Leitoscoloplos sp.	25.00	0.03
POL	Nephtyidae	Nephtys sp.	25.00	0.03
POL	Terebellidae	Nicolea zostericola	25.00	0.03

POL	Opheliidae	Ophelina n. sp.	25.00	0.03
POL	Terebellidae	Polycirrus sp.	25.00	0.03
POL	Flabelligeridae	Diplocirrus longisetosus	22.50	0.03
POL	Polynoidae	Eunoe sp.	22.50	0.03
POL	Cirratulidae	Aphelochaeta "tigrina"	20.00	0.02
POL	Flabelligeridae	Flabelligeridae	20.00	0.02
POL	Terebellidae	Lanassa nordenskioldi	20.00	0.02
POL	Ampharetidae	Lysippides sp.	20.00	0.02
POL	Maldanidae	Petaloproctus tenuis	20.00	0.02
POL	Polychaeta	Polychaeta	20.00	0.02
POL	Polynoidae	Bylgides sarsi	17.50	0.02
POL	Spionidae	Prionospio malmgreni	17.50	0.02
POL	Terebellidae	Thelepus cincinnatus	17.50	0.02
POL	Phyllodocidae	Eteone sp.	15.00	0.02
POL	Terebellidae	Lanassa sp.	15.00	0.02
POL	Spionidae	Marenzelleria wireni	15.00	0.02
POL	Nephtyidae	Nephtys longosetosa	15.00	0.02
POL	Nephtyidae	Nephtys pente	15.00	0.02
POL	Lumbrineridae	Scoletoma minuta	15.00	0.02
POL	Cirratulidae	Aphelochaeta sp. 1	10.00	0.01
POL	Terebellidae	Artacama conifera	10.00	0.01
POL	Polynoidae	Gattyana amondseni	10.00	0.01
POL	Terebellidae	Lanassa venusta	10.00	0.01
POL	Lumbrineridae	Lumbrineridae	10.00	0.01
POL	Opheliidae	Ophelina n. acuminata	10.00	0.01
POL	Paraonidae	Paraonidae	10.00	0.01
POL	Sphaerodoridae	Sphaerodoropsis n.sp.	10.00	0.01
POL	Syllidae	Syllidae	10.00	0.01
POL	Sabellidae	Euchone analis	7.50	0.01
POL	Maldanidae	Nicomache sp.	7.50	0.01
POL	Spionidae	Spionidae	7.50	0.01
POL	Spionidae	Spiophanes bombyx	7.50	0.01
POL	Polynoidae	Eunoe barbata	6.67	0.01
POL	Cirratulidae	Aphelochaeta "marioni"	5.00	0.01
POL	Spionidae	Boccardia sp.	5.00	0.01
POL	Polynoidae	Bylgides badia	5.00	0.01
POL	Polynoidae	Bylgides sp.	5.00	0.01
POL	Oenonidae	Drilonereis sp.	5.00	0.01
POL	Polynoidae	Enipo torelli	5.00	0.01
POL	Sabellidae	Euchone sp.	5.00	0.01
POL	Polynoidae	Eunoe nodosa	5.00	0.01
POL	Flabelligeridae	Flabelliderma n.sp.	5.00	0.01
POL	Oweniidae	Galathowenia oculata	5.00	0.01
POL	Spionidae	Laonice cirrata	5.00	0.01
POL	Maldanidae	Nicomache minor	5.00	0.01
POL	Orbiniidae	Orbiniidae	5.00	0.01
POL	Terebellidae	Polycirrinae	5.00	0.01
POL	Spionidae	Polydora sp.	5.00	0.01
POL	Scalibregmatidae	Polyphysia crassa	5.00	0.01
POL	Maldanidae	Praxillella affinis	5.00	0.01

POL	Spionidae	Spio filicornis	5.00	0.01
POL	Nephtyidae	Aglaophamus malmgreni	2.50	0.00
POL	Paraonidae	Aricidea suecica	2.50	0.00
POL	Capitellidae	Capitella capitata	2.50	0.00
POL	Polynoidae	Eunoe depressa	2.50	0.00
POL	Flabelligeridae	Flabelligera affinis	2.50	0.00
POL	Sabellidae	Potamilla neglecta	2.50	0.00
POR	Porifera	Porifera	15.00	0.02
POR	Halichondriidae	Halichondria panicea	5.00	0.01
PRI	Priapulidae	Priapulus caudatus	252.50	0.30
PRI	Priapulidae	Halicryptus spinulosus	35.00	0.04
PRI	Priapulidae	Priapulidae	17.50	0.02
PYC	Nymphonidae	Nymphon sp.	10.00	0.01
PYC	Pycnogonidae	Pycnogonidae	5.00	0.01
SIP	Gollfingiidae	Golfingia margaritacea	1219.17	1.44
SIP	Phascolionidae	Phascolion strombi	292.50	0.35
SIP	Sipunculida	Sipunculida	47.50	0.06
SIP	Golfingiidae	Golfingia vulgaris	30.00	0.04
TAN	Leptognathiidae	Leptognathia gracilis	55.00	0.07
UNK	Unknown	Unknown	50.00	0.06

Table A-2. A table of polychaete re-identifications with references and comments to support the changes by Leslie Harris, a polychaete taxonomist and curator at the Natural History Museum of Los Angeles County. She studied a selection of polychaetes collected on this project in summer 2010.

Problem identifications

Current identification	Old Identification	References for Re-identification	Leslie Harris Comments
Ampharete arctica	Ampharete finmarchica	Holthe 1986; Jirkov, 1989; Jirkov, 2001	A. arctica has been synonymized under A. finmarchica.
Aphelochaeta "tigrina", Aphelochaeta "marioni", Chaetozone sp. 1, Chaetozone sp. 2	Chaetozone setosa	Harris personal notes; C.A. Phillips, personal notes; Blake 1996	Specimens were examined by cirratulid specialist C.A.Phillips and found to consist of 4 distinct species, 2 of which appear to be undescribed. The other 2 seem to be described however the specimens were incomplete & lacking some characters necessary for confirmation. Quotation marks were used to denote the uncertainty of the latter 2 identifications. The geographic range of true C. setosa was recently restricted to Northern Europe in the area between the North Sea, Irish Sea, and Svalbard (Chambers et al 2007).
Arcteobia anticostiensis	Harmothoe imbricata	Uschakov, 1982	Easy to mistake for H. imbricata as this species also has ventro-lateral anterior eyes under the cephalic peaks. The areolated "half moon" pigment pattern is fairly distinctive as is the presence of 2 types of notosetae - short, blunt-tipped and long with capillary tips. Harmothoe only has 1 type o notosetae.
Barantolla sp.	Barantolla americana	Green 2002; Hutchings & Rainer 1981; Harris personal Notes	COMIDA material was compared to the types of B. americana Hartman 1963. There were differences in stain pattern & chaetal dentition between the types & the Chukchi worms plus significant differences among the Chukchi specimens so they were left as "Barantolla sp." pending further work. It is possible that Arctic records of B. americana represent an undescribed species.

Brada ?n. sp; Diplocirrus longisetosus	Flabelligera mastigophora	Jirkov & Filippova 2001; Salzar-Vallejo unpublished manuscript; Our, Bakke, & Kongsrus 2011	Some of these specimens turned out to be D. longisetosus; after consultation with Dr. Salazar-Vallejo the others were thought to be an undescribed species of Brada
Bradabyssa	Brada granulata, Brada nuda, Brada villosa, Diplocirrus longisetosus	Salazar-Vallejo unpublished manuscript	These particular specimens belong to the genus Bradabyssa Hartman 1967 as redefined by Dr. Sergio Salazar-Vallejo who is in the process of revising all genera & species in the family Flabelligeridae. They appear to belong to different species as well and will be sent to Dr. Salazar-Vallejo for re-identification.
Chone n. sp. 1	Chone sp, Sabellidae, Laonome kroyeri	Tovar-Hernandez 2007a, 2007b; Nishi et al. 2009	Does not match any described species and is probably undescribed (Dr. Mariana Tovar-Hernandez, personal communication)
Chone n. sp. 2	Chone sp	Tovar-Hernandez 2007a, 2007b; Nishi et al. 2009	Does not match any described species and is probably undescribed (Dr. Mariana Tovar-Hernandez, personal communication)
Cistenides hyperborea	Cistenides granulata	Uschakov 1955; Jirkov 2001	According to Uschakov (1955) C. granulata has 7-10 pairs of flabellum while C. hyperborea has 10-15. I counted 12 setae on each side.
Eteone longa/flava complex	Eteone longa	Pleijel 1993a	Falls into the E. longa/flava complex as discussed in Pleijel 1993a
Eteone sp.	Eteone longa	Uschakov 1972; Pleijel 1993a; Wilson 1988; Pleijel 1993b	Did not match any of the species described for the temperate-boreal North Pacific and Arctic regions in English-language literature.
Euchone n. sp. 1	Euchone sp.	Tovar-Hernandez 2007a, 2007b; Nishi et al. 2009; Banse 1970, 1972; Cochrane 2000, 2003	A small species, easily mis-identified as Chone. Appears to be an undescribed species.
Flabelliderma n. sp.	Flabelligera affinis	Salazar-Vallejo 2007	Distinctly different from F. affinis. Will be sent to Dr. Salazar-Vallejo for identification.
Glycinde wireni	Glycinde picta	Boggemann, 2005	According to Boggemann, 2005, 2 species of Glycinde have been found in the Chukchi Sea: G armigera & G. wireni Arwidsson 1899, both of which are easily distinguished from G. picta by the absence of ventral micrognaths (jaw pieces).

Heteromastus sp.	Heteromastus filiformis	Hutchings & Rainer 1982	The original type locality of H. filiformis is Mediterranean France; a neotype was erected by Hutchings & Rainer (1982) from Alexandria, Egypt. They regarded it as a cosmopolitan species. The Chukchi specimens did not quite match their re-description and given the difference in habitat (Arctic versus warm-temperate) I am reluctant to call them filiformis without direct comparison to verified specimens.
Nepthys pente	Nephtys ciliata	Rainer, 1991.	Keys to ciliata in Uschakov, 1955; keys to pente in Rainer, 1991. Pente found from Greenland to Murman coast, Labrador, North Sea. Rainer says pente "…has frequenty been identified as N. ciliata and may have a wider distribution….".
Ophelina n. sp.?	Ophelina sp.	Jirkov 2001; Rowe 2010; Parapar et al. 2011	May be new species or described in a non-English language publication.
Owenia cf. assimilis	Owenia fusiformis	Ford & Hutchings 2005; Koh & Bhaud 2003; Koh, Bhand, & Jirkov 2003.	Described from Norway, so this is a possible range extension for O. assimilis if the identification is correct. Specimens need to be compared to type or topotype material of O. assimilis.
Pholoe sp. D Harris	Pholoe minuta	Petersen 1998; Pettibone 1992; Harris, personal notes	Pholoe minuta, described from Greenland, is a strongly pigmented species which has erroneously been reported from many different regions. These specimens do not appear to be minuta nor do they match any of the NE Pacific species (P. glabra Hartman, courtneyae Blake, sp. A-B-C Harris) that I have encountered. P. assimilis Orsted has also been reported from the Chukchi Sea (MacDonald et al 2009) but I have no way of knowing if these specimens are the same species as their's or if they identified their P. assimils correctly as there isn't a good current description.
Phyllodoce groenlandica	Anaitides groenlandica	Uschakov, 1972; Pleijel, 1993a; Pleijel, 1993b	Species identified correctly; since the publication of Uschakov the genera Phyllodoce & Anaitides were synonymized.

Polyphysia crassa	Scalibregma inflatum	Worsfold, undated; Boggemann 1997	Scalibregma inflatum is nearly always orange or dark yellow in color & has dorsal & ventral cirri in the posterior body region. This animal is white & lacks dorsal & ventral cirri in the posterior. Normally P. crassa looks more maggot like but this specimen is elongated, giving it a typical S. inflatum shape which is misleading. It was the white color that made me take a closer look for the presence of parapodial cirri.
Scoletoma fragilis	Lumbrineris fragilis	Harris, personal notes; Budaeva 2005	The genus Lumbrineris has been split into several genera based on setal & jaw structure.
Scoletoma minuta	Lumbrineris fragilis	Harris, personal notes; Budaeva 2005	Misidentification.
Scoletoma sp. 1	Lumbrineris fragilis	Harris, personal notes; Budaeva 2005	Differs from S. fragilis in species-specific characters, e.g., arrangement of setae & number of teeth on jaw pieces.
Scoletoma sp. 2	Lumbrineris fragilis	Harris, personal notes; Budaeva 2005	Differs from S. fragilis in species-specific characters, e.g., arrangement of setae & number of teeth on jaw pieces.
Sphaerodoropsis n.sp.?	Sphaerodoropsis minuta	Fauchald, 1974; Reuscher & Fiege, 2011	S. minuta has 2 postsetal parapodial lobes & the ventrum is covered by small papilae; this has no postsetal lobes & no papillae on the ventrum. It did not key out in Fauchald, 1974. Using the updated species key in Reuscher & Fiege, 2011, it keyed out to S. polypapillata Hartmann-Schroder & Rosenfeldt, 1988, but does not match that Antarctic species. Probably an undescribed species.
Sternaspis n. sp.?	Sternaspis scutata	Petersen 2000	Petersen (2000) gives detailed descriptions of S. fossor (Maine), cf. fossor (California) and S. scutata (Mediterrean) and these specimens do not match any of the three. According to Petersen there are about 15 valid species many of which had been previously considered to be synonyms of S. scutata. Sendall (2006) examined all extant type material & topotype material in his revision. these specimens do not appear to match any the species he redescribes.

Syllis "oerstedi"	Syllis sp., Syllis oerstedi	Licher 1999	Syllis oerstedi is now considered a nomen dubium without an adequate description (Licher, 1999). The type cannot be found so the species cannot be redefined. Ramos, San Martin & Sikorski (2010) apparently feel it's valid & intend to establish a type & redefine the species but that hasn't been done yet. As it keys out to S. oerstedi in Uschakov 1955 I have left the specimens as "oerstedi" pending the redescription.
Syllis sp. B	Syllis sp.	Licher 2000	Does not key out to any known Syllis for the area; more work is needed to confirm if it is undescribed or not.
Terebellides n. sp.?	Terebellides stroemi	Jirkov 1989; Jirkov 2001; Williams 1984; Garraffoni, Lana & Hutchings 2005	T.stroemi was previously considered to be a cosmopolitan species. Starting with Williams (1984) authors have shown that it consists of many morphologically distinct species. The Chukchi specimens do not match any described species known for the region.
Travisia cf. forbesi	Travisia forbesii	Jirkov 2001; Rowe 2010; Kirkegaard 1996; Uschakov 1955	Several authors have suggested that T. forbesi is one of the "cosmopolitan" species which may prove to consist of multiple species. The discrepancies between descriptions in various references such as Kirkegaard 1996 & Uschakov 1955 may result from such a mix up of species.